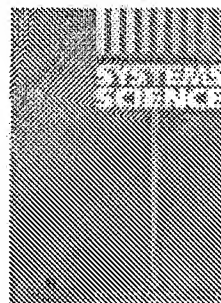


ingentaconnect

Bridge MonitoringBridge and Structural Health Monitoring -
contact us!**Alert Button for Seniors**"As Seen on TV" 24/7 Senior Alert Help
Button

Ads by Google

Next generation structural health
monitoring and its integration into
aircraft design**Author:** Boller C.¹**Source:** International Journal of Systems Science, Volume
31, Number 11, 1 November 2000 , pp. 1333-1349(17)**Publisher:** Taylor and Francis Ltd

< previous article | next article > | view table of contents

Mark item**Key:** ☐ - Free Content ☐ - New Content ☐ - Subscribed Content ☐ - Free Trial
Content**Abstract:**

Structural health monitoring (SHM) has become increasingly important with regard to ageing aircraft, required enhanced performance and the need to reduce aircraft operational cost. Affordable advanced miniaturized sensors and continuous improvement in data processing technology combined with powerful software algorithms has allowed non-destructive testing (NDT) to become an integral part of structural materials and has thus given structures a self-sensing functionality. This paper describes where to integrate SHM into the aircraft design process and how to validate the established loads monitoring process in comparison to an emerging damage monitoring solution, before more precisely describing a technology selection regarding damage monitoring. Acousto-ultrasonics is a technique being especially emphasized. Results from laboratory experiments will be shown and commented and a perspective of future trends will be given.

References: 5 references ☐ open in new window

Articles that cite this article?

Language: English**Document Type:** Research article**Affiliations: 1:** DaimlerChrysler Aerospace, Military Aircraft, D-81663
München/Germany.**The full text article is available for purchase****\$43.75 plus tax** ☒ Credit/debit card ☐ Institutional payment account

OR

< previous article | next article > | view table of contents

Table of Contents

With Suggested Relevant References and Page Numbers

Patent Fulltext Files	1
Second approach	5
Patent Abstract Files	11
Second approach	14
21/3,K/22 (Item 22 from file: 350)	20 ✓
NPL Full Text Files	22
17/3,K/27 (Item 3 from file: 624)	26 ✓
NPL Abstract Files	29
16/5/15 (Item 6 from file: 8)	40 ✓
Inventor Search	50
Patent Files Searched	50
NPL Files Searched	53
Secondary author search	56
Supplemental Resources	61
AIAA Journal	76
Other References (IEEE)	79

Patent Fulltext Files

File 348:EUROPEAN PATENTS 1978-2007

File 349:PCT FULLTEXT 1979-2007

Set	Items	Description
S1	14077	AEROELASTIC? OR AERODYNAMIC? OR AERO() ELASTIC? OR AERO()- DYNAMIC?
Limitall/s1		
S2	143	NEURAL()(NET? ? OR NETWORK? ?) OR ARTIFICIAL()INTELLIGENCE OR (VIRTUAL OR INTELLIGENT) (2N)(ROBOT? OR AGENT? ? OR SERVO? ? OR BOT OR BOTS OR SYSTEM? ?) OR SOFTBOT? OR SOFT()(BOT OR B- OTS)
S3	660	AI OR SYMBOT? OR KNOWBOT? OR INFERENCE()ENGINE? ? OR ANN OR (ARTIFICIAL () NEURAL () NETWORK?) OR (PARALLEL () DISTRIBU- TED () PROCESSING () NETWORK?)
S4	27	EXPERT () SYSTEM? ? OR INTELLIGENT () RETRIEVAL OR KNOWLE- DGE () ENGINEERING OR MACHINE ()LEARNING
S5	774	S2:S4
S6	11928	REPAIR??? OR ALTERATION? ? OR ALTER??? OR MODIFY OR MODIF- ICATION OR MODIFIED OR CORRECT??? OR BROKEN OR BREAK??? OR FI- X??? OR WORN OR MEND??? OR MALFUNCTION? OR FAILU- RE? ? OR MISFUNCTION? OR LEAK??? OR SERVICING
S9	1767	(ENTER??? OR INPUT????? OR INSERT????? OR ADD??? OR SCAN????? OR READ????) (5N) (DEVICE? ? OR MODULE? ? OR PARAMETER? ?)
S10	38	IC=(G06F-015? OR G06F-019?)
S11	230	S1 AND S5 AND S6 AND S9
S12	12	S1 (50N) S5 AND S6 AND S9
S14	12	S1 AND S5 AND S10
S15	24	S12 OR S14
S16	19	S15 AND PY=1963:2004
S17	19	IDPAT (sorted in duplicate/non-duplicate order)
S18	19	IDPAT (primary/non-duplicate records only)

18/3,K/2 (Item 2 from file: 348)
DIALOG(R)File 348:EUROPEAN PATENTS
(c) 2007 European Patent Office. All rts. reserv.

01402725

An automized blade shape designing method

PATENT ASSIGNEE:

HONDA GIKEN KOGYO KABUSHIKI KAISHA, (2060610), 1-1, Minami-Aoyama 2-chome
, Minato-ku Tokyo, (JP), (Applicant designated States: all)

INVENTOR:

Yamaguchi Yoshihiro c/o KK.Honda Gijutsu Kenkyusho, 4-1, Chuo 1-chome
Wako-shi, Saitama, (JP)

Arima Toshiyuki c/o K.K. Honda Gijutsu Kenkyusho, 4-1, Chuo 1-chome
Wako-shi, Saitama, (JP)

LEGAL REPRESENTATIVE:

Rupp, Christian, Dipl.Phys. et al (88331), Mitscherlich & Partner Patent-
und Rechtsanwälte Sonnenstrasse 33, 80331 Munchen, (DE)

PATENT (CC, No, Kind, Date): EP 1186747 A2 020313 (Basic)

APPLICATION (CC, No, Date): EP 2001120075 010821;

PRIORITY (CC, No, Date): JP 2000268316 000905

DESIGNATED STATES: AT; BE; CH; CY; DE; DK; ES; FI; FR; GB; GR; IE; IT; LI;
LU; MC; NL; PT; SE; TR

EXTENDED DESIGNATED STATES: AL; LT; LV; MK; RO; SI

INTERNATIONAL PATENT CLASS (V7): F01D-005/14

...SPECIFICATION has such a disadvantage that it is not coincident with
non-linearity and discontinuity of aerodynamic evaluation occurring in
a change of profile and therefore it has less flexibility to various...

...gradient based methods have been giving way to statistic methods using
evolutionary algorithms (EAs) and artificial neural networks (ANNs)
which are easily adjustable to the non-linearity and have a flexibility
for various...selected as the objective functions to be optimized, is
adopted. Of course, besides the above parameters, it is possible to
add, for example, the maximum slope of blade surface Mach number (or
pressure) distribution, L/D...the stagger angle (gamma) to the trailing
edge metal angel (beta)² as variables and fix the radius of leading
edge circle r1 to the solidity (sigma) as constants. According to...

18/3,K/13 (Item 13 from file: 349)
DIALOG(R)File 349:PCT FULLTEXT
(c) 2007 WIPO/Thomson. All rts. reserv.

00501611 **Image available**

AIR DATA SENSOR APPARATUS AND METHOD

Patent Applicant/Assignee:

ACCURATE AUTOMATION CORPORATION,
PAP Robert Michael,
COX Chadwick James,
LEWIS Carl Edwin III,
DONOVAN David John,
CARLTON Lindley A,
ROBINSON Timothy Wayne,

KOCHER Melvin P,
 FRISCH Joseph Clifford,
 PLATT John Carlton,
 DAVIS Joel L,

Inventor(s):

PAP Robert Michael,
 COX Chadwick James,
 LEWIS Carl Edwin III,
 DONOVAN David John,
 CARLTON Lindley A,
 ROBINSON Timothy Wayne,
 KOCHER Melvin P,
 FRISCH Joseph Clifford,
 PLATT John Carlton,
 DAVIS Joel L,

Patent and Priority Information (Country, Number, Date):

Patent: WO 9932963 A1 19990701
 Application: WO 98US27089 19981218 (PCT/WO US9827089)
 Priority Application: US 97995511 19971222

English Abstract

...the aircraft surface (3) in proximity to the conformal member to preserve the aircraft's aerodynamic shape. The associator (6) is coupled to the sensor (2) to receive the sensor signal...

...air pressure. Preferably, the associator (6) is implemented as a learning system such as a neural network, that can be trained to generate accurate air data based on the sensor signal. The...

Publication Year: 1999

Detailed Description

... if the aircraft were damaged in flight, for example.

The learning system can be a neural network coupled to receive the signal from the sensor. The learning system functions to map the...cover substantially preserves the shape of the exterior surface of the aircraft and thus maintains aerodynamic integrity.

The invented apparatus can include an interface unit coupled between the sensor and the...

...the corresponding air data signal can be derived by a learning system such as a neural network trained either in Right or in wind tunnel testing, for example. The method can also...that is shaped to conform to the aircraft's exterior surface so that it is aerodynamically integral with the aircraft surface in which it is installed. As such, the sensor adds...

...generated by the apparatus.

The associator can include a learning system 7 such as a neural network, that is trained

5

with the mapping of the sensor signal to the air data...the associator to train the learning system. If the learning system is implemented as a neural network, the weights of the neural network are adjusted preferably through back propagation or other technique using training sets mapping the sensor signals to the air data signals. The preferred neural network configuration is the well-known multilayer perceptron, and one or two hidden layers are generally...an air data signal based on

the air pressure signal.

The associator can include a neural network processor such as the NNPe commercially available from Accurate Automation™ Corporation of Chattanooga, Tennessee. The NNP is preprogrammed to implement a neural network, preferably a multilayer perceptron with one or two hidden layers and sufficient input nodes to...

...from all sensors included in the apparatus. The NNP uses the mapping programmed in its neural network to generate an air data signal based on the air pressure signal. The neural network processor, or more generally, the associator, is coupled to supply the air data signal to... is well-known in the art, by minimizing the function.

...from the input layer, through the hidden layers, to the output node(s) of the neural network implemented in the processor 7, to generate the air data signal. The specific neural network implemented in the neural network processor, preferred to be a ...known to exist in the wind tunnel. The training sets are used to train the neural network implemented in the processor 7 to accomplish the desired mapping of
20
the air pressure...

35 An apparatus as claimed in claim 1, wherein the associator includes a neural network processor, the apparatus further characterized by: an interface unit coupled between the sensor and the...

...pressure signal, and supplying the sens' A
ed
pressure signal as an input to a neural network implemented in the neural network processor, and receiving the air data signal generated by the neural network processor based on the supplied air pressure signal, and the interface unit outputting the received...

Second approach

Set	Items	Description
S1	151582	NEURAL() (NET? ? OR NETWORK? ?) OR ARTIFICIAL() INTELLIGENCE OR AI OR ANN OR (ARTIFICIAL () NEURAL () NETWORK?)
S3	224398	AEROSPACE? OR AIRCRAFT? OR AIRPLANE? OR AEROPLANE? OR AIRL- INER? OR CHOPPER? OR HELICOPTER? OR JET?
S7	588484	REPAIR??? OR ALTERATION? ? OR BROKEN OR BREAK??? OR MALFU- NCTION? OR CERTIFICATION?
S9	36	S1 (50N) S3 (50N) S7
S10	29	S9 AND PY=1963:2004
S11	29	IDPAT (sorted in duplicate/non-duplicate order)
S12	28	IDPAT (primary/non-duplicate records only)
S13	28	S12 AND PY=1963:2004

13/3,K/9 (Item 2 from file: 349)
 DIALOG(R)File 349:PCT FULLTEXT
 (c) 2007 WIPO/Thomson. All rts. reserv.

01051470 **Image available**
 METHOD AND APPARATUS FOR TACTILE CUEING OF AIRCRAFT CONTROLS
 Patent Applicant/Assignee:
 BELL HELICOPTER TEXTRON INC, P.O. Box 482, Fort Worth, TX 76101, US, US
 (Residence), US (Nationality), (For all designated states except: US)
 Patent Applicant/Inventor:
 AUGUSTIN Michael J, 6205 Glengarry Court, Fort Worth, TX 76180, US, US
 (Residence), US (Nationality), (Designated only for: US)
 BERTAPELLE Allen L, 5412 Two Jacks Court, Arlington, TX 76017, US, US
 (Residence), US (Nationality), (Designated only for: US)
 DREIER Mark E, 1803 Coventry Court, Arlington, TX 76017, US, US
 (Residence), US (Nationality), (Designated only for: US)
 LINTON Bradley D, 690 Newt Patterson Road, Mansfield, TX 76063, US, US
 (Residence), US (Nationality), (Designated only for: US)
 MCKEOWN William L, 1401 Woodridge Circle, Euless, TX 76040, US, US
 (Residence), US (Nationality), (Designated only for: US)
 YEARY Robert D, 1503 Naches Drive, Arlington, TX 76014, US, US
 (Residence), US (Nationality), (Designated only for: US)
 Legal Representative:
 WALTON James E (et al) (agent), Hill & Hunn, LLP, Suite 1440, 201 Main
 Street, Fort Worth, TX 76102, US,
 Patent and Priority Information (Country, Number, Date):
 Patent: WO 200381554 A1 20031002 (WO 0381554)
 Application: WO 2003US8998 20030321 (PCT/WO US0308998)
 Priority Application: US 2002367059 20020321; US 2002385164 20020531

Patent and Priority Information (Country, Number, Date):

Patent: ...20031002

Fulltext Availability:

Detailed Description

Publication Year: 2003

Detailed Description

... HUMS applications. This means that the addition of tactile cueing
 system 11 on an aircraft already equipped with HUMS can be achieved at
 minimum additional cost.

Referring now to Figure 5 in the drawings, a table of flight data

parameters is illustrated. Three separate polynomial neural networks (PNN) predict the torque simultaneously. These predictions are compared to the current torque, and algebraic expressions suitable for meeting software certification requirements. Each PNN uses an independent set of flight data parameters from aircraft 10. The parameters are preferably grouped into the following categories: airframe, engine and pilot. The...

13/3,K/14 (Item 7 from file: 349)
DIALOG(R)File 349:PCT FULLTEXT
(c) 2007 WIPO/Thomson. All rts. reserv.

00816701 **Image available**

A METHOD AND SYSTEM FOR SORTING INCIDENT LOG DATA FROM A PLURALITY OF MACHINES

Patent Applicant/Assignee:

GENERAL ELECTRIC COMPANY, 1 River Road, Schenectady, NY 12345, US, US
(Residence), US (Nationality)

Inventor(s):

FERA Gregory John, 5664 Rockledge Drive, Erie, PA 16511, US,
MCQUOWN Christopher M, 3516 Dominic Drive, Erie, PA 16506, US,
REICHENBACH Bryan, 2838 Zimmerman Road, Erie, PA 16510, US,
WISNIEWSKI Edward P, 613 Burkhart Avenue, Erie, PA 16511, US,

Legal Representative:

BENINATI John F (et al) (agent), General Electric Company, 3135 Easton
Turnpike W3C, Fairfield, CT 06431, US,

Patent and Priority Information (Country, Number, Date):

Patent: WO 200150210 A1 20010712 (WO 0150210)
Application: WO 2000US34626 20001219 (PCT/WO US0034626)
Priority Application: US 99173948 19991230; US 2000521328 20000309

Patent and Priority Information (Country, Number, Date):

Patent: ...20010712

Fulltext Availability:

Detailed Description

Publication Year: 2001

Detailed Description

... such as a locomotive or other complex systems used in industrial processes, medical imaging, telecommunications, aerospace applications, power generation, etc., includes elaborate controls and sensors that generate faults when anomalous operating...

...encountered. Typically, a field engineer will look at a fault log and determine whether a repair is necessary.

Approaches like neural networks, decision trees, etc., have been employed to learn over input data to provide prediction, classification

13/3,K/15 (Item 8 from file: 349)
DIALOG(R)File 349:PCT FULLTEXT
(c) 2007 WIPO/Thomson. All rts. reserv.

00811361 **Image available**

METHOD OF VERIFYING PRETRAINED NEURAL NET MAPPING FOR USE IN SAFETY-CRITICAL SOFTWARE

Patent Applicant/Assignee:

SIMMONDS PRECISION PRODUCTS INC, 3 Coliseum Centre, 2550 West Tyvola Road, Charlotte, NC 28217, US, US (Residence), US (Nationality)

• Inventor(s):

ZAKRZEWSKI Radoslaw Romuald, Apartment 18, 125 Kennedy Drive, South Burlington, VT 05403, US,

Legal Representative:

ZITELLI William E (et al) (agent), Calfee, Halter & Griswold LLP, 1400 McDonald Investment Center, 800 Superior Avenue, Cleveland, OH 44114, US,

Patent and Priority Information (Country, Number, Date):

Patent: WO 200144939 A2-A3 20010621 (WO 0144939)

Application: WO 2000US33947 20001214 (PCT/WO US0033947)

Priority Application: US 99465881 19991216

(EP) AT BE CH CY DE DK ES FI FR GB GR IE IT LU MC NL PT SE TR

Publication Language: English

Filing Language: English

Fulltext Word Count: 19827

Patent and Priority Information (Country, Number, Date):

Patent: .. 20010621

Fulltext Availability:

Detailed Description

Publication Year: 2001

Detailed Description

... software of neural nets and look-up tables from the point of view of a certification process is that bounds for values of the neural net 30 mapping function $f(x)$...

...appropriate set of testing points will be addressed. If these bounds 35 can be determined, certification of a pre-trained neural net will be equivalent to certification of a look-up table, which is a wellunderstood problem.

Verification of a Neural Net - Case of Look-Up Table Approximation

In this section, verification of input-output properties of a neural net mapping function $f(X)$, which has been trained to replace a look-up table mapping...

...and y may be the fuel quantity of at least one fuel tank on an aircraft. The goal is to verify that the trained neural network mapping function indeed approximates the given 15 look-up table in software operation. A procedure...

13/3,K/16 (Item 9 from file: 349)
DIALOG(R)File 349:PCT FULLTEXT
(c) 2007 WIPO/Thomson. All rts. reserv

00797891 **Image available**

A METHOD AND SYSTEM FOR ESTIMATING TIME OF OCCURRENCE OF MACHINE-DISABLING FAILURES

Patent Applicant/Assignee:

GENERAL ELECTRIC COMPANY, Carl A. Rowald, Esquire, 2901 East Lake Road, Building 14-522, Erie, PA 16531, US, US (Residence), US (Nationality)

Inventor(s):

JAMMU Vinay Bhaskar, 50 C3 Hillcrest Village, Niskayuna, NY 12309, US,
BLILEY Richard Gerald, 1020 Belleview Drive, Erie, PA 16504-2710, US,
SCHNEIDER William Roy, 8990 Old Wattsburg Road, Erie, PA 16510, US,

Legal Representative:

MORA Enrique J (agent), Holland & Knight LLP, P.O. Box 1526, Orlando, FL
32802-1526, US,

Patent and Priority Information (Country, Number, Date):

Patent: WO 200131449 A1 20010503 (WO 0131449)
Application: WO 2000US29322 20001024 (PCT/WO US0029322)
Priority Application: US 99162047 19991028; US 2000491939 20000126

Patent and Priority Information (Country, Number, Date):

Patent: ...20010503

Fulltext Availability:

Detailed Description

Publication Year: 2001

Detailed Description

... such as a locomotive or other complex systems used in industrial processes, medical imaging, telecommunications, aerospace applications, power generation, etc., includes elaborate controls and sensors that generate faults when anomalous operating...

...encountered. Typically, a field engineer will look at a fault log and determine whether a repair is necessary.

Approaches like neural networks, decision trees, etc., have been employed to learn over input data to provide prediction, classification

...

13/3,K/17 (Item 10 from file: 349)
DIALOG(R)File 349:PCT FULLTEXT
(c) 2007 WIPO/Thomson. All rts. reserv.

00756212

LASER DOPPLER VIBROMETER FOR REMOTE ASSESSMENT OF STRUCTURAL COMPONENTS

Patent Applicant/Assignee:

GEORGIA TECH RESEARCH CORPORATION, Office of Technology Licensing, 400
Tenth Street, Atlanta, GA 30332-0415, US, US (Residence), US
(Nationality)

Inventor(s):

SPRINGER Paul LeBaron III, 2395 Christopher's Walk, Atlanta, GA
30327-1110, US
MAHAFFEY James E, 4437 Mount Paran Parkway, Atlanta, GA 30327, US
HARLEY Ron, 803 Tanners Pointe Drive, Lawrenceville, GA 30044, US

Legal Representative:

HORSTEMEYER Scott A, Thomas, Kayden, Horstemeyer & Risley, L.L.P., Suite
1750, 100 Galleria Parkway, Atlanta, GA 30339, US

Patent and Priority Information (Country, Number, Date):

Patent: WO 200068654 A1 20001116 (WO 0068654)
Application: WO 2000US12871 20000511 (PCT/WO US0012871)
Priority Application: US 99133588 19990511

Patent and Priority Information (Country, Number, Date):

Patent: ...20001116

Fulltext Availability:

Claims

Publication Year: 2000

Claim

... vibration data set comprises 200 data points, where the 200th data point is the actual breaking strength of said structure.

36 The method of claim 26, wherein said artificial neural network is a feed-forward I O artificial neural network. ')7. The method of claim 26, wherein said artificial neural network is a self-organizing map artificial neural network.

38 The method of claim 26, wherein said structure comprises a power pole cross-arm...

...structure comprising:

a vehicle, wherein said vehicle comprises a vibratory response measuring device; and a neural network.

41 The system of claim 40, wherein said vehicle comprises an aircraft.

42 The system of claim 40, wherein said vehicle comprises an automobile. 4'). The system...

...said data set comprises 200 data points, where the 200th data point is the actual breaking strength of said structure.

53 The system of claim 40, wherein said artificial neural network is a feed-forward artificial neural network.

54 The system of claim 40, wherein said artificial neural network is a self-organizing map artificial neural network.

...in said structure and wherein said vehicle comprises a vibratory response measuring device; and a neural network, wherein said neural network evaluates said vibratory excitation.

56 The system of claim 55, wherein said vehicle comprises an aircraft.

57 The system of claim 55, wherein said vehicle comprises an automobile.

58 The system...

13/3,K/21 (Item 14 from file: 349)
DIALOG(R)File 349:PCT FULLTEXT
(c) 2007 WIPO/Thomson. All rts. reserv.

00406184 **Image available**

3-BRAIN ARCHITECTURE FOR AN INTELLIGENT DECISION AND CONTROL SYSTEM

Patent Applicant/Assignee:

WERBOS Paul J,

Inventor(s):

WERBOS Paul J,

Patent and Priority Information (Country, Number, Date):

Patent: WO 9746929 A2 19971211

Application: WO 97US9724 19970604 (PCT/WO US9709724)

Priority Application: US 9619154 19960604

Patent and Priority Information (Country, Number, Date):

Patent: ...19971211

Fulltext Availability:

Claims

Publication Year: 1997

Claim

... are numerically inefficient (i.e. too slow) in their treatment of noise; and so on. Neural network implementations of ADP also permit the use of high-throughput ANN chips, which can make it more practical to use a highly complex and intelligent control design even within the limitations of an aircraft or spacecraft.

Many analysts believe that NASA's most important mission, in the long-term, is to use research and development to break down the key barriers which support us from a true "space economy." (See Settling space...

Patent Abstract Files

File 347:JAPIO Dec 1976-2006
File 350:Derwent WPIX 1963-2007

Set Items Description
S1 18183 AEROELASTIC? OR AERODYNAMIC? OR AERO() ELASTIC? OR AERO()-
DYNAMIC?
Limitall/sl
S2 18 NEURAL() (NET? ? OR NETWORK? ?) OR ARTIFICIAL() INTELLIGENCE
OR (VIRTUAL OR INTELLIGENT) (2N) (ROBOT? OR AGENT? ? OR SERVO?
? OR BOT OR BOTS OR SYSTEM? ?) OR SOFTBOT? OR SOFT() (BOT OR B-
OTS)
S3 13 AI OR SYMBOT? OR KNOWBOT? OR INFERENCE() ENGINE? ? OR ANN OR
(ARTIFICIAL () NEURAL () NETWORK?) OR (PARALLEL () DISTRIBUTED ()
PROCESSING () NETWORK?)
S4 1 EXPERT () SYSTEM? ? OR INTELLIGENT () RETRIEVAL OR KNOWLE-
DGE () ENGINEERING OR MACHINE () LEARNING
S5 31 S2:S4
S6 4339 REPAIR??? OR ALTERATION? ? OR ALTER??? OR MODIFY OR MODIF-
ICATION OR MODIFIED OR CORRECT??? OR BROKEN OR BREAK??? OR FI-
X??? OR WORN OR MEND??? OR MALFUNCTION? OR FAILU-
RE? ? OR MISFUNCTION? OR LEAK??? OR SERVICING
S7 174 (ENTER??? OR INPUT???? OR INSERT???? OR ADD??? OR SCAN????
OR READ???) (5N) (DEVICE? ? OR MODULE? ? OR PARAMETER? ?)
S8 1 S1 AND S5 AND S6 AND S7
S9 88 MC=(T01-J15H OR T01-J16C1 OR T01-S03 OR W06-B08) OR IC=(
G06F-015? OR G06F-019?)
S10 88 S1 AND S9
S11 11 S5 AND S10
S12 12 S8 OR S11
S13 6 S12 AND PY=1963:2004
S14 6 IDPAT (sorted in duplicate/non-duplicate order)
S15 6 IDPAT (primary/non-duplicate records only)

15/3,K/1 (Item 1 from file: 350)
DIALOG(R) File 350:Derwent WPIX
(c) 2007 The Thomson Corporation. All rts. reserv.

0013624380 - Drawing available
WPI ACC NO: 2003-719896/200368
XRPX Acc No: N2003-575456

Computer implemented composite response surface construction method for
design optimization of aircraft engine, involves performing parameter based
partitioning of design space and using neural network to analyze
parameters

Patent Assignee: NASA US NAT AERO & SPACE ADMIN (USAS)

Inventor: MADAVAN N K; RAI M M

Patent Family (1 patents, 1 countries)

Patent Application

Number	Kind	Date	Number	Kind	Date	Update
US 6606612	B1	20030812	US 199896660	P	19980813	200368 B
			US 1998113310	P	19981222	
			US 1999374491	A	19990813	

Priority Applications (no., kind, date): US 199896660 P 19980813; US
1998113310 P 19981222; US 1999374491 A 19990813

Patent Details

Number Kind Lan Pg Dwg Filing Notes
 US 6606612 B1 EN 15 7 Related to Provisional US 199896660
 Related to Provisional US 1998113310

...design optimization of aircraft engine, involves performing parameter based partitioning of design space and using neural network to analyze parameters

Original Titles:

Method for constructing composite response surfaces by combining neural networks with other interpolation or estimation techniques

Alerting Abstract ...dependence of variables of interest with respect to respective design parameters is represented using a neural network and interpolation/estimation process. The output of neural network and interpolation process is combined to establish optimal condition. A feedback loop allows further processing in the neural network and interpolation process....USE - For design optimization of aerodynamic components and heat transfer structures e.g. wings, engines, transonic high pressure turbine, stator and...

...the total amount of simulation data reduces the training requirements and training times of the neural network. Permits a designer to rapidly perform variety of trade-off studies before arriving at the...

Class Codes

...Manual Codes (EPI/S-X): T01-J16C1

Original Publication Data by Authority

Original Abstracts:

...for design optimization that incorporates the advantages of both traditional response surface methodology (RSM) and neural networks is disclosed. The present invention employs a unique strategy called parameter-based partitioning of the given design space. In the design procedure, a sequence of composite response surfaces based on both neural networks and polynomial fits is used to traverse the design space to identify an optimal solution. The composite response surface has both the power of neural networks and the economy of low-order polynomials (in terms of the number of simulations needed and the network training...

...The present invention handles design problems with many more parameters than would be possible using neural networks alone and permits a designer to rapidly perform a variety of trade-off studies before arriving at the final...

Claims:

...for parallel analysis, each such parameter to be analyzed in at least one of a neural network and an estimation/interpolation process whereby an objective function that combines the output from the neural network and the estimation/interpolation process establishes a condition of optimality, and a feedback loop allows for further processing in the neural network process and the estimation/interpolation process to construct a composite response surface in a design space. Basic Derwent Week: 200368

DIALOG(R)File 350:Derwent WPIX

(c) 2007 The Thomson Corporation. All rts. reserv.

0009464737 - Drawing available

WPI ACC NO: 1999-405216/199934

XRPX Acc No: N1999-302041

Air data sensing method and apparatus for aircraft

Patent Assignee: ACCURATE AUTOMATION CORP (ACCU-N)

Inventor: CARLTON L A; COX C J; DAVIS J L; DONOVAN D J; FRISCH J C; KOCHER
M P; LEWIS C E; PAP R M; PLATT J C; ROBINSON T W

Patent Family (2 patents, 81 countries)

Patent

Application

Number	Kind	Date	Number	Kind	Date	Update
WO 1999032963	A1	19990701	WO 1998US27089	A	19981218	199934 B
AU 199923065	A	19990712	AU 199923065	A	19981218	199950 E

Priority Applications (no., kind, date): US 1997995511 A 19971222

Patent Details

Number	Kind	Lan	Pg	Dwg	Filing	Notes
WO 1999032963	A1	EN	48	46		

Regional Designated States,Original: AT BE CH CY DE DK EA ES FI FR GB GH

GM GR IE IT KE LS LU MC MW NL OA PT SD SE SZ UG ZW

AU 199923065 A EN Based on OPI patent WO 1999032963

Alerting Abstract ...the corresponding air data signal can be derived by a learning system such as a neural network trained either in flight or in wind tunnel testing, for example...

...7 Learning system e.g. neural network

Class Codes

...Manual Codes (EPI/S-X): T01-J16C1

Original Publication Data by Authority

Original Abstracts:

...the aircraft surface (3) in proximity to the conformal member to preserve the aircraft's aerodynamic shape. The associator (6) is coupled to the sensor (2) to receive the sensor signal, and maps the sensor...

...air pressure. Preferably, the associator (6) is implemented as a learning system such as a neural network, that can be trained to generate accurate air data based on the sensor signal. The invention also includes a...

...

Basic Derwent Week: 199934...

Second approach

Set Items Description
 S2 19928 NEURAL() (NET? ? OR NETWORK? ?) OR ARTIFICIAL() INTELLIGENCE
 OR AI OR ANN OR (ARTIFICIAL () NEURAL () NETWORK?)
 S3 4099046 REPAIR??? OR ALTERATION? ? OR MODIFY OR MODIFICATION OR M-
 ODIFIED OR CORRECT??? OR BROKEN OR BREAK??? OR FIX??? OR WORN
 OR MEND??? OR MALFUNCTION? OR FAILURE? ? OR SERVICING
 S4 424796 AEROSPACE? OR AIRCRAFT? OR AIRPLANE? OR AEROPLANE? OR AIRL-
 INNER? OR CHOPPER? OR HELICOPTER? OR JET?
 S15 29 S2 (50N) S3 (50N) S4
 S16 112028 INK () JET? ?
 S17 27 S15 NOT S16
 S19 26 S17 AND PY=1963:2004
 S20 26 IDPAT (sorted in duplicate/non-duplicate order)
 S21 26 IDPAT (primary/non-duplicate records only)

21/3,K/1 (Item 1 from file: 350)
 DIALOG(R)File 350:Derwent WPIX
 (c) 2008 The Thomson Corporation. All rts. reserv.

0015787567 - Drawing available
 WPI ACC NO: 2004-675761/200466
 Related WPI Acc No: 2000-490378; 2004-477652; 2007-238588
 XRPX Acc No: N2004-535517
 Computer system for flight control of aircraft has neural network
 which produces modified control signal for linear controller to provide
fixed solution for flight control to correct errors in modeling
 Patent Assignee: GUIDED SYSTEMS TECHNOLOGIES INC (GUID-N)
 Inventor: CORBAN J E
 Patent Family (2 patents, 1 countries)
 Patent Application

Number	Kind	Date	Number	Kind	Date	Update
US 20040181499	A1	20040916	US 1995510055	A	19950801	200466 B
			US 2000585105	A	20000531	
			US 2004806501	A	20040322	
US 7039473	B2	20060502	US 2004806501	A	20040322	200629 E

Priority Applications (no., kind, date): US 1995510055 A 19950801; US
 2000585105 A 20000531; US 2004806501 A 20040322

Patent Details

Number	Kind	Lan	Pg	Dwg	Filing	Notes
US 20040181499	A1	EN	19	9	Continuation of application	US 1995510055
					Continuation of application	US 2000585105
					<u>Continuation of patent US 6092919</u>	
					<u>Continuation of patent US 6757570</u>	

Computer system for flight control of aircraft has neural network
 which produces modified control signal for linear controller to provide
fixed solution for flight control to correct errors in modeling

Basic Derwent Week: 200466

21/3,K/2 (Item 2 from file: 350)
 DIALOG(R)File 350:Derwent WPIX

(c) 2008 The Thomson Corporation. All rts. reserv.

- 0014381337 - Drawing available

WPI ACC NO: 2004-570399/200455

XRPX Acc No: N2004-451136

Mechanical wave data e.g. acoustic signal, and vibration collecting method for mechanical system e.g. airplane engine, involves obtaining data from a sensor at location of mechanical system

Patent Assignee: NELSON M C (NELS-I)

Inventor: NELSON M C

Patent Family (1 patents, 1 countries)

Patent Application

Number	Kind	Date	Number	Kind	Date	Update
US 20040143398	A1	20040722	US 2003437963	P	20030103	200455 B
			US 2003437964	P	20030103	
			US 2003437967	P	20030103	
			US 2003437968	P	20030103	
			US 2004752201	A	20040105	

Priority Applications (no., kind, date): US 2003437963 P 20030103; US 2003437964 P 20030103; US 2003437967 P 20030103; US 2003437968 P 20030103; US 2004752201 A 20040105

Patent Details

Number Kind Lan Pg Dwg Filing Notes

US 20040143398	A1	EN	9	5	Related to Provisional US 2003437963
					Related to Provisional US 2003437964
					Related to Provisional US 2003437967
					Related to Provisional US 2003437968

Alerting Abstract ...airplane engine, paint sprayer in automobile assembly line, or aircraft wing and tail structure, for jet engine monitoring, failure detection and prediction in composite material, and physical security for moveable assets e.g. aircraft.

...give a substantially more reliable power spectra. The method improves the utility and reliability of artificial intelligence in vibration and acoustic monitoring data. The method provides highly reliable and detailed diagnostics for

Original Publication Data by Authority

Original Abstracts:

...mechanical events in mechanical systems, for enhancing the performance of pattern recognition including without limitation artificial intelligence methods, and for monitoring and assessing the condition of mechanical systems such as motors, structures, and structural elements. Applications include, without limitation, jet engine monitoring, failure detection and prediction in composite materials, and physical security for moveable assets such as aircraft. Basic Derwent Week: 200455

21/3,K/11 (Item 11 from file: 350)

DIALOG(R)File 350:Derwent WPIX

(c) 2008 The Thomson Corporation. All rts. reserv.

0009390519 - Drawing available

WPI ACC NO: 1999-325866/199927

XRPX Acc No: N1999-244379

Virtual sensor in military helicopters for low airspeed indication

Patent Assignee: US SEC OF NAVY (USNA)

Inventor: HAAS D J; MCCOOL K M; SCHAEFER C G

Patent Family (1 patents, 1 countries)

Patent Application

Number	Kind	Date	Number	Kind	Date	Update
US 5901272	A	19990504	US 1996736176	A	19961024	199927 B

Priority Applications (no., kind, date): US 1996736176 A 19961024

Patent Details

Number	Kind	Lan	Pg	Dwg	Filing	Notes
US 5901272	A	EN	17	8		

Original Publication Data by Authority

Original Abstracts:

The invention is directed to means, utilizing a neural network, for estimating helicopter airspeed at speeds below about 50 knots using only fixed system parameters as inputs to the neural network. The system includes: means for entering at least one initial parameter; means for measuring, in a nonrotating reference frame associated with the helicopter, a plurality of variable state parameters generated during flight of the helicopter; means for determining a plurality of input parameters based on the at least one initial parameter and the plurality...

...

Basic Derwent Week: 199927...

21/3,K/12 (Item 12 from file: 350)

DIALOG(R)File 350:Derwent WPIX

(c) 2008 The Thomson Corporation. All rts. reserv.

0009321819 - Drawing available

WPI ACC NO: 1999-253310/199921

Related WPI Acc No: 1998-297164

XRPX Acc No: N1999-188496

Helicopter airspeed information estimation system

Patent Assignee: US SEC OF NAVY (USNA)

Inventor: HAAS D J; MCCOOL K M; SCHAEFER C G

Patent Family (1 patents, 1 countries)

Patent Application

Number	Kind	Date	Number	Kind	Date	Update
US 5890101	A	19990330	US 1996740067	A	19961024	199921 B
			US 1997955970	A	19971022	

Priority Applications (no., kind, date): US 1996740067 A 19961024; US 1997955970 A 19971022

Patent Details

Number	Kind	Lan	Pg	Dwg	Filing	Notes
US 5890101	A	EN	16	8		Division of application US 1996740067

Division of patent US 5751609

Original Publication Data by Authority

Original Abstracts:

- The invention is directed to a system, utilizing a neural network, for estimating helicopter airspeed in the low airspeed flight range of below about 50 knots using only fixed system parameters as inputs to the neural network. The method includes the steps of: (a) defining input parameters derivable from variable state parameters generated during flight of the helicopter and measurable in a nonrotating reference frame associated with the helicopter; (b) determining the input parameters and a corresponding helicopter airspeed at a plurality of flight conditions representing a predetermined low airspeed flight domain of the helicopter; (c) establishing a learned relationship between the determined input parameters and the corresponding helicopter airspeed wherein the relationship is represented by at least one nonlinear equation; (d) storing the at least one nonlinear equation in a memory onboard the helicopter; (e) measuring real time values of the variable state parameters during low airspeed flight of the helicopter; (f) calculating...

Basic Derwent Week: 199921

21/3,K/17 (Item 17 from file: 350)
 DIALOG(R)File 350:Derwent WPIX
 (c) 2008 The Thomson Corporation. All rts. reserv.

0008264336 - Drawing available
 WPI ACC NO: 1997-372324/199734
 XRPX Acc No: N1997-309234

Object flow performance feature model generation for aircraft - involves coupling test database to neural network and providing test input signals representing object geometric configurations and outputs representing flow performance features

Patent Assignee: NASA US NAT AERO & SPACE ADMIN (USAS)

Inventor: JORGENSEN C; ROSS J

Patent Family (1 patents, 1 countries)

Patent Number	Kind	Date	Application Number	Kind	Date	Update
US 5649064	A	19970715	US 1995446071	A	19950519	199734 B

Priority Applications (no., kind, date): US 1995446071 A 19950519

Patent Details

Number	Kind	Lan	Pg	Dwg	Filing	Notes
US 5649064	A	EN	14	6		

Original Publication Data by Authority

Original Abstracts:

The method and apparatus includes a neural network for generating a model of an object in a wind tunnel from performance data on the object. The network...

...signals (e.g., lift, drag, pitching moment, or other performance features). In one embodiment, the neural network training method employs a modified Levenberg-Marquardt optimization technique. The model can be generated "real time" as wind tunnel testing proceeds. Once trained, the model is used to estimate performance features associated with the aircraft given geometric configuration and/or power setting input. The invention can also be applied in other similar static flow...

Basic Derwent Week: 199734...

21/3,K/18 (Item 18 from file: 350)

DIALOG(R)File 350:Derwent WPIX

(c) 2008 The Thomson Corporation. All rts. reserv.

0007972234 - Drawing available

WPI ACC NO: 1997-062946/199706

XRPX Acc No: N1997-052009

Air-fuel ratio controller for IC engine e.g. gasoline engine of vehicles - includes control correction computation unit to compute quantity of fuel jet correction corresponding to estimated fuel ratio

Patent Assignee: MATSUSHITA DENKI SANGYO KK (MATU)

Inventor: FUJIOKA N; ISHIDA A; NAKAMURA T; TAKIGAWA M

Patent Family (2 patents, 1 countries)

Patent Application

Number	Kind	Date	Number	Kind	Date	Update
JP 8312411	A	19961126	JP 1995116929	A	19950516	199706 B
JP 3144264	B2	20010312	JP 1995116929	A	19950516	200116 E

Priority Applications (no., kind, date): JP 1995116929 A 19950516

Patent Details

Number Kind Lan Pg Dwg Filing Notes

JP 8312411 A JA 8 8

JP 3144264 B2 JA 8 Previously issued patent JP 08312411

Alerting Abstract ...A converter (19) converts the signals and the converted signals are fed to the neural network based computation device, which outputs an air-fuel ratio. A control correction computation device (111) uses the air-fuel ratio output by the computation device to compute fuel jet correction, based on present engine conditions...

21/3,K/19 (Item 19 from file: 350)

DIALOG(R)File 350:Derwent WPIX

(c) 2008 The Thomson Corporation. All rts. reserv.

0007874419

WPI ACC NO: 1996-505496/199650

XRAM Acc No: C1996-158593

XRPX Acc No: N1996-425968

Evaluation of hydrocarbon fuels by near-I.R. spectroscopy - includes codifying obtd. NIR signal and comparing obtd. spectra with correlated matrix of parameter values in trained neural network.

Patent Assignee: INTEVEP SA (INVV)

Inventor: AARON R; ADRIANO P; ARROYO F; FERNANDO A; HERNAN P; PARISI A;

PARISI A F; PRIETO H; RANSON A

Patent Family (11 patents, 8 countries)

Patent Application

Number	Kind	Date	Number	Kind	Date	Update
US 5572030	A	19961105	US 1994231424	A	19940422	199650 B
			US 1996585000	A	19960111	
GB 2312741	A	19971105	GB 19968947	A	19960429	199747 NCE
DE 19617917	A1	19971113	DE 19617917	A	19960503	199751 NCE
JP 9305567	A	19971128	JP 1996112861	A	19960507	199807 NCE
NL 1003058	C2	19971110	NL 1003058	A	19960507	199807 NCE

CA 2175326 A 19971030 CA 2175326 A 19960429 199821 NCE
 BR 199602223 A 19980908 BR 19962223 A 19960510 199842 NCE
 MX 199601605 A1 19980701 MX 19961605 A 19960430 200012 NCE
 CA 2175326 C 19991116 CA 2175326 A 19960429 200014 NCE
 MX 197072 B 20000622 MX 19961605 A 19960430 200133 NCE
 DE 19617917 C2 20020529 DE 19617917 A 19960503 200237 NCE

Priority Applications (no., kind, date): US 1994231424 A 19940422; US 1996585000 A 19960111; GB 19968947 A 19960429; CA 2175326 A 19960429; MX 19961605 A 19960430; DE 19617917 A 19960503; JP 1996112861 A 19960507; NL 1003058 A 19960507; BR 19962223 A 19960510

Patent Details

Number	Kind	Lan	Pg	Dwg	Filing	Notes
US 5572030	A	EN	16	9	Continuation of application	US 1994231424
GB 2312741	A	EN	40	9		
DE 19617917	A1	DE	22	9		
JP 9305567	A	JA	13	0		
NL 1003058	C2	NL	22	0		
CA 2175326	A	EN				
BR 199602223	A	PT				
CA 2175326	C	EN				

Alerting Abstract ...method is given for evaluating hydrocarbon fuel selected from gasoline, diesel fuel, kerosene, naphtha and jet fuel to determine a desired parameter selected from Reid vapour pressure, simulated distn. values, research...

...pt. and/or smoke pt. The method comprises: (1) providing a computer configured as a neural network; (2) training the neural network to evaluate a hydrocarbon fuel from a family of fuels to determine the desired parameter...

...of the fuels; (c) codifying each of the spectra obtd. by providing a base line correction and then reducing the base line corrected spectra to a desired number of pts. corresp. to the parameters being evaluated; (d) developing...

Original Publication Data by Authority

Claims:

...method is given for evaluating hydrocarbon fuel selected from gasoline, diesel fuel, kerosene, naphtha and jet fuel to determine a desired parameter selected from Reid vapour pressure, simulated distn. values, research...

...pt. and/or smoke pt. The method comprises: (1) providing a computer configured as a neural network; (2) training the neural network to evaluate a hydrocarbon fuel from a family of fuels to determine the desired parameter, the training comprising: (a) selecting...

...of the fuels; (c) codifying each of the spectra obtd. by providing a base line correction and then reducing the base line corrected spectra to a desired number of pts. corresp. to the parameters being evaluated; (d) developing a...

...matrix from the desired number of pts., the first matrix to be inputted to the neural network; (e) obtaining a second matrix of parameter

values from an analytical evaluation of the hydrocarbon fuels; (f) processing the first and second matrices in the neural network to obtain a functional relationship between the two to develop...

...What is claimed is: ...of hydrocarbon fuels selected from the group consisting of gasoline, diesel fuel, kerosene, naphtha and jet fuel to determine a desired parameter selected from the group consisting of Reid vapor pressure...

...point, and combinations thereof, comprising the steps of: (1) providing a computer configured as a neural network; (2) training the neural network so as to evaluate a hydrocarbon fuel from the family of hydrocarbon fuels to determine the desired parameter, said training comprising...

...an NIR spectra for each of said plurality of hydrocarbon fuels; (c) codifying each of the NIR spectra obtained by providing a base line correction and thereafter reducing the base line corrected spectra to a desired number of points corresponding to the parameters being evaluated; (d) developing...

...from the desired number of points, said first matrix to be subsequently inputted to the neural network; (e) obtaining a second matrix of parameter values from an analytical evaluation of the plurality of hydrocarbon fuels; (f) processing the first matrix and the second matrix in the neural network to obtain a functional relationship between the first matrix and the second matrix so as to develop a...

Basic Derwent Week: 199650

21/3,K/22 (Item 22 from file: 350)

DIALOG(R)File 350:Derwent WPIX

(c) 2008 The Thomson Corporation. All rts. reserv.

0007137444 - Drawing available

WPI ACC NO: 1995-171093/199523

XRPX Acc No: N1995-134060

Individual aircraft working life evaluation system - uses black-box containing neural network for processing parameter values from standard aircraft instruments and ground evaluation and memory system

Patent Assignee: EUROCOPTER DEUT GMBH (EURO-N)

Inventor: BRAND E

Patent Family (2 patents, 1 countries)

Patent Application

Number	Kind	Date	Number	Kind	Date	Update
DE 4336588	A1	19950504	DE 4336588	A	19931027	199523 B
DE 4336588	C2	19990715	DE 4336588	A	19931027	199932 E

Priority Applications (no., kind, date): DE 4336588 A 19931027

Patent Details

Number Kind Lan Pg Dwg Filing Notes

DE 4336588 A1 DE 5 4

Alerting Abstract ...The evaluation system uses a neural network receiving information from the standard aircraft instruments, for storing the aircraft flight position, velocity, control angle and loading, etc.,

together with further calculated parameters, provided by..

...stored information is transferred to an evaluation memory system on the ground, for summing the aircraft usage to determine the working life and the servicing requirements...

...Pref. the values provided by the aircraft instruments are continuously interrogated by the neural network, the aircraft on-board processor used to process the stored values.

...

Basic Derwent Week: 199523...

21/3,K/24 (Item 24 from file: 350)
DIALOG(R)File 350:Derwent WPIX
(c) 2008 The Thomson Corporation. All rts. reserv.

0006147640 - Drawing available
WPI ACC NO: 1992-390268/199247
XRPX Acc No: N1992-297669
Subsystem failure analysis appts. for electronic artificial intelligence system - simulates effect of subsystem failure to test system using knowledge base, user interface and failure analysis component
Patent Assignee: BOEING CO (BOEI)
Inventor: CHAKRAVARTY A J; NAKAMURA Y
Patent Family (1 patents, 1 countries)
Patent Application
Number Kind Date Number Kind Date Update
US 5161158 A 19921103 US 1989421579 A 19891016 199247 B

Priority Applications (no., kind, date): US 1989421579 A 19891016

Patent Details

Number	Kind	Lan	Pg	Dwg	Filing	Notes
US 5161158	A	EN	18	6		

Alerting Abstract ...with the knowledge base and the simulation condition data, and generates a set of subsystem failure responses that would occur in the electronic system if the failure actually occurred. The component also performs a fault isolation analysis...

...USE/ADVANTAGE - For analysing failure effect propagation in electronic system having at least one system mode, e.g. in artificial intelligence system in aircraft, for system level failure analysis. Efficient.
Improves design, testing and maintenance of avionics systems.

NPL Full Text Files

Files Searched -	File 810:Business Wire 1986-1999/
File 275:Gale Group Computer DB(TM) 1983-2007	File 647:CMP Computer Fulltext 1988-2007
File 47:Gale Group Magazine DB(TM) 1959-2007	File 674:Computer News Fulltext 1989-2006
File 621:Gale Group New Prod.Annou.(R) 1985-2007	File 696:DIALOG Telecom. Newsletters 1995-2007
File 636:Gale Group Newsletter DB(TM) 1987-2007	File 369:New Scientist 1994-2007
File 148:Gale Group Trade & Industry DB 1976-2007	File 613:PR Newswire 1999-2007
File 624:McGraw-Hill Publications 1985-2007	File 813:PR Newswire 1987-1999
File 98:General Sci Abs 1984-2007	File 370:Science 1996-1999
File 553:Wilson Bus. Absolute 1982-2007	File 20:Dialog Global Reporter 1997-2007
File 15:ABI/Inform(R) 1971-2007	File 16:Gale Group PROMT(R) 1990-2007
File 635:Business Dateline(R) 1985-2007	File 160:Gale Group PROMT(R) 1972-1989
File 9:Business & Industry(R) Jul/1994-2007	File 484:Periodical Abs Plustext 1986-2007
File 610:Business Wire 1999-2007	File 634:San Jose Mercury Jun 1985-2007

Set	Items	Description
S1	71476	AEROELASTIC? OR AERODYNAMIC? OR AERO() ELASTIC? OR AERO()-DYNAMIC?
S2	1016	NEURAL()(NET? ? OR NETWORK? ?) OR ARTIFICIAL()INTELLIGENCE OR (VIRTUAL OR INTELLIGENT) (2N)(ROBOT? OR AGENT? ? OR SERVO? ? OR BOT OR BOTS OR SYSTEM? ?) OR SOFTBOT? OR SOFT()(BOT OR BOTS)
S3	1328	AI OR SYMBOT? OR KNOWBOT? OR INFERENCE()ENGINE? ? OR ANN OR (ARTIFICIAL () NEURAL () NETWORK?) OR (PARALLEL () DISTRIBUTED () PROCESSING () NETWORK?)
S4	154	EXPERT () SYSTEM? ? OR INTELLIGENT () RETRIEVAL OR KNOWLEDGE () ENGINEERING OR MACHINE ()LEARNING
S5	2280	S2:S4
S6	25589	REPAIR??? OR ALTERATION? ? OR ALTER??? OR MODIFY OR MODIFICATION OR MODIFIED OR CORRECT??? OR BROKEN OR BREAK??? OR FIX??? OR WORN OR MEND??? OR MALFUNCTION? OR FAILURE? ? OR MISFUNCTION? OR LEAK??? OR SERVICING
S8	776	(ENTER??? OR INPUT????? OR INSERT????? OR ADD??? OR SCAN????? OR READ????) (5N) (DEVICE? ? OR MODULE? ? OR PARAMETER? ?)
S15	52	S1 (50N) S5 (50N) (S6 OR S8)
S16	45	S15 AND PY=1963:2004
S17	31	RD (unique items)

17/3,K/9 (Item 6 from file: 16)
 DIALOG(R)File 16:Gale Group PROMT(R)
 (c) 2007 The Gale Group. All rts. reserv.

06651647 Supplier Number: 55814096 (USE FORMAT 7 FOR FULLTEXT)
 New cockpit controls, displays make everyone a pilot.
 Gonzalez, Jean
 Design News, v54, n17, p88
 Sept 6, 1999
 Language: English Record Type: Fulltext
 Document Type: Magazine/Journal; Refereed; Academic Trade
 Word Count: 1569

... damaged aircraft controllable."
 Today's flight controllers are a medley of electromechanical systems,

which signal aerodynamic control surfaces in response to pilot commands.

The intelligent flight control system employs experimental neural network software developed by NASA scientists at Moffett Field, CA and Boeing Company's Phantom Works...

...MO). Engineers at Dryden Flight Research Center in Edwards, CA are testing it on a modified F-15.

The "smart software," when fully developed, should increase safety, helping NASA reach its...

...7 million hours, with over 100 different iterations and 500 test flights to perfect. The neural network software cuts the amount of code required by a factor of 20. The neural network learns the aircraft's current operational status, checking it six times per second, sensing differences...

19990906

17/3,K/14 (Item 1 from file: 47)

DIALOG(R)File 47:Gale Group Magazine DB(TM)

(c) 2007 The Gale group. All rts. reserv.

06648685 SUPPLIER NUMBER: 108050570 (USE FORMAT 7 OR 9 FOR FULL TEXT)

Mind-expanding machines: artificial intelligence meets good old-fashioned human thought.

Bower, Bruce

Science News, 164, 9, 136(3)

August 30, 2003

ISSN: 0036-8423 LANGUAGE: English RECORD TYPE: Fulltext

WORD COUNT: 2453 LINE COUNT: 00199

... Just as it proved too difficult for early flight enthusiasts to discover the principles of aerodynamics by trying to build aircraft modeled on bird wings, Ford argues, it maybe too hard...

...computers modeled on the processes of human thought.

That's a controversial stand in the artificial intelligence community. Although stung by criticism of their failure to create the insightful computers envisioned by the field's founders nearly 50 years ago

...the Turing Test with flying colors.

"I'm skeptical of people who are skeptical" of AI research, says Rodney Brooks, who directs the Massachusetts Institute of Technology's artificial intelligence laboratory. He heads a "hard-core AI" venture aimed at creating intelligent, socially adept robots...

20030830

17/3,K/19 (Item 1 from file: 275)

DIALOG(R)File 275:Gale Group Computer DB(TM)

(c) 2007 The Gale Group. All rts. reserv.

02687205 SUPPLIER NUMBER: 98078355 (USE FORMAT 7 OR 9 FOR FULL TEXT)
Reshaping aircraft. (Transportation).

Jonietz, Erika

Technology Review (Cambridge, Mass.), 106, 2, 27(1)

March, 2003

ISSN: 1099-274X LANGUAGE: English RECORD TYPE: Fulltext

... stress; and it will use the carbon nanotubes as tiny actuators to help the machines modify their shapes in response to changing aerodynamic conditions.

In addition to developing the materials, the institute's researchers will have to create...actuators, predicts David Zimmerman, a University of Houston mechanical engineer who heads the institute's intelligent-systems group. "The theory for handling that just doesn't exist today," he says. So his...

20030301

17/3,K/20 (Item 1 from file: 484)
DIALOG(R)File 484:Periodical Abs Plustext
(c) 2007 ProQuest. All rts. reserv.

06202739 SUPPLIER NUMBER: 405312011 (USE FORMAT 7 OR 9 FOR FULLTEXT)
Mind-expanding machines
Bower, Bruce
Science News (GSCN), v164 n9, p136
Aug 30, 2003
ISSN: 0036-8423 JOURNAL CODE: GSCN
DOCUMENT TYPE: Feature
LANGUAGE: English RECORD TYPE: Fulltext; Abstract
WORD COUNT: 2413

2003

TEXT:

... Just as it proved too difficult for early flight enthusiasts to discover the principles of aerodynamics by trying to build aircraft modeled on bird wings, Ford argues, it maybe too hard...

...computers modeled on the processes of human thought.

That's a controversial stand in the artificial intelligence community. Although stung by criticism of their failure to create the insightful computers envisioned by the field's founders nearly 50 years ago

...the Turing Test with flying colors.

"I'm skeptical of people who are skeptical" of AI research, says Rodney Brooks, who directs the Massachusetts Institute of Technology's artificial intelligence laboratory. He heads a "hard-core AI" venture aimed at creating intelligent, socially adept robots...

17/3,K/22 (Item 3 from file: 484)
DIALOG(R)File 484:Periodical Abs Plustext
(c) 2007 ProQuest. All rts. reserv.

04689006 SUPPLIER NUMBER: 50915228 (USE FORMAT 7 OR 9 FOR FULLTEXT)
Metamorphic substances shape actuator, sensor system design
Kenyon, Henry S
Signal (FSIG), v54 n7, p42-45, p.4
Mar 2000
ISSN: 0037-4938 JOURNAL CODE: FSIG
DOCUMENT TYPE: Feature
LANGUAGE: English RECORD TYPE: Fulltext; Abstract

WORD COUNT: 2085

2000

TEXT:

... gains by applying these techniques in existing systems. A major focus of the work is aerodynamic and hydrodynamic control, vibration and noise reduction.

Smart materials are usually composites made up of...

...and operation. When combined with actuators, an embedded signal-sensor processing network and a control system, intelligent substances can alter a vehicle's structural performance by making modifications to compensate for damage or new mission...

17/3,K/23 (Item 4 from file: 484)
DIALOG(R)File 484:Periodical Abs Plustext
(c) 2007 ProQuest. All rts. reserv.

04070859

Estimation of aircraft lateral-directional parameters using neural networks

Ghosh, A K; Raisinghani, S C; Khubchandani, Sunil

Journal of Aircraft (FJAI), v35 n6, p876-881, p.6

Nov 1998

ISSN: 0021-8669 JOURNAL CODE: FJAI

DOCUMENT TYPE: Feature

LANGUAGE: English RECORD TYPE: Abstract

1998

...ABSTRACT: method (christened "the Delta method") of estimating aircraft parameters from flight data using feed-forward neural networks is applied for the extraction of lateral-directional parameters from simulated as well as real-flight data. The neural network is trained using aircraft motion and control variables as the network inputs and aerodynamic coefficients as the network outputs; the trained network is used to predict aerodynamic coefficients for a suitably modified input file.

17/3,K/25 (Item 1 from file: 624)
DIALOG(R)File 624:McGraw-Hill Publications
(c) 2007 McGraw-Hill Co. Inc. All rts. reserv.

01100093

NASA Chief Sees High-Tech Future

Paul Richfield

Edited By Paul Richfield

Business & Commercial Aviation, Vol. 87, No. 1, Pg 35
July, 2000
JOURNAL CODE: BCA
SECTION HEADING: BRIEFING ISSN: 0191-4642
WORD COUNT: 452

TEXT:

...safe operations -- even in zero visibility conditions.

Ultimately, Goldin expects aircraft to make use of "neural network computers able to "learn and modify" using feedback from embedded micro-sensors distributed throughout the structure, or "nano-technology that pushes the theoretical limits of performance."

"We may literally grow multi-function aircraft skins for structure, aerodynamic efficiency and control, and environmental protection," he said. "When damaged, these surfaces may self-heal..."

2000

17/3,K/26 (Item 2 from file: 624)
DIALOG(R)File 624:McGraw-Hill Publications
(c) 2007 McGraw-Hill Co. Inc. All rts. reserv.

0307544

Software Developed for Using Neural Network Techniques in Problem Solving
Aviation Week & Space Technology, Vol. 134, No. 24, Pg 216
June 17, 1991
JOURNAL CODE: AW
SECTION HEADING: International Product News ISSN: 0005-2175
WORD COUNT: 480

TEXT:

... they do not easily recognize patterns, nor can they deal with imprecise or contradictory data.

Neural networks exhibit an adaptive behavior that makes them capable of "self-learning." Instead of being programmed, neural networks are "trained" by exposing them to repeated examples. And when neural networks are trained with correct examples from available data, they can accurately "fill in the blanks" for missing information or...

... aerospace engineering application, ExploreNet can be used to predict how an aircraft will perform aerodynamically. The data could come from a combination of flight tests, wind tunnel experiments and finite element analysis on a supercomputer.

"Our experience and customers lead us to expect that neural networks can be used easily to combine algorithms and test data, combining the 'knowledge' from both..."

... KnowledgeNet uses patented technology to explain the rationale behind choices or decisions made by a neural network. It can be applied to applications that require either simple YES/NO decisions or more...

1991

17/3,K/27 (Item 3 from file: 624)
DIALOG(R)File 624:McGraw-Hill Publications
(c) 2007 McGraw-Hill Co. Inc. All rts. reserv.

0005786

USAF Awards Contracts to Develop Self-Repair Control Concepts

Robert R. Ropelewski

Aviation Week & Space Technology, Vol. 123, No. 5, Pg 65

August 5, 1985

JOURNAL CODE: AW

SECTION HEADING: AERONAUTICAL ENGINEERING ISSN: 0005-2175

WORD COUNT: 1,155

TEXT:

... for development of reconfiguration concepts permitting maximum performance of aircraft flight control systems after actuator failure or surface damage.

--Charles Stark Draper Laboratory--\$215,213 for development of a computer software...

...possible when battle damage is incurred.

--Honeywell, Inc.--\$1.7 million for development of an expert system for maintenance diagnostics that would be used by technicians at austere bases. The system would be modified as an experience base develops in the field.

--Analytical Methods, Inc., of Redmond, Wash.--\$275,000 for development of an aerodynamic model to predict stability and control parameters of an aircraft that has received substantial damage...

1985

17/3,K/28 (Item 1 from file: 635)
DIALOG(R)File 635:Business Dateline(R)
(c) 2007 ProQuest Info&Learning. All rts. reserv.

0098735 89-22567

NCUBE Unveils World's Fastest Supercomputer

Lokey, Ann

Business Wire (San Francisco, CA, US) s1 p1

PUBL DATE: 890619

WORD COUNT: 553

DATELINE: Beaverton, OR, US

TEXT:

...computer chip.

The highly advanced component contains a 64-bit floating point processor, and error-correcting memory management unit, message routing hardware and input/output processors. The VLSI circuit is a...

...said Stephen Colley, NCUBE president.

"Scientific and engineering application areas that will be revolutionized include neural networks, artificial intelligence,

robotics, structural, seismic and chemical analysis, signal processing, aerodynamics and fluid dynamics.

"The availability of the Oracle DBMS software on the NCUBE 2 will...

17/3,K/29 (Item 1 from file: 636)
DIALOG(R)File 636:Gale Group Newsletter DB(TM)
(c) 2007 The Gale Group. All rts. reserv.

01519780 Supplier Number: 42172661 (USE FORMAT 7 FOR FULLTEXT)
SMALLER BUDGETS COULD IMPEDE NEURAL NETWORK ADVANCEMENT
Defense Technology Business, v3, n13, pN/A
June 25, 1991
Language: English Record Type: Fulltext
Document Type: Newsletter; Trade
Word Count: 1336

... as well as pattern, speech and handwriting recognition. "I think the earliest significant result of neural networks as applied to conventional products will be in the area of control." The company's...

...flight control, thermal health monitoring, manufacturing process control and embedded sensors.

White, technology leader of intelligent systems development at the new aircraft products division, explained that the company is working on a neural network-based control system for the F-15. Stable flight is dependent upon an accurate aeromodel...

...something happens to the aircraft in flight (such as losing its stabilator or experiencing mechanical failure), the aeromodel changes and adapts to the aircraft's impaired condition. "The neural network basically learns, based upon in-flight data, the necessary changes to the aeromodel to provide...

...for hypersonic aircraft such as the NASA/DoD National Aerospace Plane (NASP). "We believe that neural networks will solve many of the problems concerning the monitoring and control of liquid hydrogen fuel which is pumped throughout the aircraft to cool aerodynamically heated surfaces during hypersonic flight," White explained.

Under a DARPA program investigating the use of...

19910625

Files Searched -	File 60:ANTE: Abstracts in New Tech & Eng. 1966-2007
File 2:INSPEC 1898-2007/	File 65:Inside Conferences 1993-2007
File 6:NTIS 1964-2007	File 95:TEME-Technology & Management 1989-2007
File 8:Ei Compendex(R) 1884-2007	File 99:Wilson Appl. Sci & Tech Abs 1983-2007
File 34:SciSearch(R) Cited Ref Sci 1990-2007	File 144:Pascal 1973-2007
File 35:Dissertation Abs Online 1861-2007	File 256:TecInfoSource 82-2007
File 56:Computer and Information Systems Abstracts 1966-2007	File 434:SciSearch(R) Cited Ref Sci 1974-1989
	File 266:FEDRIP 2007
	File 583:Gale Group Globalbase(TM) 1986-2002

Set Items Description

S1 252464 AEROELASTIC? OR AERODYNAMIC? OR AERO() ELASTIC? OR AERO()-
DYNAMIC?

S2 2308 NEURAL()(NET? ? OR NETWORK? ?) OR ARTIFICIAL()INTELLIGENCE
OR (VIRTUAL OR INTELLIGENT) (2N)(ROBOT? OR AGENT? ? OR SERVO?
? OR BOT OR BOTS OR SYSTEM? ?) OR SOFTBOT? OR SOFT()(BOT OR B-
OTS)

S3 591 AI OR SYMBOT? OR KNOWBOT? OR INFERENCE()ENGINE? ? OR ANN OR
(ARTIFICIAL () NEURAL () NETWORK?) OR (PARALLEL () DISTRIBU-
TED () PROCESSING () NETWORK?)

S4 620 EXPERT () SYSTEM? ? OR INTELLIGENT () RETRIEVAL OR KNOWLE-
DGE () ENGINEERING OR MACHINE ()LEARNING

S5 2886 S2:S4

S6 34438 REPAIR??? OR ALTERATION? ? OR ALTER??? OR MODIFY OR MODIF-
ICATION OR MODIFIED OR CORRECT??? OR BROKEN OR BREAK??? OR FI-
X??? OR WORN OR MEND??? OR MALFUNCTION? OR FAILU-
RE? ? OR MISFUNCTION? OR LEAK??? OR SERVICING

S7 1000 (ENTER??? OR INPUT????? OR INSERT????? OR ADD??? OR SCAN????
OR READ???) (5N) (DEVICE? ? OR MODULE? ? OR PARAMETER? ?)

S8 3 S1 AND S5 AND S6 AND S7

S13 63 S1 (10N) S5 (10N) (S6 OR S7)

S14 64 S8 OR S13

S15 41 S14 AND PY=1963:2004

S16 29 RD (unique items)

16/5/2 (Item 2 from file: 2)
DIALOG(R)File 2:INSPEC
(c) 2007 Institution of Electrical Engineers. All rts. reserv.

08549377 INSPEC Abstract Number: C2003-04-3360L-036
Title: Hierarchical approach to adaptive control for improved flight
safety
Author(s): Idan, M.; Johnson, M.; Calise, A.J.
Author Affiliation: Georgia Inst. of Technol., Atlanta, GA, USA
Journal: Journal of Guidance, Control, and Dynamics vol.25, no.6 p.
1012-20
Publisher: AIAA,
Publication Date: Nov.-Dec. 2002 Country of Publication: USA
CODEN: JGCDDT ISSN: 0731-5090
SICI: 0731-5090(200211/12)25:6L:1012:HAAC;1-O
Material Identity Number: C746-2002-007
U.S. Copyright Clearance Center Code: 0731-5090/02/\$10.00
Language: English Document Type: Journal Paper (JP)
Treatment: Theoretical (T); Experimental (X)
Abstract: Following failures of primary aerodynamic actuators, safe
flight can be maintained by introducing alternative actuation systems. An

intelligent hierarchical flight control system architecture is presented that is designed using nonlinear adaptive synthesis techniques and online learning neural networks to enhance flight safety. Pseudocontrol hedging is used for proper adaptation in the presence of actuator saturation, rate limits, and failure. The hierarchical structure incorporates nonactive secondary actuation channels that are engaged after a failure of a primary control surface is encountered. The methodology requires only the knowledge that a failure in a specific actuator has occurred. A model of the failed aircraft, the failure type, and the failure size need not to be known. The neural network element of the secondary channel will adapt to the failed actuator effect. The secondary control channels are designed to account for the typically lower authority and degraded performance that can be expected with secondary actuation systems. The proposed hierarchical flight control architecture is attractive, in particular, as a retrofit to existing certified flight control systems for enhanced flight safety. The proposed flight control architecture is evaluated in a nonlinear flight simulation environment, demonstrating its retrofit features. (22 Refs)

Subfile: C

Descriptors: actuators; adaptive control; aircraft control; hierarchical systems; intelligent control; neurocontrollers; nonlinear control systems; safety systems

Identifiers: intelligent control; hierarchical flight control system; nonlinear control system; adaptive control; flight safety; actuator saturation; aircraft control; neural network; secondary control channels

Class Codes: C3360L (Aerospace control); C1340E (Self-adjusting control systems); C1340N (Neurocontrol); C1340B (Multivariable control systems); C1340K (Nonlinear control systems); C1230D (Neural nets); C7420 (Control engineering computing); C5290 (Neural computing techniques)

Copyright 2003, IEE

16/5/3 (Item 3 from file: 2)

DIALOG(R)File 2:INSPEC

(c) 2007 Institution of Electrical Engineers. All rts. reserv.

06998161 INSPEC Abstract Number: C9809-3375-009

Title: A hybrid autopilot for BTT steering using RBF neural nets

Author(s): McDowell, D.M.; Irwin, G.W.; Lightbody, G.; McConnell, G.

Author Affiliation: Control English Res. Group, Queen's University, Belfast, UK

Conference Title: Proceedings of the 13th World Congress, International Federation of Automatic Control. Vol.P. Aerospace, Transportation Systems p.159-64

Editor(s): Gertler, J.J.; Cruz, J.B., Jr.; Peshkin, M.; Masten, M.; Mitchell, J.R.; Perrin, J.P.; Mohleji, S.C.

Publisher: Pergamon, Oxford, UK

Publication Date: 1997 Country of Publication: UK x+378 pp.

ISBN: 0 08 042924 6 Material Identity Number: XX97-02117

Conference Title: Proceedings of the 13th World Congress. Vol.P: Aerospace, Transportation Systems

Conference Date: 30 June-5 July 1996 Conference Location: San Francisco, CA, USA

Language: English Document Type: Conference Paper (PA)

Treatment: Theoretical (T); Experimental (X)

Abstract: A hybrid neural adaptive control scheme is proposed to alleviate the tracking problems associated with a bank-to-turn (BTT) autopilot. This employs a Gaussian radial basis function neural network in parallel with an independently regulated, fixed-gain lateral autopilot to adaptively compensate for roll-induced cross-coupling, time-varying aerodynamic derivatives and control surface constraints to achieve consistent tracking performance over the flight envelope. The

hybrid scheme is evaluated against realistic pitch acceleration and roll rate profiles generated from a typical guidance scenario and its performance compared with constant parameter and gain scheduled autopilot.

(13 Refs)

Subfile: C

Descriptors: adaptive control; aerodynamics; feedforward neural nets; missile guidance; neurocontrollers; tracking

Identifiers: roll autopilot; bank-to-turn steering; RBF neural nets; tracking; Gaussian radial basis function neural network; cross-coupling; aerodynamic derivatives; missile guidance; adaptive control; lateral autopilot; neurocontrol

Class Codes: C3375 (Military control systems); C3360L (Aerospace control); C1230D (Neural nets); C1340N (Neurocontrol); C1340E (Self-adjusting control systems); C3120C (Spatial variables control)

Copyright 1998, IEE

16/5/4 (Item 4 from file: 2)

DIALOG(R)File 2:INSPEC

(c) 2007 Institution of Electrical Engineers. All rts. reserv.

05595492 INSPEC Abstract Number: B9403-7600-004, C9403-7460-018

Title: Expert system for laser vulnerability analysis of aerospace structures

Author(s): Grandhi, R.V.; Chandu, S.V.L.; Rajagopalan, H.; Fautheree, D.

Author Affiliation: Wright State University, Dayton, OH, USA

Conference Title: Conference Record AUTOTESTCON '92. The IEEE Systems Readiness Technology Conference (Cat. No.92CH3148-4) p.79-87

Publisher: IEEE, New York, NY, USA

Publication Date: 1992 Country of Publication: USA xxx+463 pp.

ISBN: 0 7803 0643 0

U.S. Copyright Clearance Center Code: CH3148-4/92/0000-0079\$01.00

Conference Sponsor: IEEE

Conference Date: 21-24 Sept. 1992 Conference Location: Dayton, OH, USA

Language: English Document Type: Conference Paper (PA)

Treatment: Practical (P)

Abstract: The authors discuss the framework of a knowledge-based expert system for studying the survivability of the aerospace structures exposed to high energy lasers using VAASEL (vulnerability analysis of aerospace structures exposed to lasers) software. VAASEL is a synthesis tool built around NASTRAN and ASTROS programs. The knowledge base involves threat characterization, temperature distribution, failure prediction, linear and nonlinear statics, air loads and aeroelastic disciplines. A description of the VAASEL expert system modules, the graphics interface and the input data generator is included. (11 Refs)

Subfile: B C

Descriptors: aerospace computing; aircraft; expert systems; failure analysis; laser beam effects; mechanical engineering computing

Identifiers: linear statics; laser vulnerability analysis; aerospace structures; knowledge-based expert system; survivability; high energy lasers; VAASEL; vulnerability analysis; synthesis tool; NASTRAN; ASTROS; threat characterization; temperature distribution; failure prediction; nonlinear statics; air loads; aeroelastic disciplines; graphics interface; input data generator

Class Codes: B7600 (Aerospace facilities and techniques); B7210B (Automatic test and measurement systems); C7460 (Aerospace engineering); C6170 (Expert systems); C7440 (Civil and mechanical engineering)

16/5/5 (Item 5 from file: 2)

DIALOG(R)File 2:INSPEC

(c) 2007 Institution of Electrical Engineers. All rts. reserv.

05560927 INSPEC Abstract Number: C9402-7460-017

Title: Aircraft failure detection and identification using neural networks

Author(s): Napolitano, M.R.; Chen, C.I.; Naylor, S.

Author Affiliation: West Virginia University, Morgantown, WV, USA

Journal: Journal of Guidance, Control, and Dynamics vol.16, no.6 p. 999-1009

Publication Date: Nov.-Dec. 1993 Country of Publication: USA

CODEN: JGCDDT ISSN: 0731-5090

U.S. Copyright Clearance Center Code: 0731-5090/93/\$2.00+.50

Language: English Document Type: Journal Paper (JP)

Treatment: Practical (P)

Abstract: A neural network is proposed as an approach to the task of failure detection following damage to an aerodynamic surface of an aircraft flight control system. Several drawbacks of other failure detection techniques can be avoided by taking advantage of the flexible learning and generalization capabilities of a neural network. This structure, used for state estimation purposes, can be designed and trained on line in flight and generates a residual signal indicating the damage as soon as it occurs. From an analysis of the cross-correlation functions between some key state variables, the identification of the damage type can also be achieved. The results of a nonlinear numerical simulation for a damaged control surface are reported and discussed. (21 Refs)

Subfile: C

Descriptors: aircraft control; failure analysis; fault location; generalisation (artificial intelligence); identification; learning (artificial intelligence); neural nets

Identifiers: failure detection and identification; neural networks; aerodynamic surface; aircraft flight control system; learning; generalization; cross-correlation functions; nonlinear numerical simulation; damaged control surface

Class Codes: C7460 (Aerospace engineering); C5290 (Neural computing techniques); C3360L (Aerospace systems)

16/5/6 (Item 1 from file: 6)

DIALOG(R)File 6:NTIS

(c) 2007 NTIS, Intl Cpyrght All Rights Res. All rts. reserv.

2245687 NTIS Accession Number: N20020066785/XAB

Improving the Unsteady Aerodynamic Performance of Transonic Turbines using Neural Networks

Rai, M. M. ; Madavan, N. K. ; Huber, F. W.

National Aeronautics and Space Administration, Moffett Field, CA. Ames Research Center.

Corp. Source Codes: 019045001; NC473657

Report Number: NAS 1.15:208791; NASA/TM-1999-208791,A-99V0041

Sep 1999 26p

Languages: English

Journal Announcement: USGRDR0226; STAR4008

Order this product from NTIS by: phone at 1-800-553-NTIS (U.S. customers); (703)605-6000 (other countries); fax at (703)605-6900; and email at orders@ntis.gov. NTIS is located at 5285 Port Royal Road, Springfield, VA, 22161, USA.

NTIS Prices: PC A03/MF A01

Country of Publication: United States

Contract Number: RTOP 632-30-00

A recently developed neural net-based aerodynamic design procedure is

used in the redesign of a transonic turbine stage to improve its unsteady aerodynamic performance. The redesign procedure used incorporates the advantages of both traditional response surface methodology and neural networks by employing a strategy called parameter-based partitioning of the design space. Starting from the reference design, a sequence of response surfaces based on both neural networks and polynomial fits are constructed to traverse the design space in search of an optimal solution that exhibits improved unsteady performance. The procedure combines the power of neural networks and the economy of low-order polynomials (in terms of number of simulations required and network training requirements). A time-accurate, two-dimensional, Navier-Stokes solver is used to evaluate the various intermediate designs and provide inputs to the optimization procedure. The procedure yielded a modified design that improves the aerodynamic performance through small changes to the reference design geometry. These results demonstrate the capabilities of the neural net-based design procedure, and also show the advantages of including high-fidelity unsteady simulations that capture the relevant flow physics in the design optimization process.

Descriptors: *Aerodynamic characteristics; *Supersonic turbines; *Design optimization; *Fluid dynamics; Neural nets; Education; Navier-stokes equation; Polynomials; Simulation

Identifiers: NTISNASA

Section Headings: 51A (Aeronautics and Aerodynamics--Aerodynamics)

16/5/7 (Item 2 from file: 6)

DIALOG(R)File 6:NTIS

(c) 2007 NTIS, Intl Cpyrght All Rights Res. All rts. reserv.

2112706 NTIS Accession Number: N19990008889

Neural Net-Based Redesign of Transonic Turbines for Improved Unsteady Aerodynamic Performance

Madavan, N. K. ; Rai, M. M. ; Huber, F. W.

National Aeronautics and Space Administration, Moffett Field, CA. Ames Research Center.

Corp. Source Codes: 019045001; NC473657

Report Number: NAS 1.15:208754; NASA/TM-1998-208754,A-9900398

Nov 98 20p

Languages: English

Journal Announcement: GRAI9910; STAR3702

Presented at Propulsion, 35th, Los Angeles, CA, 20-24 Jun. 1999. American Inst. of Aeronautics and Astronautics, Reston, VA.

Order this product from NTIS by: phone at 1-800-553-NTIS (U.S. customers); (703)605-6000 (other countries); fax at (703)605-6900; and email at orders@ntis.fedworld.gov. NTIS is located at 5285 Port Royal Road, Springfield, VA, 22161, USA.

NTIS Prices: PC A03/MF A01

Country of Publication: United States

Contract Number: RTOP 519-40-12

A recently developed neural net-based aerodynamic design procedure is used in the redesign of a transonic turbine stage to improve its unsteady aerodynamic performance. The redesign procedure used incorporates the advantages of both traditional response surface methodology (RSM) and neural networks by employing a strategy called parameter-based partitioning of the design space. Starting from the reference design, a sequence of response surfaces based on both neural networks and polynomial fits are constructed to traverse the design space in search of an optimal solution that exhibits improved unsteady performance. The procedure combines the power of neural networks and the economy of low-order polynomials (in terms of number of simulations required and network training requirements). A

time-accurate, two-dimensional, Navier-Stokes solver is used to evaluate the various intermediate designs and provide inputs to the optimization procedure. The optimization procedure yields a modified design that improves the aerodynamic performance through small changes to the reference design geometry. The computed results demonstrate the capabilities of the neural net-based design procedure, and also show the tremendous advantages that can be gained by including high-fidelity unsteady simulations that capture the relevant flow physics in the design optimization process.

Descriptors: *Supersonic turbines; *Navier-stokes equation; *Fluid dynamics; *Design analysis; *Aerodynamic characteristics; Neural nets; Unsteady aerodynamics; Simulation; Polynomials; Optimization; Aerodynamics

Identifiers: NTISNASA

Section Headings: 51C (Aeronautics and Aerodynamics--Aircraft); 46B (Physics--Fluid Mechanics)

16/5/8 (Item 3 from file: 6)

DIALOG(R)File 6:NTIS

(c) 2007 NTIS, Intl Cpyrght All Rights Res. All rts. reserv.

2024266 NTIS Accession Number: N19970023679/XAB

Direct Adaptive Aircraft Control Using Dynamic Cell Structure Neural Networks

Jorgensen, C. C.

National Aeronautics and Space Administration, Moffett Field, CA. Ames Research Center.

Corp. Source Codes: 019045001; NC473657

Report Number: NAS 1.15:112198; A-976719A; NASA-TM-112198

May 97 20p

Languages: English

Journal Announcement: GRAI9723; STAR3508

Order this product from NTIS by: phone at 1-800-553-NTIS (U.S. customers); (703)605-6000 (other countries); fax at (703)321-8547; and email at orders@ntis.fedworld.gov. NTIS is located at 5285 Port Royal Road, Springfield, VA, 22161, USA.

NTIS Prices: PC A03/MF A01

Country of Publication: United States

Contract Number: RTOP 519-30-12

A Dynamic Cell Structure (DCS) Neural Network was developed which learns topology representing networks (TRNS) of F-15 aircraft aerodynamic stability and control derivatives. The network is integrated into a direct adaptive tracking controller. The combination produces a robust adaptive architecture capable of handling multiple accident and off-nominal flight scenarios. This paper describes the DCS network and modifications to the parameter estimation procedure. The work represents one step towards an integrated real-time reconfiguration control architecture for rapid prototyping of new aircraft designs. Performance was evaluated using three off-line benchmarks and on-line nonlinear Virtual Reality simulation. Flight control was evaluated under scenarios including differential stabilator lock, soft sensor failure, control and stability derivative variations, and air turbulence.

Descriptors: *Aerodynamic stability; *On-line systems; *Neural nets; *Adaptive control; *Aircraft design; *F-15 aircraft; *Real time operation; *Virtual reality; Nonlinearity; Prototypes; Failure; Flight control; Simulation

Identifiers: NTISNASA

Section Headings: 51B (Aeronautics and Aerodynamics--Aeronautics)

16/5/9 (Item 4 from file: 6)

DIALOG(R)File 6:NTIS

- (c) 2007 NTIS, Intl Cpyrght All Rights Res. All rts. reserv.

1974909 NTIS Accession Number: PB96-207428

Journal of the Chinese Institute of Engineers, Volume 19, Number 3, May

1996. Transactions of the Chinese Institute of Engineers, Series A

(Bimonthly rept)

Liou, C. T. ; Lee, S. C. ; Wu, C. K. ; Hong, H. K. ; Hsu, Y. Y.

Chinese Inst. of Engineers, Taipei (Taiwan).

Corp. Source Codes: 112211000

May 96 134p

Languages: English

Journal Announcement: GRAI9623

Figures in this document may not be fully legible in microfiche.

Summaries in Chinese. See also PB96-186580.

Order this product from NTIS by: phone at 1-800-553-NTIS (U.S. customers); (703)605-6000 (other countries); fax at (703)321-8547; and email at orders@ntis.fedworld.gov. NTIS is located at 5285 Port Royal Road, Springfield, VA, 22161, USA.

NTIS Prices: PC A08/MF A02

Country of Publication: Taiwan

;Contents: The Design of a Linear PID-Type Fuzzy Controller; A Method of Clustering Quantization for Better Training of CMAC; Numerical Modelling for Buckling of Buried Pipelines Induced by Compressive Ground Failure; Pulsatile Flow past Bileaflet Aortic Valve Prostheses; Source Number Estimator Using Neural Network; Aerodynamics of a Vibrating Square Prism in Homogeneous Turbulent Flows; A Parallel Run-Time Iterative Load Balancing Algorithm for Solution-Adaptive Finite Element Meshes on Hypercubes; Improvement of Plane Stress Solutions Using Adaptive Finite Elements; Dynamic Analysis of the Flexible Connecting Rod of a Slider-Crank Mechanism by Finite Element Method; A New Method for Texture Analysis Using Morphological Gradient Texture Histogram; Vibration Analysis and Measurement of a Rolling Stay; Dynamic Analysis of a T-Type Timoshenko Frame to a Moving Load Using Finite Element Method; and Adaptive Fractal Image Coding in Subband Domain.

Descriptors: *Research projects; *Taiwan; Computer systems; Neural networks; Control systems; Turbulent flow; Algorithms; Mathematical models; Machinery

Identifiers: NTISTFSOLO

Section Headings: 62GE (Computers, Control, and Information Theory--General); 94GE (Industrial and Mechanical Engineering--General); 70GE (Administration and Management--General)

16/5/10 (Item 1 from file: 8)

DIALOG(R)File 8:Ei Compendex(R)

(c) 2007 Elsevier English Info. Inc. All rts. reserv.

09928783 E.I. No: EIP04278251515

Title: Intelligent multi-resolution modelling: Application to synthetic jet actuation and flow control

Author: Singla, Puneet; Junkins, John L.; Rediniotis, Othon; Subbarao, Kamesh

Corporate Source: Texas A and M University 3141-TAMU, College Station, TX 77843-3141, United States

Conference Title: 42nd AIAA Aerospace Sciences Meeting and Exhibit

Conference Location: Reno, NV, United States Conference Date: 20040105-20040108

Sponsor: American Institute of Aeronautics and Astronautics, AIAA

E.I. Conference Number: 63204

Source: AIAA Paper 42nd AIAA Aerospace Sciences Meeting and Exhibit 2004.

Publication Year: 2004

Language: English

Document Type: CA; (Conference Article) Treatment: T; (Theoretical)

Journal Announcement: 0407W2

Abstract: A novel "directed graph" based algorithm is presented that facilitates intelligent learning and adaptation of the parameters appearing in a Radial Basis Function Network (RBFN) description of input output behavior of nonlinear dynamical systems. Several alternate formulations, that enforce minimal parameterization of the RBFN parameters are presented. An Extended Kalman Filter algorithm is incorporated to estimate the model parameters using multiple windows of the batch input-output data. The efficacy of the learning algorithms are evaluated on judiciously constructed test data before implementing them on real aerodynamic lift and pitching moment data obtained from experiments on a Synthetic Jet Actuation based Smart Wing. 19 Refs.

Descriptors: *Jets; Flow control; Aerodynamics; Neural networks; Frequency agility; Radial basis function networks; Time series analysis; Degrees of freedom (mechanics); Algorithms; Parameter estimation; Error correction; Problem solving; Theorem proving

Identifiers: Synthetic jet actuators (SJA); Space systems; Pitching moment coefficient; Lift coefficient

Classification Codes:

631.1 (Fluid Flow, General); 731.3 (Specific Variables Control); 651.1 (Aerodynamics, General); 716.2 (Radar Systems & Equipment); 723.4 (Artificial Intelligence); 922.2 (Mathematical Statistics); 931.1 (Mechanics); 731.1 (Control Systems); 721.1 (Computer Theory (Includes Formal Logic, Automata Theory, Switching Theory & Programming Theory))

631 (Fluid Flow); 731 (Automatic Control Principles & Applications); 651 (Aerodynamics); 716 (Electronic Equipment, Radar, Radio & Television); 723 (Computer Software, Data Handling & Applications); 922 (Statistical Methods); 931 (Applied Physics Generally); 721 (Computer Circuits & Logic Elements); 921 (Applied Mathematics)

63 (FLUID FLOW; HYDRAULICS, PNEUMATICS & VACUUM); 73 (CONTROL ENGINEERING); 65 (AEROSPACE ENGINEERING); 71 (ELECTRONICS & COMMUNICATION ENGINEERING); 72 (COMPUTERS & DATA PROCESSING); 92 (ENGINEERING MATHEMATICS); 93 (ENGINEERING PHYSICS)

16/5/11 (Item 2 from file: 8)

DIALOG(R)File 8:Ei Compendex(R)

(c) 2007 Elsevier English Info. Inc. All rts. reserv.

09271759 E.I. No: EIP03037324801

Title: A modification to particle swarm optimization algorithm

Author: Fan, Huiyuan

Corporate Source: Turbo and Jet Engine Laboratory Israel Institute of Technology, Haifa, Israel

Source: Engineering Computations (Swansea, Wales) v 19 n 7-8 2002. p 970-989

Publication Year: 2002

CODEN: ENCOEN ISSN: 0264-4401

Language: English

Document Type: JA; (Journal Article) Treatment: A; (Applications); T; (Theoretical)

Journal Announcement: 0301W3

Abstract: In this paper, a modification strategy is proposed for the particle swarm optimization (PSO) algorithm. The strategy adds an adaptive scaling term into the algorithm, which aims to increase its convergence

rate and thereby to obtain an acceptable solution with a lower number of objective function evaluations. Such an improvement can be useful in many

- practical engineering optimizations where the evaluation of a candidate solution is a computationally expensive operation and consequently finding the global optimum or a good sub-optimal solution with the algorithm is too time consuming, or even impossible within the time available. The modified PSO algorithm was empirically studied with a suite of four well-known benchmark functions, and was further examined with a practical application case, a neural-network-based modeling of aerodynamic data. The numerical simulation demonstrates that the modified algorithm statistically outperforms the original one. 17 Refs.

Descriptors: *Evolutionary algorithms; Optimization; Convergence of numerical methods; Computational methods; Computer simulation; Neural networks; Mathematical models; Aerodynamics; Statistical methods

Identifiers: Particle swarm optimization algorithm; Engineering optimization; Adaptive scaling; Nonlinear optimization algorithm

Classification Codes:

921.6 (Numerical Methods); 921.5 (Optimization Techniques); 723.5 (Computer Applications); 723.4 (Artificial Intelligence); 651.1 (Aerodynamics, General); 922.2 (Mathematical Statistics)

921 (Applied Mathematics); 723 (Computer Software, Data Handling & Applications); 651 (Aerodynamics); 922 (Statistical Methods)

92 (ENGINEERING MATHEMATICS); 72 (COMPUTERS & DATA PROCESSING); 65 (AEROSPACE ENGINEERING)

16/5/12 (Item 3 from file: 8)

DIALOG(R)File 8:Ei Compendex(R)

(c) 2007 Elsevier English Info. Inc. All rts. reserv.

09082309 E.I. No: EIP02277003298

Title: Analysis and design of advanced miniscale mechatronic systems: Synthesis of intelligent flight servos

Author: Lyshevski, Sergey Edward; Sinha, A.S.C.

Corporate Source: Dept. of Elec. and Computer English Purdue University at Indianapolis, Indianapolis, IN 46202-5132, United States

Source: International Journal of Smart Engineering System Design v 4 n 2 April/June 2002. p 115-123

Publication Year: 2002

CODEN: IJSDFJ ISSN: 1025-5818

Language: English

Document Type: JA; (Journal Article) Treatment: T; (Theoretical)

Journal Announcement: 0207W1

Abstract: The flight vehicle performance (flight and handling qualities, agility, controllability, maneuverability, etc.) depends upon flight actuators, which displace the control surfaces. Intelligent flight servos must be designed to achieve the specified criteria, requirements, and standards. Miniscale electromechanical flight actuators are actuated by electric servo-motors, and brushless permanent-magnet synchronous machines are perfectly suited due to their efficiency, reliability, high torque density, low cost and maintenance, simplicity, and ruggedness. However, conventional controllers do not ensure the dynamic performance of flight actuators in the full operating envelope under rapidly changing flight and environmental conditions and aerodynamic loads. An intelligent flight servo is designed using the developed neural networks synthesis procedure. The Hopfield equations are modified to incorporate delay for finite switching. The effect of even small delays due to finite switching for composite large networks could be significant, and, therefore, closed-loop systems may exhibit delay-induced instability. The results obtained are valid for systems without delays if the conditions of the

theorems hold. These results are applied to illustrate the application of neural network-based control systems design for advanced flight servos. It is shown that new controllers must be synthesized because synchronous servomotors are controlled taking into account the electromagnetic features, software, and hardware used. Control signals, which drive high-switching transistors (more specifically, MOSFET drivers), are developed by the DSP based upon the rotor angular displacement. The DSP performs control and decision-making through learning, adaptation, reconfiguration, scheduling, and optimization mechanisms. Other functions, such as identification, estimation, and diagnostics, can be also performed. We demonstrate that the neural network-based intelligent controllers guarantee the specified tracking accuracy, desired deflection rate, and disturbance attenuation. The system performance is documented.

12 Refs.

Descriptors: *Mechatronics; Flight simulators; Actuators; Permanent magnets; Synchronous motors; Aerodynamic loads; Neural networks; Digital control systems; Transistors; Rotors; MOSFET devices; Optimization; Decision making

Identifiers: Intelligent flight servos

Classification Codes:

705.3.1 (AC Motors)

732.1 (Control Equipment); 704.1 (Electric Components); 705.3 (Electric Motors); 651.1 (Aerodynamics, General); 723.4 (Artificial Intelligence); 731.1 (Control Systems); 714.2 (Semiconductor Devices & Integrated Circuits); 601.2 (Machine Components); 921.5 (Optimization Techniques); 912.2 (Management)

608 (Mechanical Engineering, General); 731 (Automatic Control Principles & Applications); 732 (Control Devices); 704 (Electric Components & Equipment); 705 (Electric Generators & Motors); 651 (Aerodynamics); 723 (Computer Software, Data Handling & Applications); 714 (Electronic Components & Tubes); 601 (Mechanical Design); 921 (Applied Mathematics); 912 (Industrial Engineering & Management)

60 (MECHANICAL ENGINEERING, GENERAL); 73 (CONTROL ENGINEERING); 70 (ELECTRICAL ENGINEERING, GENERAL); 65 (AEROSPACE ENGINEERING); 72 (COMPUTERS & DATA PROCESSING); 71 (ELECTRONICS & COMMUNICATION ENGINEERING); 92 (ENGINEERING MATHEMATICS); 91 (ENGINEERING MANAGEMENT)

16/5/13 (Item 4 from file: 8)

DIALOG(R)File 8: Ei Compendex(R)

(c) 2007 Elsevier English Info. Inc. All rts. reserv.

08863574 E.I. No: EIP01306591359

Title: Redesigning gas-generator turbines for improved unsteady aerodynamic performance using neural networks

Author: Madavan, N.K.; Rai, M.M.; Huber, F.W.

Corporate Source: NASA Ames Research Center, Moffett Field, CA 94035, United States

Source: Journal of Propulsion and Power v 17 n 3 May/June 2001. p 669-677

Publication Year: 2001

CODEN: JPPOEL ISSN: 0748-4658

Language: English

Document Type: JA; (Journal Article) Treatment: T; (Theoretical)

Journal Announcement: 0108W1

Abstract: A recently developed neural network-based aerodynamic design procedure is used in the redesign of gas-generator turbine stage to improve its unsteady aerodynamic performance. The redesign procedure used incorporates the advantages of both traditional response-surface methodology and neural networks by employing a strategy called parameter-based partitioning of the design space. Starting from the

reference design, a sequence of response surfaces based on both neural networks and polynomial fits is constructed to traverse the design space in search of an optimal solution that exhibits improved unsteady performance. The procedure combines the power of neural networks and the economy of low-order polynomials (in terms of number of simulations required and network training requirements). A time-accurate, two-dimensional, Navier-Stokes solver is used to evaluate the various intermediate designs and provide inputs to the optimization procedure. The procedure yields a modified design that improves the aerodynamic performance through small changes to the reference design geometry. These results demonstrate the capabilities of the neural network-based design procedure and also show the advantages of including high-fidelity unsteady simulations that capture the relevant flow physics in the design optimization process. 21 Refs.

Descriptors: *Gas turbines; Aerodynamics; Neural networks; Computer aided design; Polynomials; Navier Stokes equations; Geometry; Optimization; Computer simulation

Identifiers: Gas-generator turbines

Classification Codes:

612.3 (Gas Turbines & Engines); 651.1 (Aerodynamics, General); 461.1 (Biomedical Engineering); 723.5 (Computer Applications); 921.1 (Algebra); 921.2 (Calculus); 921.5 (Optimization Techniques)

612 (Internal Combustion Engines); 651 (Aerodynamics); 461 (Bioengineering); 723 (Computer Software, Data Handling & Applications); 921 (Applied Mathematics)

61 (MECHANICAL ENGINEERING, PLANT & POWER); 65 (AEROSPACE ENGINEERING); 46 (BIOENGINEERING); 72 (COMPUTERS & DATA PROCESSING); 92 (ENGINEERING MATHEMATICS)

16/5/14 (Item 5 from file: 8)

DIALOG(R)File 8: Ei Compendex(R)

(c) 2007 Elsevier English Info. Inc. All rts. reserv.

07978623 E.I. No: EIP98034137367

Title: Two new techniques for aircraft parameter estimation using neural networks

Author: Raisinghani, S.C.; Ghosh, A.K.; Kalra, P.K.

Corporate Source: Indian Inst of Technology, Kanpur, India

Source: Aeronautical Journal v 102 n 1011 Jan 1998. p 25-30

Publication Year: 1998

CODEN: AENJAK ISSN: 0001-9240

Language: English

Document Type: JA; (Journal Article) Treatment: T; (Theoretical)

Journal Announcement: 9805W3

Abstract: Two new techniques for estimating aircraft stability and control derivatives (parameters) from flight data using feed forward neural networks are proposed. Both techniques use motion variables and control inputs as the input file, while aerodynamic coefficients are presented as the output file for training a neural network. For the purpose of parameter estimation, the trained neural network is presented with a suitably modified input file, and the corresponding predicted output file of aerodynamic coefficients is obtained. Suitable interpretation and manipulation of such input-output files yields the estimated values of the parameters. The methods are validated first on the simulated flight data and then on real flight data obtained by digitizing analogue data from a published report. Results are presented to show how the accuracy of the estimates is affected by the topology of the network, the number of iterations and the intensity of the measurement noise in simulated flight data. One of the significant features of the proposed methods is that they

do not require guessing of a reasonable set of starting values of the parameters as a popular parameter estimator like the maximum likelihood method does. (Author abstract) 11 Refs.

Descriptors: *Aircraft; Parameter estimation; Feedforward neural networks ; System stability; Aerodynamics; Learning systems; Computer simulation; Topology; Iterative methods; Motion control

Identifiers: Aerodynamic coefficients; Flight data

Classification Codes:

652.1 (Aircraft, General); 731.1 (Control Systems); 723.4 (Artificial Intelligence); 731.4 (System Stability); 651.1 (Aerodynamics, General); 921.4 (Combinatorial Mathematics, Includes Graph Theory, Set Theory)

652 (Aircraft); 731 (Automatic Control Principles); 723 (Computer Software); 651 (Aerodynamics); 921 (Applied Mathematics)

65 (AEROSPACE ENGINEERING); 73 (CONTROL ENGINEERING); 72 (COMPUTERS & DATA PROCESSING); 92 (ENGINEERING MATHEMATICS)

16/5/15 (Item 6 from file: 8)

DIALOG(R)File 8: Ei Compendex(R)

(c) 2007 Elsevier English Info. Inc. All rts. reserv.

07502283 E.I. No: EIP96093335674

Title: Computer based expert system for battle damage repair of composite structures

Author: Gali, S.; Kressel, I.; Karuchro, Z.; Lebovitz, H.

Corporate Source: IAI Engineering Div, Ben Gurion International Airport, Isr

Conference Title: Proceedings of the 1996 5th International Conference on Computer Aided Design in Composite Material Technology

Conference Location: Udine, Italy Conference Date: 199607

E.I. Conference Number: 45312

Source: Computer Aided Design in Composite Material Technology - International Conference 1996. Computational Mechanics Publ, Southampton, Engl. p 115-121

Publication Year: 1996

CODEN: 85PMA6

Language: English

Document Type: CA; (Conference Article) Treatment: A; (Applications); T ; (Theoretical)

Journal Announcement: 9611W2

Abstract: The Computerized System, REPCOMP, developed for damage repair of composite structures is an expert system for the design of damage repair. REPCOMP provides detail repair instructions and drawings, taking into consideration strength and stiffness requirements as well as aerodynamics, weight and other design considerations. The REPCOMP expert system is being developed for the two major paths in damage repair of composite structures which are: Permanent damage repair, suitable for long term use of civil and military aircraft. A/C Battle Damage Repair (ABDR), suitable for field repair of military aircraft during battle. REPCOMP operates on portable computer (PC) using the Microsoft Windows graphical environment. It is an independent system and can be used in any field repair base. Currently the program handles the ABDR path. (Author abstract) 4 Refs.

Descriptors: *Expert systems; Composite structures; Repair; Computer aided engineering; Strength of materials; Stiffness; Aerodynamics; Military aircraft; Personal computers; Computer software

Identifiers: Computer based expert system; Battle damage repair;

Microsoft windows graphical environment

Classification Codes:

- 723.4.1 (Expert Systems)
- 723.4 (Artificial Intelligence); 408.2 (Structural Members & Shapes);
- 913.5 (Maintenance); 723.5 (Computer Applications); 651.1 (Aerodynamics, General)
- 723 (Computer Software); 408 (Structural Design); 913 (Production Planning & Control); 421 (Materials Properties); 651 (Aerodynamics)
- 72 (COMPUTERS & DATA PROCESSING); 91 (ENGINEERING MANAGEMENT); 42 (MATERIALS PROPERTIES & TESTING); 65 (AEROSPACE ENGINEERING)

16/5/16 (Item 1 from file: 34)

DIALOG(R)File 34:SciSearch(R) Cited Ref Sci

(c) 2007 The Thomson Corp. All rts. reserv.

09726143 Genuine Article#: 439XG Number of References: 7

Title: The control of shroud leakage flows to reduce aerodynamic losses in a low aspect ratio, shrouded axial flow turbine

Author(s): Wallis AM (REPRINT) ; Denton JD; Demargne AAJ

Corporate Source: Siemens Power Generat UK Ltd,CA Parsons Works,Newcastle

Upon Tyne/Tyne & Wear/England/ (REPRINT); Siemens Power Generat UK

Ltd,CA Parsons Works,Newcastle Upon Tyne/Tyne & Wear/England/; Univ

Cambridge,Whittle Lab,Cambridge//England/

Journal: JOURNAL OF TURBOMACHINERY-TRANSACTIONS OF THE ASME, 2001, V123, N2 (APR), P334-341

ISSN: 0889-504X Publication date: 20010400

Publisher: ASME-AMER SOC MECHANICAL ENG, THREE PARK AVE, NEW YORK, NY 10016-5990 USA

Language: English Document Type: ARTICLE

Geographic Location: England

Journal Subject Category: ENGINEERING, MECHANICAL

Abstract: The losses generated by fluid leaking across the shrouds of turbine blade rows are known to form a significant proportion of the overall loss generated in low aspect ratio turbines. The use of shrouds to encase the tips of turbine blades has encouraged the development of many innovative sealing nl arrangements, all of which are intended to reduce the quantity of fluid (the leakage fraction) leaking across the shroud. Modern sealing arrangements have reduced leakage fractions considerably, meaning that further improvements can only be obtained by controlling the leakage flow in such a way so as to minimize the aerodynamic losses incurred by the extraction and re-injection of the leakage flow; into the mainstream. There ai-e few published experimental investigations on the interaction between mainstream and leakage flows to provide guidance on the best means of managing the leakage flows to do this. This paper describes the development and testing of a strategy to turn the fluid leaking over shrouded turbine rotor blade rows with the aim of reducing the aerodynamic losses associated with its re-injection into the mainstream flow. The intent was to extract work from the leakage flow in the process. A four stage research turbine was used to test in detail the sealing design resulting from this strategy. A reduction in brake efficiency of 3.5 percent was measured. Further investigation suggested that much of the increase in loss could De attributed to the presence of axial gaps upstream and downstream of the shroud cavity which facilitated the periodic ingress and egress of mainstream fluid into the shroud cavity under the influence of the rotor potential field. This process was exacerbated by reductions in the leakage fraction.

Cited References:

DAWES WN, 1993, V29, P221, PROGR AEROSPACE SCI

DENTON JD, 1976, RMN848 CEGB MARCHW E
DENTON JD, 1993, 93GT435 ASME
HEIDEGGER NJ, 1996, 32 AIAA ASME SAE ASE
JEFFERSON JL, 1954, NE COAST I ENG SHIP
TRAUPEL W, 1966, THERMISCHE TURBOMASC
WALLIS AM, 1998, 98GT516 ASME

16/5/17 (Item 1 from file: 35)
DIALOG(R)File 35:Dissertation Abs Online
(c) 2007 ProQuest Info&Learning. All rts. reserv.

01729298 ORDER NO: AADAA-I9957359

Identification of aerodynamic coefficients with a neural network

Author: Richardson, Kristina Anne

Degree: Ph.D.

Year: 2000

Corporate Source/Institution: Princeton University (0181)

Adviser: Robert Stengel

Source: VOLUME 61/01-B OF DISSERTATION ABSTRACTS INTERNATIONAL.
PAGE 386. 220 PAGES

Descriptors: ENGINEERING, AEROSPACE ; ENGINEERING, MECHANICAL ;
ENGINEERING, ELECTRONICS AND ELECTRICAL ; ARTIFICIAL
INTELLIGENCE

Descriptor Codes: 0538; 0548; 0544; 0800

The components of a framework for the procurement, identification, and employment of aerodynamic coefficients are developed. The basic structure follows the estimation-before-modeling (EBM) technique. In the EBM methodology, state estimation and model determination are broken into two independent steps. An extended Kalman-Bucy filter and a modified Bryson-Frazier smoother are used to estimate state and force histories from a measurement vector. This data is used for maintenance of the aerodynamic mapping. The model satisfies the accuracy, smoothness, and differentiability requirements demanded by nonlinear control laws.

<italic>A-priori</italic> information drawn from the entire input-space is employed to establish a baseline model. Dynamic-system measurements are processed to provide the accurate state and force histories required for on-line updates of the identification model. An extended-Kalman Bucy filter provides state estimates and in combination with a random-walk model accurate force histories. A modified Bryson-Frazier smoother refines these estimates based on future measurements.

The identification scheme employs a neural network to provide models of aerodynamic coefficients during dynamic-system operation. These models are valid over the entire input-output space. Prior to flight, *<italic>a-priori</italic>* data is incorporated into a base neural network using a new design and training algorithm. This algorithm functions in the face of an eight-dimension input vector. During flight, the parameters of the base neural are fixed, and a second set of activation functions are available for learning the surface created by the difference between the base neural network and the current dynamic-system information. The new neural network is demonstrated on a longitudinal-motion aircraft model, with static and dynamic training data, and its training speed, accuracy, and parsimony abilities versus existing neural networks are established.

The identification framework is used to identify the three longitudinal-motion coefficients of a twin-jet, transport aircraft. A localized feature is introduced into the lift-coefficient surface and performance of the model. The network learns new information from the

dynamic-training data patterns, without loss of information in regions distant from the dynamic maneuvers. Approximation performance is evaluated with respect to both training and generalization data sets.

16/5/18 (Item 2 from file: 35)

DIALOG(R)File 35:Dissertation Abs Online

(c) 2007 ProQuest Info&Learning. All rts. reserv.

01139823 ORDER NO: AAD13-41097

PARAMETER ESTIMATION USING A BACK PROPAGATION NEURAL NETWORK

Author: SCHROEDER, WAYNE KEVIN

Degree: M.S.A.E.

Year: 1990

Corporate Source/Institution: THE UNIVERSITY OF TEXAS AT ARLINGTON (2502)

Supervisor: C. W. JILES

Source: VOLUME 29/01 of MASTERS ABSTRACTS.

PAGE 125. 104 PAGES

Descriptors: ENGINEERING, AEROSPACE; MATHEMATICS; COMPUTER SCIENCE

Descriptor Codes: 0538; 0405; 0984

A method to estimate the aerodynamic stability derivatives from flight test data using a modification of the classic back propagation neural network algorithm is developed. Studies are performed with a neural network based on this classic model to examine model requirements. Modifications which are original to this work are applied to the neural network's learning algorithm to enable association between time varying input patterns of vehicle response to correlated sets of stability derivatives. Convergence is achieved for a time response at a given flight condition. Simultaneous association between multiple time histories and related stability derivatives is not demonstrated due to computational limits, but proof by analogy is provided for the existence of a solution.

16/5/19 (Item 1 from file: 56)

DIALOG(R)File 56:Computer and Information Systems Abstracts

(c) 2007 CSA. All rts. reserv.

0000436910 IP ACCESSION NO: 200604-25-09333

Augmentation of a Non Linear Dynamic Inversion Scheme Within the NASA IFCS F-15 WVU Simulator

Perhinschi, M G; Napolitano, M R; Campa, G; Fravolini, M L; Massotti, L; Lando, M

West Virginia, University, Morgantown

PAGES: 1667-1672

PUBLICATION DATE: 2003

PUBLISHER: Institute of Electrical and Electronics Engineers, Inc., 445

Hoes Ln, Piscataway, NJ, 08854-1331

COUNTRY OF PUBLICATION: USA

PUBLISHER URL: <http://iee.org>

PUBLISHER EMAIL: inspec@iee.org

CONFERENCE:

2003 American Control Conference, Denver, CO, USA, 4-6 June 2003

DOCUMENT TYPE: Conference Paper

RECORD TYPE: Abstract

LANGUAGE: English

ISBN: 0780378962

FILE SEGMENT: Computer & Information Systems Abstracts

ABSTRACT:

This paper describes the results of a study focused on enhancing the performance of a non linear dynamic inversion scheme augmented with a neural network to cancell the dynamic inversion error. The approach is based on adding a pre-trained neural network providing the values of the aerodynamic stability and control derivatives required by the dynamic inversion calculations, as the aircraft moves throughout its flight envelope. Additionally, a comparison is performed using two different classes of neural networks (Sigma-Pi and EMRAN algorithms) for the cancellation of the dynamic inversion errors. The study is performed using the WVU IFCS F-15 simulation environment. The results show that the updating of the aerodynamic derivatives reduces the error compensating activity of the neural network. Performance improvements in terms of tracking error are observed for some maneuvers; however, a significant sensitivity to the update rate has been noticed.

DESCRIPTORS: Dynamic inversion; Neural networks; Flight simulators; Nonlinear systems; Flight control systems; F-15 aircraft; Control systems design; Error correction; Aircraft control; NASA programs; Performance enhancement; Aerodynamic stability; Flight envelopes; Neurocontrol
SUBJ CATG: 25, Computer Communication Networks

16/5/23 (Item 5 from file: 56)

DIALOG(R)File 56:Computer and Information Systems Abstracts

(c) 2007 CSA. All rts. reserv.

0000128781 IP ACCESSION NO: 1886597

Plan for an automated design method of airfoils.

Marazzi, R; Ghielmi, L G

L'AEROTEC. MISSILI SPAZIO., v 66, n 1, p 18-26, 1987

PUBLICATION DATE: 1987

DOCUMENT TYPE: Journal Article

RECORD TYPE: Abstract

LANGUAGE: English

FILE SEGMENT: Computer & Information Systems Abstracts

ABSTRACT:

The computer gives the possibility of automatizing the aerodynamic design for aeronautical applications. The first step in this direction is the adoption of optimization procedures. Subsequently recourse can be made to artificial intelligence languages, which permit heuristic knowledges to be implemented through a symbolic representation. This article presents a plan for the automation of the design of wing airfoils. A possible choice of objective function, geometrical and aerodynamic constraints and geometrical modification functions used in the optimization procedure applied to a concrete case are first indicated. The modification of a lifting symmetrical airfoil produced as an example, this being one of the early results obtained by the authors. The initial indications for the realization of a system expert in the design of airfoils are given in the last part of this article.

DESCRIPTORS: Airfoils; Design engineering; Automation; Modification;

- Optimization; Geometry; Aerodynamics; Aeronautics; Constraints; Hoisting; Expert systems; Concretes; Aircraft; Wings (aircraft); Aircraft components; Wings; Computer aided design; Aircraft engineering

SUBJ CATG: I 6610, AIRCRAFT ENGINEERING; C CA14.1, AERONAUTICAL ENGINEERING

16/5/24 (Item 1 from file: 65)

DIALOG(R)File 65:Inside Conferences

(c) 2007 BLDSC all rts. reserv. All rts. reserv.

01322465 INSIDE CONFERENCE ITEM ID: CN013080025

Feed Forward Neural Networks for Aerodynamic Modelling and Sensor Failure Detection

Raol, J. R.

CONFERENCE: Aeronautical Society of India-Annual general meeting; 47th

JOURNAL- AERONAUTICAL SOCIETY OF INDIA, 1995; VOL 47; NUMBER 4 P: 193-199

The Society, 1995

ISSN: 0001-9267

LANGUAGE: English DOCUMENT TYPE: Conference Preprinted papers

CONFERENCE SPONSOR: Aeronautical Society of India

CONFERENCE LOCATION: Madras, India

CONFERENCE DATE: Jan 1996 (19960)

BRITISH LIBRARY ITEM LOCATION: 4677.000000

DESCRIPTORS: aeronautical

16/5/25 (Item 2 from file: 65)

DIALOG(R)File 65:Inside Conferences

(c) 2007 BLDSC all rts. reserv. All rts. reserv.

00779767 INSIDE CONFERENCE ITEM ID: CN007617501

Neural Network Approach to Aerodynamic Coefficients Estimation and Aircraft Failure Isolation Design

Chiang, C.-Y.; Youssef, H.

CONFERENCE: Guidance, navigation and control conference

PAPERS- AMERICAN INSTITUTE OF AERONAUTICS AND ASTRONAUTICS, 1994; CP 948; NUMBER 2 P: 500-509

AIAA, 1994

ISBN: 156347087X

LANGUAGE: English DOCUMENT TYPE: Conference Papers

CONFERENCE SPONSOR: AIAA

CONFERENCE LOCATION: Scottsdale, AZ

CONFERENCE DATE: Aug 1994 (199408)

BRITISH LIBRARY ITEM LOCATION: 6369.400000

NOTE:

In 3 vols

DESCRIPTORS: AIAA; guidance; navigation; control

16/5/26 (Item 1 from file: 95)

DIALOG(R)File 95:TEME-Technology & Management

(c) 2007 FIZ TECHNIK. All rts. reserv.

01658054 20020702792

Analysis and design of advanced miniscale mechatronic systems: Synthesis of

intelligent flight servos

(Analyse und Entwurf fortgeschrittener miniaturisierter mechatronischer Systeme: Synthese intelligenter Flug-Servos)

Sinha, ASC; Lyshevski, SE

University of Indianapolis, USA

International Journal of Smart Engineering System Design, v4, n2, pp115-123, 2002

Document type: journal article Language: English

Record type: Abstract

ISSN: 1025-5818

ABSTRACT:

The flight vehicle performance (flight and handling qualities, agility, controllability, maneuverability, etc.) depends upon flight actuators, which displace the control surfaces. Intelligent flight servos must be designed to achieve the specified criteria, requirements, and standards. Miniscale electromechanical flight actuators are actuated by electric servo-motors, and brushless permanent-magnet synchronous machines are perfectly suited due to their efficiency, reliability, high torque density, low cost and maintenance, simplicity, and ruggedness. However, conventional controllers do not ensure the dynamic performance of flight actuators in the full operating envelope under rapidly changing flight and environmental conditions and aerodynamic loads. An intelligent flight servo is designed using the developed neural networks synthesis procedure. The Hopfield equations are modified to incorporate delay for finite switching. The effect of even small delays due to finite switching for composite large networks could be significant, and, therefore, closed-loop systems may exhibit delay-induced instability. The results obtained are valid for systems without delays if the conditions of the theorems hold. These results are applied to illustrate the application of neural network-based control systems design for advanced flight servos. It is shown that new controllers must be synthesized because synchronous servomotors are controlled taking into account the electromagnetic features, software, and hardware used. Control signals, which drive high-switching transistors (more specifically, MOSFET drivers), are developed by the DSP based upon the rotor angular displacement. The DSP performs control and decision-making through learning, adaptation, reconfiguration, scheduling, and optimization mechanisms. Other functions, such as identification, estimation, and diagnostics, can be also performed. It is demonstrated that the neural network-based intelligent controllers guarantee the specified tracking accuracy, desired deflection rate, and disturbance attenuation. The system performance is documented.

DESCRIPTORS: MECHATRONICS; AEROPLANES; CONTROL SYSTEMS; ARTIFICIAL NEURAL NETWORKS; TRANSFER CHARACTERISTICS; AUTOMATIC CONTROL SYSTEMS; DYNAMIC BEHAVIOUR

IDENTIFIERS: Mechatronik; intelligenter Flug-Servo

16/5/27 (Item 2 from file: 95)

DIALOG(R)File 95:TEME-Technology & Management

(c) 2007 FIZ TECHNIK. All rts. reserv.

00918757 M95080120650

Prediction of helicopter component loads using neural networks

(Die Vorhersage von Hubschrauber-Komponentenbelastungen unter Anwendung der Theorie neuronaler Netze)

Haas, DJ; Milano, J; Flitter, L

Naval Surface Warfare Center, Bethesda, USA

Journal of the American Helicopter Society, v40, n1, pp72-82, 1995

Document type: journal article Language: English

Record type: Abstract

ISSN: 0002-8711

ABSTRACT:

An artificial neural network is trained using helicopter flight test data to predict rotor system component loads during high-speed maneuvering flight. Inputs to the network include control positions and aircraft state parameters. These parameters can be measured easily in the nonrotating system, i.e., the fuselage, and vary at a relatively low frequency. A network design sensitivity study is conducted and several networks are developed for three loads: the rotor blade pushrod load, blade normal bending moment, and main-rotor damper load. Prediction accuracy is evaluated using a validation data set consisting of symmetric pullout maneuvers, rolling pullout maneuvers, and climbing turns not contained in the training data set. A traditional statistical approach, stepwise multiple linear regression, also is utilized, and the two methods are compared and contrasted. Correlation coefficients from 84 to 97 are achievable using the neural network model for all three loads. Through a unified approach involving both neural network and statistical analysis; greater accuracy and understanding of the neural network is attained.

DESCRIPTORS: GYROPLANES; FLIGHT CHARACTERISTICS; TESTING; ROTARY BLADES--ROTARY WINGS; AERODYNAMICS; SENSITIVITY; FORECAST; ARTIFICIAL NEURAL NETWORKS; INSERTION PARAMETERS; FREQUENCY RANGES; AIRCRAFT FUSELAGES; BENDING MOMENT; IMPACT STRESS; COMPUTING; COMPARISON OF SYSTEMS; REGRESSION ANALYSIS; AEROPLANES

IDENTIFIERS: Hubschrauber; Flugdaten; neuronales Netz

16/5/28 (Item 1 from file: 144)

DIALOG(R)File 144:Pascal

(c) 2007 INIST/CNRS. All rts. reserv.

15758477 PASCAL Number: 02-0471040

Online parameter estimation techniques comparison within a fault tolerant Flight Control System

SONG Yongkyu; CAMPA Giampiero; NAPOLITANO Marcello; SEANOR Brad; PERHINSCHI Mario G

Hankuk Aviation University, Kyonggido 412-791, Korea, Republic of; West Virginia University, Morgantown, West Virginia 26506-6106, United States

Journal: Journal of guidance, control, and dynamics, 2002, 25 (3)

528-537

ISSN: 0731-5090 CODEN: JGCODS Availability: INIST-19058

Number of Refs.: 26 reference

Document Type: P (Serial) ; A (Analytic)

Country of Publication: United States

Language: English

The results of a study where two online parameter identification (PID) methods are compared for application within a fault tolerant flight control system are described. One of the PID techniques is time-domain based, whereas the second is featured in the frequency domain. The time-domain method was directly suitable for the online estimates of the dimensionless aircraft stability derivatives. The frequency-domain method was modified from its original formulation to provide direct estimates of the stability derivatives. This effort was conducted within the research activities of the NASA Intelligent Flight Control System F-15 program. The comparison is performed through dynamic simulations with a specific procedure to model the aircraft aerodynamics following the occurrence of a battle damage/failure on a primary control surface. The two PID methods show

similar performance in terms of accuracy of the estimates, convergence time, and robustness to noise. However, the frequency-domain-based method outperforms the time-domain-based method in terms of computational requirements for online real-time applications. The study has also emphasized the advantages of using ad hoc short preprogrammed maneuvers to provide enough excitation following the occurrence of the actuator failure to allow the parameter estimation process.

English Descriptors: Parameter estimation; System identification; Fault tolerant system; Fault tolerance; Intelligent system; Aircraft; Intelligent control; Differential integral proportional control; Robustness; Flight; Aerodynamics; Damaging; Failures; Rupture; Dynamic model; Modeling; Frequency domain method; Time domain method

Classification Codes: 001D02D07; 001D02D09

16/5,K/1 (Item 1 from file: 2)

DIALOG(R)File 2:INSPEC

(c) 2007 Institution of Electrical Engineers. All rts. reserv.

08573218 INSPEC Abstract Number: C2003-05-1180-006

Title: A modification to particle swarm optimization algorithm

Author(s): Huiyuan Fan

Author Affiliation: Turbo & Jet Engine Laboratory, Technion-Israel Inst. of Technol., Haifa, Israel

Journal: Engineering Computations vol.19, no.8 p.970-89

Publisher: Emerald,

Publication Date: 2002 Country of Publication: UK

CODEN: ENCOEN ISSN: 0264-4401

SICI: 0264-4401(2002)19:8L:970:MPSO;1-K

Material Identity Number: N816-2002-008

DOI: 10.1108/02644400210450378

Language: English Document Type: Journal Paper (JP)

Treatment: Theoretical (T)

Abstract: In this paper, a modification strategy is proposed for the particle swarm optimization (PSO) algorithm. The strategy adds an adaptive scaling term into the algorithm, which aims to increase its convergence rate and thereby to obtain an acceptable solution with a lower number of objective function evaluations. Such an improvement can be useful in many practical engineering optimizations where the evaluation of a candidate solution is a computationally expensive operation and consequently finding the global optimum or a good sub-optimal solution with the algorithm is too time consuming, or even impossible within the time available. The modified PSO algorithm was empirically studied with a suite of four well-known benchmark functions, and was further examined with a practical application case, a neural-network-based modeling of aerodynamic data. The numerical simulation demonstrates that the modified algorithm statistically outperforms the original one. (17 Refs)

Subfile: C

Descriptors: convergence; evolutionary computation; optimisation; search problems

Identifiers: particle swarm optimization; modification strategy; search process; large scale search; convergence; genetic algorithms; adaptive scaling; global optimum; sub-optimal solution

Class Codes: C1180 (Optimisation techniques); C1230 (Artificial intelligence)

Copyright 2003, IEE

- ...Abstract: four well-known benchmark functions, and was further examined with a practical application case, a neural-network-based
- modeling of aerodynamic data. The numerical simulation demonstrates that the modified algorithm statistically outperforms the original one.

2002

Patent Files Searched

File 347:JAPIO Dec 1976-2007/
File 348:EUROPEAN PATENTS 1978-2007
File 349:PCT FULLTEXT 1979-2007
File 350:Derwent WPIX 1963-2007

Set	Items	Description
S1	20	AU=(HAUDRICH D? OR PITT D ? OR HAUDRICH, D? OR PITT, D ?)
S2	32260	AEROELASTIC? OR AERODYNAMIC? OR AERO() ELASTIC? OR AERO()- DYNAMIC?
S3	2	S1 AND S2
S4	2	IDPAT (sorted in duplicate/non-duplicate order)
S5	2	IDPAT (primary/non-duplicate records only)

5/3,K/1 (Item 1 from file: 350)
DIALOG(R)File 350:Derwent WPIX
(c) 2007 The Thomson Corporation. All rts. reserv.

0015410411 - Drawing available
WPI ACC NO: 2005-756366/200577
XRPX Acc No: N2005-624001

Aeroelastic analysis system for aircraft, has network module which
generates transformation of input parameters associated with aeroelastic
characteristics of structure, to produce aeroelastic analysis result

Patent Assignee: BOEING CO (BOEI)

Inventor: HAUDRICH D P; PITT D M

Patent Family (1 patents, 1 countries)

Patent	Application
--------	-------------

Number	Kind	Date	Number	Kind	Date	Update
US 20050234839	A1	20051020	US 2004825032	A	20040414	200577 B

Priority Applications (no., kind, date): US 2004825032 A 20040414

Patent Details

Number	Kind	Lan	Pg	Dwg	Filing	Notes
US 20050234839	A1	EN	23	11		

Aeroelastic analysis system for aircraft, has network module which
generates transformation of input parameters associated with aeroelastic
characteristics of structure, to produce aeroelastic analysis result

Original Titles:

Neural network for aeroelastic analysis

Inventor: HAUDRICH D P...

...PITT D M

Alerting Abstract ...NOVELTY - An input module receives input parameters
associated with aeroelastic characteristics of a structure. A neural
network module generates transformation of input parameters to produce
aeroelastic analysis result based on a trained neural network....
aeroelastic analysis method; and aeroelastic analysis program.

...

...USE - For analyzing aeroelastic characteristic of structure such as stabilator, wind, elevator, canard, aileron, flap, spoiler, stabilizer, tail section and rudder of aircraft...

...ADVANTAGE - Obtains aeroelastic analysis result easily at low cost.

...DESCRIPTION OF DRAWINGS - The figure shows the functional block diagram of the aeroelastic analysis system.

Title Terms/Index Terms/Additional Words: AEROELASTIC;

Original Publication Data by Authority

Inventor name & address:

Haudrich, Darin P...

Original Abstracts:

A system and method of performing aeroelastic analysis using a neural network. Input parameters, such as mass and location, contributing to aeroelastic characterization are determined and constrained. A model of a structure to be analyzed can be constructed. The model can include a number of locations where the input parameters can be varied. The aeroelastic characteristic of the structure can be analyzed using a finite element model to determine a number of output characteristics...

...of a plurality of input samples. A neural network can be generated for determining the aeroelastic characteristic based on input parameters. The input sample/output characteristic pairs can be used to train the neural network...

...neural network can be used to generate a non-linear transfer function that generates the aeroelastic characteristic in response to input parameters.

Claims:

1. An aeroelastic analysis system, the system comprising:an input module configured to receive one or more input parameters associated with aeroelastic characteristics of a structure; anda neural network module coupled to the input module, and configured to generate a transformation of the one or more input parameters to produce at least one aeroelastic analysis result, the transformation based in part on a trained neural network.

5/3,K/2 (Item 2 from file: 350)

DIALOG(R)File 350:Derwent WPIX

(c) 2007 The Thomson Corporation. All rts. reserv.

0015398675 - Drawing available

WPI ACC NO: 2005-743827/200576

XRPX Acc No: N2005-613160

Flight control circuit for mobile platform of aircraft has output which controls actuator for mobile platform in response to command from flight control system and signal representing vibration of structure in mobile platform

Patent Assignee: PITT D M (PITT-I)

Inventor: PITT D M

Patent Family (1 patents, 1 countries)

Patent Application

Number Kind Date Number Kind Date Update

US 20050224659 A1 20051013 US 2004798687 A 20040311 200576 B

Priority Applications (no., kind, date): US 2004798687 A 20040311

Patent Details

Number Kind Lan Pg Dwg Filing Notes
US 20050224639 A1 EN 10 6

Inventor: MIN M

Alerting Abstract ...ADVANTAGE - Suppresses aerodynamically induced vibrations of structures in mobile platform, thus reducing cyclic loads and improving fatigue life of structure...

Original Publication Data by Authority

Original Abstracts:

...methods for use on a mobile platform including a light control system, a structure, an aerodynamic surface, and an actuator operatively coupled to the surface to control the surface. The circuit includes a first and...
Claims:
...circuit for use on a mobile platform including a light control system, a structure, an aerodynamic surface, and an actuator operatively coupled to the surface to control the surface, the circuit comprising: a first input...

NPL Files Searched

File 2:INSPEC 1898-2007
 File 6:NTIS 1964-2007
 File 8:Ei Compendex(R) 1884-2007
 File 34:SciSearch(R) Cited Ref Sci 1990-2007
 File 434:SciSearch(R) Cited Ref Sci 1974-1989
 File 35:Dissertation Abs Online 1861-2007
 File 65:Inside Conferences 1993-2007
 File 99:Wilson Appl. Sci & Tech Abs 1983-2007

S1 214641 AEROELASTIC? OR AERODYNAMIC? OR AERO() ELASTIC? OR AERO()DYNAMIC?
 S2 4 AU=(HAUDRICH D? OR PITT D ? OR HAUDRICH, D? OR PITT, D ?)
 S3 4 S1 AND S2
 S4 4 RD (unique items)
 ? t 4/3,k/1-4

4/3,K/1 (Item 1 from file: 8)
 DIALOG(R)File 8:Ei Compendex(R)
 (c) 2007 Elsevier Eng. Info. Inc. All rts. reserv.

11807020 E.I. No: EIP073210748009

Title: Determination of the flutter critical stores configuration
 utilizing an optimized artificial neural network

Author: Pitt, Dale M.; Haudrich, Darin P.

Corporate Source: Boeing Company, St. Louis, MO 63166-0156

Conference Title: 48th AIAA/ASME/ASCE/AHS/ASC Structures, Structural
 Dynamics, and Materials Conference

Conference Location: Waikiki, HI, United States Conference Date:
 20070423-20070426

E.I. Conference No.: 70016

Source: Collection of Technical Papers - AIAA/ASME/ASCE/AHS/ASC
 Structures, Structural Dynamics and Materials Conference Collection of
 Technical Papers - 48th AIAA/ASME/ASCE/AHS/ASC Structures, Structural
 Dynamics, and Materials Conference v 8 2007.

Publication Year: 2007

CODEN: CPSCDO ISSN: 0273-4508 ISBN: 9781563478925

Language: English

Author: Pitt, Dale M.; Haudrich, Darin P.

Abstract: Aeroelasticians are tasked with determining that the basic
 air-vehicle is flutter free within 115 percent...

Descriptors: *Neural networks; Computational methods; Fighter aircraft;
Flutter (aerodynamics); Optimization; Wings

4/3,K/2 (Item 2 from file: 8)
 DIALOG(R)File 8:Ei Compendex(R)
 (c) 2007 Elsevier Eng. Info. Inc. All rts. reserv.

10768052 E.I. No: EIP05519593003

Title: Development of an artificial neural aeroelastic network (AN**2)
 for the prediction of multiple flutter crossing

Author: Pitt, Dale M.; Haudrich, Darin P.

Corporate Source: Boeing Company, St. Louis, MO 63166-0516, United States

Conference Title: 46th AIAA/ASME/ASCE/AHS/ASC Structures, Structural
 Dynamics and Materials Conference

Conference Location: Austin, TX, United States Conference Date:

20050418-20050421

E.I. Conference No.: 66173

Source: Collection of Technical Papers - AIAA/ASME/ASCE/AHS/ASC Structures, Structural Dynamics and Materials Conference Collec. of Technic. Pap. - 46th AIAA/ASME/ASCE/AHS/ASC Struct., Struct. Dynam. and Mater. Conf., 13th AIAA/ASME/AHS Adap. Struct. Conf., 7th AIAA Non-Determin. Appr. Forum, 6th AIAA GSF 1st AIAA MDOSC v 9 2005.

Publication Year: 2005

CODEN: CPSCDO ISSN: 0273-4508

Language: English

Title: Development of an artificial neural aeroelastic network (AN**2) for the prediction of multiple flutter crossing

Author: Pitt, Dale M.; Haudrich, Darin P.

Descriptors: *Flutter (aerodynamics); Wings; Neural networks; Damping; Error analysis

4/3,K/3 (Item 3 from file: 8)

DIALOG(R)File 8: Ei Compendex(R)

(c) 2007 Elsevier Eng. Info. Inc. All rts. reserv.

10351006 E.I. No: EIP05169045955

Title: Artificial neural network for multiple aeroelastic analysisAuthor: Pitt, Dale M.; Haudrich, Darin P.

Corporate Source: Boeing Company, St. Louis, MO 63166-0516, United States

Conference Title: Collect. of Pap. - 45th AIAA/ASME/ASCE/AHS/ASC Struct., Struct. Dyn. and Mater. Conf.; 12th AIAA/ASME/AHS Adapt. Struct. Conf.; 6th AIAA Non-Deterministic Approaches Forum; 5th AIAA Gossamer Spacecraft Forum

Conference Location: Palm Springs, CA, United States Conference Date: 20040419-20040422

E.I. Conference No.: 64536

Source: Collection of Technical Papers - AIAA/ASME/ASCE/AHS/ASC Structures, Structural Dynamics and Materials Conference Collect. of Tech. Pap. - 45th AIAA/ASME/ASCE/AHS/ASC Struct., Struct. Dyn. and Mater. Conf.; 12th AIAA/ASME/AHS Adapt. Struct. Conf.; 6th AIAA Non-Deterministic Approaches Forum; 5th AIAA Gossamer Spa v 4 2004.

Publication Year: 2004

CODEN: CPSCDO ISSN: 0273-4508

Language: English

Title: Artificial neural network for multiple aeroelastic analysisAuthor: Pitt, Dale M.; Haudrich, Darin P.

Descriptors: *Wings; Flutter (aerodynamics); Neural networks; Structural analysis; Elasticity; Damping; Error analysis; Finite element method; Computer simulation

Identifiers: Mach number; Structural damping; Aeroelastic stability; Modal mass

4/3,K/4 (Item 1 from file: 65)

DIALOG(R)File 65: Inside Conferences

(c) 2007 BLDSC all rts. reserv. All rts. reserv.

05653545 INSIDE CONFERENCE ITEM ID: CN058627833

AIAA-2004-1750 Artificial Neural Network for Multiple Aeroelastic Analysis

Pitt, D.; Haudrich, D.

CONFERENCE: Structures, structural dynamics, and materials conference;;

45th AIAA/ASME/ASCE/AHS/ASC 12th AIAA/ASME/AHS adaptive structures

conference: 6th AIAA non-deterministic approaches forum: 5th AIAA
gossamer spacecraft forum-45TH

• P: 2598-2605

AIAA., 2004

LANGUAGE: English DOCUMENT TYPE: Conference Papers

CONFERENCE LOCATION: Palm Springs, Calif 2004; Apr (200404)

NOTE:

Held in conjunction with 12th AIAA/ASME/AHS adaptive structures
conference, 6th AIAA non-deterministic approaches forum and 5th AIAA
gossamer spacecraft forum

AIAA-2004-1750 Artificial Neural Network for Multiple Aeroelastic
Analysis

Pitt, D.; Haudrich, D.

Secondary author search

File 14:Mechanical and Transport Engineer Abstract 1966-2007/

File 56:Computer and Information Systems Abstracts 1966-2007 File 61:Civil Engineering Abstracts. 1966-2007

Set Items Description

--- ----

S2 10 (AEROELASTIC? OR AERODYNAMIC? OR AERO() ELASTIC? OR
AERO()DYNAMIC?) AND AU=(HAUDRICH D? OR PITT D ? OR
HAUDRICH, D? OR PITT, D ?)

S3 6 RD (unique items)

3/3,K/1 (Item 1 from file: 14)

DIALOG(R)File 14:Mechanical and Transport Engineer Abstract
(c) 2007 CSA. All rts. reserv.

0000840363 IP ACCESSION NO: 200710-62-483351

Determination of the Flutter Critical Stores Configuration Utilizing an
Optimized Artificial Neural Network

Pitt, Dale M; Haudrich, Darin P

48th AIAA/ASME/ASCE/AHS/ASC Structures, Structural Dynamics, and Materials
Conference, 2007

PUBLICATION DATE: 2007

PUBLISHER: American Institute of Aeronautics and Astronautics, 1801
Alexander Bell Drive, Suite 500, Reston, VA, 20191-4344

COUNTRY OF PUBLICATION: USA

PUBLISHER URL: <http://www.aiaa.org>

CONFERENCE:

48th AIAA/ASME/ASCE/AHS/ASC Structures, Structural Dynamics, and Materials
Conference, Honolulu, HI, USA, 23-26 Apr. 2007

DOCUMENT TYPE: Conference Paper; Journal Article

RECORD TYPE: Abstract

LANGUAGE: English

ISSN: 0146-3705

REPORT NO: AIAA Paper 2007-2365

FILE SEGMENT: Mechanical & Transportation Engineering Abstracts

Pitt, Dale M; Haudrich, Darin P

ABSTRACT:

Aeroelasticians are tasked with determining that the basic air-vehicle is flutter free within 115 percent...

...DESCRIPTORS: Constraints; Artificial neural networks; Certification
testing; Aircraft; Networks; Computational efficiency; Fuel tanks;
Carriages; Mathematical models; Aeroelasticity; Flight envelopes;
Astronautics; Placement; Computation; Inertia

3/3,K/2 (Item 2 from file: 14)

DIALOG(R)File 14:Mechanical and Transport Engineer Abstract
(c) 2007 CSA. All rts. reserv.

0000837213 IP ACCESSION NO: 200709-62-465625

A Technique For Determining The Critical Flutter Configuration From

Multiple External Stores Utilizing Artificial Neural Networks

- Pitt, Dale M; Haudrich, Darin P
AUTHOR EMAIL: dale.m.pitt@boeing.com

CEAS/AIAA/DGLR International Forum on Aeroelasticity and Structural Dynamics 2005 Proceedings, 2005
PUBLICATION DATE: 2005

PUBLISHER: DGLR, Godesberger Allee 70, Bonn, D-53175
COUNTRY OF PUBLICATION: Germany
PUBLISHER URL: www.dglr.de

CONFERENCE:
CEAS/AIAA/DGLR International Forum on Aeroelasticity and Structural Dynamics 2005, Munich, Germany, 28 June-1 July 2005

DOCUMENT TYPE: Conference Paper; Journal Article
RECORD TYPE: Abstract
LANGUAGE: English
ISBN: 393218243X
FILE SEGMENT: Mechanical & Transportation Engineering Abstracts

Pitt, Dale M; Haudrich, Darin P

ABSTRACT:
... of the 'Most Critical' or lowest flutter speed. The new technique utilized an Artificial Neural Aeroelastic Network (AN 2) that was trained on flutter data to predict flutter speeds as the...

...DESCRIPTORS: Learning theory; External stores; Shape; Email; Networks; Electronic mail; Smart structures; Trains; Inertia; Fighter; Splines; Aeroelasticity; Errors

3/3,K/3 (Item 3 from file: 14)
DIALOG(R)File 14:Mechanical and Transport Engineer Abstract
(c) 2007 CSA. All rts. reserv.

0000522328 IP ACCESSION NO: 200605-62-27985
Development of an Artificial Neural Aeroelastic Network (AN 2) for the Prediction of Multiple Flutter Crossing

Pitt, Dale M; Haudrich, Darin P
Boeing Co., Saint Louis, MO

PAGES: 1-11
PUBLICATION DATE: 2005

PUBLISHER: American Institute of Aeronautics and Astronautics, The Aerospace Center, 370 L'Enfant Promenade, SW, Washington, DC, 20024
COUNTRY OF PUBLICATION: USA

CONFERENCE:
46th AIAA/ASME/ASCE/AHS/ASC Structures, Structural Dynamics, and Materials Conference, Austin, TX, USA, 18-21 Apr. 2005

DOCUMENT TYPE: Conference Paper
RECORD TYPE: Abstract
LANGUAGE: English

ISSN: 0146-3705

REPORT NO: AIAA Paper 2005-2288

FILE SEGMENT: Mechanical & Transportation Engineering Abstracts

Development of an Artificial Neural Aeroelastic Network (AN 2) for the Prediction of Multiple Flutter Crossing

Pitt, Dale M; Haudrich, Darin P

DESCRIPTORS: Aeroelastic wings; Wing oscillations; Flutter analysis; Lumped parameter systems; Artificial neural networks; Vibration damping; Error analysis...

3/3,K/4 (Item 4 from file: 14)

DIALOG(R)File 14:Mechanical and Transport Engineer Abstract

(c) 2007 CSA. All rts. reserv.

0000232856 IP ACCESSION NO: 2001-13-007092

Applications of XTRAN3S and CAP-TSD to fighter aircraft

PITT, D M; FUGLSANG, D F; DROUIN, D V
McDonnell Aircraft Co., Saint Louis, MO [PITT]

PAGES: 1340-1348

PUBLICATION DATE: 1990

PUBLISHER: Washington, DC, American Institute of Aeronautics and Astronautics

CONFERENCE:

AIAA/ASME/ASCE/AHS/ASC Structures, Structural Dynamics and Materials Conference, 31st, Long Beach, CA, Technical Papers. Part 3, UNITED STATES, 2-4 Apr. 1990

DOCUMENT TYPE: Conference Paper

RECORD TYPE: Abstract

LANGUAGE: English

REPORT NO: AIAA PAPER 90-1035

NUMBERS: A90-29359 11-39; Contract: F33615-87-C-3212; A90-29359 11-39

FILE SEGMENT: Mechanical & Transportation Engineering Abstracts

PITT, D M; FUGLSANG, D F; DROUIN, D V

ABSTRACT:

... unsteady transonic sm all-disturbance (TSD) codes, XTRAN3S and CAP-TSD, were used to perform aeroelastic analyses of four fighter aircraft configurations. The XTRAN3S code was used for a wing alone...

...a wing, launcher, and tip missile arrangement of the F/A-18. Static and dynamic aeroelastic calculations were performed using both the linear and the nonlinear forms of the small- disturbance...

...wing alone flutter results and those from a linear flutter analysis computed using Doublet Lattice aerodynamics. These comparisons show good agreement for the linear aerodynamics TSD solutions but significant changes in the flutter speed for the nonlinear aerodynamic TSD solutions. Comparisons were also made for the canard/wing/tail and the wing /launcher

...

DESCRIPTORS: Wings (aircraft); Military aircraft; Military planes;

Vibration; Mathematical models; Aerodynamics; Aeroelasticity;

- Dynamics; Missiles; Positioning; Launchers; Accuracy; Hoisting; Beaches; Geometry; Lattices; Statics; Aircraft components; Computation; *Aeroelasticity; *Computer programs; *Fighter aircraft; *Flutter analysis; *Transonic flutter; *Unsteady aerodynamics; F-15 aircraft; Linear equations; Nonlinear equations; Perturbation theory; Time marching

3/3,K/5 (Item 5 from file: 14)

DIALOG(R)File 14:Mechanical and Transport Engineer Abstract

(c) 2007 CSA. All rts. reserv.

0000131510 IP ACCESSION NO: 200212-12-009640

Theoretical prediction of dynamic-inflow derivatives

PITT, D M; PETERS, D A

Vertica, v 5, n 1, p 21-34, 1981

PUBLICATION DATE: 1981

CONFERENCE:

Royal Aeronautical Society, Society of British Aerospace Companies, and University of Bristol, European Rotorcraft and Powered Lift Aircraft Forum, 6th, University of Bristol, Bristol, England, 16-19 Sept. 1980

DOCUMENT TYPE: Conference Paper; Journal Article

RECORD TYPE: Abstract

LANGUAGE: English

FILE SEGMENT: Mechanical & Transportation Engineering Abstracts

PITT, D M; PETERS, D A

3/3,K/6 (Item 6 from file: 14)

DIALOG(R)File 14:Mechanical and Transport Engineer Abstract

(c) 2007 CSA. All rts. reserv.

0000070064 IP ACCESSION NO: 200212-13-008511

Supporting wire interference effects in supersonic near wakes of slender bodies

PITT, D M; SELBERG, B P

U.S. Army, Aviation Systems Command, St. Louis, Mo. [PITT]

Journal of Spacecraft and Rockets, v 13, p 123-126, Feb. 1976

PUBLICATION DATE: 1976

PUBLISHER: American Institute of Aeronautics and Astronautics, 1801

Alexander Bell Drive, Suite 500, Reston, VA, 20191-4344

COUNTRY OF PUBLICATION: USA

PUBLISHER URL: <http://www.aiaa.org>

CONFERENCE:

, United States

DOCUMENT TYPE: Journal Article

RECORD TYPE: Abstract

LANGUAGE: English

ISSN: 0022-4650

PITT, D.M.; SELBERG, B P

...DESCRIPTORS: tunnels; Width; Pressure measurement; *Near wakes; *Slender bodies; *Supersonic wakes; *Support interference; *Wind tunnel tests; Aerodynamic interference; Atmospheric entry simulation; Viscous flow; Wedge flow

File 14:Mechanical and Transport Engineer Abstract 1966-2007

Set	Items	Description
S2	309	NEURAL() (NET? ? OR NETWORK? ?) OR ARTIFICIAL() INTELLIGENCE OR (VIRTUAL OR INTELLIGENT) (2N) (ROBOT? OR AGENT? ? OR SERVO? ? OR BOT OR BOTS OR SYSTEM? ?) OR SOFTBOT? OR SOFT() (BOT OR BOTS)
S3	105	AI OR SYMBOT? OR KNOWBOT? OR INFERENCE() ENGINE? ? OR ANN OR (ARTIFICIAL () NEURAL () NETWORK?) OR (PARALLEL () DISTRIBUTED () PROCESSING () NETWORK?)
S4	80	EXPERT () SYSTEM? ? OR INTELLIGENT () RETRIEVAL OR KNOWLEDGE () ENGINEERING OR MACHINE () LEARNING
S7	394	S2:S4
S8	7708	REPAIR??? OR ALTERATION? ? OR ALTER??? OR MODIFY OR MODIFICATION OR MODIFIED OR CORRECT??? OR BROKEN OR BREAK??? OR FIX??? OR WORN OR MEND??? OR MALFUNCTION? OR FAILURE? ? OR MISFUNCTION? OR LEAK??? OR SERVICING
S9	208	(ENTER??? OR INPUT????? OR INSERT????? OR ADD??? OR SCAN????? OR READ???) (5N) (DEVICE? ? OR MODULE? ? OR PARAMETER? ?)
S18	5776	AEROELASTIC? OR AERO() ELASTIC?
S19	58	S18 AND S7
S20	9	S19 AND (S8 OR S9)
S21	8	S20 AND PY=1963:2004
S22	8	RD (unique items)
S23	9	S19 AND (INPUT??? OR OUTPUT???)
S26	64	S18 AND CERTIFICATION?
S27	3	S7 AND S26
S28	12	S23 OR S27
S29	6	S28 AND PY=1963:2004
S30	6	RD (unique items)

22/5/1

DIALOG(R) File 14:Mechanical and Transport Engineer Abstract
(c) 2007 CSA. All rts. reserv.

0000686594 IP ACCESSION NO: 200705-20-099469
Modeling Aircraft Wing Loads From Flight Data Using Neural Networks

Allen, Michael J
NASA Dryden

, Sept. 2003
PUBLICATION DATE: 2003

PUBLISHER: Society of Automotive Engineers, 400 Commonwealth Dr.,
Warrendale, PA, 15096
COUNTRY OF PUBLICATION: USA
PUBLISHER URL: DRL: <http://www.sae.org/servlets/productDetail?PROD>
TYP=PAPER&PROD CD=2003-01-30 25 <http://www.sae.org>

DOCUMENT TYPE: Conference Paper
RECORD TYPE: Abstract
LANGUAGE: English
REPORT NO: SAE Document 2003-01-3025
NOTES: World Aviation Congress (R) & Exposition, September 2003, Montreal,
QC, CANAD, Session: Structures
FILE SEGMENT: Mechanical & Transportation Engineering Abstracts

ABSTRACT:

This paper documents input data conditioning, input parameter selection, structure, training, and validation of neural network models of the active Aeroelastic wing aircraft. Neural networks can account for uncharacterized nonlinear effects and retain generalization capability. Model inputs include aircraft rates, accelerations, and control surface positions. Linear loads models were developed for network training starting points. The models were trained with rolls, loaded reversals, windup turns, and individual control surface doublets for load excitation. Data results from all loads models at Mach 0.90 and altitude of 15,000 ft. show an average model prediction error reduction of 18.6 percent.

DESCRIPTORS: Neural networks; Aircraft; Mathematical models; Aircraft components; Training; Control surfaces; Error reduction; Active control; Acceleration; Rolls; Networks; Wings (aircraft); Nonlinearity; Aviation; NASA; Altitude; Quality control; Excitation; Conditioning; Aeroelastic wings; Exposure; Aeronautics
SUBJ CATG: 20, Automotive Engineering (General)

22/5/2

DIALOG(R)File 14:Mechanical and Transport Engineer Abstract
(c) 2007 CSA. All rts. reserv.

0000444478 IP ACCESSION NO: 200505-61-14462
Application of Smart Materials to Composite Structures

Lee, I; Kim, D-H; Roh, J-H; Han, J-H
Korea Advanced Institute of Science and Technology

Key Engineering Materials, Part 3, v 270-273, p 2193-2198, 2004
PUBLICATION DATE: 2004

PUBLISHER: Trans Tech Publications Ltd., Brandrain 6, Zurich-Utikon,
CH-8707

COUNTRY OF PUBLICATION: Switzerland

PUBLISHER URL: <http://www.ttp.net>

PUBLISHER EMAIL: ttp@ttp.net

CONFERENCE:

Proceedings of the 11th Asiam Pacific Conference on Nondestructive Testing:
Part 3, Jeju Island, South Korea, 3-7 Nov. 2003

DOCUMENT TYPE: Journal Article

RECORD TYPE: Abstract

LANGUAGE: English

ISSN: 1013-9826

NOTES: Graphs; Spectra

NO. OF REFS.: 8

FILE SEGMENT: Mechanical & Transportation Engineering Abstracts

ABSTRACT:

Advanced structural systems are required to have specific functions associated with operating environments. This article introduces some analytic and experimental research results on the application of smart materials, especially shape memory alloy, optical fiber, and piezoelectric materials. The first part presents the thermo-mechanical responses of the shape memory alloy hybrid composite (SMAHC) cylindrical panels. SMA wires are embedded in neutral plane of the panel with residual strain so that the

recovery stress generated by shape memory effect (SME) can modify the structure stiffness and enhance the adaptability under thermal buckling.

The second one is about the application of fiber optic sensor systems to the vibration measurement and suppression. The dynamic sensing characteristics of fiber optic sensors were explored and the vibration measurement and suppression of composite structures have been performed. In addition, the stability boundary evaluation and the suppression of dynamic aeroelastic instability have been investigated utilizing piezoceramic actuators and adaptive controller based on neural-networks. (Example materials: graphite fiber reinforced plastics.)

DESCRIPTORS: Graphite fiber reinforced plastics; Graphite-epoxy composites; Hybrid composites; Shape memory alloys; Optical fibers; Neural networks; Vibration measurement; Smart materials; Composite structures; Fiber optics; Sensors; Adaptive control systems; Dynamic tests; Actuators; Piezoelectric ceramics; Thermal buckling; Stresses; Stiffness; Vibration control
SUBJ CATG: 61, Design Principles

22/5/3

DIALOG(R)File 14:Mechanical and Transport Engineer Abstract
(c) 2007 CSA. All rts. reserv.

0000407345 IP ACCESSION NO: 200304-11-0392
Neural network approach for nonlinear aeroelastic analysis

Voitcu, O; Wong, Y S
Alberta, University, Edmonton, Canada [Voitcu]

Journal of Guidance, Control, and Dynamics, v 26, n 1, p 99-105, Jan. 2003
PUBLICATION DATE: 2003

PUBLISHER: American Institute of Aeronautics and Astronautics, The
Aerospace Center, 370 L'Enfant Promenade, SW, Washington, DC, 20024
COUNTRY OF PUBLICATION: USA

CONFERENCE:
, UNITED STATES

DOCUMENT TYPE: Journal Article

RECORD TYPE: Abstract

LANGUAGE: ENGLISH

ISSN: 0731-5090

NOTES: AIAA Dispatch; Voice: 800 662 1545; Fax: 816 926 8794; E-Mail:
dispatch@aiaa.org

NO. OF REFS.: 28

FILE SEGMENT: Mechanical & Transportation Engineering Abstracts

ABSTRACT:

A new approach is proposed, based on the use of artificial neural networks, for predicting nonlinear aeroelastic oscillations. Our objective is to reconstruct the asymptotic state of the nonlinear behavior of an aeroelastic model when only a limited segment of the transient data is known. An original neural network architecture is proposed and is used to predict the nonlinear motions of an aeroelastic system modeling a self-excited two-degree-of-freedom airfoil oscillating in pitch and plunge. When a segment of the transient state of the given signal is used for training, the neural network is capable of correctly predicting the corresponding limit-cycle oscillations, damped oscillations, or unstable divergent oscillations. The network training set consists of numerically

generated data or data obtained from a wind-tunnel experiment. A neural network used in conjunction with wavelet decomposition is presented; it is shown to be capable of extracting the values of the damping coefficients and frequencies from the predicted signal. Neural networks, thus, are proving to be useful tools in nonlinear aeroelastic analysis. (Author)

DESCRIPTORS: Neural networks; Mathematical models; Numerical analysis; Airfoils; Aeroelasticity; Oscillations; Dynamic tests; Damping; Nonlinear dynamics; Mathematical analysis; Wind tunnels; *Airfoil oscillations; *Aeroelastic stability; *Neural nets; *Self excitation; *Wind tunnel tests; *Nonstabilized oscillation; *Vibration damping; Nonlinear equations; Asymptotic methods; Transient oscillations; Dynamic structural analysis; Hopfield neural network; Segments; Signals; Analyzing; Tools; Coefficients; Pitch; Conjunction; Control; Motion; Decomposition; Frequencies; Models

SUBJ CATG: 11, Aircraft

22/5/5

DIALOG(R)File 14:Mechanical and Transport Engineer Abstract
(c) 2007 CSA. All rts. reserv.

0000285510 IP ACCESSION NO: 2001-11-018534
Adaptive neural control of aeroelastic response

Lichtenwalner, Peter F; Little, Gerald R; Scott, Robert C
McDonnell Douglas Aerospace, Saint Louis, MO [Lichtenwalner

PAGES: 199-209
PUBLICATION DATE: 1996

PUBLISHER: Bellingham, WA: Society of Photo-Optical Instrumentation
Engineers (SPIE Proceedings. Vol. 2717)

CONFERENCE:
Smart structures and materials 1996: Smart structures and integrated
systems; Proceedings of the Meeting, San Diego, CA, UNITED STATES, 26-29
Feb. 1996

DOCUMENT TYPE: Conference Paper
RECORD TYPE: Abstract
LANGUAGE: English
NUMBERS: A96-38502 10-39; A96-38502 10-39; SPIE-2717
NO. OF REFS.: 13
FILE SEGMENT: Mechanical & Transportation Engineering Abstracts

ABSTRACT:

The Adaptive Neural Control of Aeroelastic Response (ANCAR) program is a joint R&D effort conducted by McDonnell Douglas Aerospace (NASA/Langley).

The goal is to cooperatively develop the smart structure technologies necessary for alleviating undesirable vibration and aeroelastic response associated with highly flexible structures. Adaptive control can reduce aeroelastic response associated with buffet and atmospheric turbulence, it can increase flutter margins, and it may be able to reduce response associated with nonlinear phenomenon like limit cycle oscillations. Phase I of the ANCAR problem involved development and demonstration of a neural network-based semi-adaptive flutter suppression system which used a neural network for scheduling control laws as a function of Mach number and dynamic pressure. This controller was tested along with a robust

fixed gain control law in NASA's Transonic Dynamics Tunnel utilizing the Benchmark Active Controls Testing wing. This paper presents the results of Phase I testing as well as the development progress of Phase II. (Author)

DESCRIPTORS: Aeroelasticity; Adaptive control systems; Vibration; Smart structures; Dynamics; Oscillations; Scheduling; Neural networks; Aerospace; Dynamical systems; Turbulence; Control equipment; Control systems; Instrumentation; Benchmarking; Aircraft; Wings (aircraft); Aircraft components; *Aircraft control; *Aeroelasticity; *Adaptive control; *Neural nets; *Vibration damping; *Aeroservoelasticity; Flight control; Flutter analysis; Active control
SUBJ CATG: 11, Aircraft

22/5/6

DIALOG(R)File 14:Mechanical and Transport Engineer Abstract
(c) 2007 CSA. All rts. reserv.

0000249260 IP ACCESSION NO: 2001-11-027972

AHS, Annual Forum, 48th, Washington, June 3-5, 1992, Proceedings. Vols. 1 & 2

ADDL. SOURCE INFO: Alexandria, VA, American Helicopter Society, 1992, p. Volume 1, 822 p.; volume 2, 786 p. (For individual items see A93-35902 to A93-36018)

PUBLICATION DATE: 1992

CONFERENCE:

Alexandria, VA, American Helicopter Society, 1992, p. Vol. 1, 822 p.; vol. 2, 786 p. (For individual items see A93-35902 to A93-36018), UNITED STATES

DOCUMENT TYPE: Conference

RECORD TYPE: Abstract

LANGUAGE: ENGLISH

NOTES: Alexandria, VA, American Helicopter Society, 1992, p. Vol. 1, 822 p.; vol. 2, 786 p. (For individual items see A93-35902 to A93-36018)

FILE SEGMENT: Mechanical & Transportation Engineering Abstracts

ABSTRACT:

Topics addressed include the development of the coupled rotor-fuselage model, maximum operational effectiveness on RAH-66 Comanche, advanced helicopter pilotage visual requirements, Navy success in modification installation management, improved static and dynamic performance of helicopter powerplant, Navier-Stokes correlations to fuselage wind tunnel test data, a Taguchi analysis of helicopter maneuverability and agility, and thermoplastic applications in helicopter components. Also discussed are Mi-26 autorotational landings, improvements in hover display dynamics for a combat helicopter, prediction of rotorcraft transmission noise, an optimal composite curing system, helicopter rotor blade flap vibratory loads, cost/weight savings for the V-22 wing stow, helicopter response to atmospheric turbulence, a hover performance analysis of advanced rotor blades, scaling of energy absorbing composite plates, an avionics troubleshooting system, and an integrated navigation system for tactical helicopters. (AIAA)

DESCRIPTORS: Helicopters; Dynamic tests; Dynamics; Troubleshooting; Management; Joining; Loads (forces); Modification; Correlation analysis ; Naval engineering; Avionics; Curing; Cost engineering; Dynamical systems; Turbulence; Energy transmission; Maneuverability; Mathematical models; Rotorcraft; Statics; Wind tunnels; Navigation systems; Weight

reduction; Helicopter rotor blades; Flaps; Thermoplastic resins; Noise; Aircraft; Absorbing; Energy conservation; Wings (aircraft); Airframes; Rotor blades; Cost analysis; Installation; *Acoustics; *Aerodynamic characteristics; *Aircraft construction materials; *Aircraft design; *Conferences; *Crew workstations; *Dynamic structural analysis; *Flight simulation; *Human factors engineering; *Military technology; *Propulsion system performance; *Rotary wing aircraft; Aeroelasticity; Composite structures; Elastic bending; Expert systems; Flight characteristics; Helicopter design; Helmet mounted displays; Night flights (aircraft); Rigid rotors; Rotor body interactions; Structural vibration; Technology transfer; Terrain analysis; Visual flight
SUBJ CATG: 11, Aircraft

22/5/7

DIALOG(R)File 14:Mechanical and Transport Engineer Abstract
(c) 2007 CSA. All rts. reserv.

0000234147 IP ACCESSION NO: 2001-11-033199

Society of Flight Test Engineers, Annual Symposium, 21st, Garden Grove, CA, Aug. 6-10, 1990, Proceedings

ADDL. SOURCE INFO: Symposium sponsored by Society of Flight Test Engineers, Boeing Aircraft Co., Endevco, et al. Lancaster, CA, Society of Flight Test Engineers, 1990, 300 p. For individual items see A92-35927 to A92-35953.
PUBLICATION DATE: 1990

CONFERENCE:

Symposium sponsored by Society of Flight Test Engineers, Boeing Aircraft Co., Endevco, et al. Lancaster, CA, Society of Flight Test Engineers, 1990, 300 p. For individual items see A92-35927 to A92-35953., UNITED STATES

DOCUMENT TYPE: Conference

RECORD TYPE: Abstract

LANGUAGE: ENGLISH

NOTES: Symposium sponsored by Society of Flight Test Engineers, Boeing Aircraft Co., Endevco, et al. Lancaster, CA, Society of Flight Test Engineers, 1990, 300 p. For individual items see A92-35927 to A92-35953.; No individual items are abstracted in this volume

FILE SEGMENT: Mechanical & Transportation Engineering Abstracts

ABSTRACT:

The present conference on flight testing encompasses avionics, flight-testing programs, technologies for flight-test predictions and measurements, testing tools, analysis methods, targeting techniques, and flightline testing. Specific issues addressed include flight testing of a digital terrain-following system, a digital Doppler rate-of-descent indicator, a high-technology testbed, a low-altitude air-refueling flight-test program, techniques for in-flight frequency-response testing for helicopters, limit-cycle oscillation and flight-flutter testing, and the research flight test of a scaled unmanned air vehicle. Also addressed are AV-8B V/STOL performance analysis, incorporating pilot-response time in failure-case testing, the development of pitot static flightline testing, targeting techniques for ground-based hover testing, a low-profile microsensor for aerodynamic pressure measurement, and the use of a variable-capacitance accelerometer for flight-test measurements. (C.C.S.)

DESCRIPTORS: Flight testing; Vehicles; Oscillations; Avionics; Computer programs; Aerospace engines; Aerodynamics; Vtol/stol aircraft; Statics; Helicopters; Accelerometers; Aircraft; Pressure measurement; Doppler

effect; *Conferences; *Flight test instruments; *Flight tests;

Aeroelasticity; Air to air refueling; Airships; Control surfaces;

Doppler radar; Flutter analysis; Global positioning system; Iff systems

(identification); Navstar satellites; Radar tracking; Real time operation

; Terrain following aircraft; Test stands; Video tape recorders; Digital

techniques; Descent; Weapon systems; Low altitude; Swept wings; Aircraft

icing; Remotely piloted vehicles; Inertial navigation; Expert systems

; Space Shuttles; Mission planning; Pilot performance; Aircraft hazards

SUBJ CATG: 11, Aircraft

22/5/8

DIALOG(R)File 14:Mechanical and Transport Engineer Abstract

(c) 2007 CSA. All rts. reserv.

0000204617 IP ACCESSION NO: 2001-11-040574

Knowledge-based (expert) systems for structural analysis and design

Felt, Larry R; Grisham, Andrew F; Dotson, Bennie F

DOTSON, BENNIE F (Boeing Military Airplane Co., Seattle, WA)

PAGES: 601-610

PUBLICATION DATE: 1987

PUBLISHER: New York, American Institute of Aeronautics and Astronautics

CONFERENCE:

Structures, Structural Dynamics and Materials Conference, 28th, Monterey,

CA, Technical Papers. Part 1, 6-8 Apr. 1987

DOCUMENT TYPE: Conference Paper

RECORD TYPE: Abstract

LANGUAGE: English

REPORT NO: AIAA PAPER 87-0836

NUMBERS: A87-33551 14-39

FILE SEGMENT: Mechanical & Transportation Engineering Abstracts

ABSTRACT:

Fourteen years ago the Boeing Company began the development of an interfaced, modular, knowledge-based structural analysis system which would

serve as a rapid, efficient and accurate design and analysis tool. This

paper describes specific details of the resulting Interfaced Structural

Analysis System (ISAS) and presents examples of its usage within the Boeing

Company. Specific applications in the multidisciplinary/structural

optimization and aeroelastic tailoring fields are included. Future

directions and current modifications, such as, the use of microcomputers in

a work station environment, are also presented. (Author)

DESCRIPTORS: Structural analysis; Design engineering; Modification;

Accuracy; Optimization; Expert systems; Aeroelasticity; Dynamics;

Aircraft components

SUBJ CATG: 11, Aircraft

30/5/3

DIALOG(R)File 14:Mechanical and Transport Engineer Abstract

(c) 2007 CSA. All rts. reserv.

0000341088 IP ACCESSION NO: 200201-62-2209

Identification and prediction of unsteady transonic aerodynamic loads by multi-layer functionals.

Marques, F D; Anderson, J
Sao Paulo, University, Brazil [Marques]

Journal of Fluids and Structures, v 15, n 1, p 83-106, Jan. 2001

PUBLICATION DATE: 2001

PUBLISHER: Academic Press, Inc. Ltd., 24-28 Oval Rd., London, NW1 7DX

COUNTRY OF PUBLICATION: UK

PUBLISHER URL: <http://www.academicpress.com>

CONFERENCE:
, UNITED KINGDOM

DOCUMENT TYPE: Journal Article

RECORD TYPE: Abstract

LANGUAGE: English

ISSN: 0889-9746

NOTES: Aerospace Dispatch; Voice: 800 662 1545; Fax: 816 926 8794; E-Mail: dispatch@aiaa.org; Graphs

NO. OF REFS.: 18

FILE SEGMENT: Mechanical & Transportation Engineering Abstracts

ABSTRACT:

Nonlinear unsteady aerodynamic effects present major modeling difficulties in the analysis and control of aeroelastic response. A

rigorous mathematical framework that can account for the complex nonlinearities and time-history effects of the unsteady aerodynamic response is provided by the use of functional representations. A recent development, based on functional approximation theory, has achieved a new functional form; namely, multilayer functionals. The development of a multilayer functional for discrete-time, finite memory, causal systems has been shown to be realizable via finite impulse response neural networks. Identification of an appropriate temporal neural network model of the nonlinear transonic aerodynamic response is facilitated via a supervised training process using multiple input-output sets, with data obtained by an Euler CFD code. The training process is based on a genetic algorithm to optimize the network architecture, combined with a random search algorithm to update weight and bias values. The approach is examined for two different multiple aerodynamic input-output data sets, and in both cases, the prediction properties of the network model establish the multilayer functional as a suitable representation of unsteady aerodynamic response. (Author)

DESCRIPTORS: Aerodynamics; Mathematical models; Neural networks; Computational fluid dynamics; Aeroelasticity; Genetic algorithms; Nonlinearity; Loads (forces); *Aeroelasticity; *Aerodynamic loads; *Prediction analysis techniques; *Parameter identification; *Unsteady aerodynamics; *Transonic flow; *Fluid-structure interaction; *Functionals

30/5/3

DIALOG(R)File 14:Mechanical and Transport Engineer Abstract

* (c) 2007 CSA. All rts. reserv.

0000341088 IP ACCESSION NO: 200201-62-2209

Identification and prediction of unsteady transonic aerodynamic loads by multi-layer functionals.

Marques, F D; Anderson, J

Sao Paulo, University, Brazil [Marques]

Journal of Fluids and Structures, v 15, n 1, p 83-106, Jan. 2001

PUBLICATION DATE: 2001

PUBLISHER: Academic Press, Inc. Ltd., 24-28 Oval Rd., London, NW1 7DX

COUNTRY OF PUBLICATION: UK

PUBLISHER URL: <http://www.academicpress.com>

CONFERENCE:

, UNITED KINGDOM

DOCUMENT TYPE: Journal Article

RECORD TYPE: Abstract

LANGUAGE: English

ISSN: 0889-9746

NOTES: Aerospace Dispatch; Voice: 800 662 1545; Fax: 816 926 8794; E-Mail: dispatch@aiaa.org; Graphs

NO. OF REFS.: 18

FILE SEGMENT: Mechanical & Transportation Engineering Abstracts

ABSTRACT:

Nonlinear unsteady aerodynamic effects present major modeling difficulties in the analysis and control of aeroelastic response. A rigorous mathematical framework that can account for the complex nonlinearities and time-history effects of the unsteady aerodynamic response is provided by the use of functional representations. A recent development, based on functional approximation theory, has achieved a new functional form; namely, multilayer functionals. The development of a multilayer functional for discrete-time, finite memory, causal systems has been shown to be realizable via finite impulse response neural networks. Identification of an appropriate temporal neural network model of the nonlinear transonic aerodynamic response is facilitated via a supervised training process using multiple input-output sets, with data obtained by an Euler CFD code. The training process is based on a genetic algorithm to optimize the network architecture, combined with a random search algorithm to update weight and bias values. The approach is examined for two different multiple aerodynamic input-output data sets, and in both cases, the prediction properties of the network model establish the multilayer functional as a suitable representation of unsteady aerodynamic response. (Author)

DESCRIPTORS: Aerodynamics; Mathematical models; Neural networks;Computational fluid dynamics; Aeroelasticity; Genetic algorithms;Nonlinearity; Loads (forces); *Aeroelasticity; *Aerodynamic loads;

*Prediction analysis techniques; *Parameter identification; *Unsteady

aerodynamics; *Transonic flow; *Fluid-structure interaction; *Functionals

; Neural nets; Euler equations of motion; Machine learning;

Optimization

SUBJ CATG: 62, Theoretical Mechanics and Dynamics

30/5/4

DIALOG(R)File 14:Mechanical and Transport Engineer Abstract
(c) 2007 CSA. All rts. reserv.

0000318991 IP ACCESSION NO: 2001-11-011038

Flutter speed prediction during flight flutter testing using neural
networks

Cooper, J E; Crowther, W J
Manchester, Victoria University, United Kingdom [Cooper

PAGES: 255-263

PUBLICATION DATE: 1999

PUBLISHER: Hampton, VA: NASA, Langley Research Center

CONFERENCE:

CEAS/AIAA/ICASE/NASA Langley International Forum on Aeroelasticity and
Structural Dynamics, Williamsburg, Proceedings. Pt. 1, UNITED STATES, 22-25
June 1999

DOCUMENT TYPE: Conference Paper

RECORD TYPE: Abstract

LANGUAGE: English

NUMBERS: A99-34276 09-39

NOTES: Proceedings. Pt. 1 (A99-34276 09-39)

NO. OF REFS.: 15

FILE SEGMENT: Mechanical & Transportation Engineering Abstracts

ABSTRACT:

Flight flutter testing is a crucial part in the certification of a prototype aircraft. The flight envelope must be expanded safely; however, there is always the pressure to complete the tests as quickly as possible. Although there will be an aeroelastic model of the system for comparison, the decision to proceed to the next test point is usually based upon the modal parameters estimated from the flutter test data. A number of different methods have been proposed to determine the speed at which flutter occurs; however, the most commonly used approach is simply to extrapolate the estimated damping ratios. In this paper, a method for the prediction of flutter speed from flutter test data is proposed based upon the use of Neural Networks. The method is demonstrated upon a simulated aeroelastic model. (Author)

DESCRIPTORS: Vibration; Mathematical models; Aeroelasticity; Neural
networks; Aircraft components; Certification testing; Prototypes;

Damping; Dynamics; Aircraft; Extrapolation; *Flutter analysis;*Prediction analysis techniques; *Neural nets; *Flight tests;*Aircraft models; Certification; Civil aviation; Matrices (mathematics)

SUBJ CATG: 11, Aircraft

30/5/5

DIALOG(R)File 14:Mechanical and Transport Engineer Abstract
(c) 2007 CSA. All rts. reserv.

0000317742 IP ACCESSION NO: 2001-11-012200

CEAS/AIAA/ICASE/NASA Langley International Forum on Aeroelasticity and
Structural Dynamics, Williamsburg, VA, June 22-25, 1999, Proceedings. Pts.
1 & 2

ADDL. SOURCE INFO: Hampton, VA, NASA, Langley Research Center, 1999, p. Pt.

1, 453 p.; pt. 2, 436 p

PUBLICATION DATE: 1999

PUBLISHER: Hampton, VA: NASA, Langley Research Center

CONFERENCE:

, UNITED STATES

DOCUMENT TYPE: CONFERENCE VOLUME - MOTHER ENTRY

RECORD TYPE: Abstract

LANGUAGE: English

REPORT NO: NASA/CP-1999-209136/PT 1 & PT 2

NOTES: For individual items see A99-34277 to A99-34347

FILE SEGMENT: Mechanical & Transportation Engineering Abstracts

ABSTRACT:

The present two-volume collection of papers on aeroelasticity and structural dynamics discusses CFD, flexible aircraft, multidisciplinary design optimization, limit cycle oscillation, test methods, tiltrotor, panel flutter, and landing dynamics. Attention is given to certification, flutter control, structural optimization, reduced-order models, nonlinearity, and linear methods. Other issues addressed include aeroelastic applications, structure and aerodynamics integration, nonlinear flutter, devices, buffet, aeroelastic tailoring, fluid-structure interaction, and system modeling. Specific topics considered include limit cycle oscillation prediction using artificial neural networks, computer-controlled normal mode tuning, multibody analysis of an active control for a tiltrotor, nonlinear transient whirl vibration analysis of aircraft brake systems, aeroelasticity simulations in turbulent flows, and a survey of shape parameterization techniques.
(AIAA)

DESCRIPTORS: Aeroelasticity; Mathematical models; Vibration; Dynamics;

Tiltrotors; Oscillations; Optimization; Aircraft; Aircraft components;

Aerial surveys; Turbulent flow; Computer simulation; Panels; Vibration

analysis; Neural networks; Aerodynamics; Brakes; Control systems;

Nonlinearity; Platinum; Design engineering; *Conferences; *

Aeroelasticity; *Structural analysis; Computational fluid dynamics;

Multidisciplinary design optimization; Airfoil oscillations; Numerical

control; Tilt rotor aircraft; Certification; Eigenvalues; Nonlinear

systems; Buffeting; Finite element method; Structural vibration; Landing

gear; Parallel computers; F-18 aircraft; Wind tunnel tests; Chaos;

Trailing edges

SUBJ CATG: 11, Aircraft

30/5/6

DIALOG(R)File 14:Mechanical and Transport Engineer Abstract

(c) 2007 CSA. All rts. reserv.

0000299280 IP ACCESSION NO: 2001-11-059045

Innovation in rotorcraft technology; Proceedings of the Royal Aeronautical Society, London, United Kingdom, June 24, 25, 1997

ADDL. SOURCE INFO: London, United Kingdom, Royal Aeronautical Society, 1997

PUBLICATION DATE: 1997

PUBLISHER: London, United Kingdom: Royal Aeronautical Society

CONFERENCE:
, UNITED KINGDOM

DOCUMENT TYPE: CONFERENCE VOLUME - MOTHER ENTRY

RECORD TYPE: Abstract

LANGUAGE: English

ISBN: 1857680839

NOTES: For individual items see A97-37540 to A97-37554

FILE SEGMENT: Mechanical & Transportation Engineering Abstracts

ABSTRACT:

The present volume on innovation in rotorcraft technology discusses high-speed alternatives to conventional rotorcraft, new perspectives on an advanced compound helicopter, design considerations for next-generation rotors, and a future multirole, mission-adaptable air-vehicle concept. Attention is given to carefree handling and control augmentation for rotorcraft, virtual reality in the Apache cockpit, prediction of usable FOV limits for future rotorcraft helmet mounted displays, and the application of Direct Voice Input to battlefield helicopters. Other topics addressed include obstacle detection for helicopters, the promise of adaptive materials for alleviating aeroelastic problems, a novel method for reducing blade-vortex interaction noise, and the main sources of helicopter vibration and noise emissions and adaptive concepts to reduce them. (AIAA)

DESCRIPTORS: Rotorcraft; Helicopters; Aeronautics; Noise; Emissions; Vibration; Virtual reality; Helmet mounted displays; Materials handling; Cockpit displays; Aeroelasticity; Rotors; *Conferences; *Rotorcraft aircraft; *Research and development; Helicopter control; Obstacle avoidance; Field of view; Combat; Blade-vortex interaction; Aircraft noise; Noise spectra; Noise reduction; Smart structures; Aerodynamic stability; Mathematical models; Artificial intelligence; Flight control; Control systems design; Feedback control; Active control; Aircraft compartments

SUBJ CATG: 11, Aircraft

Parameter estimation of an aeroelastic aircraft using neural networks

S C RAISINGHANI and A K GHOSH

Department of Aerospace Engineering, Indian Institute of Technology Kanpur,
Kanpur 208 016, India

Abstract. Application of neural networks to the problem of aerodynamic modelling and parameter estimation for Aeroelastic aircraft is addressed. A neural model capable of predicting generalized force and moment coefficients using measured motion and control variables only, without any need for conventional normal elastic variables or their time derivatives, is proposed. Furthermore, it is shown that such a neural model can be used to extract equivalent stability and control derivatives of a flexible aircraft. Results are presented for aircraft with different levels of flexibility to demonstrate the utility of the neural approach for both modelling and estimation of parameters.

Estimation of Aeroelastic Parameters of Bridge Decks Using Neural Networks

J. Engrg. Mech., Volume 130, Issue 11, pp. 1356-1364 (November 2004)

Sungmoon Jung,1 S.M.ASCE; Jamshid Ghaboussi,2 M.ASCE; and Soon-Duck Kwon3

(Accepted 4 April 2004)

A new method of estimating flutter derivatives using artificial neural networks is proposed. Unlike other computational fluid dynamics based numerical analyses, the proposed method estimates flutter derivatives utilizing previously measured experimental data. One of the advantages of the neural networks approach is that they can approximate a function of many dimensions. An efficient method has been developed to quantify the geometry of deck sections for neural network input. The output of the neural network is flutter derivatives. The flutter derivatives estimation network, which has been trained by the proposed methodology, is tested both for training sets and novel testing sets. The network shows reasonable performance for the novel sets, as well as outstanding performance for the training sets. Two variations of the proposed network are also presented, along with their estimation capability. The paper shows the potential of applying neural networks to wind force approximations.

San Diego, California June 1999

AMERICAN CONTROL CONFERENCE Paper # ACC99-AIAA0004 / FP08-1

A NEURAL NETWORK-BASED APPROACH TO ACTIVE STRUCTURAL MODE SUPPRESSION FOR FLEXIBLE TRANSPORT AIRCRAFT

Eugene Y. Lavretsky

Dennis K. Henderson

Phantom Works

The Boeing Company

2401 E. Wardlow Rd. MC CO78-0420

Long Beach, CA 90807-5309

ABSTRACT: The dynamics of the first few structural bending modes in large, flexible transport aircraft are typically characterized by low frequency and light damping. In a scenario where the frequencies of these modes are in close proximity with the rigid body modes, notch filtering yields undesirable results, and active control must be used to suppress structural excitation. This paper develops a methodology for the design of a structural mode suppression system using an ordered neural network-based approach. The resulting control system is robust over a set of linear plant models, which are used as a training set during the neural control design process for the original non-linear system.

Cited reference Rodden, W. P., and Johnson, E. H., "MSC / NASTRAN, Aeroelastic Analysis", The MacNeal-Schwendler Corporation, 1994.

Torsional Vibrations of Pre-Twisted Blades using Artificial Neural Network Technology

M. A. Rao and J. Srinivas

Department of Mechanical Engineering, Andhra University, Visakhapatnam, A.P. India

Abstract. The free torsional vibrations of a linearly tapered, twisted flexible blade, rotationally constrained at an arbitrary position along the length of blade, have been investigated using neural networks. The blade has a rectangular cross-section with equal taper in the horizontal and vertical planes, in addition to the flexibility at the root portion. The constraint is a rotational spring. The constraint on the blade at an optimum location is designed so as to increase the lowest natural frequency of the blades with considerable root flexibility. The optimum location is determined as the position of the node in the second mode shape of

the unconstrained tapered blade with flexible roots. A trained Neural Network is used to identify the location of the nodal or optimum point for a given blade-taper ratio and root flexibility parameter. The minimum stiffness of the constraint at an optimum position for a maximum raise in the first eigenfrequency is evaluated. Results are presented in tabular and graphical form.

Keywords. Artificial neural networks; Back propagation algorithm; Mode shapes; Root flexibility; Taper-rotational constraint; Torsional frequencies

Cited reference Celi, R., Friedmann, P. P. (1990) Structural optimization with Aeroelastic constraints of rotor blades with straight and swept tips. AIAA Journal, 28(5), 928-936

Reliability-based design optimization of Aeroelastic structures

Journal Structural and Multidisciplinary Optimization

Publisher Springer Berlin / Heidelberg

ISSN 1615-147X (Print) 1615-1488 (Online)

Issue Volume 27, Number 4 / June, 2004

Source: DTIC

Accession Number : ADP010520

Multi-Objective Aeroelastic Optimization

Corporate Author : DAIMLER CHRYSLER AEROSPACE MUNICH (GERMANY) MILITARY AIRCRAFT

Personal Author(s) : Stettner, M. ; Haase, W.

Report Date : JUN 2000

Abstract : The present work is aiming at an Aeroelastic analysis of the X31 delta wing and particularly at the Aeroelastic optimization problem of maximizing the aerodynamic roll rate and minimizing the structural weight at supersonic flow speeds. Results are achieved by means of a multi-objective genetic algorithm (GA) utilizing a GUI-supported software being a developed in the European-Union funded ESPRIT project FRONTIER.

Aeroelasticity

by Raymond L. Bisplinghoff, Holt Ashley and Robert L. Halfman.-- Mineola: Dover Publication, 1996

ix, 860p.

ISBN : 0-486-69189-6.

629.132362 N96 "R(T)" 177266

IDENTIFICATION AND PREDICTION OF UNSTEADY TRANSONIC AERODYNAMIC LOADS BY MULTI-LAYER FUNCTIONALS

F. D. MARQUESa and J. ANDERSONb

a Departamento de Engenharia Mecânica, Universidade de São Paulo, Cx. Postal 359, 13560-970, São Carlos, SP, Brazil

b Department of Aerospace Engineering, University of Glasgow, Glasgow, G12 8QQ, Scotland, U.K.

Received 25 June 1998; accepted 22 June 2000. ; Available online 1 March 2002.

Abstract

Nonlinear unsteady aerodynamic effects present major modelling difficulties in the analysis and control of Aeroelastic \ "hit2" \ "hit2" response. A rigorous mathematical framework, that can account for the complex nonlinearities and time-history effects of the unsteady aerodynamic response, is provided by the use of functional representations. A recent development, based on functional approximation theory, has achieved a new functional form; namely, multi-layer functionals. The development of a multi-layer functional for discrete-time, finite memory, causal systems has been shown to be realizable via finite impulse response \ "hit1" \ "hit1"neural \ "hit3" \ "hit3" networks. Identification of an appropriate temporal \ "hit2" \ "hit2"neural \ "hit4" \ "hit4" network model of the nonlinear transonic aerodynamic response is facilitated via a supervised training process using multiple input-output sets, with data obtained by an Euler CFD code. The training process is based on a genetic algorithm to optimize the network architecture, combined with a random search algorithm to update weight and bias values. The approach is examined for two different multiple aerodynamic input-output data sets, and in both cases, the prediction properties of the network model establish the multi-layer functional as a suitable representation of unsteady aerodynamic response.

Automatic updating of large aircraft models using experimental data from ground vibration testing

Structural Dynamics Section, Institute of Aeroelasticity, German Aerospace Center (DLR), Bunsenstr. 10, 37073, Göttingen, Germany

Received 21 May 2002; revised 27 June 2002; accepted 5 July 2002. ; Available online 24 October 2002.

Abstract

The Aeroelastic \ "hit2" \ "hit2" stability \ "hit1" \ "hit1" certification \ "hit3" \ "hit3" of today's civil aircraft structures requires validated analytical models which have to meet high flutter calculation, fan-blade-off and windmilling \ "hit2" \ "hit2" certification \ "hit4" \ "hit4" calculation standards. The dynamic model of the aircraft must be validated in such a way that the dynamic behaviour of the aircraft is reproduced nearly exactly in order to reflect real scenarios when infuriate extreme or flight loads on the model. In addition, the dynamic model must be an accurate representation in order to predict the behaviour of the structure with regard to different boundary conditions. In view of shorter testing times or large-scale civil aircraft this topic will increase in importance in the future since correct free-free boundary conditions are very severe to realize during ground vibration testing (GVT). The above mentioned application fields illustrate the all-important role of the validated analytical model within the scope of civil aeronautics. The aim of this study was to find a new way of updating analytical models of large aircraft by using modal data obtained by GVT in order to save time during model validation. A strategy is presented in this article for validating the finite element (FE) model of a civil four-engine aircraft using a computational model updating (CMU) method

Wing instability of a full composite aircraft

Mahmood M. Shokrieh \ "m4.cor*" \ "m4.cor*", mailto:shokrieh@iust.ac.ir mailto:shokrieh@iust.ac.ir and Fathollah Taheri Behrooz

Mechanical Engineering Department, Iran University of Science and Technology, Narmak, Tehran 16844, Iran

Aeroelastic ity of morphing wings using neural networks

by Natarajan, Anand, Ph.D., Virginia Polytechnic Institute and State University, 2002, 144 pages; AAT 3110283

Abstract (Summary)

In this dissertation, neural networks are designed to effectively model static non-linear Aeroelastic problems in adaptive structures and linear dynamic Aeroelastic systems with time varying stiffness. The use of adaptive materials in aircraft wings allows for the change of the contour or the configuration of a wing (morphing) in flight. The use of smart materials, to accomplish these deformations, can imply that the stiffness of the wing with a morphing contour changes as the contour changes. For a rapidly oscillating body in a fluid field, continuously adapting structural parameters may render the wing to behave as a time variant system. Even the internal spars/ribs of the aircraft wing which define the wing stiffness can be made adaptive, that is, their stiffness can be made to vary with time. The immediate effect on the structural dynamics of the wing, is that, the wing motion is governed by a differential equation with time varying coefficients. The study of this concept of a time varying torsional stiffness, made possible by the use of active materials and adaptive spars, in the dynamic Aeroelastic behavior of an adaptable airfoil is performed here.

Another type of Aeroelastic problem of an adaptive structure that is investigated here, is the shape control of an adaptive bump situated on the leading edge of an airfoil. Such a bump is useful in achieving flow separation control for lateral directional maneuverability of the aircraft. Since actuators are being used to create this bump on the wing surface, the energy required to do so needs to be minimized. The adverse pressure drag as a result of this bump needs to be controlled so that the loss in lift over the wing is made minimal. The design of such a "spoiler bump" on the surface of the airfoil is an optimization problem of maximizing pressure drag due to flow separation while minimizing the loss in lift and energy required to deform the bump. One Neural Network is trained using the CFD code FLUENT to represent the aerodynamic loading over the bump. A second Neural Network is trained for calculating the actuator loads, bump displacement and lift, drag forces over the airfoil using the finite element solver, ANSYS and the previously trained neural network. This non-linear Aeroelastic model of the deforming bump on an airfoil surface using neural networks can serve as a fore-runner for other non-linear Aeroelastic problems.

Artificial Neural Network prediction of aircraft Aeroelastic behavior

by Pesonen, Urpo Juhani, Ph.D., Wichita State University, 2001, 159 pages; AAT 3032139

Abstract (Summary)

An Artificial Neural Network that predicts Aeroelastic behavior of aircraft is presented. The neural net was designed to predict the shape of a flexible wing in static flight conditions using results from a structural analysis and an aerodynamic analysis performed with traditional computational tools. To generate reliable training and testing data for the network, an Aeroelastic analysis code using these tools as components was designed and validated. To demonstrate the advantages and reliability of Artificial Neural Networks, a network was also designed and trained to predict airfoil maximum lift at low Reynolds numbers where wind tunnel data was used for the training. Finally, a neural net was designed and trained to predict the static Aeroelastic behavior of a wing without the need to iterate between the structural and aerodynamic solvers.

Virtual reality saves money!

Dave Harrold. Control Engineering. Barrington: Oct 2000. Vol. 47, Iss. 11; pg. 36, 5 pgs

Abstract (Summary)

More and more companies are learning, often the hard way, that investments in simulations can save time and money. Simulations are really imitations that take on the appearance, form, or sound of something that is, or could be real. Use of simulations to assist in the design of stuff has blossomed since the proliferation of desktop personal computers, windows user environment, and modular software development techniques. An are often overlooked as a simulation candidate is business planning. Once business strategies for becoming more flexible and agile move from the handwaiving and overhead projection arena, entire business processes will ened to be designed, analyzed, and reengineered.

.....

In the United States, design simulation software from javascript:void(0);MSC.Software (Los Angeles, Calif.) is recognized by the Federal Aviation Agency as an accepted standard for design and analysis of stress, vibration, heat-transfer, acoustics, and Aeroelasticity for airframe manufacturers seeking design certification.

The MacNeal-Schwendler Corp. Issues "Call for Papers" for Second Worldwide Aerospace Conference

Business Editors. Business Wire. New York: Oct 28, 1998. pg. 1

Abstract (Summary)

Oct. 28, 1998--The MacNeal-Schwendler Corp. (NYSE:MNS)(MSC) has issued a Call for Papers to be presented at its Second Worldwide Aerospace Conference, June 7-10, 1999.

The conference will be held at the Hyatt Regency in Long Beach, Calif. Papers are being solicited in the design and certification of aerospace vehicles, covering such applications as structural dynamics, Aeroelasticity, optimization, test correlation, thermal, and stress analysis.

AIAA Journal

Neural-network-based controller for nonlinear Aeroelastic system

Ku, C-S, Hajela, P. American Institute of Aeronautics and Astronautics. AIAA Journal. New York: Feb 1998. Vol. 36, Iss. 2; pg. 249, 7 pgs

Abstract (Summary)

Attenuation of vibratory response is an important design consideration in many aeroelastic systems and active methods of vibration reduction have been studied extensively. The use of artificial neural networks is explored as an approach for developing robust control strategies.

Neural networks for inverse problems in damage identification and optical imaging

Yong Y Kim, Rakesh K Kapania. American Institute of Aeronautics and Astronautics. AIAA Journal. New York: Apr 2003. Vol. 41, Iss. 4; pg. 732

Abstract (Summary)

Artificial neural networks (ANNs) are employed in solving inverse problems in damage detection in structures, as well as detection, using optical imaging, of an anomaly in a light-diffusive media, such as a human tissue. Both of these problems, namely, identifying the damage parameters in a damaged structure and identifying the representative properties in a tissue, require solving highly complex inverse problems. The neural networks (NNs) for both problems are similar, and a method found suitable for solving one type of problem can be applied for solving the other type of problem. In the damage identification problem, the natural frequencies of a damaged beam model obtained from analytical and numerical methods were used to identify damage parameters by employing feedforward backpropagation, and also radial basis NNs. In the optical imaging problem, the tissue under investigation was illuminated by a number of near-infrared light sources placed around the circumference of the tissue. Both the location and the size of the anomaly were identified by studying the influence of the anomaly on the light intensity received at the boundary of the tissue. The near-infrared light measurements are assumed to be available at a number of light detector positions, also along the circumference of the tissue. NNs were used to determine the location and the size of the anomaly in a tissue. The direct problem for the case of optical imaging was solved using the finite element method to generate the training and testing sets for NNs.

Fault classification using pseudomodal energies and neural networks

Tshildzi Marwala. American Institute of Aeronautics and Astronautics. AIAA Journal. New York: Jan 2003. Vol. 41, Iss. 1; pg. 82

Abstract (Summary)

A new fault identification method is introduced that uses pseudomodal energies to train neural networks. The proposed procedure is tested on a simulated cantilevered beam and a population of 20 cylindrical shells, and its performance is compared to that of the procedure that uses modal properties to train neural networks. Both the cantilevered beam and cylindrical shells are divided into three substructures, and faults are introduced into these substructures. The cylinder is excited using modal hammer, and acceleration is measured using an accelerometer. Each fault case is assigned a fault identity with the presence of fault represented by a 1, whereas the absence of fault is represented by a 0. Following this fault representation scheme, a fault located in substructure 1 would have an identity of [1 0 0], with two zeros indicating the absence of faults in substructures 2 and 3. The Neural Network used is a multilayer perceptron trained using scaled conjugate method. The statistical overlap factor and principal component analysis are used to reduce the size of the input data. For both examples the pseudomodal-energy-trained neural networks provide better classification of faults than the networks trained using the conventional modal properties.

Structural integrity redesign through neural-network inverse mapping

R M Pidaparti, S Jayanti, M J Palakal, S Mukhopadhyay. American Institute of Aeronautics and Astronautics. AIAA Journal. New York: Jan 2003. Vol. 41, Iss. 1; pg. 119

Abstract (Summary)

A neural-network inverse mapping approach was used in a structural integrity redesign problem to achieve the desired strength, corrosion, and fatigue properties. Also, through the inverse-mapping procedure the relative importance of damage parameters was obtained for two trained neural-network models. The damage parameters corresponding to a given strength and corrosion rate are predicted in one network, whereas the damage parameters corresponding to a given corrosion fatigue life are predicted in the other network. The results obtained from the inverse mapping procedure are compared with actual panel configurations and environments and experimental data. The results obtained through the inverse-mapping procedure are found to agree well with the experimental data, thus demonstrating the feasibility of the approach for the structural integrity redesign of aging aircraft structures.

Material property identification of composite plates using Neural Network and evolution algorithm

Byung Joon Sung, Jin Woo Park, Yong Hyup Kim. American Institute of Aeronautics and Astronautics. AIAA Journal. New York: Sep 2002. Vol. 40, Iss. 9; pg. 1914

Abstract (Summary)

The baseline material properties of composite materials are susceptible to errors due to various defects during the manufacturing and operation. Thus, accurate estimation of the actual material properties is necessary for accurate numerical analysis.

Structural damage identification using pole/zero dynamics in neural networks

S M Yang, G S Lee. American Institute of Aeronautics and Astronautics. AIAA Journal. New York: Sep 2001. Vol. 39, Iss. 9; pg. 1805

Abstract (Summary)

Yang and Lee developed an improved method of structural damage identification, utilizing not only the change of natural frequencies (poles) but also the change of zeros. The backpropagation Neural Network with a momentum term and an adaptive learning rate was employed to construct the complex effect-to-cause mapping between the pole/zero dynamics and the damage conditions

Aerodynamic design using neural networks

Man Mohan Rai, Nateri K Madavan. American Institute of Aeronautics and Astronautics. AIAA Journal. New York: Jan 2000. Vol. 38, Iss. 1; pg. 173

Abstract (Summary)

An aerodynamic design procedure that incorporates the advantages of both traditional response surface methodology and neural networks is described.

Miniature multihole pressure probes and their neural-network-based calibration

Rediniotis, Othon K, Vijayagopal, Rajesh. American Institute of Aeronautics and Astronautics. AIAA Journal. New York:

Jun 1999. Vol. 37, Iss. 6; pg. 666, 9 pgs

Abstract (Summary)

We present the development of miniature multihole pressure probes and a novel neural-network-based calibration algorithm for them. Seven-hole probes of tip diameters as low as 0.035 in. (0.9 mm) were successfully fabricated with high tip surface quality.

Air data sensing from surface pressure measurements using a Neural Network method

Rohloff, Thomas J, Whitmore, Stephen A, Catton, Ivan. American Institute of Aeronautics and Astronautics. AIAA Journal. New York: Nov 1998. Vol. 36, Iss. 11; pg. 2094, 8 pgs

Abstract (Summary)

Neural networks have been successfully developed to estimate freestream static and dynamic pressures from an array of pressure measurements taken from ports located flush on the nose of an aircraft. Specific techniques were developed for extracting a proper set of Neural Network training patterns from an abundant archive of data.

Fatigue crack growth predictions in aging aircraft panels using optimization Neural Network

Pidaparti, R M V, Palakal, M J. American Institute of Aeronautics and Astronautics. AIAA Journal. New York: Jul 1998. Vol. 36, Iss. 7; pg. 1300, 5 pgs

Abstract (Summary)

An optimization-based Neural Network method is developed to predict fatigue crack growth and fatigue life of multiple site damage panels found in aging aircraft. The method utilizes an optimization solution to predict the probable crack path based upon the initial panel configuration and accounts for lead crack spanning, small multiple site damage, and plasticity zones. The approach of the Neural Network was motivated by the optimization analysis and the time-consuming computational analyses for multiple site damage problems.

Neural-network-based controller for nonlinear aeroelastic system

Ku, C-S, Hajela, P. American Institute of Aeronautics and Astronautics. AIAA Journal. New York: Feb 1998. Vol. 36, Iss. 2; pg. 249, 7 pgs

Abstract (Summary)

Attenuation of vibratory response is an important design consideration in many aeroelastic systems and active methods of vibration reduction have been studied extensively. The use of artificial neural networks is explored as an approach for developing robust control strategies.

Automation of some operations of a wind tunnel using artificial neural networks

Decker, Arthur J, Buggele, Alvin E. American Institute of Aeronautics and Astronautics. AIAA Journal. New York: Feb 1996. Vol. 34, Iss. 2; pg. 421

Abstract (Summary)

The results of tests of artificial neural networks for their ability at estimating sensor readings from shadowgraph patterns, shadowgraph patterns from shadowgraph patterns and sensor readings from sensor readings are presented.

Neural networks with modified backpropagation learning applied to structural optimization

Kodiyalam, Srinivas, Gurumoorthy, Ram. American Institute of Aeronautics and Astronautics. AIAA Journal. New York: Feb 1996. Vol. 34, Iss. 2; pg. 408

Abstract (Summary)

A multilayer feedforward Neural Network with a modification to the standard backpropagation training of neural nets is examined. Information on the gradients of target outputs with respect to network inputs is used in the modification.

Neuromorphic approach to inverse problems in aerodynamics

Prasanth, R K, Whitaker, Kevin W. American Institute of Aeronautics and Astronautics. AIAA Journal. New York: Jun 1995. Vol. 33, Iss. 6; pg. 1150

Abstract (Summary)

Two simple examples that show the ability of neural networks to solve inverse aerodynamic problems are offered. Each example case requires a separate Neural Network to be designed, trained and validated, but some features were common to all networks used.

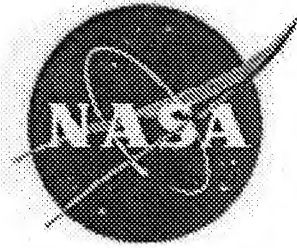
Other References (IEEE)

Raisinghani, S.C. and Gosh, A.K., "Parameter estimation of an aeroelastic aircraft using neural networks", Sadhanā, vol.25, part.2, April 2000, pp. 181-191.

Bartels, R. E.: An Elasticity Based Mesh Scheme Applied to the Computation of Unsteady Three Dimensional Spoiler and Aeroelastic Problems. Presented at 14th AIAA Computational Fluid Dynamics Conference, June 28–July 1, 1999, Norfolk, Virginia. AIAA Paper No. 99-3301.
<http://techreports.larc.nasa.gov/ltrs/PDF/1999/aiaa/NASA-aiaa-99-3301.pdf>
Organization RC RTOP 522-25-41

Whitlow, W., Jr.; and Todd, E. N. (Editors): CEAS/AIAA/ICASE/NASA Langley International Forum on Aeroelasticity and Structural Dynamics 1999. NASA/CP-1999-209136/PT2, June 1999, 419 p.

11



The Use of the Regier Number in the Structural Design With Flutter Constraints

H. J. Dunn and Robert V. Doggett, Jr.
Langley Research Center, Hampton, Virginia

*See also cited
references page 14*

August 1994

National Aeronautics and
Space Administration
Langley Research Center
Hampton, Virginia 23681-0001

Summary

This preliminary investigation introduces the use of the Regier number as a flutter constraint criterion for aeroelastic structural optimization. Artificial Neural Network approximations are used to approximate the flutter criterion requirements as a function of the design Mach number and the parametric variables defining the aspect-ratio, center-of-gravity, taper ratio, mass ratio and pitch inertia of the wing. The presented approximations are simple enough to be used in the preliminary design stage without a well defined structural model. An example problem for a low-speed, high-aspect-ratio, light-aircraft wing is presented. The example problem is analyzed for the flutter Mach number using doublet lattice aerodynamics and the PK solution method. The use of the Regier number constraint criterion to optimize the example problem for minimum structural mass while maintaining a constant flutter Mach number is demonstrated.

Introduction

The structural optimization of an airplane wing to satisfy flutter constraints is often an expensive process in terms of computer resource requirements. The typical iteration of the design through the optimization process requires repeated determination of the unsteady aerodynamic forces and subsequent flutter solutions. While the solution of the flutter equations requires little computer resources, the calculation of the unsteady aerodynamic forces often requires significant computer storage and central processor time. One means to reduce these costs, as discussed in references 1 and 2, is to use a simplified model of the unsteady aerodynamics. If the changes in the structure between adjacent iterations are small then the unsteady aerodynamic forces will be virtually unaffected and the aerodynamic model need not be updated at every iteration. A complete update might be made after, say, five iterations. Another simplified model, used in reference 3, assumes that the modal basis used to calculate the unsteady aerodynamic forces is unaffected during the optimization. This report presents an alternative approach to actually calculating the unsteady aerodynamic forces and explicitly solving the flutter equations during the optimization. The method uses a flutter criterion to evaluate the flutter susceptibility of the wing. Certain properties of the wing are compared with the criterion to assess whether or not the wing has acceptable flutter characteristics. The use of a flutter criterion is particularly attractive during preliminary design when a variety of wings are under study, and high accuracy is not required.

Although there are no flutter criteria that apply to all wings, there are criteria available that apply to many wings. For example, one flutter criterion is to

have the sectional center-of-gravity forward of the sectional aerodynamic center-of-pressure. However when this criterion is used for the design of a wing, the resulting design has excessive weight. The criterion for the flutter constraint used in this report is based on the stiffness-altitude parameter, or Regier number, which depends on the stiffness of the wing and characteristics of the fluid in which the wing is operating, in particular, the density and speed of sound. As the name stiffness-altitude implies, the value of the Regier number increases as either stiffness or altitude is increased. This parameter has been used in reference 4 to correlate the flutter results obtained from several hundred wind-tunnel, flutter-model tests.

The proposed criteria is "If the Regier number for the wing being designed is greater than a reference value, the wing is flutter free." The reference value is a calculated Regier number based on experimental flutter tests. If the Regier is substantially larger than the reference value, the wing has excess stiffness. This suggests that some material in the load bearing structure could be reduced (*i.e.* reduce the stiffness) and thus reduce the structural mass. If the Regier number is less than the reference value, then the wing will flutter. An advantage of the proposed criterion over other criterion is that this proposed criterion is easy to calculate and simple enough so that it may be used early in the design process.

The purpose of this paper is to discuss how a flutter constraint based on the Regier number can be used in optimizing an airplane wing. First the Regier number, including its background and meaning is introduced. This discussion is followed by the development of an artificial neural network (reference 5), or ANN, approximation for the reference Regier number data obtained from reference 4. Next, the procedure for using the Regier number in structural optimization is presented. Finally, the application of the Regier number criteria to an illustrative example is presented.

Symbols

ANN	artificial neural network
AR	aspect ratio
a	speed of sound
$b = \frac{\bar{c}}{2}$	reference length, wing semichord
\bar{c}	mean aerodynamic chord
$C_{L\alpha}$	lift curve slope
cg	center of gravity, % \bar{c}
ea	elastic axis position, % b
g	constraint function used in CONMIN

g	structural damping coefficient
h_a, h_f	height of aft or forward beam, Figure 8
I	input of ANN scaling function, (Equation 3)
J	objective function
k	reduced frequency
K_{AR}	ANN approximation for the AR correction factor
K_{cg}	ANN approximation for the cg correction factor
K_λ	ANN approximation for the λ correction factor
K_μ	ANN approximation for the μ correction factor
K_{r_α}	ANN approximation for the r_α correction factor
l	semispan of wing
M	Mach number
m	sectional wing mass
O	output of ANN scaling function, (Equation 7)
p	dummy argument of Equations 5 and 6
$\mathcal{R} = \frac{\omega_r b}{a} \sqrt{\mu}$	Regier number
$\bar{\mathcal{R}} = \frac{\bar{\mathcal{R}}}{\sqrt{C_{L\alpha}}}$	Frueh's modified Regier number
\mathcal{R}^*	Regier number approximation
r_α	radius of gyration, normalized by b
S_1, S_2	Nonlinear transfer function used in ANN
t_a, h_f	thickness of aft or forward beam wall, Figure 8
v	vector of structural response variables
V	velocity
$V_I = \frac{V}{b\omega_r\sqrt{\mu}}$	velocity index parameter
W	beam mass per unit length
w_a, w_f	width of aft or forward beam, Figure 8
w_j	weight parameter of neuron element (Equation 4)
Wt	mass of the support structure
x	vector of structural optimization design variables

y_j	output of a neuron element (Equation 4)
z	vertical displacement of the beam at the typical wing section
ω	frequency
$\mu = \frac{m}{m_{h,2}}$	mass ratio
ρ	mass density of fluid
ρ_s	mass density of the support structure
Λ	sweep angle
λ	taper ratio
Θ_j	bias parameter of neuron element (Equation 4)

subscripts:

α	pitch mode natural frequency
a	aft beam
\mathcal{C}	conservative approximation
d	divergence condition
\mathcal{E}	best estimate approximation
f	forward beam or flutter condition
j	j^{th} neuron element
max	maximum value
min	minimum value
r	reference
0	reference condition

The Regier Number

The Regier number, or stiffness-altitude parameter, is one of several nondimensional aeroelastic parameters that have been used to insure dynamic similarity between models (reference 6). The stiffness-altitude parameter was first suggested for use in displaying flutter data by Arthur A. Regier. Over time this parameter has become known as the Regier number, or \mathcal{R} . The expression for \mathcal{R} is

$$\mathcal{R} = \frac{\omega_r b \sqrt{\mu}}{a} \quad (1)$$

where ω_r is a reference frequency, b is the reference length, μ is the mass ratio, and a is the speed of sound. As is the case for the more familiar velocity index parameter¹ V_I , \mathcal{R} can be derived by simplifying

¹ The velocity index parameter V_I is related to \mathcal{R} by the following relationship:

$$V_I = \frac{M}{\mathcal{R}}.$$

the approximate empirical flutter formula expression given by Theodorsen and Garrick in reference 7. A modified version of \mathcal{R} is presented by Frueh in reference 8. Frueh's modified Regier number $\bar{\mathcal{R}}$ is given by

$$\bar{\mathcal{R}} = \frac{\mathcal{R}}{\sqrt{C_{L\alpha}}} \quad (2)$$

where $C_{L\alpha}$ is the lift curve slope. This expression would be attractive for use in correlating flutter data because $\bar{\mathcal{R}}$ has a smoother variation with Mach number than the Regier number does. However, in many instances $C_{L\alpha}$ information is not available, especially from research flutter model tests, so it is often not possible to use $\bar{\mathcal{R}}$. It should be pointed out the Frueh's expression can also be derived from Theodorsen and Garrick's approximate empirical formula (reference 7) recognizing that $C_{L\alpha}$ is 2π in their formula. So, in effect, Regier's formulation essentially assumes a constant lift curve slope. Recent research reports since about 1970 have not often used either \mathcal{R} or V_I because these reports tend to be problem, or wing, specific. For a specific wing, presenting the stability boundary using \mathcal{R} or V_I is not as useful as a plot of the stability boundary using dynamic pressure. However, in aeroelastic research reports prior to the 1970's the focus of the research was in parametric studies and the presenting of the data using \mathcal{R} or V_I is very common.

\mathcal{R} is also directly related to the parameters M and μ that arise from a non-dimensional considerations of flutter. The term $\frac{\omega b}{a}$ is the ratio of vibration velocity to fluid speed of sound and may be thought of as a modified Mach number. The remaining term μ is the nondimensional ratio of mass of the body to the apparent mass of the fluid surrounding it.

In reference 6 Regier describes \mathcal{R} as the square root of the ratio between the structural inertia force and the fluid force at Mach 1. Using the Regier number to define the stability boundary stresses the importance of the ratio between the inertial forces and fluid forces as a primary factor in the governing equations of motion. Two dynamically similar models that have the same Regier number will have the same ratio of structural force to fluid forces at Mach 1. If the two models are also aerodynamically similar, then the flutter stability boundary will be the same when plotted in the \mathcal{R} vs M plane. Figure 1 shows \mathcal{R} plotted against Mach number for an typical wing. When constant dynamic pressure lines are plotted against M , they appear as radial lines through the origin as shown in Figure 1. The stable no flutter region is above the boundary; the unstable flutter region is below the boundary. Unlike V_I , \mathcal{R} has the origin as an anchor point. The above properties makes \mathcal{R} an attractive parameter for correlating flutter data from different wing configurations.

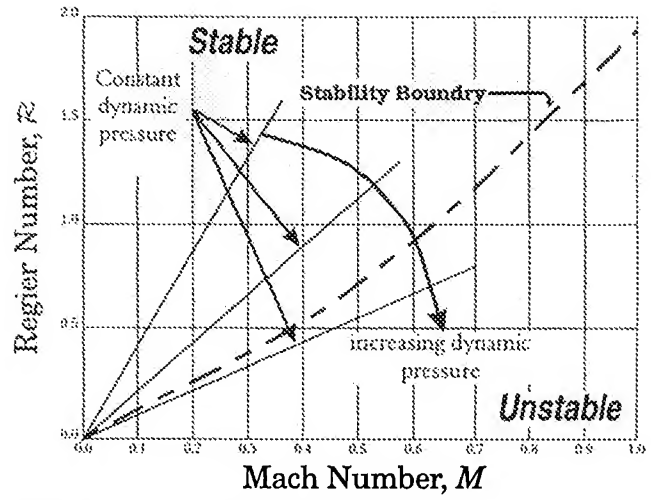


Figure 1. Regier Number Stability Plane.

For these reasons Harris (reference 4) chose \mathcal{R} to catalog flutter data from a variety of wing configurations. Reference 4 is a summary of 341 experimental and theoretical flutter studies presented as a series of flutter boundary plots of \mathcal{R} vs M and correction factors, such as the correction factor for the aspect ratio, K_{AR} vs AR . Figure 2 is a typical plot of \mathcal{R} vs M taken from reference 4 showing the flutter boundary and data points for low sweep conventional planform wings.

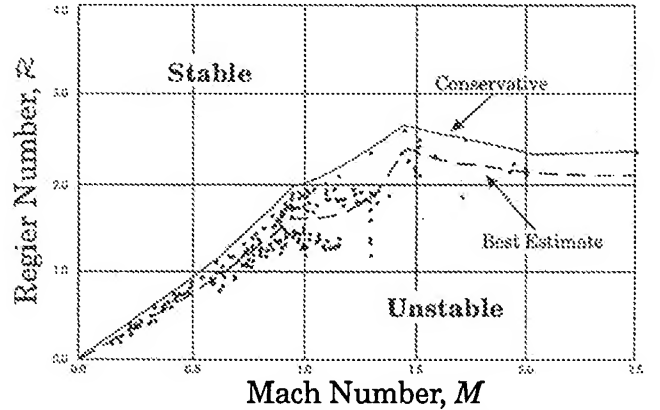


Figure 2. Regier Number vs Mach Number.

Other data plots in reference 4 are used for conventional planform wing of moderate and high sweep, and delta wing designs. The reference 4 designated "conservative estimate" and "best estimate" curves are shown in Figure 2 as solid and dashed lines, respectively. The conservative estimate curve encompasses all the experimental data whereas the best estimate curve is similar to a mean fairing through the data. The data in Figure 2 were adjusted by Harris to a nominal wing design for an average aspect ratio, center-of-gravity position, taper ratio, mass ratio, sweep angle, and radius of gyration. In practice, the data from reference 4 is adjusted for the particular AR , cg , λ , μ , Λ and r_α of the wing

design by using correction factors. The correction factors are normally a function of a single parameter with the exception of the correction factor for μ . This will be explained in the "The Regier Number Approximation" section of the paper.

To determine if a wing design has an aeroelastic problem using reference 4, the \mathcal{R} of the design calculated using Equation 1 is compared to the adjusted \mathcal{R} value calculated by using the methods and data of reference 4. A flutter condition is predicted if the \mathcal{R} calculated using Equation 1 is less than the \mathcal{R} generated by using reference 4. If the \mathcal{R} of the design is greater than the \mathcal{R} of reference 4, then addition weight savings can be achieved by removing some of the structural mass being used to generate "excess" this stiffness.

The Artificial Neural Network

Artificial neural networks (ANNs) are used in this report to approximate a number of curves in reference 4. This section serves to give the uninformed reader a brief introduction to the ANN. Further information on ANNs can be found in reference 5. ANNs are not unique to the work presented in this report and several other functions could have been used to approximate the data.

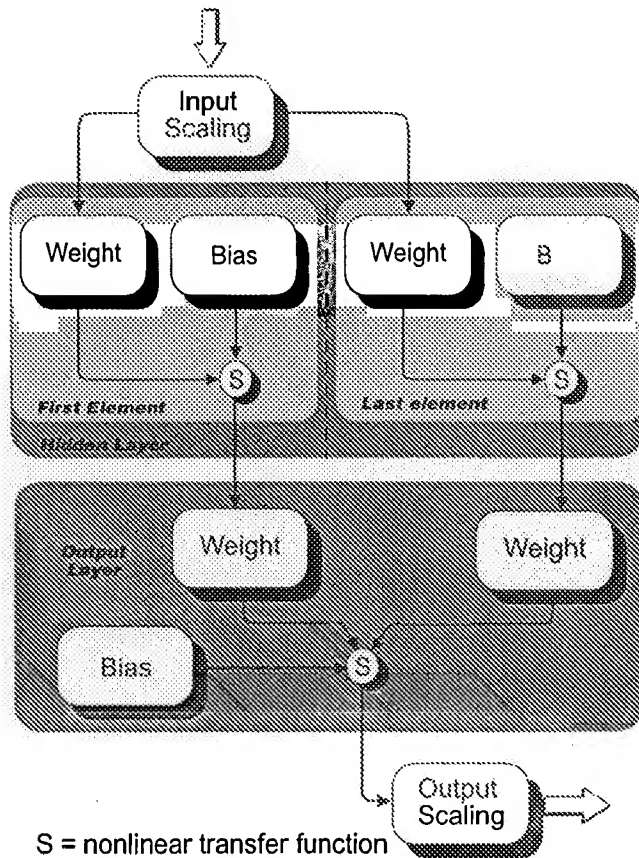


Figure 3. Artificial Neural Networks.

ANNs derive their name from trying to mimic the structure and functions of neural systems of living creatures. In general the network is composed of a number of signal processing elements, or artificial neurons. Figure 3 shows the form of the ANN using the McCulloch-Pitts neuron model (reference 5). In the conventional use of ANNs, the data is approximated by a single large ANN with several inputs and outputs. Because the data in reference 4 have been separated into several single input/output functions the conventional ANN model is not used. All of the ANNs developed in this report have a single input and output variable. The input variables are initially scaled before being passed to each neuron elements as shown in Figure 3. The individual neuron elements reside in what is commonly called the "hidden layer." The number of elements in the hidden layer determines the degree of accuracy of the approximation function. The more elements in the hidden layer the better the ANN is at approximating the original function. The output of each of the hidden layer elements is passed to the "output layer" which is also a neuron element. The output of the output layer is again scaled before being used.

The equations used for calculating the approximation are:

The input scaling function is

$$I_{scaled} = \frac{(I - I_{min})}{(I_{max} - I_{min})} * 0.8 + 0.1 \quad (3)$$

where I_{scaled} is the output of the scaling function, and I_{max} and I_{min} are the input scaling parameters.

The McCulloch-Pitts model for a single input neuron is described by

$$y_j = S_i(w_j I_{scaled} + \Theta_j) \quad (4)$$

where y_j is the output, w_j is the weight, and Θ_j is the bias of the neuron element. The function S_i defines the type of limiting or nonlinear transfer function used in the neuron. The approximations generated in this report use the following two types of nonlinear transfer functions

$$S_1(p) = \frac{1 - e^{-2p}}{1 + e^{-2p}} \quad (5)$$

$$S_2(p) = \frac{1}{1 + e^{-p}} \quad (6)$$

where p is the input to the function. The same type of nonlinear transfer function is used for all neuron elements of a particular ANN approximation.

The output scaling function is

$$O = \frac{(y_j - O_{min})}{0.8} * (O_{max} - O_{min}) + O_{min} \quad (7)$$

where O is the output of the approximation, O_{max} and O_{min} are output scaling parameters, and y_j is given by equation 4. The parameters that define the ANN are the minimum and maximum of the input and output scaling functions plus the weights and biases of the each of the neurons elements. Equations 3 – 7 are used to approximate each of the individual functions that are joined together to form the Regier number approximation as described in the next section.

The Regier Number Approximation

This section describes the approximations that are used to approximate the information contained in reference 4. Reference 4 presents the design estimates of the flutter margins as a series of basic flutter boundary plots in the form of \mathcal{R} vs M for wing configurations of specific values for AR , cg , λ , μ , Λ , and r_α . Parametric adjustment factors are presented as additional plots that are used to modify the basic boundary plots for variations in AR , cg , λ , μ , Λ , and r_α . These adjustment factors are necessary to account for wing configurations that are different from the base configuration. In Figure 4 the data and the ANN approximation function are shown for the aspect-ratio adjustment factor K_{AR} as a function of the wing aspect-ratio value AR . There are different basic flutter boundary plots for different planform designs, such as high sweep or delta platforms. The approximations calculated in this report for the base flutter boundary are for subsonic, low sweep, conventional-planform wing configurations.

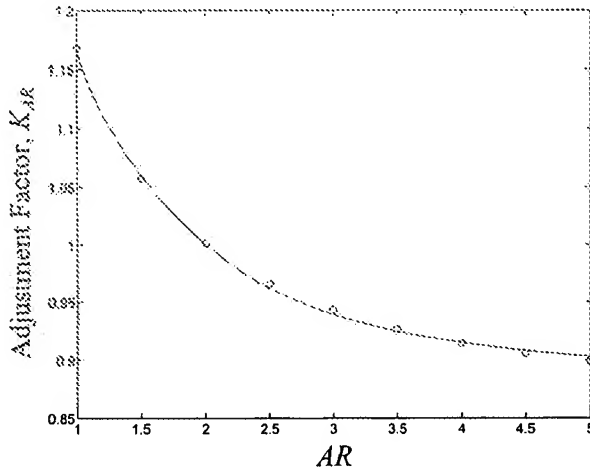


Figure 4. ANN Approximation of K_{AR} .

The K_{AR} ANN approximation function is calculated using Equation 7. The $K_{AR}(AR)$ has a value of 1 for $AR = 2$, which represents the aspect-ratio value of the base configuration wing. There are four other adjustment factors, $K_{cg}(cg)$ for the sectional wing cg

location, $K_\lambda(\lambda)$ for the taper ratio, $K_\mu(\mu, \Lambda, M)$ for mass ratio, and $K_{r_\alpha}(r_\alpha)$ for the radius of gyration. Each of the adjustment factors are calculated using Equation 7. The mass ratio adjustment factor appears to be a function of μ , Λ , and M but it is actually only a function of μ . The parameters Λ and M determine which one of 6 different functions of μ is used. The complete ANN approximation for the flutter boundaries are:

$$\mathcal{R}_C^* = \frac{\mathcal{R}_C(M)}{K_{AR}(AR)K_{cg}(cg)K_\lambda(\lambda)K_\mu(\mu, \Lambda, M)K_{r_\alpha}(r_\alpha)} \quad (8)$$

$$\mathcal{R}_E^* = \frac{\mathcal{R}_E(M)}{K_{AR}(AR)K_{cg}(cg)K_\lambda(\lambda)K_\mu(\mu, \Lambda, M)K_{r_\alpha}(r_\alpha)} \quad (9)$$

where \mathcal{R}_C and \mathcal{R}_E , each calculated using Equation 7. The functions \mathcal{R}_C^* , equation 8, and \mathcal{R}_E^* , equation 9, are best and conservative estimate ANN approximations as a function of M , AR , cg , λ , μ , r_α . The \mathcal{R}_C^* approximation is based on the envelope of \mathcal{R} whereas \mathcal{R}_E^* is based on the average value of \mathcal{R} .

Table 1 list the number elements in the hidden layer and the type of nonlinear transfer function (equations 5 or 6) used for each function. The value of zero for the K_{r_α} entry of Table 1 denotes no hidden layer. Table 2 lists the function coefficients for the ANN approximations. Note that the coefficients for K_μ entry of Table 1 is a single line in the table and is dependent on the value of Λ and M to determine which set of coefficients are used. As noted above and in Figure 3 each ANN has input and output scaling functions. Table 3 lists the scaling coefficients used in equations 3 and 7.

Equations 8 and 9 describe simple approximations that can be used with a minimum of computational effort to develop a constraint function for use in a complex structural optimization procedure or to check a design for its flutter margin.

Table 1. Regier ANN Configuration.

ANN function	Number of Elements in Hidden Layer	Nonlinear Transfer Function
\mathcal{R}_E^*	2	S_1
\mathcal{R}_C^*	2	S_1
K_{AR}	2	S_2
K_{cg}	2	S_2
K_λ	2	S_2
K_μ	1	S_2
K_{r_α}	0	S_2

Table 2. Regier ANN Coefficients.

Function	Hidden w_j	Layer Θ_j	Output w_j	Layer Θ_j
K_{AR}	-10.1802	6.4287	-2.8981	-0.2088
	11.3170	-1.6769	2.5877	
K_{cg}	-8.8731	4.6806	1.8229	-2.1408
	-12.3446	0.9841	5.6267	
K_λ	13.5425	-1.5790	-4.8732	2.6204
	-9.4929	4.8397	1.7489	
K_μ				
$M < .9$				
$A < 20^\circ$	5.6802	-2.1022	-1.4161	0.6581
$20^\circ < A < 52^\circ$	-6.1022	1.4173	2.7400	-1.0061
$A > 52^\circ$	6.0479	-1.1682	-3.4544	2.3473
$M > .9$				
$A < 20^\circ$	-6.2028	1.0579	2.7628	-0.8023
$20^\circ < A < 52^\circ$	6.3106	-0.8072	-5.0643	3.8784
$A > 52^\circ$	5.3574	0.6696	7.5510	-2.0054
K_{r_α}			5.6931	-2.8362
\mathcal{R}_C^*	-1.3377	-1.1461	-0.3777	0.6175
	1.4409	-1.2542	0.4905	
\mathcal{R}_E^*	1.3996	-0.5984	0.3697	0.7787
	1.3784	-1.0410	0.1003	

Table 3. Regier ANN Scale factors.

Function	Input		Output	
	Max	Min	Max	Min
K_{AR}	2	.2	1.5000	0.8993
K_{cg}	60	35	1.7877	0.8098
K_λ	1	0	2.2616	0.9048
K_μ	90	10	1.2390	0.7512
K_{r_α}	0.7	0.3	1.2630	0.7321
\mathcal{R}_C^*	1.8226	0	6	-6
\mathcal{R}_E^*	2.6731	0	6	-6

Structural Optimization Using the Regier Number Constraint

This section describes the use of the ANN approximation of the Regier number \mathcal{R}^* in a structural optimization procedure for the design of flutter free wing while minimizing

$$J = Wt \quad (10)$$

where J is the objective function and Wt is the mass of the support structure. Figure 5 shows the design optimization procedure used in this report. The procedure consists of two major independent computer pro-

grams. These are a MSC/NASTRAN^{®2} finite-element and sensitivity analysis program (reference 9) and, a second program denoted as **Optimizer** in Figure 5. The MSC/NASTRAN[®] analysis, denoted as (**Sensitivity & FEM Analysis**), uses a finite-element model (**FEM**) to generate the coefficients of the sensitivity equations. The **Optimizer** program calculates the objective function J , the gradient of the objective function $\frac{\partial J}{\partial x}$, and the constraint function g , for the optimization program CONMIN (reference 10). The CONMIN program is only used to solve the linear optimization problem. The design variable equations that are generated by MSC/NASTRAN[®] have the form

$$v = v_0 + \frac{\partial v}{\partial x}(x - x_0). \quad (11)$$

where v is a vector of structural design responses, v_0 is the value of the design responses at the start of the optimization step, $\frac{\partial v}{\partial x}$ is a matrix of sensitivity coefficients, x_0 is a vector of the value of the design variables at the start of the CONMIN optimization, and x is a vector of design variables used in CONMIN. The structural response vector v are functions that are computed within the MSC/NASTRAN[®] program. These responses can include weight, displacements due to specified load conditions, stress, and modal frequencies, etc. The elements of the design variable x are problem dependent and may include plate thickness, beam height, and flange width, etc. The matrix $\frac{\partial v}{\partial x}$ is computed by MSC/NASTRAN[®] using a finite-difference scheme. The sensitivities are transferred to the structural optimization program **Optimizer** as shown in Figure 5 and in more detail in Figure 6. Figure 6 shows the **Optimizer**'s internal flow as it cycles in the design space requiring the calculation of the objective function and constraint, or gradients of the objective function and constraint. As shown in Figure 6, the **Optimizer** program supplies the CONMIN program with the value of the objective function J , the constraint g , or the gradients of the objective function $\frac{\partial J}{\partial x}$. The CONMIN program calculates the gradient of g by using a finite-difference scheme.

The **Optimizer** finds the value of the design variable x that minimizes the linear cost function of Equation 10 subject to a non-linear inequality constraint

$$\mathcal{R}^* - \mathcal{R} < 0 \quad (12)$$

where \mathcal{R} is Regier number calculated using Equation 1, and \mathcal{R}^* is the required Regier number calculated from

² MSC/ is a registered trademark of The MacNeal-Schwendler Corporation. NASTRAN is a registered trademark of the National Aeronautics and Space Administration.

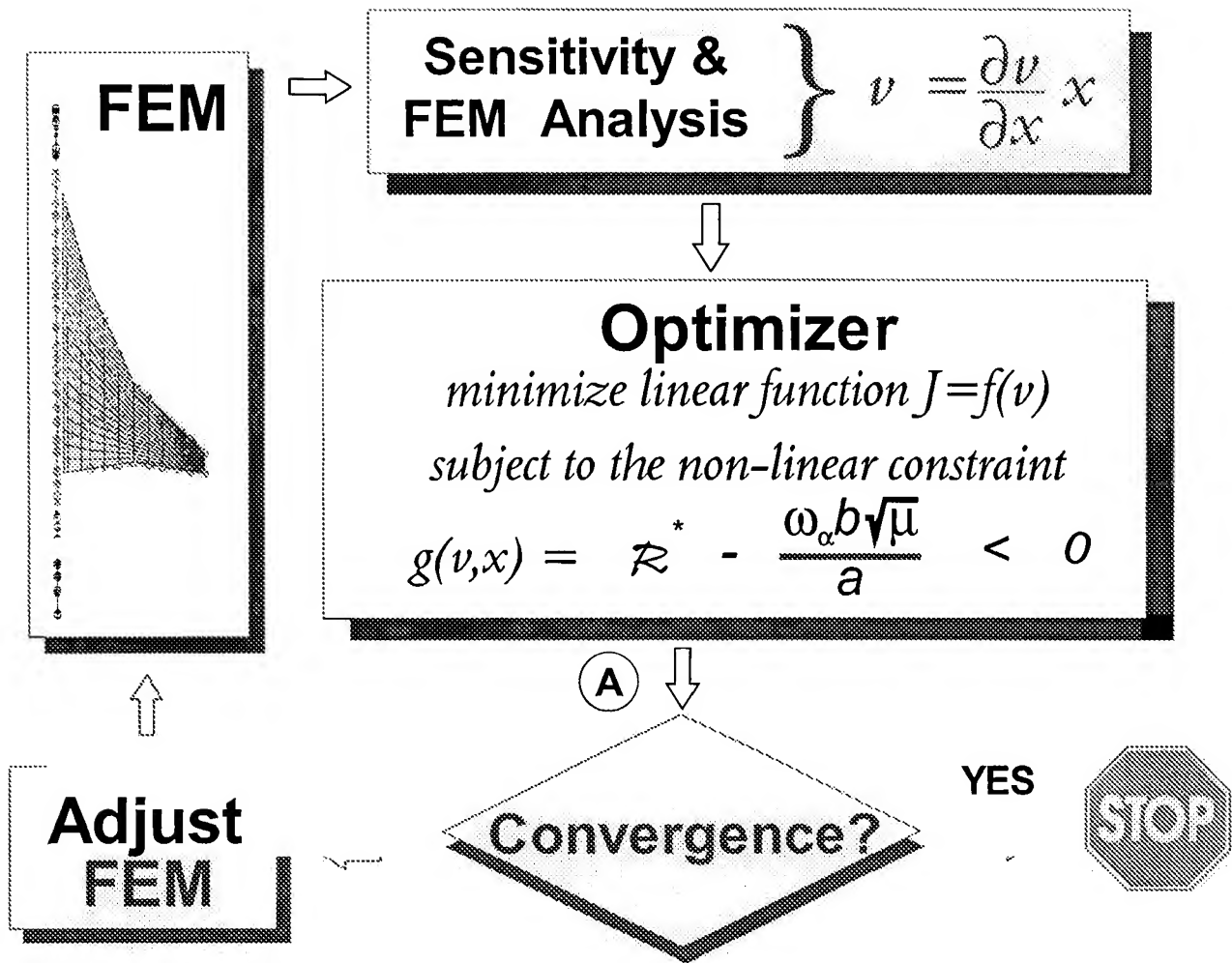


Figure 5. Design Optimization Iteration Procedure.

either Equation 8 or 9. Hereafter Equation 12 will be referred to as the Regier design constraint. \mathcal{R} is calculated using Equation 1 from the modal frequency ω_r , the wing mass m , constants dependent on the flight condition ρ and a , and if the shape optimization is being done, grid point locations of the FEM. The approximation \mathcal{R}^* is calculated using either Equations 8 or 9, and is a function of the independent variables AR , cg , λ , Λ , μ , τ_α and M . With the exception of ρ and M , all of the independent variables for calculating \mathcal{R} and \mathcal{R}^* must be calculated from the vectors v and x . The calculation of the Regier constraint from the vectors v and x is illustrated in the sample problem discussed in the next section. The values of ρ and M must be specified by the user. The CONMIN optimization program finds the value of x which will minimize the cost function, usually structural weight, subject to the Regier constraint defined by Equation 12.

A complete design iteration is a single pass around the path shown in Figure 5, executing the **Sensitivity & FEM Analysis** and **Optimizer** programs once. At the end of the CONMIN optimization program, the

design responses calculated with Equation 12 will not agree with the value calculated with the FEM analysis unless the two systems have converged. The design optimization procedure, Figure 5, must iterate between the **Sensitivity & FEM Analysis** program and the **Optimizer** program until the design responses agree, or converge. A converged design is defined when the objective function and the design variables do not change during a design iteration. The reason for the disagreement between the CONMIN and MSC/NASTRAN® design responses is that the **Sensitivity & FEM Analysis** program is calculating the responses using a nonlinear FEM of the structure and the **Optimizer** program is using a model of the structure linearized about the initial value of the design variables. At the end of the CONMIN optimization step the new values of the design responses of the linear model may not agree with the responses of the nonlinear model at the optimized value of the design variables. This behavior can be seen in the results of the sample problem in the next section. If the design has not converged, a MSC/NASTRAN® analysis is done using a new FEM based on the new

value of x and the optimization of the linear structural model is repeated. The design optimization procedure is repeated until the design responses of the sensitivity analysis agree with the value of the design response calculated with MSC/NASTRAN®, as shown in Figure 5.

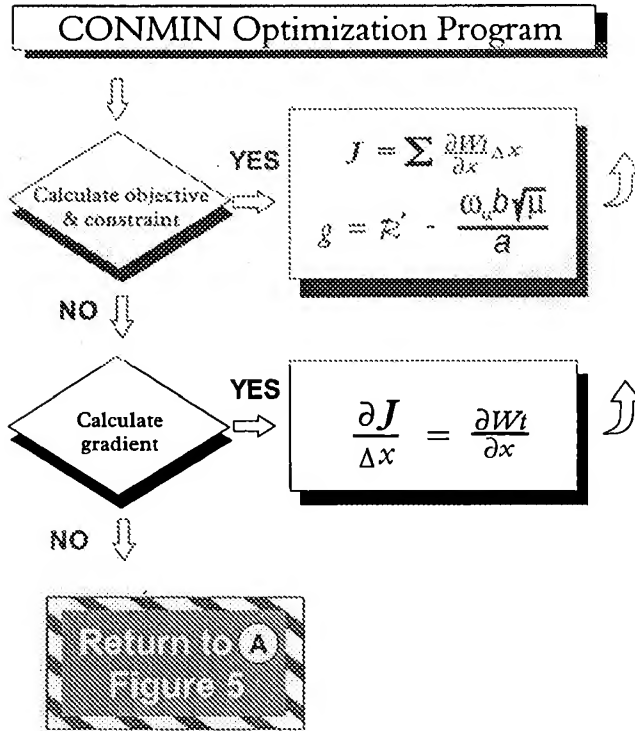


Figure 6. CONMIN Optimization Program.

Example Problem Definition, Analysis, and Optimization Results

This section describes an example problem for demonstrating the use of the Regier number constraint in the optimal design of a wing subject to a flutter requirement. The example was chosen to be complex enough to represent an actual aircraft wing. The following model specifications were selected *a priori*:

1. Shape optimization will not be done.
2. The wing will have a high AR , $AR > 5$.
3. The wing will be untapered, $\lambda = 1$.
4. The flow regime will be subsonic, and $\Lambda = 0$. The optimization will be for sea level flight condition.
5. The support structure will be two simple beams.
6. The dimensions and mass balance of the wing will be that of a typical light airplane wing that is in agreement with items 2 – 5 and designed to flutter at a subsonic M .

As a result of the above specifications R^* is a function of M , μ , r_α and cg . The optimization problem will be to design a minimum mass structure. The design

Mach number is the flutter Mach number of the initial wing design.

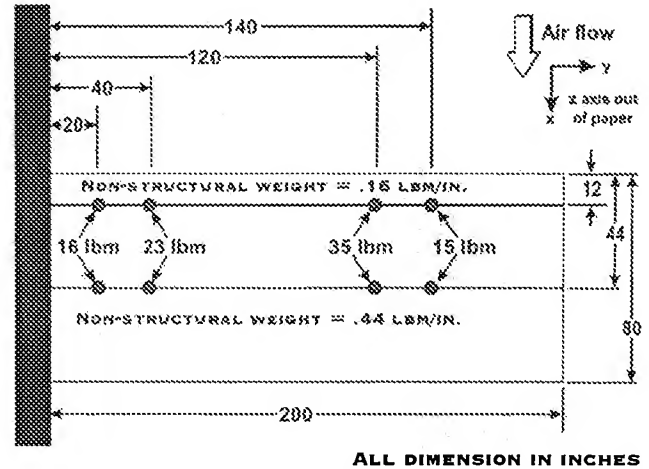


Figure 7. Example Problem: Wing Planform.

Structural Model

The planform of the example wing is presented in Figure 7. The wing is rectangular in shape with a semispan and chord of 200 and 80 in., respectively. The structure of the wing is modeled as two uniform cantilever beams. The forward and aft beam locations are placed at $0.15\bar{c}$ and $0.55\bar{c}$ to represent a typical wing box structure.

Each beam is modeled with 10 beam elements. The wing is constrained so that the aft beam is connect to the forward beam by rigid links. The forward beam is free to displace vertically and twist about its long axis. Each beam is carrying an amount of non-structural distributed mass that is proportional to the cross-sectional area from the the point midway between the beams to the leading or trailing edge of the wing. The forward beam has 0.16 lbm/in., and the aft beam has 0.44 lbm/in. of non-structural mass. To simulate the landing gear, concentrated masses of 16 and 23 lbm are located respectively on each beam at 20 and 40 in. span stations. To simulate fuel, concentrated masses of 35 and 15 lbm are located respectively on each beam at 120 and 140 in. span locations. In Figure 7, these concentrated masses are represented by small circles on each beam. Initial mass and balance information for the example wing are given in Table 4.

The design variables for the forward and aft beams are height h_f and h_a , width w_f and w_a , and wall thickness t_f and t_a of the rectangular beam section as shown in Figure 8. Table 5 summarizes the lower bound, initial, and upper bound values of the design variables.

Table 4. Example Problem: Wing Weights and Balances.

Element	Structural Mass(lbm)	Non-structural Mass(lbm)	Total Mass(lbm)
Forward Beam	23.2	32	55.2
Aft Beam	23.2	88	111.2
Fuel		100	100
Landing Gear		78	78
Total	46.4	298	344.4

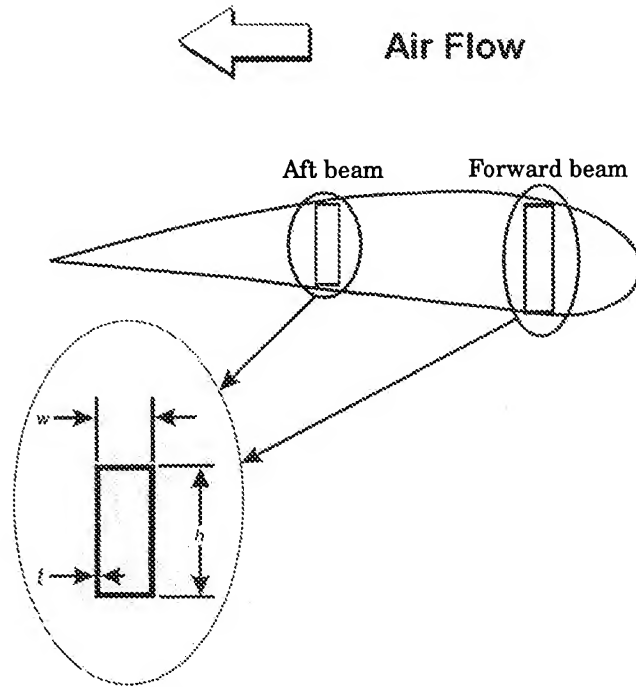


Figure 8. Example Problem: Wing Cross Section.

Table 5. Example Problem: Wing Design Parameter Values.

Parameter	Lower Bound (in.)	Initial Value (in.)	Upper Bound (in.)
w_f	1	2	3
h_f	2	4	5
t_f	0.05	0.1	0.2
w_a	1	2	3
h_a	2	4	5
t_a	0.05	0.1	0.2

Flutter Analysis

To determine the flutter Mach number design value, and to check the accuracy of the Regier constraint

criterion, a separate flutter analysis is conducted at each optimization iteration. The flutter analysis is in no way a required step in the optimization procedure. The flutter Mach number M_f for the initial wing will define the M for the design calculations. This section gives the details of how the flutter speed is calculated using the MSC/NASTRAN® computer program.

The first four vibration modes are used for the aeroelastic equations of motion. The vibration analysis results for these modes are presented in Table 6 and Figure 9. The first mode, 17 Hz, is the first bending mode. The second mode, 21 Hz, is the first torsion mode. The third mode, 46 Hz, is the second bending mode. The fourth mode, 58 Hz, is the second torsion mode. Both bending modes have significant amounts of torsion due to coupling between the plunge and pitch motion of the wing.

Table 6. Example Problem: Wing Vibration Analysis.

Mode	Frequency (Hz)	Generalized Mass	Generalized Stiffness
1 st bending	17	2.829×10^1	3.271×10^5
1 st torsion	21	1.769×10^{-1}	3.090×10^3
2 nd bending	46	1.350×10^1	1.121×10^6
2 nd torsion	58	6.760×10^{-2}	8.980×10^3

The unsteady aerodynamics are calculated using the doublet lattice method (reference 12). The aerodynamics planform, Figure 7, is divided into 10 spanwise and 5 chordwise aerodynamic boxes for the double lattice procedure. Beam spline (reference 11) interpolation is used to calculate the aerodynamic grid deflection from the motion of the forward beam. Unsteady generalized aerodynamics forces, GAFs, are calculated for the values of reduced frequency $k = [0.001, 0.1, 0.2, 0.3, 0.4, 0.5, 0.6, 0.7, 1, 5]$ and $M = [0.3, 0.6]$. Linear interpolation is used to calculate the GAFs at intervening values of k and M . The PK solution method, reference 11, is used to solve the dynamic equations of motion at $V = 600$ to 12000 in./sec in increments of 600 in./sec and $M = [0, 0.2, 0.3, 0.4, 0.5, 0.6]$. Figure 10 presents a typical results of a PK analysis for $M = 0.4$ for the above structural model with the design variables at their initial values. The data in Figure 10 indicates the 1st wing torsion mode going unstable at $V = 5000$ in./sec ($M=0.37$), $\omega = 19.5$ Hz and 1st wing bending mode diverging at $V = 9100$ in./sec, ($M=0.67$). Note, that the predicated M for the data in Figure 10 is less than the specified M for the calculated GAF data. The true instability point, often referred to as the "match point", is found by interpolating the data in Figure 10 with other results from the PK solution method ($M =$

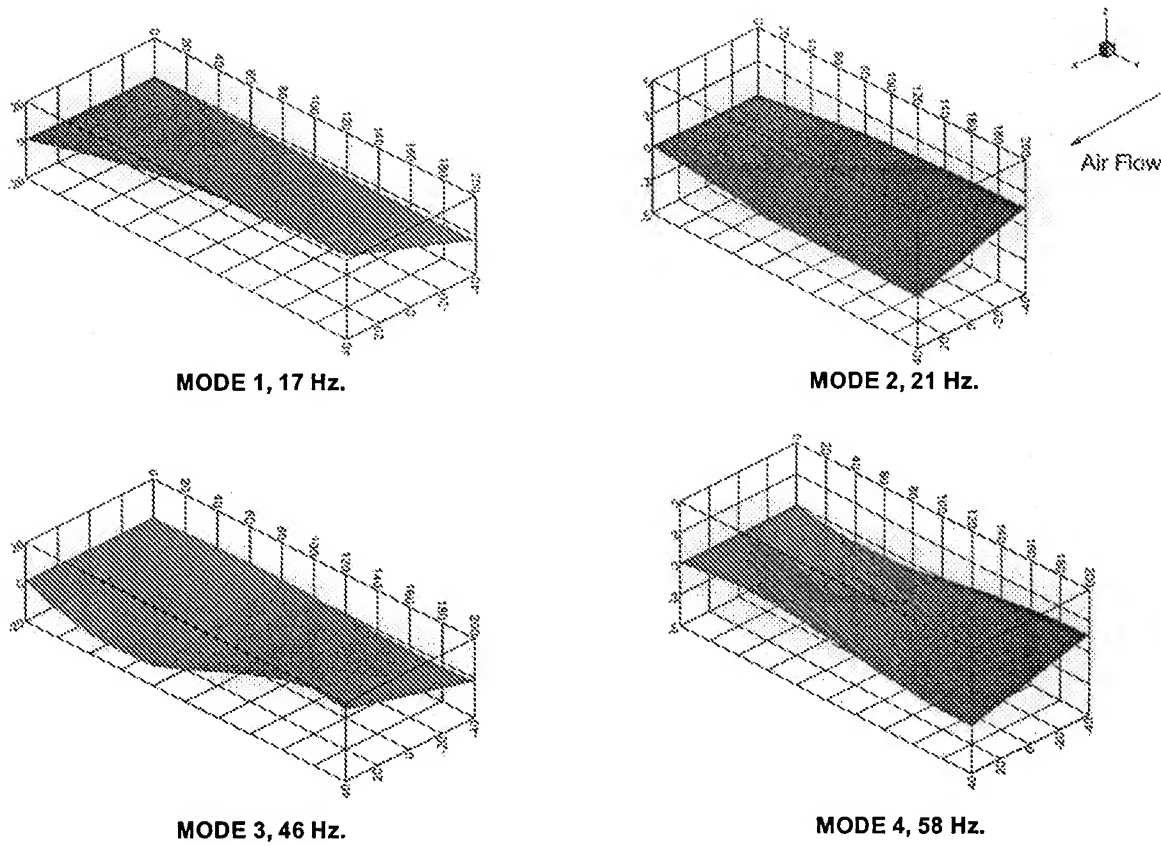


Figure 9. Example Problem: Vibration Modes.

0.3). The interpolated match point, or stability condition where ρ , M , and V are in agreement for a standard atmosphere, is $V_f = 5030$ in./sec ($M_f = 0.37$), at $\omega_f = 19.5$ Hz and $V_d = 8590$ in./sec ($M_d = 0.63$).

Regier Constraint Calculation

The Regier constraint for use in the **Optimizer**, (Figures 5 and 6), is developed in this section. The elements of the vector v in Equation 11 for this example are the variables Wt , ω_α , z_a and z_f . The required parameters in Equations 8 or 9 for the calculation of the \mathcal{R}^* are M , μ , r_α , and cg . The purpose of this section is show how these variables are calculated from the vector v . During the CONMIN optimization calculations, the design responses are approximated using Equation 11. For example, the deflection of the aft beam z_a is approximated by

$$z_a = z_{a0} + \frac{\partial z_a}{\partial x}(x - x_0) \quad (13)$$

where z_{a0} is the value of the aft beam at the start of the CONMIN program.

The Regier database in reference 4 is based on the sectional wing characteristics at the 75 percent span

location. For this example problem the nearest grid locations occur at the 80 percent span location and these grid locations are used to calculate μ , r_α , and cg . The 80 percent span was used because for this problem the parameters μ , r_α , and cg do not change between the 75 percent and 80 percent span locations.

The mass ratio for the example wing is

$$\mu = \frac{Wt + 0.6l}{\pi b^2 \rho} \quad (14)$$

where Wt is the mass of the support structure, l is the semispan of the wing, b is the wing semichord, and ρ is the density of the fluid. Note that this expression for μ contains the mass of the beams and the nonstructural mass, but does not contain the mass of the landing gear or fuel. For the values of $l=200$ in., $b=40$ in. and $\rho = 1.39 \times 10^{-4}$ lbm/in.³ Equation 14 becomes

$$\mu = \frac{Wt + 120}{44.59} \quad (15)$$

For the initial wing design $\mu = 3.69$.

The center-of-gravity cg is calculated by using

$$cg = \left(0.5 + \frac{0.05(W_a + 0.44) - 0.35(W_f + 0.16)}{W_a + W_f + 0.6} \right) \times 100 \quad (16)$$

where the sectional mass of the beams W_a and W_f are calculated by using

$$W_x = \rho_s \left(2t_x(h_x + w_x) - 4t_x^2 \right) \quad (17)$$

where ρ_s is the mass density of the support structure, and the subscript x is either a or f to denote the aft or forward beam. For the initial wing design $cg = 41.8$.

The radius of gyration r_α parameter is calculated by using

$$r_{\alpha} = \sqrt{\frac{(W_a + 0.44)(0.1 - ea)^2 + (W_f + 0.16)(0.7 - ea)^2}{W_a + W_f + 0.6}} \quad (18)$$

where ea is calculated by using the displacements z_f and z_a due to a torque applied to the wing tip. That is,

$$ea = 0.1 - 0.8 \frac{z_a}{z_a + z_f} \quad (19)$$

For the initial wing design $r_\alpha = 0.4$.

Figure 11 shows \mathcal{R}_C^* and \mathcal{R}_E^* as a function of M and the flutter analysis result (solid circle symbol) for the initial wing design. The data in Figure 11 indicate that the \mathcal{R}_E^* is a sufficiently accurate to be used in Equation 12 for \mathcal{R} . That is, the approximation of “best estimate” stability boundary is essentially the same as the doublet lattice calculated stability boundary. Substituting Equations 1 for \mathcal{R} and 9 for \mathcal{R}^* into Equation 12, with $K_{AR}(5) = 0.9029$, $K_\lambda(1) = 0.9028$, and $a = 13587$ in./sec yields the Regier constraint for an unswept wing with $AR=5$ and $\lambda=1$ as a function M , cg , μ , and r_α :

$$\frac{1.227\mathcal{R}_E^*(M)}{K_\mu(\mu)K_{cg}(cg)K_{r_\alpha}(r_\alpha)} - \frac{\omega_\alpha\sqrt{\mu}}{340} < 0 \quad (20)$$

where $K_\mu(\mu)$ represents the K_μ adjustment factor approximation for $M < .9$ and $\Lambda < 20^\circ$.

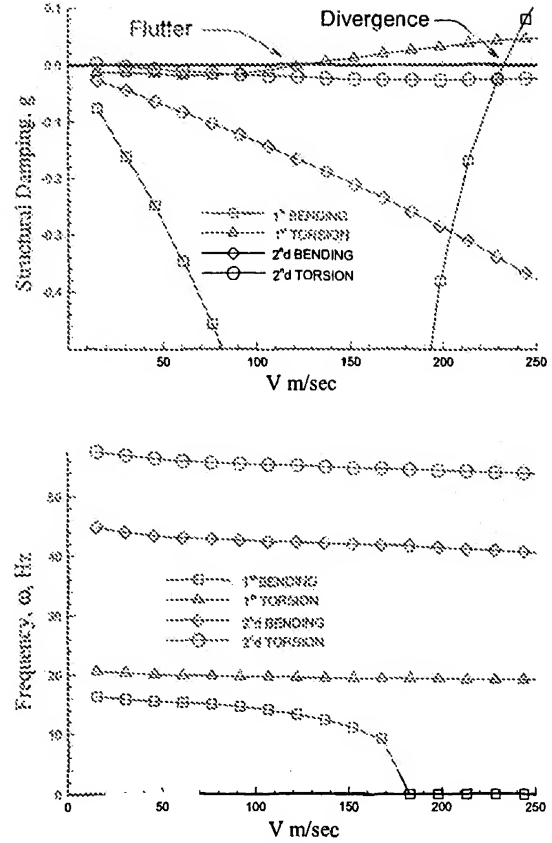


Figure 10. Example Problem: Aeroelastic Analysis.

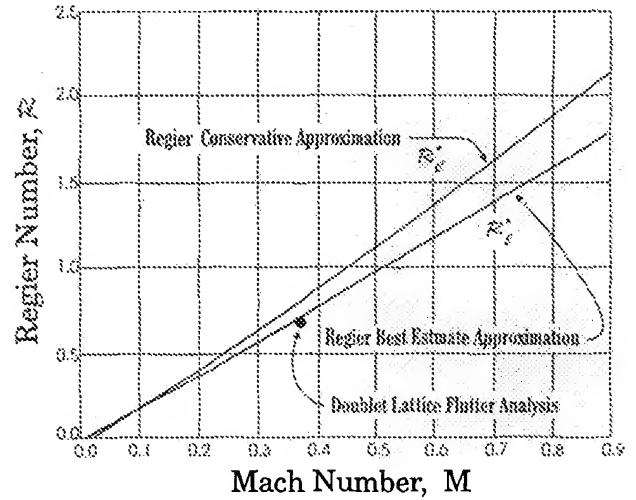


Figure 11. Example Problem: Regier Constraint Function.

Structural Optimization Results

The doublet lattice analysis predicts the initial example wing to flutter at $M = 0.37$. The objective of the optimization is to design a minimum mass wing (i.e. minimize Wt) that will be flutter free at $M = 0.37$. For

$M = 0.37$ and $\mathcal{R}_{\mathcal{E}}^* = 0.621$ Equation 20 becomes

$$\frac{0.763}{K_{\mu}(\mu)K_{cg}(cg)K_{r_{\alpha}}(r_{\alpha})} - \frac{\omega_{\alpha}\sqrt{\mu}}{340} < 0 \quad (21)$$

The design variable vector x in Equation 11 consists of the six variables w_a , w_f , h_a , h_f , t_a , and t_f . CONMIN's solution to the problem is to set all of the design variables, except h_f , to the lower design variable bounds and to find the value of h_f that satisfies the constraint function defined by Equation 21. Figure 12 is the optimization history for the design variable h_f and Table 7 lists the values of the design variables for the converged design. Figure 13 shows the optimization history of Wt . The final value of Wt is 16.6 lbm, a reduction of 29.8 lbm.

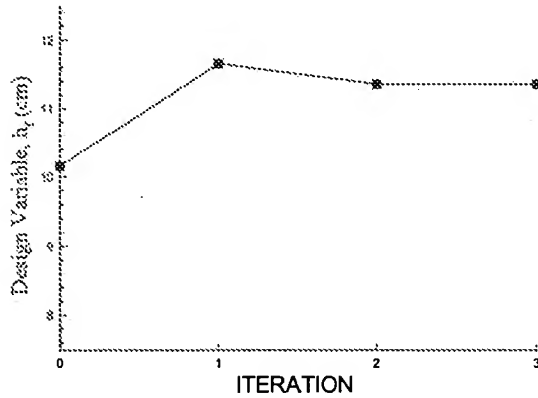


Figure 12. Optimization Results: h_f vs Iteration.

Table 7. Example Problem: Final Wing Design Variables Values.

Design Variable	Final Value (in.)
w_f	1
h_f	4.474
t_f	.05
w_a	1
h_a	2
t_a	.05

For the first and second optimization iterations in Figure 13 the discontinuous nature of the structural optimization results is quite noticeable. The first and second optimization iterations are bounded by the \square and Δ symbols. Convergence at the end of iteration 2 between the linear optimization equations and the finite element analysis equations is indicated in Figure 13 by the symbol ∇ , designating the third CONMIN

optimization step, combining with the symbol Δ , designating the second CONMIN optimization step, to give the appearance of the symbol \star .

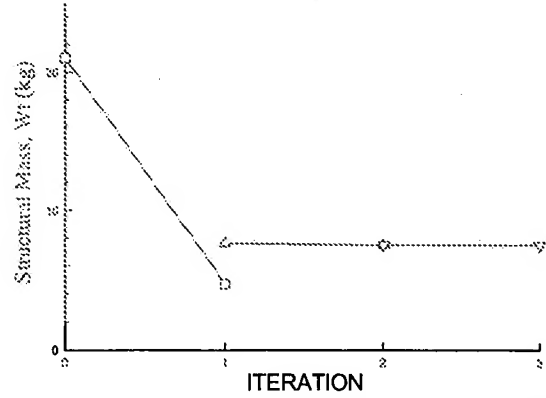


Figure 13. Optimization Results: Structure Mass vs Iteration.

Figure 14 presents the history of the \mathcal{R} and $\mathcal{R}_{\mathcal{E}}^*$ terms of the constraint function during the optimization. The solid line in Figure 14 is \mathcal{R} and the dotted line is $\mathcal{R}_{\mathcal{E}}^*$. Equation 20 is satisfied in Figure 14 whenever the solid line is above the dotted line. At the beginning of the first iteration, denoted as iteration 0 in Figure 14, the data indicates that the the structure has excess stiffness because $\mathcal{R} > \mathcal{R}_{\mathcal{E}}^*$. During the first CONMIN optimization step, i.e. between iterations 0 and 1 in Figures 12 – 14, the smallest h_f is found that satisfies the nonlinear constraint described by Equation 20. The reduction structural mass is indicated in Figure 13. At the end of the CONMIN optimization step, the MSC/NASTRAN[®] analysis results are shown at iteration 1 in Figures 12 – 14. The new constraint function indicates that a further mass savings can be made by reducing the stiffness still further during the second CONMIN optimization step. The convergence of the optimization program in two iterations is confirmed by the third segment of the results being nearly flat in Figures 12 – 14.

In Figure 15 the flutter Mach number M_f predicted by the MSC/NASTRAN[®] flutter analysis is plotted against iteration number. The variation of M_f is considered to be within the accuracy of the calculation and the optimal design is considered to meet the design specifications. However, there is no guarantee that the optimal design will have the desired aeroelastic properties because the optimization only guarantees that $\mathcal{R} > \mathcal{R}^*$.

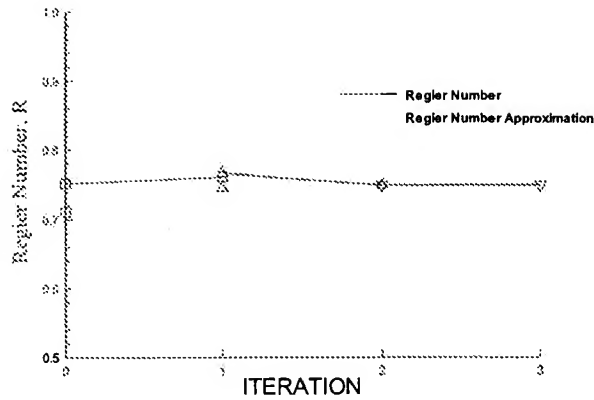


Figure 14. Optimization Results: \mathcal{R} and \mathcal{R}^* vs Iteration.

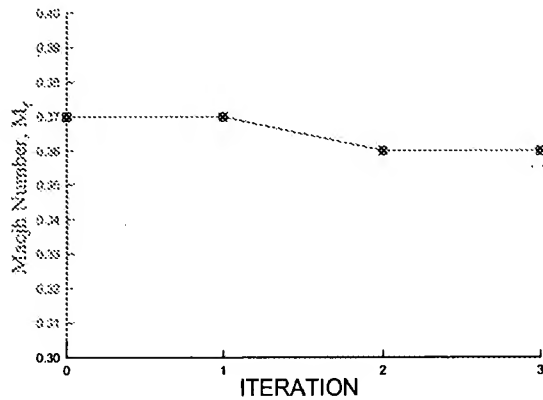


Figure 15. Optimization Results: MSC/NASTRAN® computed M_f vs Iteration.

Only a single initial value case is done in this paper because the objective of the paper is the examination of the Regier number criterion and not the optimization problem. If the structural optimization problem is of interest, several different initial conditions would have to be tested determine the existence of other minimum of the objective function in the design space.

Table 8 lists the execution times of the **Sensitivity & FEM Analysis**, **Optimizer** programs, and flutter analysis. The execution times listed in Table 8 are divided by the execution time of the flutter analysis program. Based on the data in Table 8, the Regier constraint is an efficient means for calculating an optimal structure with flutter constraint. The execution time for the structural optimization using the Regier constraint will be less than the procedure described in reference 3 since the method in reference 3 requires a calculations of the GAF at each iteration of the optimization.

Table 8. Example Problem: Program Execution Times.

Program	Relative Execution Time
Sensitivity Analysis	0.23
Optimizer	0.01
Aeroelastic Analysis	1.00

Concluding Remarks

A flutter constraint criterion based on the Regier number for aeroelastic structural optimization is introduced. The use of a constraint criterion makes it unnecessary to calculate generalized unsteady aerodynamic forces between optimization cycles as do other methods used in aeroelastic design for flutter.

The application of the method proceeds in the following manner. Existing experimental flutter data in Regier number format are approximated by using Artificial Neural Networks. This approximation is then used to develop the flutter constraint criterion. Next, the optimal flutter acceptable wing design is achieved by adjusting the design parameters to achieve the minimum of the objective function, say structural weight, while satisfying the Regier constraint criterion.

The procedure is illustrated by the application to an example problem. A simple, rectangular wing is optimized for weight at a specified Mach number while achieving a desired minimum flutter condition. The data for developing the Regier number constraint are obtained from existing experimental results of similar configurations. The solution for the illustrative problem converged in two design cycles. Because of the simplicity of the Regier number approximation, little computer resources are required.

References

1. Sobieszczanski-Sobieski, J.: Multidisciplinary Design Optimization: An Emerging New Engineering Discipline, *World Congress on Optimal Design of Structural Systems*, Rio de Janeiro, Brazil, August 2-6, 1993.
2. Chang, K. J.; Haftka, R. T.; Giles, G. L.; and Kao, P.-J.: Sensitivity Based Scaling for Correlating Structural Response from Different Analytical Models. AIAA Paper No. 91-925. Presented at AIAA/ASEM/ASCE/AHS/ASC 32nd Structures, Structural Dynamics, and Material Conference, Baltimore, MD, 1991.
3. Climent, Hector; and Johnson, Erwin H.: Aeroelastic Optimization Using MSC/NASTRAN, *International Forum on Aeroelasticity and Structural Dynamics*, May 22-26, 1993, Strasbourg, France.
4. Harris, G.: Flutter Criteria for Preliminary Design, Vought Aeronautics Report 2-53450/3R-467, September, 1963.

5. Cichocki, A.; and Unbehauen, R.: Neural Networks for Optimization and Signal Processing, John Wiley & Sons Ltd., 1993.
6. Regier, Arthur A.: The Use of Scaled Dynamic Models in Several Aerospace Vehicle Studies, *ASME Colloquium on the Use of Models and Scaling in Simulation of Shock and Vibration*, November 19, 1963, Philadelphia, Pennsylvania.
7. Theodorsen, Theodore; Garrick, I. E.: Mechanism of Flutter: T. R. No. 685, N. A. C. A., 1940.
8. Frueh, Frank J.: A Flutter Design Parameter to Supplement the Regier Number. AIAA J., vol. 2, no. 7, July 1964.
9. Moore, Greg J.: MSC/NASTRAN Design Sensitivity and Optimization User's Guide, The MacNeal Schwendler Corp. April 1992.
10. Vanderplaats, Garret N.: CONMIN: A Fortran Program for Constrained Function Minimization User's Manual, NASA TM X 62-282, Ames Research Center and U.S. Army Air Mobility R&D Laboratory, Moffett Field, CA 94035.
11. Rodden, W. P.; Harder, R. L.; and Bellinger, E. D.: Aeroelastic Addition to NASTRAN, NASA CR 3094, March 1979.
12. Giesing, J. P.; Kalman, T.P.; Rodden, W. P.: Subsonic Unsteady Aerodynamics for General Configurations, Part II, Volume I – Application of the Doublet-Lattice Method and the Method of Images to Lifting-Surface/Body Interference, Air Force Flight Dynamics Laboratory Report No. AFFDL-TR-71-5, Part II, Vol. I, April 1972.

Public reporting burden for this collection of information is estimated to average 1 hour per response, including the time for reviewing instructions, searching existing data sources, gathering and maintaining the data needed, and completing and reviewing the collection of information. Send comments regarding this burden estimate or any other aspect of this collection of information, including suggestions for reducing this burden, to Washington Headquarters Services, Directorate for Information Operations and Reports, 1215 Jefferson Davis Highway, Suite 1204, Arlington, VA 22202-4302, and to the Office of Management and Budget, Paperwork Reduction Project (0704-0188), Washington, DC 20503.

1. AGENCY USE ONLY (Leave blank)		2. REPORT DATE August 1994	3. REPORT TYPE AND DATES COVERED Technical Memorandum
4. TITLE AND SUBTITLE The Use of the Regier Number in the Structural Design with Flutter Constraints			5. FUNDING NUMBERS WU 505-63-50-06
6. AUTHOR(S) H. J. Dunn and Robert V. Daggell, Jr.			
7. PERFORMING ORGANIZATION NAME(S) AND ADDRESS(ES) NASA Langley Research Center Hampton, VA 23681-0001			8. PERFORMING ORGANIZATION REPORT NUMBER
9. SPONSORING / MONITORING AGENCY NAME(S) AND ADDRESS(ES) National Aeronautics and Space Administration Washington, DC 20546-0001			10. SPONSORING / MONITORING AGENCY REPORT NUMBER NASA TM-109128
11. SUPPLEMENTARY NOTES			
12a. DISTRIBUTION / AVAILABILITY STATEMENT Unclassified - Unlimited Subject Category 05			12b. DISTRIBUTION CODE
13. ABSTRACT (Maximum 200 words) This preliminary investigation introduces the use of the Regier number as a flutter constraint criterion for aeroelastic structural optimization. Artificial Neural Network approximations are used to approximate the flutter criterion requirements as a function of the design Mach number and the parametric variables defining the aspect-ratio, center-of-gravity, taper ratio, mass ratio and pitch inertia of the wing. The presented approximations are simple enough to be used in the preliminary design stage without a well defined structural model. An example problem for a low-speed, high-aspect-ratio, light-aircraft wing is presented. The example problem is analyzed for the flutter Mach number using doublet lattice aerodynamics and the PK solution method. The use of the Regier number constraint criterion to optimize the example problem for minimum structural mass while maintaining a constant flutter Mach number is demonstrated.			
14. SUBJECT TERMS Regier Number; Structural Optimization; Aeroelastic Vehicle Design; Flutter Design Constraint			15. NUMBER OF PAGES 15
			16. PRICE CODE A03
17. SECURITY CLASSIFICATION OF REPORT Unclassified	18. SECURITY CLASSIFICATION OF THIS PAGE Unclassified	19. SECURITY CLASSIFICATION OF ABSTRACT Unclassified	20. LIMITATION OF ABSTRACT

Public reporting burden for this collection of information is estimated to average 1 hour per response, including the time for reviewing the collection of information, searching existing data sources, gathering the data needed, and completing and reviewing the collection of information. Send comments regarding this burden estimate or any other aspect of this collection of information, including suggestions for reducing this burden, to Washington Headquarters Services, Directorate for Information Operations and Reports, 1204, Arlington, VA 22202-4302, and to the Office of Management and Budget, Paperwork Reduction Project (0106), Washington, DC 20503.

0106

urces, gathering
this collection of
Highway, Suite

1. AGENCY USE ONLY (Leave blank)		2. REPORT DATE		3. REPORT TYPE AND DATES COVERED Final 01 Nov 97 to 30 Sep 98	
4. TITLE AND SUBTITLE (T&E) Real Time Predictive Flutter Analysis and Continuous Parameter Identification of Accelerating Aircraft				5. FUNDING NUMBERS 61102F 2304/KS	
6. AUTHOR(S) Profesor Farhat					
7. PERFORMING ORGANIZATION NAME(S) AND ADDRESS(ES) Univesity of Colorado 206 Armory Campus Box B-19 Boulder CO 80309-0019				8. PERFORMING ORGANIZATION REPORT NUMBER	
9. SPONSORING/MONITORING AGENCY NAME(S) AND ADDRESS(ES) AFOSR/NM 801 North Randolph Street RM732 Arlington, VA 22203-1977				10. SPONSORING/MONITORING AGENCY REPORT NUMBER	
11. SUPPLEMENTARY NOTES					
12a. DISTRIBUTION AVAILABILITY STATEMENT APPROVAL FOR PUBLIC RELEASE; DISTRIBUTION UNLIMITED				12b. DISTRIBUTION CODE	
13. ABSTRACT (Maximum 200 words) This is a four-part final report on the research supported y the Air Force Office of Scientific Research Center under Grant F49620-98-1-0112, Real Time Predictive Flutter Analysis and Continuous Parameter Identification of Accelerating Aircraft.					
14. SUBJECT TERMS				15. NUMBER OF PAGES	
				16. PRICE CODE	
17. SECURITY CLASSIFICATION OF REPORT UNCLASSIFIED		18. SECURITY CLASSIFICATION OF THIS PAGE UNCLASSIFIED		19. SECURITY CLASSIFICATION OF ABSTRACT UNCLASSIFIED	
				20. LIMITATION OF ABSTRACT UL	

**AIR FORCE OFFICE OF SCIENTIFIC RESEARCH
GRANT F49620-98-1-0112
Final Report - February 1999**

CHARBEL FARHAT

*Department of Aerospace Engineering Sciences
Center for Space Structures and Controls
University of Colorado at Boulder
Boulder, CO 80309-0429*

SUMMARY

This is a four-part final report on the research supported by the Air Force Office of Scientific Research Center under Grant F49620-98-1-0112, **Real Time Predictive Flutter Analysis and Continuous Parameter Identification of Accelerating Aircraft**.

1. Motivations and research plan

Flutter clearance, which is part of any new aircraft or fighter weapon system development, is a lengthy and tedious process from both computational and flight testing viewpoints. An automated approach to flutter clearance that increases flight safety and reduces flight hours requires as a stepping stone the development of a real time flutter prediction capability. Such a fast analysis tool can be designed if the coupled fluid/structure aeroelastic system is represented by a simplified mathematical model that can be quickly adapted to changes in flight atmospheric conditions, aircraft mass distribution (weapon systems), fuel loading, and Mach number, and if the current parallel processing technology is exploited.

Furthermore, flight testing is always required to establish the flutter envelope of an aircraft. The traditional method for determining such an envelope uses test data extracted from the vibration response of the aircraft at fixed flight conditions. The aircraft is first trimmed to a specific flight condition (Mach number and dynamic pressure), then its aeroelastic response is deliberately excited by applying an input to a flight control surface. The frequency and damping of the excited aeroelastic response are typically extracted from

the vibration data. By repeating this test at many flight conditions, the flutter envelope can be determined. Such a traditional approach requires that the aeroelastic response be measured at many different flight conditions. This often requires a large number of flight test hours, a process which not only costs money but also exposes test pilots to proportionately increased risk. However, this test procedure can be expedited if data collected from continuously varying flight conditions can be used to extract the needed flutter damping and frequency values from an accelerating flight profile. In that case, it may be possible to greatly reduce the number of flight hours required for establishing the flutter envelope.

The Air Force Flight Test Center at the Edwards Air Force Base (AFB) has expressed great interest in the above two problems, and therefore we have proposed to conduct a three-year research effort in real time flutter analysis, and the continuous parameter identification of an accelerating aircraft. More specifically, we have proposed to develop a simplified flutter analysis method that can be run real time to provide predictive frequency and damping values for maneuvers as flown. The enabling technology of such a real time flutter analysis capability is a formulation of the aeroelastic problem that allows, among other things, partial pre-solutions and the usage of parallel processing.

We have also proposed to develop a parameter identification technique that can be used to extract frequency and damping values of an aircraft that is continuously accelerating. This technique is based on an arbitrary Lagrangian/Eulerian formulation for simulating accelerated flow problems and on windowing techniques.

Here, we report on both efforts outlined above and which have been conducted in collaboration with the researchers and engineers of the Air Force Flight Test Center at the Edwards AFB.

2. Results to date

During the fiscal year 1998, we have obtained the following results, all of which pertain to our long-term objectives described above.

2.1. A CFD based method for solving aeroelastic eigen problems in all flight regimes

In a first step, we have designed a linearized CFD method for computing an arbitrary number of eigen solutions of a given aeroelastic problem. Our method is based on the re-engineering of a three-way coupled formulation previously developed for the solution in the time domain of nonlinear transient aeroelastic problems. It is applicable in the subsonic, transonic, and supersonic flow regimes, and independently from the frequency or damping level of the target aeroelastic modes. It is based on the computation of the complex eigen solution of a carefully linearized fluid/structure interaction problem, relies on the inverse orthogonal iteration algorithm, and reutilizes existing unsteady flow solvers.

We have validated this method with the flutter analysis of the AGARD Wing 445.6 for which experimental data is available.

In a second step, we have improved the convergence of our linearized CFD method by enhancing the convergence of the inverse orthogonal iteration algorithm via the use of true second-order flow jacobians. We have simultaneously improved the convergence of our iterative solver applied to the solution of the underlying systems of equations. Both enhancements have allowed us to improve the overall CPU solution time of our method by a factor ranging between 4 and 10, depending on the given problem.

Some aspects of this specific progress are documented in the following reports, which have also been submitted and accepted for publication in archival journals:

M. Lesoinne and C. Farhat, "A CFD Based Method for Solving Aeroelastic Eigenproblems in all Flight Regimes," *Journal of Aircraft*, (submitted for publication).

M. Lesoinne, M. Sarkis, U. Hetmaniuk, and C. Farhat, "A Linearized Method for Extracting Eigen Solutions of Aeroelastic Systems," *Computer Methods in Applied Mechanics and Engineering*, (in press).

X.-C. Cai, C. Farhat and M. Sarkis, "A Minimum Overlap Restricted Additive Schwarz Preconditioner and Applications in 3D Flow Simulations," *Contemporary Mathematics*, Vol. 218, pp. 478-484 (1998).

2.2. Continuous parametric identification of an accelerating aeroelastic system

The traditional flutter testing approach implies a relatively large number of flight test hours, a process which is not only expensive, but also exposes test pilots to increased risks. One way to expedite this test procedure is to develop a method for expanding the flutter envelope of an aircraft that can use data collected from continuously varying flight conditions. By extracting the needed flutter damping and frequency values from an accelerating flight profile, it may be possible to substantially reduce the number of flight hours required for establishing the flutter envelope of an aircraft. However, we have determined that two fundamental issues must be addressed before a method for the continuous parametric identification of an accelerating aircraft can be developed.

The first issue deals with how the aeroelastic properties of an aircraft can be affected by a constant acceleration in a level flight or during maneuvering. In particular, is it possible to relate in a simple way the aeroelastic parameters measured in an accelerated flight to those measured in stabilized flight conditions? To the best of our knowledge, this issue has not yet been addressed in the literature.

The second issue is related to the fact that most if not all identification methods used in practice implicitly assume that the given aeroelastic system is linear and non-varying in time. Whether these methods can still be used to analyze accelerated flight data, or whether new methods are required for this purpose remains an open question.

During the first year of funding, we have addressed preliminary aspects of the above two issues by performing appropriate CFD based numerical simulations. More specifically,

we have considered a typical NACA 0012 wing section and investigated the effects of a horizontal acceleration on the aeroelastic response of this system. For this purpose, we had to upgrade our computational aeroelasticity capability to handle accelerated flight, which was by itself an interesting and rewarding research. We have reported on the aeroelastic results simulated in both cases of stabilized flight conditions and accelerated flight. We have compared these results and formulated preliminary conclusions regarding the theoretical feasibility of extracting the flutter envelope of an aircraft from an accelerated flight data.

This specific progress is documented in the following AIAA paper:

D. Rixen, C. Farhat, and L. Peterson, "Simulation of the Continuous Parametric Identification of an Accelerating Aeroelastic System," *37th Aerospace Sciences Meeting and Exhibit*, Reno, Nevada, January 12-15 (1999).

Motivated by our success for the NACA0012 airfoil, we have repeated our simulations of the continuous parameter identification of an accelerating aeroelastic system for a typical F16 wing section. We have designed this wing section from geometrical and structural data obtained from the Edwards AFB. The continuous parameter identification was simulated for the F16 typical wing section in accelerated flights with up to 0.05 Mach per second and for flight regimes extending from subsonic to supersonic. As shown in Figure 1, the aeroelastic parameters identified in accelerated flight are almost identical to those obtained in stabilized flight conditions. This work shows that the accelerated flight methodology is also applicable to a non-symmetric supersonic airfoil. In particular, the effectiveness of the accelerated flight approach remains good in the transonic region where the aeroelastic behaviour is highly non-linear. It was however not possible to match *perfectly* our numerical simulation results for the typical wing section with actual test results for the F16 (see Figure 1) because the available test data are for a loaded wing, whereas our typical wing model was derived from a clean wing model, and because the typical wing section approach is valid only for uniform, straight and high aspect ratio wings. However, the typical wing section properties can be tuned so that the numerical simulation results are closer to the flight test data (e.g. in Figure 2 we show the influence of the position of the elastic center). Further work will apply the accelerated flight methodology to a full 3-D aeroelastic model.

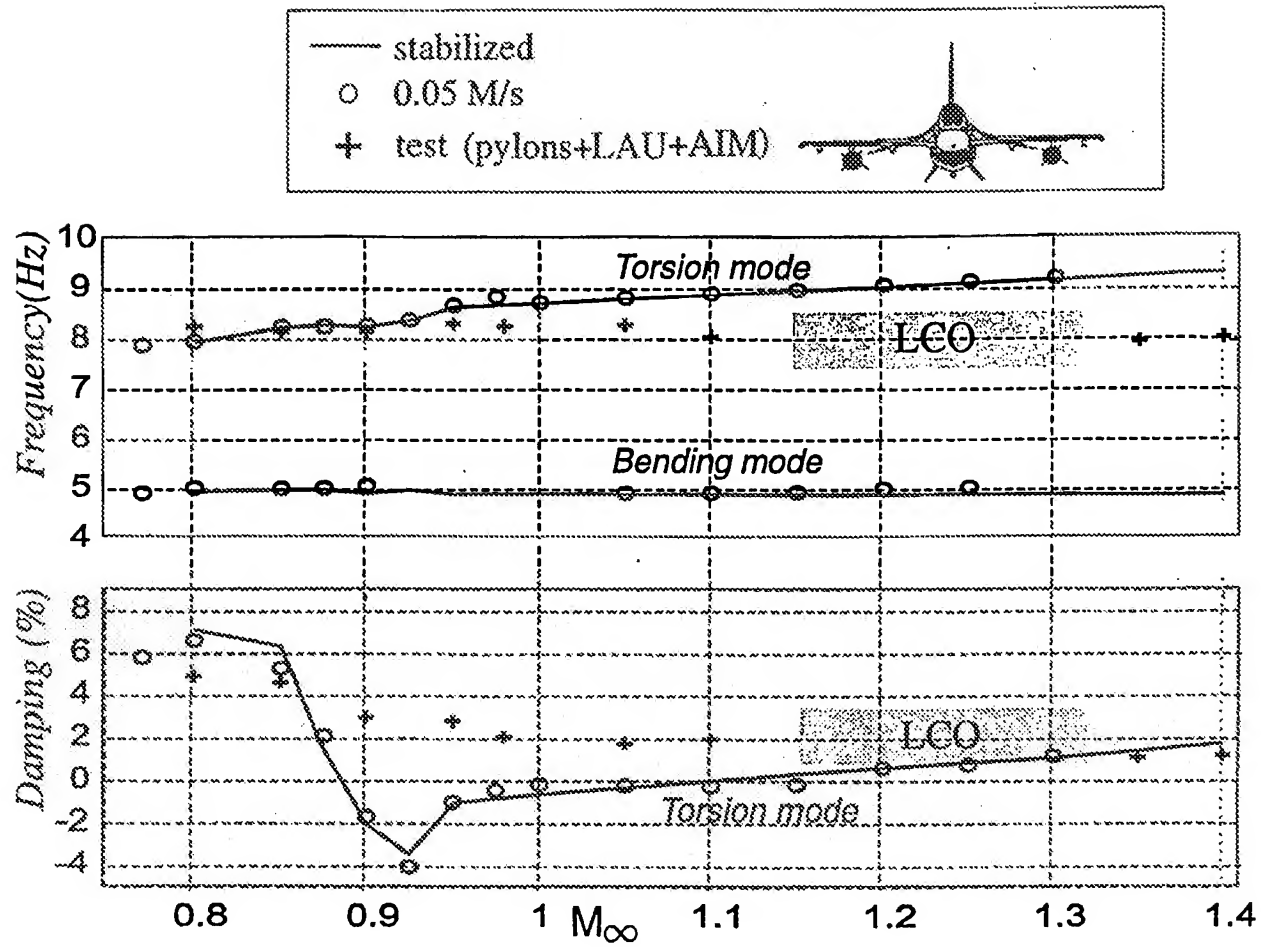


Figure 1. : identification on F16 typical wing section

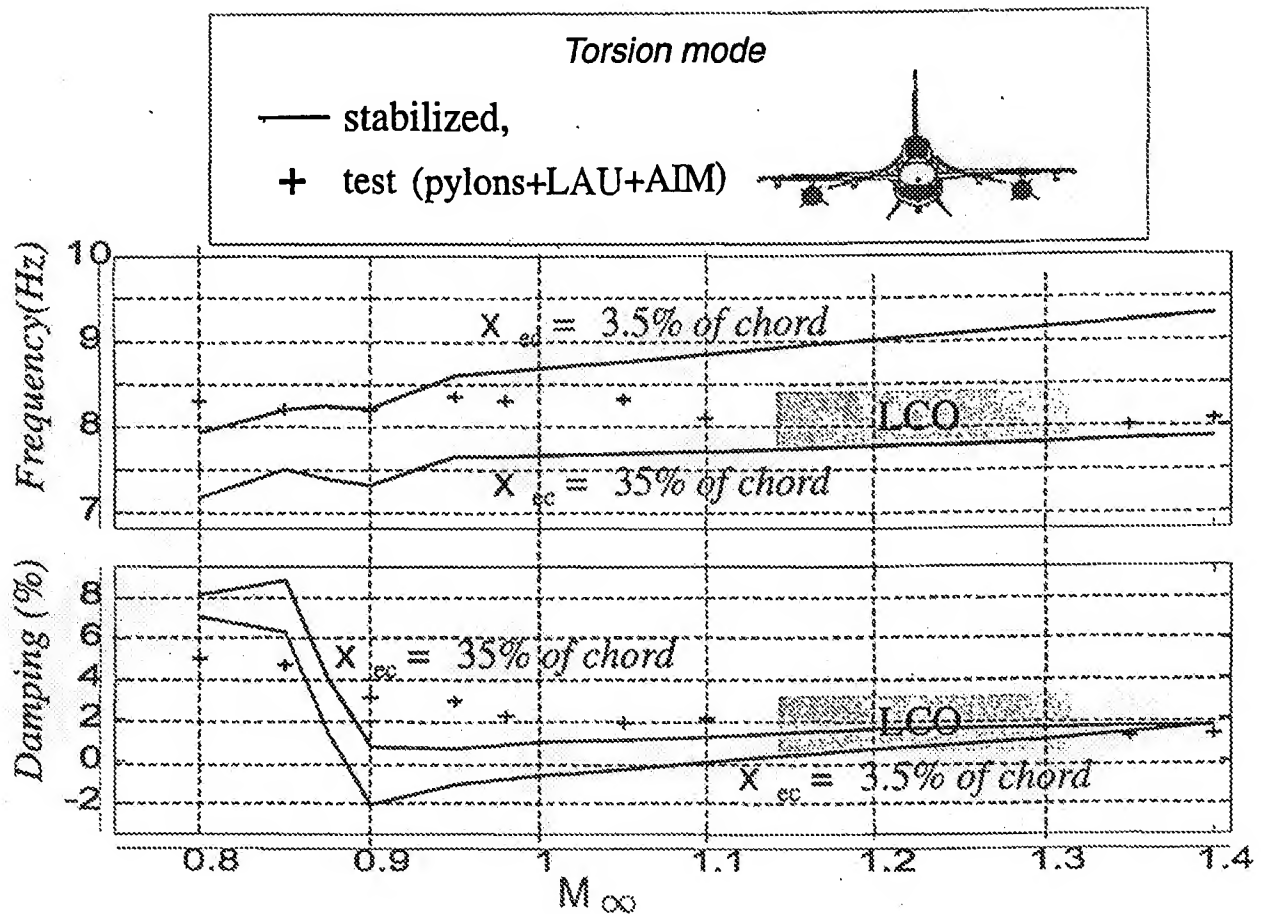


Figure 2. : model tuning

2.3. Design of an F16 advanced aeroelastic model

Because we envision applying our methods to an F16 fighter for which flight test data will be given to us by the Edwards AFB, we have acquired from Lockheed-Martin two different finite element models of an F16 aircraft version Block 50. The first model is a static one and therefore does not contain the mass distribution. The second model is a linear dynamic model which contains the needed mass information but is not adequate for stress analysis. We have begun converting these models to our software modules, refining them for more advanced aeroelastic computations, and combining the best of their features to construct a unified and advanced aeroelastic dynamic finite element model.

2.4. Interaction with the Air Force Flight Test Center at the Edwards AFB

During the first year of funding, we have had three meetings at the University of Colorado at Boulder with three representatives of the Flight Test Center at the Edwards AFB. During these meetings, we have reported on our progress, communicated our findings and conclusions, discussed technical details, and improved our understanding of some important issues related to our research and Air Force technical needs in these areas. We have also been in permanent contact with Flight Test Center personnel by phone and e-mail to acquire flight test and other data, and various grids and models.

3. Future work

Next, we plan to focus on the following activities:

Towards real time flutter analysis. The behavior of the fluid can be uniquely characterized by the Mach number and the angle of attack. Furthermore, using the approach advocated in the original proposal (Section 2.1.4), one can completely characterize the aerodynamic forces acting on an aeroelastic system by computing a specific set of canonical functions. Once these functions are determined for a given Mach number and a given angle of attack, the eigen solutions of the coupled aeroelastic problem can be computed for any value of the altitude, speed of sound, and any distribution of the structural mass and stiffness. Hence, we are currently working on developing the strategy for precomputing the canonical functions, expanding them for various Mach numbers and angles of attack using a discrete or other approximate form such as least-square fitting with exponential series or storing them using a compressed Laplace transform. Then, we will exploit them as needed to compute the eigen solutions of a target aeroelastic problem. Next, we plan to investigate two approaches for handling in real time changes in the Mach number and the angle of attack: a sensitivity based scheme, and curve fitting.

Continuous parameter identification of an F16 aeroelastic system. Motivated by our success for the F16 typical wing section, we are currently planning our simulations of the continuous parameter identification of an accelerating aeroelastic system for complete F16 (three-dimensional) configurations, with maneuvers.

4. Publications that have resulted from the first year of support

1. M. Lesoinne and C. Farhat, "A CFD Based Method for Solving Aeroelastic Eigenproblems in all Flight Regimes," *Journal of Aircraft*, (submitted for publication)
2. M. Lesoinne, M. Sarkis, U. Hetmaniuk, and C. Farhat, "A Linearized Method for Extracting Eigen Solutions of Aeroelastic Systems," *Computer Methods in Applied Mechanics and Engineering*, (in press)
3. X.-C. Cai, C. Farhat and M. Sarkis, "A Minimum Overlap Restricted Additive Schwarz Preconditioner and Applications in 3D Flow Simulations," *Contemporary Mathematics*, Vol. 218, pp. 478-484 (1998)
4. M. Lesoinne and C. Farhat, "Re-engineering of an Aeroelastic Code for Solving Eigen Problems in All Flight Regimes", ed. by K. D. Papailiou, D. Tsahalis, J. Périaux, C. Hirsch, and M. Pandolfi, *Computational Fluid Dynamics' 98, Proceedings of the Fourth European Computational Fluid Dynamics Conference*, Athens, Greece, pp. 1052-1061 (1998)
5. D. Rixen, C. Farhat, and L. Peterson, "Simulation of the Continuous Parametric Identification of an Accelerating Aeroelastic System," *37th Aerospace Sciences Meeting and Exhibit*, Reno, Nevada, January 12-15 (1999)

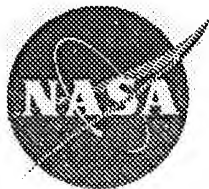
NASA Technical Memorandum 107681

1N-39
120378
P-87

**A STATE-OF-THE-ART ASSESSMENT
OF ACTIVE STRUCTURES**

Active Structures Technical Committee

September 1992



(NASA-TM-107681) A
STATE-OF-THE-ART ASSESSMENT OF
ACTIVE STRUCTURES (NASA) 87 p

N92-33580

Unclass

G3/39 0120878

National Aeronautics and
Space Administration
Langley Research Center
Hampton, Virginia 23665-5225

Preface

This report is prepared by the Active Structures Technical Committee of the NASA Langley Research Center. The committee reports to Dr. Michael F. Card, Chief Scientist at the Center. Members of the committee are:

Dr. Harry F. Benz
Dr. John D. Buckley
Mike C. Fox
Jennifer Heeg
Dr. C. Garnett Horner, chairperson
Dr. Seun K. Kahng
Henry L. Kelley
Charles J. Magurany
W. Hewitt Phillips
Dr. Robert S. Rogowski
Richard J. Silcox

Contents

Preface.....	1
Contents.....	2
Executive Summary.....	5
Acronyms.....	6
1 Introduction.....	8
2 Actuation Materials.....	10
2.1 Piezoelectric Materials.....	10
2.1.1 Benefits and Drawbacks.....	10
2.1.2 Configurations.....	10
2.1.2.1 Bimorph Bender Element.....	10
2.1.2.2 Out-of-Plane or Monomorph Element.....	11
2.1.2.3 Discretely Attached Elements.....	11
2.1.3 Piezoelectric Composites.....	11
2.1.4 Applications.....	11
2.1.5 Issues.....	13
2.2 Magnetostriction Materials.....	13
2.2.1 Benefits and Drawbacks.....	13
2.2.2 Configurations and Applications.....	14
2.3 Shape Memory Alloys.....	14
2.3.1 Benefits and Drawbacks.....	14
2.3.2 Configurations and Applications.....	15
2.4 Electrorheological Fluids.....	15
2.4.1 Benefits and Drawbacks.....	15
2.4.2 Configurations and Applications.....	16
2.5 Electrostriction Materials.....	17
2.5.1 Benefits and Drawbacks.....	17
2.5.2 Configurations and Applications.....	17
2.6 References.....	17
3 Sensory Materials.....	20
3.1 Fiber Optic Sensors.....	20
3.1.1 Introduction.....	20
3.1.2 Cure Monitoring.....	20
3.1.3 Structural monitoring.....	21
3.1.4 Non-Destructive Evaluation and Damage Detection.....	23
3.1.5 References.....	25
3.2 Dielectric Loss Sensors.....	29
3.2.1 Definition.....	29
3.2.2 Historical Perspective.....	29
3.2.3 Property Change.....	29
3.2.4 Weight and Torque.....	30
3.2.5 Electromagnetic Radiation and Heat Transfer.....	30
3.2.6 References.....	30
3.3 Piezoelectric Sensors.....	31

3.3.1 Overview.....	31
3.3.2 PE Materials/Applications.....	31
3.3.2.1 PE Film.....	31
3.3.2.2 PE Composites.....	32
3.3.2.3 Hydrophones.....	33
3.3.2.4 Ultrasonic Imaging.....	34
3.3.2.5 Vibration and Shape Control.....	34
3.3.3 References.....	35
3.4 Applications of Embedded Sensors in Aircraft.....	37
3.4.1 Introduction.....	37
3.4.2 Certification Tests.....	37
3.4.3 In-Flight Structural Monitoring.....	38
3.4.4 Load History Recording.....	39
3.4.5 Sensing of Feedback Quantities for Control.....	39
3.4.6 Aeronautical and Structural Research.....	41
3.4.7 References.....	41
3.5 Smart/Intelligent Sensors.....	42
3.5.1 Time-Frequency Analysis.....	44
3.5.2 Prediction of Dynamic Loads using Neural Networks.....	44
3.5.3 References.....	44
4 Control of Smart/Intelligent Structures.....	46
4.1 Introduction.....	46
4.2 Modern Control Approaches.....	49
4.2.1 Model Based Feedback Control Approaches.....	49
4.2.2 Active Vibration Control.....	50
4.2.3 Stochastics.....	50
4.2.4 Adaptive Control.....	50
4.2.5 Integrated Controls-Structures Design.....	51
4.3 Adaptive Feedforward Control Systems.....	51
4.4 Artificial Neural Networks.....	55
4.5 Modeling Requirements for Verification and Simulation.....	57
4.5.1 Non-Linear Properties.....	57
4.5.2 Modeling and Embedment Effect.....	57
4.5.3 Simulation and Verification.....	58
4.5.4 Zero-Gravity Issues.....	58
4.5.5 Modal Analysis.....	59
4.6 References.....	59
5 Recommendations for Future Research.....	67
5.1 Actuation Materials.....	67
5.2 Smart/Intelligent Sensors.....	67
5.3 Information Management.....	68
5.4 Applications.....	68
5.5 Research Environment.....	69
Appendix A. Proposed Structure Types.....	70
Appendix B. Piezoelectric Materials.....	71

Appendix C. Effect of Expansion and Contraction of the Surfaces on Shape of a Wedge-Shaped Trailing Edge.....	73
Appendix D. Comparisons of Adaptive Materials	77
Appendix E. Typical Applications of Piezoelectric Film (PVDF).....	79
Appendix F. Typical Properties of Piezoelectric Film (PVDF).....	82
Appendix G. Measured and calculated properties of (Pb, Ca)TiO ₃ ceramic	83
Appendix H. Piezoelectric Properties	84
Appendix I. Fatigue Loading Schedules.....	85

2. Donegan, James J., and Huss, Carl R.: Study of Some Effects of Structural Flexibility on the Longitudinal Motions and Loads as Obtained from Flight Measurements of a Swept-Wing Bomber. NACA RM L54L16, May 20, 1955.
3. Rhyne, Richard H.: Measurements of the Motions of a Large Swept-Wing Airplane in Rough Air. NACA TN 4310, Sept., 1958.
4. Rhyne, Richard H., and Murrow, Harold W.: Effects of Airplane Flexibility on Wind Strains in Rough Air at 500 Feet as Determined by Flight Tests of a Large Swept-Wing Airplane. NACA TN 4107, Sept., 1957.
5. Burris, P. M. and Bender, M. A.: - Aircraft Load Alleviation and Mode Stabilization (LAMS). AFFDL-TR-68-158, April , 1969.
6. Byrdsong, Thomas A., Adams, Richard R., and Sandford, Maynard C.: close Range Photogrammetric Measurement of Static Deflections of an Aeroelastic Supercritical Wing. NASA TM 4194, Dec., 1990.

3.5 Smart/Intelligent Sensors

A smart/intelligent sensor or an intelligent system of sensors/instruments is a critical element of a smart/intelligent structure. Definition of the words "Smart Sensor" has been evolving and expected to change its evolutionary processes with time. A smart sensor [1,2,3,4] may be considered as one that is capable of: (1) converting some form of environmental stimulus into an electrical signal; (2) providing signal conditioning; (3) executing commands and logical functions; (4) communicating through a bi-directional digital bus; (5) making solid decisions based on incomplete information gathered from multiple sensor inputs using fuzzy logic; and (6) performing such functions as health monitoring and auto-calibration.

Technology for the first five capabilities are already available, namely very large scale integration (VLSI) and micromachining/microtechnology. Some commercial sensors with such capabilities are already on the market, such sensors are CMOS based monolithic capacitive pressure sensors with signal conditioning circuit and micromachined silicon accelerometer with digital circuitry on the same chip. These sensors are inherently small and well suited for embedding as an integral part of a smart structure.

A new type of an acoustic transducer array [5] has been developed using polyvinylidene difluoride (PVF2) as a sensing material which is placed on a metal-oxide-semiconductor field-effect transistor (MOSFET). A linear 34-element receiving transducer array has been built and evaluated. A radio frequency (RF) telemetry system for powering and control of smart sensor has been reported [6]. The sensor is a single channel implantable microstimulator for neuromuscular stimulator with a 12 volt rechargeable battery which is periodically charged using a

suppress flutter. A flutter mode could be destabilized by means of a weight on the wing, resulting in flutter within the normal flight envelope. The automatic system was used to stabilize the flutter mode. In case of failure of the automatic system, the weight could be dropped to restore stability. The results of this project are given in references [5].

While the LAMS project was intended to demonstrate the feasibility of in-flight flutter suppression, it was limited in its capabilities by the state of the art of servomechanism design, since it depended on analog systems. More complex instrumentation and on-board calculation is required to make such a system feasible. As yet, no service airplanes have appeared with automatic flutter suppression systems. Among the problems of a practical installation is the separation of structural oscillations due to rough air from those due to flutter. It is possible that the greater capabilities provided by embedded sensors would make such a system feasible.

3.4.6 Aeronautical and Structural Research

The difficulty of instrumenting an airplane for research purposes has already been pointed out. If the distributed instrumentation were incorporated in the materials used in the structure, the airplane could be equipped for many types of studies not contemplated at the time of the original design. Even wind-tunnel models could benefit from these techniques. A study in reference [6] describes an optical system for measuring the static deflections of a wing in the tunnel. Obtaining and evaluating the data by this method is a long and tedious process. Embedded instrumentation would allow computer analyses of the data, and might give sufficient coverage to obtain these results.

The measurement of pressure distribution is very important subject in aeronautical research. As yet, pressure sensors have not been developed that can be incorporated in the materials used in the structure. If such sensors were developed, many capabilities would be presented of value both for research and service operations. Pressure capsules attached to embedded conductors might also simplify installations, but the capsules would have to be very thin and smooth to avoid disturbing a laminar boundary layer. The use of embedded devices for pressure measurements is a desirable subject for future research.

3.4.7 References

1. Skopinski, T. H., Aiken, William S. Jr., and Houston, Wilber B.: Calibration of Strain-Gage Installations in Aircraft Structures for the Measurement of Flight Loads. NACA TN 2993, Aug., 1953.

source of unreliability. All of this equipment is provided in triplicate or quadruplicate, with voting to rule out failed components, in order to provide the high reliability required in a control system.

Although the redundancy provided in an modern airplane required a great deal of design effort and installation difficulty, the degree of redundancy is negligible compared to that in the nervous systems of living creatures. Feedback sensors are provided for every hair and muscle fiber. The destruction of large numbers of these sensors, though it gives warning of a problem in the form of pain, may not interfere with normal activities. Such a picture forms a goal for the use of embedded sensors in airplanes. Modern techniques using distributed sensors give the possibility to emulate the capabilities of living creatures, as well as possibly to reduce the installation problems of providing a control system separate from the primary structure.

A field of research that has received considerable emphasis is the design of active systems to damp structural oscillations or to suppress flutter. Before such systems can be considered, however, it is necessary to have instrumentation to measure in flight the oscillation mode shapes and stresses throughout the structure. As soon as large, flexible airplanes became available, the NACA undertook studies to investigate the techniques required to obtain such data. A series of tests were conducted on an instrumented B-47 airplane, starting in 1952, to measure wing motions and stresses in dynamic maneuvers involving structural oscillations. The airplane was instrumented by installing strain gages on the front and rear spars at four stations on the span, in addition to an optical instrument to measure structural displacements at these stations and at various locations on the fuselage and tail. The standard research instrumentation to measure airplane rigid-body motions was also installed. The installation of equipment was very difficult because of the lack of accessibility to many parts of the structure. Installing the wiring and strain gages in the wing required over a year's work at Langley, after which flight tests were conducted at the High-speed Flight Research Center (now the Dryden Flight Research Facility) at Edwards, California.

A number of reports were published on the techniques of strain-gage instrumentation and on the B-47 tests. The method of calibration of strain gages is presented in ref. [1]. Presumably, similar techniques could be used in the case of distributed instrumentation. Some results of the flight tests on the B-47 are given in references [2-4].

An important application of measurements of dynamic oscillations of an airplane structure is the prevention of flutter at speeds beyond the flutter speed of the uncontrolled vehicle. Such a system might be desirable because it could result in lower structural weight or give the designer more freedom in choosing a configuration. A research study of this possibility was made by the Air Force in the LAMS project, an acronym for "load alleviation and mode stabilization". A B-52 was fitted with instrumentation and servomechanisms to operate the controls to

airplane structure are difficult to inspect, however, and a crack may go unnoticed until it causes failure of member. Corrosion is even more insidious, because it can attack a large number of rivets or other members simultaneously without visible effects. Some method to monitor such deterioration on a continuous basis would be very desirable.

In airplanes with composite structures, the possibility exists to install distributed sensors in the form of optical fibers or other devices in sufficient numbers to give a detailed coverage of the structure. Such sensors could have multiple uses, but one simple application would be to detect cracks that break the sensors in a localized region. In this way, cracks could be detected on a continuing basis and repairs could be made before the condition became serious. ✓

3.4.4 Load History Recording

Recording the history of loads experienced by an airplane in flight is a traditional method to obtain data applicable to the design of new airplanes. Instruments such as VG and VGH recorders have been distributed by NACA and NASA to the airplanes and military services to obtain data in service operations. Usually, only a few airplanes in a fleet can be so outfitted. In more recent times, flight recorders are carried by all commercial airplanes. These instrumented record on a continuous tape so that only the last half hour of flight is available on the record. Usually these records are examined only in case of an accident.

Continuous recording of data from distributed sensors would allow a much more detailed study of service loads. These data would be of particular interest for study of fatigue, because the many smaller loads as well as the few large loads would be recorded. Also, many parts of the structure susceptible to fatigue loads, but not usually investigated in service airplanes, could be studied. These members could include hinge brackets, wing ribs, control rods, etc. With the availability of such data, future airplanes could be designed with less excess weight now required to provide for the margin of error in knowledge of the loads.

3.4.5 Sensing of Feedback Quantities for Control

Control of the rigid-body motions of an airplane is usually accomplished by using a set of instruments located in the cockpit area. These instruments, measuring quantities such as airplane attitude, accelerations, angular velocities, etc. form the nerve center of the airplane and are used to provide feedback signals for the control system as well as to provide cockpit displays for the pilot. Many quantities required in modern airplane control systems, however, can not be measured at a central location and require remote sensors connected by wiring, or, in the case of digital systems, a data bus, to the central computer. For example, angle of attack is measured using a sensor either in the nose or on the wing, sideslip is measured by vanes under the fuselage, control positions are measured with pickups on the control surfaces, etc. These remote sensors and their associated wiring form a major

3.4.2 Certification Tests

Each new airplane is required to go through certification tests to verify that it meets its requirements for strength, performance, maneuverability, and handling qualities. These tests are hazardous because the limits of the flight envelope are being explored while the airplane is still new and untried. Present methods to minimize danger consist in gradually increasing the limits of the flight envelope, while examining the data on motions and loads with specially installed instrumentation. The instrumentation is expensive and may be rather minimal in its coverage because the difficulty of fitting additional equipment in an already crowded airframe. It is quite possible that a critical problem may be missed because of inadequate measurements.

The rationale of the certification tests is that the load distribution, stability, and stalling characteristics have been predicted by theory and by wind-tunnel testing. As a result, at a given load factor the distribution of structural loads can be predicted. Measurements at a few points can be considered to validate the adequacy of the entire structure. In practice, however, the load distribution in flight may be different from that predicted. Structural failures may therefore occur at localized regions where the loads have been predicted incorrectly. In general, there is no method to measure the detailed load distribution during certification tests.

Further problems may occur during dynamic maneuvers because of aeroelastic distortions or structural oscillations. Such problems may be noted by the test instrumentation, but the detailed analysis of the problem to determine a cure requires knowledge of mode shapes that cannot be measured by the limited test instrumentation.

The availability of distributed sensors with on-line analysis of the data would greatly enhance the safety of testing, while eliminating the expense of special test instrumentation. In general, even if not all the sensors could be hooked up at once, detailed studies of localized trouble spots could be made, and mode shapes of the entire structure could be measured to enable checks of dynamic stability predicted from previous analysis and simulation studies.

3.4.3 In-Flight Structural Monitoring

When an airplane is placed in service following completion of the certification tests, the assumption is made that airplanes build to the same design will be free from structural failure. In most cases, the loads encountered in service are less than the values successfully demonstrated, so that the airplane does not often encounter catastrophic failure in flight. More subtle forms of failure due to fatigue and corrosion are, however, a source of concern. The method of checking for fatigue cracks is to inspect the airplane at periodic intervals, using magnetic or x-ray techniques, to locate incipient cracks before they become serious. Many parts of an

23. S. Im and S.N. Atluri, "Effects of a Piezo-Actuator on a Finitely Deformed Beam Subjected to General Loading," *AIAA J.*, 27 (12), 1800-1807, (1989).
24. B.K. Wada, J.L. Fanson and E.F. Crawley, "Adaptive Structures," *Mechanical Engineering*, Vol. 112, No. 11, pp. 41-46, Nov. (1990).
25. D.W. Miller, S.A. Collins, and S.P. Peltzman, "Development of Spatially Convolution Sensors for Structural Applications," *Proc. of the 31st AIAA/ASME/ASCE/AHS Structures, Structural Dynamics and Materials Conf.*, Long Beach, Ca., April 2-4, Paper No. AIAA-90-0949, (1990).
26. Fanson, Anderson, Rapp, "Active Structures for use in Precision Control of Large Optical Systems," *Optical Engr.*, vol. 29 No. 11, 1320, (1990).
27. C.K. Lee, "Laminated Piezopolymer Plates for Torsion and Bending Sensors and Actuators," *J. Acoustical Society of America*, Vol. 85, No. 6, pp. 2432-2439, (1989).
28. Piezo Systems Product Catalog, Piezo Systems, Inc., Cambridge, Ma., (1990).

3.4 Applications of Embedded Sensors in Aircraft

3.4.1 Introduction

One of the promising applications of new techniques and materials involved in the field of smart structures is the provision of embedded sensors in the structure. Because of the small dimensions of these devices and ability to install them during construction of the airplane, the sensors could conceivably be much more numerous and widely distributed than the presently used discrete sensors. Such devices are currently in the research stage, and are not available for service use. This discussion is intended to show possible desirable applications of these techniques.

The applications of embedded sensors considered herein are as follows:

- Certification tests
- In-flight structural monitoring
- Load history recording
- Sensing of feedback quantities for control
- Aeronautical and structural research

Much of the discussion is based on earlier experience in flight research on instrumented airplanes. Because of the need for more extensive instrumentation in these tests than in service use, some of the applications have been explored, or at least studied in a preliminary way. The availability of distributed sensors, together with the data-handling capability of present-day computers, would allow routine use of techniques that have previously been considered only in research projects.

10. J. de Luis and E. Crawley, "Experimental Results of Active Control on a Prototype Intelligent Structure," in *31st AIAA SDM Dynamics Spec. Conf. Proc.* AIAA paper 90-1163 (1990).
11. R.E. Newnham, Q.C. Xu, S. Kumar, "Smart Ceramics," *Ferroelectrics*, 102, 259-266, (1990).
12. R.Y. Ting, "The Hydroacoustic Behavior of Piezoelectric Materials," *Ferroelectrics* 102, 215-224 (1990).
13. Collins, Padilla, H. von Flotow, "Design, Manufacture, and Application to Space Robotics of Distributed Piezoelectric Film Sensors," *31st Structures, Structural Dynamics and Materials Conference*, AIAA paper, (1990).
14. H. Takeuchi, H. Masuzawa, C. Nakaya and Y. Ito, "Relaxor Ferroelectric Transducers," *Proc. IEEE Ultrasonics Symp.*, pp. 697-705 (1990).
15. R.C. Buchanan, "Ceramic Materials for Electronics," 2nd edition, Marcel Dekker, Inc. (1991).
16. A. Preumont, J. Dufour, and C. Malekian, "Active Damping by a Local Force Feedback with Piezoelectric Actuators," *AIAA/ASME/ASCE/AHS/ASC Structures, Structural Dynamics, and Materials Conference*, 32nd, Baltimore, MD, Apr. 8-10, (1991).
17. T. W. Lim, "Sensor Placement for On-Orbit Modal Testing," *AIAA/ASME/ASCE/AHS/ASC Structures, Structural Dynamics, and Materials Conference*, 32nd, Baltimore, MD, Apr. 8-10, 1991.
18. R.E. Newnham, G.R. Ruschau, "Smart Electroceramics," *J. Am. Ceram. Soc.*, 74 (3), 463-480, (1991).
19. R.E. Newnham, Q.C. Xu, S. Kumar and L.E. Cross, "Smart Ceramics," *J. Wave-Material Interaction*, 4, 3-10, (1989).
20. J. Fanson, G. Blackwood, and C. Chu, "Active Member Control of Precision Structures," in *30th AIAA SDM Conf. Proc.*, AIAA paper 89, 1329, (1989).
21. T. Bailey and J.E. Hubbard, "Distributed Piezoelectric-Polymer Active Vibration Control of a Cantilever Beam," *J. Guidance Control and Dynamics*, 8 (5), 605-611, (1985).
22. E.H. Anderson, D.M. Moore, and J.L. Fanson, "Development of an Active Member Using Piezoelectric and Electrostrictive Actuation for Control of Precision Structures," *AIAA SDM Conf.*, Part 4, April 2-4, (1990).

For the U.S. Army, Georgia Tech researchers have been working on ways to improve helicopter blades. PE film sensors and shape memory alloy have been bonded to beam models of the blades. By inducing appropriate twisting effects, smart helicopter blades can vibrate less and be quieter.

Boeing has also embedded PE ceramic sensor/actuators in an aluminum beam and has demonstrated active damping. Their research topics include developing attachment adhesive at the piezoelectric interface which will improve feedforward response, reducing piezoelectric fatigue and microcracking, coating thin piezoelectric material on graphite fibers, and integrating piezoelectric materials with electronics.

3.3.3 References

1. W.A. Smith, "The Role of Piezocomposites in Ultrasonic Transducers," *Proc. IEEE Ultrasonics Symp.*, pp. 755-766 (1990).
2. S. Hanagud, M.W. Obal, and A.J. Calise, "Optimal Vibration Control by the Use of Piezoceramic Sensors and Actuators," *28th AIAA SDM Dynamics Specialists Conf. Proc.*, AIAA paper 87-987 (1987).
3. Anderson, Moore, Fanson, "Development of an Active Truss Element for Control of Precision Structures," *Optical Engr.*, vol. 29 No 11, 1333, (1990).
4. Kynar Piezo Film Technical Manual, *Atochem Sensors, Inc.* Valley Forge, Pa. (1991).
5. E. Crawley and K. Lazarus, "Induced Strain Actuation of Isotropic and Anisotropic Plates," in *30th AIAA SDM Conf. Proc.*, AIAA paper 89-1326 (1989).
6. W.A. Smith, A.A. Shaulov and B.A. Auld, "Design of Piezocomposites for Ultrasonic Transducers," *Ferroelectrics*, 91, 155-162 (1989).
7. R.Y. Ting, A.A. Shaulov and W.A. Smith, "PE Properties of 1-3 Composites of a Calcium Modified Lead Titanate in Epoxy Resins," *Proc. IEEE Ultrasonics Symp.*, pp. 707-710 (1990).
8. "Green Fiber Fabrication Method for PE Composites;" ONR contract # N00014-91-C-0036 to Ceramics Process Systems, Milford, Mass. (1991).
9. H. Takeuchi, H. Masuzawa, C. Nakaya and Y. Ito, "Medical Ultrasonic Probe Using Electrostrictive-Ceramics/Polymer Composite," *Proc. IEEE Ultrasonics Symp.*, pp. 705-708 (1989).

sintered into highly dense ceramic filaments and rods. Any sinterable ceramic or metal powder can be used in this process to produce a variety of monofilament shapes and sizes. Fiber can be spun into various diameters (3 to 50 mil) and cross-sectional shapes, such as hollow tubes, square and rectangular, and others. These fibers are used to make d_{33} piezocomposites. After the epoxy casting and cure the PE composite is sliced, ground and polished. Air-dried silver is applied to the composites flat surface followed by poling in an oil bath at 1.6 KV/MM, 120°C for 15 min. Piezoelectric measurements of this system were conducted at the Materials Research Laboratory, Pennsylvania State University, and are shown in Appendix H. The effect of varying fiber/resin type, volume fraction, and fiber diameter size (among other factors) on the resulting PE properties is an exciting area of research.

3.3.2.4 Ultrasonic Imaging

A PE fiber/epoxy composite has been developed for medical ultrasonic imaging applications [9]. The PZT fiber volume is greater than 65%. This gives the material a high electromechanical coupling coefficient (k_t) for needed high sensitivity. The low compliance polymer allows a relatively low acoustic impedance to match that of tissue for medical imaging. The requirements for this application can not be met by monolithic PZT (high coupling coefficient/ high acoustic impedance) or PE polymers (low acoustic-impedance/low coupling coefficient) alone.

3.3.2.5 Vibration and Shape Control

Smart strut technology for application to spacecraft vibration using embedded PE sensors and actuators in graphite/epoxy structures (d_{13} actuation) is being studied at MIT, TRW, and Boeing, among others. At MIT, a composite panel with embedded actuation was constructed and tested. The graphite/epoxy plate contains 32 PE actuators and localized PE sensors and accelerometers, incorporated into the structure by making small cutouts in individual graphite/epoxy plies during layup. Test results indicate that the PE ceramics and connecting wires caused only 20% tensile strength reduction in composite beams that could be excited or damped with these inserted materials. MIT has also developed FEA models to strategically locate PE actuators/sensors in high-strain regions of the structure. Their models also aid in the selection of ceramic modulus, most compatible with the structure.

TRW has embedded thin PZT actuator and sensor wafers in graphite/epoxy, polycyanate, and thermoplastic members. These have then been subjected to fatigue and thermal cycling. It was found that fatigue loading, at less than 1500 microstrain, actually enhanced the actuator/sensor feedforward by 1-10% (see Appendix I). This is most likely due to the degraded stiffness of the laminate being pushed upon. Beyond 1500 microstrain, a deterioration of 12% feedforward resulted. Greater deterioration to feedforward resulted from thermal cycling (10-30%), indicating the design need to lower the coefficient of thermal expansion mismatch of materials.

3.3.2.2 PE Composites

PE composites may generally be described as multiple-phase systems in which the overall PE properties that result from the composition can not be obtained from any known single-phase material. A PE composite may be designed to have unique properties that are best suited to a specific application. These properties include the dielectric constant, PE coefficients (d_{ij}), voltage coefficients (g_{ij}), PE coupling factors (k_{ij}), density and degree of brittleness, among others. Monolithic PE ceramics, although having excellent electromechanical coupling qualities, are too brittle for hydrophone use and have too high an acoustic impedance for ultrasonic imaging devices. However selected properties from these ceramics may be derived by incorporating them into a composite design. This typically involves a PE ceramic in the form of a rod, fiber or powder embedded in a resin matrix. The ceramic provides the electromechanical coupling required while the matrix compliance may be tailored to the application through proper resin selection. Some of the developments in this area are discussed as follows.

3.3.2.3 Hydrophones

A considerable amount of work has been done through The Office of Naval Research (ONR) and Penn State University toward the development of piezocomposites for hydrophones [6]. A hydrophone is an underwater transducer used to detect sound. The "figure of merit" for hydrophone performance is the product of the hydrostatic piezoelectric coefficient, d_h , times the hydrostatic voltage coefficient, g_h . Other desirable properties for a hydrophone are low density for better acoustical matching with water, little or no variation of the hydrostatic piezoelectric coefficient and the hydrostatic voltage coefficient with pressure, temperature or frequency, and high compliance and flexibility so the transducer can withstand mechanical shock and conform to any surface. A recent study of calcium doped PbTiO₃ (PT) rods in two types of epoxy polymers showed that the hydrostatic piezoelectric coefficient of the composites increased with increasing ceramic volume fraction (see Appendix G and reference 8). For 20% PT rod loading, the hydrostatic voltage coefficient values at room temperature were 67 mV-m/N with the stiffer epoxy and 50 mV-m/N with the more compliant epoxy. These values compare to 30 mV-m/N for the monolithic ceramic PT and 2 to 3 mV-m/N for monolithic PZT. The hydroacoustic response of the composite was found to be frequency independent from 100 Hz to 6 kHz. These results suggest that piezoelectric composites represent a class of promising new materials for underwater acoustic applications.

Another form of piezocomposites, being considered for sonar detection is being developed using PE fibers. CPS Superconductor, Milford Ma. has developed a process to fabricate PE fiber. Commercially available PZT 5H powder is compounded with a proprietary polymer system and extruded at an elevated temperature (melt spun "green fiber"). The polymer is removed by heating and the ceramic powder is

Polymeric PE films are the most recently discovered PE material and the most widely used as sensing devices [4]. They convert a mechanical force to an electrical response and, conversely, an electrical signal to a mechanical motion. They are more pliant, flexible, tough and lightweight than previously known piezoelectric materials. The most widely used PE film is based on polyvinylidene difluoride (PVDF), which has the highest PE and pyroelectric activities of any known polymer (Appendix E). High PE response is associated with the polar form of the polymer in which the hydrogen and fluorine atoms are arranged to give the maximum dipole moment per unit molecular cell. This arrangement is produced by means of treating the material in an intense electric field. The resulting product exhibits a large net polarization which gives the film its high PE activity. The level of PE activity is defined by the piezoelectric strain and stress constants, d_{31} and g_{31} respectively. By definition, the first subscript refers to the axis of polarization and the second to the axis of induced stress or strain. Typical properties of PE film (PVDF) are listed in Appendix F. A discussion of some applications follows.

In aircraft concepts designers have been studying ways to change the shape and stiffness of wings according to flight conditions. The current Air Force "smart skins" program deals with the incorporation of sensors and actuators within composite aircraft panel structures. Researchers at MIT spatially distributed PVDF film, bounded to a steel beam structure, such that the output was selectively proportional to a particular deformation pattern [5]. In this manner, the PE film served as "modal sensors" capable of supplying information on individual dynamic mode shapes. This direct measurement of the natural modes of vibration could help eliminate control system estimation techniques based on complex algorithms that decompose a vibration into these natural modes. These techniques are often limited in accuracy and dynamic response.

Innovative Dynamics, Ithaca, NY has proposed an in-flight aircraft deicing system using PE film to sense changes in wing-vibration signature that result from ice build-up. If the system detects ice, it triggers an eddy-current actuator to "ping" the wing, knocking the ice loose. The flexible PE film remained intact, whereas the ridged PE ceramics were subject to breakage when the wing was pinged. Innovative Dynamics is also applying PE films for acoustic-signature mapping of aging aircraft structures. Eddy-current actuators are used to "ping" the structure, while the flexible PE film monitors vibrations, sending an electric signal proportional to the pressure of the vibration. Changes in the acoustic-signature map are used to detect rivet-line corrosion, fatigue cracks, loosening engine mounts and attachments. At Westinghouse Electric Corp., PE ceramics are placed on waveguides and embedded into composite structures representative of submarine hulls. Acoustic signals generated by cracking or delamination of the composite are transmitted by the wave guides to the PE ceramics which convert the impulses to electric signals allowing location of the fault. PE film is suggested for vibration-damping systems in air-conditioning ducts, fuselage noise-and vibration control, and sound damping of large truck bodies.

6. Gast, Th.: Thermal Analysis, Vol. 1, *Proceedings Third Icta Davos* (1971), p. 235-241.
7. Gast, Th. and Koppe, K.: "Simultaneous Measurement of Weight and Torque in Controlled Atmospheres By Magnetic Suspension," *Journal of Vacuum Science Technology*, 15(2), (March/April 1978).
8. Burdick, G.A. and Hickman, T.G.: "Technique For Measuring Dielectric Loss Tangent," *The Review of Scientific Instruments*, Vol. 37, No. 8 (August 1966).

3.3 Piezoelectric Sensors

3.3.1 Overview

Considerable research has been conducted by aerospace and commercial industries in the development of piezoelectric (PE) materials as sensors for a wide range of applications. Defense applications include submarine hull hydrophones for detecting sonar and active noise suppression [1], acoustic-signature health monitoring for aging aircraft, in-flight deicing and aeroelastic tailoring, vibration suppression for helicopter blades [2], detonators and shock wave gages, to name a few. Some of the many commercial uses of PE sensors/actuator systems are shown in Appendix E.

Some of NASA's future space missions will require challenging material and design developments. Structures composed of antennas, reflectors, optical benches, telescopes, optical interferometers and truss members will require high dimensional control, on the order of nanometers (in some cases picometers) over very large distances, up to a 100 meters [3]. These will require precision pointing, shape control and rapid retargeting. Once initial alignment is attained, precision will have to be maintained in the face of on-board disturbances and temperature variations. For truss structure, the active strut member must be able to carry normal loads while also able to sense and damp out disturbances through actuation. Since deflection levels may not exceed a few micrometers at a maximum, strain sensing/actuation is considered the most effective approach. Candidate materials include piezoelectrics, electrostrictors, and magnetostrictors. More details of PE uses as sensors follows.

3.3.2 PE Materials/Applications

3.3.2.1 PE Film

PE films may be fabricated from ceramic or polymeric material. PE ceramic films are being developed for memory devices and data storage, which requires deposition in thin film form for application in silicon circuits. PE ceramic films/plates are also being studied as actuators in structural composites.

3.2.4 Weight and Torque

Some years ago, Gast reported on an electromagnetic balance which was combined with an electrostatic attachment for measuring torque [6]. Conceivable applications of an instrument would include measurement of density and viscosity, determination of permittivity and dielectric loss, and other combinations of properties that are functions of temperature, pressure, and other variables.

Additional work has been performed by using a magnetic suspension balance system to measure weight and torque [7]. This can be accomplished simply by using a pair of mutually attracting horseshoe magnets where the poles are kept at a predetermined distance by automatic control. The lower magnet carries two vanes of copper sheet, aligned in a horizontal plane, which are in the sensitivity range of symmetrically arranged inductive sensors fixed to the upper magnets. The sensors are connected in a Wheatstone bridge in such a manner that the distance and angular position of the vanes under load can be measured simultaneously giving weight and torque. For more details and further explanation, see Reference [7].

3.2.5 Electromagnetic Radiation and Heat Transfer

A technique for measuring dielectric loss tangents has been developed in connection with measuring various parameters of pyroelectric materials. These materials have the potential as detectors of electromagnetic radiation and sensors in heat transfer measurements. This technique uses well-known concepts and requires only conventional laboratory equipment. The technique allows for measuring dielectric loss tangents in the range of 0.1 to 2 with frequencies from 15 Hz to the megahertz range. Additional information is found in Reference [8].

3.2.6 References

1. Senturia, S.D. and Sheppard, N.F., Jr: "Dielectric Analysis of Thermoset Cure," *Advances in Polymer Science*, Vol. 80, 1, (1986).
2. Kienle, R.H. and Race, H.H.: "The Electrical, Chemical and Physical Properties of Alkyd Resins," *Trans. Electrochem. Soc.*, 65,87,(1934).
3. Gotro, Jeffery and Yandrasits, Michael: "Simultaneous Dielectric and Dynamic Mechanical Analysis of Thermosetting Polymers," *Polymer Engineering and Science*, Vol. 29, No. 5, (March 1989).
4. Senturia, S. and Garverick, S.: US Patent No. 4,423,371.
5. Senturia, S., Sheppard, N., Lee, H., and Day, D.: (*J. Phys. D*), 1, 117, (1968).

3.2 Dielectric Loss Sensors

3.2.1 Definition

Dielectric loss sensors function as the name implies; they measure the change in the electric field for a specified material or specimen. The sensor works similar to a parallel capacitor in that it senses loss or change in current or properties. Dielectric measurements are performed by placing a sample of the material to be studied between two conducting electrodes, applying a time-varying voltage between the electrodes, and measuring the resulting time-varying current. For further explanation of dielectric measuring techniques, see Reference [1].

3.2.2 Historical Perspective

Measurements of dielectric properties have been used to monitor chemical reactions in organic materials for more than fifty years. In 1934, Kienle and Race [2] reported the use of dielectric measurements to study polyesterification reactions. Many of the major issues were identified in that early paper, such as the fact that ionic conductivity often dominates the observed dielectric properties, the correlation between viscosity and conductivity early in the curing process, and the possible contribution of orientable dipoles and sample heterogeneities to measured dielectric properties.

Many other papers were written since 1934 documenting these types of techniques to measure chemical change. The description of some of these findings as it relates to the curing of thermosets can be found in Reference [1].

3.2.3 Property Change

In recent years, dielectric measurements have been utilized to study the curing of thermosets. Efforts have been made to develop a method to simultaneously measure the viscosity and dielectric properties during various cure schedules to understand the relationships [3]. A commercially available, interdigitated comb electrode dielectric sensor [4,5] was used for the dielectric measurements for the studies of Reference [3]. The Micromet Eumetric System II microdielectrometer was embedded in the material and was capable of operation in a frequency range of 0.005 to 10,000 Hz.

Reference [3] explains the usefulness of measuring the dielectric loss factor during the curing process as it relates to ionic concentration and mobility. The ion mobility is a direct function of the polymer segment mobility which change dramatically as the resin cures. Therefore by monitoring the dielectric loss, the cure process can be tracked.

Additional information on dielectric loss sensors related to thermosets can be found in Reference [1].

34. Rowe, W. J., Rausch, E. O. and Dean, P. D., "Embedded Optical Fiber Strain Sensor For Composite Structure Applications," *Proceedings SPIE*, Vol. 718, 1987, p. 266.
35. Safaai-Jazi, A. and Claus, R. O. "Synthesis of interference patterns in few-mode optical fibers," *Proceedings SPIE*, Vol. 986, 1988, p. 180 .
36. Schoenwald, J. S. and Beckham, P. M., "Distributed fiber-optic sensor for passive and active stabilization of large structures," *Review of Progress in Quantitative Nondestructive Evaluation*, Vol. 7, edited by D. O. Thompson and D. E. Chimenti, Plenum Press, New York, 1988, p. 565.
37. Senturia, S. D. et. al., "In-situ Measurement of the Properties of Curing Systems with Microdielectrometry", *Journal of Adhesion*, Vol. 15, 1982, p.69.
38. Sirkis, J. S. and Haslach, H. W., Jr., "Strain Component Separation in Surface-Mounted Interferometric Optical Fiber Strain Sensors," *Proceedings SPIE*, Vol. 1170, 1989, in press.
39. Spillman, W. B. Jr., Fuhr, P. L. and Anderson, B. L. "Performance of integrated source/detector combinations for smart skins incoherent optical frequency domain reflectometry (IOFDR) distributed fiber optic sensors," *Proceedings SPIE*, Vol. 986, 1988, p. 106.
40. Sun, K. J. and Winfree, W. P., "Propagation of Acoustic Waves in a Copper Wire Embedded in a Curing Epoxy," *Proceedings of the IEEE Ultrasonics Symposium*, 1987, p. 439.
41. Takahashi, K., "Sensor Materials for the Future: Intelligent Materials," *Sensors and Actuators*, Vol. 13, 1988, p. 3.
42. Udd, Eric, Fiber Optic Smart Structures and Skins, *Proceedings SPIE*, Vol. 986, The International Society for Optical Engineering, Bellingham, Washington, 1988.
43. Waite, S. R. and Sage, G. N., "The Failure of Optical Fibres Embedded in Composite Materials," *Composites*, Vol. 19, 1988, p. 288.
44. Zimmermann, B. D., Murphy, K. A. and Claus, R. O. "Local strain measurements using optical fiber splices and time domain reflectometry," *Review of Progress in Quantitative Nondestructive Evaluation*, Vol. 7, edited by D. O. Thompson and D. E. Chimenti, Plenum Press, New York, 1988, p. 553.

23. Hofer, B., "Fibre Optic Damage Detection in Composite Structures ", *Composites*, September, 1987, p. 309.
24. Kranbuehl, D., Delos, S., Hoff, M., Haverty, P., Hoffman, R., Godfrey, J. and Freeman, W., "Frequency Dependent Impedance Analysis: Monitoring the Chemistry and Rheology During Cure", *Proceedings of the Society of Plastics Engineers*, Vol. 45, 1987, p. 1031.
25. Leka, L. G. and Bayo, E., " A Close Look at the Embedment of Optical Fibers into Composite Structures," *Journal of Composites Technology and Research*, Vol. 11, 1989, p. 106.
26. Levy, R. L., "A New Fiber-Optic Sensor for Monitoring the Composite-Cure Process", *Polymeric Materials Science and Engineering*, Vol. 54, 1986, p.321.
27. Levy, R. L. and Schwab, S. D., "Performance Characteristics of the Fluorescence Optrode Cure Sensor (FOCS)", *Polymeric Materials Science and Engineering*, Vol. 56, 1987, p. 169.
28. Measures, R. M., Glossop, N. D. W., Lymer, J., Leblanc, M., West, J., Dubois, S., Tsaw, W. and Tennyson, R. C., "Structurally integrated fiber optic damage assessment system for composite materials," *Proceedings SPIE*, Vol. 986, p. 120.
29. Mermelstein, M. D., "All Fiber Polarimetric Sensor . " *Applied Optics*, Vol. 25, 1986, p. 1256.
30. Reddy, M., Bennett, K. D. and Claus, R. O., "Embedded optical fiber sensor of differential strain in composites," *Review of Progress in Quantitative Nondestructive Evaluation*, Vol. 6, edited by D. O. Thompson and D. E. Chimenti, Plenum Press, New York, 1987, p. 1241.
31. Rogowski, R. S., Heyman, J. S., Holben, M. S., Jr., and Sullivan, P., "A method for monitoring strain in large structures: Optical and radio frequency devices", *Review of Progress in Quantitative Nondestructive Evaluation*, Vol. 6, edited by D. O. Thompson and D. E. Chimenti, Plenum Press, New York, 1987, p. 559.
32. Rogowski, R. S., Heyman, J. S., Holben, M. S., Jr., Dehart, D. W. and Doederlein, T., "Sensor Technology for Smart Structures," *Proceedings of the 35th International Instrumentation Symposium*, 1989, p. 177.
33. Rogowski, R. S., Heyman, J. S., Holben, M. S., Jr., and Dehart, D. W., "Fiber Optic Strain Measurements in Filament Wound Graphite-Epoxy Tubes Containing Embedded Fibers, " *Proceedings SPIE*, Vol. 986, 1988, p. 194 .

11. Claus, R. O. and Wade, J. C., "Distributed Strain Measurement in a Rectangular Plate Using An Array of Optical Fiber Sensors," *Journal of Nondestructive Evaluation*, Vol. 4, 1985, p. 23.
12. Cozens, J. R., Green, M. and Yi, G., "Special Fibers for Sensing," *Proceedings SPIE*, Vol.1011, 1988, p. 62.
13. Crane, R., Macander, A. B. and Gagorik, J., "Fiber Optics for a Damage Assessment System for Fiber Reinforced Plastic Composite Structures," *Review of Progress in Quantitative Nondestructive Evaluation*, Vol. 2, edited by D. O. Thompson and D. E. Chimenti, Plenum Press, New York, 1983, p. 1419.
14. Culshaw, B., "Optical Fibres in NDT: A Brief Review of Applications," *NDT International*, Vol. 18, 1985, p. 265.
15. DePaula, R. P. and Udd, E., Editors, "Fiber-Optic and Laser Sensors IV," *Proceedings SPIE*, Vol. 718, The International Society for Optical Engineering, Bellingham, Washington, 1987.
16. Druy, M. A., Elandjian, L. and Stevenson, W. A., "Composite Cure Monitoring With Infrared Transmitting Fibers," *Proceedings SPIE*, Vol. 986, 1988, p. 130.
17. Druy, M. A. and Elandjian, L., "In-Situ (Autoclave) Cure Monitoring of Composites With IR Transmitting Optical Fibers," *Review of Progress in Quantitative Nondestructive Evaluation*, Vol. 9, edited by D. O. Thompson and D. E. Chimenti, Plenum Press, New York, 1990, in press.
18. Druy, M. A., Young, P. R., Stevenson, W. A. and Compton, D. A., "In-Situ Composite Cure Monitoring Using Infrared Transmitting Optical Fibers," *SAMPE Journal*, Vol. 25, 1989, p. 11.
19. Dunphy, J. R., Meltz, G. and Elkow, R. M., "Distributed Strain Sensing with a Twin-core Fiber Optic Sensor," *Instrument Society of America Transactions*, Vol. 26, 1987, p. 7.
20. Friedlander, G. D., "Smart Structures," *Mechanical Engineering*, Vol. 110, 1988, p. 78.
21. Griffiths, W. R. and Lamson, R. C., "Adoption of an Electro-Optic Monitoring System to Aerospace Structures," *Proceedings SPIE*, Vol. 838, 1987.
22. Harrold R. T. and San jana, Z. N., "Nondestructive Evaluation of the Curing of Resin Prepreg Using an Acoustic Waveguide Sensor," *Review of Progress in Quantitative Nondestructive Evaluation*, Vol. 6, edited by D. O. Thompson and D. E. Chimenti, Plenum Press, New York, 1987, p. 1277.

already been applied to monitoring oil pipelines for long distances and represent an emerging and enabling sensor technology.

Future advances in opto-electronics and signal processing will very likely open new avenues for sensing and make this technology an important part of NDE for assuring the safety and reliability of aircraft and spacecraft.

3.1.5 References

1. Afromowitz, M.A. and Lam, K. Y., "Fiber Optic Cure Sensor For Thermoset Composites," *Review of Progress in Quantitative Nondestructive Evaluation*, Vol. 8, edited by D. O. Thompson and D. E. Chimenti, Plenum Press, New York, 1989, p. 1467.
2. Bennett, K. D., Claus, R. O. and Pindera, M. J., "Internal Monitoring of Acoustic Emission in Graphite-Epoxy Composites Using Imbedded Optical Fiber Sensors," *Review of Progress in Quantitative Nondestructive Evaluation*, Vol. 6, edited by D. O. Thompson and D. E. Chimenti, Plenum Press, New York, 1987, p. 331.
3. Bennett, K. D., McKeeman, J. C. and May, R. G. "Full-field analysis of modal domain sensor signals for structural control," *Proceedings SPIE*, Vol. 986, 1988, p. 85.
4. Brennan, B. W., "Dynamic Polarimetric Strain Gauge Characterization Study," *Proceedings SPIE*, Vol. 986, 1988, p. 77.
5. Butter, C. D. and Hocker, G. B., "Fiber Optic Strain Gauge," *Applied Optics*, Vol. 17, 1978, p. 2867.
6. Charnek, R., Guo, Y. F., Bennett, K. D. and Claus, R. O., "Interferometric Measurements of Strain Concentrations Induced By an Optical Fiber Embedded in a Fiber Reinforced Composite," *Proceedings SPIE*, Vol. 986, 1988, p. 43.
7. Claus, R. O. and Bennett, K. D. "Smart structures program at Virginia Tech," *Proceedings SPIE*, Vol. 986, 1988, p. 12.
8. Claus, R. O. and Bennett, K. D., "Optical fiber modal domain detection of stress waves," *Proc. 1986 IEEE Ultrasonics Symp.* (Williamsburg, Va).
9. Claus, R. O. and Cantrell, J. H., Jr., "Detection of Ultrasonic Waves - Interferometer," *IEEE Ultrasonics Symposium*, 1980, p. 719.
10. Claus, R. O., Jackson, B. S. and Bennett, K. D., "Nondestructive Evaluation of Composite Materials by OTDR in Embedded Optical Fibers," *Proceedings SPIE*, Vol. 566, 1985.

Fiber optic sensor technology can be combined with advanced material and structural concepts to produce a new class of materials with internal sensors for health monitoring - providing the opportunity for smart structures. There are many potential uses of such materials in aircraft and spacecraft, especially where critical structural components have been identified and using the new materials proves cost effective. Space Station will require some type of sensing system to monitor the vibrations of the structure and feedback information to control mechanisms. A fiber optic sensor system for monitoring strain seems ideally suited for this application since the structure is large and flexible and requires a method for dynamic control. At least some parts of future aircraft will have fiber optic sensors for monitoring strain and impact damage. Commercial aircraft may be able to extend their useful life through proper monitoring of load spectra directly from the fiber optic sensor. In addition, the cost of maintenance may be reduced through "maintenance for cause" based on actual environmental history rather than air time. Certainly, military aircraft would benefit from having a damage detection and evaluation capability during engagements. The information would be invaluable to the pilot for deciding on a course of action after suffering damage to the aircraft.

To realize these benefits some important issues must be addressed. Very little has been done to determine the effect of embedding fibers on the strength of the material. Czarnek has reported very different strain fields around an optical fiber depending on the orientation of the fiber with respect to adjoining plies in the graphite/epoxy composite.[6] The effect of fiber coatings on the response of the embedded fiber to various environmental parameters must be investigated. There is some evidence that polyimide coated fibers are more suitable for strain measurements than standard acrylate coatings.[25] Also strain fields induced in the optical fiber from forces surrounding it when embedded or attached must be understood.[38]

Most of the early work has been done with standard communication fibers, but custom fibers with numerical apertures unsuitable for high speed communications may be more appropriate for sensing applications.[12]

Investigation of radiative properties of specialty optical fibers, as they relate to mechanical stress, may be of benefit for local strain measurements along an embedded fiber. Specially coated fibers may be useful for monitoring corrosion and aging in materials. Atomic oxygen is very corrosive to composite materials in near-earth orbit. Research is underway in our laboratory to measure the effects of atomic oxygen on composites and to monitor atomic oxygen with a fiber optic sensor.

Other exciting uses of this technology may be in monitoring strain in large structures such as buildings, ships, storage tanks, pressure vessels, dams and bridges.[20,41] The optical fibers with their low attenuation can literally span a bridge for miles and return information regarding structural integrity. The fibers may also find application to geodynamic monitoring as a low cost, large area sensors for strain/vibration associated with earthquake prediction. Fiber sensors have

$$\Delta L/L = -\Delta F/F$$

where L is the effective path length (optical plus electronic) and F is the nominal frequency value.

The optical phase locked loop has been applied to the measurement of dynamic strain in a cantilever beam [32] and quasi-static and dynamic strain with an optical fiber implanted in a filament wound graphite/epoxy tube.[33] Rowe, et. al. have used similar radio frequency modulation techniques to monitor strain in composite materials.[34]

3.1.4 Non-Destructive Evaluation and Damage Detection

Embedded optical fibers allow not only cure monitoring and in-service lifetime measurements but may also be used to non-destructively evaluate material degradation and damage as the material ages. The modal domain sensing system described above has been applied specifically to the detection of acoustic emission in loaded composite specimens.[2] An optical fiber used as an acoustic transducer has a very wide bandwidth compared to conventional transducers. The electronic processing of such signals using conventional acoustic emission analysis procedures is complicated because the impulse response function of the fiber exhibits a much stronger low frequency response than piezoelectric ultrasonic transducers.[7]

Some level of damage detection may also be afforded using embedded optical fiber sensor methods which locate excessive internal strain by the breakage of optical fibers arranged in a two dimensional array.[13,23,28,43] The disadvantage of such techniques is that levels of damage that do not break fibers cannot be detected and once fibers are broken no additional data may be gathered.

The capability of this type of damage detection system has been extended to additionally allow the quantitative determination of two dimensional strain in materials using several methods. First, the two dimensional strain field may be determined using single mode optical fibers embedded in a grid array, with interferometric techniques used to measure strain along the individual fiber lengths, and numerical methods used on the multiple output signals to construct the strain field. This method has been applied to the measurement of quasi-static loads and impact induced residual stresses in simply supported graphite/epoxy composite panels.[11] Alternatively, optical intensity modulation caused by microbending can be used as the sensing mechanism.[36] Loading in a composite specimen causes changes in the microbend characteristics of embedded fibers and thus in the transmitted optical intensity. Similar numerical methods would be required to map two dimensional strain fields from multiple linear measurements obtained using this method.[14,15]

or attached optical fiber sensors allow the measurement of distributed strain and vibrational modes for the entire structure and would indicate deviations from the norm by comparison with a historical data base. In addition, the fiber optic sensors can provide feedback for control of structural vibrations.

Strain and vibration measurements have been demonstrated in several laboratories using different fiber interrogation methods. These include modal domain interference,[3,8,35] optical time domain reflectometry,[10] optical polarization changes,[4,29] optical interferometry,[5,9,19,30] frequency domain reflectometry [39] and an optical phase locked loop.[25]

Optical time domain methods were first used to determine external loading in composites by Claus and co-workers [10] and improved time and frequency domain methods have subsequently been used by several investigators.[36,39,44] A method has been developed which uses in line optical fiber splices as time domain markers for optical time domain reflectometry (OTDR). An optical source generates a train of fast risetime optical pulses which propagate in the fiber. Partially reflecting splices, inserted at intervals along the length of the fiber, produce a series of regularly spaced signals and if the fiber is strained the spacing between the signals changes indicating the strain on the fiber between splices.[44] The strain resolution of this OTDR based system is limited by the rise times of the optical input pulses and the detection electronics. Currently available systems, for example, allow discrimination of locations spaced as close as 0.1mm.

Distributed structural vibration measurements may be achieved using a modal domain sensing method. The technique is based on the principle that different modes in a waveguide having slightly different propagation times produce interference patterns. If a waveguide that supports two or three modes is attached to or embedded in a structure, it can sense bends in the structure through the interference conditions between the modes. Claus et. al. have demonstrated that such methods may be used to evaluate structural vibrations of beams.[7] Specifically the mode shape amplitudes of such vibrations may be determined by appropriate processing of the time domain modal interference signals.[35]

Rogowski et.al. have investigated the use of a modulated laser diode system to measure phase modulation in an optical fiber. The system is an optical phase locked loop.[31] A voltage controlled oscillator is used to directly modulate a GaAlAs laser and to provide a reference signal to a double balanced mixer. The laser radiation passes through a multimode optical fiber, is detected, amplified, and mixed with the reference signal to generate an error voltage. The phases of the two signals are maintained at quadrature by feedback of the DC error voltage from the mixer to the oscillator. A filter removes the radio frequency component coming from the mixer. With this configuration, any change in the phase of the modulation is compensated by a change in the modulation frequency. A change in phase length, ΔL , of the optical fiber will produce a change in frequency, ΔF , according to:

vary from point to point due to variable geometry. Variations in the starting material from batch to batch and differences in handling during prepreg layup result in different degrees of cure for identical curing conditions. Enhanced quality assurance can be achieved with the use of sensors for in-situ cure monitoring. During the lifetime of the structure these in-situ sensors can also serve the purpose of monitoring the integrity of the structure. For example an optical fiber implanted in the composite for cure monitoring can be the same fiber that is interrogated later to measure strain, temperature, acoustic emission, and other parameters that are potential indicators of structural health.

Several methods have been investigated for monitoring the cure state of a composite. The most notable of these is the system developed by Drury, which measures the FTIR spectrum of the resin during cure with an optical fiber.[16] The change in the infrared spectrum indicates the degree of conversion of the resin to the cured polymer. The system has been demonstrated for epoxy and polyimide materials with fluoride, chalcogenide and sapphire fibers.[17,18] Since the method monitors chemical changes during cure it will be useful for production as well as for optimizing curing programs for new resins.

Other techniques involve monitoring physical properties related to the state of cure. Afromowitz [1] has shown that an epoxy fiber which has been fully cured can serve as an indicator of degree of cure when embedded in a graphite/epoxy composite. Since the refractive index of the cured polymer is greater than that of the uncured resin, the embedded fiber behaves as an optical waveguide until the composite is fully cured. When the fully cured state is reached, the refractive indices are identical and the fiber no longer transmits light.

Fluorescence spectra of curing composites have been measured with in-situ optical fibers to indicate cure state.[26] The sensor can later be used as a monitor for composite aging and water absorption.[27]

Acoustic waveguides embedded in curing composites have been used to measure propagation properties of ultrasonic signals. Sun and Winfree have shown that the acoustic amplitude in a copper wire embedded in a curing epoxy is related to the temperature and cure state.[40] Similar acoustic behavior has been observed for polyester-fiberglass waveguides embedded in thermosetting materials.[22]

Dielectric devices have also been investigated for cure monitoring taking advantage of the change of dielectric loss as the resin cures.[24,37]

3.1.3 Structural monitoring

The ultimate performance, safety and reliability of future aircraft and spacecraft will depend upon the capability of the crew or an automated control system to respond to adverse situations that may jeopardize the mission. Smart structural components may provide the data required for an appropriate response. Embedded

3 Sensory Materials

3.1 Fiber Optic Sensors

3.1.1 Introduction

The concept of smart structures involves the incorporation of sensors into a structural material to serve as a nervous system for health monitoring of the final product.[42] The sensors are implanted in the material at the time of processing and remain intact and available for interrogation during use.

The most common sensors being investigated for implanting in materials are fiber optic. Fiber optic sensors have been developed that can measure many physical and chemical properties and in many cases are more sensitive than alternative techniques. Considering many of the unique characteristics optical fibers possess, such as low mass, immunity to electromagnetic interference, compatibility with advanced fiber reinforced composites and the potential of a single optical fiber performing a multiple role (e.g., communication and a multiple sensor function), it is not surprising to see the emphasis on these sensors. Hence, the major portion of this section will be devoted to a review of research on fiber optic sensors for smart structures applications with a brief description of other types of sensors that may also be useful.

If we intend to monitor the health of a structure, we must consider which parameters should be measured to assure structural integrity. Carrying the analogy of a nervous system for structures a step further, we might say we want to sense "pain". That's the signal that warns an organism that something is wrong. However, what constitutes "pain" in an inanimate material? In fact we are a long way from anything resembling that sort of indicator in a structure. The question has rather been posed as, "What can we measure in a structure and would it be useful as an indicator of structural integrity?"

Ultimately, smart materials and structures will contain sensor elements that can monitor in-situ chemical and physical properties, including: state of cure, temperature, strain and vibration, acoustic emission, impact damage assessment, corrosion and aging. Aerospace applications of this emerging technology will be discussed and issues related to further advancement and timely deployment of smart structures will be considered.

3.1.2 Cure Monitoring

The curing cycle, consisting of precision programmed temperature and pressure regimes, is a critical step in the processing of fiber reinforced composite materials. The mechanical properties of the final product depend on the degree of cure. Fabrication of large parts is especially troublesome because the degree of cure may

17. Umland, J.W. and Chen, G-S., Active Member Vibration Control for a 4 Meter Primary Reflector Support Structure, 33rd AIAA/ASME/ASCE/AHS/ASC Structures, Structural Dynamics and Materials Conference, April 1992.
18. Chaudhry, Z. and Rogers, C.A., Enhanced Structural Control with Discretely Attached Actuators, 33rd AIAA/ASME/ASCE/AHS/ASC Structures, Structural Dynamics and Materials Conference, April 1992.
19. Watson, R.E., Comparison of the Response of Shape Memory Alloy Actuators Using Air-Cooling, M.S. Thesis, Naval Postgraduate School, Dec. 1984.
20. Rogers, C.A., Liang, C. and Burke, D.K., Dynamic Control Concept Using Shape Memory Alloy Reinforced Plates, "Smart Materials, Structures and Mathematical Issues", Sept. 1988.

6. Silcox, R.J., Lefebvre, S., Metcalf, V.L., Beyer, T. and Fuller, C.R.; "Evaluation of Piezoceramic Actuators for Control of Aircraft Interior Noise," AIAA paper no. 92-02-091, Proceedings of the 14th AIAA Aeroacoustics Conference, Aachen, Germany, May, 1992
7. Fuller, C.R., Gibbs, G.P. and Silcox, R.J., "Simultaneous Active Control of Flexural and Extensional Waves in Beams," *J. of Intelligent Material Systems and Structures*, vol. 1, no. 2, pp 235-247, April 1990.
8. Weisshaar, T.A., and Ehlers, S.M., Adaptive Static and Dynamic Aeroelastic Design, Proceedings of the 1991 International Forum on Aeroelasticity and Structural Dynamics, *Workshop on Smart Material Systems and Structures*, Aachen Deutschland, June 1991.
9. Ehlers, S.M., and Weisshaar, T.A., Static Aeroelastic Behavior of an Adaptive Laminated Piezoelectric Composite Wing, *Proceedings of the AIAA/ASME/ASCE/AHS/ASC 31st Structure, Structural Dynamics, and Materials Conference*, Part III pp 2340-2350, Long Beach, CA, April 1990.
10. Lazarus, K.B., Crawley, E.F., and Lin, C.Y., Fundamental Mechanisms of Aeroelastic Control with Control Surface and Strain Actuation, *Proceedings of the AIAA/ASME/ASCE/AHS/ASC 32nd Structure, Structural Dynamics, and Materials Conference*, Part III pp 1817-1831, Baltimore MD, April 1991.
11. Scott, R.C., Control of Flutter Using Adaptive Materials, M.S. Thesis, Purdue University, May 1990.
12. Heeg, J., An Analytical and Experimental Study to Investigate Flutter Suppression via Piezoelectric Actuation, M.S. Thesis, George Washington University, August 1991.
13. Newnham, R. E., and Ruschau, G. R., Smart Electroceramics, *Journal of the American Ceramic Society*, Vol 74, No. 3, March 1991.
14. Anderson, E.H., and Crawley, E.F., Piezoceramic Actuation of One- and Two-Dimensional Structures, Space Systems Laboratory, Massachusetts Institute of Technology, Cambridge, MA.
15. Carlson et. al. U.S. Patent No. 4,923,057 May 8, 1990.
16. Obal, M., Sater, J.M., Adaptive Structures Programs for the Strategic Defense Initiative Organization, 33rd AIAA/ASME/ASCE/AHS/ASC Structures, Structural Dynamics and Materials Conference, April 1992.

2.5 Electrostriction Materials

2.5.1 Benefits and Drawbacks

Electrostrictive materials change dimensionally when an electric field is applied or generate voltage when loaded, like piezoelectric ceramics do. However, the induced strain of an electrostrictor is proportional to the square of the electric field, which creates unidirectional displacement regardless of polarity. Strains comparable to PZTs can be obtained with electrostrictive ceramics similar to PMN, and without the troubling hysteretic behavior shown by PZTs under high voltage fields. The nonlinear relation between strain and electric field in electrostrictive transducers can be used to tune the piezoelectric coefficient and the dielectric constant. [13]

2.5.2 Configurations and Applications

The most noted application of electrostrictive ceramics is the micron-level manipulation of deformable mirror-surface contours to create or correct optical effects. This is utilized for focusing space communication system optical mirrors and lasers.

Electrostrictive transducers have been used in a number of applications including adaptive optic system, scanning tunneling microscopes, and precision micropositioners. [13]

2.6 References

1. Ehlers, S.M., *Aeroelastic Behavior of an Adaptive Lifting Surface*, Ph.d Dissertation, Purdue University, 1991.
2. Miller, S. E. and Hubbard, J., *Smart Components for Structural Vibration Control*, *American Control Conference*, 1988, Atlanta, GA.
3. Spangler, R.L., *Piezoelectric Actuators for Helicopter Rotor Control*, M.S. Thesis, Massachusetts Institute of Technology, February, 1989.
4. Barrett, R., *Intelligent Rotor Blade and Structures Development Using Directionally Attached Piezoelectric Crystals*, M.S. Thesis University of Maryland Department of Aerospace Engineering, 1990.
5. Lefebvre, S., *Active Control of Interior Noise Using Piezoelectric Actuators in a Large Scale Composite Fuselage Model*, M.S. Thesis, Virginia Polytechnic Institute & State University, June 1991.

particles in fiber like branches in the direction of the applied field. [13] ER fluids are suspensions consisting of hydrophilic (polarizable high-dielectric-constant) particles in a hydrophobic (dielectric) liquid.[1] In the absence of an electric field, ER fluids exhibit Newtonian flow characteristics; their strain rate is directly proportional to applied stress. However, when a sufficient electric field is applied, a yield stress phenomenon occurs such that no flow takes place until the stress exceeds a yield value which rises with increasing electric field strength. Because electrorheological fluids change their characteristics very rapidly when electric fields are applied or removed, they possess great potential for providing rapid response interface in controlled mechanical devices.[15]

2.4.2 Configurations and Applications

Typically, ER fluids have been utilized in mechanical systems such as electromechanical clutches, fluid-filled engine mounts, high speed valves and active dampers. Typical examples demonstrate the use of an electro-viscous or magneto-viscous fluid within a damper mount. The fluid is provided between opposing walls of a cavity in the mount member. The mount member is coupled between load elements to control the motion condition between them.

Control of the overall dynamic properties of structures is not easily or efficiently accomplished by localized damping, and in many cases cannot be accomplished to the extent desired by localized damping. Even for a simple plate-like structure of finite size there are an infinite number of frequencies at which resonance can occur. For each resonance, there is a different arrangement of nodal lines and points of maximum vibration over the surface of the plate.

Electronic actuator devices are placed at locations within the structure which produce amplified, tuned vibrations which responsively cancel the input motion vibration.

Damping of helicopter rotor blade vibrations by embedding ER fluids has been evaluated. The proposed system consists of a composite helicopter rotor containing pockets of ER fluid with top and bottom electrodes.

An active engine mount system has been proposed utilizing ER fluids. A system senses the dominant vibration frequency band and adjusts the viscosity and thus the stiffness of the fluid. Thus, the natural frequency of the system has been modified. This same concept can be applied for manned space structures, automobile engines, and robots.

An electrostrictive ceramic (PMN) has also been found to exhibit shape memory effects, but with an electric field being the stimulus.

There are several major concerns which need be addressed before SMAs can be used as actuators. They exhibit large amounts of hysteresis and have a very low bandwidth during the cooling half-cycle. The cooling problem has been investigated by Watson, [19]. The speed of an actuator is limited by the cooling rate. Water cooling is much faster but the power increase necessary is in most cases prohibitive; though water cooling provides a 10 times increase in bandwidth, the power is increased by approximately 20 times.

The nickel-titanium family of SMAs exhibits good force output and high resistivity along with comparatively low hysteresis in copper-modified alloys.

2.3.2 Configurations and Applications

Shape memory alloy reinforced composites use shape memory alloys as fiber reinforcements which can be stiffened or controlled by the addition of heat. Prior to embedding the shape memory alloy fibers within the resin, they are plastically elongated and constrained from contracting to their memorized length. A possible configuration of the SMA reinforced composite material is where the shape memory alloy fibers are embedded in the resin at a distance from the neutral axis. When the fibers are heated, they try to contract to their normal length and thus generate a uniformly distributed shear load along their entire length. This off-axis shear load causes the structure to bend. Transient and steady state vibration control can be accomplished with these composites as well as active buckling control and shape control.[20]

There are many fields which are currently investigating using shape memory alloys for a variety of applications. Shape memory alloys have been used since 1970 as the joining device in the hydraulic control lines of the F-14 Grumman Navy fighter. Goodyear Aerospace Corporation has been developing Nitinol for spacecraft antennae. A wire hemisphere of the material is crumpled into a tight ball less than 5 cm across. When heated above 77°C, the ball opens into its original shape, a fully formed antenna.[13] A system has also been proposed for active vibration damping and shape control on adaptive space structures.

2.4 Electrorheological Fluids

2.4.1 Benefits and Drawbacks

Electrorheological (ER) fluids exhibit coupling between their fluid dynamic and electrical behavior. When exposed to an electrical field, their viscosity, damping capability and shear strength increase. ER fluids are typically suspensions of fine particles in a liquid medium; the viscosity of the suspension can be changed dramatically by applying an electrical field. The electric field causes alignment of the

significantly below what Terfenol-D produces, but has an advantage in that it can be manufactured as a foil for easy embedding in composites.

Advantages of magnetostrictors over piezoelectric ceramics have been detailed in Appendix D. They include reliability, stable material properties, easier manufacturing and flexibility.

2.2.2 Configurations and Applications

Terfenol-D has been proposed by Grumman as a means of activating a control surface to optimize the lift performance of an aircraft wing under varying flight conditions. The wing changes shape. Ribs and spars are replaced with active members containing rods of Terfenol-D. In order to maximize the displacement obtainable, a diamond-shape structure was constructed which can deflect the trailing edge by 60°. Terfenol-D has superior strength, higher modulus and wider operational bandwidth than shape memory alloys. It can generate enough force to overcome the aerodynamic loads and has low magnetic field requirements. Magnetostriction materials are currently under evaluation for shape change of torpedo control surfaces, gimbaling cockpit simulators, and vibration damping of optical benches.

An integrated actuation system for individual control of helicopter main rotor blades using Terfenol-D actuators was proposed and evaluated in a small business innovative research (SBIR) investigation for the U.S. Army Aviation Laboratory, Fort Eustis, Virginia (see Appendix D). The purpose of adding the flaps was to provide higher harmonic control of the individual blades to cancel rotor-induced vibration, long a major concern for helicopters. The goal of the program is to reduce vibration by 90% which would represent a major improvement in helicopter technology.

2.3 Shape Memory Alloys

2.3.1 Benefits and Drawbacks

The ability of a material to recover its shape when activated by an external stimulus is termed the shape memory effect. Nitinol is the most common shape memory metal. Heat is the activating stimulus for this material. This material undergoes a change in crystal structure known as a reversible austenite to martensite phase transformation at a specific transformation temperature, dependent upon alloy composition. Young's modulus increases by almost a factor of 3. Shape memory alloys are capable of directly transforming heat into mechanical work. The heat can be produced by fluids, gases, or electricity. If the heating and cooling is controlled by pulsed direct electric current, repeated cyclic motions with high degrees of accuracy can be achieved.

using full state feedback. Reference [12] detailed the application of plates in a bimorph bender configuration to actively suppress flutter.

See Appendix C for an analysis of the expansion and contraction of the surface of an aircraft wing. A potential application of piezoelectric ceramics might be to attach ceramic wafers to the surfaces of a wing to cause the wing surface to expand or contract which will effect the control of the aircraft. Several experiments have used PZT wafers as actuation devices to statically reshape plate structures to increase aerodynamic forces such as lift. High-strain shape memory alloy (SMA) materials are being considered to effect larger static shape changes.

There has been much work done on vibration suppression and modal control with in truss structures using piezoelectric stacks, an example of which is given in reference [17].

Production applications of piezoelectric ceramics are found in the automobile industry. An example of their use is in controlling compliance in Toyota's electronic modulated suspension system. The system is a road stability and shock adjuster which detects bumps, dips, rough pavement and sudden lurches by the vehicle and then rapidly adjusts the shock absorbers to apply a softer or firmer damping force. The shock absorbers are continuously readjusted as the road conditions change so that rocking or wobbling is eliminated.[13]

2.1.5 Issues

Notable undesirable material characteristics are nonlinear response at high voltage levels, hysteresis and aging. These are more noticeable problems in piezoceramics. The properties of piezoelectric materials are nonlinear. A linearity assumption is valid for low applied voltages and small deformations. Nonlinearities of these materials have been well-documented by references [3,12,14]. Several nonlinear properties which have been found to have significance are the amplitude dependence of the field-strain relationship, creep, variations with mechanical strain, and depoling. These issues will not be addressed in detail here.

Yet another concern is that very high voltages may be required to deform thick actuating plates. This problem can be avoided by utilizing a multilayer configuration instead of increasingly thick single layer plates.

2.2 Magnetostriction Materials

2.2.1 Benefits and Drawbacks

Ferromagnetic materials allow for the creation of an elastic strain when subjected to an external magnetic field. This effect is called magnetostriction. Terfenol-D is the most commonly-known magnetostrictive material. It is capable of inducing strains up to .2%. Metglas is another magnetostrictive material. The maximum strain is

As previously mentioned, piezoelectric polymers are rarely utilized as actuating mechanisms. Reference [2] employed polyvinylidene fluoride (PVDF), a polymer, in both a sensing and actuating role for vibration control of flexible beam elements.

Ceramics are more commonly used as actuators. Reference [16] provides a glimpse at the current activities of the strategic defense initiative office (SDIO) in this area, focusing on vibration control. In the area of rotorcraft, two distinctly different actuator configurations have been examined for higher harmonic control [3,4]. The first used directionally attached plates to torsionally activate blade sections and actuate a trailing edge flap. The magnitude of flapping vibrations was significantly reduced using active controls. The second utilized a push-pull configuration of bender elements.

Another actuating application, also detailed in Reference [4], is the active damping of truss members for large space structure applications. This study used commercially available actuators which utilize the d_{33} effect (the expansion direction coincides with the direction of polarization) to limit the vibration amplitude and settling time of transients induced by dynamic perturbations to the structure such as crew motion.

In the acoustics field, recent work [5] has focused on reducing cabin noise by applying active forces produced by bonded PZT actuators to the fuselage walls or frame. Finite impulse response (FIR) filters were utilized in a least means square minimization algorithm to control both an acoustic resonance and a structural resonance at two different frequencies. Reference [6] described the use of piezoelectric plates as independent actuators (bimorph configuration) on an aluminum beam in conjunction with an adaptive controller to attenuate flexural and extensional vibrations with frequencies up to 1100 Hz.

Reference [7] details experiments and analyses of a composite beam with distributed embedded actuators controlling structural modes from 11 to 150 Hz. Through feedback of velocity, structural damping increases of an order of magnitude were obtained. Results available from aeroelastic applications of piezoceramics are very limited. Static aeroelasticity has been the subject of investigations by Ehlers and Weisshaar [1,8,9]. They conducted analytical studies on laminated composite wings with embedded actuators, looking at pure torsional, and bending deformations. They reported that through feedback to embedded adaptive material layers, the divergence speed is altered, implying also that lift effectiveness is influenced. The augmentation or replacement of conventional aerodynamic control surfaces with strain actuation for aeroelastic control has been the focus of an analytical investigation of a typical section by Lazarus, Crawley and Lin [10]. They found that strain actuation via piezoelectric elements may provide a viable and effective alternative to articulated control surfaces for controlling aeroelastic response. Investigation of flutter suppression for lifting surfaces and panels has been done by Scott [11]. This analytical study considered controlling flutter at supersonic speeds

2.1.2.2 Out-of-Plane or Monomorph Element

The intended application may suggest creative configurations for these materials. Designs for out-of-plane displacement actuators have been evaluated. Utilizing the piezoelectrics in monolithic modes, a high stiffness is achieved, however, the displacement achieved is very small. Composite structures have also been evaluated, which produced significantly more displacement, but were less stiff than the monolithic configurations. One of these utilized only the out-of-plane displacement of the piezoelectric. The second utilized both the out-of-plane and the in-plane displacements of the piezoelectric disc. This is the moonie configuration which is discussed in Reference [13]. Bender configurations have also been examined. In one instance, the bender elements were constrained at the periphery of the disc and allowed to operate as an oil can does to achieve the out-of-plane displacements. The stiffness of the configuration was lessened, but more significant displacement results were obtained. Bimorph benders have been found to be 10 times more effective than monomorph benders.

2.1.2.3 Discretely Attached Elements

In structural control, induced strain actuators are utilized generally by bonding them or embedding them in a structure. With these configurations used for inducing flexure, the developed in-plane force contributes indirectly through a locally-generated moment; control authority is thus limited by actuator offset distance. These actuators deform along with the structure. By attaching strain actuators to the structure only at discrete points, as opposed to being bonded or embedded, they are free to deform independently from the structure. The in-plane force of the actuator results in an additional moment on the structure and enhanced control [18].

2.1.3 Piezoelectric Composites

By incorporating piezoelectric rods into a composite material, directional actuation can be achieved with reduced weight. Assuming that the matrix is dielectric, and aligning the 1-direction of the PZT with the fiber direction and the 3-direction perpendicular to the direction of the ply (see Appendix B), and a 65% fiber volume fraction: the elastic properties are similar to a glass/matrix unidirectional fibrous composite. The density is reduced from the monolithic PZT but still twice that of aluminum. The anisotropy of the electromagnetic coupling provides for shear strain actuation through proper ply orientation [1]. Application of this configuration could include actuation of an adaptive wing (i.e. shape control).

2.1.4 Applications

In an actuating application, the converse piezoelectric effect is utilized as the actuators deform in response to a control signal or applied voltage.

2 Actuation Materials

2.1 Piezoelectric Materials

2.1.1 Benefits and Drawbacks

Piezoelectricity is the ability of a material to develop an electrical charge when subjected to a mechanical strain. The converse piezoelectric effect, the development of mechanical strain when subjected to an electrical field, can be utilized to actuate a structure. A local strain is produced in the structure which induces forces and moments. Thus, actuation of a structure may be accomplished at the material level. Lead-zirconate-titanate (PZT) is a piezoelectric ceramic in which the electric sub-domains have been aligned using a very large electric field. Strain is linearly proportional to the electric field in a fully poled piezoelectric material which means that the piezoelectric coefficient is a constant and cannot be electrically tuned with a bias field (see Appendix B for further discussion of piezoelectric materials).

Choosing the proper piezoelectric material to use for a given application is based on stiffness properties, flexibility, electromechanical coupling coefficients and limits on applied voltage. A piezoelectric material's ability to actuate a structure is a function of its stiffness, the limit on the voltage which can be applied, and the electromechanical coupling coefficients. Polymers have high voltage limits, yet they have low stiffness and low electromechanical coupling coefficients. Ceramics on the other hand are much stiffer and have large coupling coefficients and are thus better-suited for actuator applications.

Low density and stiffness have, in most cases, prevented the serious consideration of piezoelectric polymers for use as actuators. Ceramics have sufficiently high electromechanical coupling and stiffness that they lend themselves better to actuation applications.

2.1.2 Configurations

2.1.2.1 Bimorph Bender Element

Piezoelectric plates can be configured in different ways to accentuate the displacements or forces being generated. The in-plane expansion and contraction of adaptive materials may be utilized by bonding actuating plates to either side of a center shim. One is expanded and one is contracted; the net result is a bending displacement much greater than the length deformation of either of the two layers. This configuration, which takes advantage of the d_{31} effect (see Appendix B), is referred to as a bimorph or a bender element.

In chapter 4, control approaches for smart structures are discussed and in chapter 5, recommendations for future research are given.

1 Introduction

This report is a state-of-the-art assessment of active structures authored by the members of the active structures technical committee. The emphasis in this assessment was towards the applications in aeronautics and space. It is felt that since this technology area is growing at such a rapid pace in many different disciplines, it is not feasible to cover all of the current research but only the relevant work as relates to aeronautics and space.

Before discussing further the subject of active structures, this committee has adopted the terminology as depicted in Appendix A. Domain A contains all structures that have a sensory system. So that in addition to the usual load carrying capability of a structure, the structure also contains some type of sensory system that could be either integrated into the structural material or added on to the structure as a separate sensor.

Next, we define a B domain of structures that contain an actuation function in addition to the load carrying capability. These structure types are called adaptive because they are changeable in a predictable way. Again the actuation function may be contained within the material of the structure or it may be some attached actuator.

The intersection of the A and B domains contains three types of structures. Domain C is the type of structures that have attached sensors, actuators and processors. Examples of a class C system would be a structure with attached accelerometers, attached thrusters or proof mass actuators and an attached processor. As you go from class C to D to E, the degree of integration of the sensor and actuator with the structural material increases. An example of a type D structure would be a truss mechanism with variable length struts. These variable length struts could be hydraulically actuated or ball screw actuated telescoping cylinders. An example of a type E structure might be a structural composite material with embedded piezoelectric ceramic powder. An application of these embedded materials could be for flutter suppression in an aircraft wing or for vibration suppression in a truss strut.

At this time it does not appear that the technology exists to embed processors into structural materials. The silicon median that constitutes the processor is brittle and not compatible with the flexibility and toughness of current structural composites.

This report covers research in smart actuation materials, smart sensors, control of smart/intelligent structures. In smart actuation materials, piezoelectric, magnetostrictive, shape memory, electrorheological, and electrostrictive materials are covered. For sensory materials, fiber optics, dielectric loss, and piezoelectric sensors are examined. Applications of embedded sensors and smart sensors are discussed.

PVF2	Polyvinylidene fluoride
PZT	Lead-zirconate-titanate
RF	Radio frequency
SAMPE	Society for Advanced Materials and Process Engineering
SBIR	Small business innovation research
SDIO	Strategic Defense Initiative Office
SDM	Structures, Structural Dynamics and Materials
SERC	Space and Engineering Research Center
SMA	Shape memory alloy
SPIE	Society of Photo-Optical Instrumentation Engineers
TRW	Thompson-Ramo-Woolridge
VG	Velocity and acceleration
VGH	Velocity, acceleration, and altitude
VLSI	Very large scale integration
VPI&SU	Virginia Polytechnic Institute and State University

Acronyms

ACESA	Advanced composites with embedded sensors and actuators
AHS	American Helicopter Society
AIAA	American Institute of Aeronautics and Astronautics
ANN	Artificial neural network
ASAC	Active structural acoustic control
ASC	American Society for Composites
ASCE	American Society of Civil Engineers
ASIC	Application specific integrated circuit
ASME	American Society of Mechanical Engineers
ASSP	Acoustics, Speech and Signal Processing
CMOS	Complementary metal oxide silicon
CPU	Central processing unit
CSI	Control Structure Integration
DARPA	Defense advanced research projects agency
DoD	Department of Defense
DSP	Digital signal processor
ER	Electro-rheological
FEA	Finite element analysis
FIR	Finite impulse response
FTIR	Fourier transform infrared
ICASE	Institute for Computer Applications in Science and Engineering
IEEE	Institute of Electrical and Electronic Engineers
IIR	Infinite impulse response
IOFDR	Incoherent optical frequency domain reflectometry
LMS	Least mean square
LQG	Linear quadratic Gaussian
LQR	Linear quadratic regulator
MCM	Multiple chip module
MIMO	Multi-input multi-output
MIT	Mass. Institute of Technology
MOSFET	Metal oxide silicon field effect transistor
MSME	Masters of Science in Mechanical Engineering
NACA	National Advisory Committee for Aeronautics
NASA	National Aeronautics and Space Administration
NASTRAN	NASA structural analysis
NDE	Non-destructive evaluation
NDT	Non-destructive testing
NRL	Naval Research Laboratory
ONR	Office of Naval Research
OTDR	Optical time domain reflectometry
PE	Piezoelectric
PMN	Lead metaniobate
PVDF	Polyvinylidene fluoride

Executive Summary

Many types of smart materials and applications for potential use in aircraft and spacecraft have been examined. It is the opinion of this committee that aircraft and spacecraft performance can be improved by incorporating the use of these materials into their design. Before these materials are more widely accepted by designers of commercial and flight vehicles, more research in the testing and evaluation of these materials is needed.

The essence of this report is captured in the following list of recommendations which cover; actuation materials, smart sensors, information management, applications and research environment.

Actuation Materials

- Langley should focus on the integration of smart materials (piezoceramics, magnetostrictors, and shape memory alloys) into concepts with composites which ultimately will improve vehicle performance and reliability while decreasing fabrication costs.
- Capability, limiting performance, and design approaches of smart materials should be better understood.

Smart/Intelligent Sensors

- Micro-sensors with built-in processors for aircraft and spacecraft applications should be further developed.

Information Management

- A concept for a network that supports multiple smart subsystems and includes processing (either centrally or distributed) for improved vehicle performance and reliability needs attention.

Applications

- More areas of potential use of smart materials for improving aircraft and spacecraft performance needs encouragement. These are ideas that are hidden within the minds of researchers at Langley and it is hoped that the proper stimulants will bring forth these innovations.

Research Environment

- Build upon Langley's capability in materials and structural dynamics modeling and promote cross-directorate communications of research activities.

RF telemetry system. In addition to these smart features, an inclusion of sleep/wake mode for the smart structure would be desirable for saving on-board power source.

As many sensors and actuators are distributed over a structure, a bilateral communication bus for the sensors and actuators and processors becomes an important part of the smart structure. An architecture and interface for a process controller has been investigated [7] for a number of fundamental issues in system partitioning, controller architecture, sensor function, and sensor testing/compensation. The sensor bus interface is addressable, programmable, self-testing, compatible with a bi-directional digital sensor bus, and offers 12-bit accuracy.

Integration of current technologies in VLSI, micromachining, and system architecture for a distributed sensor/actuator structure will result in a miniature/microscale smart sensor/actuator system that is most suitable for embedment of smart sensors and actuators into a smart structure. Many of these technologies are already available but they need to be integrated to realize a smart structure. Major areas of these technology areas are listed below.

- 1) Micromachining
- 2) Specialized mixed signal silicon device integrated circuit fabrication (application specific integrated circuit)(ASIC)
- 3) Architecture and interface system design and implementation
- 4) Embedment technology

The second technology area, ASIC, is the most costly area though the ASIC technology is readily available, a technology that integrate micromachining and VLSI circuits is a specialized area which is beginning to appear within semiconductor industry, due to an increased demand of accelerometers, pressure sensors, and flow meters from the automobile industry. As an alternative and less expensive approach, use of multiple chip module (MCM) hybrid circuits in place of ASIC devices will be the most reasonable alternative avenue to pursue before a total monolithic ASIC system is sought.

The above discussions center on the implementation of the sensor hardware. However, sensor information may be augmented by incorporating data processing, information extraction and decision making capability as part of the sensor design. These elements may dictate the design of the sensor element. In many ways then the structure may become the sensor element as the response of the structure is defined and compared to previous measurements or predictions. For applications such as condition monitoring, it is desirable to monitor large none instrumented sections of a structure quickly and on a regular basis. By using discrete sensor elements and mapping the response in time and space, the transfer of vibrational energy through a structure may be defined.

Several new techniques have evolved in recent years that combine signal analysis with discrete sensor information to yield information about none instrumented

sections of a structure by correlating excitation and response measurements at discrete points. These measurements are functions of the loading distribution and the structural characteristics for those parts of the structure that carry energy between the measurement points. This approach in effect makes the structure the sensor by modeling and/or monitoring the multidimensional path of the structural response and comparing such to a previously defined response.

3.5.1 Time-Frequency Analysis

The work of Bolton and Wahl [8,9] makes use of a time-frequency analysis of structural impulse responses to reveal the wave types and paths carrying significant energy through a structure. Since each wave-type (i.e. flexural, torsional, extensional...) is characterized by its own dispersion relation, each wave-type may be associated with particular features appearing in the time-frequency domain representation of the impulse response. In this work the Wigner Distribution is used as a means for obtaining the time-frequency representations. Other methods use sonograms[10] and the Choi-Williams distribution[11].

By using a fixed excitation distribution, pattern recognition technology will allow feature extraction from this type of data that may be related to the structural parameters. In this way, changes in the characteristics of the structure between measurements made at different times may be determined. Using a distribution of sensors and/or actuators, changes in parameters may be isolated to decreasingly smaller sections of the structure for problem identification.

3.5.2 Prediction of Dynamic Loads using Neural Networks

Condition monitoring often is implemented by a recording of loading as a function of time. This however requires the use of an extensive array of sensors to provide the required information. A method of indirectly monitoring component loads through common flight variables is demonstrated which requires only an a priori model of the response/excitation relationship. This method will allow for both linear and non-linear responses.

An artificial neural network model learns these response/excitation relationships through exposure to a database of measured records on a test vehicle for a range of load histories. The ANN model, utilizing standard recorded flight variables as inputs, is trained to predict time-varying and oscillatory loads on critical components. Interpolative and extrapolative capabilities have been demonstrated[12] with agreement between predicted and measured loads on the order of 90% to 95%.

3.5.3 References

1. Najafi, K., "Smart Sensors," J. Micromechanics and Microtechnology, Vol. 1., pp 86-102, 1991
2. Brignell, J. E., "1989 Smart Sensors, A Comprehensive Survey," edited by W. Gopel, J. Hesse and J.N. Zemel, vol. 1, (New York, N.Y.)
3. Giachino, J.M., "1986 Smart Sensors," Sensors and Actuators, vol. 10, 239-248
4. Juds, S.M., "Toward a Definition of Smart Sensors," Sensors, pp 2-3, July, 1991
5. Swartz, R.G. and Plummer, J.D., "Integrated Silicon-PVF2 Acoustic Transducer Arrays," IEEE Trans. Electron Devices, vol. ED-26, No. 12, December 1979
6. Akin, T., Ziaie, B., and Najafi, K., "RF Telemetry and Control of Hermetically Sealed Integrated Sensors and Actuators," IEEE Solid-State Sensor and Actuator Workshop, Technical Digest, pp 145-9, Hilton-Head, SC, 1990
7. Najafi, N and Wise, K.D., "an Organization and Interface for Sensor-Driven Semiconductor Process Control Systems," IEEE Trans. Semiconductor Manufacturing, vol. 3, No. 4, November 1990
8. Wahl, T.J. and Bolton, J.S.; "Identification of Structureborne Noise Components by the Use of Time-Frequency Filtering," AIAA paper no. 90-3967, presented at 13th AIAA Aeroacoustic Conference, Tallahassee, FL, October 1990.
9. Wahl, T.J. "The prediction and analysis of transient structural responses," MSME Thesis, School of Mechanical Engineering, Purdue University, 1990.
10. Hodges, C.H., Power, J. and Woodhouse, J.; "The Use of the Sonogram in Structural Acoustics and an Application to the Vibration of Cylindrical Shells," J. of Sound and Vibration vol. 101, pp 203-218, 1985.
11. Choi, H.I. and Williams, W.J. "Improved time-frequency distributions: Theory and Applications," IEEE Trans. ASSP 37(6), pp 862-871, 1989.
12. Cook, A. B. et al; "The Prediction of Non-linear dynamic loads on helicopters from flight variables using artificial neural networks," AIAA 14th Aeroacoustic Conference, Aachen Germany, May 11-14, 1992

4 Control of Smart/Intelligent Structures

4.1 Introduction

This chapter provides an overview of current techniques and concepts to implement control concepts on real systems. Many technologies and approaches are currently under study and it is not feasible to mention all of the current activities for control system implementation on smart/intelligent structures. It is intended to examine the current trends of this field and to highlight those expected to be important to future progress.

Generally, the intent of adding control to structural elements is to extend the functional capability of the primary structure in some way. This may include a change in structural strength, dynamic properties, or geometry which may provide noise, vibration or flutter control, dynamic margin, maneuverability enhancement or gust alleviation. These are by no means inclusive of the control purposes. Other mission criteria include condition monitoring and damage tolerance (survivability) and redundant system design. Not only is it possible to determine the extent of a failure or predict it, but structural elements may be included such that loads may be routed around a damaged subsection. An intelligent structure of this nature would require a new type of collocated sensor and actuator system including a processor for local control of the structure and mutual communication to the central processor which is the global controller.

Using present technology, these systems generally include discrete sensors, actuators and controllers. These are currently implemented as add-on transducers and external control systems. This approach requires an extensive maze of interconnecting wires to provide the necessary communication between these elements, provides little weight or structural utilization of the control elements and limits integration of the system. Ideally, it is desirable to integrate the transducer elements into the structure such that they contribute to the overall static and dynamic load capability or damping properties. Sensors and actuators may be the integral parts of load bearing members of the structure. Consequently, design of a given structure requires to be coordinated with that of sensors, structures, and local processors as well as communication media. An approach of discrete component design/construction may be no longer applicable in many cases. An integrated design/construction approach will be a logical one to pursue

There are many approaches to control law design for structural systems. These include the state-space approach, classical control design methods and neural networks. Although some of these methods do not require an explicit model of the system to be controlled, they cannot be applied as a black box with control inputs and outputs. All of the approaches are governed by the same laws of observability and controllability. These require that the motions to be controlled be observed by the sensor system without violating temporal or spatial sampling criteria. It also

requires that the control system can couple effectively into these motions or modes in order to exercise control. For instance, a time domain processor can effectively provide a rate variable from the time history of the displacement. However, this approach cannot provide additional modal information or improved spatial resolution from a limited number of transducers.

It is not likely that any one method of control is the best suited control approach for any given situation as the strengths differ for each control strategy. However, one may envision an integrated approach blending best technologies into a distributed hierarchical control over concurrent processors with anthropomorphic intelligence.

The state space approach relies heavily upon an accurate modeling of the structural system and control elements to derive an analytical model. The performance and stability depends intricately upon the accuracy of this model and errors introduced due to measurements, environment, or an inadequate number of states being considered can have catastrophic results. However this approach integrates a more complete understanding of the control problem than all of the other approaches. Every aspect of the physical structure and the control system is modeled. The effect of all parameters of the system can be investigated as well as the excitation. The stability margins can be defined as well as any limits of the excitation bounds. This modeling criteria however is a major shortcoming of this approach however. It is generally very difficult to derive an accurate model for a complicated physical system. These systems work primarily at lower frequencies because the order of the numerical models generally used is tractable. For higher order modes, it is generally difficult to specify their resonant frequencies to the required degree of accuracy.

Systems that use a simple feedback of velocity or displacement can be made quite effective, even for multiple input/output (MIMO) systems. A feedback gain is defined between a sensing element and an actuator element that provides the required control. However, it is generally required that these systems have a negligible time delay of the system response in the frequency range for which control is to be exercised. Often, for low frequencies, this is not an unreasonable restriction. However, for most cases that have been implemented, the sensor and actuator are collocated on the structure. For more complicated structures, higher frequencies, wider bandwidth or where it is not convenient to collocate the transducers, this approach is not viable.

Controllers based upon measured open loop transfer functions have been implemented. A measurement of the response to be controlled is measured by a sensing element. The transfer function measured between this sensing element and a controller excitation is known a priori and is used to calculate the controller input required to exercise control over the response. Variations allow this approach to define the transfer function on-line using coherence methods. These systems can be quite useful for harmonic disturbances as an estimate of the disturbance can often be derived or sensed and the system loop closed. However, these systems are quite sensitive to changes in their environment and excitation spectra. In addition, these

systems are often found to be unstable. One approach to this problem is to add some adaptability to the model and provide an on-line estimate of the system parameters using various system identification approaches.

Adaptive closed loop controllers have emerged in recent years that are based upon a real time least means squares (LMS) minimization algorithms. These systems are generally based upon linear digital filter models, in which the filter parameters (coefficients) are treated as the free variables of a minimization procedure. The object of the procedure is to minimize some error function related to the difference between the measured system response and the desired system response. This approach is extended and generalized to higher order and non-linear systems with the emergence of neural network based controllers. These systems however do not explicitly integrate any system model into the controller. The limits on the implementation due to traditional controllability and detectability issues must be derived separately and integrated from an intuitive viewpoint. Finally, general stability criteria are typically not addressed in this approach.

Artificial neural networks expand and generalize upon the above concept. Neural networks were part of the attempts towards artificial intelligence initially developed in the 1950's and 1960's. These early studies diverged through the 1960's into engineering approaches that implemented statistical pattern classification, control theory and adaptive filters; and symbolic manipulation representations of artificial intelligence and cognitive science. The engineering approaches will be stressed in this survey. This approach has provided algorithms for a broad range of practical problems. Neural networks are used to classify information (temporal and/or spatial) into ranges of classes for decision making (i.e. pattern recognition). Using the general ability of mapping from one large set of variables such as sensor systems to another such as control actions, they have demonstrated the capability to capture critical behavior for very complex functions. This capability extends to multi-variable non-linear processes and may include both feedforward and/or feedback systems. A wide range of approaches is evolving in this technology area and the areas of highest potential are not well delineated.

Finally, modeling of system components is critical to the performance of the control system and essential for the system simulation. Any experimental work on control of a complex smart/intelligent system is expected to be very costly and time consuming, an extensive system simulation before any attempt of experimental evaluation is preferred. Modeling of sensors and actuators are as important as those of basic system structure. Modeling areas includes: 1) finite element model and system identification 2) model identification using hardware 3) state space model for sensors and actuators 4) modeling of environmental and aging effects of components 5) modeling of nonlinear properties of sensors and actuators 6) modal analysis.

4.2 Modern Control Approaches

This section overviews control algorithm approaches that are model based. This means an analytical model is developed that integrates the plant dynamics into a controller that performs the desired control function. In a state space formulation, a numerical procedure is typically used to integrate through the governing equations to predict the desired controller output from known system states. For rate feedback methods, the model is used to derive controller gains (frequency response functions) that operate on input rate information. These gains are typically fixed but adaptive systems are now quite common that monitor the system characteristics and change the parameters in the model as needed. These techniques encompass many methods and variations and this section is not meant to be all inclusive but merely an indication of available technologies.

4.2.1 Model Based Feedback Control Approaches (State Space)

Jacques, et al. [1] presented control design of an experimental testbed with assumptions of collocated disturbance source and actuator and that of performance metric and sensor. Control design method includes measurement of transfer function from actuator to sensor, use of nonlinear curve fitting technique to obtain state space model of the system, reduction of model order, design of linear quadratic Gaussian (LQG) controller, and removal of dynamics from controller that do not contribute to stability and affect the performance slightly.

Allen, Lauffer, and Marek [2] present design implementation of structural control of a flexible truss structure with a multiple input-output control processor and piezoelectric sensors and actuators. Structural control performed with reduced LQG design technique required model accuracy which is much greater than the accuracy required for response analysis or structural design purposes. A NASTRAN finite element model was used as the basis for the control design model. The optimal projection controller showed good correlation between the analytical and experimental performances. System identification techniques proved to be invaluable for the finite element model improvement. Hardware implementation of structural control design and techniques is highly recommended as the analytical study results are highly prone to the modeling and analysis assumptions.

Murotsu, Senda, and Hisaji [3] present optimal configuration control of the adaptive truss structures. The optimal configuration has been formulated with minimizing performance index corresponding to the demanded task. However, it was stated that the computational burden is too excessive to be an effective real-time tool. Two alternative approaches were presented with the relaxed conditions of optimality, that is local optimal configuration and the specified asymptotic convergence of the work vector.

4.2.2 Active Vibration Control

Hyland, Collins, Phillips, and King [4] present the highlights of control design process and performance obtained from the ACES and Mini-MAST structures of NASA using both centralized and decentralized controllers. The paper also discusses about the design procedure and describes the substantial performance improvement achieved with a decentralized control for active vibration suppression of flexible structures. Hong, Varadan, and Varadan [5] performed a series of active vibration control of a thin plate. Coupled multi-mode optimal control procedures for the plate have been developed using Rayleigh-Ritz method to obtain the approximated mode shape constant. A proportional type damping has been implemented to obtain a closed-form solution of the differential eigenvalue problem for the damping system. Experimental verification of uni-disc type collocated sensors and actuators was made, and theoretical and experimental work on transducer sizes and positions has been presented.

Hanagud, Babu, Stalford, and Won [6] present an adaptive structure that can adopt to failures such as debonding of the sensor during its life and take into account unmodeled dynamics. The controller is designed with several assumptions such as reduced degrees of freedom, uncertainty bounds, extent of debonding, Euler-Bernoulli beam theory and flawless beam.

4.2.3 Stochastics

Jacques and Miller [7] present use of low order models to identify and study four mechanisms through which a structural change might influence the controlled performance. Interaction of the structures and the control has been discussed by formulating a cost function in terms of structural parameters and control gains. H-2 and H-infinity performance metrics are considered for a preliminary design of the control structures. Huang and Knowles [8] uses H-infinity optimization technique as the control design methodology for the control of a large space structure. It is also pointed out that a test of a large scale structure in 1-g conditions is difficult to be carried out for verification of the control design.

Athans, Agguiero, Bielecki, Boker, Douglas, Gilpin, and Lublin, [9] discuss novel robust LQR control strategy under assumption of full state feedback and uncertain energy interpretation. Extension to robust H-2/H-infinity approach with output feedback and dynamic compensation is considered with its application to MACE. Motivation of this effort is to design of robust multi-variable controllers, obtain a state-space model of system for design, and derive a minimal multi-variable model.

4.2.4 Adaptive Control

Trent and Pak [10] present their work on the development of the methodology to design and test controllers that will provide stable environments for payloads mounted on space platforms. Difficulties of obtaining accurate models of structural

dynamics of large space structures are pointed out along with structural characteristics that may change during the spacecraft lifetime due to hardware failures and operational or environmentally induced changes. Adaptive control techniques with on-line system identification approach is presented with various concerns about controls-structures interaction (CSI) issues.

Sekine, Shibayama, Iwasawa, and Tagawa [11] describes the adaptive control system of flexible truss structures with a piezoelectric actuator as an active member. The active member actuator prove to be effective in controlling flexible truss structures statically and dynamically.

Melcher and Wimmel [12] describe modern controllers which are based on digital real-time filters, adaptation algorithms and high speed signal processor systems. It is intended to show the stringent controller requirements can be met with the use of modern adaptive signal processing containing sophisticated adaptive algorithm routines of an up-to-date software environment and high speed computational hardware system.

4.2.5 Integrated Controls-Structures Design

Maghami, Joshi, Price, Lim, Walz, Armstrong, and Gupta [13,14,15,16] proposed an approach of integrated design methodology of the structural and control system. This approach has been applied to the integrated design of a class of flexible spacecraft, a geostationary platform and a ground-based flexible structure. An optimization-based approach has been developed with a set of design variables consist of both control and structural design variables. The approach of static and dynamic dissipative control laws are used to provide robust stability in the presence of both parametric and nonparametric uncertainties. The substantially superior numerical results have been obtained with the integrated design approach compared to that of the conventional approach. It was noted that standard high performance model-based controllers such as H-2 or H-infinity are generally not robust to deal with parametric uncertainties of unmodeled dynamics and certain types of actuator and sensor nonlinearities. Iwatsubo, Kawamura, Adachi, and Ikeda [17] made an approach to the simultaneous optimum design of the structural and control system of a flexible structure. This paper describes that the gradients of the characteristic values and shape of the structure are taken as structural design variables, while the number of the structural design variables is constant, and the numerical example of this simultaneous optimum design is presented.

4.3 Adaptive Feedforward Control Systems

Control systems implementations based upon the pioneering work of Widrow [18,19] emerged from a digital signal processing approach. This work had its origins in the need to provide noise and echo rejection in long distance phone lines [20]. Because of its origins in digital signal processing, this work grew up as a separate entity from traditional or modern controls approaches which accounts for its

conflicting definitions and conventions. The term adaptive here refers to ability of the controller to change its parameters in order to minimize a specified function. This it does without regard to any previous specified system model. It simply modifies the coefficients of an a priori specified digital filter to attain this goal. This is in contrast to a modern controls approach to adaptive control discussed earlier.

The original physical system was all electronic and the disturbance to be rejected was broad band noise correlated with the desired signal but delayed in time. For all of these implementations, it is assumed that a signal (input) that is correlated with the disturbance is available for feeding forward in the controller. The frequency range over which control was to be exercised was the primary voice bandwidth, from about 500 Hz to 5000 Hz. Because of the high frequency range to be controlled, it was found that transients imposed by changes in the controller state decayed quickly. Therefore, the adaptive process of the controller is considered to be going from one steady state to another steady state. In formulating the LMS adaptive process, it is also assumed that an instantaneous estimate of error function may be substituted for the true value of the error function. Using this assumption, the algorithm was implemented such that at every sample update, the controller updates all of its parameters. Because this occurs at 10,000 times a second, the algorithm is found to converge in the mean. Thus, it often does not matter that the error estimate may have a great deal of uncertainty.

In the early to mid 1980's, this work was picked up by Burgess working in acoustical noise control [21] as a means to implement what is now commonly referred to as active noise control. From the early work of Lueg [22] and Olsen [23] using analog controllers, the use of destructive interference for noise control achieved limited success. Work in the 1970's and early 1980's utilized analog controllers and sensing arrays to implement control systems typically with analog controllers and early digital controllers. This work is reviewed extensively by Ffowcs-Williams [24] and Warnaka [25]. The emergence of special purpose digital signal processing CPU's by Texas Instruments, AT&T and Motorola in the 1980's allowed this technology to progress rapidly as digital filters and adaptive algorithms could be implemented in real time on widely available, cheap systems.

The control algorithms that have been developed based upon Widrow's work [18] operate in the time domain. The optimization process updates the digital filter coefficients based upon an algorithm that samples the error function and reference signal continuously. This work has been extended to multiple input/output systems by Elliott et al [26]. This algorithm operates in the time domain such that the coefficients of an array of finite impulse response (FIR) filters, whose outputs are linearly coupled to another array of error detection points, are adapted so that the sum of all the mean square error signals is minimized. A special case of this adaptive controller is for control of a periodic, synchronously sampled response. The implementation of the above LMS algorithm for this case can be made very efficient as described in Reference [27]. Furthermore, its behavior can be represented exactly as that of a linear time-invariant comb filter.

The above work all applied finite impulse response filters as the central algorithm of the controller. Using this approach, it was much easier to insure stability of the control system. However, for controllers with a strong frequency dependence, i.e. resonant systems, this would typically require many filter coefficients (degrees of freedom) to provide the required control. Another approach to this problem was to use infinite impulse response (IIR) filters as the controller element. This allows a more complicated frequency response function to be approximated with significantly fewer coefficients (degrees of freedom). However, stability much more difficult to insure. These issues were discussed extensively by Johnson [28]. Current work by Eriksson [29] utilizes an IIR based control algorithm in a variation of Widrow's approach. This system is available commercially and has been working in industrial noise control applications for several years.

The first applications of this technology was control of low frequency plane wave noise propagation in ducts [30,31] to more recent work demonstrating control of random multi-modal modes in ducts [32]. The approach of the Roure [31] and Silcox [32] utilized an adaptive algorithm based in the frequency domain, although the controller was implemented in the time domain as a digital FIR filter.

More recent work by Bullmore, et. al. [33] and Silcox, et. al. [34] has investigated the control of interior noise in aircraft cabins. Typical noise problems in propeller and turbofan powered aircraft are harmonic in content and quite amenable to adaptive feedforward control. A tachometer signal from the turbomachinery provides the necessary reference signal and the limited harmonic content allows relatively simple controllers to be used. Two flight tests by Elliott, et. al. [35] and Ross, et. al. [36] on a British Aerospace 748 demonstrated significant noise reduction using distributions of acoustic sources. These flight tests utilized adaptive feedforward control and an open loop transfer function approach respectively. However, they required up to 32 control sources and 64 error sensors to provide this control. Similar result were obtained by Boeing Aircraft on a deHavilland Dash 8 aircraft in unpublished results.

Recent work has demonstrated a more efficient approach for controlling low to mid frequency structural sound radiation, termed active structural acoustic control (ASAC). In contrast to using acoustic control transducers, ASAC applies control forces directly to the structure such that some estimate of the radiated pressure field is minimized. The primary advantage of this approach is that effective control can be implemented with fewer control actuators. Other advantages are related to the physical implementation of the control in that the transducers can be arranged to be reasonably compact, or integrated as part of the structure.

Early work in ASAC was carried out at NASA Langley and VPI&SU [37] in 1985 where it was demonstrated that sound transmission into cylinders could be controlled by point forces applied to the cylinder wall. Again, the application was to develop advanced techniques for controlling interior noise in aircraft. It was shown

that only certain structural modes couple or radiate to the interior space and it thus was necessary to control only these modes. This effect was termed modal suppression. As the structural motion that gives rise to the pressure response is being controlled, the interior sound field is reduced globally independent of its modal shape. This work was extended at Douglas Aircraft on a full scale DC-9 fuselage. Global control of structure-borne interior noise transmitted through the engine pylons using only two point force control actuators was demonstrated [38]. Weight, mounting considerations and control spillover effects has led to recent cooperative work at NASA and VPI&SU to study the use of piezoceramic actuators bonded to structural elements [39]. On a full scale composite fuselage model, a 4 actuator, 6 sensor system has achieved interior global attenuation of 8 to 15 dB over a range of test conditions for exterior airborne excitations [40]. Optimization of the transducer size and distribution is expected to significantly improve performance [41,42].

Another important application of ASAC is in controlling marine hull radiated sound and is being investigated under research funded by ONR/DARPA. Early work in this area studied control of free field radiation from lightly loaded panels [43]. It was demonstrated that sound radiated into a free-field could also be globally attenuated with a limited number of control actuators [44]. However, another mechanism of control was observed. For the off-resonant cases examined, a reduction in sound radiation occurred with little (or an increase) change in the averaged structural response. It was concluded that the residual or closed loop structural response has a lower radiation efficiency for the same level of response [43]. This effect was termed modal restructuring. More recently it was demonstrated that modal suppression corresponds to a decrease in all structural wave-number components while modal restructuring corresponds to a reduction only in the supersonic (radiating) components; the subsonic components are largely unaffected [45]. The significance of modal restructuring is that large attenuations of radiated sound can be achieved by an appropriate change in the controlled structural mode shapes without affecting the overall amplitude. This approach is shown to require significantly less control energy.

Other work on free field application of ASAC have centered on using optimally shaped piezoelectric sensors and actuators bonded or embedded in the structure [46] (an adaptive or smart structure). Emphasis has been placed on shaping the sensors so that the radiating components of the structural motions are observed, i.e. the sensor acts as a structural wave number filter. Good reductions in radiated sound levels for both on and off resonance conditions were observed. This work has now been extended to include the influence of heavy fluid loading on structural motions [47]. Experiments performed cooperatively between VPI&SU and NRL have shown that the ASAC technique still provides high global attenuations when the radiation loading induces significant modal coupling.

4.4 Artificial Neural Networks

Artificial neural networks encompass a broad class of concepts relating to classification, prediction, control and decision making. These systems as implemented in engineering environments are generalizations of adaptive controllers. The systems are generally implemented such that they "learn" about their control functions by example. This is generally accomplished through a process where the neural network is given a series of input and resulting outputs. The systems attempt to predict the supplied output (result) by operating on the input vector and adjusting the internal parameters of the neural network. In this way, it operates much like an adaptive digital filter except that it is not restricted to linear systems. The method which is used to train the system is a subject of much debate. The most common approach uses a back propagation algorithm which employs gradient information about the neural net model to adjust the weights of the model [48]. This technique is often cited as being slow to converge and requires a large data base to train. An extension to this technique is termed dynamic back propagation and is discussed by Narendra [49]. This approach attempts to optimize the structure of the neural network as well as the network parameters themselves. Hoskins and Vagners [50] discuss stability criteria for a closed loop system using neural controllers based on approximate models of the plant.

Barron [51] bases a general adaptive polynomial neural network upon mathematical approximation theory and statistical decision theory. In this approach, the algorithm adaptively grows the structure using the observed data using a well defined model selection criteria. The use of polynomial networks was found to provide a structure that is not limited in its approximating capability. This approach was used by Barron et al [52] to provide fault detection, isolation, estimation function and reconfiguration strategies for flight control systems. This paper outlines the design procedure (i.e. database preparation, extraction of wave form features and network synthesis) and the architecture of the system for a control reconfigurable combat aircraft. A similar approach is used in defining an optimum real time, two point boundary value problem for guidance of tactical weapons [53].

Chen and Khalil [54] showed how neural networks may be used to linearize the feedback control problem for non-linear systems. The neural network learned the non-linearities of the system on-line. The output of the controller is then used in a conventional linear control scheme. Fuller et al [55] showed that a nonlinear system could be controlled directly using a neural network as the control element. This was for a simple electronic op amp driven to saturation. However, a comparatively simple neural control was implemented in real time to several hundred hertz.

Jorgensen and Schley [56] discuss the requirements for a neural network based system for an aircraft automatic landing system. It is expected that the flight envelope which is presently very limited may be expanded using such a system. Rather than applying the linear control systems with limited inputs presently in

use, a neural network system may be expected to utilize a wide range of input parameters to "learn" the operational responses of pilots in critical situations. Simulations of a sample controller is presented along with the structure of the controller.

An experimental evaluation of neural networks for control of autonomous undersea vehicles is presented by Herman et al [57]. The design of such a system is presented as well as a discussion of the issues relating to intelligent control and the hierarchical control system architecture. An extensive survey of the use of neural networks for the control of other vehicles and robotic motion is included in subsequent chapters of this reference.

The speed and simplicity of neural networks is used by Thursby et al [58] to implement smart electromagnetic structures that provide an adaptive electromagnetic environment to the structure on which they are mounted. By incorporating a neural network into the control structure of a single microstrip patch element, an antenna's performance characteristics may be varied in real time in response to a received signal. This has a payoff of improving receiver characteristics in a frequency agile environment as well as reducing the manufacturing and siting tolerance requirements normally placed on such antennas.

A real-time feedforward neural network controller implemented multiple input, multiple output control of broad band vibration on a built up structure. The controller adaptively learned to control the vibration at multiple sensor locations. Reductions up to 20 dB were attained as reported by Bozich and MacKay [59].

Parker et al [60] describes a broad band controller based on polynomial neural networks to control the vibration generated by the interaction of an elastic structure with both laminar and/or turbulent boundary layers. This work employs recursive elements in a feedback control system to provide control of a stationary random process.

Caball et al [61] use a neural network in an analytical investigation of a nonlinear temporal and spatial optimization problem. The optimum inputs and positions of an array of actuators used for active control of noise transmission are derived. It is shown that this approach is in good agreement with conventional approaches to numerical optimization. Schemes to reduce the required degrees of freedom are illustrated. It is shown that performance of the control system is only marginally affected by the reduced channels in the control system.

Midkiff and McHenry [62] discuss the design of multi-computer networks to meet the processing requirements of smart structures. Methods for mapping neural network computational models onto multi-computer networks are discussed in the context of integrating sensor, control and communication requirements for implementation on real hardware. The structure of the multi-computer processing

nodes, interconnection networks and a hierarchical model are studied and alternatives discussed.

Mazzu et al [63] present an approach for the design of intelligent structural monitoring systems. The approach consists of integrating artificial neural networks and knowledge based expert systems in order to achieve maximum benefit from both. In this work, strain measurements are processed through parallel neural networks and expert systems are used to evaluate the results.

Finally, Protzel [64] et al discuss the fault-tolerance of artificial neural networks (ANN). In particular, the fault-tolerance characteristics of time recurrent ANNs that can be used to solve optimization problems are studied. It is demonstrated that although these networks do not perform as well as conventional optimization methods, they perform with a more graceful performance degradation when confronted with various system failures without the additional redundancy required for the conventional systems. This may be especially desirable on long-term, unmanned space missions, where component failures have to be expected but no repair or maintenance can be provided.

4.5 Modeling Requirements for Verification and Simulation

4.5.1 Non-Linear Properties

Joshi [65] presents a concise formulation of relevant nonlinear constitutive relations of piezoelectric materials suitable for sensor and transducer applications. This paper extends the widely accepted linear relations of piezoelectric materials available for structural applications to the electroelastic constitutive behavior that is critical to predicting the response of a structure with embedded piezoelectric materials.

4.5.2 Modeling and Embedment Effect

MIT researchers [66] discuss finite element modeling of ADINA model. Important attributes of the work are one beam element per strut, use of consistent mass matrix, node flexibility incorporated through measured strut component test data, wires modeled as distributed masses, and modal damping included in post processing.

Anderson and Hagood [67] discuss selection of sensors and actuators to minimize impact of model inaccuracies on achievable performance and stability. It is stated that placement and performance/stability are related to the models of the transducers, and method of achieving closed-loop performance or robustness should incorporate model uncertainty information into open or closed loop placement algorithms. Also presented are recent work in the embedded electronics for intelligent structures to establish potential advantages of distributing and embedding large numbers of sensors, actuators and processors for precision control of flexible structures.

Anders and Rogers [68] present an analytical modeling technique which uses the Ritz method, classical laminated plate theory, and finite panel acoustic radiation theory to predict the modal and structural acoustic behavior of locally activated shape memory alloy hybrid composite panels.

Davidson [69] considers the modeling of stress and strain fields around and within optical fibers embedded in carbon reinforced composites. It is stated that the fiber sensor must produce a minimum perturbation in the distribution of reinforcing fibers, not significantly alter the mechanical characteristics of the composite, and match impedance so as not to attenuate sensing signal. Jensen, Pascual, and August [70] present their investigation of the significance of the orientation of embedded optical fibers on the tensile behavior of graphite/bismaleimide laminates. It is reported that optical fibers have a detrimental effect on the tensile behavior of graphite/bismaleimide laminates. Bronowicki, Betros, Nye, McIntyre, Miller and Dvorsky [71] have made mechanical validation of embedded lead-zirconate-titanate (PZT) sensor and actuators in a composite materials. The embedded transducers have been subjected to tension and compression loading at a level of fatigue and to the vacuum and thermal environment of space. Two standard Navy PZT compositions, type I and II, embedded in graphite/epoxy or a graphite/thermoplastic laminate were evaluated.

Bronowicki, Mendenhall, Betros, Wyse and Innis [72] present phase III of the advanced composites with embedded sensors and actuators (ACESA) program.

4.5.3 Simulation and Verification

Wu and Tzeng [73] investigated active vibration control of smart structural materials using the numerical simulation and the experimental testing. The control mechanisms of Lyapunov's second method has been verified to be an effective controller for smart material systems with piezoelectric sensors and actuators for the experimental analysis and the numerical simulation. The piezoelectric active damper is effective for transient vibration control, while it is not sufficient enough to suppress large steady-state oscillation.

Hanks [74] presents ground verification of a large flexible spacecraft and analytical investigation of on-orbit dynamic tests of Space Station Freedom. Difficulties of verifying a large flexible spacecraft on earth are presented with a possible alternative of using scale models to substitute the real model ground tests.

4.5.4 Zero-Gravity Issues

Swanson, Yuen, and Pearson [75] report about the dynamics of test structures on a laboratory suspension system that were compared with the dynamics during zero-gravity parabolic flights on a NASA KC-135 aircraft. It is reported that parabolic aircraft flights can adequately measure the effects of the ground suspension friction and restraint, and that accurate modal measurements can be made. Lawrence, Lurie,

Chen and Swanson [76] performed an active member vibration control experiment in a KC-135 reduced gravity environment. The results of flight tests were well correlated to those of the ground tests. Crawley, Alexander and Rey [77] discuss about gravity effects on sensors and actuators, which affect control performance of the system. Both direct and indirect effects of gravity are presented with application to the middeck active control experiment (MACE).

4.5.5 Modal Analysis

Su, Rossi, Knowles and Austin [78] used a digital signal processing (DSP) based workstation to identify modal parameters and vibration control of a cantilever beam. The workstation with DSP as the main processor, it estimated the modal parameters of a cantilever beam after the modes were detected using stochastic methods. The workstation also analyzes the data from 34 piezoceramic sensors of acceleration and strain, and generates control signals to the 18 actuators for vibration control.

4.6 References

1. Jacques, R., Blackwood, G., MacMartin, D., How, J., and Anderson, E., "Control Design For the SERC Experimental Testbeds", MIT Workshop on Control Structures Technology, Jan 22-23, 1992, Cambridge, Mass.
2. Allen, J.J., Lauffer, J.P., and Marek, E.L., "The Sandia Structural Control Experiments," First Joint S.S./Japan Conference of Adaptive Structures, November 13- 15, 1990, Maui, Hawaii.
3. Murotsu, Y., Senda, K., and Hisaji, K., "Optimal Configuration of Control of an Intelligent Truss Structure," First Joint S.S./Japan Conference of Adaptive Structures, November 13-15, 1990, Maui, Hawaii.
4. Hyland, D.C., Collins, E.G., Phillips, D.J., and King, J.A., " Decentralized Control Experiments: Implications for Smart Structures," An International Symposium & Exhibition on Active Materials and Adaptive Structures, November 4-8, 1991, Alexandria, VA.
5. Hong, S.Y., Varadan, V.V., and Varadan, V.K., "Experiments on Active Vibration Control of a thin Plate Using Disc Sensors and Actuators," An International Symposium & Exhibition on Active Materials and Adaptive Structures, November 4-8, 1991, Alexandria, VA.
6. Hanagud, S., Babu, G.L.N., Stalford, H.L., and Won, C.C., "Robustness Issues in the Design of Smart Structures," First Joint S.S./Japan Conference of Adaptive Structures, November 13-15, 1990, Maui, Hawaii.

7. Jacues, Robert N. and Miller, David W., "Preliminary Design of Optimal H-2 and H-infinity Controlled Structures," An International Symposium & Exhibition on Active Materials and Adaptive Structures, November 4-8, 1991, Alexandria, VA.
8. Huang, Chien Y. and Knowles, Gareth J., "Control of Grumman Large Space Structure using H-infinity Optimization, An International Symposium & Exhibition on Active Materials and Adaptive Structures, November 4-8, 1991, Alexandria, VA.
9. Athans, M., Agguiero, F., Bielecki, E., Bokor, J., Douglas, J., and Lublin, L., "Summary of Additional Research in Multivariable Identification and Control," SERC Steering Committee Workshop, January 22-23, 1992, Cambridge, MA.
10. Trent, C.L. and Pak, Y.H., "Control of Space Structures Using Active Piezoelectric Members," An International Symposium & Exhibition on Active Materials and Adaptive Structures, November 4-8, 1991, Alexandria, VA.
11. Sekine, K., Shibayama, Y., Iwasawa, N., Tagawa, N., Sunahara, S., Yoshida, s., and Arikabe, T., "Identification and adaptive Control of Flexible Truss Structures," First Joint S.S./Japan Conference of Adaptive Structures, November 13-15, 1990, Maui, Hawaii.
12. Melcher, J. and Wimmel, R., "Modern Adaptive Real-Time Controller for Actively Reacting Flexible Structures," First Joint S.S./Japan Conference of Adaptive Structures, November 13-15, 1990, Maui, Hawaii.
13. Maghami, Peiman G., Joshi, Suresh M., and Price, Douglas B., "Integrated Controls- Structures Design Methodology for a Flexible Spacecraft," 15th Annual AAS Guidance and Control Conference, February 8-12, 1992, Keystone, CO.
14. Maghami, P.G., Joshi, S.M., and Lim, K.B., "Integrated controls-Structures Design: A Practical Design Tool for Modern Spacecraft," 1991 American Control Conference, June 26-28, 1991, Boston, MA.
15. Maghami, P.G., Joshi, S.M., Walz, J.E., and Armstrong, E.S., "Integrated Controls-Structures Design Methodology Development for a Class of Flexible Spacecraft," Third Air Force/NASA symposium on Recent Advances in Multi-disciplinary Analysis and Optimization, September 24-26, 1990, San Francisco, CA.
16. Maghami, P.G., Joshi, S.M., and Gupta, S., "Integrated Controls-Structures Design for a Class of Flexible Spacecraft," Fourth NASA/DoD CSI Technology Conference, November 5-7, 1990, Orlando, FL.

17. Iwatsubo, T., Kawamura, S., Adachi, K., and Ikeda, M., "Simultaneous Optimum Design of Structural and Control System," First Joint S.S./Japan Conference of Adaptive Structures, November 13-15, 1990, Maui, Hawaii.
18. Widrow, B. and Stearns, S.D. "Adaptive Signal Processing", Prentice-Hall, Englewood Cliffs, N.J. 1985.
19. Widrow, B. et al: "Adaptive Noise Canceling: Principles and Applications," Proc. of the IEEE, vol 63, no. 12, Dec. 1975.
20. Widrow, B. and Hoff, M.E.; "Adaptive Switching Circuits," IRE WESCON Convention Rec. Pt. 4, pp 96-104, 1960.
21. Burgess, J.C., "Active Adaptive Sound Control in a Duct: A Computer Simulation," J. Acoust. Soc. Amer., vol 70, pp 715-726, 1981.
22. Lueg, P.; "Process of Silencing Sound Oscillations," U.S. Patent no. 2,043,416, Filed: March 8, 1934, Patented: June 9, 1936.
23. Olsen, H.F. and May, E.G.; "Electronic Sound Absorber," Jour. Acoust. Soc. Am. vol. 25(6) pp 1130-1136, 1953.
24. Ffowcs-Williams, J.E.: "Anti-sound," Proc. R. Soc. Lond. A 395, 63-88, 1984
25. Warnaka, G. "Active Attenuation of Noise - State of the Art," Noise Control Engineering, pp 100-109, vol. 18(3), May-June 1982.
26. Elliott, S.J., Stothers, I.M. and Nelson, P.A.: "A multiple Error LMS Algorithm and Its Application to the Active Control of Sound and Vibration" IEEE Trans. on Acoustics, Speech and Signal Processing, Vol. ASSP-35, No. 10, October 1987.
27. Elliott, S. J. and Darlington, P.: "Adaptive Cancellation of Periodic, Synchronously Sampled Interference" IEEE Trans. on Acoustics, Speech and Signal Processing, Vol. ASSP-33, No. 3, June 1985.
28. Johnson, C.R.; "Adaptive IIR Filtering: Current Results and Open Issues," IEEE Trans. on Information Theory, vol. IT-30, no.2, March 1984.
29. Eriksson, L.J.; "Development of the filtered-U algorithm for active noise control," J. Acoustical Soc. Amer. vol. 89(1), January 1991.
30. Ross, C.F.; "An Adaptive Digital Filter for Broadband Active Sound Control," J. Sound and Vibration, vol. 89, pp 381-388, 1982

31. Roure, A.; "Self-Adaptive Broadband Active Sound Control System," J. Sound and Vibration, vol.101, no. 3, pp 429-441.
32. Silcox, R. J.; "Frequency Domain Adaptive Algorithms for Active Control," Proc. Internoise 91, pp 173-176, Sydney, Australia, 2-4 Dec, 1991.
33. Bullmore, A.J. et al; "Models for Evaluating the Performance of Propeller Aircraft Active Noise Control Systems," AIAA paper no. 87-2704
34. Silcox, R.J., Fuller, C.R., and Lester, H.C.; "Mechanisms of Active Control in Cylindrical Fuselage Structures," AIAA Journal, vol 28, no 8, August 1990.
35. Elliott, S.J. et al; "In-flight Experiments on the Active Control of Propeller-Induced Cabin Noise," J. of Sound and Vibration, vol. 140(2), pp219-238, 1990.
36. Dorling, C.M. et al;"A demonstration of active noise reduction in an aircraft cabin," Jour. of Sound and Vibration, vol. 128(2), January 22, 1989.
37. C.R. Fuller and J.D. Jones, "Experiments on Reduction of Propeller Induced Interior Noise by Active Control of Cylinder Vibration", J. Sound Vib. 112(2), 389 (1987)
38. M. Simpson et al, "Full Scale Demonstration of Cabin Noise Reduction using Active Vibration Control", AIAA J. Aircraft 28(3), 208 (1991).
39. C.R. Fuller et al, "Active Control of Interior Noise in Model Aircraft Fuselages Using Piezoelectric Actuators", AIAA Paper no. 90--3922 (1990)
40. R.J. Silcox et al, "Evaluation of Piezoceramic Actuators for Control of Aircraft Interior Noise", presented at 14th AIAA Aeroacoustics Conf. May 1992, AIAA paper no. 92-02-091.
41. V.R. Sonti and J.D. Jones, Proc of Recent Advances in Active Control of Sound and Vibration, Blacksburg, VA (Technomic Press, PA) 27 (1991)
42. H.C. Lester and S. Lefebvre, Proc of Recent Advances in Active Control of Sound and Vibration, Blacksburg, VA (Technomic Press, PA) 3 (1991)
43. C. R. Fuller, "Active Control of Sound Transmission/Radiation from Elastic Plates by Vibration Inputs, I: Analysis", J. Sound Vib. 136(1), 1 (1990)
44. V.L. Metcalf et al, "Active Control of Sound Transmission/Radiation from Elastic Plates by Vibration Inputs, II: Experiments", J. Sound Vib. 152(3) (1992)

45. R.L. Clark and C.R. Fuller, Proc of Recent Advances in Active Control of Sound and Vibration, Blacksburg, VA (Technomic Press, PA) 507 (1991)
46. C. R. Fuller, C.A. Rogers and H.H. Robertshaw, "Active Structural Acoustic Control with Smart Structures", Proc. of SPIE Conf., vol. 1170, 338 (1989)
47. Y. Gu and C. R. Fuller, "Active Control of Sound Radiation from a Uniform Rectangular Fluid-Loaded Plate", J. Acoust. Soc. Am. 89(4) Pt.2, 1915 (1991)
48. Werbos, P.J. "Backpropagation: past and future," proceeding of IEEE International Conference on Neural Networks, IEEE Press, I:343-353, 1988.
49. Narendra, K.S. and Parthasarathy, K.; "Gradient Methods for the Optimization of Dynamical Systems Containing Neural Networks," IEEE Trans on Neural Networks, vol. 2, no.2, pp 252-262, March 1991.
50. Hoskins, D.A. and Vagners, J.; "A Neural Network Based Explicit Model Reference Adaptive Controller," proc. 29th Conf. on Decision and Control, Honolulu, Hawaii, pp. 1725-1729, Dec. 1990.
51. Barron, A.R. and Barron, R.L. "Statistical Learning Networks: A Unifying Approach," Computing Science and Statistics: 1988 Proc. of the 20th Symposium on the Interface, pp 192-203.
52. Barron, R.L. et al, "Application of Polynomial Neural Networks to FDIE and Reconfigurable Flight Control," National Aerospace Electronics Conference, Dayton OH, May 23-25, 1990.
53. Barron, R.L. and Abbott D.W.; "Use of Polynomial Networks in Optimum, Real Time, Two-Point Boundary Value Guidance of Tactical Weapons," presented at Military Computing Conference, May 3-5, 1988, Anaheim, CA.
54. Chen, F.C. and Khalil, H.K.; "Adaptive Control of Non-Linear Systems Using Neural Networks," proc. 29th Conference on Decision and Control, pp 1707-1712, Honolulu, Hawaii, Dec. 1990.
55. Fuller, C.R., Caball, R. and Brown, D.; proc. Internoise 91, Sydney, Australia, Dec. 1991.
56. Jorgensen C.C. and Schley, C.; "A Neural Network Baseline Problem for Control of Aircraft Flare and Touchdown," pp. 403-425, Neural Networks for Control, MIT Press, Cambridge MA 1990.

57. Herman, M. et al; "Intelligent Control for Multiple Autonomous Undersea Vehicles," pp. 427-474, Neural Networks for Control, MIT Press, Cambridge MA 1990.
58. Thursby, M. et al; "Neural Control of Smart Electromagnetic Structures," proc. of An International Symposium & Exhibition on Active Materials & Adaptive Structures, Alexandria VA, Nov 1991.
59. Bozich, D.J. and MacKay, H.B.; "Neurocontrollers Applied to Real-Time Vibration Cancellation at Multiple Locations," Proc. of Conf. on Recent Advances in Active Control of Sound and Vibration, pp 326-337, VPI&SU, Blacksburg, VA April 1991.
60. Parker, B.E. et al; "Adaptive Nonlinear Polynomial Neural Networks for Control of Boundary Layer/Structural Interaction," NASA CR-189645, 1992.
61. Caball, R. et al; "The Optimization of Force Inputs for Active Structural Acoustic Control using a Neural Network," NASA TM-107627, 1992.
62. Midkiff, S.F. and McHenry, J.T.; "Multicomputer Networks for Smart Structures," Proc. of An International Symposium & Exhibition on Active Materials & Adaptive Structures, Alexandria VA, Nov 1991.
63. Mazzu, J.M., Allen, S.M. and Caglayan, A.K.; "Neural Network/ Knowledge Based Systems for Smart Structures," Proc. of An International Symposium & Exhibition on Active Materials & Adaptive Structures, Alexandria VA, Nov 1991.
64. Protzel, P.W., Palumbo, D.L. and Arras, M.K.; "Performance and Fault-Tolerance of Neural Networks for Optimization," NASA CR-187582, ICASE Report No. 91-45. June 1991.
65. Joshi, S.P., "Nonlinear Constitutive Relations for Piezoceramic Materials," An International Symposium & Exhibition on Active Materials and Adaptive Structures, November 4-8, 1991, Alexandria, VA.
66. How, J.P., Blackwood, B., Anderson, E., and Balmes, E., "Finite Element Model and Identification Procedure", SERC Steering Committee Workshop, Jan 22-23, 1992, Cambridge, MA.
67. Anderson, E. and Hagood, N.W., "Sensor and Actuator Technology Development," SERC Steering Committee Workshop, January 22-23, 1992, Cambridge, MA.

68. Anders, W.S. and Rogers, C.A., "Vibration and Low Frequency Acoustic analysis of Piecewise-Activated Adaptive Composite Panels," First Joint S.S./Japan Conference of Adaptive Structures, November 13-15, 1990, Maui, Hawaii.
69. Davidson, R., "Do Embedded Sensor systems Degrade Mechanical Performance of Host Composites?" An International Symposium & Exhibition on Active Materials and Adaptive Structures, November 4-8, 1991, Alexandria, VA.
70. Jensen, D.W., Pascual, J., and August, J.A., "Tensile Strength and stiffness Reduction Graphite/Bismaleimide Laminates with Embedded Fiber Optic Sensors," An International Symposium & Exhibition on Active Materials and Adaptive Structures, November 4-8, 1991, Alexandria, VA.
71. Bronowicki, A., Retros, R., Nye, T., McIntyre, L., Miller, L., and Dvrosky, G., "Mechanical Validation of Smart Structures," SDIO Workshop on Advanced Piezoelectric Actuation Materials for Space Applications", Institute for Defense Analyses, Feb. 25, 1992, Alexandria, VA.
72. Bronowicki, A.J., Mendenhall, T.L., Betros, R.S., Wyse, R.E., and Innis, J.W., "ACESA Structural Control System Design," First Joint S.S./Japan Conference of Adaptive Structures, November 13-15, 1990, Maui, Hawaii.
73. Wu, W.B. and Tzeng, M.J., "Active Vibration Control of Smart Structural Materials," First Joint S.S./Japan Conference of Adaptive Structures, November 13-15, 1990, Maui, Hawaii.
74. Hanks, B.R., "Research on the Structural Dynamics and Control of Flexible Spacecraft," An International Symposium & Exhibition on Active Materials and Adaptive Structures, November 4-8, 1991, Alexandria, VA.
75. Swanson, A.D., Yuen, W., and Pearson, J., "Zero-Gravity Dynamics of Space Structures in Parabolic Aircraft Flight," First Joint S.S./Japan Conference of Adaptive Structures, November 13-15, 1990, Maui, Hawaii.
76. Lawrence, C.R., Lurie, B.J., Chen, G-S., and Swanson, A.D., "Active Member Vibration Control Experiment in a KC-135 Reduced Gravity Environment," First Joint S.S./Japan Conference of Adaptive Structures, November 13-15, 1990, Maui, Hawaii.
77. Crawley, E.F., Alexander, H., and Rey, D., "The Middeck Active Control Experiment: Gravity and Suspension Effects," SERC Steering Committee Workshop, January 22-23, 1992, Cambridge, MA.

78. Su, J., Rossi, M., Knowles, G., and Austin, F., "Piezoceramic/DSP-Based Integrated Workstation for Modal Identification and Vibration Control," An International Symposium & Exhibition on Active Materials and Adaptive Structures, November 4-8, 1991, Alexandria, VA.

5 Recommendations for Future Research

The recommendations for future research in active (smart) structures at Langley emphasize Langley's strengths so that significant contributions might be achieved. The recommendations are in the following areas:

- 1) actuation materials
- 2) smart/intelligent sensors
- 3) information management
- 4) applications

5.1 Actuation Materials

In the materials area, the integration of smart materials such as piezoelectric ceramics into composite materials is seen as a research area in which Langley can make significant technical contributions. By incorporating the sensing and actuation function within the composite material, weight reductions, decreased volumes, increased reliability (fewer parts) and improved performance (better sensing and actuation) may be achieved in future aircraft and spacecraft designs. Potential research areas are piezoelectric polymeric films and coatings, integration of piezoelectric ceramic powders and metallic powders into composites, and piezoelectric fibers. The use of magnetostrictive materials, such as Metglas and Terfenol-D, with composites is another research area that should be pursued. These magnetostrictive materials have large force outputs and use low voltage inputs.

Piezoelectric ceramic powders and polymers may be film cast into thin sheets for various applications. Likewise, Terfenol-D powder and polymers could also be film cast for applications in various structural concepts.

More ways of integrating sensing materials into composites needs to be investigated. This would allow for more and better information about the structural environment that could lead to improved performance and understanding of structural behavior.

For aircraft, the current designs use the lightest materials and strongest configurations available. A goal of these smart actuation materials should be to develop stiffnesses comparable to current engineering materials.

5.2 Smart/Intelligent Sensors

Any intelligent aspect of a smart structure should come from its ability to receive and process external disturbances and command actuators based upon a control strategy resident in the control processors. A smart structure can only be as smart as its built-in intelligence level.

Areas of smart sensors which are applicable to various aspects of parameter measurements should be pursued, such areas as, acceleration, strain and strain rate, force, pressure, temperature and displacement. These measurands should be converted to signals that are suitable for signal processing and subsequent communication to the smart structure information management system.

The use of smart sensors to measure pressure and loads on wing surfaces during wind tunnel tests and flight tests should be pursued. In wind tunnel testing, the use of smart sensors could reduce the cost of design and fabrication.

5.3 Information Management

The networking of smart structural subsystems within a structure is seen as a very important research area which has not received attention by researchers. Concepts need to be developed and evaluated for performance and applications. A general architecture for information management is needed within which the network resides. Research in smart/intelligent structures at this time has dealt with a single system or subsystem. Some understanding of how these subsystems will be integrated on an aircraft or spacecraft should be addressed. It is possible that individual autonomous smart subsystems could give conflicting commands to cause performance to degrade. Thus an overall information management system including the networking architecture should be developed.

5.4 Applications

It is hoped that the development of new smart materials and the supporting technologies (electroding, poling and testing) will form a critical mass of people capable of interfacing with other researchers here at the Center. The exchange of ideas is important and we can only suggest a few ways in which smart materials could be used in aircraft and spacecraft.

In aircraft the use of smart materials in aircraft wing designs can be used to suppress flutter, control winglets, change control surfaces, and extend laminar flow region. It may be possible to develop a gust load alleviation system for general aviation. Improved sensing of performance related parameters in aircraft wings should be emphasized. Use of new smart materials should be pursued for noise suppression in transports.

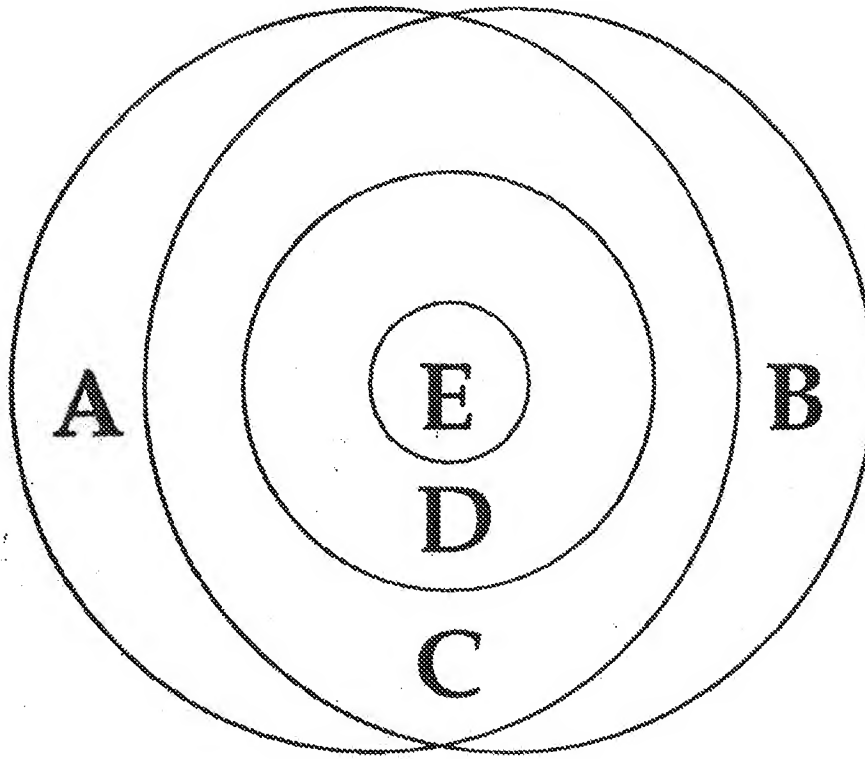
Force balances for supporting wind tunnel models could benefit from the smart materials area. A single variable stiffness support could accommodate the testing requirements of different size models which have different load ranges. This would allow other components to be properly sized so that the measured force and moments are sensitive to the wind induced loads.

5.5 Research Environment

A strong requirement for implementation of innovative structural systems is an understanding of the physics of the system to be controlled. The advanced structural dynamic modeling capabilities at Langley provide a firm foundation for future development. Additionally, for aeronautical applications, dynamic modeling of fluid structural coupling effects should be emphasized for innovative applications of smart structures.

It is hoped that a coordinated effort in active structures will be more formally established here at the Center. The research areas discussed in this report are multidisciplinary and require the cooperation of several organizations. With research activities in aeronautics and space at the Center, the management could help foster the research environment by advising the active structures technical committee of research in their organization in active structures. It would then be the intention of the technical committee to have the researcher present his or her results and engage in an exchange of ideas.

Proposed Structure Types



A Sensory

B Adaptive

C Controllable

D Active

E Intelligent

Piezoelectric Materials

Piezoelectric material are materials which generate a mechanical strain when an electrical voltage is applied or vice versa generate an electrical voltage when they are mechanically deformed. There are manmade materials which may be poled such that they will exhibit piezoelectric properties. This is accomplished by applying a large inducing voltage across the material. The dipoles within the material align themselves such that the positive ends of the dipoles are oriented toward the negative poling voltage. The electric field is held on the material for a certain time and then removed. The dipoles maintain their orientation. When subsequent smaller voltages are applied to the same piece of material, the dipoles will respond by attempting to reorient themselves.

To utilize the material once it has been poled, a charge is applied across the material. The dipoles within the piezoelectric ceramic will attempt to align themselves such that the positive ends of the dipoles will be attracted by the negative applied current and vice versa.

The electromechanical coupling coefficient is called d , followed by subscripts. The first subscript corresponds to the direction of the applied voltage and the second corresponds to the direction of deformation.

Figure 1 shows the electrodes attached to the ceramic in the same manner as the original inducing voltage was applied. This is the 3-direction. The in-plane directions are defined as the 1 and 2 -directions. When the voltage is applied as shown in the figure, the negative ends of the dipoles are pulled by the positive voltage and the positive ends are pulled by the negative voltage. This causes a stretching of the material in the direction of poling. The figure on the left shows this effect, which is termed the d_{33} effect.

Figure 2 illustrates that in response to a voltage applied in the 3-direction, a deformation occurs in the in-plane direction. Note that the d_{33} and d_{31} effects occur simultaneously. The d_{31} effect can be thought of as a Poisson-like effect.

Figure 3 shows the d_{15} effect which occurs when the electrodes and thus the applied voltage are oriented at 90 degrees to the direction of the polarization. The resultant deformation is a shear effect as the tops of the dipoles pull to the left and the bottoms strain to the right.

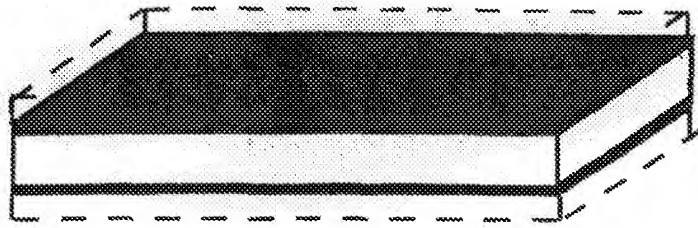


Figure 1 Thickening Effect (d_{33} effect)

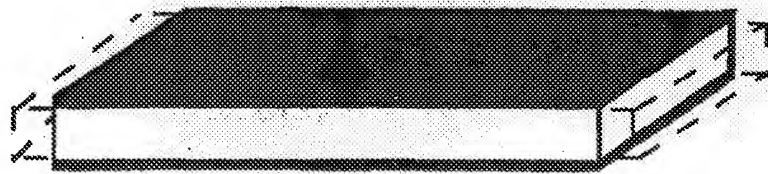


Figure 2 Lengthening Effect (d_{31} , d_{32} effect)

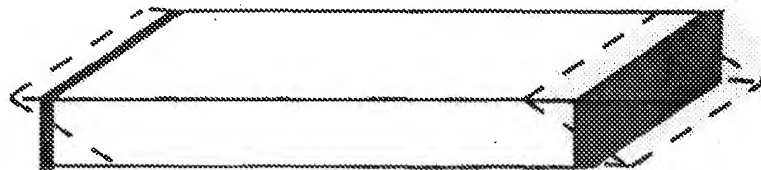
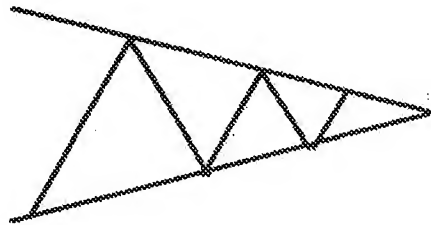


Figure 3 Shearing Effect (d_{15} effect)

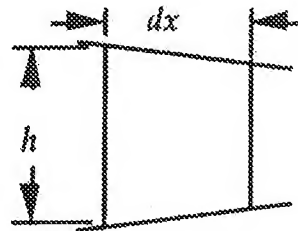
Effect of Expansion and Contraction of the Surfaces on Shape of a Wedge-Shaped Trailing Edge

A very effective means of control for subsonic airplanes is deflection of the trailing edge of an airfoil. Determination of the effect of expansion and contraction of the skins on the shape of a trailing edge is therefore of interest. A means of accomplishing the expansion and contraction could be a surface mounted piezoelectric ceramic.

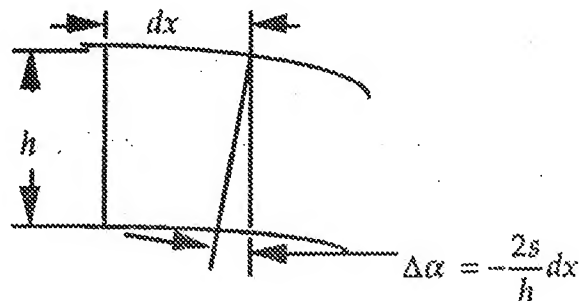
Consider a trailing edge with flat upper and lower surfaces. The skins can expand or contract longitudinally. As shown in the following sketch, the interior structure may be considered to be a Warren truss that resists shear but offers no resistance to expansion or contraction of the skins.



An element of the trailing edge of height h and length dx is shown below:



If the upper surface expands and the lower surface contracts, the change in length of each surface element is plus or minus sdx , where s is the strain of each surface. The change in angle of the rear of the section as a result of this deformation is



The thickness of the wedge-shaped trailing edge is defined by the formula:

$$h = h_0 - Kx = h_0 - \frac{h_0}{x_m} x = \frac{h_0}{x_m} (x_m - x)$$

If this value is substituted the preceding expression, then the slope of the mean line may be determined by the expression:

$$\Delta\alpha = -\frac{2sdx}{h_0/x_m(x_m - x)}$$

Integrating this expression:

$$\alpha = -\frac{2s}{h_0/x_m} \int_0^{x_i} \frac{dx}{(x_m - x)}$$

or

$$\alpha = \frac{dy}{dx} = \frac{2s}{h_0/x_m} \ln\left(\frac{x_m - x}{x_m}\right)$$

the displacement is then:

$$y = \int \frac{dy}{dx} dx = \frac{2s}{h_0/x_m} \int_0^{x_i} \ln\left(\frac{x_m - x}{x_m}\right) dx$$

let

$$u = \frac{x_m - x}{x_m}, \quad du = -\frac{dx}{x_m}, \quad \text{or } dx = -x_m du$$

then

$$\begin{aligned} y &= \frac{2s}{h_0/x_m} (-x_m) \int_1^{\frac{x_m - x_i}{x_m}} \ln(u) du \\ &= \frac{2s}{h_0/x_m} (-x_m) \left[u \ln(u) - u \right]_1^{\frac{x_m - x_i}{x_m}} \\ &= \frac{2s}{h_0/x_m} (-x_m) \left[\frac{x_m - x_i}{x_m} \ln\left(\frac{x_m - x_i}{x_m}\right) - \frac{x_m - x_i}{x_m} - (\ln(1) - 1) \right] \end{aligned}$$

simplifying:

$$\frac{y}{x_m} = -\frac{2s}{h_0/x_m} \left[\left(1 - \frac{x_i}{x_m}\right) \ln \left(1 - \frac{x_i}{x_m}\right) + \frac{x_i}{x_m} \right]$$

A plot of 2 times the quantity in brackets (for $0 \leq x_i/x_m \leq .9$) is shown in figure 1.

Discussion

The mean line is seen to bend with increasing slope as the trailing edge is approached. In practice, the finite thickness of the trailing-edge skin would prevent the use of this theory too close to the trailing edge. Also, the small angle approximations made in the derivation become invalid when the slope is too large. In the case of no small-angle approximations and the mathematical idealization of infinitely thin skin, an exact solution would show the mean line spiraling around an infinite number of times as the trailing edge is approached. This behavior is an interesting example of Zeno's paradox, but has no practical significance.

As an example, consider the trailing edge to be rigid (because of finite skin thickness) for the rear 10 percent of the wedge-shaped section considered. Then, as shown in figure 1 (with a linear function from $.9 \leq x_i/x_m \leq 1$ which is tangent to the curve at the point $x_i/x_m = .9$), the deflection at the trailing edge would be approximately:

$$\frac{y}{x_m} = -1.8 \frac{s}{h_0/x_m}$$

For a value of $h_0/x_m = 0.1$ and a value of $x_m = 1$ foot, the value of y at the trailing edge would be as follows for several values of the strain, s .

s	y , in.
0.01	2.16
0.001	0.216
0.0001	0.0216

A value of strain of about 0.01 would be required with the method studied to give a trailing-edge deflection comparable to that obtained with a conventional control surface.

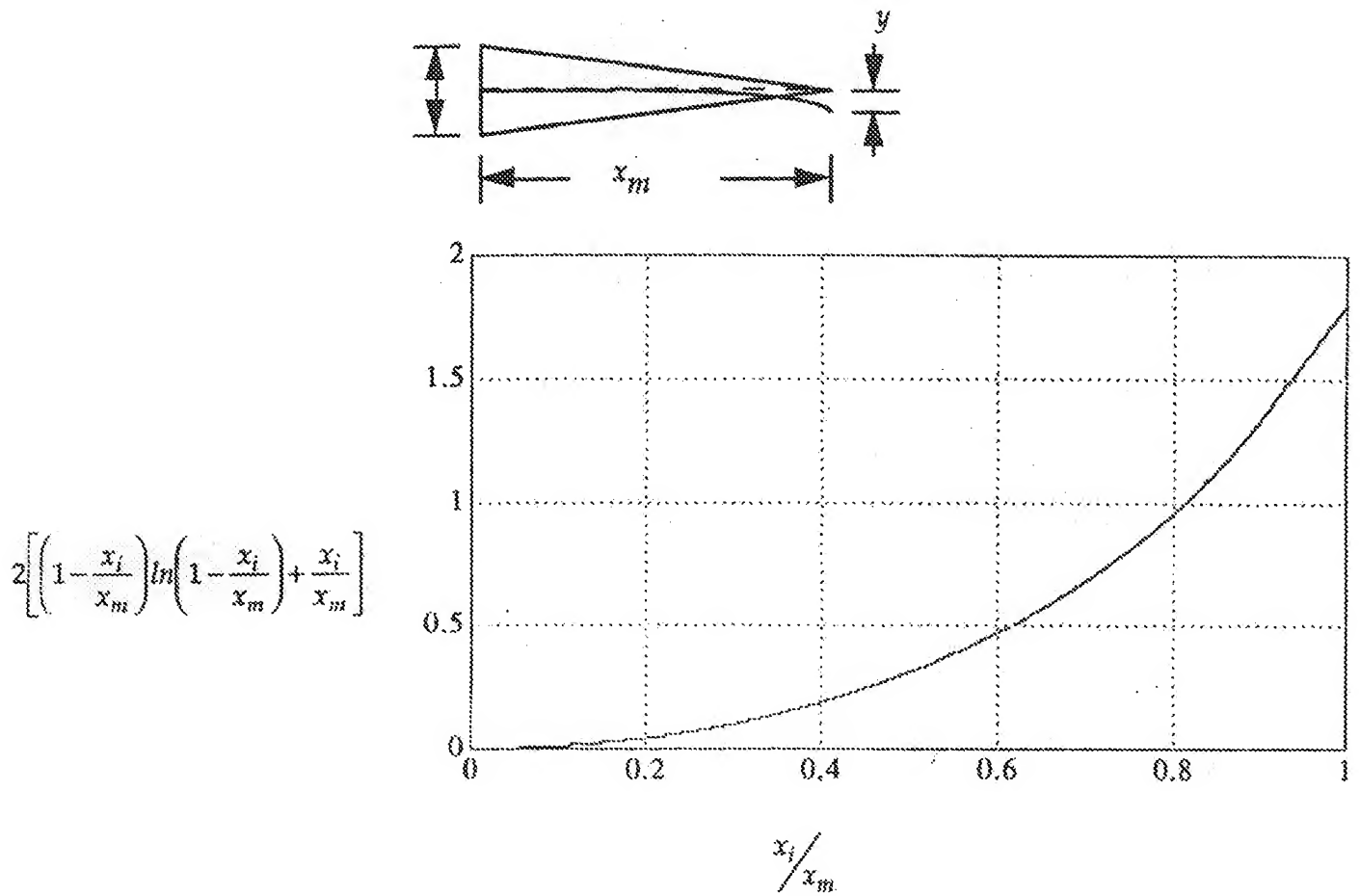


Figure 1 Function showing shape of mean line of trailing edge caused by expansion and contraction of surfaces

Comparisons of Adaptive Materials

The following information was presented by Dr. Ralph Fenn of SatCon Technology Corp. at NASA Langley Research Center on February 6, 1992.

Qualitative Comparison of Adaptive Materials

Magnetostrictive foil is superior to piezoelectric ceramics in four areas.

1. RELIABILITY:

- o No inaccessible embedded leads to break.
- o Physical continuity of large electrodes is not required.
- o Minimized short circuits due to conductive laminations.
- o Low voltage power improves reliability.

2. STABLE PROPERTIES:

- o Low temperature sensitivity of magnetostriction.
- o Low creep.
- o No "bleeding" like piezoelectrics where initial elongation decays.
- o Will not depole or break down like piezoelectric materials in high operating fields.

3. MANUFACTURABILITY:

- o Tough Metglas ribbon can be wound onto mandrels at high speed.
- o Pre-anneal Metglas is flexible enough to follow very tight curves.
- o Interlacing of electrodes and active material is not required so process is simpler.

4. FLEXIBILITY:

- o Adaptive material shape response can be altered by changing field shape using interchangeable coils.

Quantitative Comparison of Adaptive Materials

	<u>PZT-G-1195</u> <u>Piezoceramic</u>	<u>PVDF</u> <u>Piezo Film</u>	<u>PMN-BA</u> <u>Electrostr.</u>	<u>Nitinol</u> <u>Shp Mem.</u>	<u>Terfenol-D</u> <u>Magnetostr.</u>
Max. Strain (ppm)	300	300	600	20000 AC	1800
E (lb/in ²) × 10 ⁻⁶	9	0.3	17	8	7
T max (°C)	360	100	high	45	380
Hysteresis (%)	10	>10	<1	5	2
Bandwidth	kHz	kHz	kHz	1 Hz	100 Hz
Temp. Sen. (%/°C)	0.05	0.8	0.9	-	0.3

Comparison of Magnetostrictive Materials

	<u>Nickel</u>	<u>Metglas</u>	<u>Terfenol-D</u>
Maximum strain	50 ppm	50 ppm	1800 ppm
Field required	6,000 G	1 G	500 G
Resistivity	7×10 ⁻⁸ Ωm	1×10 ⁻⁶ Ωm	6×10 ⁻⁷ Ωm
Available in foil	yes	yes	no

Conclusions:

1. Nickel and most magnetostrictive materials require large fields for actuation.
2. Metglas has same maximum strain as traditional magnetostrictive materials but requires three orders of magnitude lower fields.
3. Terfenol-D has 35 times larger strains than Metglas but can not be laid into composites.

Typical Applications of Piezoelectric Film (PVDF)

COMPUTER INPUT/OUTPUT

Keyboards

Keypads and Arrays

X-Y Coordinates

Digitizer

Interactive Touch Screen

Mouse

Joystick

Printers

Impact Flight Time

Ink Drop Generation and Detection

Copiers

Switches

Paper Path Switches

Toner Level

Disc Drives

Accelerometers

Ferroelectric Memory

INDUSTRIAL

Switches

Solid State

Snap Action

Cantilever Beam

Keypad/Keyboard

Vandal-Proof

Intrinsically Safe

CMOS Wake-up

Low-Deflection

Singing Switch

Coin Counter

Acoustic Switch

Shaft Rotation

Magnetic Reed

Physical Security Energy Management

180 Degree Passive Infrared Sensors

Vidicon

Glass Break Detectors

Floor/Mat Sensor (STEP SWITCH II)

Penetration Detection

Contact Microphone

Piezo Cable Perimeter Protection

Pyrometer/Flame Sensor

Robotics

Tactile Sensor

Micropositioner

Safety Mats & Switches

Bumper Impact

Fans

Solid State

Microfan

Flow/Level

Vortex

Fluidic Oscillator

HVAC Air Flow

Doppler Ultrasound

Solid State Fluid Level

Densometer

Laminar/Turbulent Boundary Layer

INSTRUMENTATION

Machine Health Monitor

Accelerometers

Contact Microphones

Hi-Strain Dynamic Strain Gages

Weather Sensors

Rain Intensity

Hail Detection

Wind Velocity

Defouling

Hull

Water Supply

Active Vibration Damping

Strain Gages Sensor Arrays

Actuator Arrays

Non Destructive Eng.

Flexible Contact NDT Probes for Composites

NDT Arrays

Acoustic Emission Sensors

Air Ranging Ultrasound

Safety
Speed
Distance

Adaptive Optics

Fiber Optic Shutters/Modulators
Deformable Mirrors
Laser Scanners

Oil Exploration

Hydrophones
Seismic Geophones

Membranes

Active (Defouling) Membranes

Micropositioners

Tactile Microgrippers
Micromotors
Micropumps
Microfans

Power Generation

Ocean Wave
Wind Energy
Photoelectric (Solar)

MEDICAL

Diagnostics

Apnea Monitor
Ambulatory/Gait Monitors
Blood Pressure Cuff
Pressure Point Mattress
Pulse Counter
Stethoscope
Sleep Disorder Monitors
Respiratory Air Flow
Instant Thermometer
Isokinetics

Therapy

Transdermal Drug Administration
Pressure Ulcer Therapy
Osteogenesis
Wound Healing
Nerve Regeneration

Ultrasound

Near Field Imaging
Prostate
Transdermal
Transluminal
Coronary Arterial

Breast
Lithotripter
Hydrophone Calibration Probes

Handicapped Aides

Switches
Prosthesis
Braille Reader
Hearing Aid
Speech Intensification

Biological and Chemical

Thermometric Bioanalytical Sensors

Sample Analysis

Mass Change Measurement
Reactive Microstrain Measurement

Implantables

Pacemaker Activity Monitor
Implantable Switch
Vascular Graft Monitor
Micropump
Artery Monitor
Micropower Source

Instrumentation

Intravenous Drop Counter
IV Air Bubble Detection
Laser Switch/Modulator

TELECOMMUNICATIONS

*Keyboard, Microphones, Speakers,
Security*

Keypads, Hook switches
Handset, Squawk-box
Headset, Credit Card
Tone Generators
Cable Security

AUTOMOTIVE

Air Bag

Crash Sensor
Crush Sensor
Accelerometer
Occupancy Seat Sensor

Suspension

Active Suspension

Switches

Passenger Compartment Switches

Horn Switch
Control Panel

Fuel Level, Tire Rotation, Security
Keyless Entry
Motion (theft) Sensor
Passive Infrared Sensor

CONSUMER

Musical Instruments
Pick-up
Drum Trigger

Sports Equipment
Target Location (Baseball, Golf, Tennis,
Basketball, etc.)
Speed
Reaction Time
Foul Line
Force (Karate Impact,
Football Sled, Jump Force)
Sweet Spot

Toys/Games
Switches
Proximity (Passive Infrared)

Audio
Tweeter
Balloon Speakers
Novelty Speakers (Visor, Poster)
Microphone

MILITARY/GOVERNMENT

Hydrophones
Towed Cable Array
Hull Mounted Arrays
Sonobuoys
Active Noise Suppression

Ballistics
Safety and Arming Fuses
Shock Wave Gages
Detonators
Target Coordination Detection
Smart Munition Pyroelectric Sensors
Seismic Accelerometers

Physical Security
Perimeter
Seismic/Geophones
Covert Microphones

Traffic Sensors
Vehicle Classification
Weight-In-Motion
Speed
Lane Designation
Toll Booth

Appendix F

Typical Properties of Piezoelectric Film (PVDF)

Thickness	$9,28,52,110 \times 10^{-6}$ meter
Piezoelectric Strain Constant - d_{31}	$23 \times 10^{-12} \frac{\text{m}}{\text{m}}$ V/m
Piezoelectric Strain Constant - d_{33}	$-33 \times 10^{-6} \frac{\text{m}}{\text{m}}$ V/m
Piezoelectric Stress Constant - g_{31}	$216 \times 10^{-3} \frac{\text{V}}{\text{m}}$ N/m^2
Piezoelectric Stress Constant - g_{33}	$-339 \times 10^{-3} \frac{\text{V}}{\text{m}}$ N/m^2
Electromechanical Coupling Factor	12% (@ 1 kHz) 19% (@1 kHz)
Capacitance	380 pF/cm ² for 28×10^{-6} meter film
Young's Modulus	2×10^9 n/m ²
Speed of Sound	$1.5 - 2.2 \times 10^3$ m/s (transverse thickness)
Pyroelectric Coefficient	$-25 \times 10^{-6} \text{C/m}^2\text{°K}$
Permittivity	$106 - 113 \times 10^{-12} \text{F/m}$
Relative Permittivity	12 - 13
Mass Density	$1.78 \times 10^3 \text{kg/m}^3$
Volume Resistivity	10^{13} ohm meters
Surface Metallization Resistivity	2.0 ohms/square for CuNi 0.1 ohms/square for Ag ink
Loss Tangent	0.015 - .02 (@ $10 - 10^4$ Hz)
Compressive Strength	$60 \times 10^6 \text{N/m}^2$ (stretch axis)
Tensile Strength	$160 - 300 \times 10^6 \text{N/m}^2$ (Transverse axis)
Temperature Range	-40°C to 80°C
Water Absorption	< 0.02% H ₂ O
Max. Operating Voltage	750 V/mil = $30 \text{V}/10^{-6}\text{m}$
Breakdown Voltage	2000 V/mil = $100\text{V}/10^{-6}\text{m}$

**Measured and calculated properties of (Pb, Ca)TiO₃ ceramic
and stycast composites**

Contains 25 percent ceramic by volume. Underlined quantities are measured directly. Others are inferred.

	Ceramic Measured	Composite	
		Meas'd	Calc'd
ϵ_{33}^t	<u>207</u>	55	55
d_{33} (pC/N)	<u>70</u>	49	57
d_{31} (pC/N)	<u>-2.4</u>	<u>-8.5</u>	-13
k_{31} (%)	<u>2.1</u>	4.9	6.8
d_h (pC/N)	<u>65</u>	32	31
g_h (MV-m/N)	35	66	64
$d_h g_h$ ($10^{-15} \text{m}^2/\text{N}$)	2280	2100	1980

Appendix H

Piezoelectric Properties

Sample	Rod diced from ¹ Sintered Pellet	Rod #1	Composite N-1	Composite #2
Size	1mm x 1mm	Dia. 0.8mm	Dia. 30mm	Dia. 4mm
Density (g/cm ³)	7.4	7.5	1.8	3.62
Dielectric Constant, K ₃₃ ^T	3200	3000	320	420
d ₃₃ (pC/N)	593	610	400 on Rod 230 between Rod	310
K ₃₃ (K _t)	0.75 ²	0.65	0.55	0.61
C ^D (m/s)			2800	3520
d _h (pC/N)			40	52
g _h (10 ⁻³ vm/N)			14 ³	14 ³
Impedance (MRayl)			5.0	12.7

¹ Data from FMI, parts fabricated by Vernitron

² Data from Vernitron literature

³ Constant up to hydrostatic pressure 1050 PSI, equipment limit

Fatigue Loading Schedules

Type-Schedule	Load lb	Strain m-e	Percent of Limit	Number of Cycles
1-a	1,500	360	60%	100
1-b	2,500	600	100%	10
	2,000	480	80%	50
	1,500	360	60%	800
11-a	4,200	900	60%	100
11-b	7,000	1,500	100%	10
	5,600	1,200	80%	50
	4,200	900	60%	800

REPORT DOCUMENTATION PAGE

Form Approved
OMB No. 0704-0188

Public reporting burden for this collection of information is estimated to average 1 hour per response, including the time for reviewing instructions, searching existing data sources, gathering and maintaining the data needed, and completing and reviewing the collection of information. Send comments regarding this burden estimate or any other aspect of this collection of information, including suggestions for reducing this burden, to Washington Headquarters Services, Directorate for Information Operations and Reports, 1215 Jefferson Davis Highway, Suite 1204, Arlington, VA 22202-4302, and to the Office of Management and Budget, Paperwork Reduction Project (0704-0188), Washington, DC 20503.

1. AGENCY USE ONLY (Leave blank)		2. REPORT DATE September 1992	3. REPORT TYPE AND DATES COVERED Technical Memorandum
4. TITLE AND SUBTITLE A State-of-the-Art Assessment of Active Structures			5. FUNDING NUMBERS WU 590-14-41
6. AUTHOR(S) Active Structures Technical Committee			
7. PERFORMING ORGANIZATION NAME(S) AND ADDRESS(ES) NASA Langley Research Center Hampton, VA 23681-0001			8. PERFORMING ORGANIZATION REPORT NUMBER
9. SPONSORING/MONITORING AGENCY NAME(S) AND ADDRESS(ES) National Aeronautics and Space Administration Washington, DC 20546-0001			10. SPONSORING/MONITORING AGENCY REPORT NUMBER NASA TM-107681
11. SUPPLEMENTARY NOTES Garnett Horner, Chairperson, Active Structures Technical Committee, Langley Research Center, Hampton, Virginia			
12a. DISTRIBUTION/AVAILABILITY STATEMENT Unclassified - Unlimited Subject Category 39			12b. DISTRIBUTION CODE
13. ABSTRACT (Maximum 200 words) This report is a state-of-the-art assessment of active structures with emphasis towards the applications in aeronautics and space. It is felt that since this technology area is growing at such a rapid pace in many different disciplines, it is not feasible to cover all of the current research but only the relevant work as relates to aeronautics and space. The report covers research in smart actuation materials, smart sensors, control of smart/intelligent structures. In smart actuation materials, piezoelectric, magnetostrictive, shape memory, electrorheological, and electrostrictive materials are covered. For sensory materials, fiber optics, dielectric loss, and piezoelectric sensors are examined. Applications of embedded sensors and smart sensors are discussed. Control approaches for smart structures are discussed and recommendations for future research are given.			
14. SUBJECT TERMS Embedded Actuators Smart Structures and Systems Embedded Sensors Control Systems Active Structures			15. NUMBER OF PAGES 86
			16. PRICE CODE A05
17. SECURITY CLASSIFICATION OF REPORT unclassified	18. SECURITY CLASSIFICATION OF THIS PAGE unclassified	19. SECURITY CLASSIFICATION OF ABSTRACT unclassified	20. LIMITATION OF ABSTRACT UL

DAMAGE DETECTION IN SIMULATED AGING-AIRCRAFT PANELS USING THE ELECTRO-MECHANICAL IMPEDANCE TECHNIQUE

Victor Giurgiutiu* and Andrei Zagrai**

Department of Mechanical Engineering

University of South Carolina, Columbia, SC 29208

Phone: 803-777-8018, FAX: 803-777-0106, E-mail: victorg@sc.edu

ABSTRACT¹

The aging of aerospace structures is a major current concern of civilian and military aircraft operators. PZT active sensors offer special opportunities for developing sensor arrays for in-situ health monitoring of aging aircraft structures. In this paper, we examine the structural health monitoring of aging aircraft structures with the electro-mechanical (E/M) impedance method. Local impedance methodology as well as damage detection strategy were developed. The detection of damage due to corrosion, structural cracks, and active sensor self-diagnostics with electro-mechanical (E/M) impedance method are discussed. The paper emphasis is sensor fabrication and installation procedures. Consistency and repeatability of sensor fabrication and installation were perfected and confirmed by statistical tests on a number of nominally identical specimens. Experiments on simple metallic beams were then performed and the results were compared with readily available theoretical predictions. Experiments on square plates manufactured from aircraft grade thin-gage stock followed. Statistical analysis of plate data confirmed that consistent and repeatability results could be achieved with our methodology. Finally, experiments on realistic aircraft panels with simulated crack and corrosion damage were performed. An array of four sensors were installed along a line emanating at a right angle from the crack, and E/M impedance readings were collected from all sensors. Consistency of sensor readings was verified. Also, the tendency of frequency to shift in the vicinity of the crack was noticed. However, further data processing, and detailed FEM modeling are still needed before full understanding of the correlation between crack presence and sensors readings is achieved.

ELECTRO-MECHANICAL (E/M) IMPEDANCE METHOD

The impedance method is a damage detection technique complementary to the wave propagation techniques. Ultrasonic equipment manufacturers offer, as options, mechanical impedance analysis (MIA) probes and equipment (Staveley NDT Technologies, 1998). The mechanical impedance method consists of exciting vibrations of bonded plates using a specialized transducer that simultaneously measures the applied normal force and the induced velocity. Cawley (1984) extended Lange's (1978) work on the mechanical impedance method and studied the identification of local disbonds in bonded plates using a small shaker. Though phase information was not used in Cawley's analysis, present day MIA methodology uses both magnitude and phase information to detect damage.

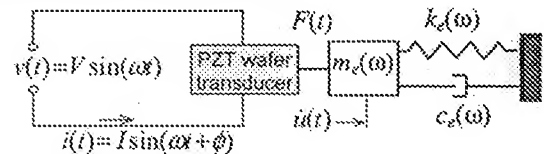


Figure 1 Electro-mechanical coupling between the PZT active sensor and the structure.

The electro-mechanical (E/M) impedance method (Rogers and Giurgiutiu, 1997) is an emerging technology that offers distinctive advantage over the mechanical impedance method. While the mechanical impedance method uses normal force excitation, the E/M impedance method uses in-plane strain. While the mechanical impedance transducer measures mechanical quantities (force and velocity/acceleration) to indirectly calculate the mechanical impedance, the E/M impedance active sensor measures the E/M impedance directly as an electrical quantity. The principles of the E/M impedance technique are illustrated in Figure 1. The effect of a piezo-electric active sensor affixed to the structure is to apply a local strain parallel to the surface that creates stationary elastic waves in the structure. The structure presents to the active sensor the drive-point impedance,

*) Associate Professor, Member ASME

**) Graduate Research Assistant, Student Member ASME

$Z_{str}(\omega) = i\omega m_e(\omega) + c_e(\omega) - ik_e(\omega)/\omega$. Through the mechanical coupling between the PZT active sensor and the host structure, on one hand, and through the electro-mechanical transduction inside the PZT active sensor, on the other hand, the drive-point structural impedance gets directly represented in the effective electrical impedance as seen at the active sensor terminals. The apparent electro-mechanical impedance of the piezo-active sensor as coupled to the host structure is:

$$Z(\omega) = \left[i\omega C \left(1 - \kappa_{31}^2 \frac{Z_{str}(\omega)}{Z_{PZT}(\omega) + Z_{str}(\omega)} \right)^{-1} \right], \quad (1)$$

where $Z(\omega)$ is the equivalent electro-mechanical admittance as seen at the PZT active sensor terminals, C is the zero-load capacitance of the PZT active sensor, κ_{31} is the electro-mechanical cross coupling coefficient of the PZT active sensor ($\kappa_{31} = d_{13}/\sqrt{s_{11}\epsilon_{33}}$), Z_{str} is the impedance of the structure, and Z_{PZT} is the impedance of the PZT active sensor. The electro-mechanical impedance method is applied by scanning a predetermined frequency range in the hundreds of kHz band and recording the complex impedance spectrum. By comparing the impedance spectra taken at various times during the service life of a structure, meaningful information can be extracted pertinent to structural degradation and the appearance of incipient damage. It must be noted that the frequency range must be high enough for the signal wavelength to be significantly smaller than the defect size.

Giurgiutiu and Rogers (1997, 1998) presented an extensive review of the state of the art in E/M impedance health monitoring of structures. Recent developments in this method focus on finding an effective damage metric to compare the E/M impedance spectra of pristine and damaged structures. Quin *et al.* (1999) developed an E/M impedance damage index (DI) scheme based on the differences of the piecewise integration of the frequency response curve between the damaged and undamaged cases. In addition, improved characterization of the structure is achieved by the separation of transverse and longitudinal outputs through directionally attached piezoelectrics (DAP). Lopes *et al.* (1999) used neural network techniques to process high-frequency E/M impedance spectra. In analytical simulation studies, a three level normalization scheme was applied to the E/M impedance spectrum based on the resonance frequencies. When applied to actual E/M experiments, the neural network approach was modified to another set of normalized values: (i) the area between damaged and undamaged impedance curves; (ii) the root mean square (RMS) of each curve; and (iii) the correlation coefficient between damaged and undamaged curves. These values were calculated for both real and imaginary parts of the impedance spectrum. Good identification of damage location and damage amplitude was reported.

DAMAGE DETECTION STRATEGY

The real part of the E/M impedance reflects the state of structural health in the local area under the influence of the excited sensor. The integrity of the sensor itself is confirmed by the E/M impedance imaginary part

Consider an array of 4 active sensors as presented in Figure 2. Each active sensor has its own sensing area resulting from the application of the localization concept. This sensing area is

characterized by a sensing radius and the corresponding sensing circle. Inside the sensing area, the sensor capability decreases as the distance from the sensor to the damage increases. A damage feature that is placed in the near field of the sensor is expected to create a larger disturbance in the sensor response than a damage feature placed in the far field. Effective area coverage is ensured when the sensing circles overlap. The diagnostics of the adjacent structure is performed using the active (real) part of the E/M impedance ($\text{Re } Z$). Incipient damage changes taking place in the structure are reflected in the drive-point structural impedance. Our experience has indicated that the change in the structural drive-point impedance extensively affects the real part of the effective electro-mechanical impedance of the piezo-electric active sensor affixed or embedded in the structure (Giurgiutiu and Rogers, 1998).

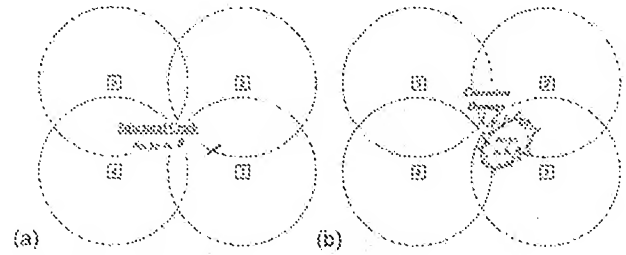


Figure 2 Damage detection using an array of 4 piezoelectric active sensors and E/M impedance method: (a) detection of structural cracks; (b) detection of corrosion damage. The circles represent the sensing radius of each active sensor.

E/M Impedance Detection of Structural Cracks

Figure 2a features a structural crack placed in the sensing circle of active sensor 1. The crack presence modifies the structural field and effective drive-point structural impedance as seen by sensor 1. In the same time, the crack also belongs to the sensing circle of sensor 2, but it is right at the periphery of this circle. By this token, we expect that the effective drive-point structural impedance as seen by sensor 2 to be also affected, but to a much lesser extent than for sensor 1. Regarding sensors 3 and 4, the structural crack is outside their sensing circles, hence their drive-point structural impedance will be almost unchanged. In virtue of Equation (2), these changes in the drive-point structural impedance will be directly reflected in the E/M impedance of the sensor. In conclusion, the crack illustrated in Figure 1a is expected to strongly modify the E/M impedance of sensor 1, to slightly modify that of 2, and to leave unchanged those of 3 and 4.

E/M Impedance Detection of Corrosion Damage

Figure 2b features a patch of corrosion damage placed in the sensing circle of active sensor 1. In the same time, the corrosion damage also belongs to the sensing circles of sensors 2 and 4, but to a lesser extent. (For sensor 2, only half of the corrosion damage is inside its sensing circle; for sensor 4, the corrosion damage only touches the periphery of its sensing circle.) We expect that the effective drive-point structural impedance seen by sensor 1 will be strongly modified, that seen by sensor 2 will be somehow modified, and that of sensor 4 will be slightly modified. The drive-point impedance of sensor 3 will remain virtually

unmodified. In virtue of Equation (2), these changes in the drive-point structural impedance will be directly reflected in the E/M impedance of the sensor. In conclusion, the corrosion damage (Figure 2b) is expected to strongly modify the E/M impedance of sensor 1, to somehow modify that of 2, slightly modify that of 4, and to leave unchanged that of 3.

Active Sensor Self-diagnostics

Piezo-electric wafer transducers affixed to, or embedded into, the structure play a major role in the successful operation of the health monitoring and damage detection system. Integrity of the transducer and consistency of the transducer/structure interface are essential elements that can "make or break" an experiment. The general expectation is that, once the transducers have been placed on or into the structure, they will behave consistently throughout the duration of the health monitoring exercise. For real structures, the duration of the health monitoring exercise is extensive and can span several years. It also will encompass various service conditions and several loading cases. Therefore, in-situ self-diagnostics methods are mandatory. The transducer array should be scanned periodically as well as prior to any damage detection cycle. Self diagnostic methods for assessing active sensor integrity are readily available with the E/M impedance technique. The piezo-electric active sensor is predominantly a capacitive device that is dominated by its reactive impedance $1/i\omega C$. Our preliminary tests have shown that the reactive (imaginary) part of the impedance ($\text{Im } Z$) can be a good indication of active sensor integrity. Base-line signatures taken at the beginning of endurance experiments when compared with recent reading could successfully identify defective active sensors. Figure 3 compares the $\text{Im } Z$ spectrum of a well-bonded PZT sensor with that of a disbonded (free) sensor. The appearance of sensor free-vibration resonance, and the disappearance of structural resonances constitute un-ambiguous features that can be used for automated sensor self-diagnostics.

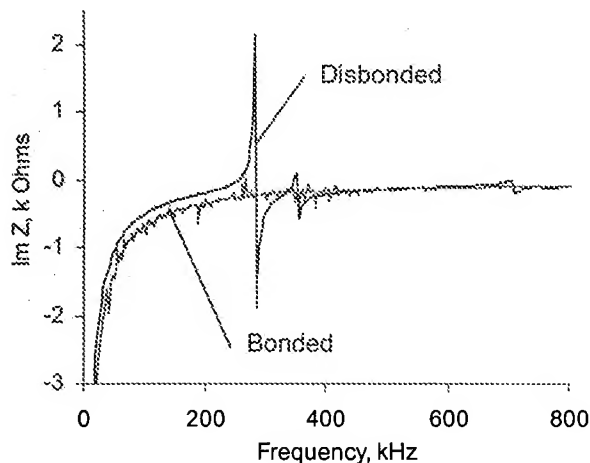


Figure 3 Active sensor self diagnostic using the imaginary part of the E/M impedance: when sensor is disbonded, new free-vibration resonance features appear at ~267 kHz.

ACTIVE SENSORS FABRICATION

Previous efforts (Giurgiutiu *et al.*, 2000) have shown that sensor intrinsic behavior can significantly affect the E/M impedance readings, and that consistent sensor fabrication and installation procedures are needed for the E/M impedance method to be successful. Hence, the analysis of the sensor fabrication and identification/elimination of faults and shortcomings was one of our major concerns of the present investigation. In order to save costs, previous efforts attempted to fabricate the small 6-mm sq. sensors out of large PZT sheet using conventional tooling. This process, though inexpensive, was producing significant variation in sensor size and geometry that affected the E/M impedance readings. In order to reduce uncertainties, we desired to seek small-size commercially available piezoelectric wafers, produced with precision technologies. Several vendors that can supply small PZT wafers were identified. The small PZT wafers produced by American Piezo Ceramics, Inc. were selected based on their low cost and good manufacturing tolerances (Table 1).

Table 1 Manufacturing tolerances for APC, Inc. small piezoelectric wafers (www.americanpiezo.com)

Dimension	Units (mm)	Standard Tolerance
Length or Width of Plates	<13mm	+/-0.13mm
Thickness of All Parts	0.20mm to 0.49mm	+/-0.025mm

Table 2 Properties of piezoelectric ceramic APC-850 (as from company website www.americanpiezo.com)

PROPERTY	UNIT	SYMBOL	APC-840	APC-841	APC-880	APC-850	APC-855	APC-856
Relative Dielectric Constant	1	$\epsilon_{33}^T/\epsilon_0$	1250	1350	1050	1750	3250	4100
Dielectric Factor Measured @ 1 Hz @ Low Field	%	tan δ	5.4	0.35	0.35	1.4	2	2.7
Cure Temperature	$^{\circ}\text{C}$	T_c	325	320	310	360	195	150
Coupling Coefficients	1	k_{31}	0.59	0.60	0.50	0.63	0.65	0.65
		k_{32}	0.72	0.68	0.62	0.72	0.74	0.73
		k_{31}	0.35	0.33	0.30	0.36	0.32	0.36
		k_{15}	0.70	0.67	0.53	0.68	0.66	0.65
Piezoelectric Coefficient	10^{-12} C/N or m/V	d_{33}	290	275	215	400	580	620
		$-d_{31}$	125	109	95	175	270	260
		d_{32}	480	450	330	580	720	710
Piezoelectric Coefficients	10^{-3} V-m/N or m ² /C	g_{33}	28.5	27.5	25	26	19.5	18.5
		$-g_{31}$	11	10.3	10	12.4	2.8	3.1
		g_{32}	38	35	22	36	27	25
Young's Modulus	10^{10} N/m ²	Y_{33}^E	8	7.6	9	4.3	6.1	5.8
		Y_{32}^E	6.8	6.3	7.2	5.4	4.8	4.5
Frequency Constants	Ht-m or m/s	N_L	1534	1700	1725	1509	1475	---
		N_T	2005	2005	2110	2030	1930	1930
		N_R	2120	2055	2080	1980	1920	---
Electric Compliance	10^{-12} m ² /N	S_{33}^E	11.8	11.7	10.8	15.3	14.8	15.0
		S_{32}^E	17.4	17.3	15.0	17.3	16.7	17.0
Density	g/cc	ρ	7.6	7.6	7.6	7.7	7.5	7.5
Mechanical Quality Factor	1	Q_m	500	1400	1000	80	75	72

A batch of 25 APC-850 piezoelectric wafers (7 mm sq., 0.2 mm thick, silver electrodes on both sides) was acquired and subjected to statistical evaluation. In this process, we started with the mechanical and electrical properties declared by the vendor and then conducted our own measurements to verify the vendor data and evaluate its veridicality. The mechanical tolerances of

these wafers, as presented by the vendor on their website, are given in Table 1. The material properties of the basic PZT material are given in Table 2. The tolerances declared by the vendor for some standard electrical properties were $\pm 5\%$ in resonance frequency, $\pm 20\%$ in capacitance and $\pm 20\%$ in the d_{33} constant. Standardized test methods for in process quality assurance of active sensor fabrication process were developed based on the following measurements:

- Geometrical dimensions
- Electrical capacitance
- Free-free E/M impedance and admittance spectra.

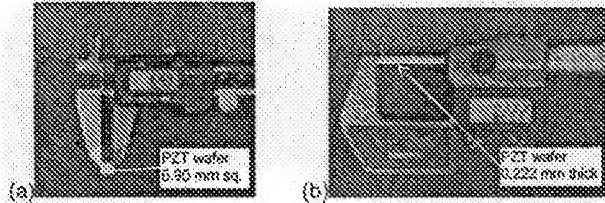


Figure 4 The dimensions of the APC-850 piezoceramic PZT wafers were measured with: (a) Mitutoyo Corp. CD-6" CS digital caliper; and (b) Mitutoyo Corp. MCD - 1" CE digital micrometer.

Geometric measurements

Twenty-five nominally identical APC-850 wafers were measured with precision instrumentation consisting of Mitutoyo Corp. CD - 6" CS digital caliper (0.01-mm precision) and Mitutoyo Corp. MCD - 1" CE digital micrometer (0.001-mm precision). Length, width, and thickness were measured and recorded (Figure 4). The results of the statistical analysis of the data obtained from these measurements are presented in Figure 5. Good agreement with the theoretical Normal distribution (Gauss law) was observed. Mean and standard deviation values for length/width and thickness were 6.9478 mm, $\pm 0.5\%$, and 0.2239 mm, $\pm 1.4\%$, respectively.

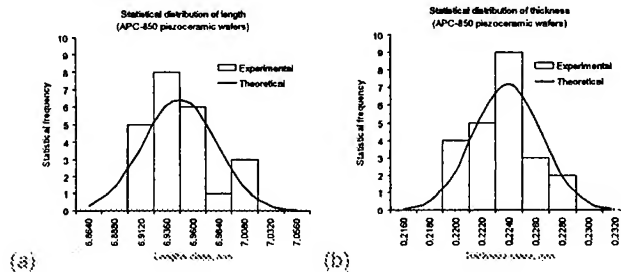


Figure 5 Statistical distributions of geometrical dimensions of APC-850 piezoceramic wafers: (a) length; (b) thickness.

Electrical Measurements

Electrical capacitance was measured with a BK Precision® Tool Kit™ 27040 digital multimeter (Figure 6a) with a resolution of 1pF. Capacitance measurements were selected as a in-process quality check to be applied during each step of sensor development and also during the sensor installation process.

Direct capacitance tests using metallic ground plate.

Capacitance of the basic PZT sensors was measured directly by putting the PZT square on a flat metallic ground plate. The negative probe was connected to the plate in a semi-permanent

fashion (hole, bolt + nut + washer, short multifilament lead, alligator clip), and the top of the PZT square was touched with the positive probe. Then, data was taken when the tester readings had converged to a stable value. At least 6 readings were recorded and the average was taken. The process was iteratively improved until consistent results were obtained. At least 6 readings were taken to a form statistical set of data. Mean and standard deviation values were 3.276 nF, $\pm 3.8\%$. While this method has clear advantages, it also has the shortcoming that instability in electrical readings may occur due to lack of a firm electrical connection through mechanical clamping of the parts in contact. To compensate for this shortcoming, we tried two alternatives: (a) a mechanical clamp; and (b) conductive adhesive tape.

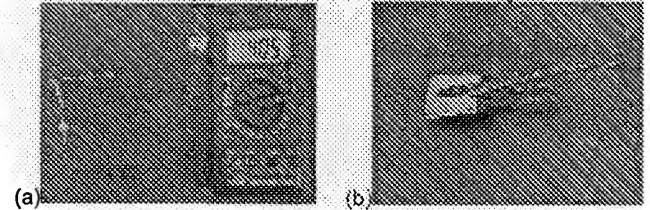


Figure 6 In process quality check equipment: (a) BK Precision® Tool Kit™ 27040 digital multimeter; (b) PZT test clamp.

Capacitance tests using a mechanical clamp

As an alternative, a test clamp was designed, constructed, and utilized to measure the capacitance of the PZT wafer (Figure 6b). During these measurements, slow convergence of the capacitance values was observed. The reasons for such slow convergence are not fully understood, but we believe that they are associated with the parasitic capacitance of the clamp, the unscreened portion of the cable, etc. Hence, this method was later abandoned.

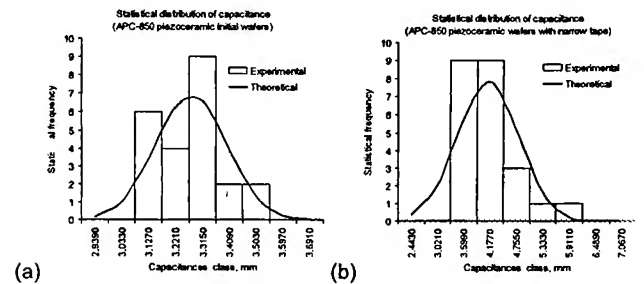


Figure 7 Statistical distribution of APC-850 piezoceramic wafers capacitance: (a) as measured on metallic ground plate; (b) as measured with narrow conductive tape.

Capacitance tests using conductive adhesive tape

The use of conductive adhesive tape as an alternative means of connections was also investigated. We used single coated 3M® Cu foil conductive tape with 0.034mm foil thickness, 0.086-mm total thickness, and 0.032 Ohms/cm² electrical resistance through the adhesive. This tape works on the principle of producing electrical conductivity through a pressure-sensitive acrylic adhesive. As the tape is applied, conductive particles in the adhesive bridge the gap between the back-up Cu foil and the piezoceramic. We used two tape widths: (a) wide, i.e., as received with a width of 6.3-mm; and (b) narrow, i.e., 2-mm wide strips cut out of the as received tape. The length of the connection with the PZT wafer was (a) 7-mm for the wide tape; and (b) 3-mm for

the narrow tape. The use of adhesive tape exhibited the same slow-convergence problems previously reported with the use of a mechanical clamp. When narrow tape was used, somehow better results were obtained, but the convergence of capacitance readings was still slow. The values measured during these tests are presented in Figure 7b. Mean and standard deviation values of 4.126 nF , $\pm 16.4 \%$ were recorded. The data shows capacitance values are significantly different from those obtained using a metallic ground plate. It was concluded that the use of conductive tape, though convenient, poses some electrical problems that need to be studied further. Hence this method was also abandoned.

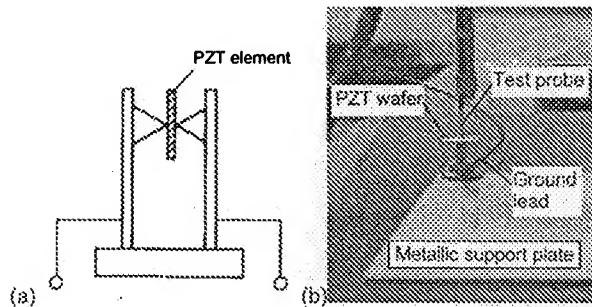


Figure 8 (a) Test jig for dynamic measurement of PZT elements (J. W. Waanders, 1991 "Piezoelectric ceramic", p.82, Fig 8.7); (b) aluminum plate with metallic bolt head used for measurement of E/M impedance and admittance spectra of the PZT active sensors.

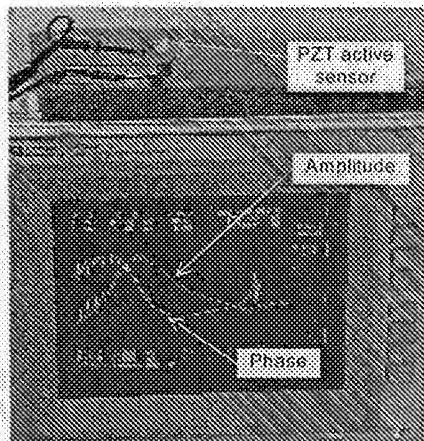


Figure 9 Experimental set up for measuring the impedance and admittance characteristics of the PZT with HP 4194A Impedance Phase-Gain Analyzer.

Measurements of the intrinsic E/M impedance and admittance spectra of the PZT active sensor

The intrinsic E/M impedance and admittance spectra of the PZT active sensors, before being attached to the structure, was measured with the HP 4194A Impedance Phase-Gain Analyzer. Three possible methods for electrically connecting the PZT wafer to the test equipment were considered: (a) clamping at center; (b) attaching conductive adhesive tape leads; and (c) attaching soldered wire leads. It was found that (a) and (c) give practically identical results, while (b) clearly different. Hence, method (b) was discontinued, and method (a) was adopted as standard procedure for its expedience. The testing fixture for implementing the method (a) was designed following Waanders (1991) concept

shown on Figure 8(a). We used a metallic plate with a lead connected at one corner (Figure 8b). The PZT wafer was centered on the bolt head and held in place with the probe tip. Thus, center clamping conditions were simulated, and the wafer could perform free vibrations while being tested.

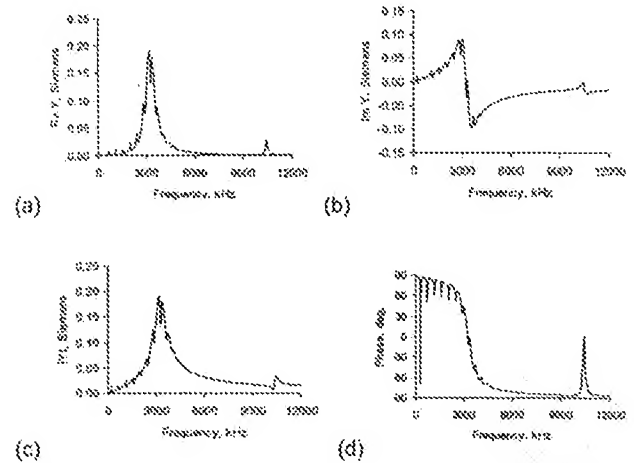


Figure 10 Amplitude and phase characteristic of a free-free sensor vs. frequency in terms of admittance: (a) real part of admittance; (b) imaginary part of admittance; (c) amplitude of admittance; (d) phase of admittance

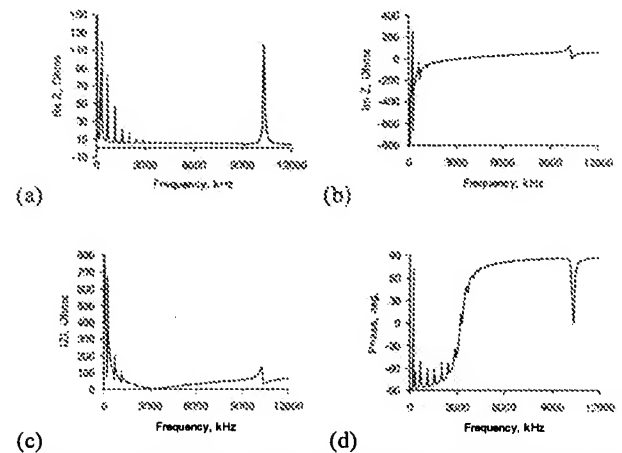


Figure 11 Amplitude and phase characteristic of a free-free sensor vs. frequency in terms of impedance: (a) real part of impedance; (b) imaginary part of impedance; (c) amplitude of impedance; (d) phase of impedance.

To obtain the intrinsic E/M impedance and admittance spectra, the PZT active sensors were tested in the 100Hz — 12MHz frequency range using the HP 4194A Impedance Analyzer (Figure 9). The data was collected through the GPIB interface and processed in MS Excel. Typical admittance and impedance frequency spectra are given in Figures 10 and 11. The PZT wafer resonance frequencies were identified from the E/M admittance spectra. It was found that since the length and the width of the PZT wafers are nearly identical, the corresponding lengthwise and widthwise frequencies are coalescent, forming twin-peaks of in-plane vibration resonances. The first, second, and third in-plane resonance frequencies, as well as the out-of-plane (thickness) resonance (which is at much higher frequency) were

identified and recorded. Also recorded were the values of the corresponding resonance peaks. Statistical distributions of the resonance frequencies and resonance amplitudes are given in Figure 12. Mean values of 251kHz and 67.152 mS, and standard deviations of $\pm 1.2\%$ and $\pm 21\%$, respectively, were obtained. These results proved that the basic APC-850 piezoelectric wafers had acceptable quality with a narrow dispersion band in resonance frequency.

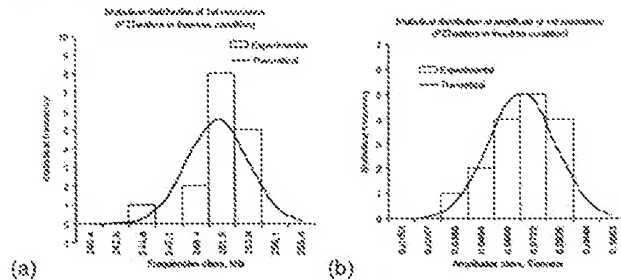


Figure 12 Statistical distribution of (a) 1st resonance frequencies and (b) admittance amplitudes on 1st resonance of APC-850 piezoceramic wafers.



Figure 13 The installation kit for strain gages (Measurements Group, Inc) was used in the bonding of piezoelectric active sensors.

ACTIVE SENSORS INSTALLATION

Sensors installation on the health-monitored structure is an important step that may have significant bearing on the success of the health monitoring tests. The development of a reliable and repeatable installation method, which would provide consistent results was one of our major preoccupations. In the installation process, the adhesive used to bond the sensor to the structure plays a crucial role. The thickness and stiffness of the adhesive layer can significantly influence the sensor capability to excite the structure and may affect the quality and veridicality of the E/M impedance signatures. Using published data (e.g., Bergman, Quattrone, 1999) and personal communications with piezoceramic vendors we concluded that cyanoacrylate adhesives are appropriate and convenient for short-term experiments, though their performance may degrade under prolonged environmental exposure. For long-term environmental exposure, other adhesive types (e.g., epoxy) may be more appropriate. Some

investigators also reported the use of conductive epoxy, but we found that the adhesive conductivity is not necessary as long as the adhesive layer is sufficiently thin to allow physical contact between the PZT wafer surface “asperities” and the substrate. The cyanoacrylate adhesive used was M-Bond 200 from Measurements Group, Inc. The accompanying strain-gage installation Instruction Bulletin 309D (Measurements Group Inc., 1992) and installation kit (Figure 13) were also used.

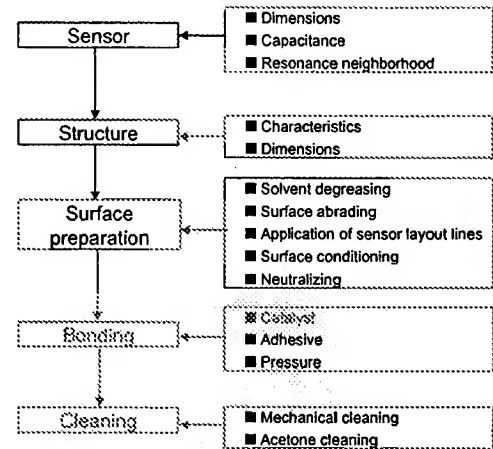


Figure 14 Diagram for installation procedure for piezoelectric active sensors.

The sensor installation procedure followed the general steps mentioned in the strain gage installation Instruction Bulletin, with some modifications introduced to account for the rigidity and fragility of the PZT material. Changes in sensor handling, cleaning, and cure pressure requirements were introduced. The complete procedure that we elaborated for bonding piezoelectric active sensors is diagrammatically presented in Figure 14. After the bonding procedure is finished, sensors edges were cleaned up to eliminate spills of cyanoacrylate adhesive that may short circuit the sensor. This mechanical and chemical procedure was performed with fine tools and acetone. After installation, the sensor capacitance was measured again and checked for consistency against the on-file free-sensor capacitance.

BEAM EXPERIMENTS To better understand the relationship between structural resonances and the frequencies displayed by the E/M admittance/impedance spectrum of the PZT active sensor attached to the structure we performed experiments on simple beam and plate specimens. Structural modeling, performed in parallel, was used to predict the structural resonance frequencies and mode shapes. The theoretical and experimental results were compared, and validation of the theoretical prediction was achieved. Further, statistical processing of several “identical” specimens allowed us to estimate the method’s variability and expected intrinsic spread when applied on more-complex structures.

One-dimensional beam structures are easy to model, and the prediction of their natural frequencies is fairly well understood (Inman, 1996). Hence, our first experiments concentrated on beam specimens. A number of small steel beams various thickness and width values were fabricated. All beams were 100mm long, but their width varied from 19.6 mm (wide beams) to 8mm (narrow beams). The nominal thickness of the specimen

was 5.2mm; by gluing two specimens back-to-back, we were also able to create double thickness specimens. Thus, four beam types were used (Figure 15): narrow-thin, narrow-thick, wide-thin, and wide-thick.

Table 3 Theoretical and experimental results for wide and narrow beams with single and double thickness.

Narrow Beam, 1t			Narrow Beam, 2t			Wide Beam, 1t			Wide Beam, 2t						
Mode	Theory kHz	Exp. kHz	A%	Mode	Theory kHz	Exp. kHz	A%	Mode	Theory kHz	Exp. kHz	A%	Mode	Theory kHz	Exp. kHz	A%
1	1.388	1.371	98.8	1	2.776	2.758	99.4	1	1.388	1.369	98.6	1	2.776	2.757	99.3
2	2.776	2.757	99.3	2	5.552	5.514	98.4	2	2.776	2.757	99.3	2	5.552	5.513	98.4
3	4.164	4.145	99.5	3	8.328	8.289	99.5	3	4.164	4.145	99.5	3	8.328	8.289	99.5
4	5.552	5.533	99.7	4	13.784	13.745	99.7	4	5.552	5.533	99.7	4	13.784	13.745	99.7
5	6.940	6.921	99.9	5	20.820	20.781	99.8	5	6.940	6.921	99.9	5	20.820	20.781	99.8
6	8.328	8.309	99.9	6	27.760	27.721	99.9	6	8.328	8.309	99.9	6	27.760	27.721	99.9
7	9.716	9.697	99.9	7	34.704	34.665	99.9	7	9.716	9.697	99.9	7	34.704	34.665	99.9
8	11.104	11.085	99.9	8	41.648	41.609	99.9	8	11.104	11.085	99.9	8	41.648	41.609	99.9
9	12.492	12.473	99.9	9	48.592	48.553	99.9	9	12.492	12.473	99.9	9	48.592	48.553	99.9
10	13.880	13.861	99.9	10	55.536	55.497	99.9	10	13.880	13.861	99.9	10	55.536	55.497	99.9
11	15.268	15.249	99.9	11	62.480	62.441	99.9	11	15.268	15.249	99.9	11	62.480	62.441	99.9
12	16.656	16.637	99.9	12	69.424	69.385	99.9	12	16.656	16.637	99.9	12	69.424	69.385	99.9
13	18.044	18.025	99.9	13	76.368	76.329	99.9	13	18.044	18.025	99.9	13	76.368	76.329	99.9
14	19.432	19.413	99.9	14	83.312	83.273	99.9	14	19.432	19.413	99.9	14	83.312	83.273	99.9
15	20.820	20.801	99.9	15	90.256	90.217	99.9	15	20.820	20.801	99.9	15	90.256	90.217	99.9
16	22.208	22.189	99.9	16	97.200	97.161	99.9	16	22.208	22.189	99.9	16	97.200	97.161	99.9
17	23.596	23.577	99.9	17	104.144	104.105	99.9	17	23.596	23.577	99.9	17	104.144	104.105	99.9
18	24.984	24.965	99.9	18	111.088	111.049	99.9	18	24.984	24.965	99.9	18	111.088	111.049	99.9
19	26.372	26.353	99.9	19	118.032	117.993	99.9	19	26.372	26.353	99.9	19	118.032	117.993	99.9
20	27.760	27.741	99.9	20	124.976	124.937	99.9	20	27.760	27.741	99.9	20	124.976	124.937	99.9
21	29.148	29.129	99.9	21	131.920	131.881	99.9	21	29.148	29.129	99.9	21	131.920	131.881	99.9
22	30.536	30.517	99.9	22	138.864	138.825	99.9	22	30.536	30.517	99.9	22	138.864	138.825	99.9
23	31.924	31.905	99.9	23	145.808	145.769	99.9	23	31.924	31.905	99.9	23	145.808	145.769	99.9
24	33.312	33.293	99.9	24	152.752	152.713	99.9	24	33.312	33.293	99.9	24	152.752	152.713	99.9
25	34.700	34.681	99.9	25	159.696	159.657	99.9	25	34.700	34.681	99.9	25	159.696	159.657	99.9
26	36.088	36.069	99.9	26	166.640	166.601	99.9	26	36.088	36.069	99.9	26	166.640	166.601	99.9
27	37.476	37.457	99.9	27	173.584	173.545	99.9	27	37.476	37.457	99.9	27	173.584	173.545	99.9
28	38.864	38.845	99.9	28	180.528	180.489	99.9	28	38.864	38.845	99.9	28	180.528	180.489	99.9
29	40.252	40.233	99.9	29	187.472	187.433	99.9	29	40.252	40.233	99.9	29	187.472	187.433	99.9
30	41.640	41.621	99.9	30	194.416	194.377	99.9	30	41.640	41.621	99.9	30	194.416	194.377	99.9
31	43.028	43.009	99.9	31	201.360	201.321	99.9	31	43.028	43.009	99.9	31	201.360	201.321	99.9
32	44.416	44.397	99.9	32	208.304	208.265	99.9	32	44.416	44.397	99.9	32	208.304	208.265	99.9
33	45.804	45.785	99.9	33	215.248	215.209	99.9	33	45.804	45.785	99.9	33	215.248	215.209	99.9
34	47.192	47.173	99.9	34	222.192	222.153	99.9	34	47.192	47.173	99.9	34	222.192	222.153	99.9
35	48.580	48.561	99.9	35	229.136	229.097	99.9	35	48.580	48.561	99.9	35	229.136	229.097	99.9
36	49.968	49.949	99.9	36	236.080	236.041	99.9	36	49.968	49.949	99.9	36	236.080	236.041	99.9
37	51.356	51.337	99.9	37	243.024	242.985	99.9	37	51.356	51.337	99.9	37	243.024	242.985	99.9
38	52.744	52.725	99.9	38	250.000	249.961	99.9	38	52.744	52.725	99.9	38	250.000	249.961	99.9
39	54.132	54.113	99.9	39	256.944	256.905	99.9	39	54.132	54.113	99.9	39	256.944	256.905	99.9
40	55.520	55.501	99.9	40	263.888	263.849	99.9	40	55.520	55.501	99.9	40	263.888	263.849	99.9
41	56.908	56.889	99.9	41	270.832	270.793	99.9	41	56.908	56.889	99.9	41	270.832	270.793	99.9
42	58.296	58.277	99.9	42	277.776	277.737	99.9	42	58.296	58.277	99.9	42	277.776	277.737	99.9
43	59.684	59.665	99.9	43	284.720	284.681	99.9	43	59.684	59.665	99.9	43	284.720	284.681	99.9
44	61.072	61.053	99.9	44	291.664	291.625	99.9	44	61.072	61.053	99.9	44	291.664	291.625	99.9
45	62.460	62.441	99.9	45	298.608	298.569	99.9	45	62.460	62.441	99.9	45	298.608	298.569	99.9
46	63.848	63.829	99.9	46	305.552	305.513	99.9	46	63.848	63.829	99.9	46	305.552	305.513	99.9
47	65.236	65.217	99.9	47	312.496	312.457	99.9	47	65.236	65.217	99.9	47	312.496	312.457	99.9
48	66.624	66.605	99.9	48	319.440	319.401	99.9	48	66.624	66.605	99.9	48	319.440	319.401	99.9
49	68.012	67.993	99.9	49	326.384	326.345	99.9	49	68.012	67.993	99.9	49	326.384	326.345	99.9
50	69.400	69.381	99.9	50	333.328	333.289	99.9	50	69.400	69.381	99.9	50	333.328	333.289	99.9
51	70.788	70.769	99.9	51	340.272	340.233	99.9	51	70.788	70.769	99.9	51	340.272	340.233	99.9
52	72.176	72.157	99.9	52	347.216	347.177	99.9	52	72.176	72.157	99.9	52	347.216	347.177	99.9
53	73.564	73.545	99.9	53	354.160	354.121	99.9	53	73.564	73.545	99.9	53	354.160	354.121	99.9
54	74.952	74.933	99.9	54	361.104	361.065	99.9	54	74.952	74.933	99.9	54	361.104	361.065	99.9
55	76.340	76.321	99.9	55	368.048	368.009	99.9	55	76.340	76.321	99.9	55	368.048	368.009	99.9
56	77.728	77.709	99.9	56	375.000	374.961	99.9	56	77.728	77.709	99.9	56	375.000	374.961	99.9
57	79.116	79.097	99.9	57	381.944	381.905	99.9	57	79.116	79.097	99.9	57	381.944	381.905	99.9
58	80.504	80.485	99.9	58	388.888	388.849	99.9	58	80.504	80.485	99.9	58	388.888	388.849	99.9
59	81.892	81.873	99.9	59	395.832	395.793	99.9	59	81.892	81.873	99.9	59	395.832	395.793	99.9
60	83.280	83.261	99.9	60	402.776	402.737	99.9	60	83.280	83.261	99.9	60	402.776	402.737	99.9
61	84.668	84.649	99.9	61	409.720	409.681	99.9	61	84.668	84.649	99.9	61	409.720	409.681	99.9
62	86.056	86.037	99.9	62	416.664	416.625	99.9	62	86.056	86.037	99.9	62	416.664	416.625	99.9
63	87.444	87.425	99.9	63	423.608	423.569	99.9	63	87.444	87.425	99.9	63	423.608	423.569	99.9
64	88.832	88.813	99.9	64	430.552	430.513	99.9	64	88.832	88.813	99.9	64	430.552	430.513	99.9
65	90.220	90.201	99.9	65	437.496	437.457	99.9	65	90.220	90.201	99.9	65	437.496	437.457	99.9
66	91.608	91.589	99.9	66	444.440	444.401	99.9	66	91.608	91.589	99.9	66	444.440	444.401	99.9
67	92.996	92.977	99.9	67	451.384	451.345	99.9	67	92.996	92.977	99.9	67	451.384	451.345	99.9
68	94.384	94.365	99.9	68	458.328	458.289	99.9	68	94.384	94.365	99.9	68	458.328	458.289	99.9
69	95.772	95.753	99.9	69	465.272	465.233	99.9	69	95.772	95.753	99.9	69	465.272	465.233	99.9
70	97.160	97.141	99.9	70	472.216	472.177	99.9	70	97.160	97.141	99.9	70	472.216	472.177	99.9
71	98.548	98.529	99.9	71	479.160	479.121	99.9	71	98.548	98.529	99.9	71	479.160	479.121	99.9
72	99.936	99.917	99.9	72	486.104	486.065	99.9	72	99.936	99.917	99.9	72	486.104	486.065	99.9
73	101.324	101.305	99.9	73	493.048	493.009	99.9	73	101.324	101.305	99.9	73	493.048	493.009	99.9
74	102.712	102.693	99.9	74	500.000	499.961	99.9	74	102.712	102.693	99.9	74	500.000	499.961	99.9
75	104.100	104.081	99.9	75	506.944	506.905	99.9	75	104.100	104.081	99.9	75	506.944	506.905	99.9
76	105.488	105.469	99.9	76	513.888	513.849	99.9	76	105.488	105.469	99.9	76	513.888	5	

specimens (100-mm square, 1-mm thick) were constructed from aircraft-grade aluminum stock. Each plate was instrumented with one 7-mm square PZT active sensor placed at its center (Figure 17). The previously described sensor installation procedure was employed. Thus, a sample of 25 nominally identical plate specimens were obtained. Data was taken on 5 of these identical specimens using the HP 4194A Impedance Analyzer.

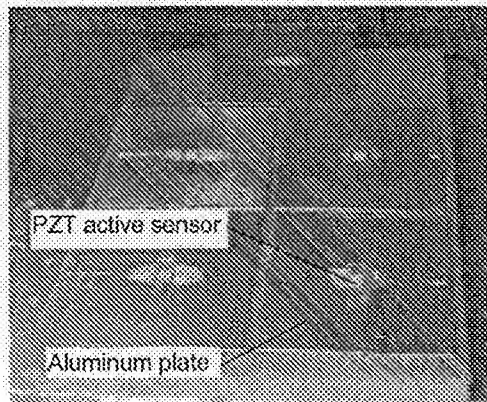


Figure 17 Thin-gage aluminum plate specimens (100-mm square, 1-mm thick), with centrally located piezoelectric sensors.

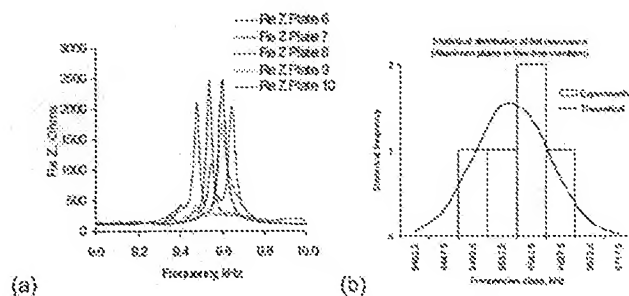


Figure 18 (a) E/M impedance spectrum around the 6th plate resonance; (b) bell-shape statistics for 5 plates.

During the experiments, the specimens were supported on commercially available packing foam to simulate free-free conditions. Thus, plate resonance frequencies could be identified from the E/M impedance real part spectra. Figure 18 presents a typical case for the identification of the 6th plate frequency. Superposed in Figure 18a are the spectrum peaks from 5 identical plates. It can be appreciated that they fall in a narrow frequency band, with mean and standard deviation values of 9.952 kHz, and $\pm 0.577\%$, respectively. The corresponding bell-shaped statistics is given in Figure 18b. Similar results were also obtained for the higher frequencies. The resonance-frequency data was statistically processed, and the mean and standard deviation of each resonance frequency were computed (Table 4). Since rectangular plates do not have closed form solutions for natural frequency calculation (Inman, 1996), no theoretical predictions were performed, and no theoretical data could be inserted in Table 4 for comparison with the experimental data. However, analysis of the experimental data presented in Table 4 indicates that frequency identification of thin-gage metallic plates using the E/M impedance method and PZT active sensors can be achieved consistently and with a good repeatability. The E/M impedance method is more convenient to use than traditional modal analysis methods that require separate instrumentation for excitation (e.g.,

impact hammer) and recording of structural response (e.g., accelerometers). The embedded PZT active sensors are much smaller size, un-obtrusive, and can be permanently attached to the structure, thus permitting in service structural health monitoring.

EXPERIMENT WITH AGING AIRCRAFT PANEL

Realistic aerospace panel specimens containing simulated crack and corrosion damage representative of aging-aircraft structures, designed and constructed at Sandia National Labs (Giurgiutiu *et al.*, 2000), were instrumented with PZT active sensors and subjected to E/M impedance evaluation. The results obtained during the present investigation were compared with previous results (Giurgiutiu *et al.*, 2000) obtained during investigations in which standardized sensor fabrication and installation procedures were not yet available. The sensors were applied to the simulated aircraft panels to detect the change of E/M impedance spectrum induced by the proximity of a simulated crack. Figure 19 shows sensors installation: the sensors are placed along a line, perpendicular to a 10-mm crack originating at a rivet hole. The sensors are 7-mm square and are spaced at 7-mm pitch. E/M impedance readings were taken of each sensor in the 200 – 2600 kHz range. Figure 20 shows the frequency spectrum of the E/M impedance real part. The spectrum reflects clearly defined resonances that are indicative of the coupled dynamics between the PZT sensors and the frequency-dependent pointwise structural stiffness as seen at each sensor location. The spectrum presented in Figure 20 shows high consistency. The dominant resonance peaks are consistently in the same frequency range, and the variations from sensor to sensor are consistent with the variations previously recorded in the simple plate experiments. These observations indicate that the sensor fabrication and installation methodology has achieved a high degree of repeatability and consistency, which represents an important step forward from the scattered results obtained with the unrefined sensor fabrication/installation reported by Giurgiutiu *et al.* (2000).

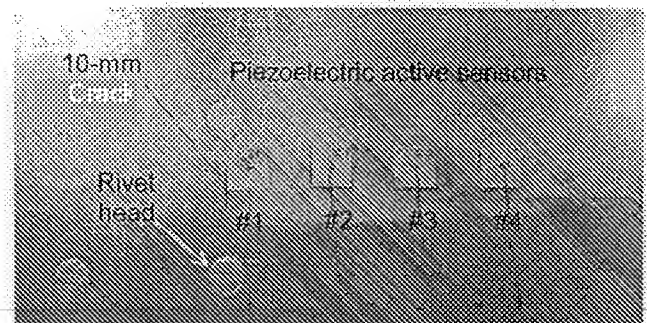


Figure 19 Piezoelectric sensors installed on the aircraft panel with aging damage simulated by a 10-mm crack originating from a rivet.

Examination of Figure 20 indicates that, out of the four E/M impedance spectra, that of sensor 1 (closest to the crack) has lower frequency peaks, which could be correlated to the damage presence. However, this argument is not entirely self-evident since the spectra in Figure 20 also show other sensor-to-sensor differences that are not necessarily related to the crack presence. In order to better understand these aspects, further investigations were performed at lower frequencies, in the 50 – 1000 kHz range (Figure 21). In this range, we can identify changes due to the

crack presence as features in the sensor 1 spectrum that do not appear in the other sensors. For example, sensor 1 presents an additional frequency peak at 114 kHz that is not present in the other sensors. It also shows a downward shift of the 400 kHz main peak. These features are indicative of a correlation between the particularities of sensor 1 spectrum and the fact that sensor 1 is placed closest to the crack. However, at this stage of the investigation, these correlations are not self evident, nor are they supported by theoretical analysis and predictive modeling of the structure under consideration. For these reasons, we conclude that further investigations are required to fully understand the correlation between the spectral features of the E/M impedance response and the presence of structural damage in the sensor vicinity. Both further signal processing and adequate modeling (e.g., with the dynamic Finite Element Method) are needed.

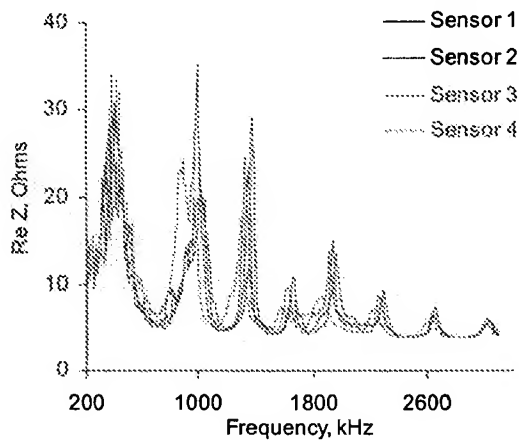


Figure 20 Real part of impedance for sensors bonded on aging aircraft structure (200-2600 kHz range).

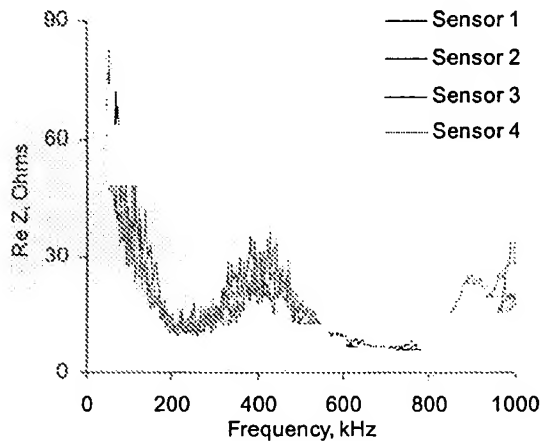


Figure 21 Real part of impedance for sensors bonded on aging aircraft structure (zoom into the 50-1000 kHz range).

CONCLUSIONS

The work reported in this paper has shown that unobtrusive permanently attached PZT active sensors can be successfully used to identify the intrinsic dynamics of a structure through the examination of the recorded E/M impedance spectrum. The

advantages of this approach over traditional structural identification methods (e.g., impact hammer/accelerometer combination) are self-evident and need not be elaborated upon.

A methodology for the fabrication and installation of PZT active sensors on metallic structures typical of aging airframes has been developed and validated through statistical tests.

Experiments on small steel beams instrumented with PZT active sensors have shown that the E/M impedance method is capable of accurately sensing the structural dynamics. The measured results compared well with theoretical predictions. Frequency increase with thickness reduction was experimentally confirmed. This observation could be directly used in the detection of corrosion damage in metallic structures, and of disbonding/delaminations in adhesively bonded and composite structures.

Experiments conducted on a statistical lot of thin-gage aluminum plates instrumented with PZT active sensors have proven that the sensor fabrication and installation procedures, reported in this paper, are sufficiently refined to give consistent and repetitive results on aircraft grade material.

Experiments on aircraft type panels using an array of PZT active sensors indicate that the sensor fabrication and installation methodology has achieved a high degree of repeatability and consistency, which represents an important step forward from the scattered results obtained with the unrefined sensor fabrication/installation reported by Giurgiutiu *et al.* (2000). The effect of simulated damage in the form of a 10-mm crack was noticed as a left shift in the natural frequencies for the sensor closest to the crack, and the appearance of a new frequency peak at around 114 kHz. However, complete understanding of the relationship between the sensor location and the changes in the E/M spectrum has not yet been fully achieved. Further efforts consisting in advanced signal processing, identification of spectrum features that are sensitive to the crack presence, and adequate modeling and simulation (e.g., via the dynamic Finite Element Method) are needed.

ACKNOWLEDGMENTS

The financial support of Department of Energy through the Sandia National Laboratories, contract doc. # BF 0133 is thankfully acknowledged. Sandia National Laboratories is a multi-program laboratory operated by Sandia Corporation, a Lockheed Martin Company, for the United States Department of Energy under contract DE-AC04-94AL85000.

REFERENCES

1. Bartkowicz, T. J., Kim, H. M., Zimmerman, D. C., Weaver-Smith, S. (1996) "Autonomous Structural Health Monitoring System: A Demonstration", *Proceedings of the 37th AIAA/ASME/ASCE/AHS/ASC Structures, Structural Dynamics, and Materials Conference*, Salt-Lake City, UT, April 15-17, 1996
2. Blanas, P., Wenger, M. P., Rigas, E. J., and Das-Gupta, D. K. (1998) "Active Composite Materials as Sensing Element for Fiber Reinforced Smart Composite Structures", *Proceedings of the SPIE North American Conference on Smart Structures and Materials*, SPIE Vol. 3329, San-Diego, CA, March 1-5, 1998.
3. Blitz, Jack; Simpson, Geoff (1996) *Ultrasonic Methods*

- of *Non-Destructive Testing*, Chapman & Hall, 1996.
4. Boller, C., Biemans, C., Staszewski, W., Worden, K., and Tomlinson, G. (1999) "Structural Damage Monitoring Based on an Actuator-Sensor System", *Proceedings of SPIE Smart Structures and Integrated Systems Conference*, Newport CA. March 1-4, 1999
5. Cawley, P. (1997) "Quick Inspection of Large Structures Using Low Frequency Ultrasound", *Structural Health Monitoring – Current Status and Perspective*, Fu-Kuo Chang (Ed.), Technomic, Inc., 1997.
6. Cawley, P., 1984, "The Impedance Method for Non-Destructive Inspection", *NDT International*, Vol. 17, No. 2, pp. 59-65.
7. Chang, F.-K. (1998) "Manufacturing and Design of Built-in Diagnostics for Composite Structures", *52nd Meeting of the Society for Machinery Failure Prevention Technology*, Virginia Beach, VA, March 30 – April 3, 1998.
8. Deng, X., Wang, Q., and Giurgiutiu, V. (1999) "Structural Health Monitoring Using Active Sensors and Wavelet Transforms", Paper # 3667-35, *SPIE's 6th Annual International Symposium on Smart Structures and Materials*, 1-5 March 1999, Newport Beach, CA
9. Duke, J. C. Jr., *Acousto-Ultrasonics – Theory and Applications*, Plenum Press, 1988.
10. Giurgiutiu, V., and Rogers, C. A. (1997) "Electro-Mechanical (E/M) Impedance Method for Structural Health Monitoring an Non-Destructive Evaluation", *Int. Workshop on Structural Health Monitoring*, Stanford University, CA, Sep. 18-20, 1997, pp. 433-444
11. Giurgiutiu, V., and Rogers, C. A. (1998) "Recent Advancements in the Electro-Mechanical (E/M) Impedance Method for Structural Health Monitoring and NDE", *Proceedings of the SPIE's 5th International Symposium on Smart Structures and Materials*, 1-5 March 1998, Catamaran Resort Hotel, San Diego, CA, SPIE Vol. 3329, pp. 536-547
12. Giurgiutiu, V.; Redmond, J.; Roach, D.; Rackow, K. (2000), "Active Sensors for Health Monitoring of Aging Aerospace Structures", Paper # 3985-32, *SPIE's 7th Annual International Symposium on Smart Structures and Materials*, 5-9 March 2000, Newport Beach, CA, SPIE Vol. 3985, pp. 294-305.
13. Giurgiutiu, V.; Rogers, C. A. (2000) "Modal Expansion Modeling of the Electro-Mechanical (E/M) Impedance Response of 1-D Structures" *European COST F3 Conference on System Identification & Structural Health Monitoring*, Universidad Politecnica de Madrid, Spain, 6-9 June 2000.
14. Kawiecki, G. (1998) "Piezogenerated Elastic Waves for Structural Health Monitoring", *Proceedings of SMART-98, NATO Advanced Research Workshop*, June 16-19, Pultusk, Poland
15. Keilers, C. H., Chang, F.-K. (1995) "Identifying Delaminations in Composite Beams Using Built-in Piezoelectrics: Part I - Experiments and Analysis; Part II An Identification Method", *Journal of Intelligent Material Systems and Structures*, Vol. 6, pp. 649-672, September, 1995.
16. Krautkramer, Josef; Krautkramer, Herbert (1990) *Ultrasonic Testing of Materials*, Springer-Verlag, 1990.
17. Lakshmanan, K. A. and Pines, D. J. (1997) "Modeling Damage in Composite Rotorcraft Flexbeams Using Wave Mechanics", *Journal of Smart Materials and Structures* (in press)
18. Lemistre, M.; Gouyon, R.; Kaczmarek, H.; Balageas, D. (1999) "Damage Localization in Composite Plates Using Wavelet Transform Processing on Lamb Wave Signals", *2nd International Workshop of Structural Health Monitoring*, Stanford University, September 8-10, 1999, pp. 861-870.
19. Lopes Jr., V., Park, G., Cudney, H., and Inman, D., (1999) "Smart Structures Health Monitoring Using Artificial Neural Network", *2nd International Workshop of Structural Health Monitoring*, Stanford University, September 8-10, 1999, , pp. 976-985.
20. Measurements Group Inc., (1992) "Student Manual for Strain Gage Technology", Bulletin 309D, 1992
21. Moetakef, M., Joshi, S., and Lawrence, K., (1996) "Elastic Wave Generation by Piezoceramic Patches", *AIAA Journal* Vol. 34, No. 10. October 1996, pp. 2110-2117.
22. Noor, A. K., Venneri, S. L., Paul, D. B., and Chang, J. C. I., (1997) "New Structures for New Aerospace Systems", *Aerospace America*, November 1997, pp. 26-31.
23. Pugachev, S. I.; Ganapol'sky, V. V.; Kasatkin, B. A.; Legusha, F. F.; Prud'ko, N. I. (1984) Handbook "Piezoceramic Transducers", Sudostroenie, St.-Petersburg, (In Russian)
24. Rogers, C. A. and Giurgiutiu, V. (1997) "Electro-Mechanical (E/M) Impedance Technique for Structural Health Monitoring and Non-Destructive Evaluation", *Invention Disclosure No. 97162*, University of South Carolina Office of Technology Transfer, July 1997.
25. Viktorov, I. A., 1967, *Rayleigh and Lamb Waves*, Plenum Press, New York, 1967
26. Waanders, J. W. (1991) "Piezoelectric Ceramic, Properties and Applications", Philips Components, Eindhoven, Netherlands, 1991.

AUTOMATION FOR NONDESTRUCTIVE INSPECTION OF AIRCRAFT

M. W. Siegel*
Carnegie Mellon University
Pittsburgh PA 15213-3891

Abstract

We discuss the motivation and an architectural framework for using small mobile robots as automated aids to operators of nondestructive inspection (NDI) equipment. We review the need for aircraft skin inspection, and identify the constraints in commercial airlines operations that make small mobile robots the most attractive alternative for automated aids for NDI procedures. We describe the design and performance of the robot (ANDI) that we designed, built, and are testing for deployment of eddy current probes in prescribed commercial aircraft inspections. We discuss recent work aimed at also providing robotic aids for visual inspection.

I. Background

Our goal is to replicate and enhance the capability of aircraft skin inspectors who use hand-held instruments (and their own senses and intelligence) to detect and classify flaws in aging aircraft. Our underlying concept is to use mobile robots, automated control, and automated interpretation of sensors and instruments to make *difficult measurements in difficult environments*. Potential application areas include not only airplane skins, the subject of this paper, but also problems such as bombs in luggage, contraband in cargo containers, verification of disarmament treaty compliance, characterizing environmentally contaminated sites, and a variety of manufacturing problems, e.g., measuring composition gradients in large process tanks, transportation problems, e.g., bridge inspection, and scientific research problems, e.g., checking the integrity, alignment, etc., of large instruments such as radio telescopes and particle accelerators. These few examples just begin to suggest the universe of potential application areas and specific

A general hierarchical paradigm for the common issues of *measurement*, *manipulation*, *mobility*, and *monitoring* characteristic of all these problems is illustrated explicitly for the aging aircraft problem in Figure 1.

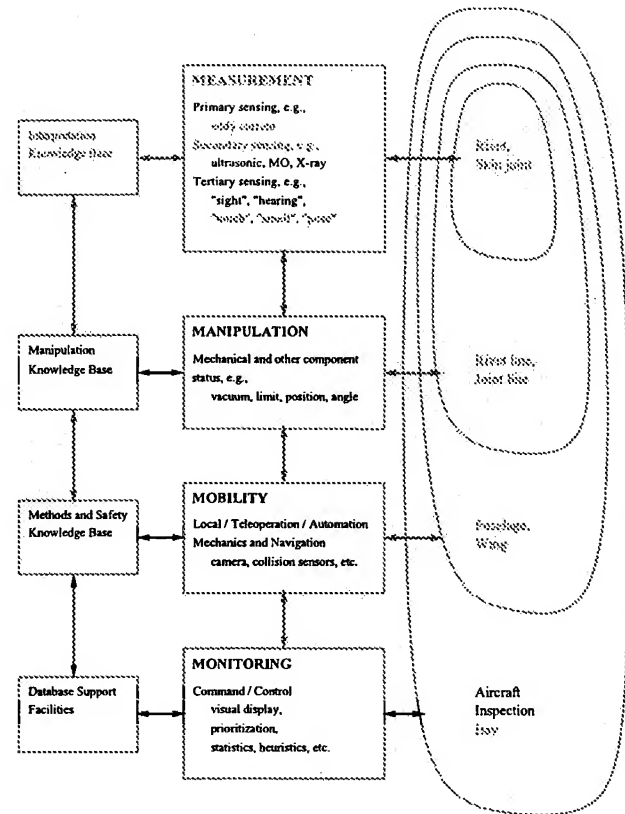


Figure 1: The 4M-s of automation for aircraft inspection.

II. Inspection of Aging Aircraft

Aircraft skins inflate and deflate with each cycle of pressurization and depressurization. The resulting stress causes several kinds of damage, primarily radial cracks around rivets, delamination of skin joints, and subsurface cracks in the structural members to which the skin is attached. Delamination is exacerbated by corrosion, which is particularly prevalent in warm moist climates. Cracks and corrosion, accelerated by island-hopping operation, resulted in April 1988 in a large section of skin tearing off the top of the fuselage of an Aloha Airlines Boeing 737. The resulting press coverage of the airplane's seemingly miraculous safe landing brought these problems prominently to the attention of the public,

*Senior Research Scientist, The Robotics Institute, School of Computer Science

and resulted in an aggressive prevention, detection, and remediation program by aircraft operators in close cooperation with each other, the aircraft manufacturers, and the FAA^{1,2,3}. Structural effects of aging in other areas, such as engines, fuel tanks, landing gear, etc, possibly will be the subjects of future automation research, but for the present our program is concentrating on skin and the immediate supporting substructures.

Through programs of periodic inspection of known problem areas on each aircraft type, skin cracks and corrosion are typically found well before they reach hazardous size. The problem areas are specified by "service bulletins" issued by aircraft manufacturers, and by "airworthiness directives" issued by the FAA. Compliance with airworthiness directives is mandatory. Compliance with service bulletins is at the airline operators discretion, but we are told that in practice they are treated as mandatory.

About 90% of skin inspection is visual, by inspectors trained for the task, most of the remainder is by eddy current probes, and a fraction of a percent is by other instrumentation of which the best known is probably ultrasonic. Our program is focused in its initial phases on automation as an aid to skin inspection using eddy current probes. Initially we will use machine vision to aid probe placement and robot navigation and to update the navigation database with descriptions of patches and other deviations from "as designed". We are beginning to investigate automated aids to visual inspection via a new program in which a small limited functionality robot will be used deploy 3D-stereoscopic cameras. Working with experienced visual inspectors, we will evaluate the acceptability of computer aided remote (teleoperated) visual inspection.

Eddy Current Inspection

The eddy current method⁴ uses a transmitting coil and a receiving coil (they may physically be one coil) coupled electromagnetically through the metal under inspection. Eddy current probes vary in tip area from several square centimeters to about one square millimeter, obviously trading off decreasing areal coverage for increasing sensitivity to small flaws as the size decreases. Anomalies in the impedance that characterizes the coupling indicate cracks, corrosion thinning, and other flaws. Inspectors generally watch an x-y oscilloscope display whose x-axis represents the in-phase (resistive) part of the impedance and whose y-axis represents the quadrature-phase (inductive or capacitive) part of the impedance. Figure 2 illustrates a probe, and Figure 3 illustrates typical impedance plane signals. The inspectors compare patterns traced out on the screen when

the probe is passed over a potential flaw with the pattern traced out when the same probe is passed over a calibration standard manufactured with a machined flaw in the simulated local structure. The probe geometry, operating frequency, scan path, etc, are chosen to optimize sensitivity to each anticipated flaw. High operating frequencies are attenuated in a short distance, and thus probe only the surface. Low operating frequencies penetrate deeper, and in some geometries can penetrate the skin entirely and probe for cracks in the supporting framework. Under typical operating conditions power levels are sufficiently low that the method is extremely linear, so it is possible to operate a probe with a composite multi-frequency transmitted waveform and to separate electronically the high-frequency surface-sensitive received signal components from the low-frequency substructure-sensitive components.

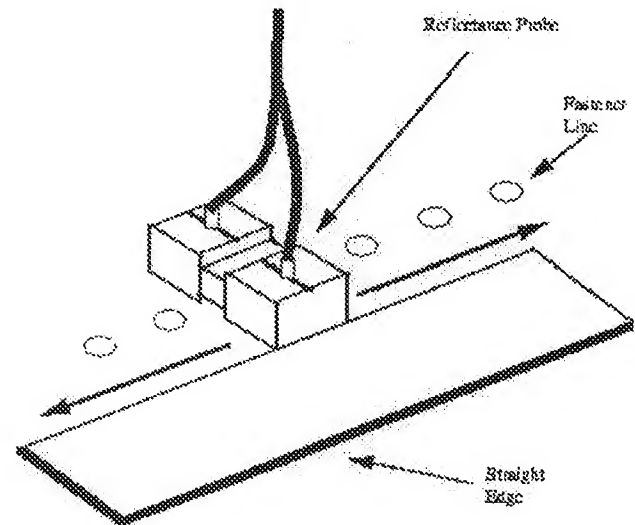


Figure 2: "Reflectance" or "pitch-catch" eddy current probe.

Modern eddy current systems can be set to alarm on traces that enter or fail to enter preset rectangular windows in complex impedance space. Initially we will rely on these alarms to alert the inspector to potential flaws indicated by anomalous signals. These areas will be marked for easy identification by the inspector, e.g., by daubing suspect rivet heads with a washable paint. Pattern recognition integrated with rule based systems is an accepted method for automating interpretation and classification of eddy current signals in other applications, e.g., inspection of heat exchanger tubes in nuclear power plants⁵. Neural network methods have been similarly successful in similar applications⁶. As the program progresses we will add additional software to implement promising approaches to automated and improved eddy current signal interpretation and classification.

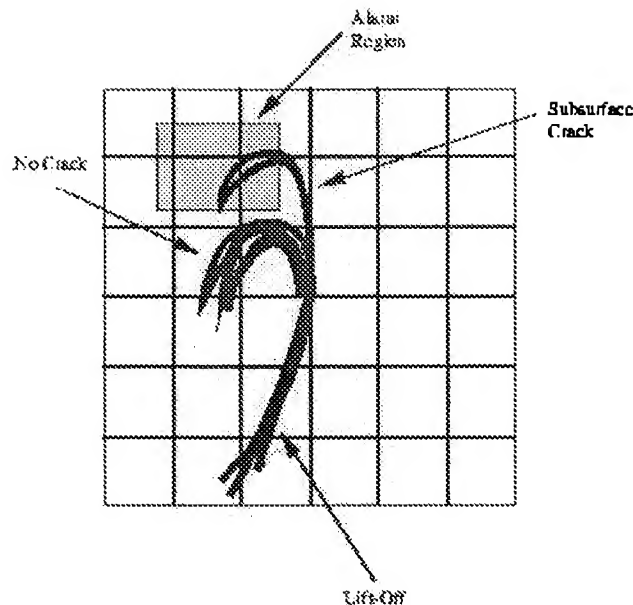


Figure 3: Eddy current signals in the complex impedance plane.

III. Automated NonDestructive Inspector

We considered many approaches to automation-assisted eddy current probe deployment, with three primary variants: the gantry-based "car wash", the vehicle-based "cherry picker", and the self-contained "window washer". The pros and cons of these alternatives have been discussed in detail elsewhere^{7, 8, 9, 10, 11, 12, 13, 14, 15}; in summary, the "window washer" design that we eventually chose for the system is dictated by the pragmatics of fitting NDI nondisruptively into the flow of passenger aircraft maintenance operations. These constraints suggest a small (under one meter maximum dimension) mobile platform that is able to walk or crawl over most if not all of the aircraft skin, whatever its orientation. This capability we achieve with active (vacuum assisted) suction cups. A concept sketch for the resulting robot (ANDI, the Automated NonDestructive Inspector) is shown in Figure 4. It is not the easiest approach, but it is the most acceptable, and incidentally it is the approach that requires the most interesting enabling research.

Cruciform Design

Because there is generally more fore-aft than circumferential inspection path, the robot is designed with a cruciform geometry that enables it to move along fore-aft paths most rapidly; this results in a design in which it moves on circumferential paths somewhat more slowly, and in skew directions adequately, but a bit awkwardly. The mechanical design is sketched in Figure 5 and shown

Aircraft Skin Inspection Robot

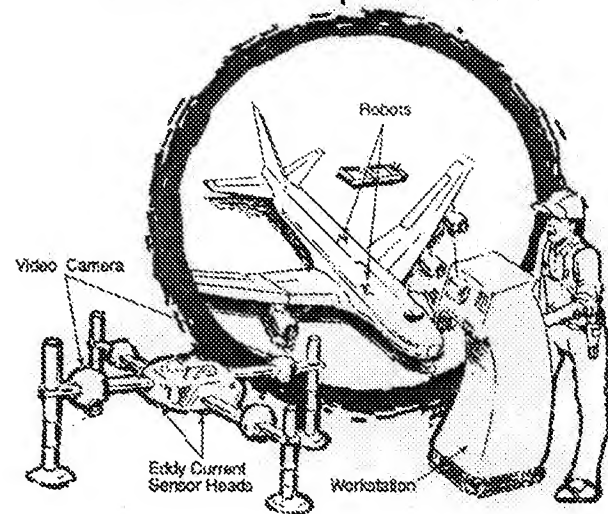


Figure 4: Concept sketch for ANDI.

close-up (with eddy current probe in the foreground and a graphical depiction of the probe output on the computer monitor screen in the background) in Figure 6. It has many features in common with the class of mobile robots known in the literature as "beam walkers"^{16, 17}. However unlike most beam walkers our robot is able to side step almost as easily as it can walk forward or backward. The two cross members ("bridges") are normally locked at right angles to the main longitudinal member ("spine"), but they can be released to pivot freely by about 15° in either direction; this permits the robot to steer and thus to travel along paths that are neither strictly fore-aft nor strictly circumferential. Pneumatically actuated up-down degrees of freedom on the four suction cups at the ends of the bridges enable the walking motion, and another pneumatic actuator enables the raising and lowering of the eddy current probe. The sliding motions of the bridges along and perpendicular to the spine are actuated by electric motors.

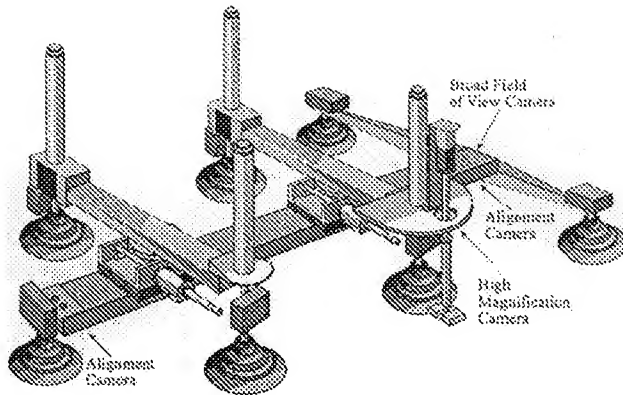


Figure 5: Mechanical features of ANDI, showing four camera mounting points.

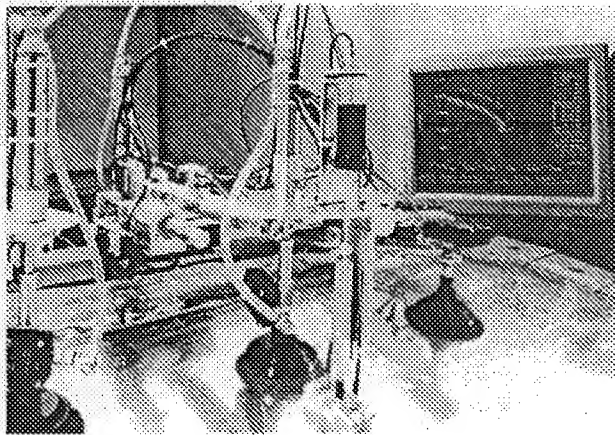


Figure 6: ANDI, showing eddy current probe and its signal on the computer monitor.

Alternative Designs

It is regrettably easy to confuse ANDI, particularly given its multiply anthropomorphic name**, with the much larger and more complex system of which it is essentially just the mechanical end effector. It is thus appropriate to emphasize explicitly that ANDI is just the first prototype mechanical end effector of a large and complex system (most of which is black boxes full of electronics and computers) that can accommodate many different end effectors. ANDI is designed to demonstrate the feasibility of using robots to assist inspectors of aging aircraft. But ANDI is not the last end effector that will ever be needed for this task. There are places on an airplane skin where ANDI cannot adhere, e.g., sharply curved regions around the nose, tail, and leading and trailing edges of the wings and horizontal and vertical stabilizers. There are places where ANDI can adhere but may turn out to be

insufficiently agile to deploy the eddy current sensor in an effective pattern, e.g., perhaps around doors, windows, repair patches, etc. Our goal is to demonstrate what ANDI can do. We guess it can do something like 80% of the mandated and recommended eddy current inspections on DC-9 or Boeing 737 and larger aircraft. If ANDI proves its technical and economic worth in these applications, we are confident that we (and others!) will be able to design as many specialized mechanical end effectors as are needed to cover the applications ANDI cannot.

A block diagram of the currently envisioned complete system is shown in Figure 7.

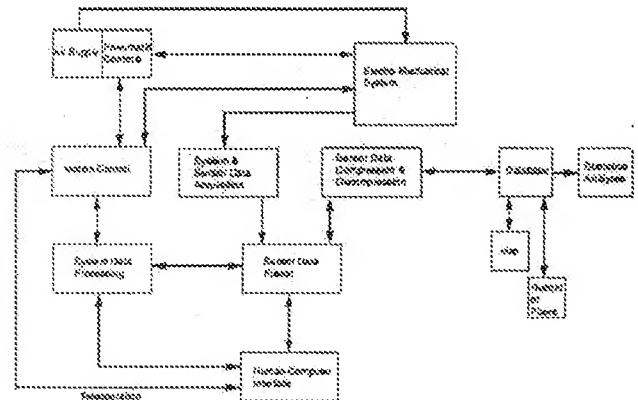


Figure 7: Block diagram of planned complete system.

Special Purpose Actuators

Our initial eddy current sensor deployment demonstration is targeted on part of a mandated inspection on the fuselage of a DC-9 that uses a "reflectance" or "pitch-catch" probe with mechanically independent but electrically coupled transmit and receive coils. This particular inspection has both a surface crack and a subsurface crack component which we address simultaneously by composite dual frequency operation. The reflectance probe geometry is sensitive to integrated conditions over a fairly large patch of skin (a few square millimeters), so it is forgiving of small errors in placement relative to the rivets under examination. Under these circumstances it is adequate to deploy the probe with a simple up-down lifter mechanism and let it self-align with the skin under the influence of a constant-force spring. Another part of the planned demonstration inspection uses a "pencil" probe with a single coil that has a much smaller sensitive area. It must thus be placed and scanned more accurately, e.g., along a path that is tangential to each rivet, which may require closed loop

**Messrs Andrew Carnegie and Andrew Mellon both suggest ANDI

guidance. Another small but necessary part of the demonstration inspection requires moving a pencil probe completely around the circumference of several rivets. The more complex probe paths that this inspection component requires can in principle be achieved by coordinating the motions of bridge-along-spine and bridge-perpendicular-to-spine, but we anticipate that obtaining the necessary mechanical precision and simplicity of control may require adding some nominally redundant special purpose degrees of freedom, e.g., a rotary mechanism for precisely circumnavigating individual rivets.

Path Control

The path control system addresses mechanical positioning of the eddy current probe and the robot at four distance scales corresponding to the tasks of *alignment*, *guidance*, *navigation*, and *path planning*.

Alignment means the relative position of the eddy current or alternative probe and the rivet or other component under inspection. The inspection protocol is predicated on the assumption that the probe will be moved along a precise short path relative to the part geometry. Signal classification can be done meaningfully only if this path is followed.

Guidance means, for rivet inspection, moving the probe from one rivet to the next and arriving there in correct alignment. For other inspections, e.g., for corrosion somewhere along a skin joint, it means following the required inspection path. In this case it differs from alignment only in distance scale.

Navigation means coordinating walking and probe guidance so that an inspection that spans multiple robot steps proceeds smoothly and certainly.

Path planning means being able to traverse as rapidly as possible, without inspecting, long distances between areas that require inspection. This is the scale at which collisions with undocumented parts of the airplane (e.g., a non-standard antenna), expected parts in an unexpected state (e.g., an access hatch left open during maintenance), and other maintenance equipment (e.g., a wrench left on a bolt head) are potentially serious problems.

We expect to achieve the necessary position accuracy by dead-reckoning using high mechanical precision motion over short distances between map database landmarks and using machine-vision-based correction at each landmark. The obvious landmarks are the rivets themselves, each of which is in principle individually identifiable in the aircraft design database. The eddy current signals themselves then provide an additional and perhaps finer level of correction: misalignment signatures are

recognizable and quantifiable, although some sign ambiguities would have to be resolved by active sensing. Skin joints and skin joint intersections provide additional landmarks. They are particularly appropriate for navigation and path planning, in contrast with the rivets, which are particularly appropriate for alignment and guidance. Skin joints are farther apart than rivets, a disadvantage in terms of dead-reckoning error accumulation, but their existence is more consistent from airplane to airplane (of the same type) since their locations are less likely to be changed by modifications and repairs. The skin joints and skin joint intersections, referenced in terms of the underlying longeron (or stringer) and spar (or body station) identification numbers, are in fact the features in terms of which mandated and recommended inspections are defined.

In principle the map databases are all on-line at the factory for as-designed and as-built, and on-line at the hangar for as-modified and as-repaired. In practice the data are still on paper for all aircraft except the generation now in gestation, e.g., the Boeing 777, and we expect we will have to use ANDI to bootstrap populating its own map and exception database.

Vision System

ANDI will have at least four cameras in the alignment, guidance, navigation, and path planning system. Cameras will also have roles in visual flaw detection, but not until a later phase of the program.

Macro Camera

The first camera will be mounted on the same platform as the eddy current probe, with a macro capability giving it a field-of-view of approximately one rivet. It will be used for fine alignment and for the inspector's visual observation of the appearance of the rivet and the adjacent skin at high magnification. In some inspections that require precision probe alignment the alignment control loop may incorporate the eddy current sensor signal as well. In later phases image understanding will be incorporated for visual flaw detection, and possibly as an adjunct to eddy current or other NDI probes. For example, a particular eddy current probe that has a radially symmetric field geometry may sensitively indicate the presence of a radial crack, but will obviously be blind to its orientation; it may then be useful to use the high magnification camera to find its orientation.

Alignment Cameras

The second and third cameras, each with medium magnification fields of view of about 10 cm x 15 cm, or a line of four to six rivets, will be mounted at the head and tail of the spine. These cameras will be used to locate line segments of rivets. A robust best-fit¹⁸ to the head and tail line segments will guide the eddy current sensor along a scan line. This guidance functionality is required early, so these will be the first cameras installed on ANDI. Guidance is actually required before alignment, because the initial eddy current probe is of the "pitch-catch" or "reflectance" type, which is sufficiently tolerant of misalignment that little alignment (fine adjustment about the guidance line) is likely to be needed. The imagery from these cameras will also be made available to the inspector for opportunistic flaw detection of, for example, lightning holes and small dents. As in the case of the high magnification camera, automation of the flaw detection role for these cameras will come in a later project phase. However, we have already made substantial progress prototyping the computer vision based automation of the alignment function. Several rivet finding algorithms have been tried, including edge detection followed by region growing, gray level variance, and a trained neural network, yielding the general conclusion that even with uncontrolled lighting, low contrast, and interference from specular reflectances, any scale-sensitive operator that has the actual rivet size hard wired into it will succeed. A conventional robust line-fitting algorithm based on minimizing the mean absolute deviation almost always correctly draws the desired line through three, four, or five rivets even for the most ghastly poor images. Early results are discussed and illustrated in the following section.

Zoom Lens Camera

The fourth camera, with an ordinary zoom lens's range of focal lengths and working distances, will be mounted on a motorized pan-tilt head high above ANDI's tail end. In the initial experiments, before general purpose navigation and path planning algorithms are in place, ANDI will be teleoperated between inspection stations. Thus the fourth camera will initially be the inspector's eye on the robot's actual configuration, possible interferences or collisions, sensible paths between inspection stations, and gross visual flaws, e.g., pillowing due to extensive subsurface corrosion. As the program progresses machine vision algorithms will increasingly use this camera for proprioception (visually confirming that the actual robot pose corresponds to the control system's model of the pose), collision avoidance and footfall decisions (new radio antennas, skin patches, or raised head replacement rivets will have to be found, avoided, and entered into the database), long distance path planning between inspection

stations, and opportunistic detection of large flaws.

Vision Based Alignment

While there are important exceptions that we will eventually have to address, most of the time rivets line up neatly in evenly spaced rows and columns. ANDI is designed to take maximum advantage of this design rule: what ANDI can do most effortlessly and precisely is to scan an eddy current sensor along a straight line segment parallel to and almost the full length of its spine. The essential alignment problem is thus to align the spine parallel to the line segment under inspection. The approach we are developing is to best-fit visually a short line segment near each end of the spine, best-fit the long line segment to the two short line segments, and scan along the long line segment open loop unless the eddy current data show features that suggest the rivet line wiggles enough that transverse corrections are needed.

On the assumption that if a computer vision algorithm works well with terrible looking images it will probably work better with better looking images, we developed our approach on a sequence of images that we collected with uncontrolled lighting, uncontrolled surroundings (which are obvious in specular reflection), poorly controlled camera standoff from the riveted surface (a test panel with a radius of curvature and other features comparable to a Boeing 737 or DC-9), and a consumer grade 8 mm camcorder camera that we scanned over the test panel by hand. We digitized to 8 bits x 3 colors about 80 frames grabbed from the tape at about 1.5 sec intervals. Each frame was digitized into 480 pixels x 512 lines x 3 colors, then averaged in 8 x 8 blocks into 60 pixel x 64 line x 3 color working images. At the lowered resolution the rivet line segment finding pipeline runs at approximately real-time (1.5 sec/frame) on a workstation. With the camera parameters and resolution we used, rivets are circular blobs that generally fit into a 7 x 7 block. A typical frame, with gray levels computed by averaging the RGB values, is shown in Figure 8.

Conventional Algorithm

As mentioned in the previous section, finding rivets is easy even when the images are as ugly as this one: any sensible operator with a scale length matched to the rivet size works fine. Under these circumstances a useful strategy is to choose an operator that rarely misses a real rivet even at the price of occasionally finding a false rivet, provided that one or more downstream modules can be tailored to reliably reject false rivets. Finding all real rivets plus some non-rivets we can in fact do with a Canny edge detector¹⁹. Next we observe that specular reflections, the main potential source of false rivets, look

Figure 10: Line fit to t

Neural Network Algorithm

An alternative algorithm was network simulated in software the problem by saying that re finding suitable discriminati ranges intuitively, relevant par found mechanically by syst parameters of a generalized in reliably behaves as a rivet applied to an operator-representative of the problem adequately representative of th trained network will also be

outputs, and digital input and with various sensors (e.g., s actuators (e.g., solenoid valve cylinders). The second PC probe system and its display. is on an independent proprietary now supports alignment of the : Its permanent successor will su system requirements outlined a

As development continues th displays will be rationalized. processing power (which will with on-board computing power etc), and to coalesce the mu powerful windowing system to to controls, signals, images, an A rudimentary interim data function during laboratory tests eddy current sensor scanning walking between scanned locat

Database and Archiving

Aircraft skin inspections are r requirement to record anomalies In practice, we are told, ai detected flaws, even those t recommended thresholds. Even pass/fail recording would not thresholds have substantial sal good growth models²² for pred will repair be necessary. These circumstances notwithstanding that the predictive capabilities archiving and statistical analysis results will facilitate main potentially increase safety. T database. with an architectu

IV. Visual Inspection

As mentioned earlier, close to 90% of aircraft inspection is visual; our choice of eddy current inspection for the first demonstration of automation to aid aircraft inspectors was driven by the relative simplicity of automating deployment of eddy current probes (and NDI probes in general) in comparison with visual inspection. Unlike NDI, where the goal is usually to detect a flaw whose location and nature is known in advance (from previous experience or from computer modelling), visual inspection has a substantial opportunistic component. The visual inspector's goal is to find not only the anticipated failures, but "everything else" as well: dents, lightning strikes, and other kinds of damage of an unpredictable nature in unpredictable locations. The open-ended quality of this task makes it an unlikely candidate for a level of automation approaching the level we are planning for NDI.

However discussions with airline management and NDI inspection personnel suggest that an integral visual inspection capability may be perceived as an indispensable component of any economically viable system of automated aids to NDI.

In response to this perception, a mobile end-effector like ANDI does suggest itself as a teleoperable platform from which ground-based visual inspection might efficiently be conducted. If this could be accomplished, it would be valuable for many of the same reasons that ground-based NDI is valuable: reduced set-up time, human-factors issues of inspector performance in a difficult environment, inspector safety, database access, data archiving, etc. The question is whether remote cameras can provide sufficiently high quality (presumably meaning primarily high resolution) imagery to satisfy the notoriously fussy (we are comforted to say) visual inspectors. We recently began a program whose goal is to answer this question. This program combines elements of the FAA-sponsored ANDI project with salient elements of an ARPA-sponsored project in 3D-Stereoscopy Technologies for image and graphics visualization.

One of the costs of human inspection is attributable to the difficulty of safely getting the inspector to the right place on the airplane: it involves erecting scaffolding, providing safety harnesses, etc, all of which can take more time than the inspection per se. ANDI can be placed on an airplane fuselage at human chest level, and directed to move to any area requiring inspection without erecting scaffolding and without endangering the human inspector. Thus even a teleoperated capability, with only the most rudimentary elements of automation (e.g., computer coordination of gait), could permit the inspector rapidly and safely to perform the necessary visual inspections. With

appropriately selected cameras and actuators thus could clearly be done at the required variety of points-of-view, magnifications, lighting conditions, etc.

3D-Stereoscopic Vision

We are particularly interested in the prospect of providing the visual inspector with binocular 3D-stereoscopic vision. Stereoscopic perception appears to be important to the visual inspectors who we have observed on the job. We speculate that this may be because of its importance both in perceiving and in rejecting the effects of specular reflection off the mirror-like aircraft skin. Specular reflection appears to be important to inspectors looking for the presence or absence of specific flaws: they often move their heads and lights as they look for an expected tell-tale glint. Specular reflection is particularly apparent in binocular 3D-stereoscopic imagery because the sharply directed reflection appears much brighter in one or the other image, in contrast to the diffuse reflections, whose intensities are evenly balanced in the two images. [For this reason waterfalls and fast running streams, which are notoriously difficult to photograph (and paint) well, look spectacularly realistic in 3D-stereoscopic imagery.] Furthermore, the depth perception provided by 3D-stereoscopic imagery also makes it easy to reject artifacts of the environment that are reflected by the aircraft skin. Without depth perception it is impossible to know (except by high-level knowledge of the context) whether features of the imagery are in the skin or in the environment and seen in reflection. With depth perception, image features that are not in the plane of the skin can be rejected straightforwardly, even automatically.

The components required in a 3D-stereoscopic system are (1) a matched pair of cameras (analogous to the human's two eyes), (2) suitable and suitably controllable lighting, and (3) a display that is capable of directing the image corresponding to the right camera to the operator's right eye and the image corresponding to the left camera to the operator's left eye. There is no ideal way to accomplish (3). Special video taping equipment is also needed if the imagery is to be recorded. A variety of commercially available solutions have pros and cons that we are evaluating in context of the visual inspection application. Available solutions include frame, field, and subfield sequential methods with active shuttering eyewear, field and sequential methods with interline-polarization and passive eyewear, and "virtual reality" approaches using head-mounted displays. We have one subfield sequential and one interline-polarization system operational, so will conduct our initial experiments with these systems.

We are building for these experiments a simple mobile manipulator that will move over an airplane panel test

surface according to the inspector's instructions mediated by a computer that will support a suitably high-level interface. A simple mobile manipulator (in contrast to ANDI) will suffice because (unlike ANDI) it will have to operate, for these evaluation experiments, only on a more-or-less horizontal surface.

Acknowledgements

The opportunity to automate aging aircraft inspection was suggested by Stephen A. George. The inspection system concept was developed in collaboration with William M. Kaufman. The design and construction of the ANDI system was done in collaboration with Kaufman, Christopher J. Alberts, Court L. Wolfe, Christopher W. Carroll, and John J. Hudak at Carnegie Mellon Research Institute (CMRI), and Alan D. Guisewite and Ian Davis of the Robotics Institute. The image processing examples are Davis's. Russell Jones and Roy Weatherbee of USAir, and William Keil, formerly of USAir, provided invaluable insight and advice about operating and inspecting commercial aircraft. The design of the 3D-stereoscopic inspection testbed was done primarily by Gregg W. Podnar at the Robotics Institute. The ANDI project is supported by the FAA Aging Aircraft Research Program via FAA Research Grant 93-G-013 and Bureau of Mines Grant G0319014. The 3D-stereoscopic visual inspection project is supported by the Ben Franklin Technology Center of Western Pennsylvania and Aircraft Diagnostics Corporation (ADC) via Grant RR10032 (1993-94). The 3D-Stereoscopic Technologies project is supported by ARPA under the High Definition Systems Program Grant MDA 972-92-J-1010.

References

1. Nelson J. Miller, "FAA Initiatives in Aging Aircraft Research for Assurance of Continued Airworthiness", Tech. report, FAA Technical Center, 1991.
2. *1991 International Conference on Aging Aircraft and Structural Airworthiness (Washington, DC)*, Federal Aviation Administration (FAA) and NASA, Charles E. Harris, Nov 1991.
3. Richard Johnson, "Aging aircraft and airworthiness", *Aerospace Engineering*, Jul 1992, pp. 23-30.
4. Robert C. McMaster (editor emeritus), Paul McIntire (editor), Michael L. Mester (technical editor), editors, *Electromagnetic testing: eddy current, flux leakage, and microwave nondestructive testing*, American Society for Nondestructive Testing, Columbus OH, Nondestructive testing handbook, Vol. 4, No. xxiii, 1986.
5. Soon-Ju Kang, Nam-Seok Park, and Yong-Rae Kwon, "A Hybrid Expert System for Eddy Current based Inspection of Steam Generator Tubes in Nuclear Power Plant", *Third Symposium on Expert Systems Application to Power Systems (Tokyo-Kobe, JAPAN)*, Korea Atomic Energy Research Institute and Korea Advanced Institute of Science and Technology, Dajeon City and Seoul, Korea, Apr 1991, pp. 144-151.
6. Kil-Yoo Kim, et al., "Eddy Current Signal Recognition Using Neural Network", *Third Symposium on Expert Systems Application to Power Systems (Tokyo-Kobe, Japan)*, Korea Atomic Energy Research Institute, Artificial Intelligence Department, Dajeon-City, KOREA, Apr 1991.
7. C. J. Alberts, W. M. Kaufman, M. W. Siegel, "The Development of a Robotic System to Assist Aircraft Inspectors", *Proceedings of the ATA NonDestructive Testing Forum*, ATA, Airlines Transport Association, Scottsdale, AZ, September 1993, pp. ???.
8. M. W. Siegel, W. M. Kaufman, C. J. Alberts, "Mobile Robots for Difficult Measurements in Difficult Environments: Application to Aging Aircraft Inspection", *Robotics and Autonomous Systems*, Vol. 11, 1993, pp. 187-94.
9. M. W. Siegel, "Robotics for Difficult Measurements in Difficult Environments: Application to Aging Aircraft Inspection", Robotics Institute Annual Review.
10. Ian Davis and M. W. Siegel, "Automated NonDestructive Inspector of Aging Aircraft", *Proceedings of the Wuhan meeting*, SPIE, Second International Symposium of Measurement Technology and Intelligent Instruments, Wuhan China, October 1993, pp. 190-201.
11. Ian Davis, M. W. Siegel, "Vision algorithms for guiding the Automated NonDestructive Inspector of aging aircraft skins", *Proceedings of the San Diego Meeting*, SPIE, SPIE, Bellington WA, July 1993, pp. 133-44.
12. W. M. Kaufman, C. J. Alberts, M. W. Siegel, "Automated Inspection of Aircraft", *Proceedings of the Fifth Conference*, Deutsche Gesellschaft fur Luft- und Raumfahrt e.V. (DGLR), International Conference on Structural Airworthiness of New and Aging Aircraft, Hamburg, Germany, June 1993.
13. M. W. Siegel, W. M. Kaufman, and C. J. Alberts,

- “Mobile Robots for Difficult Measurements in Difficult Environments: Application to Aging Aircraft Inspection”, *Proceedings of the Pittsburgh Meeting*, C. Thorpe, ed., IAS Conference, International Conference on Intelligent Autonomous Systems: IAS-3, Pittsburgh PA 15213, February 1993, pp. 156-63.
14. C. J. Alberts, W. M. Kaufman, M. W. Siegel, “Automated Inspection of Aircraft”, *Aerospace '92, Dallas TX*, SME, SME, June 1992.
 15. W. M. Kaufman, M. W. Siegel, C. J. Alberts, “Robot for Automation of Aircraft Skin Inspection”, *Proceedings of the International Workshop on Inspection and Evaluation of Aging Aircraft*, Benham Bahr, ed., Federal Aviation Administration (FAA) hosted by Sandia National Laboratories, Albuquerque NM, May 1992, pp. VII 13-18.
 16. W. Chun, S. Price, and A. Spiessbach, “Design and Construction of a Quarter Scale Model of the Walking Beam”, *Proceedings of the Twentieth Annual Pittsburgh Conference (Pittsburgh, PA)*, Instrument Society of America, Martin Marietta Space Systems Co., Denver, CO, May 1989, pp. 785-788, Modeling and Simulation, Volume 20, Part 2
 17. W. Chun, S. Price, and A. Spiessbach, “Terrain interaction with the quarter scale Beam Walker”, *Mobile Robots IV (Philadelphia, PA)*, SPIE, Martin Marietta Space Systems Co., Denver, CO, Nov 1989, pp. 98-103.
 18. W. H. Press, B. P. Flannery, S. A. Teukolsky, and W. T. Vetterling, *Numerical Recipes in C*, Cambridge University Press, Cambridge, 1990.
 19. J. Canny, “Finding Edges and Lines in Images”, Technical Report 720, MIT AI Laboratory, June 1983.
 20. R. Duda and P. Hart, *Pattern Classification and Scene Analysis*, Wiley and Sons, 1973.
 21. D. E. Rumelhart, J. L. McClelland, and the PDP Research Group, *Parallel Distributed Processing*, The MIT Press, Cambridge MA, 1986.
 22. Regis Pelloux, “Tracking Cracks in Aviation Safety - The Facts on Fuselage Fatigue”, *MIT Industrial Liaison Program*, No. A1191-056, Nov 1991.



Pergamon

Computers Ind. Engng. Vol. 30, No. 2, pp. 257-267, 1996

Copyright © 1996 Elsevier Science Ltd

Printed in Great Britain. All rights reserved

0360-8352/96 \$15.00 + 0.00

0360-8352(95)00170-0

USING NEURAL NETWORKS TO PREDICT COMPONENT INSPECTION REQUIREMENTS FOR AGING AIRCRAFT*

HUAN-JYH SHYUR,¹ JAMES T. LUXHOJ¹ and TREFOR P. WILLIAMS²

¹Department of Industrial Engineering and ²Department of Civil Engineering, Rutgers University, P.O. Box 909, Piscataway, NJ 08855-0909, U.S.A.

Abstract—Currently under development by the Federal Aviation Administration (FAA), the Safety Performance Analysis System (SPAS) will contain indicators of aircraft safety performance that can identify potential problem areas for inspectors. The Service Difficulty Reporting (SDR) system is one data source for SPAS and contains data related to the identification of abnormal, potentially unsafe conditions in aircraft or aircraft components/equipment. A higher expected number of SDRs suggests a greater possibility of a maintenance problem and may be used to alert Aviation Safety Inspectors (ASIs) of the need for preemptive safety or repair actions.

The preliminary SDR performance indicator in SPAS is not well defined and is too general to be of practical value. In this study, an artificial neural network model is created to predict the number of SDRs that could be expected by part location using sample data from the SDR database that have been merged with aircraft utilization data. The predictions from the neural network models are then compared with results from multiple regression models. The methodological comparison suggests that artificial neural networks offer a promising technology in predicting component inspection requirements for aging aircraft.



USING NEURAL NETWORKS TO PREDICT COMPONENT INSPECTION REQUIREMENTS FOR AGING AIRCRAFT*

HUAN-JYH SHYUR,¹ JAMES T. LUXHOJ¹ and TREFOR P. WILLIAMS²

¹Department of Industrial Engineering and ²Department of Civil Engineering, Rutgers University,
P.O. Box 909, Piscataway, NJ 08855-0909, U.S.A.

Abstract—Currently under development by the Federal Aviation Administration (FAA), the Safety Performance Analysis System (SPAS) will contain indicators of aircraft safety performance that can identify potential problem areas for inspectors. The Service Difficulty Reporting (SDR) system is one data source for SPAS and contains data related to the identification of abnormal, potentially unsafe conditions in aircraft or aircraft components/equipment. A higher expected number of SDRs suggests a greater possibility of a maintenance problem and may be used to alert Aviation Safety Inspectors (ASIs) of the need for preemptive safety or repair actions.

The preliminary SDR performance indicator in SPAS is not well defined and is too general to be of practical value. In this study, an artificial neural network model is created to predict the number of SDRs that could be expected by part location using sample data from the SDR database that have been merged with aircraft utilization data. The predictions from the neural network models are then compared with results from multiple regression models. The methodological comparisons suggest that artificial neural networks offer a promising technology in predicting component inspection requirements for aging aircraft.

1. INTRODUCTION

Large scale service systems, such as air and surface transport systems, require well designed maintenance management programs to effectively compete in a global economy. These repairable systems are subject to aging mechanisms, such as wear, fatigue, creep and stress corrosion. Inspection and diagnostic activities are integral components of an effective maintenance strategy in an attempt to ensure system safety, reliability and availability.

Due to the significant growth in the number of aircraft in the U.S., there is an increasing number of structural components for the Federal Aviation Administration (FAA) to monitor. There is a need to develop new techniques for maintaining airworthiness of aging aircraft and for improved methods for accurate prediction of residual life of repaired structures. The use of new prediction methods, such as artificial neural networks, may prove useful for forecasting of removal and inspection dates for aircraft engines, assemblies and components.

The Safety Performance Analysis System (SPAS), currently under development by the FAA, will be an analytical tool designed to support Aviation Safety Inspectors (ASIs) [1, 2] and will contain indicators of safety performance that can signal potential problem areas for inspector consideration [3–5]. It will also enable inspectors to access existing FAA data sources in a timely manner, and will function as a decision support tool to assist inspectors in identifying airlines and/or aircraft that present a greater safety risk and warrant further surveillance.

The Flight Standards Information System (FSIS) is a comprehensive program that contains all Flight Standards automation efforts. SPAS and Flight Standards Automation are components of FSIS. The SPAS Project Management Plan was proposed in March 1991. SPAS is a novel research program for FAA inspection activities, since it will integrate data relating to air operator, air agencies, aircraft types and personnel and shifts away from the current use of decentralized databases.

*This article is based on research performed at Rutgers University. The contents of this paper reflect the view of the authors who are solely responsible for the accuracy of the facts, analyses, conclusions, and recommendations presented herein, and do not necessarily reflect the official view or policy of the Federal Aviation Administration.

The FAA has established a Center for Computational Modeling of Aircraft Structures (CMAS) at Rutgers University. One CMAS research project has focused on analyzing the contribution of the Service Difficulty Reporting (SDR) database to SPAS. The SDR subsystem contains data related to the identification of abnormal, potentially unsafe conditions in aircraft or aircraft components/equipment. The *major objectives* of this research project are:

- To develop meaningful indicators that establish national air operator profiles for comparison purposes.
- To identify national SDR trends and inputs to improve the FAA's surveillance system.
- To provide guidelines for the efficient scheduling of FAA safety inspectors.

A significant effort of SPAS is to develop safety performance indicators that will identify and define critical safety characteristics for airline operators. The 13 performance indicators that are currently defined in SPAS will assist in diagnosing an airline's safety profile compared with others in the same class. The preliminary SDR performance indicator in SPAS is too general to be of practical value. The result of this CMAS research effort is that more refined, specific SDR performance indicators have been generated. The tracking of performance indicators facilitates the identification of unfavorable trends, thus enabling a safety inspector to focus attention on airlines most in need of closer examination. Such heightened tracking enhances efficient scheduling of inspections under budgetary and staffing constraints.

Models to predict the *overall* number of SDRs, and the number of SDRs for cracking and corrosion cases by aircraft type have been developed using both multiple regression analysis and neural networks. The "best" models from these two modeling approaches have been compared and are reported in Luxhoj *et al.* [6]. Neural networks have proven to be a very effective model-free regression methodology to predict the expected number of SDRs. For creating more useful safety performance indicators, this paper attempts to predict the number of SDRs that could be expected by *part location* based on the SDR database. This is the first step to construct an indicator to signal potential problem areas by *component type* for inspector consideration. These alert indicators can be used to define upper and lower control limits and to monitor adverse trends in component performance. Efficient inspection activities will facilitate timely aircraft maintenance and minimize the cost of aircraft unavailability.

While it is true that prediction models for determining aircraft *maintenance* requirements could be based on simply forecasting aggregate failure rates by aircraft type for all planes repaired at the same depot or forecasting failure rates for each plane assigned to a different, regional repair facility, the primary purpose of the CMAS research focuses on the composite *inspection* activities of a regulatory agency.

2. RESEARCH METHODOLOGY

While there exist many prediction methods in the literature, this research focuses on two modeling approaches to develop more refined SDR performance indicators for aircraft component types: multiple regression and neural networks. Multiple regression represents a "classical" approach to multivariate data analysis while the emerging field of neural networks represents a "new" approach to nonlinear data analysis. Multiple regression is a general statistical technique used to analyze the relationship between a single dependent (predicted) variable and several independent (predictor or regressor) variables. Multiple linear regression produces a linear approximation to the data. Variable transformations allow, to some extent, the linear regression methods to handle nonlinear cases as well. However, such transformations may make the interpretation of the results difficult. One could always find a polynomial of higher degree that would give a perfect fit to a specified data set. However, this results in overfitting and an inability of the regression model to generalize. Also, regression models do not learn incrementally, and must be re-estimated periodically.

Neural networks attempt to simulate the functioning of human biological neurons. Neural networks have been particularly useful in pattern recognition problems that involve capturing and learning complex underlying (but consistent) trends in data. Neural networks are highly nonlinear, and in some cases, are capable of producing better approximations than multiple regression which

Table 1. Sample SDR and ARS "merged" data [10]

Aircraft model	SDR date	Part name	Part location	Part condition	Estimated age	Estimated flight hr	Estimated landing
DC9	84-03-22	Skin	E + E compt	Cracked	17.74	32,619.03	53,999.20
DC9	84-03-22	Skin	Aft bag bin	Cracked	17.74	32,619.03	53,999.20
DC9	86-07-07	Skin	Fuselage	Cracked	20.03	36,836.23	60,980.56
DC9	80-06-20	Skin	Galley door	Cracked	13.24	34,396.44	33,888.77
DC9	81-12-01	Skin	FS625	Corroded	14.69	38,160.55	37,597.32
DC9	87-05-11	Skin	RT wheel well	Cracked	20.14	52,299.10	51,527.19
DC9	87-05-11	Skin	STA 580-590	Cracked	20.14	52,299.10	51,527.19

produces a linear approximation [7–9]. However, as noted above, variable transformations do allow, to some extent, the regression methods to handle nonlinearity. Neural network learning supports incremental updating and is easier to embed in an intelligent decision system since batch processing is not required. While neural networks offer an alternative to regression that will learn functional relationships among variables to predict an outcome measure, neural network outcomes lack a simple interpretation of results. For instance, the modeling technique does not provide objective criteria to decide what set of predictors is more important for the prediction. Neural networks may also suffer from overfitting of the data and lack of prediction generality. The limitations of neural networks with respect to outliers, multicollinearity and other problems inherent in real world data have received scant attention.

Knowledge of the expected numbers of SDRs by aircraft component type will have value to Aviation Safety Inspectors (ASIs) when attempting to efficiently schedule field inspection workload requirements. Moreover, the identification of unfavorable inspection trends will enable the FAA to specify that the airlines take preemptive maintenance measures.

2.1. Data description

The CMAS research team was provided with a subset of the SDR database that had been merged with the Aircraft Utilization (ARS) database. This merged database was created by Rice [10] and consisted of 1308 observations for the DC-9 aircraft for the period April 1974 to March 1990. Table 1 displays sample data. Estimated flight hours and estimated landings are derived values based upon the original delivery date of the first operator, the date of the ARS data reference and the SDR date. The equations developed by Rice [10] for these derived values are presented in Fig. 1.

3. NEURAL NETWORK MODELS

Neural networks are computing systems that incorporate a simplified model of the human neuron, organized into networks similar to those found in the human brain [7]. Instead of

$$\begin{aligned} & \cdot \text{AGE} \\ & \cdot \text{ESTFHRS} = (\text{SDRDATE} - \text{SERVICE}) / (\text{ARSDATE} - \text{SERVICE}) * \text{FHSCUM} \\ & \cdot \text{ESTLDGS} = (\text{SDRDATE} - \text{SERVICE}) / (\text{ARSDATE} - \text{SERVICE}) * \text{LDGSCUM} \end{aligned}$$

where

ESTFHRS = Estimated flying hours at SDRDATE

ESTLDGS = Estimated landings at SDRDATE

SDRDATE = Date of SDR (from SDR database)

SERVICE = Original delivery date (first operator, ARS)

ARSDATE = Date of ARS data reference

FHSCUM = Cumulative fuselage flying hours (ARS)

LDGSCUM = Cumulative fuselage landings (ARS)



Fig. 1. Derived predictor variables [10].

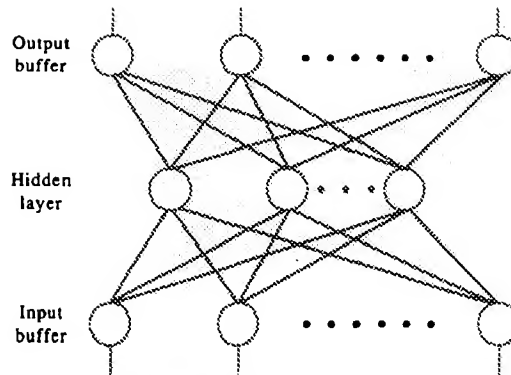


Fig. 2. An example three-layer backpropagation neural network.

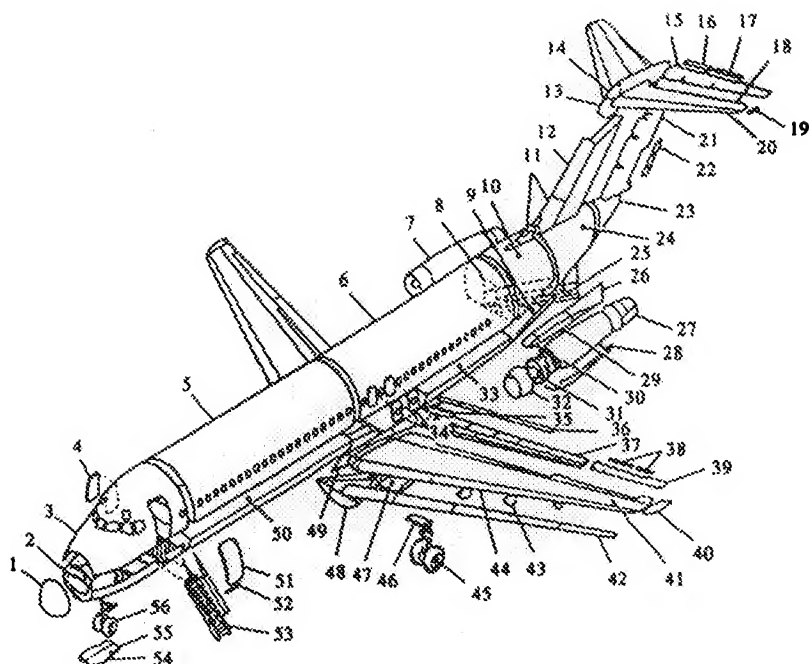
programming the neural network, it is “taught” to give acceptable results. Artificial neural networks are computer simulations of biological neurons. Neural networks can be layered into many levels, with or without hidden layers exhibited between an input and an output layer. Figure 2 displays a network of neurons that are organized into a three-layer hierarchy. The ability of artificial neural networks to capture underlying, complex trends in data has been researched and documented in a significant number of research papers since the “rebirth” of neural networks in 1982 when researchers “rediscovered” their important characteristics [11–15]. The large number of research papers available on these characteristics prohibits their documentation here, but as an indication of their diverse cognitive power, there have been applications of neural networks in varied areas from stock market price prediction and credit rating approval to engineering applications such as pattern/image recognition, digital signal processing and automated vehicle guidance [13].

This research attempts to take advantage of the ability of artificial neural networks to capture and retain complex underlying relationships that exist between an aircraft’s operations data and SDR inspection reporting profiles.

There are six broad categories and approx. 50 different types of neural network architectures in use today [16]. Backpropagation neural networks are the most commonly used neural network architectures. These neural networks are especially good for pattern recognition. Figure 2 shows the basic configuration of the three-layer backpropagation network. To develop a backpropagation model, a training set of data patterns which consist of both inputs and the actual outputs observed must be developed. During training, the neural network processes patterns in a two-step procedure. In the first or forward phase of backpropagation learning, an input pattern is applied to the network, and the resulting activity is allowed to spread through the network to the output layer. The program compares the actual output pattern generated for the given input to the corresponding training set output. This comparison results in an error for each neurode in the output layer. In the second, or backward phase, the error from the output layer is propagated back through the network to adjust the interconnection weights between layers. This learning process is repeated until the error between the actual and desired output converges to a predefined threshold [17]. A trained neural network is expected to predict the output when a new input pattern is provided to it.

3.1. SDR part location neural networks

A structural schematic of the DC-9 aircraft is presented in Fig. 3. For the 1308 sample data observations from the period 1974–90, there are only 569 data observations for cracking cases for the DC-9, and only 390 observations identify the part location. There is insufficient and incomplete input data for each part location, so the part locations were categorized into 11 larger “groupings” as presented in Table 2. The corresponding sample sizes for each major part grouping is superscripted in parentheses. Note that the part location numbers in Table 2 do not correspond to the part location numbers in Fig. 3 due to the “grouping” strategy. The frequency of reporting by part location is graphically portrayed in the frequency histogram of Fig. 4. For the given data, approx. 70% of cracking cases occurred in the aircraft main fuselage areas and the “Fuselage STA 588 to 996 (recoded as “Part 3”)” includes 22.2% of cracking cases.



NO.	Description	NO.	Description	NO.	Description
1.	Radome	20.	Horizontal stabilizer leading edge	39.	Aileron
2.	Fuselage nose lower structure	21.	Rudder	40.	Wing tip
3.	Fuselage nose upper structure	22.	Rudder tab	41.	Wing main structure
4.	Forward service door	23.	Tail cone	42.	Wing slat
5.	Fuselage STA 229 to 588 upper structure	24.	Fuselage tail structure	43.	Flap hinge fairing
6.	Fuselage STA 588 to 996 upper structure	25.	Passenger AFT entrance door stairway	44.	Wing leading edge
7.	Upper cowl door	26.	Pylon AFT panel	45.	Main gear
8.	Passenger AFT entrance stairwell door	27.	Thrust reverser cowl	46.	Main gear outboard door
9.	Fuselage STA 996 to 1087 lower structure	28.	Lower cowl door	47.	Main gear inboard door
10.	Fuselage STA 996 to 1087 upper structure	29.	Pylon center panel	48.	Keel
11.	Dorsal fin	30.	Pylon leading edge	49.	Wing-to-fuselage fillet
12.	Vertical stabilizer	31.	Engine	50.	Fuselage STA 229 to 588 lower structure
13.	Vertical stabilizer tip	32.	Nose cowl	51.	Passenger forward entrance door
14.	Removable tip fairing	33.	Fuselage STA 756 to 996 lower structure	52.	Forward stairwell door
15.	Elevator	34.	Overwing emergency exits	53.	Passenger forward entrance stairwar
16.	Elevator control tab	35.	Flap vane	54.	Forward nose gear doors
17.	Elevator geared tab	36.	Spoiler	55.	AFT nose gear doors
18.	Horizontal stabilizer AFT section	37.	Wing flap	56.	Nose gear
19.	Horizontal stabilizer tip assembly	38.	Aileron tabs		

Fig. 3. Structural schematic of the DC-9 aircraft (Douglas Aircraft Co., Inc, *DC-9 Structure Repair Manual*).

Table 2. Backpropagation neural networks for DC-9 part locations (cracking cases)

Initial parameters		
Learning rate = 0.01	Input layers = 3 (Avg-age, Avg-flight hours, Avg-landings)	
Momentum = 0.05	Hidden layers = 21	
Initial weight = 0.3	Output layer = 11 (No. of SDR for each part location)	
Patterns = 20		
Part No.	Part description (-):No. of observations	R^2 value
1	Fuselage nose structure ⁽³¹⁾	0.8563
2	Fuselage station 229 to 588 ⁽³⁷⁾	0.8329
3	Fuselage station 588 to 996 ⁽⁸¹⁾	0.8504
4	Fuselage station 996 to 1087 ⁽⁶⁸⁾	0.7382
5	Fuselage tail structure ⁽⁹⁹⁾	0.6837
6	Rudder ⁽¹³⁾	0.7832
7	Pylon aft panel ⁽⁷⁾	0.4926
8	Wing ⁽¹⁵⁾	0.5773
9	Passenger fwd entrance door ⁽²⁷⁾	0.7948
10	Cargo door ⁽⁷⁾	0.8373
11	Aft press blkhd ⁽²⁰⁾	0.8744

Based on the current SDR data base which presents one SDR for one aircraft record, a prediction model is created that can be used to signal potential problem areas by homogeneous aircraft type. The expected number of SDRs in a certain part location is used as an index that indicates the possibility of failure in the area. A higher expected number of SDRs suggests a greater possibility that a maintenance problem exists.

To generate the model, current data have been grouped by aircraft age or flight hours to calculate the average number of SDRs in each part location. For example, in the age "cohort" or grouping of $10 \text{ yr} \leq \text{aircraft age} \leq 10.5 \text{ yr}$, if it is observed that there are two aircraft with three part No. 2 failures and three aircraft with six part No. 3 failures, then we can argue that one aircraft in that age range has 1.5 SDRs (3 SDRs/2 aircraft) for part No. 2 or 2 SDRs (i.e. 6 SDRs/3 aircraft) for part No. 3. Moreover, the average age, flight hours and number of landings in this age "cohort" is also calculated to create a complete training data record.

In an attempt to create "robust" SDR prediction models, different data "grouping" strategies were surveyed. Currently, the data with aircraft age less than 16 yr are grouped by age in increments of 0.5 yr and the remaining data are grouped by flight hours in increments of 4000 hr. This grouping strategy is suggested by a multiple regression approach as reported by Luxhoj *et al.* [6]. The SAS regression procedure "STEPWISE" with significance level 0.05 is used in Ref. 6 to find explanatory variables (such as age, flight hours and number of landings) for an *overall* SDR prediction model that included both cracking and corrosion cases. This overall model did not identify part locations. If the observed data with aircraft age less than 16 yr are grouped by flight hours, then no independent variables are selected for a regression model using the backwards stepwise procedure.

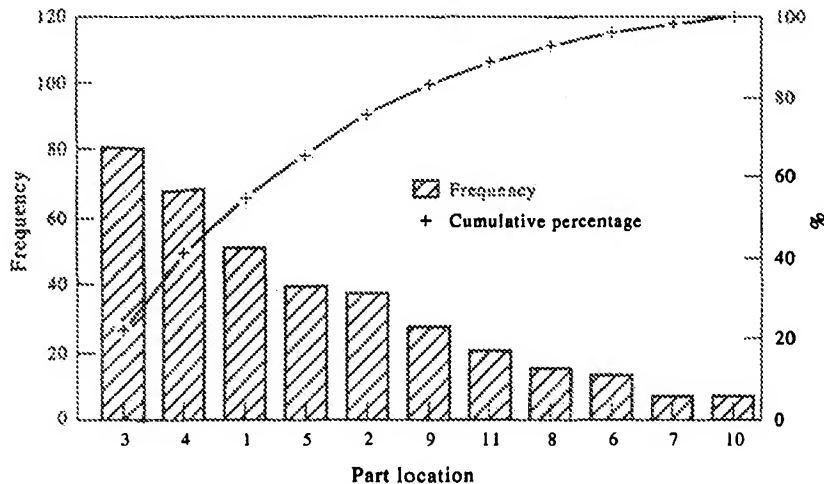


Fig. 4. Frequency histogram of part locations.

Table 3. Sample training patterns for neural network models

Age (input)	Flight hours (input)	Landings (input)	Part-1 (output)	Part-2 (output)	Part-3 (output)	...	Part-11 (output)
7.85	18,690.47	20,802.41	0	0	0		0
9.89	23,196.85	22,131.14	0	0	1		0
10.22	26,628.15	29,868.82	0	0	1		0
14.54	38,342.68	39,529.86	0	0	2		0
15.48	20,389.20	21,082.51	0	1	0		0
16.10	7648.51	8747.93	0	0	0		0
16.59	9847.38	11,650.02	0	0	0		0
19.71	14,890.32	17,608.92	1	1	1		0
20.49	18,417.62	22,897.46	0	1	1	...	1
21.27	21,193.82	28,295.16	0	0	1		0
21.22	25,934.51	30,647.01	0	1	1		1
21.18	30,354.34	33,997.60	1	0	1		1
20.93	34,201.58	41,745.07	1	1	1		1
20.47	37,618.85	41,610.96	1	1	1		1
19.95	41,831.14	46,925.22	1.333	1	1		1
20.85	46,138.41	50,187.29	1	1.333	1.083		1
21.28	49,973.60	56,181.93	1.25	1.5	1		1
21.41	53,329.71	60,088.01	1	1	1.583		1
21.84	57,753.52	65,016.48	1.222	1	1.273		0
21.87	61,351.04	56,383.35	1	1	1		0

However, if the data are grouped by age, then it appears that age is a significant explanatory variable for this model. Furthermore, we can also identify that data with aircraft age greater than 16 yr should be grouped by flight hours as this can be a significant explanatory variable in the prediction model. When using the data grouping strategy of flight hours in the SDR data base, the suggested interval grouping size is 4000 flight hours [6].

A three-layer backpropagation architecture is used to classify SDR cracking cases for part location data grouped by the above data partitioning strategy. Previous research by Luxhoj *et al.* [6] on the sensitivity of using different neural network architectures for the SDR problem domain suggests that the three-layer backpropagation architecture yields the best results for the given SDR data. This observation is consistent with Maren *et al.* [13] who report on successful applications of three-layer backpropagation architectures for fault diagnosis. For the component data, the number of SDRs for one aircraft in a certain age group is calculated. As Luxhoj *et al.* [6] demonstrate, the use of “ungrouped” data results in poor prediction models for both the multiple regression and neural network techniques. However, due to the age “grouping” strategy, only 18 input patterns can be used to train the neural network model. The model includes three input neurons (i.e. operations data, such as aircraft age, flight hours and number of landings) and 11 output neurons that identify the number of SDRs in 11 different part locations. These patterns are created in an attempt to capture underlying relationships between aircraft operations data and the “mix” of expected number of SDRs by component type. The sample training patterns are presented in Table 3, and the designed backpropagation neural network model is shown in Fig. 5. The numbers in the 11 “output” columns represent the “average” number of SDRs per airplane for

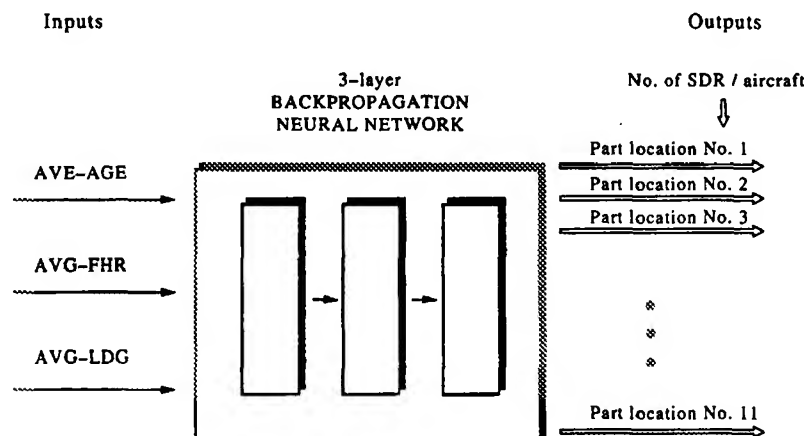


Fig. 5. Backpropagation neural network model for SDR part locations.

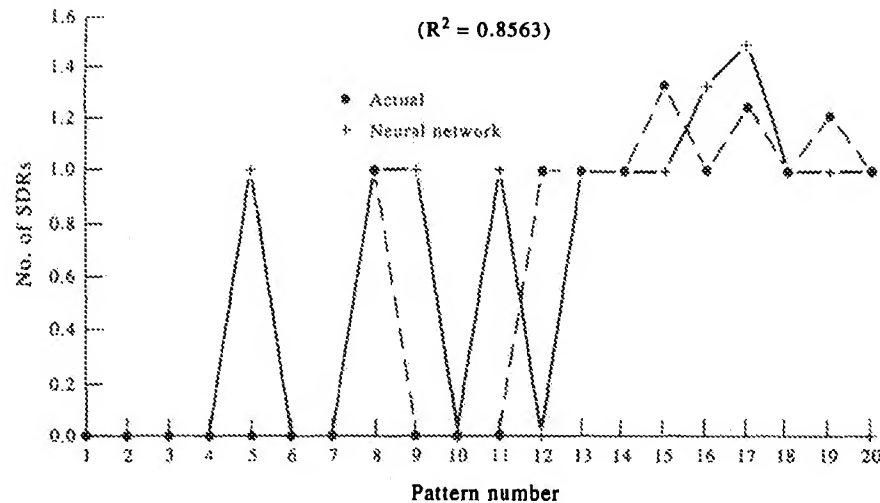


Fig. 6. Model performance of the fuselage nose structure (part location No. 1).

that part location and were obtained using the “cohort” data grouping strategy as previously discussed.

The prediction model is trained using the *NeuroShell 2* [18] computer program, which requires Microsoft Windows, a minimum of 4 MB of RAM, and at least a 386SX microprocessor. In addition, this commercial software program implements several different types of neural network architectures, and supports easy import/export of files, model building and testing, and the creation of run-time versions of trained networks all via a friendly graphical user interface. Backpropagation neural network “learning” parameters include the “learning rate” which is used to specify the magnitude of the weight changes, the “momentum” factor which specifies the proportion of the last weight change that is added to the new weight change, and an “initial weight” that is used to initialize the weights between the network’s connections prior to “training”.

In neural network modeling, the R^2 value compares the accuracy of the model to the accuracy of a trivial benchmark model where the prediction is simply the mean of all the sample patterns. A perfect fit would result in an R^2 value of 1, a very good fit near 1, and a poor fit near 0. If the neural network model predictions are worse than one could predict by just using the mean of the sample case outputs, the R^2 will be 0. Although not precisely interpreted in the same manner as the R^2 value or coefficient of multiple determination in regression modeling, nevertheless, the R^2 value from a neural network model may be used as an approximation when evaluating model adequacy.

Plots of the actual value vs the predicted value from the network for two of the part locations are exhibited in Figs 6 and 7. These parts are the Fuselage Nose Structure (Part No. 1) and the Fuselage Station 588–996 (Part No. 3). Corresponding R^2 values for each of the 11 part location models are provided in Table 2. Eight of the 11 models have R^2 values about 0.7 which suggests that a backpropagation neural network is very effective in predicting the number of SDRs for major structural groupings of part locations. Five of the 11 models have R^2 values of 0.8 or higher. The “best” part location backpropagation models in this study are for the AFT Press BULKHEAD ($R^2 = 0.8744$), fuselage nose structure ($R^2 = 0.8563$), fuselage stations 588 to 996 ($R^2 = 0.8504$), cargo door ($R^2 = 0.8371$) and fuselage stations 229 to 588 ($R^2 = 0.8329$).

The accuracy of neural network models will be affected by the input training patterns. The number of the observations for each of the 11 part locations is one major factor that has influence on the accuracy and efficiency of the model. For a small number of observations, the neural network model cannot provide an effective prediction for some part locations. For example, the Pylon AFT panel model ($R^2 = 0.4926$) is based on only seven observations. Even for some cases that have a relatively high R^2 value but with only few observations, there is still insufficient evidence to conclude that the model provides a reasonable prediction in this part location. The cargo door neural network model is one of these cases.

3.2. Comparison with multiple regression models

An alternative approach to estimate the number of SDRs by part location is the use of multiple regression. However, one multiple regression model can only predict one dependent variable. To predict the number of SDRs for 11 different part locations, 11 different multiple regression models should be created. The following list of possible explanatory variables was used in creating the multiple regression models: age, flight hours, number of landings, age², flight hours², number of landings², age \times flight hours, age \times number of landings, flight hours \times number of landings, flight hours/age, and number of landings/age. Quadratic terms were considered in an inherently linear model to evaluate any nonlinear relationships. The regression models were examined for multicollinearity, since a high degree of multicollinearity makes the results not generalizable as the parameter estimates in the model may not be stable due to the high variance of the estimated coefficients. Since flight hours, number of landings and age of an aircraft are interrelated, multicollinearity is inherent in the independent variables.

Two statistical measures of multicollinearity are the tolerance (TOL) value and the variance inflation factor (VIF) (Hair *et al.* [19]). The tolerance value is equal to one minus the proportion of a variable's variance that is explained by the other predictors. A low tolerance value indicates a high degree of collinearity. The variance inflation factor is the reciprocal of the tolerance value, so a high variance inflation factor suggests a high degree of collinearity present in the model. The VIF and TOL measures assume normality and are typically relative measures. A high tolerance value (above 0.10) and a low VIF value (below 10) usually suggest a relatively small degree of multicollinearity (Hair *et al.* [19]).

Due to the lack of observed data in two cases (i.e. sample sizes of seven), only nine multiple regression models are created to estimate the number of SDRs for major structural groupings of part locations. The VIF and TOL values were examined for each model to reduce the multicollinearity. A sample model to predict the expected number of SDRs for the major structural grouping of "Fuselage Station 588–996 (Part No. 3)" is provided below:

$$\text{No. of SDRs (Part No. 3)} = -6.192868 + (0.341556 \times \text{age}) - (0.000004097 \times \text{age} \times \text{flight hours}) + (0.001897 \times \text{age}/\text{flight hours}).$$

This model has an R^2 value of 0.7844 and the relative measures of multicollinearity are reported as:

Independent variable	TOL	VIF
age	0.05040	19.839
age \times flight hours	0.03395	29.455
age/flight hours	0.06052	16.522

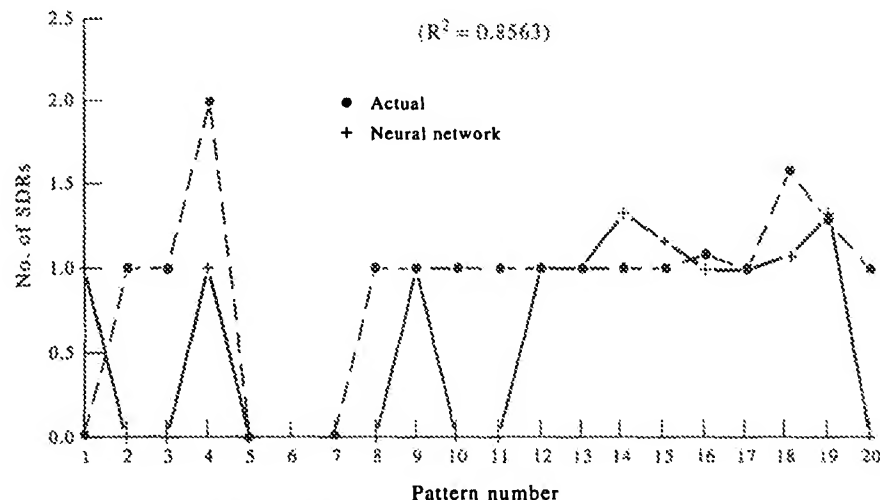


Fig. 7. Model performance of the fuselage stations 588–996 (part location No. 3).

Table 4. Comparison of neural network and multiple regression models

Part No.	Part description (-):No. of observations	NN		MR	
		R^2	MSE	R^2	MSE
1	Fuselage nose structure ⁽⁵¹⁾	0.8383	0.043	0.6723	0.123
2	Fuselage station 229 to 588 ⁽³⁷⁾	0.8329	0.048	0.5314	0.170
3	Fuselage station 588 to 996 ⁽⁴¹⁾	0.8304	0.039	0.7844	0.070
4	Fuselage station 996 to 1087 ⁽⁴⁴⁾	0.7382	0.078	0.5435	0.171
5	Fuselage tail structure ⁽³⁹⁾	0.6837	0.099	0.6303	0.145
6	Rudder ⁽¹³⁾	0.7832	0.054	0.4699	0.164
7	Pylon aft panel ⁽⁷⁾	0.4926	0.107	---	---
8	Wing ⁽¹⁵⁾	0.5771	0.101	0.4453	0.166
9	Passenger fwd entrance door ⁽²⁷⁾	0.7948	0.051	0.6801	0.099
10	Cargo door ⁽⁷⁾	0.8371	0.034	---	---
11	Aft press blkhd ⁽²⁰⁾	0.8744	0.047	0.6593	0.158

The multicollinearity measures suggest that some degree of multicollinearity is present in this model, but these values are close to the generally recommended threshold values of $VIF \leq 10$ and $TOL \geq 0.10$.

Table 4 presents the R^2 values for the nine regression models as compared with the R^2 values for the corresponding neural network models. Although not interpreted precisely in the same manner, nevertheless, analyzing the R^2 values from neural network and multiple regression facilitates approximate comparisons. Only one multiple regression model has an R^2 value above 0.7.

Since the goal is to maximize the precision of the SDR predictions, the mean square error (MSE) is also used for comparative purposes. The MSE is defined as:

$$MSE(\beta) = E(\hat{\beta} - \beta)^2,$$

where β is some arbitrary parameter. The above expression is equivalent to:

$$MSE = [\text{bias}(\hat{\beta})]^2 + \text{var}(\hat{\beta}).$$

The criterion of minimizing the MSE thus considers the variance and the square of the bias of the estimator. Comparing the results of the two approaches reveals that neural network modeling provides better fits to the SDR part location data in all cases than does regression modeling. Also, it appears that neural networks may be more useful for predictive purposes, in some cases, when there are sparse data sets, an observation that has been reported in Luxhoj and Shyur [20] in their analysis of helicopter part reliability data. However, the general predictive capability and statistical confidence of neural networks given small sample sizes still requires investigation across varied characterizations of data sets.

4. CONCLUSIONS AND RECOMMENDATIONS

In this study, promising results are achieved when using three-layer backpropagation neural networks to predict SDR reporting profiles by part location for major structural components for the DC-9 aircraft. Prediction of the number of SDRs for each part location is helpful to Aviation Safety Inspectors (ASIs) and may be used to signal potential problem areas based upon aircraft operating conditions and age. Using neural networks, one can obtain the expected number of SDRs for a major structural grouping of components whenever the operating conditions are known. These current results are encouraging, but additional data are required to validate the generality of the modeling approach.

The part location data "grouping" strategy is useful to provide efficient input patterns to create a reasonable neural network model. However, some information hidden in the data set is lost in the process of "grouping". Due to this strategy, the difficulty to maintain the current neural network will also increase. A new approach to replace the current "grouping" strategy should be developed.

Another recommendation is to develop the entire probability mass function from the neural network for major part locations. This would then provide aircraft safety inspectors with the most likely category of failure, the second most likely etc. based upon the operating conditions and age of the aircraft. Attempts to refine the management reporting from the neural network models are underway.

Neural network modeling, a model-free regression technique, is easy to develop, maintain and use. However, it should possess one set of reasonable and useful input buffers. In the SDR reporting profiles, only three different input buffers (age, flight hours and number of landings) can be used in this model. Other factors that affect the components, such as engine hours and flight cycles, are still not exhibited in the SDR reporting profiles. If these data can be collected and merged to the current data base, then more promising and meaningful models can be created.

Acknowledgements—The authors of this report would like to acknowledge the support of the SPAS program and Mr John Lapointe and Mr Michael Var.

REFERENCES

1. *Safety Performance Analysis Subsystem*. Functional description document. U.S. Department of Transportation, Volpe National Transportation Systems Center, Cambridge, MA, March (1992).
2. *Safety Performance Analysis Subsystem*. Prototype concept document. U.S. Department of Transportation, Volpe National Transportation Systems Center, Cambridge, MA, April (1992).
3. *Safety Performance Analysis Subsystem*. Indicators suggested for SPAS prototype (DRAFT). U.S. Department of Transportation, Volpe National Transportation Systems Center, Cambridge, MA, August (1992).
4. *Safety Performance Analysis Subsystem*. Continuing analysis: indicator graphs and tables. U.S. Department of Transportation, Volpe National Transportation Systems Center, Cambridge, MA, October (1992).
5. *Safety Performance Analysis Subsystem*. Continuing analysis: additional indicator definitions (DRAFT). U.S. Department of Transportation, Volpe National Transportation Systems Center, Cambridge, MA, October (1992).
6. T. Luxhoj, T. P. Williams and H.-J. Shyur. Prediction of inspection profiles for aging aircraft. Rutgers University, Center for Computational Modeling of Aircraft Structures, Technical Report (1994).
7. P. Simpson. *Artificial Neural Systems*. Pergamon Press, New York (1990).
8. P. D. Wasserman and T. Schwartz. Neural network, part 1: what are they and why is everybody so interested in them now? *IEEE Expert* 2, 10–13 (1987).
9. A. Weigend, B. A. Huberman and D. E. Rumelhart. Predicting the future: a connectionist approach. *Int. J. Neural Syst.* 1, 193–210 (1990).
10. R. C. Rice. Repair Database Assessment. Battelle Summary Report, Contract No. DTRS-57-89-C-00006, March (1991).
11. J. J. Hopfield. Neural networks and physical systems with emergent collective abilities. *Proc. Natl Acad. Sci.* 79, 2554–2558 (1982).
12. J. J. Hopfield. Neurons with graded response have collective computational properties like those of two-state neurons. *Proc. Natl Acad. Sci.* 81, 3088–3092 (1984).
13. A. J. Maren, C. T. Harston and R. M. Pap. *Handbook of Neural Computing Applications*. Academic Press, New York (1990).
14. W. S. McCulloch and W. Pitts. A logical calculus of ideas immanent in nervous activity. *Bull. Mathl Biophys.* 5, 115–133 (1943).
15. D. L. Reilly, L. N. Cooper and C. Elbaum. A neural model for category learning. *Biol. Cybernet.* 45, 35–41 (1982).
16. R. Hecht-Nielsen. Neurocomputing: picking the human brain. *IEEE Spectrum* 25, 36–41 (1988).
17. M. Caudil. Neural network training tips and techniques. *AI Expert* 6, 56–61 (1991).
18. *NeuroShell 2*. Ward Systems Group, Inc., Frederick, MD (1993).
19. J. F. Hair, R. E. Anderson, R. L. Tatham and W. C. Black. *Multivariate Data Analysis*, 3rd edn. Macmillan, New York (1992).
20. J. T. Luxhoj and H.-J. Shyur. Reliability curve fitting for aging helicopter components. *Reliab. Eng. Syst. Safety* 48, 229–234 (1995).

Active Control of Wind-Tunnel Model Aeroelastic Response Using Neural Networks

Robert C. Scott*

NASA Langley Research Center, Hampton, VA 23681

Under a joint research and development effort conducted by the National Aeronautics and Space Administration and The Boeing Company (formerly McDonnell Douglas) three neural-network based control systems were developed and tested. The control systems were experimentally evaluated using a transonic wind-tunnel model in the Langley Transonic Dynamics Tunnel. One system used a neural network to schedule flutter suppression control laws, another employed a neural network in a predictive control scheme, and the third employed a neural network in an inverse model control scheme. All three of these control schemes successfully suppressed flutter to or near the limits of the testing apparatus, and represent the first experimental applications of neural networks to flutter suppression. This paper will summarize the findings of this project.

Keywords: neural network, adaptive control, aeroelasticity, flutter suppression

Introduction

ACTIVE control of aeroelastic phenomena will become more prevalent on future flight vehicles. One of the key issues in gaining acceptance of such systems is reliability. Systems that can reliably adapt to sensor and actuator failures or plant changes will improve system reliability. Since neural networks can be trained to model dynamic systems, their use has been suggested for adaptive control and many studies proposing a variety of control system architectures have been studied. Some common types of algorithms include model reference control where the neural network is used to model the plant and inverse control where the neural network is used to model the inverse of the plant. Studies to investigate the aeronautical applications of neural networks have been much more limited. References 1, 2, and 3 describe analytical studies where neural networks were applied to flight controls in either fixed wing or rotorcraft applications. These studies have focused on utilizing neural networks to achieve improvements in trajectory tracking. Studies to investigate the application of neural networks to controlling aeroelastic response (flutter and gust load alleviation, for example) have, however, been even more limited. The purpose of the present research is to investigate the use of neural networks for controlling aeroelastic response.

The work described in this paper is part of the Adaptive Neural Control of Aeroelastic Response (ANCAR) project. ANCAR was a joint research and development

effort conducted by the National Aeronautics and Space Administration, Langley Research Center and The Boeing Company (formerly McDonnell Douglas) under a Memorandum of Agreement. The goal of the program was to develop and demonstrate neural-network based adaptive control systems using the Benchmark Active Controls Technology (BACT) wind-tunnel model. The ANCAR program consisted of two phases. Phase I was the development and demonstration of a neural network gain scheduled flutter suppression system. Under Phase II, two adaptive neural-network based control systems were to be developed and demonstrated. These systems used predictive control and inverse model control methodologies. This paper will summarize all the accomplishments of the ANCAR project; however, the majority of the paper will focus on the neural-network based inverse model system which has not previously been reported.

The work presented in this paper was an exploratory study. Additional research is required to determine the merits of using neural networks for aeroelastic control. In addition to the neural-network based control systems, there were several other control systems tested using the BACT wind-tunnel model. These control systems include those described in references 4 and 5. The control systems described in these papers were designed using classical or modern methods. While the performance of these control systems was not directly compared with the neural-network based control systems, it was apparent that they were significantly more robust than either the neural predictive or inverse model control systems. The neural gain scheduled system is based on classical

*Research Engineer, Aeroelasticity Branch, Structures and Materials Competency.

control law design and its performance was qualitatively similar to the systems in references 4 and 5.

Apparatus

Transonic Dynamics Tunnel

Wind-tunnel testing was conducted in the NASA Langley Transonic Dynamics Tunnel (TDT).⁶ The TDT is a single-return variable-density transonic wind tunnel. The slotted test section is 16 ft by 16 ft square with cropped corners. The speed and pressure are independently controllable over a range of Mach number from 0.0 to 1.2 (unblocked), and a range of stagnation pressures from near zero to one atmosphere. Either air or a heavy gas can be used as the test medium. The heavy gas used in these wind-tunnel tests was R-12, but the TDT has since been modified to use R134a as the heavy gas. The TDT is also equipped with quick-opening bypass valves which can be activated to rapidly reduce test-section dynamic pressure and Mach number when flutter occurs. The combinations of large scale, high speed, high density, variable pressure, and the bypass-valve system make the TDT ideally suited for aeroelastic testing.

Wind-Tunnel Model

The BACT wind-tunnel model is a rigid, rectangular wing with an NACA 0012 airfoil section. It is equipped with a trailing-edge (TE) control surface and upper- and lower-surface spoilers, all independently controllable. The model is attached to a flexible mount system, the Pitch And Plunge Apparatus (PAPA), that allows both pitch and plunge degrees-of-freedom. An image of the model mounted in the TDT and a separate image showing only the model and mount system are shown in figure 1. The model is extensively instrumented with pressure transducers and accelerometers to measure surface pressures and model dynamic response, and the mount system is instrumented with strain gauges to measure normal force and pitching moment. Parameters which could be varied during the test include Mach number, dynamic pressure, model angle-of-attack, and control surface deflection. Reference 7 contains a more detailed description of this wind-tunnel model.

Neural Networks

Neural networks have been studied for many years in a variety of fields. These fields include speech and image recognition, credit and insurance policy evaluation, and trajectory control to name a few. They have also been studied extensively for use in controlling dynamic systems. The MATLAB Neural Network Toolbox Manual⁸ provides an excellent overview of neural network applications with many references. While numerous control system architectures and network types have been investigated, this section of the paper will provide a brief

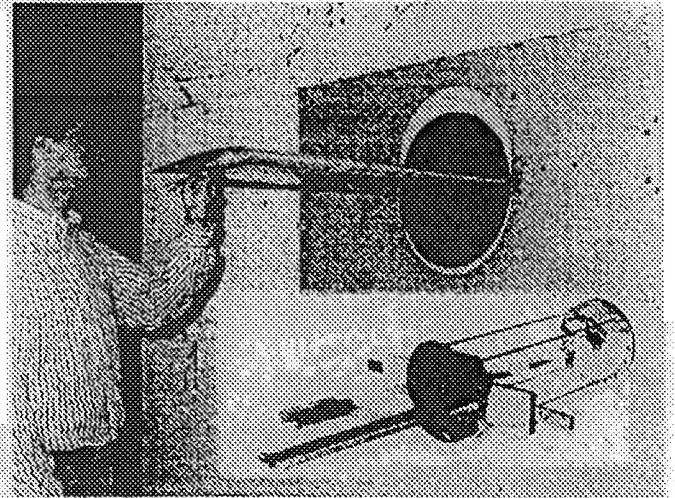


Fig. 1 BACT wind-tunnel model.

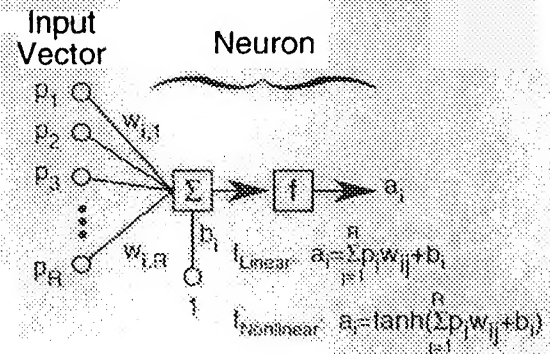


Fig. 2 Neural network computational element or neuron.

summary of only the neural networks applied in this paper.

The name neural network comes from the fact that the networks emulate the structure of the brain. In biological nervous systems, the output of one neuron is connected to many other neurons. It is these connections that determine the function of the network. In practice, neural networks are composed of many computational elements or neurons operating in parallel. The general structure of an individual neuron is shown in figure 2. The function of each neuron is to sum the weighted inputs (w_{ij}) and the bias (b_j) and process this sum through a transfer function (f). The transfer functions considered in this study will be limited to the two shown in figure 2: a linear transfer function or a sigmoid transfer function (\tanh). The use of a \tanh or tan-sigmoid transfer function allows the modeling of nonlinear effects.

Two or more neurons can be used to form a layer and one or more layers forms a neural network. An example of the network structure used in this paper is shown in figure 3. This network consists of an input vector and two layers of neurons, a hidden layer and an output layer.

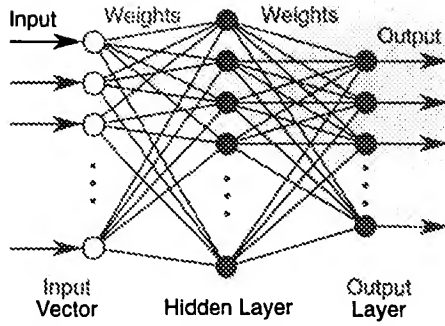


Fig. 3 Neural network with one hidden layer.

Typically the output layer uses linear transfer functions and the hidden layer uses linear or tan-sigmoid transfer functions. This network structure is the simplest form of multilayer feedforward network. More hidden layers can be used, but no more than one hidden layer was used in this paper. Given sufficient neurons on the hidden layer, this type of network can approximate most functions arbitrarily well.

Neural networks must be trained prior to use as predictive models. Training is a common term in the field of neural networks and simply refers to the process by which the network weights and biases are selected. The training process begins by selecting or acquiring training data, a set of input and output data for the plant or function to be approximated with the network. During the training process the weights and biases are adjusted until the error between the training data output and the network output is minimized. There are several methods or algorithms for adjusting the network weights and biases. A common training method, and the one used in this paper, is backpropagation. Backpropagation is a gradient descent optimization algorithm that can be used on multilayer networks as long as the neurons have differentiable transfer functions.

Gain Scheduler

This section of the paper will summarize the implementation and findings of the neural network gain scheduled flutter suppression system described in reference 9. The objective of this system was to use a neural network to schedule flutter suppression control laws. The approach taken in this study was to use a series of state-space models of the BACT wind-tunnel model to design classical single input single output (SISO) flutter suppression control laws. The state-space models were generated using the Integrated Structures, Aerodynamics, and Controls (ISAC) code.¹⁰ The state-space models all used the same structural and aerodynamic models with Mach number (M) and dynamic pressure (q) being varied. In all, fifty six state-space models were used where Mach number varied from 0.3 to 0.9 and dynamic pres-

sure varied from 75 to 250 psf. These models were used to design a fixed-gain control law and to design a series of control laws optimized to minimize accelerometer output for each combination of M and q. A neural network was used to schedule the series of 56 optimized control laws.

Fixed-Gain Control Law

The fixed-gain feedback control law was designed to stabilize and minimize the wing response over the entire range of the state-space models. A washout filter was included in the compensation to eliminate any drift due to bias errors in the accelerometers. Root-locus pole and zero placement methods were used to design the fixed-gain robust feedback control law given below.

$$\frac{s(s^2 + 12s + 520)}{s^4 + 27s^3 + 491s^2 + 4515s + 13050}$$

Neural-Network Scheduled Control Laws

For the neural-network scheduled control laws, the control law described above was tailored for the pole-zero dynamics of each state-space model. Fifty-six custom designs were generated for the various M and q condition state-space models. All of the resulting control laws had the same order numerator (3 zeros) and denominator (4 poles) as the robust fixed-gain control law. The general form of these control laws is given below:

$$k \frac{s^3 + a_2 s^2 + a_1 s}{s^4 + b_3 s^3 + b_2 s^2 + b_1 s + b_0}$$

The neural network, shown in the lower portion of figure 4, was trained using backpropagation to output the two numerator coefficients, the four denominator coefficients, and the overall gain as functions of M and q. The control law parameters used to train the neural network were in the continuous domain, rather than the discrete domain. This was required because continuous-domain coefficients vary smoothly as a function of M and q and do not require the high numerical precision of discrete-domain control law coefficients. The neural network outputs were transformed into the discrete domain before being transferred to the digital controller.

Experimental Results

The control system architecture that was implemented in the 1995 BACT wind-tunnel test is shown in figure 4. The trained neural network and Tustin (continuous-to-discrete) transformation was implemented on a Macintosh computer. As M and q were varied, the Macintosh computer transferred control laws to the real time system. The Active Digital Controller (ADC)¹¹ was used as the real-time digital control system operating at a rate of 200 Hz. The fixed-gain control law was also implemented on the ADC.

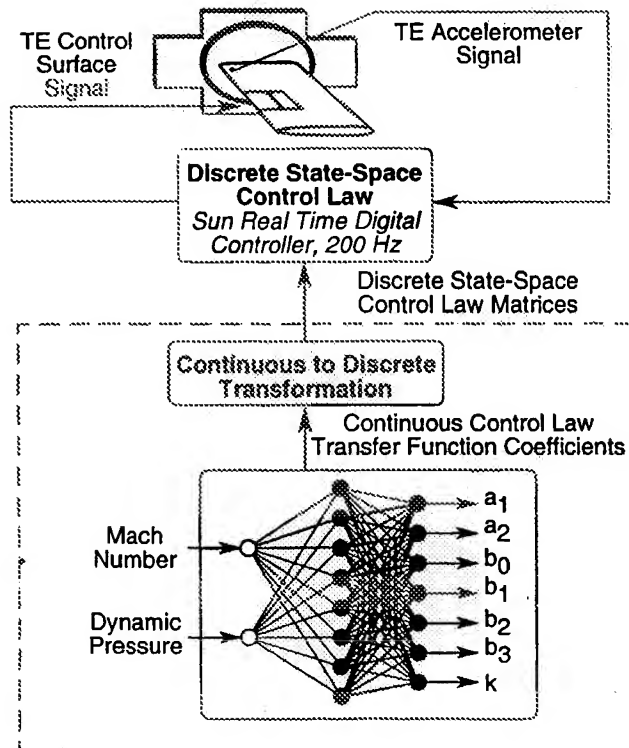


Fig. 4 Neural network gain scheduling system architecture.

The control systems were tested along four constant total-pressure lines which define test paths within the TDT. These H-lines and the BACT model open-loop flutter boundary are shown in figure 5. Each H-line is determined by the total pressure of the gas in the tunnel, and conditions are varied along each H-line by varying the motor RPM. For three of the four H-lines, open-loop unstable conditions were encountered and the control laws successfully suppressed flutter. For each H-line, data was collected for open-loop, fixed-gain closed-loop, and neural-network gain-scheduled closed-loop configurations. The open-loop tests were terminated as soon as classical flutter was encountered.

While both the fixed-gain and neural-network gain scheduled controllers provided effective flutter stabilization, the neural network system was able to achieve lower Root Mean Square (RMS) wing acceleration across the range of M and q conditions. The relative performance improvement is illustrated in figure 6 which plots the RMS wing acceleration versus dynamic pressure for the third H-line. The open-loop flutter boundary is indicated here by the sharp increase in open-loop response around $q=160$ psf.

Predictive Control

The neural predictive control system described in reference 12 will be summarized in this section. The goal

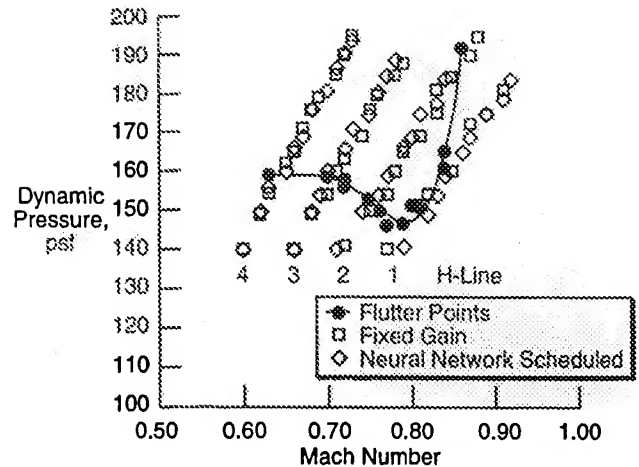


Fig. 5 Data acquired for fixed and gain scheduled systems.

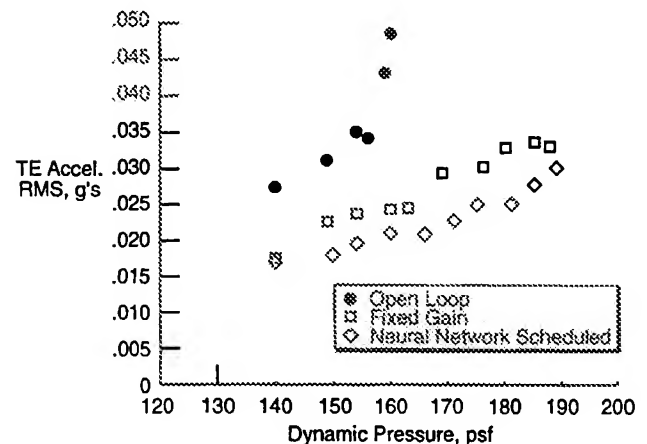


Fig. 6 Fixed and gain scheduled system response.

of this control system was to demonstrate the use of a neural network in a Model-Based Predictive Control (MBPC) system. MBPC utilizes a model of the plant to predict future physical model responses to future control inputs. A search algorithm is typically used to select the best control input. In this application, the objective of the search algorithm was to minimize model response. The plant model can be a linear or a nonlinear network, and the control system can include the ability to update the plant model. The system implemented in this study used a linear plant model. The control system trains the plant model using experimental data and the plant model can be retrained to adapt to changes in the physical plant. This algorithm is called Neural Predictive Control (NPC).

NPC Algorithm Description

A simplified block diagram of the NPC architecture is shown in figure 7. The NPC system can use either

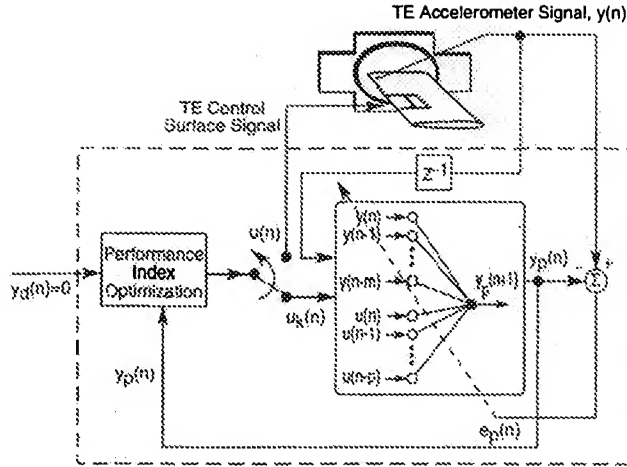


Fig. 7 Neural predictive control system architecture

a linear single layer network or neural-network plant model. As depicted in this figure, the NPC system implemented in this study used a linear plant model to capture the input/output dynamics of the BACT model. This predictive plant model is then utilized in an on-line optimization scheme to select the optimal control values for each control cycle. This system used a sample rate of 100 Hz, and each cycle had a duration of 0.01 seconds. The plant model can initially be trained by exciting the actuators, measuring the sensor response, and training the plant model. This model can then be updated on-line to handle with changing conditions and time-varying plant dynamics. The plant model training portion of this system is performed in parallel with the closed-loop portion and is depicted by the error feedback to the plant model in figure 7.

The method implemented for flutter suppression involves minimizing a cost function. The cost function, or performance index, is typically a quadratic function of the regulation/tracking error and required control input power. Consequently, NPC is an optimal controller in the same sense that the Linear Quadratic Regulator (LQR) is optimal. The advantage of NPC over LQR lies in its capability to be easily extended to nonlinear systems and to explicitly account for plant constraints in real time.

A step-by-step description of the NPC algorithm is given below:

1. Generate a reference trajectory, $y_d(n)$, which represents the desired value of the future plant output ($y_d(n) = 0$ for flutter suppression).
2. Predict the future plant output, $y_p(n+1)$, using the plant model. This prediction is based on the current and past values of the plant input and output, $u(n)$ and $y(n)$, and a new trial input value, $u_k(n)$. For the

BACT model u is the TE control surface command and y is the TE accelerometer signal.

3. Evaluate the performance of the trial input value according to a performance index based on the cost of regulation/tracking error and the required control input power.
4. Repeat steps 2 and 3 with an optimization scheme until the termination criteria (desired performance or iteration limit) is achieved.
5. Output the trial control value selected by the optimization process to the plant. This is where the switch in figure 7 is moved from the down position to the up position so that the TE control surface command can be sent to the physical model. After the signal is sent the switch is returned to the down position for the next control cycle.
6. If on-line learning is engaged, update the plant model using a set of input/output data and an appropriate training algorithm.
7. Repeat the entire process for each control cycle.

The inputs to the plant model consist of time-delayed samples of the plant inputs, $u(n)$, and outputs, $y(n)$, as shown in figure 7. For nonlinear control applications, a multi-layer neural network architecture with backpropagation training can be used. For linear plants, a linear autoregressive moving average (ARMA) model is used. The NPC architecture was implemented using a Pentium 60 MHz PC with a plug-in Alacron neural accelerator board and analog input/output boards. The Pentium host CPU is responsible for all NPC computations and data transfer to the input/output and neural accelerator boards. The neural accelerator board performs the on-line model adaptation which occurs in parallel with the host CPU control loop computations. Due to several limitations of this hardware and software, only the linear ARMA plant models were considered in this study.

Simulation Results

The simulation studies were performed to design the appropriate plant model architecture, evaluate the robustness of the controller, and validate the real time control software. Successful adaptation and control was demonstrated across the range of simulated wind tunnel conditions, with the NPC system running at a rate of 100 Hz. One representative simulation time history is illustrated in figure 8 for an open-loop unstable condition, $M=0.75$ and $q=175$ psf. Starting with an untrained network, a white noise excitation signal was sent to the TE control surface for four seconds and the accelerometer response recorded providing 400 data points for neural

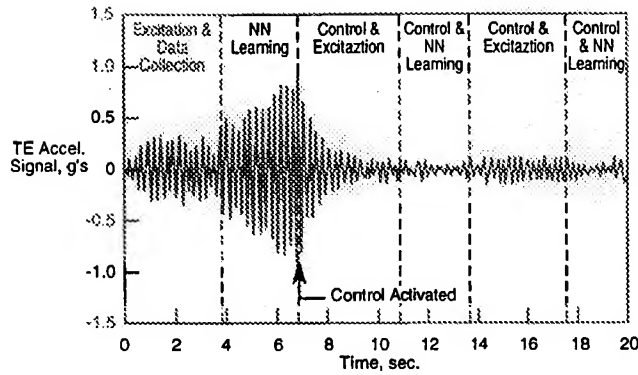


Fig. 8 NPC simulation time history.

network learning. The learning then occurred during the next 2.7 seconds, allowing control to be activated at about 6.7 seconds. As shown in the figure, from $t=3.9$ to $t=6.7$, the wing response grew steadily due to open-loop flutter until the controller was initiated for flutter suppression. Once the system was activated, learning and control occur simultaneously, allowing model updates to occur every 6.7 seconds. The length of this time interval is determined by the speed of the processors, the control cycle rate, and the amount of data needed for accurate plant modeling.

Experimental Results

The NPC system was tested at several M and q conditions along two H-lines. Testing began at the lower end of the H-line, in the open-loop stable region, with plant model learning activated. Dynamic pressure and Mach number were then gradually increased to conditions well beyond the open-loop flutter boundary. The continuous adaption of the plant model, which was one goal of the project, was not reliable enough to use for long periods of time. Periodically, the plant model generated by the on-line learning algorithm was not accurate enough and resulted in an unstable control system. Additional analysis is necessary to isolate the root of the problem, but it may be related to the level of random noise used to excite the wing dynamics, the amount of data used for training, or tuning of the performance index used by the NPC system.

After several unsuccessful attempts to operate in a fully adaptive mode, it was decided to activate learning only when a new model was required. Thus, for each H-line the plant model was generated at the low end of the H-line at an open-loop stable condition, and then learning was turned off, thereby freezing the plant model parameters. This arrangement was used to successfully suppress flutter along two H-lines as shown in figure 9.

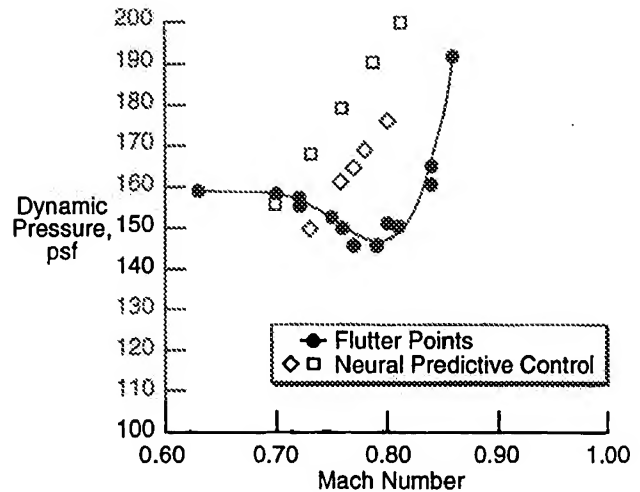


Fig. 9 NPC wind-tunnel data points.

Inverse Model Control

This section of the paper will provide a detailed description of the application of neural networks and inverse modelling to the control of aeroelastic response.

Architecture

The inverse modelling control architecture used in this study borrows elements from several proposed control schemes. This section of the paper will describe the relevant aspects of these systems and the system architecture implemented here. Inverse modelling control has generally been applied to trajectory tracking applications. References 13, 14, and 15 describe several approaches to inverse modelling control and introduce several elements applicable to the present problem. In general, the key assumption in inverse model control is that an unknown plant can be made to track an input command signal when this signal is applied to a controller whose transfer function approximates the inverse of the plant's transfer function. An adaptive control system can be created by applying an adaptive inverse modelling process to the plant. A simple form of such a system is depicted in figure 10. The upper portion of this figure shows the training procedure. Here the arrow passing through the network box indicates the feedback of the error for training of the network using back propagation. The lower portion of figure 10 shows the implementation of the inverse model. In practice the adaptive inverse model will be continuously updated. Thus, no direct feedback is used, except that the plant output is monitored and utilized to adapt the parameters of the controller.

The type of system just described is only suitable for minimum phase systems. The introduction of a time delay on the plant input used in the inverse modelling process allows one to obtain an approximate delayed in-

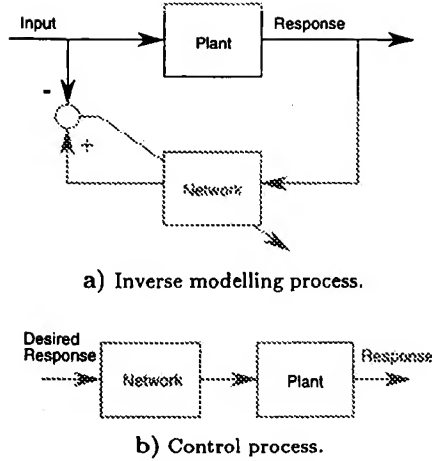


Fig. 10 Generic inverse model control block diagram.

verse model to both minimum and non-minimum phase plants. Reference 14 also suggests using a prefilter on the plant input signal. Both the time delay and prefilter concepts will be employed in this study to generate inverse plant models. As the aeroelastic control application investigated here is not a trajectory following problem, the actual implementation of the inverse model in the control system will be different than that proposed by Widrow.¹³⁻¹⁵ The implementation of the inverse model in a closed-loop system is discussed next.

The inverse model can take numerous forms including the one used here, a neural network. The implementation of the neural-network inverse model used in this study is similar to that proposed in reference 16. Unlike many other studies, reference 16 suggests a relatively simple implementation where the neural network inputs and outputs are connected directly to the plant like a standard feedback controller. The present implementation will use this approach. However, unlike reference 16 which used perceptron neural networks trained using genetic algorithms, the present application will use a two-layer feed-forward neural network trained using back-propagation.

The present implementation of the inverse modelling approach is shown in figure 11. The upper part of the figure shows the acquisition of training data and the off-line network training procedure. The input to the network is one of the BACT model's accelerometer signals. As indicated on the figure, the input to the network is made up of the current and delayed values of this signal. The number of time-delayed inputs used can be varied. Also, as discussed earlier, the model input signal used to train the network is delayed and filtered prior to used. The data acquisition was performed using the ADC¹¹ sampling at 200 Hz. The network training was performed off-line using the MATLAB software. The time delay

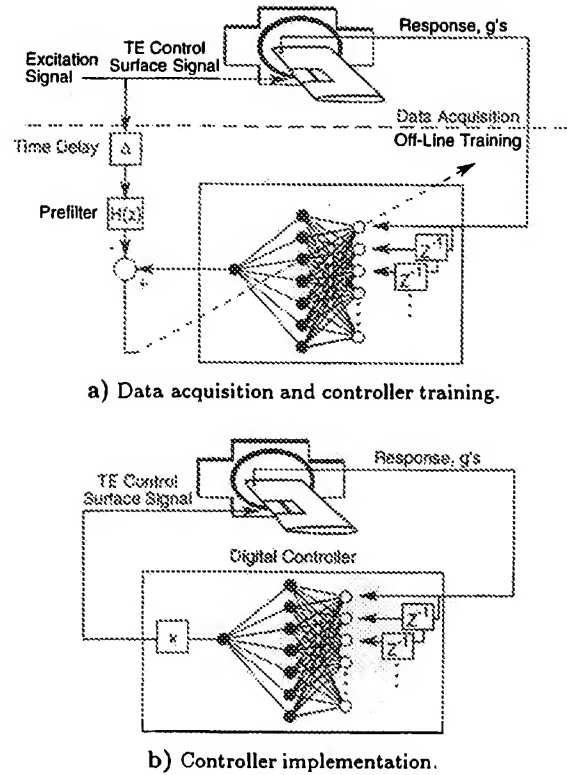


Fig. 11 Inverse model control system architecture.

(Δ) was an integer number of time steps. The prefilter was implemented using the MATLAB FILTFILT function. This function digitally filters the data in both the forward and reverse directions. The result has zero phase distortion with a magnitude modified by the square of the filter's magnitude response. The prefilter is tailored to have a peak magnitude near the frequency of the physical phenomenon to be controlled. For flutter suppression, the flutter frequency is used.

The lower portion of figure 11 shows the implementation of a trained network. Here the network is inserted in the control loop with the the BACT model's TE control surface command as the output of the network. This control system also was implemented on the ADC¹¹ sampling at 200 Hz. The gain, k , on the output signal could be varied on-line.

The following steps summarize the operation of this system.

1. Send excitation signal to the BACT model recording both the excitation (TE control surface command) and the model response (accelerometer signal).
2. Train the network using delayed and filtered excitation signal and BACT accelerometer response time history.
3. Implement trained network on the real-time system.

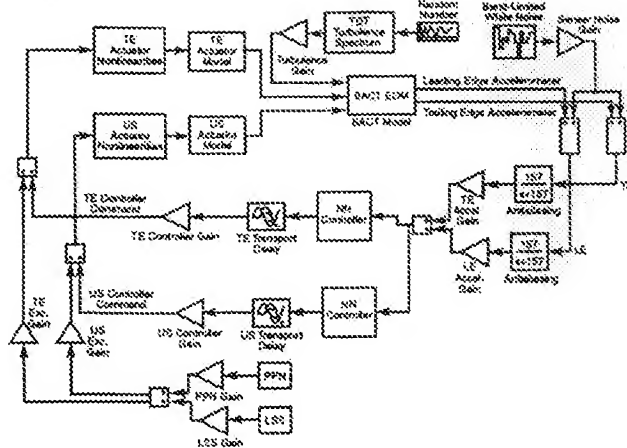


Fig. 12 Inverse model control system simulation block diagram.

Prior to implementation of this system, many parameters were explored using the simulation model discussed in the next section.

Simulation Model

The simulation model developed by Waszak^{17,18} was used in this study. The model was formed by combining the equations of motion for the BACT wind-tunnel model with actuator models and a model of wind-tunnel turbulence. Wherever possible, the numerical model parameters were determined experimentally. The mass and inertia parameters were obtained by measuring the mass, stiffness, and damping properties of the BACT flexible mount. The static aerodynamic parameters were determined from experimental data when the BACT model was mounted to a five-degree-of-freedom balance.⁷ The dynamic derivatives were obtained computationally using ISAC.¹⁰ The numerical values for the static and dynamic stability and control derivatives are only valid at a single Mach number of 0.77; however, the dynamic pressure for the model could be changed. The analytical flutter boundary for this simulation model occurs at a dynamic pressure of 150.8 psf. Figure 12 shows the version of the simulation model used in this study. The BACT equations of motion and actuator models developed by Waszak are contained in the appropriately labeled blocks. The turbulence model in the upper left portion of the model is based on a Dryden spectrum with parameters tuned to match power spectrum data obtained in the TDT. The other elements of the block diagram were added for this investigation.

The primary changes to the model developed by Waszak included the addition of the neural-network control blocks and numerous other gain blocks. The control system studies in this investigation were SISO so the gain blocks were included to allow the same SIMULINK¹⁹

model to be used for either accelerometer signal (trailing edge or leading edge) or either control surface (TE control surface of upper spoiler) without changing the model. For instance, if the gains on the upper spoiler control signal and the gain on the leading edge accelerometer signal are both zero, the resulting system would be SISO utilizing the TE control surface and the TE accelerometer. This was the configuration considered in this investigation. In addition, excitation generators and their associated gains were introduced for obtaining training data and for studying the effects of noise and turbulence.

Several parameters that could also be varied but are not shown in figure 12, include the number of hidden layers on the neural network and the number of time-delayed network inputs. The hidden layer could be either linear or nonlinear.

Parametric Variations

This section of the paper will present results from several parametric variations using the simulation model described above. First, a few words about how these parametric studies were performed. The primary objective of this system is flutter suppression and the performance of the control system will be evaluated at a dynamic pressure where the model is open-loop unstable, 175 psf. The data for training the network must be obtained initially at a dynamic pressure where the model is open-loop stable. The initial training was obtained from an open-loop simulation using a dynamic pressure of 133 psf where a pseudo-random noise (PPN) or linear sign sweep (LSS) input was used to drive the TE control surface. Both excitation signals had frequency content between 0 and 12 Hz. The prefilter for the flutter suppression applications was selected to have peak magnitude of unity in the vicinity of the flutter frequency of the BACT model. The prefilter used for flutter suppression control laws is shown below.

$$\frac{-431.1s}{s^3 + 19.6s^2 + 811.6s + 2529.8}$$

It has a peak magnitude of unity at 4 Hz and significant washout below and rolloff above this target frequency.

In all the parametric results presented, the RMS values of the TE accelerometer and the TE control surface will be plotted against the parameter being varied. Lower is better and values off the scale of the plot indicate that the system is not stable. The value of Δ , the number of time delays used in training the network, is a very important parameter and will often be used as the independent variable in these plots. The nominal simulation parameters are as follows

Network Controller:

Hidden Nodes = 6

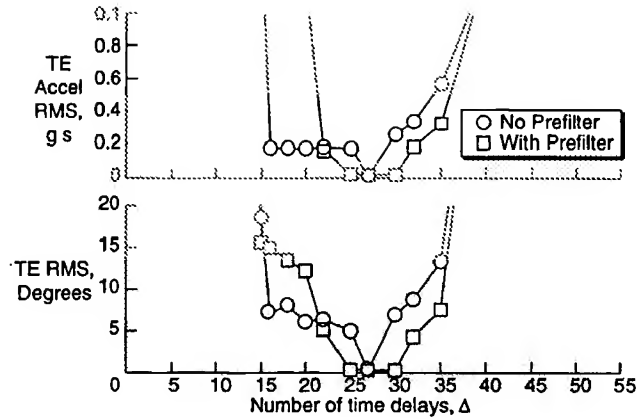


Fig. 13 Comparison of linear inverse model control system response with and without the use of the prefilter.

Time Delayed Inputs = 25

$\Delta = 25$

Training Data Simulation:

$q = 133.0$ psf

Turbulence Gain = 3.0

Simulation Time = 30 seconds

TE Control Surface Excitation = PPN

Controller Evaluation Simulation:

$q = 175.0$ psf

Turbulence Gain = 3.0

Simulation Time = 30 seconds

Control Law Gain, $k = 2.0$

The first issue to be explored is the use of the prefilter. Figure 13 shows a comparison of linear controller performance where the linear network controllers were trained with and without the prefilter. The comparison shows that a controller that will suppress flutter can be obtained without using the prefilter, but it will have poor robustness properties. Typically, an acceptable flutter suppression control system will have control surface RMS values significantly below unity. Without the prefilter, only one value of Δ achieves acceptable control system performance.

The next parametric variation considered a linear network where Δ and the turbulence gain were varied. The turbulence gain was varied for the open-loop simulations where the training data was acquired. A gain of three was used to evaluate the closed-loop performance. This data is shown in figure 14. From these data, it is apparent that a time delay between 25 and 35 achieves the best performance. It can also be observed that moderate levels of turbulence improve the performance of the network controllers.

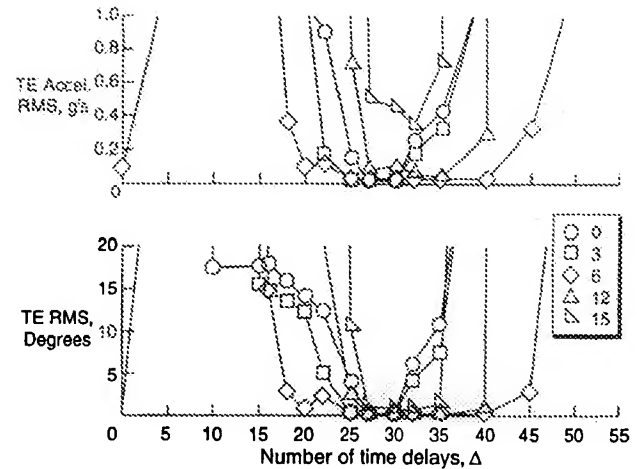


Fig. 14 Linear network inverse model controller performance for varying Δ and turbulence gain.

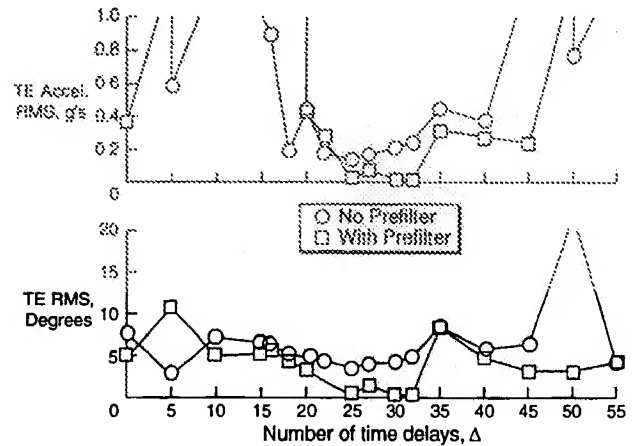


Fig. 15 Comparison of nonlinear inverse model control system response with and without the use of the prefilter.

The use of a nonlinear network (sigmoid transfer function on the hidden layer) is now considered. Figure 15 shows a comparison between nonlinear networks trained with and without a prefilter as a function of Δ . An important feature of the nonlinear result is that while the system may become unstable, the control command is limited by the saturation of the sigmoid transfer functions. Otherwise, the linear and nonlinear network controllers achieve similar levels of performance. To further explore the use of nonlinear network controllers, the turbulence gain and prefilter were varied. Figure 16 shows a comparison of the performance of nonlinear network controllers where the training data was obtained using various values of the turbulence gain. As with the linear case, moderate levels of turbulence were found to be desirable.

The next parameter to be considered in this study

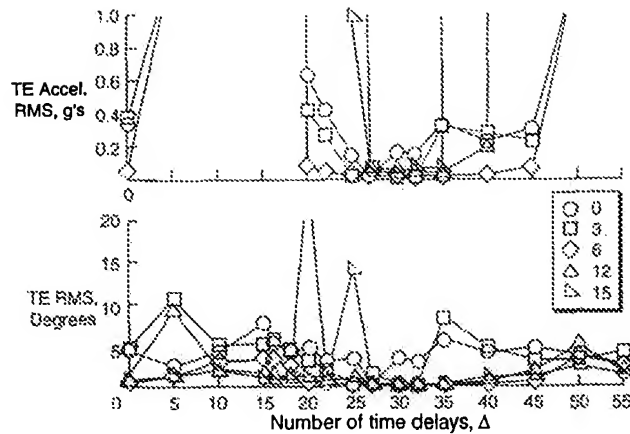


Fig. 16 Nonlinear network inverse model controller performance for varying Δ and turbulence gain.

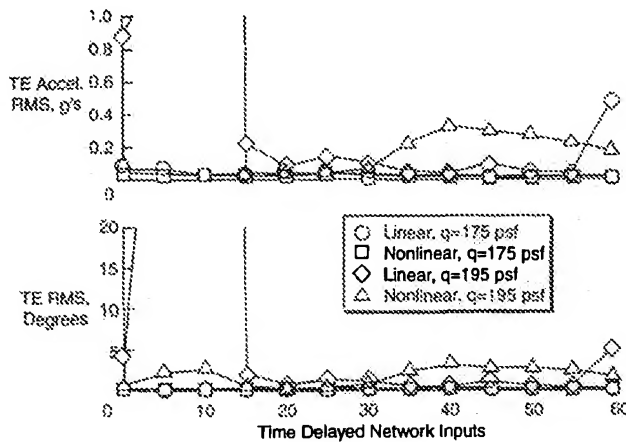


Fig. 17 Inverse model controller performance as a function of the number of delayed network inputs. $\Delta=25$.

was the number of delayed inputs to use on the network controller. Figure 17 shows a comparison of performance of a linear and nonlinear network where the number of time-delayed inputs was varied from 0 to 60. The value of Δ in these analyses was 25. The systems were evaluated at two dynamic pressures, 175 psf and 195 psf. At 175 psf dynamic pressure, the performance of the system was insensitive to the number of time delays, but at 195 psf dynamic pressure, a minimum value of 15 time delays was required.

The final parameter considered is the excitation type used to obtain the training data. So far only a PPN excitation has been used. A comparison of PPN results with those obtained using a LSS excitation is presented in figure 18 for both linear and nonlinear controllers. Both types of excitations yield controllers with similar performance, but the PPN excitation appears to have a slight advantage over the LSS excitation.

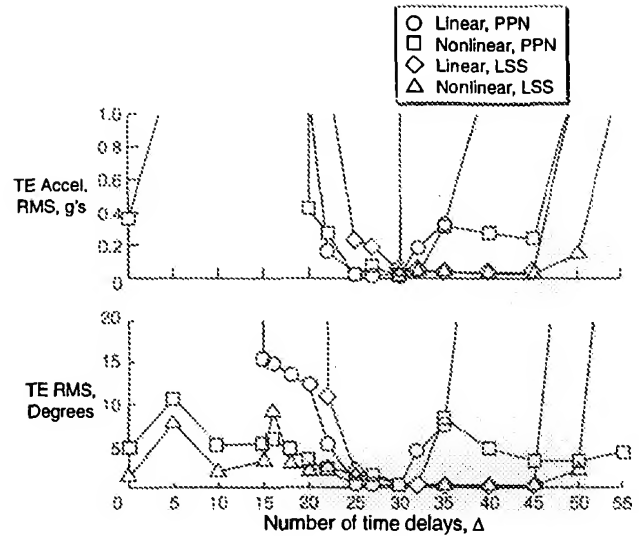


Fig. 18 Linear and nonlinear inverse model controllers trained using PPN and LSS excitation.

This completes the discussion on the inverse model control parametric studies. Note that not all parameters were varied. Future studies should consider the use of the leading accelerometer sensor and the use of the spoiler. The amplitude of the control surface excitation was not varied, and sensor noise was not considered at all. The only control systems considered were SISO, yet the simulation model can be modified to use both leading-edge and trailing-edge accelerometers as input signals to the controller. Finally, a truly adaptive system needs to continually re-acquire data and train new inverse model controllers as the plant changes. This was not considered in the present study.

Experimental Results

This section of the paper describes experimental results for application of inverse modelling control to the BACT model during the 1996 wind-tunnel test. The networks used during this wind-tunnel test all had 25 time-delayed inputs to the network and 6 nodes on the hidden layer. These controllers were SISO with the input coming from the TE accelerometer and the output being sent to the TE control surface. Unless otherwise noted, the prefilter used is the same as that described in the preceding subsection. Due to time constraints only a limited number of parameter variations were explored experimentally.

Two inverse model flutter suppression control systems were demonstrated. Figure 19 shows a portion of the TDT operating envelope with the BACT open-loop flutter boundary superimposed. The two inverse model control systems are designated A and B. System A was trained using data acquired at conditions well below the open-loop flutter boundary ($M=0.65$, $q=133$ psf).

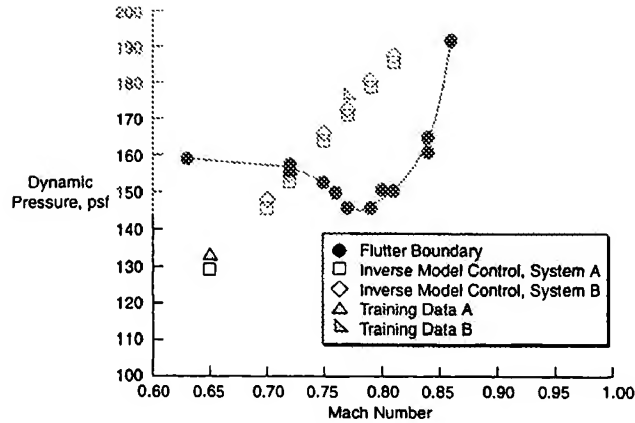


Fig. 19 Inverse model flutter suppression data points acquired. Linear networks. $\Delta=25$. $k=3.0$

System B was trained using data acquired above the open-loop flutter boundary ($M=0.77$, $q=177$ psf) with the loop closed. In both cases a PPN excitation was sent to the TE control surface when the training data was acquired. Both systems A and B used linear networks. As indicated in figure 19, both systems successfully suppressed flutter in excess of 35 psf above the open-loop flutter boundary. The response of the model for both systems was similar indicating that a fully adaptive system may be feasible as successful network controllers can be synthesized from data acquired with the loop closed above the open-loop flutter boundary.

Inverse model controllers were explored for reducing the turbulence response subcritically (below the BACT open-loop flutter boundary). In this application, both the training data and closed-loop data were acquired at approximately the same tunnel conditions. For these experiments, the TDT Flow Oscillating Vanes⁶ were used and data was acquired at several discrete vane frequencies. Figure 20 shows the open- and closed-loop response RMS of the model as a function of vane frequency. The open-loop response is indicated by the solid line with two distinct natural frequencies apparent. The inverse model controllers were both linear, and both systems significantly reduced model response between 3 and 4 Hz. The only difference between the two systems was the value of Δ used in the training. The larger value of Δ appeared to favor the frequencies below 3.5 Hz, while the smaller value favored the frequencies above 3.5 Hz.

The final experimental data to be discussed will be the use of nonlinear networks to reduce turbulence response. Figure 21 shows the open- and closed-loop response RMS of the model as a function of vane frequency. Unlike the previous experimental results, these systems were trained using a prefilter that had a peak frequency of 3.2 Hz. Training data acquired with PPN and LSS were used. Both systems reduced the turbulence response in

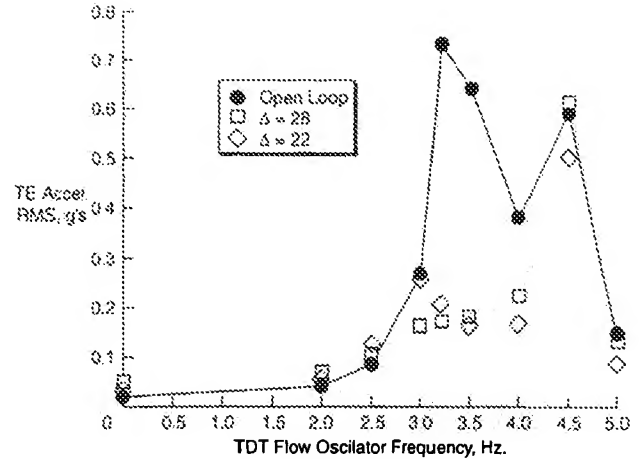


Fig. 20 Open- and closed-loop response to TDT flow oscillator system. Linear networks. $k=4.5$. Training data acquired at $M=0.7$ and $q=102$ psf. Response data acquired at $M=0.7$ and $q=101$ psf.

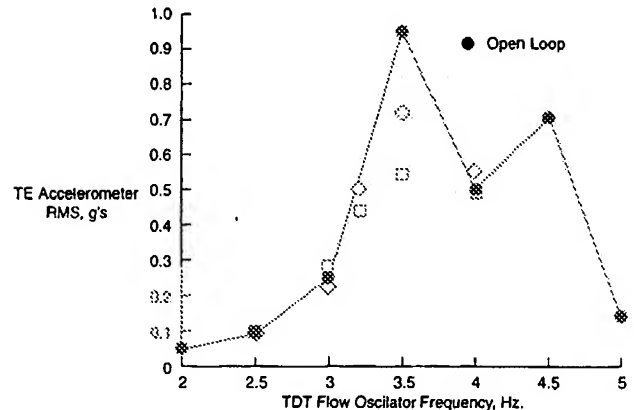


Fig. 21 Open- and closed-loop response to TDT flow oscillator system. Nonlinear networks. $\Delta=28$. $k=2$. Training data acquired at $M=0.7$ and $q=102$ psf. Response data acquired at $M=0.7$ and $q=101$ psf.

the vicinity of the target frequency. At vane frequencies above 4 Hz, the TE control surfaced angle remained virtually fixed and the model behaved as if open-loop. The PPN training yielded a control system that has lower response than the control system synthesized using the LSS data. This trend is consistent with the simulation results presented in figure 18 where for $\Delta = 25$ the response levels are lower for controllers trained using PPN excitation than for those trained using LSS excitations.

Concluding Remarks

This paper has presented an exploratory application of neural networks to the control of aeroelastic response. The project was joint research and development effort conducted by the National Aeronautics and Space Ad-

ministration and The Boeing Company (formerly McDonnell Douglas). The objective of this project was to develop adaptive neural-network based control systems. Three neural-network based control systems were developed and tested. The control systems were experimentally evaluated using the Benchmark Active Controls Technology (BACT) transonic wind-tunnel model in the Transonic Dynamics Tunnel (TDT). One system used a neural network to schedule flutter suppression control laws, another employed a neural network in a predictive control scheme, and the third employed a neural network in an inverse model control scheme.

The gain scheduling control systems simply used a neural network to schedule classically-designed SISO control system parameters as a function of tunnel conditions (Mach number and dynamic pressure). The neural network was trained to output control system parameters which were then transferred to the real-time digital controller. The system successfully suppressed flutter and reduced system response.

The predictive control system was implemented using a linear network to model the plant. The plant model was synthesized on-line using experimental data, and the system successfully suppressed flutter. Of the three systems tested, this was the only truly adaptive system. The system was, however, only partially successful in the fully adaptive mode. The hardware and software required to implement this system with a nonlinear network was not available for this investigation. For additional work in this area see references 20, 21, and 22.

Linear and nonlinear inverse model controllers were successfully used to control aeroelastic response on the BACT wind-tunnel model. In each case, network control laws were synthesized directly from the time histories of model input and output data. Experimentally, an increase in flutter dynamic pressure of at least 20 psf was achieved, and a reduction in the RMS response of over 40% at the target frequency was achieved.

It is important to note that this was an exploratory study, and significant further study is required to determine the merits of using neural networks for aeroelastic control. The control systems discussed in this paper were just a few of the many control systems tested using the BACT model, and in general the performance of these neural network systems was poor compared with conventional control systems designed using classical and modern methods. Furthermore, the BACT model is an extremely simple and robust aeroelastic model and successful implementation using this model does not guarantee success with a more realistic plant.

References

- ¹Leitner, J., Prasad, J., and Calise, A., "Nonlinear Control of Rotorcraft Using Approximate Feedback Linearization and On-line Neural Networks," *AIAA Guidance, Navigation and Control Conference*, No. 94-3693, Scottsdale, AZ, Aug. 1994.
- ²Troudet, T., Garg, S., and Merrill, W., "Design and Evaluation of a Robust Dynamic Neurocontroller for a Multivariable Aircraft Control Problem," *Nasa tm 105579*, June 1992.
- ³Steck, J. E. and Rokhsaz, K., "Use of Neural Networks in Control of High Alpha Maneuvers," *30th Aerospace Sciences Meeting and Exhibit*, No. 92-0048, Reno, NV, Jan. 1992.
- ⁴Mukhopadhyay, V., "Transonic Flutter Suppression Control Law Design, Analysis and Wind Tunnel Results," *CEAS/AIAA/ICASE/NASA-Langley International Forum on Aeroelasticity and Structural Dynamics*, June 1999.
- ⁵Waszak, M. R., "Robust Multivariable Flutter Suppression for the Benchmark Active Control Technology (BACT) Wind-Tunnel Model," *Proceedings of the Eleventh Symposium on Structural Dynamics and Control*, Blacksburg, VA, May 1997.
- ⁶"The Langley Transonic Dynamics Tunnel," *Langley Working Paper LWP-799*, Sept. 1969.
- ⁷Scott, R. C., Hoadley, S. T., Wieseman, C. D., and Durham, M. H., "The Benchmark Active Controls Technology Model Aerodynamic Data," *Proceedings of the 35th Aerospace Sciences Meeting and Exhibit*, No. 97-0829, Reno, NV, Jan. 1997.
- ⁸Demuth, H. and Beale, M., *Neural Network Toolbox*, The Math Works, Inc., Jan. 1998.
- ⁹Lichtenwalner, P., Little, G., and Scott, R., "Adaptive Neural Control of Aeroelastic Response," *SPIE 1996 Symposium on Smart Structures and Materials*, San Diego, CA, Feb. 1996.
- ¹⁰Peele, E. L. and Adams, W. M., "A Digital Program for Calculating the Interaction Between Flexible Structures, Unsteady Aerodynamics, and Active Controls," *NASA TM 80040*, Jan. 1979.
- ¹¹Hoadley, S. T. and McGraw, S. M., "The Multiple-Function Multi-Input/Multi-Output Digital Controller System for the AFW Wind-Tunnel Model," *AIAA 92-2083*, April 1992.
- ¹²Lichtenwalner, P., Little, G., Pado, L., and Scott, R., "Adaptive Neural Control for Active Flutter Suppression," *SPIE 1997 Symposium on Smart Structures and Materials*, San Diego, CA, March 1997.
- ¹³Widrow, B., McCool, J. M., and Medoff, B. P., "Adaptive Control By Inverse Modelling," *Fifteenth Asilomar Conference on Circuits, Systems and Computers*, Nov. 1978, pp. 90-94.
- ¹⁴Widrow, B., Shur, D., and Shaffer, S., "On Adaptive Inverse Control," *Fifteenth Asilomar Conference on Circuits, Systems and Computers*, Pacific Grove, CA, Nov. 1981, pp. 185-189.
- ¹⁵Widrow, B. and Bilello, M., "Nonlinear Adaptive Signal Processing for Inverse Control," *World Congress On Neural Networks*, San Diego, CA, June 1994.
- ¹⁶Ichikawa, Y. and Sawa, T., "Neural Network Application for Direct Feedback Controllers," *IEEE Transactions on Neural Networks*, Vol. 3, No. 2, March 1992, pp. 224-231.
- ¹⁷Waszak, M. R., "BACT Simulation User Guide," *NASA TM 97-206252*, Nov. 1997.
- ¹⁸Waszak, M. R., "Modeling the Benchmark Active Control Technology Wind-Tunnel Model for Application to Flutter Suppression," *AIAA 96-3437*, July 1996.
- ¹⁹The Math Works, Inc., *Simulink - Dynamic System Simulation for Matlab*, Dec. 1996.
- ²⁰Pado, L. E. and Lichtenwalner, P. F., "Neural Predictive Control for Active Buffet Alleviation," No. 99-1319, 1999.
- ²¹Pado, L. E., Lichtenwalner, P. F., Liguore, S. L., and Drouin, D., "Neural Predictive Control for Active Buffet Alleviation," *SPIE 1998 Symposium on Smart Structures and Materials*, San Diego, CA, Feb. 1998.
- ²²Pado, L. E. and Damle, R. R., "Predictive Neuro Control of Vibration in Smart Structures," *SPIE 1996 Symposium on Smart Structures and Materials*, San Diego, CA, Feb. 1998.



A bibliography of neural network business applications research: 1994–1998

Bo K. Wong^{a,*}, Vincent S. Lai^b, Jolie Lam^c

^a*Department of Information Systems, Lingnan University, Tuen Mun, N.T., Hong Kong*

^b*Chinese University of Hong Kong, Hong Kong*

^c*City University of Hong Kong, Hong Kong*

Abstract

The purpose of this paper is to present a comprehensive bibliography of neural network application research in business during the period of 1994–1998. Our extensive literature searches have identified a total of 302 research articles. A classification of these articles by year reveals that a large amount of research has been published in the last five years. Production/operations, finance, marketing/distribution, and information systems were found as the most popular application areas. Information on neural network development language/tool, learning paradigm, computing operating environment, journals and authors are included. An in-depth comparison with the previous survey findings and potential future research trend in the neural network business research are discussed.

Scope and purpose

Due to the breakthrough of the neural network technology, there has been an increasing amount of neural network application research in the last decade. As a result, a considerable amount of published research has appeared, with a significant portion focusing on actual neural network development for business applications. But a comprehensive bibliography of these research published in the last five years is not documented. © 2000 Published by Elsevier Science Ltd. All rights reserved.

Keywords: Neural network; Bibliography

1. Introduction

Neural network computing is an approach that attempts to mimic certain processing capabilities of the brain. This machine learning technology has the ability to represent knowledge based on

* Corresponding author. Tel.: + 852-2616-8096, fax: + 852-2892-2442.

E-mail address: bokwong@ln.edu.hk (B.K. Wong)

massive parallel processing and recognize patterns based on experience. Since the 1980s, the drastic breakthrough of the computing technology has led to an increasing amount of neural network research on a wide variety of business functional applications. Most of these research findings pointed out that neural network technology could be successfully used in business and most of the time is superior to other techniques or technologies. A bibliography of these research studies published during the period of 1988–September 1994 was documented in Wong et al. [1]. The purpose of this paper is to present a comprehensive bibliography of these neural network business applications published after this period, compare the major changes of the research between the two periods, and discuss the future potential research trend.

2. Research methodology

The literature search process involved three major steps. First, both ABI/INFORM database and *Business Periodical Index* (BPI) were searched using the keyword ‘neural network’ for the period covering 1994–1998. The ABI/INFORM database was the most important step in our literature retrieval process since it included more than 800 different business-related international journals. In this database, we were able to retrieve about 920 abstracts from the specified period.

Second, a reference search of textbooks on neural networks and related topics was conducted. We considered a total of 14 textbooks: Bose and Liang [2], Browne [3], Chen [4], De Wilde [5], De Wilde [6], Golden [7], Goonatillake and Treleaven [8], Hagan et al. [9], Hunt et al. [10], Irwin et al. [11], Korn [12], Parks [13], Rzempoluck [14], and Van Rooif et al. [15]. However, these books were not that helpful since most references were on scientific applications.

Third, 10 additional journals were also included in our manual search. The rationale was that (1) several prestigious journals known to publish neural network articles were either partially or not included in the ABI/INFORM database or BPI, and (2) some of these journals were deemed as being important in the MIS discipline [16–18]. These 10 journals were *ACM DATABASE*, *AI Expert*, *Communications of the ACM*, *Expert Systems: The International Journal of Knowledge Engineering and Neural Networks*, *IEEE Expert* (renamed as *IEEE Intelligent Systems & Their Applications* in 1998), *IEEE Transactions on Software Engineering*, *IEEE Transactions on Systems, Man, and Cybernetics*, *Information Systems Research*, *International Journal of Human-Computer Studies*, and *International Journal of Production Research*.

Not all the articles retrieved were included in our survey. Two criteria were applied in the selection process of the articles. Each article (1) should present the application of neural network in business and discussed either a prototype or a fully developed system, and (2) should have a stringent research methodology and have detailed discussions on the development process of neural networks. A large number of articles were eliminated because they were not business application types of research.

3. Results

We have identified a total of 302 journal articles. The Refs. [19–320] present the bibliography of these neural network business applications. Fig. 1 shows the distribution of articles published by year, including years 1988–1993.

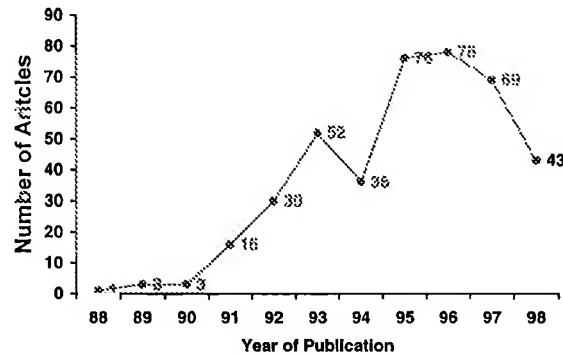


Fig. 1. Distribution of articles by year.

Table 1 shows 302 articles by area of application. Production/operations had the largest number of applications, followed by finance, marketing/distribution, information systems, accounting/auditing, and human resources. In production/operations, the most popular research areas were part family/machine grouping, job shop scheduling, cellular manufacturing system design, and equipment/machine fault diagnosis/detection. Bankruptcy prediction of banks/firms was the most common application in the area of finance.

The language/tool used in the development, the learning paradigm, and the type of computer operating environment of each neural network application are presented in Table 2. It is not surprising to find that the most common programming language was C/C++, and the most common tools were NeuralWorks Professional, NeuroShell, and BrainMaker. In addition, back-propagation, ART, Hopfield and Radial Basis Function were the most popular learning paradigms of these neural networks.

There were a total of 94 articles reporting the types of computing platform. Approximately 62.8% (59 articles) reported the use of microcomputer, 35.1% (33 articles) reported the operation on minicomputer or mainframe, and 2.1% (2 articles) reported the utilization of both.

Table 3 lists the journals that published the most neural network business applications. Journals such as *Computers and Industrial Engineering*, *International Journal of Production Research*, *European Journal of Operational Research*, *Computers in Industry*, *Journal of Manufacturing*, and *Computers and Operations Research* are the more popular journals. The reason is quite obvious since there are many neural network applications in the area of production/operations, and these journals are more suitable for publishing in this area.

These 302 articles were written by a total of 601 authors. Six authors did not report their affiliations. Out of 595 authors, approximately 87.1% (518 authors) were affiliated with 219 different academic institutions and 12.9% (77 authors) were affiliated with 60 non-academic or business-related institutions. Also, approximately 47.5% (104 institutions) of the academic institutions were US institutions and 52.5% (115 institutions) were non-US institutions. Thirty-one of the 60 business-related institutions (51.7%) were US institutions and the remaining 29 (48.3%) were non-US institutions.

Table 1
Distribution of articles by application area^a

Accounting/auditing

- Audit judgement task supporting [88]
- Auditor's going concern uncertainty decision prediction [178]
- Fraud risk assessment [115]
- Preliminary control risk assessment [87]
- Quarterly accounting earnings forecasting [49]

Total: 5

Finance

- Acquired and liquidated firms discrimination [214]
- Bankruptcy prediction of banks/firms [42,62,133,175,188,194,289,309]
- Bond trading [97,231,232,259]
- Capital market index forecasting [313]
- Change card default risk assessment [280]
- Commercial bank's market efficiency assessment [27]
- Commercial loan credit worthiness evaluation [111]
- Commodity future trading [216]
- Company failure analysis [251]
- Construction contract bond claims prediction [279]
- Corporate health estimation [166]
- Country risk rating prediction [58]
- Credit authorization [91]
- Credit evaluation [227]
- Credit scoring [177]
- Derivative securities pricing and hedging [129]
- Distress financial firms classification [161]
- Exchange rate forecasting [106,138]
- Federal reserve decision making [264]
- Financial distress forecasting [24]
- Financial prediction and trading strategies [221]
- Financial risk classification [226]
- Financial statement analysis and interpretation [158]
- Future spot rates predication [277]
- Futures trading volume forecasting [142]
- Initial public offering forecasting [119]
- Initial public offering pricing [136]
- Insurance problem examination [295]
- Insurer insolvency prediction [43]
- Interest rate prediction [215]
- Intermarket analysis [244]
- International equity risk premium prediction [94]
- Investment banking hiring prediction [192]
- Investment behavior investigation [98]
- Investment management [239]
- Loan classification [90]
- Mutual fund net asset value forecasting [67]
- Non-life insurance companies evaluation [157]
- Nonpayment prediction [206]
- Portfolio optimization [127,270]

Table 1 (continued)

Real estate appraisal [314]
Residential property values evaluation [78]
Shipbuilding's scheduling system development [173]
Spot exchange rates prediction [222]
Stock market index prediction [152,281]
Stock market holding period return investigation [312]
Stock market indexes structure testing [19]
Stock market volatility forecasting [44,92]
Stock performance/selection prediction [34,316]
Stock's systematic risk forecasting [311]
Successful new ventures identification [137]
T-bond market prediction [245]
Total: 67
<i>Human resource</i>
Salesperson hiring [308]
Total: 1
<i>Information systems</i>
Character recognition for personal digital assistant [315]
Computer assess security [218]
Computer program risk analysis engineering [147]
Computer users authentication [242]
Computer viruses recognition and classification [93,282]
Database tables clustering [139]
Document semantic indexing [60]
Information retrieval [81,185]
Intelligent networks' feature interaction management [284]
Internet user modeling [201]
Knowledge discovery and concept exploration [59]
Organizations' IT adoption identification [252]
Production systems' information integration [99]
Software cost estimation [169,247]
Software development [269]
Software development effort estimation [103,310]
Software fault prediction [255]
Software maintenance task effort prediction [140]
Software quality prediction [168]
Text-editing goals identification [296]
Total: 24
<i>Marketing/distribution</i>
Competitive retail coffee market structure identification [118]
Consumer choice prediction [306]
Consumer segments identification [86]
Franchising decision making improvement [187]
Future order forecasting [204]
Gasoline demand forecasting [174]
Industrial market segmentation [104]
International airline passenger forecasting [212]
Long distance telephone usage [253]

(continued on next page)

Table 1 (continued)

Market responses prediction [292]
 Market segmentation [31]
 Market share forecasting [20]
 New investment product promotion [108]
 Product design [30]
 Product purchase frequency prediction [97]
 Relationship quality investigation [37]
 Sales forecasting [25,163,164,189]
 Solo mailing [317]
 Target marketing [318,319]
 Telephone interview response analysis [205]

Total: 24

Production/operations

Abrasive flow machining operation [223]
 Acoustic emission behaviors evaluation [66]
 Adaptive optimal controlling [155]
 Aging aircraft component inspection prediction [257]
 Aging aircraft safety prediction [190]
 Aircraft and machine tool pattern recognition [176]
 Arm trajectory formation [195]
 Automated guided vehicle system optimization [74]
 Automated material handling [121]
 Barley malting process [102]
 Beam landing adjustment [229]
 Bean vibration minimization [46]
 Bearing faults prediction [268]
 Boundary defect recognition [154]
 Building text's automatic content recognition [200]
 Capacity allocation [113]
 Car sequencing [262,263]
 Cell formation [71]
 Cellular manufacturing system design [70,165,237,238]
 Cerebellum motor learning [146]
 Charts pattern identification [22]
 Cold bending steel reinforcing bars automation [96]
 Colored object recognition [304]
 Complex grinding processes controlling [256]
 Computer vision inspection [55]
 Computer vision precise measurement [271]
 Control charts pattern recognition [131,132,260]
 Cost estimation [39,40,83,89]
 Cost estimation predictive modelling [261]
 Cost flow forecasting [41]
 Cutting tool monitoring [202]
 DC motor speed controlling [243]
 DOF stanford manipulator design [208]
 Design retrieval [29]
 Electricity demand prediction [79]
 Equipment/machine fault diagnosis/detection [85,109,156,184]

Table 1 (continued)

Facility layout optimization [285]	
Featured-based product cost estimation [320]	
Flexible beam's torque control [287]	
FMS designed analysis [191]	
Gas furnace identification [33]	
Group technology [143]	
Image inspection and verification [117]	
Incipient object slippage detection [51]	
Integrated circuit fabrication [272]	
Intelligent manufacturing control [124]	
Intelligent package [29]	
Job scheduling [123]	
Job shop scheduling [45,135,170,224,233,246,248,258]	
Lime granule quality inspection [53]	
Machine design [95]	
Machine fault diagnosis [126]	
Machine performance degradation measurement [171]	
Machine tools' thermal deformation [293]	
Machinery diagnosis [63]	
Machining knowledge acquisition [82]	
Manufacturing diagnosis [236]	
Manufacturing process control and monitoring [35]	
Manufacturing process parameter change detection [235]	
Manufacturing processes simulation [141]	
Manufacturing system simulation optimization [128]	
Manufacturing systems design and real-time reconfiguration [198]	
Manufacturing systems prediction [153]	
Material selection [112]	
Message passing system [160]	
Multi-objective FMS scheduling [149,199]	
Multicriteria solid transportation optimization [181]	
Multiple I/O data network routing optimization [288]	
Musculo-skeletal system modelling [150]	
Naphtha cut point prediction [297]	
Nonlinear process control improvement [274]	
Non-stationary manufacturing process tracking [299]	
Oil quality rating [194]	
Part family grouping [75,148]	
Part family/machine grouping [47,61,84,100,144,159,182,275,276,294]	
Part positioning [54]	
Part-tool grouping [26]	
Peg-into-hole assembly operation [217]	
Plant identification and control [33]	
Plant location classification [38]	
Plant location optimization [291]	
Plasma etch processing [241]	
Process control [64,101]	
Process mean shift detection and classification [57]	
Process modelling and controlling [307]	
Process planning [197]	

(continued on next page)

Table 1 (continued)

Product manufacturability controlling [73]
Products quality modelling [120]
Progressive die design [186]
Quality control [191]
Quality controller [68]
Raw material purchasing [151]
Resource constrained scheduling [266]
Retrieving systems design [56]
Road tunnel ventilation controlling [107]
Robot arm impedance controlling [286]
Robot manipulator controlling [179]
Robot tracking controlling [219]
Robotic die polishing [162]
Robotic grasping system design [209]
Rolling mill - process control [107]
Rotating-Machinery performance analysis [183]
Schedule assessment [114]
Sheet metal parts classification [116]
Signal monitoring system [145]
Single machine mean tardiness [246]
Slip resistance prediction [290]
Star-LAN design optimization [110]
Statistical process control [65,80]
Steel manufacturing [249]
Steel mill prediction scheduling [302]
Steel plant's real-time process control [250]
Steel temper mill presetting [225]
Surface flows identification [298]
System reliability estimation [77]
Tandem cold mill production model [69]
Three-link robot's smooth trajectory tracking [130]
Tool path planning [273]
Tool wear monitoring [230]
Touch trigger probes' travel map establishment [254]
Toys and consumer electronics' speech processing [210]
Trickling filter performance prediction [228]
Unit commitment and power demand prediction [36]
Vehicle controller [32]
Vehicle detection [193]
Vehicle driving comfort prediction [48]
Vehicle routing problem [283]
Waste treatment [267]
Wave soldered joints inspection [134]
Wear equation identification [211]
Welding quality improvement [203]

Total: 163

Others

- Airline passenger volume prediction [213]
- Autoregressive moving average model identification [172]

Table 1 (continued)

Business value and organizational variables identification [234]
Construction firms' subcontractor rating [23]
Consumer's expenditure forecasting [76]
Economic growth forecasting [21]
Electronic meeting output classification [220]
Expenditure system model estimation [301]
Forecasting method selection [72]
Forecasting model selection [240,265]
Industrial production index analysis [105]
Organizational decision making [303]
Organizational structure modelling [300]
Real-time macroeconomic forecasting [278]
Residential construction demand forecasting [125]
Risky projects' economic analysis [28]
Simultaneous equation systems forecasting [52]
Strategic business planning [180]
Time series analysis [50]
Time-series forecasting [122,167]
Time-tabling problem [196]
Total health care costs prediction [207]
Warranty claims forecasting [305]
Total: 25

^aThere are two applications in article [29,33,97,107,191,194,246].

4. Comparisons with the previous survey [1]

Overall, the amount of research has been increasing in the last decade. It should be noted here that the number of research studies has stayed almost the same in years 1995–97 and has dropped significantly in 1998. We believe that it is not that simple to draw any conclusion on this situation. The possible explanation is that researchers are beginning to have more interest to conduct research in other artificial intelligence techniques, such as genetic algorithm and fuzzy logic. Also, some new journals that published neural network applications might not be included in the scope of our search.

As compared with the last survey, production/operations and finance were still the most common research application areas. It is interesting to find that the number of research studies in marketing/distribution and information systems has significantly increased. On the other hand, there were still only a few research studies in accounting/auditing and human resources, and their number of articles stayed approximately the same.

In the area of production/operations, the most popular research applications were still part family/machine grouping, job shop scheduling, and equipment/machine fault diagnosis/detection. However, less amount of research has been conducted on the area of process control.

Bankruptcy prediction of banks/firms remained a common research area in finance, but there was a sharp decrease in the number of studies on stock performance/selection prediction in comparison with the previous survey. Instead, our survey indicated that there were more in-depth

Table 2
Neural network characteristics by article^a

Article	Language/tool	Learning paradigm	Computer operating environment
[19]	LENNS	NR	Fujitsu VPX 240/10 Vector Processor
[20]	MATLAB	Backpropagation	NR
[21]	NeuroForecaster	NR	NR
[22]	NR	ART-1	NR
[23]	NeuralWorks Professional II	Backpropagation	NR
[24]	NR	Backpropagation	NR
[25]	NR	Backpropagation	NR
[26]	NR	NR	NR
[27]	NR	Backpropagation	NR
[28]	NeuralWorks Professional II	Backpropagation	NR
[29]	C++	ART-1	Microcomputer
[30]	NR	Backpropagation	NR
[31]	NR	Frequency-Sensitive Competitive Learning	NR
[32]	NR	Backpropagation	NR
[33]	NR	Backpropagation	NR
[34]	BrainMaker, NeuralWorks Professional II/Plus	Backpropagation	486 Microcomputer
[35]	C++	Backpropagation	NR
[36]	Professional II	Backpropagation	NR
[37]	NR	Backpropagation	NR
[38]	ANSim, NeuroShell	Backpropagation, ART-2	NR
[39]	NR	Backpropagation	486 56 MHz Microcomputer
[40]	NR	Backpropagation	NR
[41]	NR	Backpropagation	NR
[42]	NR	Backpropagation	NR
[43]	NR	Backpropagation	NR
[44]	NR	NR	NR
[45]	NR	NR	NR
[46]	NR	NR	486 Microcomputer
[47]	NR	Fuzzy ART	486 Microcomputer
[48]	NeuralWares Professional II/Plus	Radial Basis Function, Backpropagation	NR
[49]	NR	Backpropagation	NR
[50]	NR	NR	NR
[51]	NR	Backpropagation	386 100 MHz Microcomputer
[52]	NR	Genetic Adaptive NN Training Algorithm	NR
[53]	NR	Backpropagation	NR
[54]	Borland C++	Backpropagation	486 DX 66 MHz Microcomputer
[55]	Parallel Distributed Processing Software	NR	ITEX 100 Image Processing System with Microcomputer
[56]	C	ART-1	486 DX 50 MHz Microcomputer
[57]	NR	Backpropagation	NR
[58]	NeuralWares Explorer	Backpropagation, Counter Propagation Network	NR

Table 2 (continued)

Article	Language/tool	Learning paradigm	Computer operating environment
[59]	C	NR	DEC Station 5000/120
[60]	C	Hopfield	UNIX
[61]	NR	ART-1	NR
[62]	NeuralWorks Professional II/Plus	NR	NR
[63]	NR	Radial Basis Function	NR
[64]	Turbo C	Backpropagation	486 with a Math Coprocessor Microcomputer
[65]	NR	Backpropagation, Modular	486 Microcomputer
[66]	C	Backpropagation	NEC EWS 4800 Workstation
[67]	C, SAS	Backpropagation	Apollo Workstation
[68]	NR	Backpropagation, Radial Basis Function	NR
[69]	NR	Backpropagation	Sun Sparc 20 Workstation
[70]	NR	Backpropagation	Sun Sparc, Pentium Dos Machine
[71]	Basic, Turbo C	Interactive Activation and Competition	586 Microcomputer
[72]	Basic, BrainMaker	Backpropagation	Microcomputer 8 MHz
[73]	NR	Backpropagation	NR
[74]	FORTRAN	NR	NR
[75]	NR	Backpropagation	Microcomputer
[76]	NR	Backpropagation	NR
[77]	NR	Backpropagation	NR
[78]	NR	Backpropagation	NR
[79]	NR	NR	NR
[80]	NR	Radial Basis Function	NR
[81]	NR	NR	Macintosh Quadra, DEC Station 5000/200
[82]	NR	NR	NR
[83]	PlaNet	NR	NR
[84]	NR	NR	HP-Apollo Workstation
[85]	FORTRAN	Backpropagation	Microcomputer
[86]	NR	Backpropagation	NR
[87]	NR	Backpropagation	NR
[88]	NR	Backpropagation	NR
[89]	NR	NR	NR
[90]	NeuralWorks Professional II/Plus	Backpropagation	486 33 MHz Microcomputer
[91]	NR	NR	NR
[92]	NR	NR	NR
[93]	C	NR	Microcomputer
[94]	NR	Backpropagation	NR
[95]	NR	Backpropagation	NR
[96]	NR	Backpropagation	NR
[97]	NR	Backpropagation	Microcomputer 20 MHz
[98]	NeuralWares Professional II, NeuralWares Predict	Backpropagation, Cascade Correlation	NR

(continued on next page)

Table 2 (continued)

Article	Language/tool	Learning paradigm	Computer operating environment
[99]	NETS, PlaNet v5.6	NR	NR
[100]	CNAPS-C	ART-1	CNAPS Neurocomputer
[101]	NR	Backpropagation	NR
[102]	NR	Backpropagation	Sun Ultrasparc 1
[103]	NR	Backpropagation	NR
[104]	NeuroForecaster	NR	486 50 MHz Microcomputer
[105]	NR	NR	486 Microcomputer
[106]	NR	NR	NR
[107]	NR	NR	NR
[108]	NR	Backpropagation	386 Microcomputer
[109]	MS C version 6.0	Backpropagation	Microcomputer
[110]	NR	Boltzmann Machine	NR
[111]	NR	Adaptive Linear Element (ADALINE), Adaptive Non-linear Element (ADANLINE), Backpropagation, Pocket Algorithm with Ratchet	NR
[112]	C++	Backpropagation	Microcomputer
[113]	NR	NR	NR
[114]	MATLAB, CELESTIN	Backpropagation	NR
[115]	NeuroShell 2	Backpropagation	NR
[116]	NR	ART-2	NR
[117]	NR	NR	NR
[118]	Microsoft Visual Basic 3.0, Ward System Group Neuro Windows	Backpropagation	NR
[119]	Gauss ANN	NR	NR
[120]	NR	NR	NR
[121]	FORTTRAN	Kohonen's Self Organizing Feature Map	Sun Sparc Station 330
[122]	NR	Backpropagation	NR
[123]	C	Backpropagation	NR
[124]	C++ for Windows	NR	486 66 MHz Microcomputer
[125]	NR	Backpropagation	NR
[126]	Turbo C++ , Logical Systems C	ARTMAP	486 33 MHz Microcomputer
[127]	NeuroShell	Backpropagation	NR
[128]	NR	Backpropagation	NR
[129]	NR	Backpropagation	Sun Sparc Workstation II
[130]	NR	Adaptive Heuristic Critic	NR
[131]	NR	NR	NR
[132]	NR	ART	NR
[133]	NR	Ontigenic	NR
[134]	C	Backpropagation	386 Microcomputer
[135]	NR	Hopfield, Backpropagation	486 333 MHz Microcomputer

Table 2 (continued)

Article	Language/tool	Learning paradigm	Computer operating environment
[136]	NR	NR	NR
[137]	NeuralWorks Professional II/Plus	Backpropagation	486 Microcomputer
[138]	NR	Backpropagation	NR
[139]	NR	Kohonen	NR
[140]	PlaNet v5.6	NR	NR
[141]	C, SNNS	Backpropagation	Sun Sparc 5 Workstation
[142]	NTRAIN	NR	486 DX 266 MHz Microcomputer
[143]	NR	ART-1	386 Microcomputer
[144]	NR	ART-1/KS, ART-1/KSC, Fuzzy ART	NR
[145]	NR	ART-2, ART-2A, Cascade Correlation	NR
[146]	NR	Backpropagation, Parallel Layer Weight Recursive Least-Squares, QR Decomposition Algorithm	NR
[147]	NR	Backpropagation	NR
[148]	C++	NR	IBM RS/6000
[149]	NR	Kohonen	NR
[150]	NR	NR	NR
[151]	NR	Backpropagation	NR
[152]	NR	Backpropagation, Probabilistic Neural Network, Recurrent Neural Network	NR
[153]	NR	NR	NR
[154]	NR	Backpropagation, Hopfield	NR
[155]	NR	Backpropagation	NR
[156]	NR	ART-2	NR
[157]	Pascal	Backpropagation	NR
[158]	C	Boltzmann Machine	Sun Sparc, SLC, NeXT computer
[159]	C++	NR	IBM RS/6000
[160]	NR	Backpropagation, Neocognitron, Hopfield	NR
[161]	NR	Backpropagation	NR
[162]	NR	Backpropagation	Microcomputer
[163]	NR	NR	NR
[164]	NR	Backpropagation	NR
[165]	NR	Backpropagation	NR
[166]	C	NR	NR
[167]	Hybrid Backpropagation, Turbo-Pascal, Turbo Vision	NR	486 50 MHz Microcomputer

(continued on next page)

Table 2 (continued)

Article	Language/tool	Learning paradigm	Computer operating environment
[168]	Freeware Program Developed at U. of Bari	Backpropagation	NR
[169]	NR	NR	NR
[170]	NR	Backpropagation	SIMD Type of Parallel Computer with 256 Processor
[171]	NR	CMAC	NR
[172]	NR	Backpropagation	NR
[173]	UNIK-NEURO	NR	Sun Sparc
[174]	UNIK-NN	Backpropagation	NR
[175]	NeuralWorks Professional v5.0	SOFM, LVQ	NR
[176]	NR	Backpropagation	486 DX 66 MHz Microcomputer
[177]	NR	Backpropagation	HNC neurocomputer
[178]	N-NET	NR	Microcomputer
[179]	NR	Hebbian, Backpropagation	NR
[180]	Visual Basic	Backpropagation	Microcomputer
[181]	<i>Mathematica</i> tool	NR	Pentium 133 MHz Microcomputer
[182]	Turbo C	ART-1	NR
[183]	NR	Enhanced CMAC	486 Microcomputer
[184]	C	Backpropagation	NR
[185]	NR	Kohonen's Feature Map Algorithm	Cray Super Computer
[186]	NR	Backpropagation	NR
[187]	BrainMaker	Backpropagation	386 DX 40 Microcomputer
[188]	NR	NR	NR
[189]	NeuroShell 2	Backpropagation, General Regression NN	386 Microcomputer
[190]	NeuroShell 2	Backpropagation, General Regression NN, Probabilistic Neural Network	NR
[191]	C, SIMAN	Fuzzy ARTMAP	Intel's Personal Supercomputer (IPSC)
[192]	NR	NR	NR
[193]	NR	Radial Basis Function	NR
[194]	NeuralWorks Professional II	NR	NR
[195]	NR	NR	NR
[196]	C	Hopfield	486 33 MHz Microcomputer
[197]	NR	NR	NR
[198]	NR	Backpropagation	NR
[199]	MATLAB	Kohonen	NR
[200]	KBS-Class	NR	NR
[201]	NR	Backpropagation	NR
[202]	NR	Kohonen's Unsupervised Feature-Maps, Backpropagation	NR
[203]	SAS	Backpropagation	Microcomputer
[204]	NeuralWorks Professional II	NR	NR
[205]	CATPAC	Clustering Algorithm	NR

Table 2 (continued)

Article	Language/tool	Learning paradigm	Computer operating environment
[206]	NR	General Regression NN, Backpropagation	NR
[207]	NR	General Regression NN	NR
[208]	NR	Backpropagation	NR
[209]	NR	NR	NR
[210]	NR	Backpropagation	NR
[211]	NR	Neuro-Fuzzy GMDH algorithm	NR
[212]	NR	NR	NR
[213]	NR	Backpropagation	NR
[214]	NR	Backpropagation	NR
[215]	C	NR	NR
[216]	NR	Backpropagation	NR
[217]	NR	Reinforcement Network	NR
[218]	C	Backpropagation, Sum-of-Product Algorithm, Hybrid Sum-of-Products Algorithm	486 Microcomputer
[219]	NR	NR	486 Microcomputer
[220]	NR	Kohonen SOM	NR
[221]	NR	NR	NR
[222]	NR	NR	NR
[223]	BrainMaker	Backpropagation	486 DX 66 MHz Microcomputer
[224]	NR	Backpropagation	NR
[225]	NR	Backpropagation	NR
[226]	NR	Modified Backpropagation	Sun-4 Machine
[227]	NR	Backpropagation	Convex-C240
[228]	NETS Software	NR	386 SX 25 Microcomputer
[229]	NR	NR	NR
[230]	NR	Backpropagation	NR
[231]	NR	NR	NR
[232]	NR	NR	NR
[233]	NR	NR	NR
[234]	NeuroShell	NR	NR
[235]	NR	NR	NR
[236]	NR	Backpropagation	NR
[237]	NR	NR	NR
[238]	NR	Cluster Centre Seeking (CCS) Algorithm	NR
[239]	NR	Backpropagation	NR
[240]	FORTTRAN	NR	IBM Mainframe
[241]	NR	Backpropagation	NR
[242]	NR	NR	NR
[243]	NR	Extension to Hopfield, Cohen-Grossberg	NR
[244]	NR	Back-Percolation Algorithm	NR
[245]	Predict	NR	NR
[246]	C	Modified Hopfield Network	Sun Sparc 2 Workstation
[247]	NR	CMAC	NR

(continued on next page)

Table 2 (continued)

Article	Language/tool	Learning paradigm	Computer operating environment
[248]	NR	Hopfield, Boltzmann	NEC PC-980/DA
[249]	NR	NR	NR
[250]	Quick C, NeuralWares Nworks Explorer	Backpropagation	NR
[251]	NR	SOFM	NR
[252]	NR	Backpropagation, Newton-Raphson Algorithm	NR
[253]	GRG2-Based System	Backpropagation	IBM RS/6000 model 530
[254]	BrainMaker	Backpropagation	Microcomputer 90 MHz
[255]	NR	NR	NR
[256]	NR	Radial Basis Function	NR
[257]	NeuroShell 2	Backpropagation	386 Microcomputer
[258]	NR	Backpropagation	386 33 MHz Microcomputer
[259]	Pascal	Quickprop Algorithm, Cascade-Correlation	NR
[260]	NR	NR	NR
[261]	NR	Backpropagation	NR
[262]	NR	SOF, Hopfield	NR
[263]	NR	Hopfield	NR
[264]	NR	NR	NR
[265]	BrainMaker	NR	Microcomputer
[266]	NR	Backpropagation, ART	NR
[267]	NR	NR	NR
[268]	NR	Cascade Correlation	NR
[269]	NR	Backpropagation	386 Microcomputer
[270]	NR	Probabilistic Neural Networks	NR
[271]	Parallel Distributed Processing Software	NR	486 DX2 Microcomputer
[272]	NR	ART	Microcomputer
[273]	NR	SOM	486 Microcomputer
[274]	NR	NR	NR
[275]	FORTAN 77	Fuzzy ART, ART-1	IBM 4381 Mainframe
[276]	NR	Fuzzy ART	Notebook
[277]	NR	NR	NR
[278]	NR	General Regression NN	NR
[279]	C	NR	DEC Station 5000/200 Ultrix Work- station
[280]	WinNN™	Backpropagation	Microcomputer
[281]	NR	Radial Basis Function	NR
[282]	NR	Backpropagation	NR
[283]	C	SOFM	Sun Sparc 10 Workstation
[284]	ASPIRIN/MIGRAINES	NR	NR
[285]	NR	Backpropagation	Sun Sparc 10, HP9000/710 computer
[286]	NR	Backpropagation	NR

Table 2 (continued)

Article	Language/tool	Learning paradigm	Computer operating environment
[287]	NR	Backpropagation	NR
[288]	NR	NR	NR
[289]	NR	Backpropagation	NR
[290]	NR	NR	NR
[291]	NR	Hopfield-Tank Network	NR
[292]	NR	NR	NR
[293]	MATLAB	Backpropagation	NR
[294]	NR	Competitive Learning, ART, SOFM	Microcomputer
[295]	C	NR	NR
[296]	SunNet Simulator	Backpropagation	SUN 4
[297]	NR	Backpropagation	486 DX2 33 MHz Microcomputer
[298]	NR	Backpropagation	NR
[299]	NR	Radial Basis Function	NR
[300]	NR	NR	NR
[301]	NR	Monotonic Backpropagation	NR
[302]	NR	Monotonic Backpropagation	NR
[303]	NR	Backpropagation	NR
[304]	NR	NR	NR
[305]	NR	Backpropagation	NR
[306]	NR	Backpropagation	NR
[307]	C	Counterpropagation	SUN Microsystem
[308]	NR	Convergence Algorithm	NR
[309]	BrainMaker	Backpropagation	Microcomputer
[310]	NR	Backpropagation	NR
[311]	NR	General Regression NN	NR
[312]	NR	NR	NR
[313]	NevProp Software	Backpropagation	NR
[314]	@Brain, NeuroShell	NR	486 33 MHz Microcomputer
[315]	NR	Backpropagation	NR
[316]	C	Backpropagation	VAX 11/750
[317]	NR	NR	NR
[318]	NR	Backpropagation	NR
[319]	NR	Backpropagation	NR
[320]	MATLAB	Backpropagation	NR ^a

^aNR = not reported.

studies on stock market, including stock market index prediction [152,281], stock market holding period return investigation [312], stock market indexes structure testing [19], stock market volatility forecasting [44,92], stock's systematic risk forecasting [311].

In the information system area, there was only one study on software application in the last survey. However, our review had eight software application related studies, including software cost

Table 3
Top journals publishing neural network applications

Journal	Count
Computers and Industrial Engineering	37
International Journal of Production Research	30
Computers in Industry	23
European Journal of Operational Research	21
Decision Support Systems	18
IEEE Transactions on Systems, Man, and Cybernetics	16
Journal of Manufacturing Systems	10
IEEE Expert (Intelligent Systems & Their Applications)	9
Computers and Operations Research	8
IIE Transactions	8

estimation [169,247], software development [269], software development effort estimation [103,310], software fault prediction [255], software maintenance task effort prediction [140], and software quality prediction [168].

In terms of the computer platform, approximately 60% of the research studies used microcomputer in both surveys. Of 53 applications reporting the types of languages in this survey, only three (5.7%) studies used Pascal to develop neural networks. Since there was 29.2% in the last review, it is quite obvious that Pascal is not a popular language anymore. Instead, the percentage of using C/C++ has increased from 50% to approximately 67.9% (36 articles). It is also interesting to find that NeuralWorks Professional, NeuroShell, and BrainMaker remained the most popular tools, and backpropagation, ART, Hopfield, and Radial Basis Function were still the most common learning paradigms.

Both *Computers & Industrial Engineering* and *International Journal of Production Research* remained the most popular journals publishing neural network business applications in both surveys. Interestingly, *European Journal of Operational Research* was not in the ranking list in the last survey, but became the third most popular journal in this survey.

The majority of authors still came from academic institutions and remained almost the same percentage as compared with the last review. However, the percentage of US institutions has dropped from approximately 70 percent to less than 50 percent.

5. Future trend

There is no doubt that production/operations and finance will still be the most common research areas in the future. Three possible reasons are accounting for this: (1) production/operations and finance usually involve a lot of difficult, complex, and non-linear applications, and neural networks technology is a tool that can handle these problems efficiency and effectively; (2) the accessibility of raw data is relatively easy; and (3) there are many potential real-world applications in the area of production/operations and can, therefore, simulate academics' and practitioners' interest in conducting research.

Marketing/distribution is also a fast growing research area. More marketing researchers and practitioners are beginning to become aware of the value of neural networks in classification and forecasting since they have been applying this technology successfully in market segmentation and sales forecasting. In fact, some studies pointed out that neural networks could outperform other techniques/technologies traditionally used in the marketing analysis (e.g. [20,25,37,163]).

Academics and practitioners will be more interested in applying neural networks to explore real world applications and to conduct in-depth applications analysis, as evidenced by those applications in computer software and market segmentation/forecasting in our survey. This trend will probably continue since neural networks become a mature technology after more than 10 years' research in the business area.

Since there are many powerful neural network tools developed for the microcomputer platform, many researcher/developers still prefer to use microcomputers even though its processing speed could be a concern in some sophisticated applications. It should be noted here that these neural network tools always have upgrade versions with additional capabilities, such as NeuralWorks professional II/Plus v5.23, NeuralShell 2, and BrainMaker v3.7. This also explains why they can remain the most popular tools for development.

Those journals publishing production/operations will probably still dominate in the future since there are a variety of potential research applications in this area. Also, the relatively ease of accessing raw data and the actual implementation of real-world application simulate a lot of neural network research studies in the manufacturing environment.

Although there is an increasing percentage of non-US institutions involved in the development of neural network applications, the authors speculate that such growth will not persist. This is due to the fact that many countries' information technologies are not as advanced as that of US, and their adoption of neural network technology can lag behind a few years. Therefore, such an increase only reflects the fact that neural networks have started catching the attention of the non-US researchers/developers in the last five years.

6. Limitations of the study

Readers should be cautious in interpreting the results of this survey, since the findings are based on data collected only from journal articles. The results therefore do not include all actual neural network applications. Second, due to the lengthy journal review process, the neural networks reported in our surveyed articles are likely to lag behind the actual adoption of neural networks in the real world. Third, we have reviewed academic/professional journal articles only. Conference proceedings and doctoral dissertations are excluded, as we assume that high-quality research is eventually published in academic/professional journals. Also, many foreign journals and new journals might not be included in our review since they were not within the scope of our computer/manual search.

7. Conclusion

Our literature survey results and the comparisons with the previous review has revealed some insights into the trends of neural network research. It is hoped that this can help

researchers/practitioners to better understand the current status of this state-of-the-art technology in the business applications.

Acknowledgements

The authors would like to acknowledge Dr. Li Jiang, Ms. Yuen Chiu Yim, and Ms. Pui Sze So, for their assistance in this project.

References

- [1] Wong BK, Bodnovich TA, Selvi Y. A bibliography of neural network business applications research: 1988–September 1994. *Expert Systems* 1995;12:253–62.
- [2] Bose NK, Liang P. *Neural network fundamentals with graphs, algorithms, and applications*. New York: McGraw-Hill, 1996.
- [3] Browne A. *Neural network analysis, architectures, and applications*. Bristol, UK: Institute of Physics Publishing Company, 1997.
- [4] Chen CH. *Fuzzy logic and neural network handbook*. New York: McGraw-Hill, 1996.
- [5] De Wilde P. *Neural network models: an analysis*. UK: Springer, 1996.
- [6] De Wilde P. *Neural network models: theory and projects*. UK: Springer, 1997.
- [7] Golden RM. *Mathematical methods for neural network analysis and design*. Cambridge, MA: MIT Press, 1996.
- [8] Goonatilake S, Treleaven P. *Intelligent systems for finance and business*. Chichester: Wiley, 1995.
- [9] Hagan MT, Demuth HB, Beale MH. *Neural network design*. Boston: PWS Publishing Company, 1996.
- [10] Hunt KJ, Irwin G, Warwick K. *Neural network engineering in dynamic control systems*. Berlin: Springer, 1995.
- [11] Irwin GW, Warwick K, Hunt KJ. *Neural network applications in control*. UK: Institution of Electrical Engineers, 1995.
- [12] Korn GA. *Neural networks and fuzzy-logic control on personal computers and workstations*. Cambridge, MA: MIT Press, 1995.
- [13] Parks RW. *Fundamentals of neural network modeling: neuropsychology and cognitive neuroscience*. Cambridge, MA: MIT Press, 1998.
- [14] Rzepoluck EJ. *Neural network data analysis using simulnet*. Berlin: Springer, 1998.
- [15] Van Rooij AJF, Jain LC, Johnson RP. *Neural network training using genetic algorithms*. Singapore: World Scientific, 1996.
- [16] Gillenson M, Stutz J. Academic issues in MIS: journal and books. *MIS Quarterly* 1991;15:447–52.
- [17] Hamilton S, Ives B. The journal communication system for MIS research. *Database* 1983;14:3–14.
- [18] Hardgrave BC, Walstrom KA. Forums for MIS scholars. *Communications of the ACM* 1997;40:119–24.
- [19] Abhyankar A, Copeland LS, Wong W. Uncovering nonlinear structure in real-time stock-market indexes: the S&P 500, the DAX, the Nikkei 225, and the FTSE-100. *Journal of Business and Economic Statistics* 1997;15:1–14.
- [20] Agrawal D, Schorling C. Market share forecasting: an empirical comparison of artificial neural networks and multinomial logit model. *Journal of Retailing* 1996;72:383–407.
- [21] Aiken M, Krosp J, Vanjani M, Govindarajulu C, Sexton R. A neural network for predicting total industrial production. *Journal of End User Computing* 1995;7:19–23.
- [22] Al-Ghanim A. An unsupervised learning neural algorithm for identifying process behavior on control charts and a comparison with supervised learning approaches. *Computers and Industrial Engineering* 1997;32:627–39.
- [23] Albino V, Garavelli AC. A neural network application to subcontractor rating in construction firms. *International Journal of Project Management* 1998;16:9–14.
- [24] Altman EI, Marco G, Varetto F. Corporate distress diagnosis: comparisons using linear discriminant analysis and neural networks (the Italian experience). *Journal of Banking and Finance* 1994;18:505–29.

- [25] Ansuj AP, Camargo ME, Radharamanan R, Petry DG. Sales forecasting using time series and neural networks. *Computers and Industrial Engineering* 1996;31:421–4.
- [26] Arizono I, Kato M, Yamamoto A, Ohta H. A new stochastic neural network model and its application to grouping parts and tools in flexible manufacturing systems. *International Journal of Production Research* 1995;33:1535–48.
- [27] Athanassopoulos AD, Curram SP. A comparison of data envelopment analysis and artificial neural networks as tools for assessing the efficiency of decision making units. *Journal of the Operational Research Society* 1996;47:1000–16.
- [28] Badiru AB, Sieger DB. Neural network as a simulation metamodel in economic analysis of risky projects. *European Journal of Operational Research* 1998;105:130–42.
- [29] Bahrami A, Lynch M, Dagli CH. Intelligent design retrieval and packaging system: application of neural networks in design and manufacturing. *International Journal of Production Research* 1995;33:405–26.
- [30] Balakrishnan N, Chakravarty AK, Ghose S. Role of design-philosophies in interfacing manufacturing with marketing. *European Journal of Operational Research* 1997;103:453–69.
- [31] Balakrishnan PV, Cooper MC, Jacob VS, Lewis PA. Comparative performance of the FSCL neural net and K-means algorithm for market segmentation. *European Journal of Operational Research* 1996;93:346–57.
- [32] Baluja S. Evolution of an artificial neural network based autonomous land vehicle controller. *IEEE Transactions on Systems, Man, and Cybernetics* 1996;26:450–63.
- [33] Barada S, Singh H. Generating optimal adaptive fuzzy-neural models of dynamical systems with applications to control. *IEEE Transactions on Systems, Man, and Cybernetics — Part C: Applications and Reviews* 1998;28:371–91.
- [34] Barr DS, Mani G. Using neural nets to manage investments. *AI Expert* 1994;9:6–21.
- [35] Barschdorff D, Monostori L, Wöstenkühler GW, Egresits C, Kádár B. Approaches to coupling connectionist and expert systems in intelligent manufacturing. *Computers in Industry* 1997;33:5–15.
- [36] Bataineh S, Al-Anbuky A, Al-Aqtash S. An expert system for unit commitment and power demand prediction using fuzzy logic and neural networks. *Expert Systems* 1996;13:29–40.
- [37] Bejou D, Wray B, Ingram TN. Determinants of relationship quality: an artificial neural network analysis. *Journal of Business Research* 1996;36:137–43.
- [38] Benjamin CO, Chi S-C, Gaber T, Riordan CA. Comparing BP and ART II neural network classifiers for facility location. *Computers and Industrial Engineering* 1995;28:43–50.
- [39] Bode J. Decision support with neural networks in the management of research and development: concepts and application to cost estimation. *Information and Management* 1998;34:33–40.
- [40] Bode J. Neural networks for cost estimation. *Cost Engineering* 1998;40:25–30.
- [41] Boussabaine AH, Kaka AP. A neural networks approach for cost flow forecasting. *Construction Management and Economics* 1998;16:471–9.
- [42] Brockett PL, Cooper WW, Golden LL, Pitaktong U. A neural network method for obtaining an early warning of insurer insolvency. *The Journal of Risk and Insurance* 1994;61:402–24.
- [43] Brockett PL, Cooper WW, Golden LL, Xia X. A case study in applying neural networks to predicting insolvency for property and casualty insurers. *Journal of the Operational Research Society* 1997;48:1153–62.
- [44] Brooks C. Predicting stock index volatility: can market volume help?. *Journal of Forecasting* 1998;17:59–80.
- [45] Bugnon B, Stoffel K, Widmer M. FUN: a dynamic method for scheduling problems. *European Journal of Operational Research* 1995;83:271–82.
- [46] Burke L, Flanders S. Using ontogenic classification networks in a smart structures application. *Computers and Operations Research* 1995;22:871–81.
- [47] Burke L, Kamal S. Neural networks and the part family/machine group formation problem in cellular manufacturing: a framework using fuzzy ART. *Journal of Manufacturing Systems* 1995;14:148–59.
- [48] Burke LI, Storer RH, Lansing LL, Flanders SW. A neural-network approach to prediction of vehicle driving comfort. *IIE Transactions* 1996;28:439–52.
- [49] Callen JL, Kwan CCY, Yip PCY, Yuan Y. Neural network forecasting of quarterly accounting earnings. *International Journal of Forecasting* 1996;12:475–82.
- [50] Canarelli P. Analysing the past and managing the future using neural networks. *Futures* 1995;27:325–38.

- [51] Canepa G, Petrigliano R, Campanella M, de Rossi D. Detection of incipient object slippage by skin-like sensing and neural network processing. *IEEE Transactions on Systems, Man, and Cybernetics — Part B: Cybernetics* 1998;28:348–56.
- [52] Caporaletti LE, Dorsey RE, Johnson JD, Powell WA. A decision support system for in-sample simultaneous equation systems forecasting using artificial neural systems. *Decision Support Systems* 1994;11:481–95.
- [53] Carvalho P, Costa N, Ribeiro B, Dourado A. Industrial visual inspection of lime granules by neural networks. *Computers and Industrial Engineering* 1998;35:539–42.
- [54] Chang CA, Lo CC, Hsieh K-H. Neural networks and fourier descriptors for part positioning using bar code features in material handling systems. *Computers and Industrial Engineering* 1997;32:467–76.
- [55] Chang CA, Su C-T. A comparison of statistical regression and neural network methods in modeling measurement errors for computer vision inspection systems. *Computers and Industrial Engineering* 1995;28:593–603.
- [56] Chang CA, Tsai CY. Using ART1 neural networks with destructive solid geometry for design retrieving systems. *Computers in Industry* 1997;34:27–41.
- [57] Chang SL, Aw CA. A neural fuzzy control chart for detecting and classifying process mean shifts. *International Journal of Production Research* 1996;34:2265–78.
- [58] Chattopadhyay SP. Neural network approach for assessing country risk for foreign investment. *International Journal of Management* 1997;14:159–67.
- [59] Chen H, Ng T. An algorithmic approach to concept exploration in a large knowledge network (Automatic Thesaurus Consultation): symbolic branch-and-bound search vs. connectionist hopfield net activation. *Journal of the American Society for Information Science* 1995;46:348–69.
- [60] Chen H, Zhang Y, Houston AL. Semantic indexing and searching using a hopfield net. *Journal of Information Science* 1998;24:3–18.
- [61] Chen SJ, Cheng CS. A neural network-based cell formation algorithm in cellular manufacturing. *International Journal of Production Research* 1995;33:293–318.
- [62] Chen SK, Mangiameli P, West D. The comparative ability of self-organizing neural networks to define cluster structure. *Omega: The International Journal of Management Science* 1995;23:271–9.
- [63] Chen Y, Li X, Orady E. Integrated diagnosis using information-gain-weighted radial basis function neural networks. *Computers and Industrial Engineering* 1996;30:243–55.
- [64] Cheng C-S. A multi-layer neural network model for detecting changes in the process mean. *Computers and Industrial Engineering* 1995;28:51–61.
- [65] Cheng C-S. A neural network approach for the analysis of control chart patterns. *International Journal of Production Research* 1997;35:667–97.
- [66] Cheng R, Tozawa T, Gen M, Kato H, Takayama Y. AE behaviors evaluation with BP neural network. *Computers and Industrial Engineering* 1996;31:867–71.
- [67] Chiang WC, Urban TL, Baldrige GW. A neural network approach to mutual fund net asset value forecasting. *Omega: The International Journal of Management Science* 1996;24:205–15.
- [68] Chinnam RB, Kolarik WJ. Neural network-based quality controllers for manufacturing systems. *International Journal of Production Research* 1997;35:2601–20.
- [69] Cho S, Jang M, Yoon S, Cho Y, Cho H. A hybrid neural-network/mathematical prediction model for tandem cold mill. *Computers and Industrial Engineering* 1997;33:453–6.
- [70] Christodoulou M, Gaganis V. Neural networks in manufacturing cell design. *Computers in Industry* 1998;36:133–8.
- [71] Chu C-H. An improved neural network for manufacturing cell formation. *Decision Support Systems* 1997;20:279–95.
- [72] Chu C-H, Widjaja D. Neural network system for forecasting method selection. *Decision Support Systems* 1994;12:13–24.
- [73] Chu X, Holm H. Product manufacturability control for concurrent engineering. *Computers in Industry* 1994;24:29–38.
- [74] Chung Y, Fischer GW. A neural algorithm for finding the shortest flow path for an automated guided vehicle system. *IIE Transactions* 1995;27:773–83.
- [75] Chung Y, Kusiak A. Grouping parts with a neural network. *Journal of Manufacturing Systems* 1994;13:262–75.

- [76] Church KB, Curram SP. Forecasting consumers' expenditure: a comparison between econometric and neural network models. *International Journal of Forecasting* 1996;12:255–67.
- [77] Coit DW, Smith AE. Solving the redundancy allocation problem using a combined neural network/genetic algorithm approach. *Computers and Operations Research* 1996;23:515–26.
- [78] Collins A, Evans A. Aircraft noise and residential property values an artificial neural network approach. *Journal of Transport Economics and Policy* 1994;28:175–97.
- [79] Connor JT. A robust neural network filter for electricity demand prediction. *Journal of Forecasting* 1996;15:437–58.
- [80] Cook DF, Chiu C-C. Using radial basis function neural networks to recognize shifts in correlated manufacturing process parameters. *IIE Transactions* 1998;30:227–34.
- [81] Cortez EM, Park SC, Kim S. The hybrid application of an inductive learning method and a neural network for intelligent information retrieval. *Information Processing and Management* 1995;31:789–813.
- [82] Cox LD, Al-Ghanim AM, Culler DE. A neural network-based methodology for machining knowledge acquisition. *Computers and Industrial Engineering* 1995;29:217–20.
- [83] Creese RC, Li L. Cost estimation of timber bridges using neural networks. *Cost Engineering* 1995;37:17–22.
- [84] Dagli C, Huggahalli R. Machine-part family formation with the adaptive resonance theory paradigm. *International Journal of Production Research* 1995;33:893–913.
- [85] D'Antone I. A parallel neural network implementation in a distributed fault diagnosis system. *Microprocessing and Microprogramming* 1994;40:305–13.
- [86] Dasgupta CG, Dispensa GS, Ghose S. Comparing the predictive performance of a neural network model with some traditional market response models. *International Journal of Forecasting* 1994;10:235–44.
- [87] Davis JT. Experience and auditors' selection of relevant information for preliminary control risk assessments. *Auditing: A Journal of Practice and Theory* 1996;15:16–37.
- [88] Davis JT, Massey AP, Lovell RER II. Supporting a complex audit judgment task: an expert network approach. *European Journal of Operational Research* 1997;103:350–72.
- [89] De la Garza JM, Rouhana KG. Neural networks versus parameter-based applications in cost estimating. *Cost Engineering* 1995;37:14–8.
- [90] Desai VS, Crook JN, Overstreet GA. A comparison of neural networks and linear scoring models in the credit union environment. *European Journal of Operational Research* 1996;95:24–37.
- [91] Didner RS. Intelligent systems at American Express. In: Goonatilake S, Treleaven P, editors. *Intelligent systems for finance and business*. Chichester: Wiley, 1995. p. 31–7.
- [92] Donaldson RG, Kamstra M. Forecast combining with neural networks. *Journal of Forecasting* 1996;15:49–61.
- [93] Doumas A, Mavrouidakis K, Gritzalis D, Katsikas S. Design of a neural network for recognition and classification of computer viruses. *Computers and Security* 1995;14:435–48.
- [94] Dropsy V. Do macroeconomic factors help in predicting international equity risk premia? testing the out-of-sample accuracy of linear and nonlinear forecasts. *Journal of Applied Business Research* 1996;12:120–32.
- [95] Dunk K, Lee C, Martin P. An attribute design method: a new approach to flexible welding machine design. *International Journal of Production Research* 1994;32:2525–40.
- [96] Dunston PS, Ranjithan S, Bernold LE. Neural network model for the automated control of springback in rebars. *IEEE Expert* 1996;11:45–9.
- [97] Dutta S, Shekhar S, Wong WY. Decision support in non-conservative domains: generalization with neural networks. *Decision Support Systems* 1994;11:527–44.
- [98] Eakins SG, Stansell SR, Buck JF. Analyzing the nature of institutional demand for common stocks. *Quarterly Journal of Business and Economics* 1998;37:33–48.
- [99] Eberts R, Habibi S. Neural network-based agents for integrating information for production systems. *International Journal of Production Economics* 1995;38:73–84.
- [100] Enke D, Ratanapan K, Dagli C. Machine-part family formation utilizing and ART1 neural network implemented on a parallel neuro-computer. *Computers and Industrial Engineering* 1998;34:189–205.
- [101] Eppinger SD, Huber CD, Pham VH. A methodology for manufacturing process signature analysis. *Journal of Manufacturing Systems* 1995;14:20–34.

- [102] Espuña A, Delgado A, Puigjaner L. Improved batch process performance by evolutionary modelling. *Computers in Industry* 1998;36:271–8.
- [103] Finnie GR, Witting GE, Desharnais J-M. A comparison of software effort estimation techniques: using function points with neural networks, case-based reasoning and regression models. *Journal of Systems Software* 1997;39:281–9.
- [104] Fish KE, Barnes JH, Aiken MW. Artificial neural networks: a new methodology for industrial market segmentation. *Industrial Marketing Management* 1995;24:431–8.
- [105] Franses PH, Draisma G. Recognizing changing seasonal patterns using artificial neural networks. *Journal of Econometrics* 1997;81:273–80.
- [106] Franses PH, Homelen PV. On forecasting exchange rates using neural networks. *Applied Financial Economics* 1998;8:589–96.
- [107] Funabashi M, Maeda A, Morooka Y, Mori K. Fuzzy and neural hybrid expert systems: synergetic AI. *IEEE Expert* 1995;10:32–40.
- [108] Furness P. Neural networks for data-driven marketing. In: Goonatilake S, Treleaven P, editors. *Intelligent systems for finance and business*. Chichester: Wiley, 1995. p. 73–6.
- [109] Gan R, Yang D. Case-based decision support system with artificial neural network. *Computers and Industrial Engineering* 1994;27:437–40.
- [110] Gen M, Tsujimura Y, Ishizaki S. Optimal design of a star-LAN using neural networks. *Computers and Industrial Engineering* 1996;31:855–9.
- [111] Glorfeld LW, Hardgrave BC. An improved method for developing neural networks: the case of evaluating commercial loan creditworthiness. *Computers and Operations Research* 1996;23:933–44.
- [112] Goel V, Chen J. Application of expert network for material selection in engineering design. *Computers in Industry* 1996;30:87–101.
- [113] Gong D, Gen M, Yamazaki G, Xu W. Neural network approach for allocation with capacity. *Computers and Industrial Engineering* 1996;31:849–54.
- [114] Grabot B. Objective satisfaction assessment using neural nets for balancing multiple objectives. *International Journal of Production Research* 1998;36:2377–95.
- [115] Green BP, Choi JH. Assessing the risk of management fraud through neural network technology. *Auditing: A Journal of Practice and Theory* 1997;16:14–28.
- [116] Greska W, Franke V, Geiger M. Classification problems in manufacturing of sheet metal parts. *Computers in Industry* 1997;33:17–30.
- [117] Griffiths BJ, Wilkie B. A low-cost vision system combining conventional and artificial intelligence techniques for complex image inspection and verification. *International Journal of Production Research* 1995;33:2133–46.
- [118] Gruca TS, Klemz BR. Using neural networks to identify competitive market structures from aggregate market response data. *Omega: the International Journal of Management Science* 1998;26:49–62.
- [119] Haefke C, Helmenstein C. Forecasting Austrian IPOs: an application of linear and neural network error-correction models. *Journal of Forecasting* 1996;15:237–51.
- [120] Hanna MM, Buck A, Smith R. Fuzzy petri nets with neural networks to model products quality form a CNC-milling machining centre. *IEEE Transactions on Systems, Man, and Cybernetics* 1996;26:638–45.
- [121] Hao G, Lai KK. Solving the AGV problem via a self-organizing neural network. *Journal of Operational Research Society* 1996;47:1477–93.
- [122] Hill T, O'Connor M, Remus W. Neural network models for time series forecasts. *Management Science* 1996;42:1082–92.
- [123] Hill T, Remus W. Neural network models for intelligent support of managerial decision making. *Decision Support Systems* 1994;11:449–59.
- [124] Holter T, Yao X, Rabelo LC, Jones A, Yih Y. Integration of neural networks and genetic algorithms for an intelligent manufacturing controller. *Computers and Industrial Engineering* 1995;29:211–5.
- [125] Hua GB. Residential construction demand forecasting using economic indicators: a comparative study of artificial neural networks and multiple regression. *Construction Management and Economics* 1996;14:25–34.
- [126] Huang H-H, Wang H-PB. Machine fault diagnostics using a transputer network. *Computers and Industrial Engineering* 1996;30:269–81.

- [127] Hung S-Y, Liang T-P, Liu VW-C. Integrating arbitrage pricing theory and artificial neural networks to support portfolio management. *Decision Support Systems* 1996;18:301–16.
- [128] Hurriion RD. An example of simulation optimization using a neural network metamodel: finding the optimum number of kanbans in a manufacturing system. *Journal of Operational Research Society* 1997;48:1105–12.
- [129] Hutchinson JM, Lo AW, Poggio T. A nonparametric approach to pricing and hedging derivative securities via learning networks. *The Journal of Finance* 1994;49:851–89.
- [130] Hwang KS, Lin CS. Smooth trajectory tracking of three-link robot: a self-organizing CMAC approach. *IEEE Transactions on Systems, Man, and Cybernetics — Part B: Cybernetics* 1998;28:680–92.
- [131] Hwarng HB. Proper and effective training of a pattern recognizer for cyclic data. *IIE Transactions* 1995;27:746–56.
- [132] Hwarng HB, Chong CW. Detecting process non-randomness through a fast and cumulative learning ART-based pattern recognizer. *International Journal of Production Research* 1995;33:1817–33.
- [133] Ignizio JP, Soltys JR. Simultaneous design and training of ontogenic neural network classifiers. *Computers and Operations Research* 1996;23:535–46.
- [134] Jagannathan S. Automatic inspection of wave soldered joints using neural networks. *Journal of Manufacturing Systems* 1997;16:389–98.
- [135] Jain AS, Meeran S. Job-shop scheduling using neural networks. *International Journal of Production Research* 1998;36:1249–72.
- [136] Jain BA, Nag BN. Artificial neural network models for pricing initial public offerings. *Decision Sciences* 1995;26:283–302.
- [137] Jain BA, Nag BN. Performance evaluation of neural network decision models. *Journal of Management Information Systems* 1997;14:201–16.
- [138] Jamal AMM, Sundar C. Modeling exchange rates with neural networks. *Journal of Applied Business Research* 1997;14:1–5.
- [139] Johnson A, Fotouhi F. Adaptive indexing in very large databases. *Journal of Database Management* 1995;6:4–12.
- [140] Jørgensen M. Experience with the accuracy of software maintenance task effort prediction models. *IEEE Transactions on Software Engineering* 1995;21:674–81.
- [141] Jula P, Houshyar A, Severance FL, Sawhney A. Application of artificial neural networks in interactive simulation. *Computers and Industrial Engineering* 1996;31:417–20.
- [142] Kaastra I, Boyd MS. Forecasting futures trading volume using neural networks. *The Journal of Futures Markets* 1995;15:953–70.
- [143] Kamal S, Burke LI. Fact: a new neural network-based clustering algorithm for group technology. *International Journal of Production Research* 1996;34:919–46.
- [144] Kaparathi S, Suresh NC. Performance of selected part-machine grouping techniques for data sets of wide ranging sizes and imperfection. *Decision Sciences* 1994;25:515–39.
- [145] Keyvan S, Durg A, Nagaraj J. Application of artificial neural networks for the development of a signal monitoring system. *Expert Systems* 1997;14:69–79.
- [146] Khemaissia S, Morris A. Use of an artificial neuroadaptive robot model to describe adaptive and learning motor mechanisms in the central nervous system. *IEEE Transactions on Systems, Man, and Cybernetics — Part B: Cybernetics* 1998;28:404–16.
- [147] Khoshgoftaar TM, Lanning DL. A neural network approach for early detection of program modules having high risk in the maintenance phase. *Journal of Systems Software* 1995;29:85–91.
- [148] Kiang MY, Kulkarni UR, Tam KY. Self-organizing map network as an interactive clustering tool — an application to group technology. *Decision Support Systems* 1995;15:351–74.
- [149] Kim C-O, Min H-S, Yih Y. Integration of inductive learning and neural networks for multi-objective FMS scheduling. *International Journal of Production Research* 1998;36:2497–509.
- [150] Kim J, Hemami H. Coordinated three-dimensional motion of the head and torso by dynamic neural networks. *IEEE Transactions on Systems, Man, and Cybernetics — Part B: Cybernetics* 1998;28:653–66.
- [151] Kim JK, Park KS. Neural network-based decision class analysis for buliding topological-level influence diagram. *International Journal of Human — Computer Studies* 1997;47:513–30.
- [152] Kim SH, Chun SH. Graded forecasting using an array of bipolar predictions: application of probabilistic neural networks to a stock market index. *International Journal of Forecasting* 1998;14:323–37.

- [153] Kim SH, Lee CM. Nonlinear prediction of manufacturing systems through explicit and implicit data mining. *Computers and Industrial Engineering* 1997;33:461–4.
- [154] Kim T, Kumara SRT. Boundary defect recognition using neural networks. *International Journal of Production Research* 1997;35:2397–412.
- [155] Kim W, Lee JK. UNIK-OPT/NN neural network based adaptive optimal controller on optimization models. *Decision Support Systems* 1996;18:43–62.
- [156] Ko TJ, Cho DW, Jung MY. On-line monitoring of tool breakage in face milling using a self-organized neural network. *Journal of Manufacturing Systems* 1995;14:80–90.
- [157] Kramer B. N.E.W.S.: a model for the evaluation of non-life insurance companies. *European Journal of Operational Research* 1997;98:419–30.
- [158] Kryzanowski L, Galler M. Analysis of small-business financial statements using neural nets. *Journal of Accounting, Auditing and Finance* 1995;10:147–70.
- [159] Kulkarni UR, Kiang MY. Dynamic grouping of parts in flexible manufacturing systems — a self-organizing neural networks approach. *European Journal of Operational Research* 1995;84:192–212.
- [160] Kumar MJ, Patnaik LM. Mapping of artificial neural networks onto message passing systems. *IEEE Transactions on Systems, Man, and Cybernetics* 1996;26:822–35.
- [161] Kumar N, Krovi R, Rajagopalan B. Financial decision support with hybrid genetic and neural based modeling tools. *European Journal of Operational Research* 1997;103:339–49.
- [162] Kuo R-J. A robotic die polishing system through fuzzy neural networks. *Computers in Industry* 1997;32:273–80.
- [163] Kuo R-J, Xue KC. A decision support system for sales forecasting through fuzzy neural networks with asymmetric fuzzy weights. *Decision Support Systems* 1998;24:105–26.
- [164] Kuo R-J, Xue KC. An intelligent sales forecasting system through integration of artificial neural network and fuzzy neural network. *Computers in Industry* 1998;37:1–15.
- [165] Kusiak A, Lee H. Neural computing-based design of components for cellular manufacturing. *International Journal of Production Research* 1996;34:1777–90.
- [166] Lacher RC, Coats PK, Sharma SC, Fant LF. Theory and methodology a neural network for classifying the financial health of a firm. *European Journal of Operational Research* 1995;85:53–65.
- [167] Lachtermacher G, Fuller JD. Backpropagation in time-series forecasting. *Journal of Forecasting* 1995;14:381–93.
- [168] Lanubile F, Visaggio G. Evaluating predictive quality models derived from software measures: lessons learned. *Journal of Systems Software* 1997;38:225–34.
- [169] Lee A, Cheng CH, Balakrishnan J. Software development cost estimation: integrating neural network with cluster analysis. *Information and Management* 1998;34:1–9.
- [170] Lee HC, Dagli CH. A parallel genetic-neuro scheduler for job-shop scheduling problems. *International Journal of Production Economics* 1997;51:115–22.
- [171] Lee J. Measurement of machine performance degradation using a neural network model. *Computers in Industry* 1996;30:193–209.
- [172] Lee JK, Jhee WC. A two-stage neural network approach for ARMA model identification with ESACF. *Decision Support Systems* 1994;11:461–79.
- [173] Lee JK, Lee KJ, Park HK, Hong JS, Lee JS. Developing scheduling systems for Daewoo shipbuilding: DAS project. *European Journal of Operational Research* 1997;97:380–95.
- [174] Lee JK, Yum CS. Judgmental adjustment in time series forecasting using neural networks. *Decision Support Systems* 1998;22:135–54.
- [175] Lee KC, Han I, Kwon Y. Hybrid neural network models for bankruptcy predictions. *Decision Support Systems* 1996;18:63–72.
- [176] Lee S-K, Jang D. Translation, rotation and scale invariant pattern recognition using spectral analysis and hybrid genetic-neural-fuzzy networks. *Computers and Industrial Engineering* 1996;30:511–22.
- [177] Leigh D. Neural networks for credit scoring. In: Goonatilake S, Treleaven P, editors. *Intelligent systems for finance and business*. Chichester: Wiley, 1995. p. 61–9.
- [178] Lenard MJ, Alam P, Madey GR. The application of neural networks and a qualitative response model to the auditor's going concern uncertainty decision. *Decision Sciences* 1995;26:209–27.
- [179] Lewis FL. Neural network control of robot manipulators.. *IEEE Expert* 1996;11:64–75.

- [180] Li X, Ang CL, Gay R. An intelligent scenario generator for strategic business planning. *Computers in Industry* 1997;34:261–9.
- [181] Li Y, Ida K, Gen M, Kobuchi R. Neural network approach for multicriteria solid transportation problem. *Computers and Industrial Engineering* 1997;33:465–8.
- [182] Liao TW, Lee KS. Integration of a feature-based CAD system and an ART1 neural model for GT coding and part family forming. *Computers and Industrial Engineering* 1994;26:93–104.
- [183] Lin C-C, Wang H-P. Performance analysis of rotating machinery using enhanced cerebellar model articulation controller (E-CMAC) neural networks. *Computers and Industrial Engineering* 1996;30:227–42.
- [184] Lin H, Yih Y, Salvendy G. Neural-network based fault diagnosis of hydraulic forging presses in China. *International Journal of Production Research* 1995;33:1939–51.
- [185] Lin X. Map displays for information retrieval. *Journal of the American Society for Information Science* 1997;48:40–54.
- [186] Lin Z-C, Chang H. Application of fuzzy set theory and back-propagation neural networks in progressive die design. *Journal of Manufacturing Systems* 1996;15:268–81.
- [187] Lu L-C, Chen W-H, Kim D, Hwang C-P. Artificial neural systems improve franchising decision making. *International Journal of Management* 1996;13:25–32.
- [188] Luther RK. An artificial neural network approach to predicting the outcome of Chapter 11 bankruptcy. *The Journal of Business and Economic Studies* 1998;4:57–73.
- [189] Luxhøj JT, Riis JO, Stensballe B. A hybrid econometric-neural network modeling approach for sales forecasting. *International Journal of Production Economics* 1996;43:175–92.
- [190] Luxhøj JT, Williams TP, Shyur H-J. Comparison of regression and neural network models for prediction of inspection profiles for aging aircraft. *IIE Transactions* 1997;29:91–101.
- [191] Malkani A, Vassiliadis CA. Parallel implementation of the fuzzy ARTMAP neural network paradigm on a hypercube. *Expert Systems* 1995;12:39–53.
- [192] Mann LH. Gaining global insights: using neural networks for marketing research can give you access to uncharted territories. *Marketing Research* 1997;9:24–30.
- [193] Mantri S, Bullock D, Garrett J. Vehicle detection using a hardware-implemented neural net. *IEEE Expert* 1997;12:15–21.
- [194] Markham IS, Ragsdale CT. Combining neural networks and statistical predictions to solve the classification problem in discriminant analysis. *Decision Sciences* 1995;26:229–42.
- [195] Massone LLE, Myers JD. The role of plant properties in arm trajectory formation: a neural network study. *IEEE Transactions on Systems, Man, and Cybernetics* 1996;26:719–32.
- [196] Mautser HE, Magazine MJ. Comparison of neural and heuristic methods for a timetabling problem. *European Journal of Operational Research* 1996;93:271–87.
- [197] Mei J, Zhang H-C, Oldham WJB. A neural network approach for datum selection in computer-aided process planning. *Computers in Industry* 1995;27:53–64.
- [198] Mezgár I, Egresits C, Monostori L. Design and real-time reconfiguration of robust manufacturing systems by using design of experiments and artificial neural networks. *Computers in Industry* 1997;33:61–70.
- [199] Min H-S, Yih Y, Kim C-O. A competitive neural network approach to multi-objective FMS scheduling. *International Journal of Production Research* 1998;36:1749–65.
- [200] Modin J. KBS-CLASS: a neural network tool for automatic content recognition of building texts. *Construction Management and Economics* 1995;13:411–6.
- [201] Moghrabi C, Eid MS. Modeling users through an expert system and a neural network. *Computers and Industrial Engineering* 1998;35:583–6.
- [202] Monostori L, Egresits C. On hybrid learning and its application in intelligent manufacturing. *Computers in Industry* 1997;33:111–7.
- [203] Moon H-S, Na S-J. A neuro-fuzzy approach to select welding conditions for welding quality improvement in horizontal fillet welding. *Journal of Manufacturing Systems* 1996;15:392–403.
- [204] Moon YB, Janowski R. A neural network approach for smoothing and categorizing noisy data. *Computers in Industry* 1995;26:23–39.
- [205] Moore K, Burbach R, Heeler R. Using neural nets to analyze qualitative data by reducing the complexity of text data, automated coding saves time and money. *Marketing Research* 1995;7:35–9.

- [206] Morrison J, Lee T. Forecasting nonpayment behavior of customers for a mail order company. *The Journal of Business Forecasting* 1996;15:11–4.
- [207] Morrison JR, Johnson JD, Barnes JH, Summers K, Szeinbach SL. Predicting total health care costs of medicaid recipients: an artificial neural systems approach. *Journal of Business Research* 1997;40:191–7.
- [208] Moussa MA. An experiment in approximating an end effector positional error of a 6 D.O.F. manipulator using neural network. *Computers and Industrial Engineering* 1998;35:547–50.
- [209] Moussa MA, Kamel MS. Requirements and design of a grasping system for personal robots. *Computers and Industrial Engineering* 1998;35:475–8.
- [210] Mozer MC. Neural-network speech processing for toys and consumer electronics. *IEEE Expert* 1996;11:4–5.
- [211] Nagasaka K, Ichihashi H, Leonard R. Neuro-fuzzy GMDH and its application to modelling grinding characteristics. *International Journal of Production Research* 1995;33:1229–40.
- [212] Nam K, Schaefer T. Forecasting international airline passenger traffic using neural networks. *Logistics and Transportation Review* 1995;31:239–51.
- [213] Nam K, Yi J, Prybutok VR. Predicting airline passenger volume. *The Journal of Business Forecasting* 1997;16:14–6.
- [214] Nath R, Rajagopalan B, Ryker R. Determining the saliency of input variables in neural network classifiers. *Computers and Operations Research* 1997;24:767–73.
- [215] Nikolopoulos C, Fellrath P. A hybrid expert system for investment advising. *Expert Systems* 1994;11:245–50.
- [216] Ntungo C, Boyd M. Commodity futures trading performance using neural network models versus ARIMA models. *The Journal of Futures Markets* 1998;18:965–83.
- [217] Nuttin M, Brussel HV. Learning the peg-into-hole assembly operation with a connectionist reinforcement technique. *Computers in Industry* 1997;33:101–9.
- [218] Obaidat MS, Macchiarolo DT. A multilayer neural network system for computer access security. *IEEE Transactions on Systems, Man, and Cybernetics* 1994;24:806–13.
- [219] Oh S-Y, Part H-G, Nam S-H. A neural network-based real-time robot tracking controller using position sensitive detectors. *Expert Systems* 1995;12:115–22.
- [220] Orwig RE, Chen H, Nunamaker JF. A graphical, self-organizing approach to classifying electronic meeting output. *Journal of the American Society for Information Science* 1997;48:157–70.
- [221] Pantazopoulos KN, Tsoukalas LH, Bourbakis NG, Brün MJ, Houstis EN. Financial prediction and trading strategies using neurofuzzy approaches. *IEEE Transactions on Systems, Man, and Cybernetics — Part B: Cybernetics* 1998;28:520–31.
- [222] Parhizgari AM, De Boyrie ME. Predicting spot exchange rates in a nonlinear estimation framework using futures prices. *The Journal of Futures Markets* 1997;17:935–56.
- [223] Petri KL, Billo RE, Bidanda B. A neural network process model for abrasive flow machining operations. *Journal of Manufacturing Systems* 1998;17:52–64.
- [224] Philipoom PR, Rees LP, Wiegmann L. Using neural networks to determine internally-set due-date assignments for shop scheduling. *Decision Sciences* 1994;25:825–51.
- [225] Pican N, Alexandre F, Bresson P. Artificial neural networks for the presetting of a steel temper mill. *IEEE Expert* 1996;11:22–7.
- [226] Piramuthu S, Ragavan H, Shaw MJ. Using feature construction to improve the performance of neural networks. *Management Science* 1998;44:416–30.
- [227] Piramuthu S, Shaw MJ, Gentry JA. A classification approach using multi-layered neural networks. *Decision Support Systems* 1994;11:509–25.
- [228] Pu H-C, Hung Y-T. Use of artificial neural networks: predicting trickling filter performance in a municipal wastewater treatment plant. *Environmental Management and Health* 1995;6:16–27.
- [229] Purnomo MH, Tada A, Shimizu E. Beam landing adjustment for color purity of integrated tube component using artificial neural network. *Computers and Industrial Engineering* 1995;29:153–7.
- [230] Purushothaman S, Srinivasa YG. A procedure for training an artificial neural network with application to tool wear monitoring. *International Journal of Production Research* 1998;36:635–51.
- [231] Quah T-S, Tan C-L, Raman KS, Srinivasan B. Towards integrating rule-based expert systems and neural networks. *Decision Support Systems* 1996;17:99–118.

- [232] Quah T-S, Tan C-L, Raman KS, Teh H-H, Srinivasan BS. A shell environment for developing connectionist decision support systems. *Expert Systems* 1994;11:225–34.
- [233] Quiroga LA, Rabelo LC. Learning from examples: a review of machine learning, neural networks and fuzzy logic paradigms. *Computers and Industrial Engineering* 1995;29:561–5.
- [234] Raggad BG. Neural network technology for knowledge resource management. *Management Decision* 1996;34:20–4.
- [235] Ramirez-Beltran ND, Montes JA. Neural networks for on-line parameter change detections in time series models. *Computers and Industrial Engineering* 1997;33:337–40.
- [236] Ransing RS, Lewis RW. A semantically constrained neural network for manufacturing diagnosis. *International Journal of Production Research* 1997;35:2639–60.
- [237] Rao HA, Gu P. Expert self-organizing neural network for the design of cellular manufacturing systems. *Journal of Manufacturing Systems* 1994;13:346–58.
- [238] Rao HA, Gu P. A multi-constraint neural network for the pragmatic design of cellular manufacturing systems. *International Journal of Production Research* 1995;33:1049–70.
- [239] Refenes AN, Zaprainis AD, Connor JT, Bunn DW. Neural networks in investment management. In: Goonatilake S, Treleaven P, editors. *Intelligent systems for finance and business*. Chichester: Wiley, 1995 p. 177–208.
- [240] Reynolds SB, Mellichamp JM, Smith RE. Box-jenkins forecast model identification. *AI Expert* 1995;10:15–28.
- [241] Rietman EA, Patel SH, Lory ER. Modeling and control of a semiconductor manufacturing process with an automata network: an example in plasma etch processing. *Computers and Operations Research* 1996;23:573–85.
- [242] Rogers J. Neural network user authentication. *AI Expert* 1995;10:29–33.
- [243] Rovithakis GA, Christodoulou MA. Neural adaptive regulation of unknown nonlinear dynamical systems. *IEEE Transactions on Systems, Man, and Cybernetics* 1997;27:10–22.
- [244] Ruggiero MA. Training neural nets for intermarket analysis. *Futures* 1994;23:42–4.
- [245] Ruggiero MA. Build a real neural net. *Futures* 1995;24:44–6.
- [246] Sabuncuoglu I, Gurgun B. A neural network model for scheduling problems. *European Journal of Operational Research* 1996;93:288–99.
- [247] Samson B, Ellison D, Dugard P. Software cost estimation using an albus perceptron (CMAC). *Information and Software Technology* 1997;39:55–60.
- [248] Satake T, Morikawa K, Nakamura N. Neural network approach for minimizing the makespan of the general job-shop. *International Journal of Production Economics* 1994;33:67–74.
- [249] Schlang M, Poppe T, Gramchow O. Neural networks for steel manufacturing. *IEEE Expert* 1996;11:8–9.
- [250] Schmidt DC, Haddock J, Marchandon S, Runger GC, Wallace WA, Wright RN. A methodology for formulating, formalizing, validating, and evaluating a real-time process control advisor. *IIE Transactions* 1998;30: 235–45.
- [251] Serrano-Cinca C. Self organizing neural networks for financial diagnosis. *Decision Support Systems* 1996;17:227–38.
- [252] Setiono R, Thong JYL, Yap C-S. Symbolic rule extraction from neural networks an application to identifying organizations adopting IT. *Information and Management* 1998;34:91–101.
- [253] Shanker M, Hu MY, Hung MS. Effect of data standardization on neural network training. *Omega: The International Journal of Management Science* 1996;24:385–97.
- [254] Shen Y, Moon S. Mapping of probe pretravel in dimensional measurements using neural networks computational technique. *Computers in Industry* 1997;34:295–306.
- [255] Sherer SA. Software fault prediction. *Journal of Systems Software* 1995;29:97–105.
- [256] Shin YC, Vishnupad P. Neuro-fuzzy control of complex manufacturing processes. *International Journal of Production Research* 1996;34:3291–309.
- [257] Shyr HJ, Luxhøj JT, Williams TP. Using neural networks to predict component inspection requirements for aging aircraft. *Computers and Industrial Engineering* 1996;30:257–67.
- [258] Sim SK, Yeo KT, Lee WH. An expert neural network system for dynamic job shop scheduling. *International Journal of Production Research* 1994;32:1759–73.
- [259] Siriopoulos C, Perantonis S, Karakoulos G. Artificial intelligence models for financial decision making. *Information Strategy: The Executive's Journal* 1994;11:49–54.

- [260] Smith AE. X-bar and R control chart interpretation using neural computing. *International Journal of Production Research* 1994;32:309–20.
- [261] Smith AE, Mason AK. Cost estimation predictive modeling: regression versus neural network. *The Engineering Economist* 1997;42:137–61.
- [262] Smith K, Palaniswami M, Krishnamoorthy M. A hybrid neural approach to combinatorial optimization. *Computers and Operations Research* 1996;23:597–610.
- [263] Smith K, Palaniswami M, Krishnamoorthy M. Traditional heuristic versus hopfield neural network approaches to a car sequencing problem. *European Journal of Operational Research* 1996;93:300–16.
- [264] Smith PA, MacLin OH. Have presidents influenced monetary policy: new evidence from an artificial neural network. *Studies in Economics and Finance* 1995;16:23–45.
- [265] Sohl JE, Venkatachalam AR. A neural network approach to forecasting model selection. *Information and Management* 1995;29:297–303.
- [266] Song IR, Yang T, Chen JJ-G. Enhanced exchange heuristic based resource constrained scheduler using ARTMAP. *Computers and Industrial Engineering* 1997;33:469–72.
- [267] Spall JC, Cristion JA. A neural network controller for systems with unmodeled dynamics with applications to wastewater treatment. *IEEE Transactions on Systems, Man, and Cybernetics* 1997;27:369–75.
- [268] Spoerre JK. Application of the cascade correlation algorithm (CCA) to bearing fault classification problems. *Computers in Industry* 1997;32:295–304.
- [269] Srinivasan K, Fisher D. Machine learning approaches to estimating software development effort. *IEEE Transactions on Software Engineering* 1995;21:126–37.
- [270] Steiner M, Wittkemper H-G. Portfolio optimization with a neural network implementation of the coherent market hypothesis. *European Journal of Operational Research* 1997;100:27–40.
- [271] Su C-T, Chang CA, Tien F-C. Neural networks for precise measurement in computer vision systems. *Computers in Industry* 1995;27:225–36.
- [272] Su C-T, Tong L-I. A neural network-based procedure for the process monitoring of clustered defects in integrated circuit fabrication. *Computers in Industry* 1997;34:285–94.
- [273] Suh S-H, Shin Y-S. Neural network modeling for tool path planning of the rough cut in complex pocket milling. *Journal of Manufacturing Systems* 1996;15:295–304.
- [274] Sun G, Dagli CH, Thammano A. Dynamic neuro-fuzzy control of the nonlinear process. *Computers and Industrial Engineering* 1997;33:413–6.
- [275] Suresh NC, Kaparthi S. Performance of fuzzy ART neural network for group technology cell formation. *International Journal of Production Research* 1994;32:1693–713.
- [276] Suresh NC, Slomp J, Kaparthi S. The capacitated cell formation problem: a new hierarchical methodology. *International Journal of Production Research* 1995;33:1761–84.
- [277] Swanson NR, White H. A model-selection approach to assessing the information in the term structure using linear models and artificial neural networks. *Journal of Business and Economic Statistics* 1995;13:265–75.
- [278] Swanson NR, White H. A model selection approach to real-time macroeconomic forecasting using linear models and artificial neural networks. *Review of Economics and Statistics* 1997;79:540–50.
- [279] Taha MA, Park SC, Russell JS. Knowledge-based DSS for construction contractor prescreening. *European Journal of Operational Research* 1995;84:35–46.
- [280] Tana SS, Koh HC. A multi-layer perceptron model of credit scoring for assessing default risk in charge card applicants. *International Journal of Management* 1997;14:250–5.
- [281] Teixeira JC, Rodrigues AJ. An applied study on recursive estimation methods, neural networks and forecasting. *European Journal of Operational Research* 1997;101:406–17.
- [282] Tesauro GJ, Kephart JO, Sorkin GB. Neural networks for computer virus recognition. *IEEE Expert* 1996;11:5–6.
- [283] Torki A, Somhom S, Enkawa T. A competitive neural network algorithm for solving vehicle routing problem. *Computers and Industrial Engineering* 1997;33:473–6.
- [284] Tsang S, Magill EH. Learning to detect and avoid run-time feature interactions in intelligent networks. *IEEE Transactions on Software Engineering* 1998;24:818–30.
- [285] Tsuchiya K, Bharitkar S, Takefuji Y. A neural network approach to facility layout problems. *European Journal of Operational Research* 1996;89:556–63.

- [286] Tsuji T, Ito K, Morasso PG. Neural network learning of robot arm impedance in operational space. *IEEE Transactions on Systems, Man, and Cybernetics* 1996;26:290–8.
- [287] Tsuji T, Xu BH, Kaneko M. Adaptive control and identification using one neural network for a class of plants with uncertainties. *IEEE Transactions on Systems, Man, and Cybernetics — Part A: Systems and Humans* 1998;28:496–505.
- [288] Tsujimura Y, Gen M, Ishizaki S. Optimal routing in multiple I/O data network using neural network with perturbed energy function. *Computers and Industrial Engineering* 1997;33:477–80.
- [289] Tsukuda J, Baba S-I. Predicting Japanese corporate bankruptcy in term of financial data using neural network. *Computers and Industrial Engineering* 1994;27:445–8.
- [290] Twomey JM, Smith AE, Redfern MS. A predictive model for slip resistance using artificial neural networks. *IIE Transactions* 1995;27:374–81.
- [291] Vaithyanathan S, Burke LI, Magent MA. Massively parallel analog tabu search using neural networks applied to simple plant location problems. *European Journal of Operational Research* 1996;93:317–30.
- [292] Van Wezel MC, Baets WRJ. Predicting market responses with a neural network: the case of fast moving consumer goods. *Marketing Intelligence and Planning* 1995;13:23–30.
- [293] Vanherck P, Dehaes J, Nuttin D. Compensation of thermal deformations in machine tools with neural nets. *Computers in Industry* 1997;33:119–25.
- [294] Venugopal V, Narendran TT. Machine-cell formation through neural network models. *International Journal of Production Research* 1994;32:2105–16.
- [295] Versaggi MR. Understanding conflicting data. *AI Expert* 1995;10:21–5.
- [296] Villegas L, Eberts RE. A neural network tool for identifying text-editing goals. *International Journal of Human — Computer Studies* 1994;40:813–33.
- [297] Wadi I. Neural network model predicts naphtha cut point. *Oil and Gas Journal* 1996;25:67–70.
- [298] Wang C, Huang S-Z. A refined flexible inspection method for identifying surface flaws using the skeleton and neural network. *International Journal of Production Research* 1997;35:2493–507.
- [299] Wang G-N, Go YC. On-line neuro-tracking of non-stationary manufacturing processes. *Computers and Industrial Engineering* 1996;30:449–61.
- [300] Wang S. A dynamic perspective of differences between cognitive maps. *Journal of the Operational Research Society* 1996;47:538–49.
- [301] Wang S. Nonparametric econometric modeling: a neural network approach. *European Journal of Operational Research* 1996;89:581–92.
- [302] Wang S. Neural networks in generalizing expert knowledge. *Computers and Industrial Engineering* 1997;32:67–76.
- [303] Wang S, Archer NP. A neural network based fuzzy set model for organizational decision making. *IEEE Transactions on Systems, Man, and Cybernetics — Part C: Application and Reviews* 1998;28:194–203.
- [304] Wang YS, Griffiths BJ, Wilkie BA. A novel system for coloured object recognition. *Computers in Industry* 1996;32:69–77.
- [305] Wasserman GS, Sudjianto A. A comparison of three strategies for forecasting warranty claims. *IIE Transactions* 1996;28:967–77.
- [306] West PM, Brockett PL, Golden LL. A comparative analysis of neural networks and statistical methods for predicting consumer choice. *Marketing Science* 1997;16:370–91.
- [307] Whittaker AD, Cook DF. Counterpropagation neural network for modelling a continuous correlated process. *International Journal of Production Research* 1995;33:1901–10.
- [308] Wilson RL. A neural network approach to decision alternative prioritization. *Decision Support Systems* 1994;11:431–47.
- [309] Wilson RL, Sharda R. Bankruptcy prediction using neural networks. *Decision Support Systems* 1994;11:545–57.
- [310] Wittig G, Finnie G. Estimating software development effort with connectionist models. *Information and Software Technology* 1997;39:469–76.
- [311] Wittkemper H-G, Steiner M. Using neural networks to forecast the systematic risk of stocks. *European Journal of Operational Research* 1996;90:577–88.

- [312] Wong SQ, Long JA. A neural network approach to stock market holding period returns. *American Business Review* 1995;13:61–4.
- [313] Wood D, Dasgupta B. Classifying trend movements in the MSCI U.S.A. capital market index — a comparison of regression, arima and neural network methods. *Computers and Operations Research* 1996;23:611–22.
- [314] Worzala E, Lenk M, Silva A. An exploration of neural networks and its application to real estate valuation. *The Journal of Real Estate Research* 1995;10:185–201.
- [315] Yoeger L. Neural networks provide robust character recognition for Newton PDAs. *IEEE Expert* 1996;11:10–1.
- [316] Yoon Y, Guimaraes T, Swales G. Integrating artificial neural networks with rule-based expert systems. *Decision Support Systems* 1994;11:497–507.
- [317] Zahavi J, Levin N. Issues and problems in applying neural computing to target marketing. *Journal of Direct Marketing* 1995;9:33–45.
- [318] Zahavi J, Levin N. Issues and problems in applying neural computing to target marketing. *Journal of Direct Marketing* 1997;11:63–75.
- [319] Zahavi J, Levin N. Applying neural computing to target marketing. *Journal of Direct Marketing* 1997;11:76–93.
- [320] Zhang YF, Fuh JYH, Chan WT. Feature-based cost estimation for packaging products using neural networks. *Computers in Industry* 1996;32:95–113.

Bo K. Wong is currently an associate professor of Information Systems (IS) in the Department of IS, Lingnan University. His current research interests are in neural network and genetic algorithm business applications. He has published extensively in a variety of journals, including articles in *Journal of Decision Support Systems*, *European Journal of Operational Research*, *Information and Management*, *International Journal of Operations & Production Management*, and other professional Journals. Dr. Wong has also involved in consulting activities in many organizations, including 3M Company, Commercial Intertech Corporation, Delpi Packard Electric Systems, and The Open University of Hong Kong. He received the Most Distinguished Research Paper Award in the Society for the Advancement of Information Systems in 1996 and was listed in *Who's Who* in 1993.

Lai is an associate professor of MIS at the Chinese University of Hong Kong. His research focuses on database design, network management, business processing reengineering, and technology management. His articles on these topics have been published in the *Communications of the ACM*, *Data Base*, *Decision Support Systems*, *European Journal of Information Systems*, *IEEE Transactions on Engineering Management*, *Information and Management*, and many others.

Jolie Lam is currently a Ph.D. candidate in Management Information Systems at the City University of Hong Kong.

Adaptive neural control of aeroelastic response

Peter F. Lichtenwalner and Gerald R. Little

McDonnell Douglas Aerospace
McDonnell Douglas Corporation
St. Louis, Missouri 63166

and

Robert C. Scott

NASA Langley Research Center
Hampton, Virginia 23681

ABSTRACT

The Adaptive Neural Control of Aeroelastic Response (ANCAR) program is a joint research and development effort conducted by McDonnell Douglas Aerospace (MDA) and the National Aeronautics and Space Administration, Langley Research Center (NASA LaRC) under a Memorandum of Agreement (MOA). The purpose of the MOA is to cooperatively develop the smart structure technologies necessary for alleviating undesirable vibration and aeroelastic response associated with highly flexible structures. Adaptive control can reduce aeroelastic response associated with buffet and atmospheric turbulence, it can increase flutter margins, and it may be able to reduce response associated with nonlinear phenomena like limit cycle oscillations. By reducing vibration levels and loads, aircraft structures can have lower acquisition cost, reduced maintenance, and extended lifetimes.

Phase I of the ANCAR program involved development and demonstration of a neural network-based *semi-adaptive* flutter suppression system which used a neural network for scheduling control laws as a function of Mach number and dynamic pressure. This controller was tested along with a robust fixed-gain control law in NASA's Transonic Dynamics Tunnel (TDT) utilizing the Benchmark Active Controls Testing (BACT) wing. During Phase II, a *fully adaptive* on-line learning neural network control system has been developed for flutter suppression which will be tested in 1996. This paper presents the results of Phase I testing as well as the development progress of Phase II.

Keywords: Neural Networks, Active Vibration Control, Flutter Suppression, Smart Structures, Aeroservoelasticity

1. INTRODUCTION

The Adaptive Neural Control of Aeroelastic Response (ANCAR) program is a joint research and development effort conducted by McDonnell Douglas Aerospace (MDA) and the National Aeronautics and Space Administration, Langley Research Center (NASA LaRC) under a Memorandum of Agreement (MOA). The purpose of the MOA is to cooperatively develop and demonstrate the smart structure technologies necessary for alleviating undesirable vibration and aeroelastic response associated with highly flexible structures. Implementation of these technologies, which include neural networks, fiber optics, and adaptive materials, will enable future aircraft to be more lightweight and flexible, thereby increasing affordability.

1.1 Background

Aeroservoelasticity (ASE) is a multidisciplinary technology that deals with the interactions of an aircraft's flight control system, its flexible structure, and the aerodynamic forces resulting from its rigid-body and flexible motions. A major focus of ASE research and development has been the demonstration of advanced active control concepts that interact with and/or exploit the aeroelastic characteristics of flexible structures. Over the past quarter century, NASA LaRC has been involved in several wind tunnel test programs specifically focused on the demonstration of active control systems for flutter suppression.¹

These active flutter suppression (AFS) systems can be categorized as (1) non-adaptive (fixed-gain), (2) semi-adaptive, and (3) fully adaptive. All of these systems make use of feedback control techniques which utilize sensors for measuring the wing response and actuators for affecting the wing response. With the non-adaptive method, the control law is fixed for all time. The semi-adaptive method utilizes a variable gain controller which schedules the control law as a function of relevant parameters such as flight conditions. The fully adaptive method requires no prior knowledge and self-organizes to suppress flutter under a changing environment. This method is hence the most attractive, since it offers the greatest potential for overall performance, robustness, fault tolerance, and reduced control system design cost. A linear fully adaptive AFS system was developed and tested by General Dynamics using a 1/4 scale F-16 wind tunnel model with conventional sensors and actuators. Their final report² provides an excellent summary of the issues involved in developing adaptive AFS systems.

The motivation behind the ANCAR program lies in the application of smart structures technology for enabling future aircraft to be more lightweight and flexible. Smart structures utilize embedded fiber optics, piezoelectric transducers, shape memory alloys, and other advanced techniques for achieving widely distributed sensing and actuation within the structure. Advanced algorithms and processors are required to efficiently utilize the massive amount of data provided by a smart structure. Artificial neural networks, which provide effective large scale parallel processing and adaptation performance, are extremely attractive for implementing the "brain" of a smart structure. For this reason, the ANCAR MOA was drafted by NASA and MDA to cooperatively develop and test the neural network technology required for application of a smart structure flutter suppression system.

1.2 Program Objectives

The ANCAR program has been divided into three phases, with each phase defined below:

I. *Semi-Adaptive* Neural Control of Flutter on a Simple Wing with Conventional Aerodynamic Control Surfaces

II. *Fully Adaptive* Neural Control of Flutter on a Simple Wing with Conventional Aerodynamic Control Surfaces

III. *Fully Adaptive* Neural Control of Flutter on a *Smart Structure* Wing with Smart Material and Conventional Aerodynamic Actuators

The specific objective of Phase I was to apply neural network technology to improve control performance over that of a conventional fixed-gain controller. Implementing a semi-adaptive, pre-trained neural network controller was a low risk, conservative first step. The objective of Phase II is to use on-line learning neural networks to implement a fully adaptive, self-optimizing controller for AFS. Both Phases I and II are using NASA's Benchmark Active Controls Testing (BACT)³ wing, which is a simple wing model with conventional control surfaces. Phase III will utilize NASA's Piezoelectric Aeroelastic Response Tailoring Investigation (PARTI)⁴ wing with smart material sensing and actuation. This phased approach allows gradual development and testing of neural network-based control beginning with semi-adaptive control of a simple wing model and ending with fully adaptive control of a smart structure wing.

1.3 Approach

The approach to the Phase I objective of developing a neural network-based semi-adaptive flutter suppression system was to train a neural network to schedule single-input/single-output (SISO) control laws as a function of Mach number (M) and dynamic pressure (q). This neural network then provided control law parameters to a real-time digital controller for stabilizing the BACT wing using one accelerometer sensor and one trailing edge flap. The approach to meeting the Phase II objective of fully adaptive flutter suppression was to develop and implement a Model Predictive Control (MPC) architecture using an on-line learning neural network for the internal model.

The following sections describe the test article, the Phase I semi-adaptive control system architecture and wind tunnel test results, and the Phase II fully adaptive control system architecture and simulation results. The Phase II system will be tested in the wind tunnel in early 1996.

2. EXPERIMENTAL TEST SETUP

The Benchmark Active Controls Testing (BACT) wing model was chosen as the test article for the first and second phases of the program since it is a simple, well understood model which exhibits classical flutter phenomena, at a frequency of approximately 4-5 Hz, that develops very gradually and can be easily extinguished with a mechanical snubber system. The BACT wing, shown in Figure 1, is a rigid wing attached to a flexible mount system known as the Pitch And Plunge Apparatus (PAPA). The trailing edge aileron was used as the control surface and the inboard trailing edge accelerometer was used as the feedback sensor. A pair of independently actuated upper and lower-surface spoilers are also available for control and may be used in future testing.

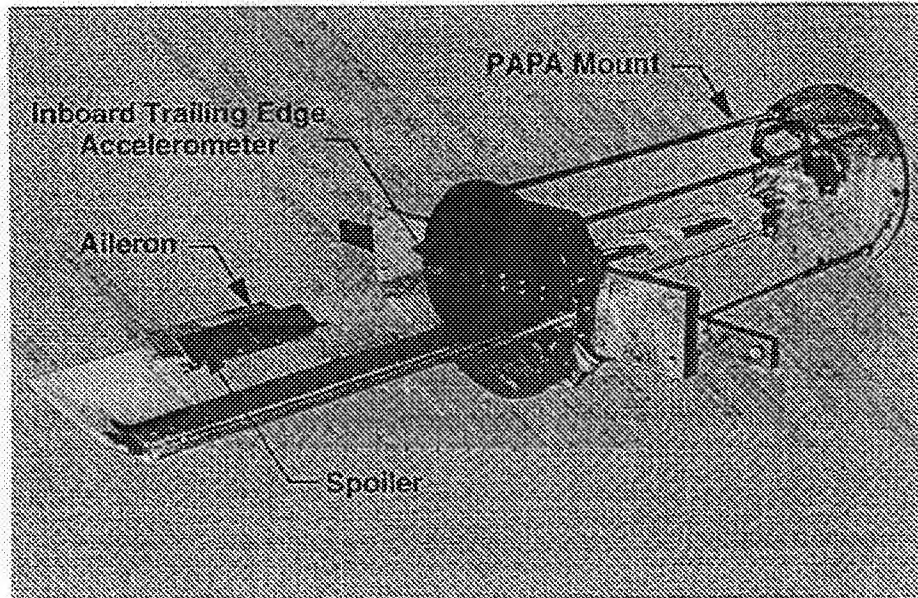


Figure 1. Benchmark Active Controls Testing (BACT) Wing Model

Wind-tunnel testing was conducted in the NASA Langley Transonic Dynamics Tunnel (TDT)⁵. The TDT is a single-return variable-density transonic wind tunnel. The slotted test section is 16 ft. by 16 ft. square with cropped corners. The speed and pressure are independently controllable over a range of Mach number from 0.0 to 1.2 (unblocked), and a range of stagnation pressure from near zero to one atmosphere. Either air or a heavy gas (R-12) can be used as the test medium. The TDT is also equipped with quick-opening bypass valves which can be activated to rapidly reduce test-section dynamic pressure and Mach number when flutter occurs. The combinations of large scale, high speed, high density, variable pressure, and the bypass-valve system make the TDT ideally suited for aeroelastic testing. The open-loop flutter boundary for the BACT wing in the TDT is shown in Figure 2.

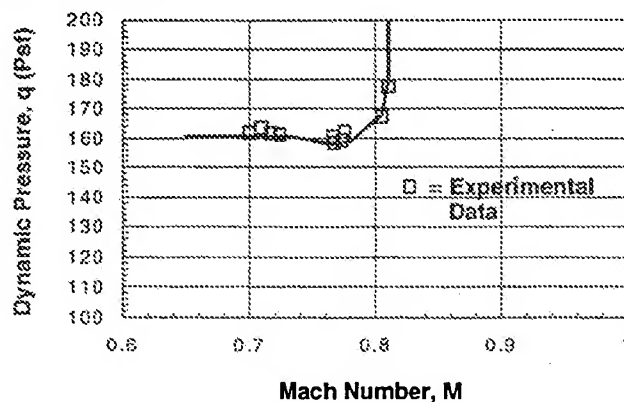


Figure 2. BACT Wing Open-Loop Flutter Points

3. SEMI-ADAPTIVE ACTIVE FLUTTER SUPPRESSION SYSTEM (PHASE I)

This section describes the semi-adaptive control system architecture developed during Phase I, and discusses the associated wind tunnel testing and performance results obtained.

3.1 Control Architecture

The architecture of the semi-adaptive control scheme is illustrated in Figure 3. The NASA Active Digital Controller (ADC)⁶, hosted on a Sun workstation, was used as the real-time digital control system, operating at a rate of 200 Hz. The trained neural network was implemented on a Macintosh computer which downloaded the scheduled control laws to the ADC. As shown in Figure 3, the output of the neural network consisted of control law parameters in the continuous time domain. These parameters were then converted to discrete state space matrix coefficients through a standard Tustin continuous-to-discrete transformation.

Using state-space models of the BACT wing developed by NASA with the Integrated Structures and Aerodynamics and Controls (ISAC) code⁷, a single optimized control law was designed at each specific M and q condition using the MATLAB Control Toolbox and SIMULINK simulation software. The neural network was then trained with M and q as inputs and control law parameters as outputs. As the wind tunnel operating conditions were varied, new values of M and q resulted in a new control law as interpolated by the trained neural network. This new control law then provided updated parameters for the real time SISO discrete state space control implementation. A robust, fixed-gain control law was also designed to operate across the entire range of M and q conditions. The performance of these systems was evaluated first in simulation and then finally in the NASA wind tunnel.

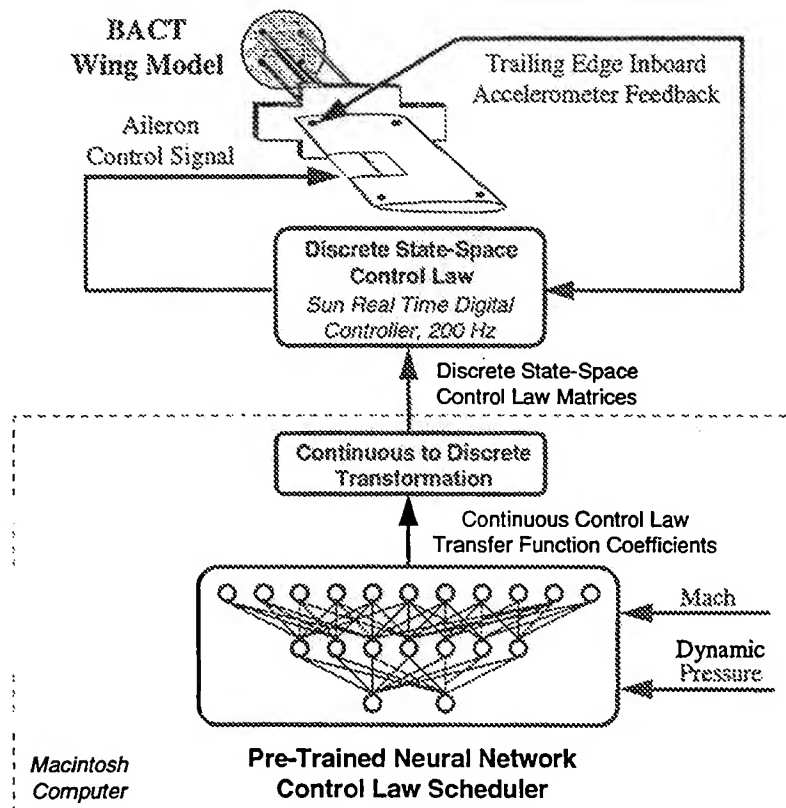


Figure 3. Neural Network-Based Semi-Adaptive Control Architecture

3.1.1 Fixed-Gain Control Law

The fixed-gain robust feedback control law was designed to stabilize and minimize the RMS wing motion over the entire dynamic range of the state space models furnished by NASA ($M=0.3, q=75$ to $M=0.9, q=250$). In addition to this compensation, the overall feedback transfer function included the necessary analog antialiasing filter and the transport lag introduced by the discrete digital computer implementation of the control law. A rigid body washout filter was included in the compensation to eliminate any drift due to bias errors in the accelerometers. Root-locus pole and zero placement methods were used to design the fixed-gain robust feedback control law given below:

$$H_c(s) = \frac{s(s^2 + 12s + 520)}{s^4 + 27s^3 + 491s^2 + 4515s + 13050}$$

The fixed-gain compensation provided four poles at -5, -10, and $-6 \pm 15i$ and three zeros at 0 and $-6 \pm 22i$. To illustrate the qualitative effect of this compensation, consider the BACT wing dynamics for a typical open-loop flutter condition ($M=0.77, q=162$ psf). While the state space models were of order 14 (14 poles and 14 zeros), eight zero-pole pairs can be effectively canceled due to their relatively close locations far from the imaginary axis. This results in a reduced order BACT model composed of six poles and six zeros. The locations of these poles and zeros in the complex s -plane are illustrated in Figure 4. Note that at this tunnel condition, two poles are slightly to the right of the imaginary axis, resulting in an unstable open-loop plant. The plant is also non-minimum phase, with right-half-plane zeros.

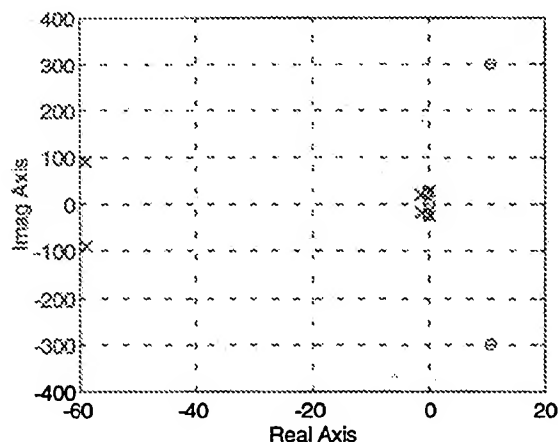


Figure 4. BACT Wing Open-Loop Poles and Zeros

Figure 5(a) illustrates the movement of the closed-loop poles obtained with the robust fixed-gain compensation. The slot-filter, composed of the pole at -6 ± 15 and the zero at -6 ± 22 , pulls the closed-loop pole significantly farther into the left-half plane, resulting in greater damping. The location of the slot-filter was designed to minimize the RMS wing motion over the entire dynamic range of M and q .

3.1.2 Neural Network Scheduled Control Laws

For the neural network scheduled control laws, the slot-filter described above was tailored for the wing model pole-zero dynamics at each particular M and q . Figure 5(b) illustrates the location of the slot-filter and resulting root locus for the open-loop flutter condition example discussed above ($M=0.77$ and $q=162$ psf). This custom slot-filter, located at -6 ± 29.5 and -6 ± 24.2 , pulls the root locus significantly farther into the left-half plane. The gain can then be chosen as desired to minimize the RMS wing motion or to maximize damping. Fifty-six custom designs were generated for the various M and q condition state space models: $M = 0.3, 0.5, 0.65, 0.75, 0.77, 0.82$, and 0.9 at q values of 75, 100, 125, 150, 175, 200, 225, and 250 psf. As described in the example above, the slot-filter was designed for each condition, resulting in the same order numerator

(3 zeros) and denominator (4 poles) as the robust fixed-gain control law. Therefore the general form of the neural network control law is given below:

$$K \frac{s^3 + a_2 s^2 + a_1 s}{s^4 + b_3 s^3 + b_2 s^2 + b_1 s + b_0}$$

A multi-layer perceptron (MLP) neural network⁸, shown in Figure 6, was trained with backpropagation to output the two numerator coefficients, the four denominator coefficients, and the overall gain as a function of M and q. The gain was chosen to minimize the RMS wing motion as excited by the wind tunnel turbulence. The neural network was then able to schedule the control laws and achieve near optimal flutter suppression as the wind tunnel conditions were varied. The control law parameters in the continuous domain, rather than the discrete domain, were chosen to be the outputs of the neural network since they vary smoothly as a function of M and q and don't require the high numerical precision of discrete domain control law coefficients. Consequently, the neural network outputs were transformed into the discrete domain before being used by the digital controller.

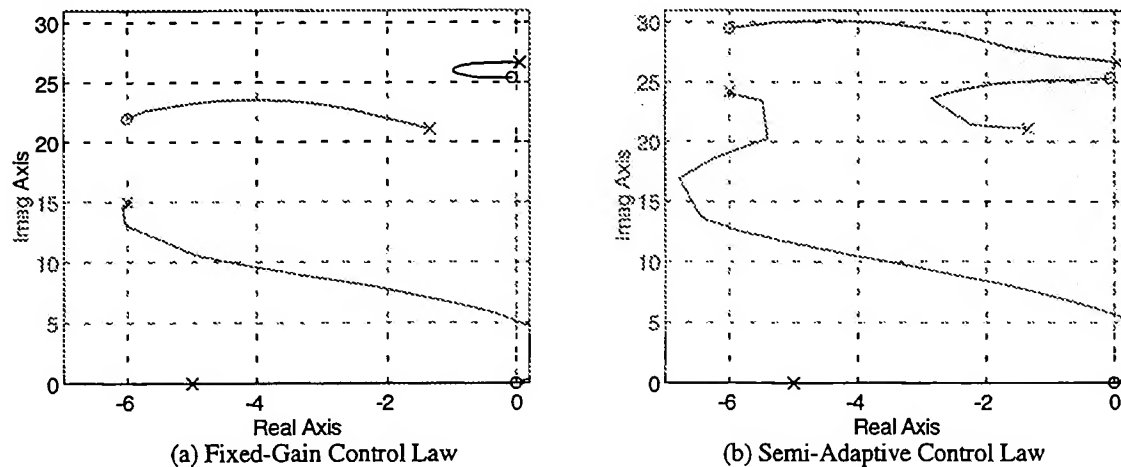


Figure 5. Root Locus for Typical Open-Loop Flutter Condition (M=0.77, q=162 psf)

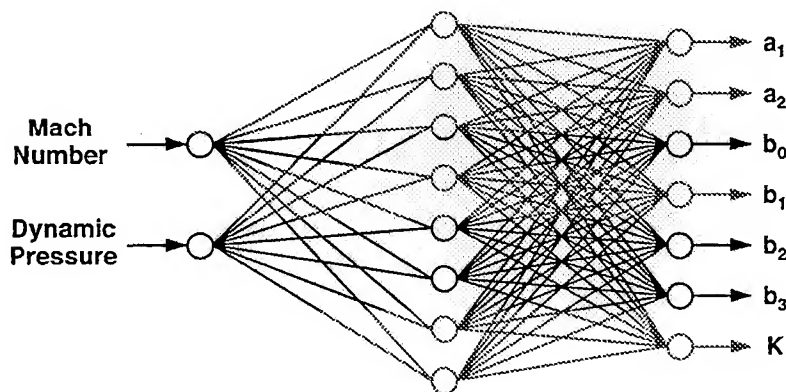


Figure 6. Neural Network Used for Control Law Scheduling

3.2 Wind Tunnel Test Results

Testing of the neural network-based semi-adaptive AFS system occurred in the NASA LaRC TDT on 1/31/95 and 2/1/95. This section describes the test conditions and summarizes the overall control performance results.

3.2.1 Test Conditions

Four tests were conducted, in which q was varied from 140 psf to 190 psf along four constant total pressure lines (h-lines). These h-lines are presented graphically along with the open-loop flutter boundary in Figure 7. As shown in Figure 7, h-line #1 remained inside the open-loop flutter boundary. Subsequent h-lines progressed to include an increasing number of flutter condition points. For each h-line, data was collected for open-loop, fixed-gain non-adaptive closed-loop, and neural network semi-adaptive closed-loop conditions. The open-loop tests were terminated as soon as classical flutter was experienced.

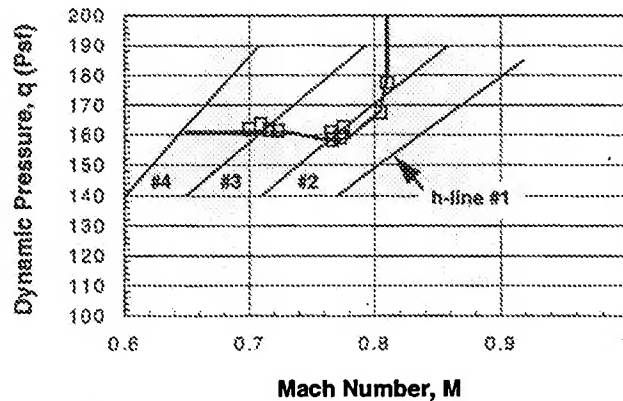


Figure 7. H-Line Mach Number and Dynamic Pressure Profiles

3.2.2 Test Results

Time history data was collected at all of the test points described above. While both the fixed-gain and neural network semi-adaptive controllers provided effective flutter stabilization, the neural network control was able to achieve lower RMS wing acceleration across the range of M and q conditions. This relative performance improvement is illustrated in Figure 8 which plots the RMS wing acceleration versus dynamic pressure for the third h-line. Representative time history plots of the BACT wing's acceleration response are given in Figure 9 for both below flutter boundary (open-loop stable) and above flutter boundary (open-loop unstable) conditions.

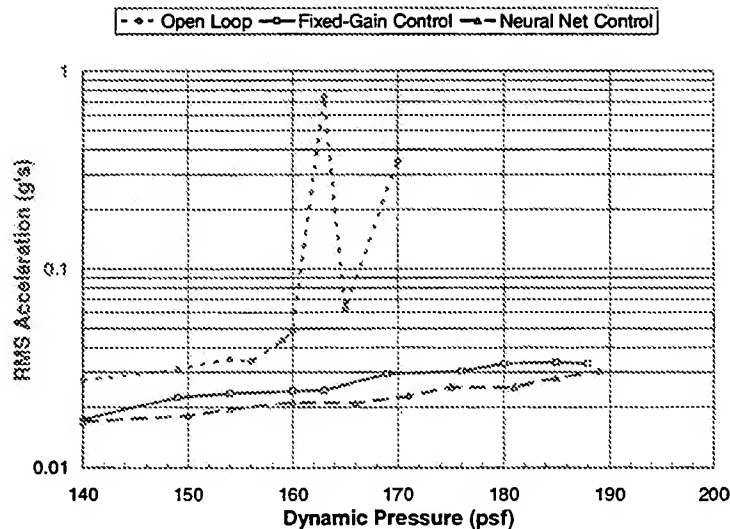
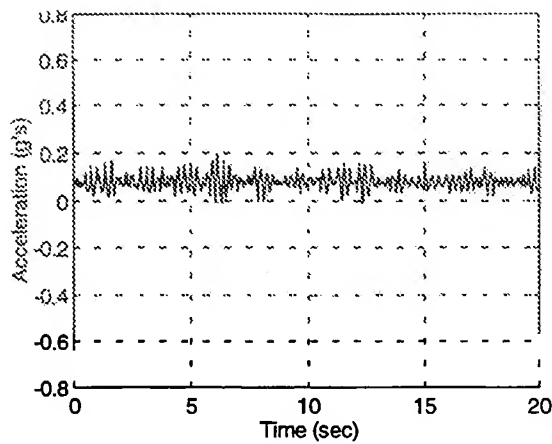
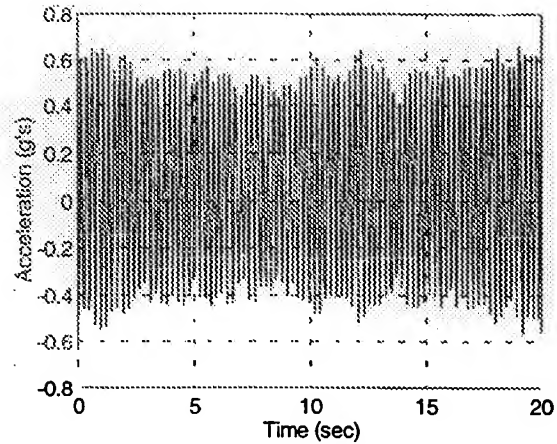


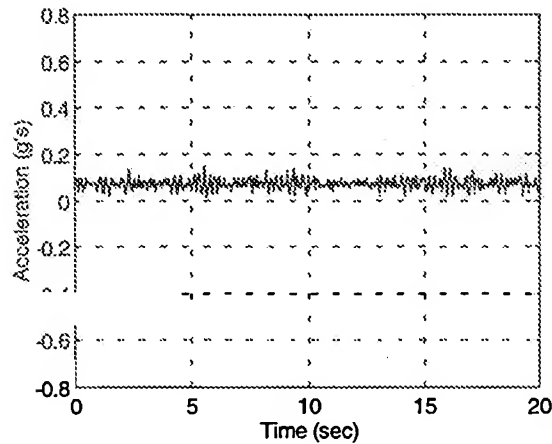
Figure 8. BACT Wing RMS Acceleration versus Dynamic Pressure



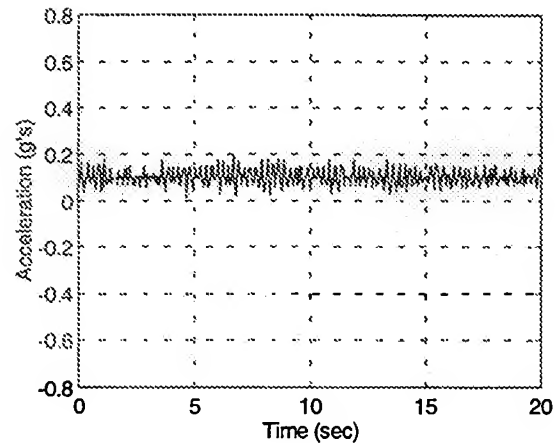
(a) Open Loop, Below Flutter Boundary
($M = 0.72$, $q = 140$ psf; RMS = 0.032)



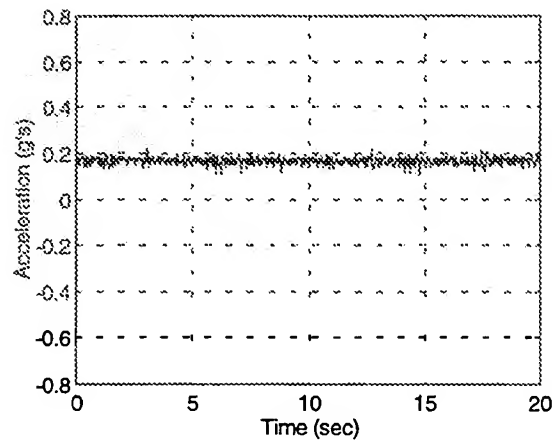
(b) Open Loop, Above Flutter Boundary
($M = 0.78$, $q = 162$ psf; RMS = 0.364)



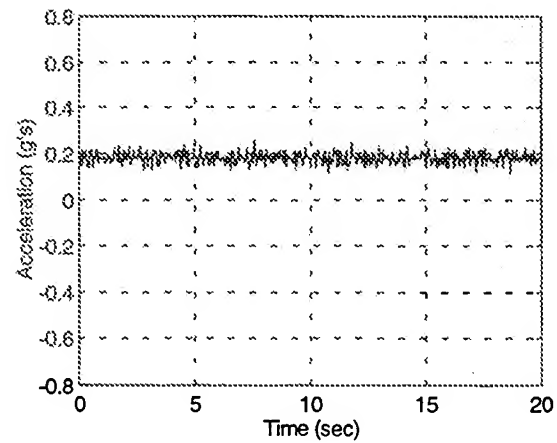
(c) Fixed-Gain Control, Below Flutter Boundary
($M = 0.72$, $q = 141$ psf; RMS = 0.023)



(d) Fixed-Gain Control, Above Flutter Boundary
($M = 0.78$, $q = 160$ psf; RMS = 0.031)



(e) Neural Net Control, Below Flutter Boundary
($M = 0.71$, $q = 140$ psf; RMS = 0.020)



(f) Neural Net Control, Above Flutter Boundary
($M = 0.77$, $q = 159$ psf; RMS = 0.025)

Figure 9. BACT Wing Acceleration Response Time Histories

FULLY ADAPTIVE ACTIVE FLUTTER SUPPRESSION SYSTEM (PHASE II)

The completion of Phase I objectives provided the foundation necessary for achieving the Phase II goal of developing a fully adaptive active flutter suppression (AFS) system. Based on several years of experience in applying neural network based control to manufacturing⁹ and active vibration suppression, it was decided to use a very general approach based on the Model Predictive Control (MPC)^{10,11} architecture. Using a neural network for the plant model enables the approach to be applied to a wide variety of complex, nonlinear systems due to the nonlinear modeling capability of neural networks. It also provides a direct method of control system adaptation by allowing the neural network model to be trained on-line. This architecture, which uses a neural network model within an MPC framework, is referred to as Neural Predictive Control (NPC)¹². Reference 12 provides a detailed description of the NPC architecture developed at MDA and its performance on a benchmark cantilevered beam vibration suppression problem. Similar control system architectures involving neural network-based MPC have been used successfully in the chemical processing industry as well.¹³

4.1 Control Architecture and Implementation

A top level view of the NPC architecture is shown in Figure 10. As depicted in this figure, the NPC system uses a neural network to model the input/output dynamics of the plant to be controlled. This predictive plant model is then utilized in an on-line optimization scheme to select the optimal control values for each control cycle. The plant model can be pre-trained by exciting the actuators, measuring the sensor response, and training the neural net model. This model can then be further updated on-line to cope with changing flight conditions and changing plant dynamics. In the Phase II wind tunnel test, this system will be tested in NASA's TDT on the BACT wing model. The main goal of this test is to demonstrate the applicability of NPC for active flutter suppression and the ability of the NPC system to self-configure through on-line learning.

The NPC architecture has been implemented for real time control in a Pentium 60MHz PC with a plug-in neural accelerator board and analog input/output boards. The Pentium host CPU is responsible for all NPC computations and data transfer to the input/output and neural accelerator boards. The neural accelerator board performs the on-line model adaptation which occurs in parallel with the host CPU control loop computations. Real time adaptive single-input/single-output (SISO) control has been demonstrated at rates up to 500 Hz with this hardware.

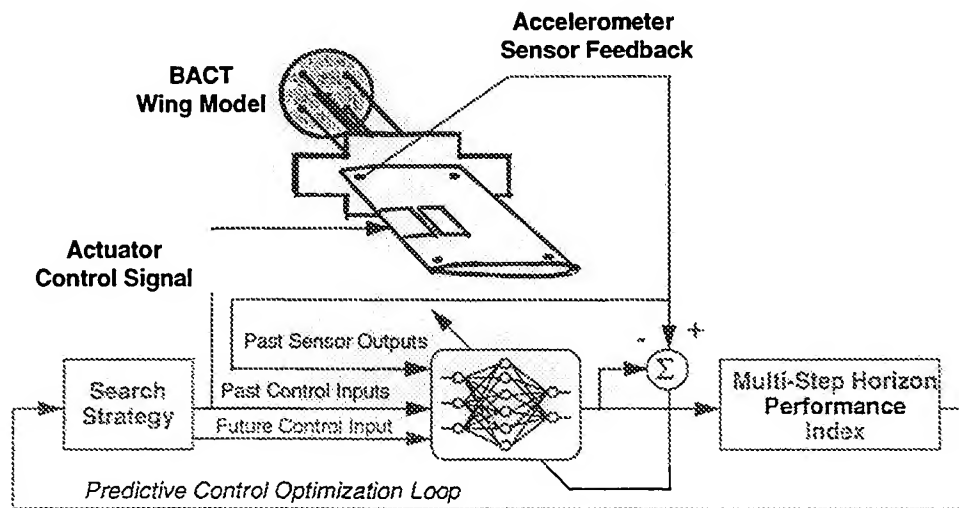


Figure 10. Neural Predictive Control (NPC) System Architecture

4.2 Simulation Results

The PC-based NPC system, running at a rate of 100 Hz, has been tested and verified in simulation using the state space models of the BACT wing provided by NASA. Successful adaptation and control has been demonstrated across the range of wind tunnel conditions. One representative simulation time history is illustrated in Figure 11 for an open loop unstable condition ($M = 0.75$, $q = 175$ psf). Starting with an untrained network, a white noise excitation signal is sent to the aileron for

four seconds, providing 400 data points for neural network learning. The learning then occurs during the next 2.7 seconds, allowing control to be activated at about 6.7 seconds. As shown in the figure, the wing vibration grows steadily until the controller is initiated for flutter suppression. Once the AFS system is activated, learning and control will occur simultaneously, allowing model updates to occur every 6.7 seconds. The length of this time interval is determined by the speed of the processors, the control cycle rate, and the amount of data needed for accurate plant modeling. Further analysis is being conducted to determine the optimum settings for the level of excitation, the amount of data needed for learning, and the performance index used by the NPC optimization loop. Additional analysis is focusing on evaluating the overall robustness of this adaptive control scheme.

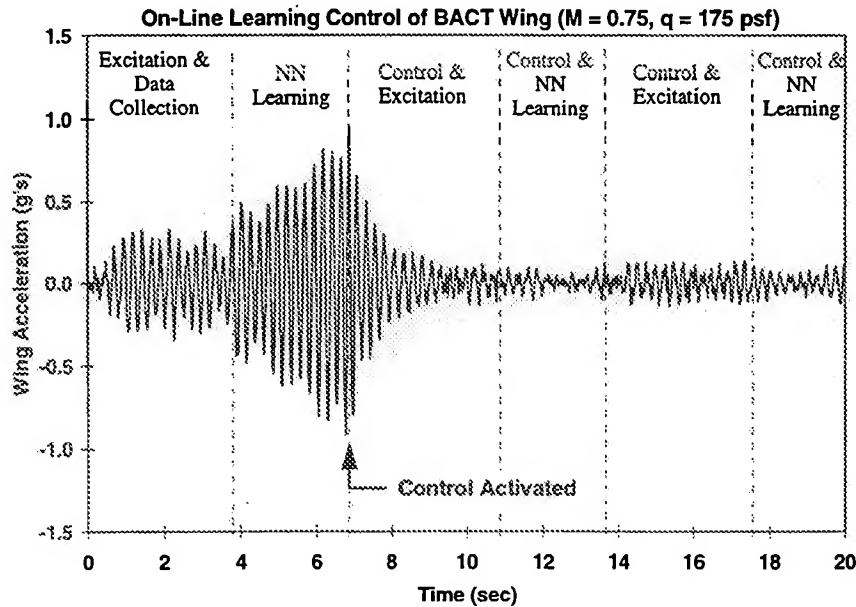


Figure 11. Simulation Results for NPC Fully Adaptive Active Flutter Suppression System

5. CONCLUSIONS

Under the ANCAR program, MDA and NASA have demonstrated the benefits of neural network technology for both semi-adaptive and fully adaptive active wing flutter suppression. During Phase I, a neural network was trained and implemented to provide a semi-adaptive control law. The usefulness of the neural network's ability to generalize/interpolate control laws as a function of wind tunnel parameters (M and q) was demonstrated. At the midway point of Phase II, a general and robust architecture for fully adaptive neural network-based control has been developed and is ready to be tested in the wind tunnel during 1996 on a simple wing model with conventional actuator control surfaces.

This Neural Predictive Control (NPC) architecture will be scaled up for application to a smart structure wing model during Phase III of the program. Adaptive neural network-based control is considered to be an enabling technology for both lightweight flexible wing and reconfigurable control systems which will provide extended aircraft life, reduced acquisition costs, and reduced operation and support costs for future aerospace systems.

6. REFERENCES

1. T. E. Noll, B. Perry III, and M. W. Kehoe, "A Quarter Century of NASA Wind-Tunnel and Flight Experiments Involving Aeroservoelasticity," AGARD Specialists Meeting on Advanced Aeroservoelastic Testing and Data Analysis, Rotterdam, Netherlands, May 8-12, 1995.
2. R. P. Peloubet Jr., R. M. Bolding, and K. B. Penning, "Adaptive Flutter Suppression Wind Tunnel Demonstration," AFWAL-TR-87-3053, October 1987.

3. R. Bennet, et al., "The Benchmark Aeroelastic Models Program - Description and Highlights," AGARD Conference, Transonic Unsteady Aerodynamics and Aeroelasticity, San Diego, CA, October 7-11, 1991.
4. J. Heeg, A. McGowan, E. Crawley, and C. Lin, "The Piezoelectric Aeroelastic Response Tailoring Investigation: A Status Report," Proceedings of the SPIE Smart Structures and Materials Conference, San Diego, CA, March 2-3, 1995.
5. Aeroelasticity Branch Staff, "The Langley Transonic Dynamics Tunnel," NASA Langley Working Paper, LWP-799, September, 1969.
6. S. T. Hoadley and S. M. McGraw, "The Multiple-Function Multi-Input/Multi-Output Digital Controller System for the AFW Wind-Tunnel Model," AIAA Paper 92-2083, April 1992.
7. E. L. Peele and W. M. Adams, "A Digital Program for Calculating the Interaction Between Flexible Structures, Unsteady Aerodynamics, and Active Controls," NASA TM-80040, January 1979.
8. D. E. Rumelhart, J. L. McClelland, and the PDP Research Group, *Parallel Distributed Processing, Vol. 1, Foundations*, Cambridge, MA, MIT Press, Ch. 8, 1986.
9. P. F. Lichtenwalner, "Neural-Network Based Control for the Fiber Placement Composite Manufacturing Process," *Journal of Materials Engineering and Performance*, pp. 687-692, October 1993.
10. M. Morari, "Model Predictive Control: Multivariable Control Technique of Choice in the 1990s?," *Advances in Model-Based Predictive Control*, Oxford University Press Inc., New York, 1994.
11. R. Soeterboek, *Predictive Control - A Unified Approach*, Prentice Hall, Cambridge, Great Britain, 1992.
12. L. Pado and R. Damle, "Predictive Neuro Control of Vibration in Smart Structures," To be Published in the Proceedings of the SPIE 1996 Symposium on Smart Structures and Materials, San Diego, CA, February 26-29, 1996.
13. A. Draeger, S. Engell, and H. Ranke, "Model Predictive Control Using Neural Networks," *IEEE Control Systems*, Vol. 15, No. 5, pp. 61-66, October 1995.

Controlled aeroelastic response and airfoil shaping using adaptive materials and integrated systems

Jennifer L. Pinkerton, Anna-Maria R. McGowan, Robert W. Moses, Robert C. Scott, Jennifer Heeg

Aeroelasticity Branch, NASA Langley Research Center
Hampton, Virginia 23681-0001

ABSTRACT

This paper presents an overview of several activities of the Aeroelasticity Branch at the NASA Langley Research Center in the area of applying adaptive materials and integrated systems for controlling both aircraft aeroelastic response and airfoil shape. The experimental results of four programs are discussed: the Piezoelectric Aeroelastic Response Tailoring Investigation (PARTI); the Adaptive Neural Control of Aeroelastic Response (ANCAR) program; the Actively Controlled Response of Buffet Affected Tails (ACROBAT) program; and the Airfoil THUNDER Testing to Ascertain Characteristics (ATTACH) project. The PARTI program demonstrated active flutter control and significant reductions in aeroelastic response at dynamic pressures below flutter using piezoelectric actuators. The ANCAR program seeks to demonstrate the effectiveness of using neural networks to schedule flutter suppression control laws. The ACROBAT program studied the effectiveness of a number of candidate actuators, including a rudder and piezoelectric actuators, to alleviate vertical tail buffeting. In the ATTACH project, the feasibility of using Thin-Layer Composite-Unimorph Piezoelectric Driver and Sensor (THUNDER) wafers to control airfoil aerodynamic characteristics was investigated. Plans for future applications are also discussed.

Keywords: piezoelectric actuators, active controls, flutter suppression, subcritical response tailoring, buffet load alleviation, neural networks, airfoil shaping

1. INTRODUCTION

Since the Wright brothers' first successful flight, designers have searched for ways to improve both the efficiency and performance of aircraft. Two key research areas that have arisen are controlling aircraft aeroelastic response and controlling airfoil shape. Historically, the use of passive techniques, such as increasing structural stiffness, mass balancing, or modifying geometry, has been the approach for preventing the onset of flutter, buffet, and other undesirable aeroelastic phenomena. The approach originally spawned by airfoil shaping research sought to achieve design-point airfoil camber control through the deflection of conventional wing control surfaces. Although these approaches have been effective, the passive solutions penalize aircraft designs by increasing both weight and cost while decreasing overall performance. However, utilization of existing control surfaces introduces no such additional penalties; thus, secondary applications for these devices have been sought.

When fuel economy became a more important design driver in the early 1970's, aircraft designers expanded the airfoil shaping application of the control surfaces to improve the off-design performance of aircraft during the clean-wing phases of flight.¹⁻³ One technique called flap scheduling used predetermined flap deflections at specific flight conditions to produce more optimal aerodynamic shapes.¹ During the past twenty years, considerable research has also been devoted to developing active flutter suppression concepts that utilize conventional control surfaces.⁴⁻⁷ And more recently, use of these surfaces has been studied for alleviating buffeting.⁸ For these latter applications, active use of control surfaces eliminates most of the penalties associated with the passive techniques and provides flexibility since any method of control employed can be varied with configuration or flight condition.

However, there are difficulties with using conventional control surfaces in such secondary applications. These include: (1) adequately addressing system redundancy, reliability, and maintainability, (2) avoiding compromising the control surface authority available to maneuver an aircraft, (3) obtaining adequate control effectiveness, and (4) not overshadowing performance improvements with increased complexity and structural weight.² Because of these concerns, alternatives to utilizing the aerodynamic control surfaces are being studied. The use of adaptive materials as control effectors is one such alternative.

Building upon the rich history of the conventional control surface research efforts discussed above and more recent accomplishments in the application of adaptive materials are four programs in the Aeroelasticity Branch at the NASA Langley Research Center (LaRC) that are attempting to advance the state-of-the-art in controlling both aeroelastic response and airfoil shape. One of these programs is the Piezoelectric Aeroelastic Response Tailoring Investigation (PARTI) program. To date,

most applications of adaptive materials to wing flutter suppression have focused on the use of piezoelectric materials. Results available from this application focus primarily on analytical study, with a few reports documenting experimental work. Weisshaar provides a summary of these efforts and a considerable reference list in reference 9. The PARTI program sought to validate and extend the results from such previous wing flutter suppression studies by being the first to wind-tunnel test a relatively large, multi-degree-of-freedom aeroelastic testbed.

The control of active flutter suppression systems is the focus of another research effort at NASA LaRC called the Adaptive Neural Control of Aeroelastic Response (ANCAR) program. At this time, numerous studies, like those discussed and referenced in reference 10, have been conducted on the use of neural networks; however, experiments applying this technology to the control of undesirable aeroelastic phenomena are limited. The ANCAR program seeks to experimentally demonstrate, for the first time ever, an adaptive neural-network-based flutter suppression system.

The application of adaptive materials to buffeting alleviation research is relatively recent. One of the first feasibility studies for this application was conducted by Heeg, *et al.* at NASA LaRC in a table-top wind tunnel.¹¹ Another study at NASA LaRC, called the Actively Controlled Response of Buffet Affected Tails (ACROBAT) program, extended this application in 1995, seeking to demonstrate for the first time the effectiveness of using piezoelectric actuators in alleviating vertical tail buffeting at high angles of attack on a large-scale aircraft model.

Airfoil shaping studies incorporating adaptive materials began in the mid-1980's. The first attempt at active aerodynamic shape control was conducted by Crawley, Warkentin, and Lazarus and involved the use of piezoelectric actuators to generate twist and camber on the surface of a plate.¹² More recent studies, primarily analytical, have focused on assessing the capability of the available adaptive materials to create significant skin deflections. Although promising results have been obtained, many researchers have concluded that most adaptive materials lack the strength and out-of-plane displacement capability needed for this application.¹³⁻¹⁵ However, another research effort at NASA LaRC, called the Airfoil THUNDER Testing to Ascertain Characteristics (ATTACH) project, has recently initiated the investigation of a new adaptive material for this application.

The purpose of this paper is to briefly present background information on piezoelectric adaptive materials and to highlight the progress, current status, and future plans of the four programs mentioned above: the Piezoelectric Aeroelastic Response Tailoring Investigation (PARTI), the Adaptive Neural Control of Aeroelastic Response (ANCAR) program, the Actively Controlled Response of Buffet Affected Tails (ACROBAT) program, and the Airfoil THUNDER Testing to Ascertain Characteristics (ATTACH) project.

For the purposes of this paper, the following definitions will be utilized. "Adaptive materials" are materials that alter their shapes when exposed to an external stimulus. When actuators made of these materials are embedded within or affixed to a host structure and then stimulated to create forces on that structure, the result is an "active structure." An "adaptive structure," or equivalently a "smart structure," is then produced when an active structure is commanded by an adaptive control law, which may employ a neural network.¹⁶ An "integrated system" is formed when a control effector (either an adaptive material or a control surface), host structure, sensor, and controller work together to achieve the same functional goal.

2. EXPERIMENTAL APPARATUS

2.1 Wind tunnels

The programs described herein utilized the two wind tunnels operated within the Aeroelasticity Branch: the Transonic Dynamics Tunnel (TDT), a very large and complex facility, and the Flutter Research and Experiment Device (FRED), a simple table-top device. The TDT, shown in Figure 1, is a 16-foot-by-16-foot test section, closed-circuit, continuous flow wind tunnel capable of testing over a range of stagnation pressures from near zero to atmospheric and Mach numbers from near zero to 1.2, using either an air or heavy gas medium, and has the capability to reduce wind speed rapidly in the event of an instability.¹⁷ Designed specifically for aeroelastic testing, the TDT has been used for decades to conduct numerous aircraft and rotorcraft aeroelastic and aeroservoelastic tests. The PARTI, ANCAR, and ACROBAT models were tested in the TDT. The ATTACH model was tested in the FRED wind tunnel, which is shown in Figure 2. FRED is a table-top, open-circuit tunnel with a 6-inch-by-6-inch fully removable acrylic glass test section. Powered by a 2-hp motor, the wind tunnel is capable of operating at a maximum velocity of 38.1 m/s (125 ft/s). A single honeycomb screen at the beginning of the contraction duct helps to smooth the flow before it reaches the test section. This tunnel was also used to test earlier aeroelastic applications of adaptive materials.^{11,18}

2.2 Piezoelectric materials

Piezoelectric materials, which develop a strain when subjected to an electric field and vice versa, are one of the most popular adaptive materials used today. Currently, these materials are divided into two groups, which differ by the direction that they are able to affect a host structure. The first group, commonly called strain actuators, exhibit an in-plane displacement capability. The second group is a new generation of actuators specifically designed to have an out-of-plane displacement capability.

The conventional configuration for an in-plane displacement piezoelectric actuator consists of a single piezoelectric wafer sandwiched between two electrodes. The relationship between an applied electric field and the corresponding behavior of a piezoelectric actuator is well documented.^{16,18,19} Increased in-plane actuation can be obtained by several means, including grouping multiple wafers into multiple layers. An actuator possessing some out-of-plane displacement capability can also be created by stacking several of the in-plane piezoelectric wafers.²⁰

Two of the new generation of piezoelectric actuators specifically designed to have an out-of-plane displacement capability are RAINBOW (Reduced And Internally Biased Oxide Wafer)²¹ and THUNDER (Thin-Layer Composite-Unimorph Piezoelectric Driver and Sensor).²² Both devices have a monolithic structure and are pre-stressed during fabrication to set the direction of their displacement. RAINBOW, the first of these actuators to be developed, possesses 10 times the displacement capability of the in-plane actuators previously discussed. THUNDER, which was developed in house at NASA LaRC, exhibits an even larger displacement capability.

2.3 Actuator selection methodology

In general, the selection of an appropriate actuator for use with each program presented in this paper was based on four criteria: (1) bandwidth, (2) force, (3) displacement capability, and (4) ease of application. For flutter suppression and buffeting alleviation, bandwidth, force, and ease of application are the major criteria, and commercially available in-plane actuators suffice. However, for airfoil shaping, the driving criteria are force, displacement capability, and ease of application. Thus, out-of-plane displacement actuators, such as piezoelectric stacks, RAINBOW wafers, and THUNDER wafers, are typically used for this application.

3. RESEARCH PROGRAMS

3.1 The Piezoelectric Aeroelastic Response Tailoring Investigation (PARTI) program

The Piezoelectric Aeroelastic Response Tailoring Investigation (PARTI) program was the first study in the area of aeroelastic control using adaptive materials to use a relatively large, multi-degree-of-freedom aeroelastic testbed. The PARTI program was a cooperative effort between the NASA Langley Research Center and the Massachusetts Institute of Technology. The objectives of this program were to demonstrate active control of aeroelastic response at subcritical speeds (conditions below the wing flutter speed) and wing flutter suppression using a large-scale aeroelastic wind-tunnel model with distributed piezoelectric actuators and to develop detailed experimental and analytical techniques. In this program, a wind-tunnel model was designed and fabricated, aeroservoelastic analyses were performed, and the model was ground and wind-tunnel tested in the TDT. As a result of this program, an extensive database of experimental information has been gathered that is instrumental in understanding the many issues associated with applying strain actuation technology to dynamic problems. The PARTI model was first tested in March 1994 to obtain basic flutter characteristics and transfer functions relating the model response to piezoelectric actuator input for various tunnel conditions. A closed-loop wind-tunnel test of the PARTI model was completed in November 1994. Preliminary results have been previously published regarding data collected during these tests.²³ Analysis and design of several control laws along with preliminary test data have also been published.²⁴ Further discussion of wind-tunnel testing results and a discussion of experimental methodologies can be found in reference 25. The current paper will present a brief description of the PARTI model and wind-tunnel testing.

3.1.1 Wind-tunnel model

The model is a five-foot long, high aspect ratio semi-span wing designed to flutter at low speeds to simplify aerodynamic analyses and wind-tunnel testing. The model consists of two primary structures: an exterior fiberglass shell used to obtain aerodynamic lift and an interior composite plate that contains the piezoelectric actuators and acts as the main load carrying member. The fully assembled model mounted in the TDT is shown in Figure 3. Figure 4 shows the interior construction of the model. The interior plate is composed of an aluminum honeycomb core sandwiched by graphite epoxy face sheets.

The face sheets are of $[-20^\circ/0^\circ]$ laminate, referenced to the wing quarter-chord which is swept aft 30° . The unsymmetric, unbalanced composite lay-up provides a static bend/twist coupling. The model has two additional components: a trailing-edge aerodynamic control surface and a wing-tip flutter-stopper device. The flutter-stopper tip-mass assembly was constructed as a safety device for wind-tunnel testing. Piezoelectric actuators cover the inboard 60% of the span of the internal composite plate and account for 7.3% of the total wing weight. Fifteen groups of piezoelectric actuator patches are adhered to the top and bottom of the interior plate. The actuators are configured to impart differential bending moments to the plate; however, the ply orientation of the graphite epoxy and the wing sweep angle make it possible for piezoelectric actuation to affect both the bending and torsion natural modes of the model. The piezoelectric patches were only used for actuation; ten strain gages and four accelerometers were used as sensors. The complete design of the PARTI model is documented by Reich and Crawley.²⁶

3.1.2 Wind-tunnel testing

The PARTI model was ground tested and wind-tunnel tested during two entries in the TDT. Ground vibration tests were conducted to determine the dynamic characteristics of the model at zero-airspeed and to validate analytical models. Experimental flutter characteristics and open-loop time-history data at subcritical conditions were obtained during the first wind-tunnel test in March 1994. Time history data was acquired at several dynamic pressures by actuating each of the 15 groups of piezoelectric actuators individually as well as in five sets of several actuator groups. The open-loop data were used to construct state-space models for control law design, to examine the linearity of piezoelectric actuation, and to verify analytical models and techniques. A time domain system identification method was used to generate the state-space models from the time histories obtained during wind-tunnel testing. Using system identification, all of the PARTI model dynamics were fully captured using a math model with 120 states; however, state-space models with as little as 40 states were used as well. The open-loop data were also used to examine the linearity of piezoelectric actuation. Despite the presence of nonlinearities, the results indicate that superposition can be used to combine the responses of individual piezoelectric actuator groups. Furthermore, preliminary results show that there is a linear increase in model response with a linear increase in piezoelectric command voltage.

Twenty-eight control laws designed to increase flutter speed and reduce response at subcritical conditions were tested during the second wind-tunnel test. A variety of control law design techniques were used and both single-input/single-output (SISO) and multi-input/multi-output (MIMO) control laws were designed utilizing up to five inputs and nine outputs. The PARTI model can be represented by up to 15 control outputs (15 groups of piezoelectric actuators) and 14 control inputs (10 strain gages and 4 accelerometers). However, several piezoelectric actuator groups receiving the identical output signal were considered as one control output. The most successful flutter suppression control law was also effective in reducing response at subcritical speeds, demonstrating a 12% increase in flutter dynamic pressure and a 75% reduction in the power spectral density of peak response at subcritical speeds as shown in Figures 5 and 6. This was a SISO control law that used all 15 piezoelectric actuator groups. Another SISO control law that used strain gage 4 for feedback and piezoelectric actuator groups 3, 4, 6, 7, and 10 successfully increased flutter speed 8%.

The PARTI program successfully demonstrated active flutter suppression and reduced response at subcritical speeds using piezoelectric actuation on a five-foot span wind-tunnel model. Through this program, a number of issues associated with applying piezoelectric actuation to aeroelastic problems have been addressed; however, there exist several issues that require further study, some of which are planned as follow-on studies to the present research. These include an examination of scaling laws, power consumption, increasing control effectiveness through optimal actuator and sensor selection and placement, and the analytical development of state-space models.

3.2 Adaptive Neural Control of Aeroelastic Response (ANCAR) program

An important aspect in the development of a smart structure or integrated system is the corresponding development of an adaptive controller. The Adaptive Neural Control of Aeroelastic Response (ANCAR) program is a cooperative effort between NASA LaRC and McDonnell Douglas Aerospace to develop and demonstrate an integrated flutter suppression system that uses an adaptive neural network controller. The ANCAR program is comprised of three phases. Phases I and II use the LaRC Benchmark Active Controls Testing (BACT) wind-tunnel model. The Phase I objectives were to develop and demonstrate a hybrid control system that incorporated conventional control algorithms and neural networks to suppress flutter. Wind-tunnel testing for this phase took place in January 1995. The Phase II objectives are to develop and demonstrate an adaptive neural-network-based flutter suppression system during a January 1996 wind-tunnel entry. Phase III objectives are to combine the neural adaptive control system with an active structure like the PARTI model. Currently, wind-tunnel testing for this phase is scheduled for 1998. This section of the paper will focus on the results of Phase I and the plans for Phase II.

3.2.1 BACT wind-tunnel model

The BACT model²⁷ was originally developed as part of the Benchmark Models Program (BMP).²⁸ The BMP was a NASA LaRC program that included a series of models which were used to study different aeroelastic phenomena and to validate aeroelastic, aeroservoelastic, and computational fluid dynamic methods in several wind-tunnel tests. Because the BACT model dynamics are well understood and it has control surfaces and relatively benign flutter mechanisms, it is an ideal testbed for initial testing of new control schemes, including neural-based systems.

The BACT model is depicted in Figure 7. The model is a rigid, rectangular wing with a NACA 0012 airfoil section. It is equipped with a trailing-edge control surface and upper- and lower-surface spoilers, all independently controllable. The model, shown in the figure, is attached to a mount system called the pitch-and-plunge apparatus (PAPA) that allows both pitch and plunge degrees-of-freedom. The model is extensively instrumented with pressure transducers and accelerometers to measure surface pressures and model dynamic response, and the mount system is instrumented with strain gages to measure normal force and pitching moment.

3.2.2 Phase I

The schematic for the Phase I neural network control system is shown in Figure 8. This is a hybrid control system that uses a neural network to gain schedule conventional control law parameters with varying Mach number and dynamic pressure. Figure 8 shows how the system was implemented. The neural network was trained to use Mach number and dynamic pressure as input and provide the coefficients of the control law as output. After conversion from continuous to discrete time, the control laws could be downloaded and run on a real time digital controller.

The neural network was trained by using fifty-six different state-space analytical models, each corresponding to a different combination of Mach number and dynamic pressure, which ranged from 0.3 to 0.9 and 75 psf to 250 psf, respectively. These models were used to generate fifty-six 3-zero and 4-pole, single-input/single-output control law designs, each optimized to achieve minimum RMS model response to tunnel turbulence. For each of the fifty-six control laws, there were 7 parameters that could be varied with Mach number and dynamic pressure, and a multi-layer perceptron neural network was trained with backpropagation to output these seven control law parameters as a function of Mach number and dynamic pressure. For comparison purposes, the same design strategy was used to generate a fixed-gain flutter suppression control law to provide the best possible performance over the whole flight envelope.

In the TDT, testing is accomplished easily and conveniently by first choosing a tunnel stagnation pressure and then varying drive motor RPM, which simultaneously changes Mach number and dynamic pressure. During Phase I testing, four different stagnation pressures were chosen, resulting in wide-ranging combinations of Mach number and dynamic pressure within the training space. Data was acquired at each of the four constant stagnation pressure conditions for the open-loop system, for the closed-loop fixed-gain system, and for the closed-loop neural-network-scheduled system. The RMS of the trailing edge accelerometer response for one of the stagnation pressures is shown in Figure 9. For this pressure, open-loop flutter occurs at a dynamic pressure of 161 psf. Here, the neural-network-scheduled system has the lowest response.

3.2.3 Phase II

The goal of Phase II is to incorporate neural networks into adaptive flutter suppression systems. Unlike the Phase I controller, the Phase II neural systems will not use conventional control designs. Instead, they will adapt, on-line, to changing test conditions. A variety of adaptive neural-network-based systems will be tested during the January 1996 test. Several of the algorithms to be tested use a predictive control algorithm. Predictive control algorithms require generation of a math model for the system being controlled. Once the model is complete, the loop can be closed and a search or optimization algorithm can be used to select the control input commands that further minimize response over some time interval. In this application, a neural network is trained using experimental data acquired in the wind tunnel to create a neural model of the system that can be used to predict future responses to future control inputs.²⁹ A neural network realization of predictive control is shown in Figure 10.

This experimental study is investigating the use of neural networks for adaptive control of flutter with the BACT wind-tunnel model. During Phase I testing, a hybrid control system using a neural network to gain schedule conventional control law parameters was implemented for the first time, demonstrating slightly better flutter suppression than a fixed-gain control system. Demonstration of an advanced neural network that can adapt to changing conditions is the goal for Phase II.

3.3 The Actively Controlled Response of Buffet Affected Tails (ACROBAT) program

The goal of the Actively Controlled Response of Buffet Affected Tails (ACROBAT) program was to demonstrate the feasibility of using active control for alleviating buffeting caused by leading edge extension (LEX) vortex burst. This phenomenon is shown in Figure 11. For this program, an existing 1/6-scale rigid full-span model of the F/A-18 A/B aircraft was refurbished, and three new flexible and two new rigid vertical tails were fabricated. The model, shown in Figure 12, was tested during July 1995 and November 1995 with each of the new flexible tail surfaces at a Mach number of 0.09 in a test medium consisting of air at atmospheric pressure. The three flexible tails were fabricated from a 1/8-inch thick aluminum plate and covered with balsa wood to produce the desired airfoil shape. The three flexible vertical tails used: (1) a rudder surface; (2) a tip vane configured with a slotted cylinder; 3) an embedded slotted cylinder; or (4) piezoelectric actuation devices. For the vertical tail with piezoelectric actuation, a hatch cover was incorporated in the design to cover the plate-mounted piezoelectric devices while maintaining the proper airfoil shape. The piezoelectric actuator arrangement itself, shown in Figure 13, consisted of three root actuators, two tip actuators, and two central actuators per side. Each of the tip and central actuators was comprised of two stacks of two layers of piezoelectric wafers, while each root actuator utilized two stacks of four layers for added effectiveness. The response of each flexible vertical tail was measured using a root bending strain gage and two tip accelerometers. Pressure transducers were surface mounted on both sides of all tails, excluding the tail with piezoelectric actuation.

3.3.1 Accomplishments

During the open-loop entry in July 1995, transfer functions were acquired for the response of the vertical tail to rudder (and buffet) inputs, to piezoelectric actuator (and buffet) inputs, to tip vane (and buffet) inputs, and to embedded cylinder (and buffet) inputs. Surface pressure data was also acquired. Based on the open-loop data, the rudder and the piezoelectric actuators appeared the most effective candidates. In addition to these open-loop measurements, several preliminary control laws were tested using the rudder, where in each case, the control law was designed using classical control methods. Data for several of these preliminary rudder-based control laws reduced the RMS response in the first bending mode by as much as 35%. This preliminary closed-loop result gave valuable insight into active buffeting alleviation for the November 1995 closed-loop entry. During the November entry, sixteen control laws were tested for the rudder while six control laws were tested for the piezoelectric actuators. Each control law reduced the power spectral density of the first bending mode by as much as 60% using gains well below the actuators' physical limits. The results of one control law for the piezoelectric actuators are shown in Figure 14. Pressure measurements were acquired on both surfaces of the flexible and rigid vertical tails during numerous open-loop and closed-loop conditions at various angles of attack.

The results of these wind-tunnel tests illustrate that buffeting alleviation of vertical tails can be accomplished using active control of the rudder or of piezoelectric actuators. A better understanding of control law design for active buffeting alleviation has been gained from this investigation. The pressure measurements offer insight into the flowfield around the tail during buffet.

3.3.2 Future plans

Tests in the TDT to investigate potential adaptive control concepts for buffeting alleviation are planned for later this decade. In addition to wind-tunnel investigations, the United States Air Force (USAF) and NASA, through the auspices of The Technical Cooperative Program (TTCP), have initiated a collaborative buffeting alleviation study involving research organizations and industry from the United States, Australia, and Canada. The objective of this program is to ground test a full-scale F-18 vertical tail that incorporates a buffeting alleviation system employing piezoelectric actuators. The ground tests are expected to be performed in Australia at the Aeronautical and Maritime Research Laboratory in Melbourne. Plans are to pursue a flight test demonstration of the concept at NASA Dryden Flight Research Center in 1999 if the ground test program proves successful.

3.4 Airfoil THUNDER Testing to Ascertain Characteristics (ATTACH) project

The Airfoil THUNDER Testing to Ascertain Characteristics (ATTACH) project was a feasibility study that focused on identifying (1) the material characteristics, such as creep, hysteresis, and fatigue, and (2) the airfoil shaping effectiveness of the new THUNDER piezoelectric technology under aerodynamic loading. Characterization of the material behavior of THUNDER was the objective for Phase I, while Phase II examined its ability to reduce drag over an airfoil. The following sections present both the approach and preliminary findings of both phases of testing.

The testbed used for both phases of testing in the ATTACH project was the 0.25-inch thick, 1.5-inch wide, 5-inch long, generic, roughly-symmetric airfoil shown in Figure 15. This airfoil was supported by two 0.25-inch thick, 10-inch long sidewalls that extended through 85% of the length of the test section, creating a nearly two-dimensional flow condition. A single 1.5-inch wide, 2.5-inch long rectangular wafer of THUNDER was placed near the leading edge of the airfoil to act as the first half of the upper surface. To smooth the airfoil/wafer interface, a sheet of thin fiberglass material was wrapped over the upper surface of the airfoil/wafer combination and held in place by a flexible latex membrane. A photograph of the installed model is shown in Figure 16.

3.4.1 Phase I testing

The initial series of tests conducted during the ATTACH project were performed to identify the creep, hysteresis, and fatigue characteristics of a THUNDER wafer under aerodynamic loading. For this experiment, a total of 60 conditions were tested, consisting of combinations of the following parameters: five angles of attack (-2° , 0° , $+2^\circ$, $+4^\circ$, $+6^\circ$), four steady-state input voltages (-102 V, $+102$ V, -170 V, $+170$ V), and three tunnel velocities (wind-off, 20 m/s, 35 m/s).

The data obtained during this experiment conclusively identified the presence of both creep and hysteresis of the wafer under wind-on (loaded) and wind-off (unloaded) conditions. An example of wafer displacement in response to five cycles of applied voltage is shown in Figure 17. The test conditions were wind-off with the model at zero degrees angle of attack. In the figure, creep is characterized by the increasing positive (up) and negative (down) displacements exhibited by the wafer while under the constant applied voltages of ± 102 V, respectively. Hysteresis appears as the repeatable symmetric "loops," which in this case are offset slightly due to creep. Figure 18 provides a comparison of the wafer displacement responses for the wind-off and 20 m/s conditions, again at zero degrees angle of attack. Creep and hysteresis are still apparent for the wind-on condition, but the presence of the flow contributes to smaller positive displacements (compared to wind-off) for the same applied voltage. Wafer displacements are smaller at lower tunnel velocities (not shown) and higher at higher angles of attack (also not shown).

During this phase of testing, the health of the wafer was frequently checked to gain a preliminary understanding of material fatigue. After two weeks of testing, the performance of the wafer began to noticeably degrade. During subsequent examination, no visible flaws were found, but a 33% drop in capacitance was discovered, and repoling returned the wafer to its full capabilities. Thus, similar to other piezoelectric adaptive materials, the performance of THUNDER appears to be a function of capacitance.

3.4.2 Phase II testing

With the objective of determining the ability of the THUNDER wafer to reduce drag over the airfoil, tests were conducted at the 40 wind-on conditions described above. For purposes of this feasibility study, it was assumed that variations in drag were directly proportional to velocity changes in the wake of the model. Comparisons of wake velocity for different test conditions, therefore, provided qualitative indications of the drag reducing potential of this piezoelectric actuator for this subscale model. Velocity measurements were taken by traversing a hot film anemometer velocity probe in 0.125-inch increments through the center of the test section sufficiently aft of the airfoil trailing edge to allow the wake to return to tunnel static pressure.

Results from this phase of testing were consistent with the results from Phase I. Velocity and angle of attack had the anticipated effect on drag. Positive applied voltages, which expanded the upper surface of the airfoil up to meet the flow, had the effect of reducing drag. Negative applied voltages produced the opposite effect. These results were obtained using only 32% of the maximum unloaded capability of the wafer. Thus, greater drag reductions would be expected if that percentage is increased.

The results of this research effort indicate that the new THUNDER actuator technology is a promising candidate for future airfoil shaping investigations. Despite decreases in the displacements of the wafer due to aerodynamic loading, noticeable drag reductions were obtained.

4. CONCLUDING REMARKS

This paper has presented brief descriptions of four innovative in-house research programs from the Aeroelasticity Branch at the NASA Langley Research Center. In these programs, adaptive materials and integrated systems are used for either active aeroelastic control or passive aerodynamic shape control. Active wing flutter suppression and reduction in wing response at speeds below flutter were demonstrated in the PARTI program using piezoelectric actuators. Demonstration of an integrated

flutter suppression system using adaptive neural network control is being studied through the ANCAR program. The ACROBAT program demonstrated reduced buffeting of the vertical tails of an F-18 scale model using piezoelectric actuators and an active rudder. And the airfoil shaping potential of a new piezoelectric actuator technology called THUNDER was demonstrated in the ATTACH project.

5. REFERENCES

1. Renken, J. H., "Mission - Adaptive Wing Camber Control Systems for Transport Aircraft," *AIAA-85-5006*, AIAA 3rd Applied Aerodynamics Conference, Colorado Springs, Colorado, October 14-16, 1985.
2. Szodruch, J. and Hilbig, R., "Variable Wing Camber for Transport Aircraft," *Progress in Aerospace Sciences*, Vol. 25, pp. 297-328, 1988.
3. Redeker, G.; Wichmann, G.; and Oelker, H. C., "Aerodynamic Investigations Toward an Adaptive Airfoil for a Transonic Transport Aircraft," *Journal of Aircraft*, Vol. 23, No. 5, pp. 398-405, May 1986.
4. Sanford, M. C.; Abel, I.; and Gray, D. L., *Development and Demonstration of a Flutter Suppression System Using Active Controls*, NASA TR R-450, December 1975.
5. Newsom, J. R. and Abel, I., *Active Control of Aeroelastic Response*, NASA TM-83179, July 1981.
6. Waszak, M. R. and Srinathkumar, S., "Active Flutter Suppression: Control System Design and Experimental Validation," *AIAA Paper No. 91-2629*, August 1991.
7. Hwang, C.; Winther, B. A.; and Mills, G. R., *Demonstration of Active Wing/Store Flutter Suppression Systems*, AFFDL TR-78-65, June 1980.
8. Ashley, Holt; Rock, Stephen M.; Digumarthi, Ramarao; Chaney, Kenneth; and Eggers, Alfred J., Jr., *Active Control for Fin Buffet Alleviation*, WL-TR-93-3099, January 1994.
9. Weisshaar, T. A., "Aeroservoelastic Control with Active Materials - Progress and Promise," *Proceedings of the CEAS International Forum on Aeroelasticity and Structural Dynamics*, Manchester UK, June 1995.
10. Lichtenwalner, P. F. and Little, G. R., "Adaptive neural control of aeroelastic response," *SPIE Vol. 2717: Smart Structures and Integrated Systems*, Publication pending.
11. Heeg, J.; Miller, J. M.; and Doggett, R. V., *Attenuation of Empennage Buffet Response Through Active Control of Damping Using Piezoelectric Material*, NASA TM-107736, February 1993.
12. Crawley, E. F.; Warkentin, D. J.; et al., *Feasibility Analysis of Piezoelectric Devices*, MIT-SSL 5-88, Space Systems Laboratory, Massachusetts Institute of Technology, Cambridge, Mass., January 1988.
13. Leeks, Tamara J. and Weisshaar, Terrence A., "Optimization of unsymmetric actuators for maximum panel deflection control," *SPIE Vol. 2443: Smart Structures and Integrated Systems*, pp. 62-74, San Diego, CA, February 27-March 3, 1995.
14. Weisshaar, Terrence A., "Active Aeroelastic Tailoring with Advanced Materials," *31st Aircraft Symposium*, pp. 34-45, Gifu, Japan, Nov. 10-11, 1993.
15. Layton, Jeffrey B., "An Analysis of Flutter Suppression Using Adaptive Materials Including Power Consumption," *AIAA-95-1191-CP*, pp. 299-305, 1995.
16. Weisshaar, T. A., "Aeroservoelastic Control Concepts with Active Materials," *ASME International Mechanical Engineering Congress Exposition, Special Symposium on Aeroelasticity and Fluid/Structure Interaction Problems*, Proceedings of the 1994 ASME Winter Meeting, November 1994.
17. *The NASA Langley Transonic Dynamics Tunnel*, LWP-799, September 1969.
18. Heeg, J., *Analytical and Experimental Investigation of Flutter Suppression by Piezoelectric Actuation*, NASA TP-3241, March 1993.
19. Crawley, Edward F. and Anderson, Eric H., "Detailed Models of Piezoceramic Actuation of Beams," *Journal of Intelligent Material Systems and Structures*, Vol. 1., pp. 4-25, January 1990.
20. Takahashi, Sadayuki., "Longitudinal Mode Multilayer Piezoceramic Actuators," *Ceramic Bulletin* 65, The American Ceramic Society, pp. 1156-1157, 1986.
21. Haertling, Gene H., "Rainbow Ceramics -- A New Type of Ultra-High-Displacement Actuator," *American Ceramic Society Bulletin*, Vol. 73, No. 1, pp. 93-96, January 1994.
22. Hellbaum, Richard F., et al., Patent Application Number LAR15348-1.
23. Heeg, J.; McGowan, A-M. R.; Crawley, E. F.; and Lin, C. Y., "The Piezoelectric Aeroelastic Response Tailoring Investigation: Analysis and Open-Loop Testing," *Proceedings of the CEAS International Forum on Aeroelasticity and Structural Dynamics*, Manchester UK, June 1995.
24. Lin, C. Y.; Crawley, E. F.; and Heeg, J., "Open-Loop and Preliminary Closed-Loop Results of a Strain Actuated Active Aeroelastic Wing," *Proceedings of the 36th AIAA/ASME/ASCE/AHS/ASC Structures, Structural Dynamics, and Materials Conference*, New Orleans, LA, April 1995.
25. McGowan, Anna-Maria Rivas; Heeg, Jennifer; and Lake, Renee C., "Results From Wind-Tunnel Testing from the Piezoelectric Aeroelastic Response Tailoring Investigation," *Proceedings of the 1996 SDM Conference*, Publication pending.

26. Reich, G. W. and Crawley, E. F., *Design and Modeling of an Active Aeroelastic Wing*, SERC #4-94, Massachusetts Institute of Technology, February 1993.
27. Durham, Michael H.; Keller, Donald F.; Bennett, Robert M.; Wieseman, Carol D., *A Status Report on a Model for Benchmark Active Controls Testing*, NASA TM-107582, April 1991.
28. Rivera, Jose A., Jr.; Dansberry, Bryan E.; *et al.*, "Experimental Flutter Results with Steady and Unsteady Pressure Measurements of a Rigid Wing on a Flexible Mount System," *AIAA 91-1010*, April 1991.
29. Soloway, D. and Haley, P., *Neural Generalized Predictive Control*, NASA TM pending publication, 1996.

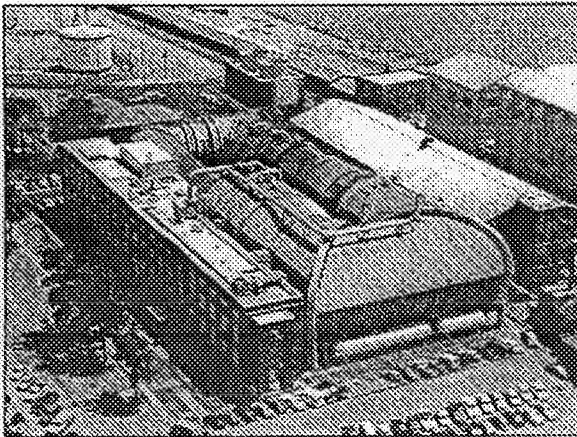


Figure 1. The NASA Langley Transonic Dynamics Tunnel (TDT).

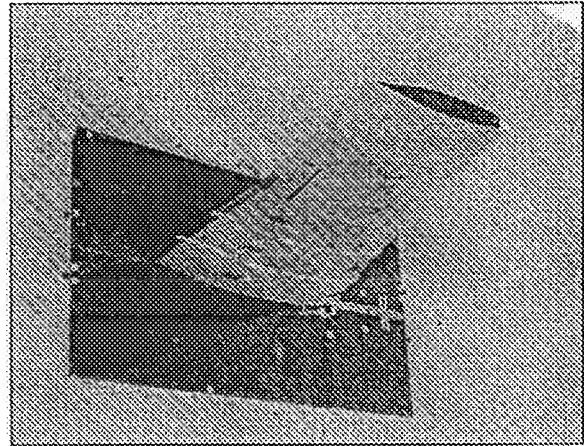


Figure 3. Photograph of the PARTI wind-tunnel model mounted in the TDT.

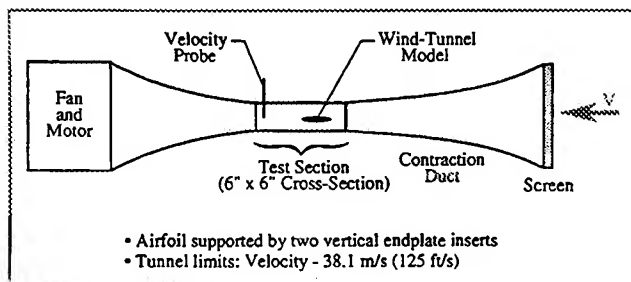


Figure 2. The Flutter Research and Experiment Device (FRED) wind tunnel.

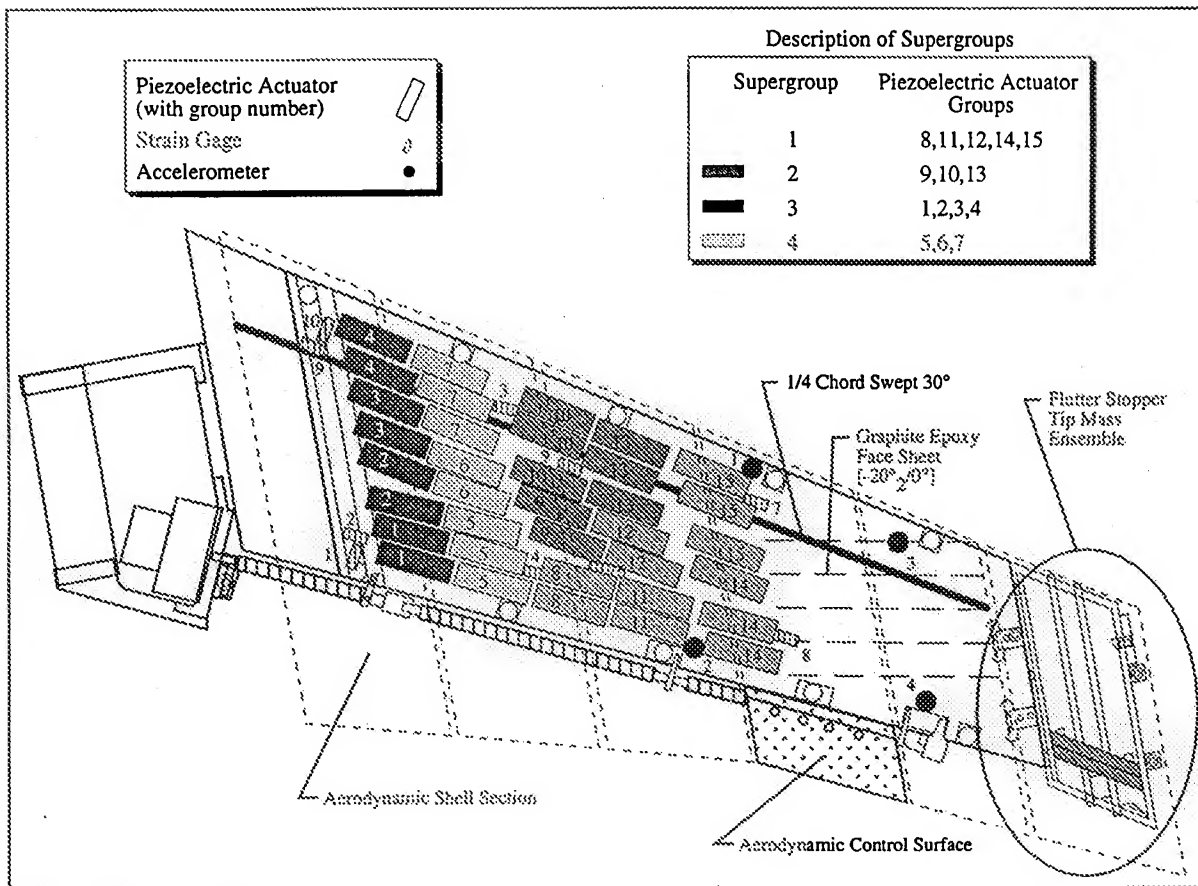


Figure 4. Drawing of the major components on the PARTI wind-tunnel model.

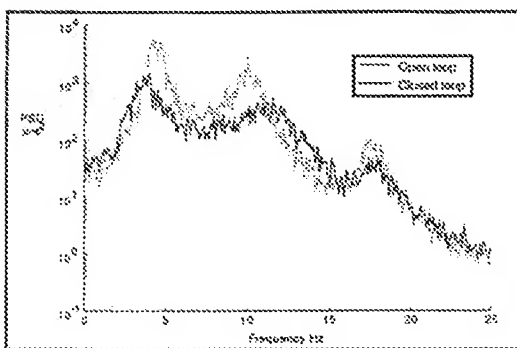


Figure 5. Results of subcritical response tailoring: Power spectral density functions.

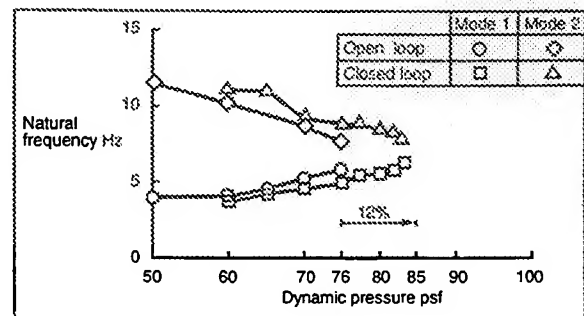


Figure 6. Comparison of natural frequency migration for open-loop and closed-loop systems.

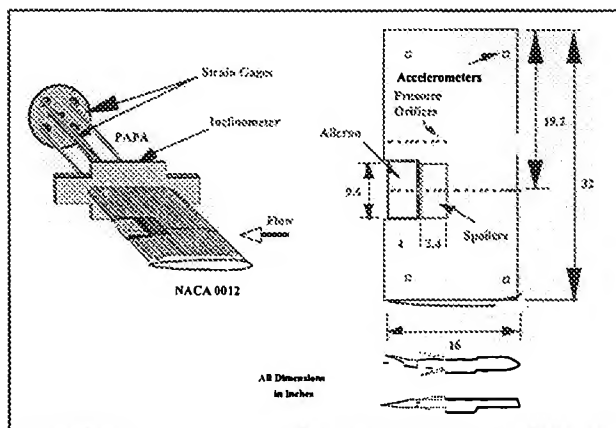


Figure 7. BACT wind-tunnel model.

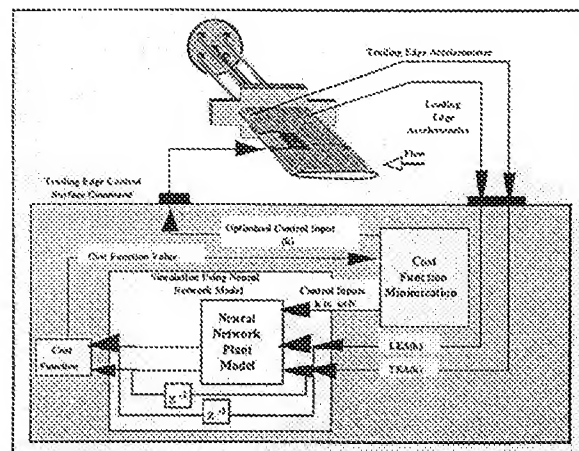


Figure 10. Neural network realization of predictive control.

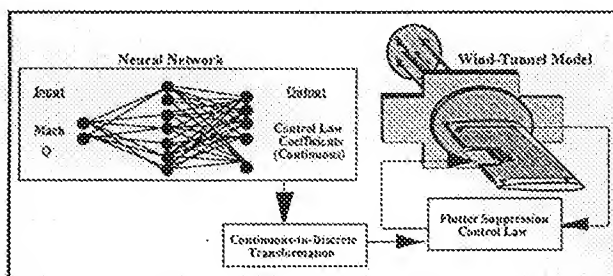


Figure 8. Neural-network-scheduled flutter suppression system.

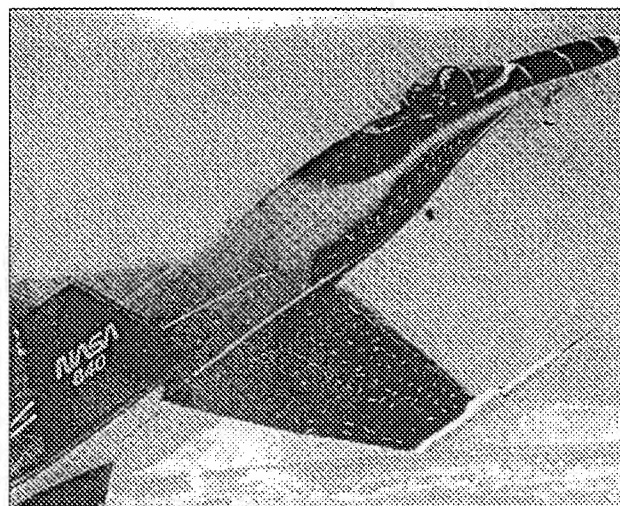


Figure 11. Flow visualization of LEX core breakdown.

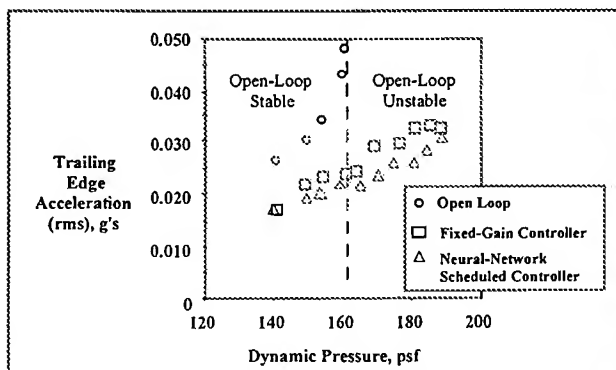


Figure 9. Comparison of neural-network-scheduled and fixed-gain closed-loop systems and the open-loop system.

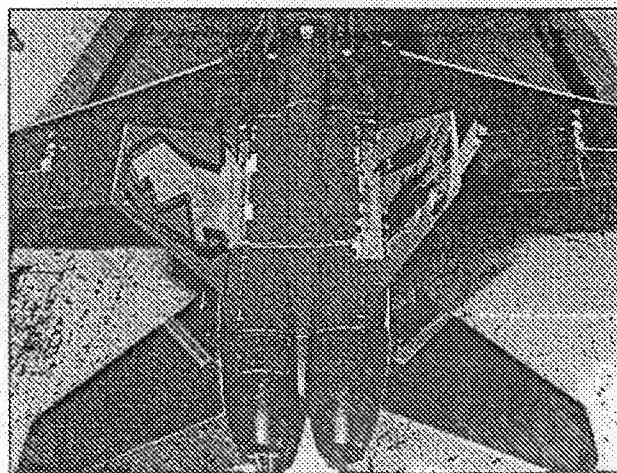


Figure 12. 1/6-scale F/A-18 A/B model installed in the TDT.



Figure 13. Piezoelectric actuator configuration.

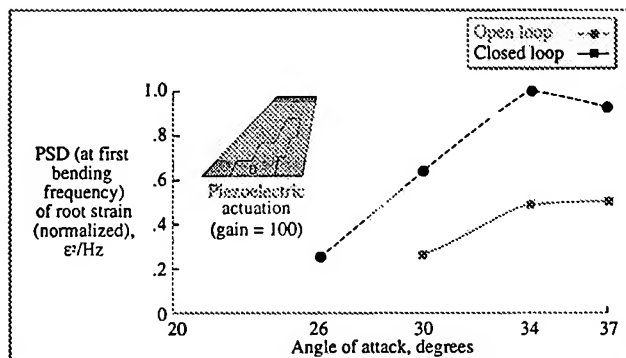


Figure 14. Buffeting alleviation results second entry (November 1995): first bending mode.

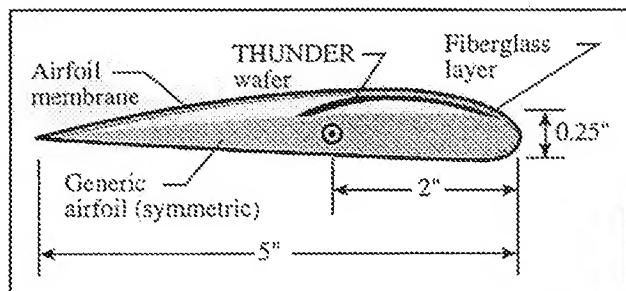


Figure 15. ATTACH testbed.

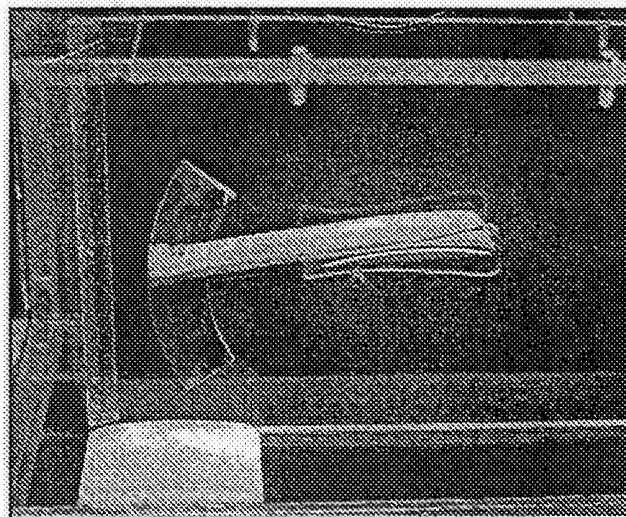


Figure 16. Photograph of the ATTACH model in FRED.

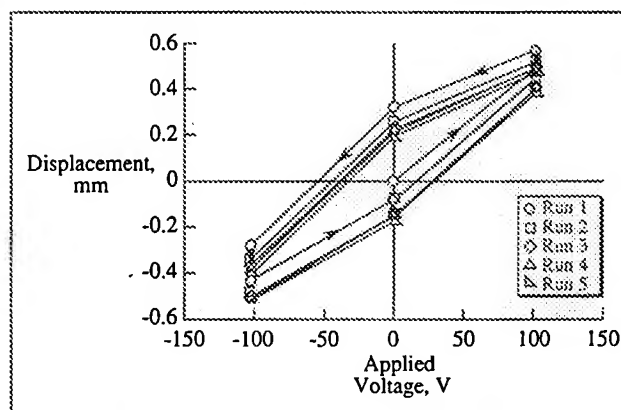


Figure 17. Typical wafer displacement pattern in response to five cycles of applied voltage (+/- 102 V).

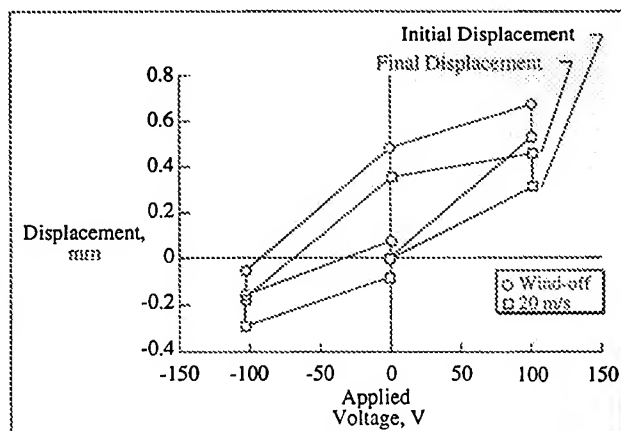


Figure 18. Changes in wafer displacement due to aerodynamic loading.

Neural Predictive Control for Active Buffet Alleviation

Lawrence E. Pado, Peter F. Lichtenwalner, Salvatore L. Liguore, Donald Drouin

The Boeing Company
St. Louis, Missouri

ABSTRACT

The Adaptive Neural Control of ~~Aeroelastic~~ Response (ANCAR) and the Affordable Loads and Dynamics Independent Research and Development (IRAD) programs at the Boeing Company jointly examined using ~~neural network based active~~ control technology for alleviating undesirable vibration and aeroelastic response in a scale model aircraft vertical tail. The potential benefits of adaptive control includes reducing aeroelastic response associated with buffet and atmospheric turbulence, increasing flutter margins, and reducing response associated with nonlinear phenomenon like limit cycle oscillations. By reducing vibration levels and thus loads, aircraft structures can have lower acquisition cost, reduced maintenance, and extended lifetimes.

Wind tunnel tests were undertaken on a rigid 15% scale aircraft in Boeing's mini-speed wind tunnel, which is used for testing at very low air speeds up to 80 mph. The model included a dynamically scaled flexible tail consisting of an aluminum spar with balsa wood cross sections with a hydraulically powered rudder. Neural Predictive Control (NPC) was used to actuate the vertical tail rudder in response to strain gauge feedback to alleviate buffeting effects. First mode RMS strain reduction of 50% was achieved.

The Neural Predictive Control system was developed and implemented by the Boeing Company to provide an intelligent, adaptive control architecture for smart structures applications with automated synthesis, self-optimization, real-time adaptation, nonlinear control, and fault tolerance capabilities. It is designed to solve complex control problems through a process of automated synthesis, eliminating costly control design and surpassing it in many instances by accounting for real world non-linearities.

Keywords: Neural Networks, Active Vibration Control, Buffet Load Alleviation, Smart Structures, Aeroservoelasticity

1.0 INTRODUCTION

The Boeing Company examined using neural network based active control technology for alleviating undesirable vibration and aeroelastic response in a scale model aircraft vertical tail. Adaptive control can reduce aeroelastic response associated with buffet and atmospheric turbulence, it can increase flutter margins, and it may be able to reduce response associated with nonlinear phenomenon like limit cycle oscillations. By reducing vibration levels and loads, aircraft structures can have lower acquisition cost, reduced maintenance, and extended lifetimes. The focus of this current program is to demonstrate the use of an active rudder using Neural Predictive Control (NPC) to reduce buffet response. This report documents a wind tunnel experiment using a 15% aerodynamics model with a flexible vertical tail. The vertical tail was designed with a movable rudder that was controlled using an imbedded hydraulic actuator. The model was installed on a strut that was controlled to pitch the model up to 7 deg/sec for a range of angle of attack up to 45°.

2.0 BACKGROUND

Buffet is defined as random loadings which arise from pressure fluctuations. Early investigations of buffet date back as far as 1931, when it was determined that buffeting due to an up-draft and sudden increase in angle of attack, was the source of destruction of a Junkers F13 at Moephan, England on July 21, 1930¹. As time passed, aircraft flew faster and between 1940 and 1960 many studies were performed on wing buffet; such as, the Bristol Bagshot Type 95². After 1968, emphasis was placed on maneuverability, agility and high angle of attack flight, all of which exposed the empennage to random aerodynamic loadings.

In recent times, modern combat aircraft have become faster, more agile, and are demanded to fly in conditions of separated flow. Under these demanding flight environments, the aircraft is often subjected to severe buffet which can drastically reduce the fatigue life of the aircraft structure and increase structural design requirements, cost, and weight.

Various methods for alleviating buffeting have been explored. Perhaps the most common one is strengthening the structure which can increase the fatigue life of the structure but increases weight and is very likely to chase the fatigue failures to un-strengthened adjacent structures. Other techniques attempted to control the vortex³. These attempts either have undesirable side effects such as added weight or are not effective enough.

Other groups have performed research on using active control to alleviate buffet. The first thought of using an actively controlled rudder to reduce the strain at the root of a tail caused by aerodynamic loads was Ashely⁵ in 1992. The actual first attempt was successfully demonstrated by Moses⁴ in 1995. Tests were performed on a 1/6 scale F-18 wind tunnel model in NASA's Transonic Dynamics Tunnel. In that test, the starboard vertical tail was equipped with an active rudder and the port vertical tail was equipped with piezoelectric actuators. Root Mean Square (RMS) values of root strain were reduced by as much as 19% using the piezo actuators. Results using the rudder reduced strains in once instance by 18%⁶.

In 1993, Boeing (formerly McDonnell Douglas Aerospace) began looking for an adaptive control architecture for smart structures applications with automated synthesis, self-optimization, real-time adaptation, nonlinear control, and fault tolerance capabilities. The nonlinear and adaptability requirements immediately suggested the use of neural network technology. After examining forward-inverse control which showed promise in simulation, it was eventually dropped due to its low tolerance to noise when creating the neural network based model.

A more suitable paradigm was based on a model predictive control framework⁷. These types of controllers generally use state space representations as the model⁸. The development work performed at Boeing was based on how to integrate a neural network model into this framework to replace the more ordinary linear state space model. Using the neural network as the plant model enables the model based predictive control approach to be applied to a wide variety of complex, nonlinear systems due to the nonlinear modeling capability of neural networks. It also provides a direct method of control system adaptation by allowing the neural network model to be trained on-line. This architecture, which uses a neural network model within an MPC framework, is hence referred to as Neural Predictive Control (NPC). A description of the NPC architecture developed at Boeing (formerly MDA) and its performance on a benchmark cantilevered beam vibration suppression problem is given by Pado and Damle⁹ (1996). Results of applying the NPC system for active flutter suppression is given by Lichtenwalner et al¹⁰ (1996). NASA is currently working on a similar approach called Neural Generalized Predictive Control (NGPC) for nonlinear control applications¹¹. Other control system architectures involving neural network-based MPC have been used successfully in the chemical processing industry as well¹² (Draeger, et al., 1995). These types of process based controllers are far too inefficient to be used in real time vibration control systems.

The focus of this current program is to demonstrate active buffet suppression on a vertical tail with an active rudder using NPC. This method has the advantages of both being effective and adding little additional mass. The paper briefly documents a wind tunnel test and the successful results.

3.0 PHYSICAL TEST SETUP

The wind tunnel test was performed on a 15% scale model aircraft. Testing was done in the Boeing St. Louis Mini-Speed Wind Tunnel test Facility. The mini-speed wind tunnel is used for testing at very low wind speeds up to 80mph in an open jet test section 15 feet high by 20 feet wide by 20 feet long. The model was configured with a dynamically scaled flexible vertical tail, mounted on the left-hand side of the model. All other parts on the model were "rigid". Instrumentation was installed on the flexible vertical tail to monitor internal dynamic loads and accelerations due to vortex impingement.

The flexible tail is a flutter model design with an aluminum spar and balsa wood cross sections, as depicted in Figure 1 and Figure 2. The balsa wood sections are non-structural and give the tail its aerodynamic shape. A hydraulic actuator is incorporated into the tail to move the rudder during the controlled runs. The flexible vertical tail is instrumented with both strain gauges and accelerometers placed to be sensitive to strain and acceleration both inboard and outboard of the tail. These sensors were used for quantifying the bending and torsion moments and for providing real-time feedback to the active control

system. The actuator was designed and built to specifications in the Boeing wind tunnel fabrication facilities. The pump and servo-value were connected to the model through tubing above the wind tunnel setup.



Figure 1. Flex Tail Aluminum Spar with Hydraulic Actuator

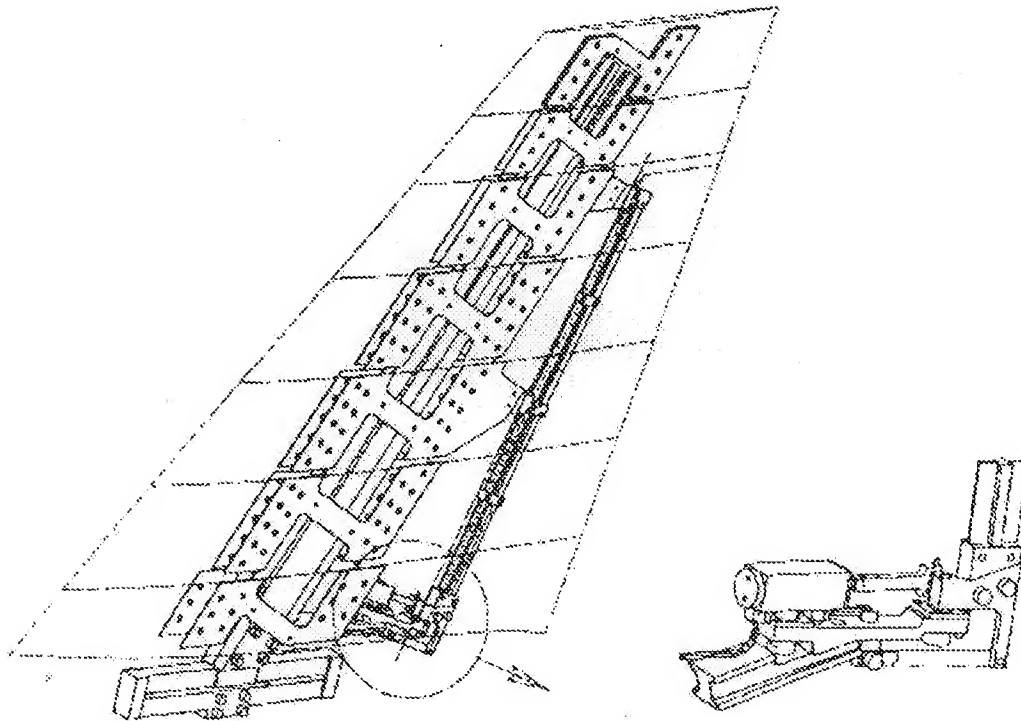


Figure 2. Schematic of Flex Tail with Active Rudder

4.0 ENVIRONMENT AND MODEL CHARACTERISTICS

Buffet causes structural fatigue leading to costly repairs. A rule of thumb is that a 10% decrease in RMS vibration leads to a doubling of fatigue life. The magnitude of buffeting encountered is a function of dynamic pressure (Q) and Angle of Attack (AOA) as shown in Figure 3. Based on the information in Figure 3, selected Qs between 3.5 and 10 and AOAs between 28 and 38 degrees were used as the flight conditions to examine the utility of using Neural Predictive Control for buffet alleviation. When these conditions are scaled up to full size, over 80% of the damage takes place in these regimes.

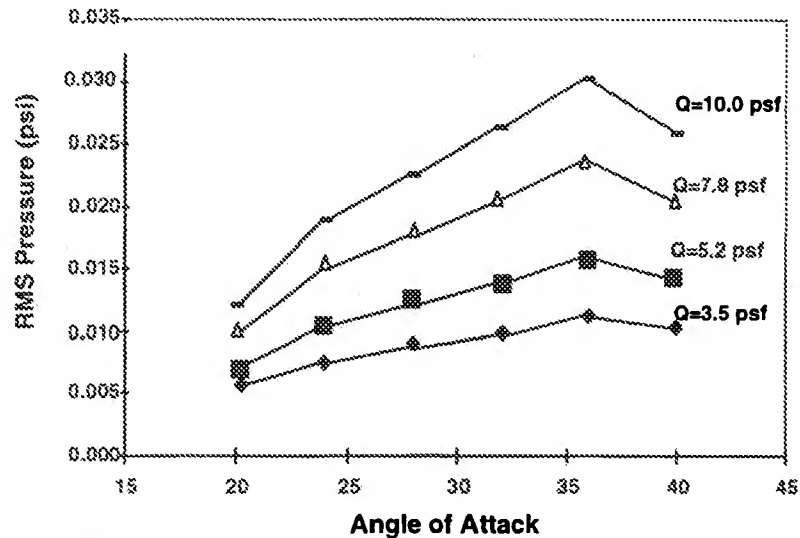


Figure 3 - Dynamic pressure effects on open loop root bending RMS

There were two modes of interest in this test - first mode bending response at 16.4Hz and a torsion mode response at 38.3 Hz as shown in Figure 4.

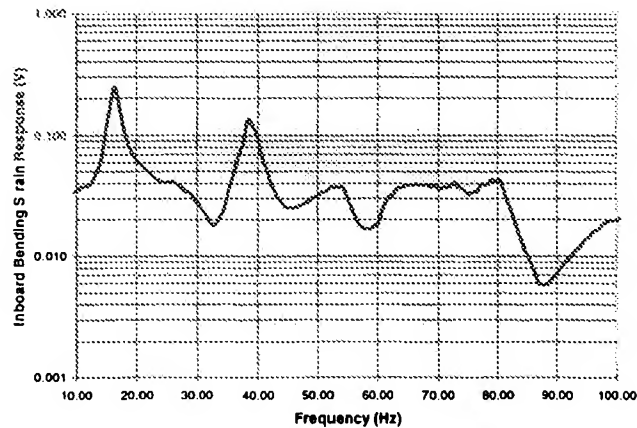


Figure 4 – Commanded rudder to strain transfer function as measured by a strain sensor located at the inboard base

An important goal of the test was to control the torsion mode of the tail as well as the bending mode. As can be seen in Figure 5, authority as measured by the Rotational Variable Displacement Transducer (RVDT), was sharply curtailed

beginning at about 35Hz. Although mode 2 authority was reduced by a factor of four, it was felt that there was still enough bandwidth to attempt control of the torsion mode.

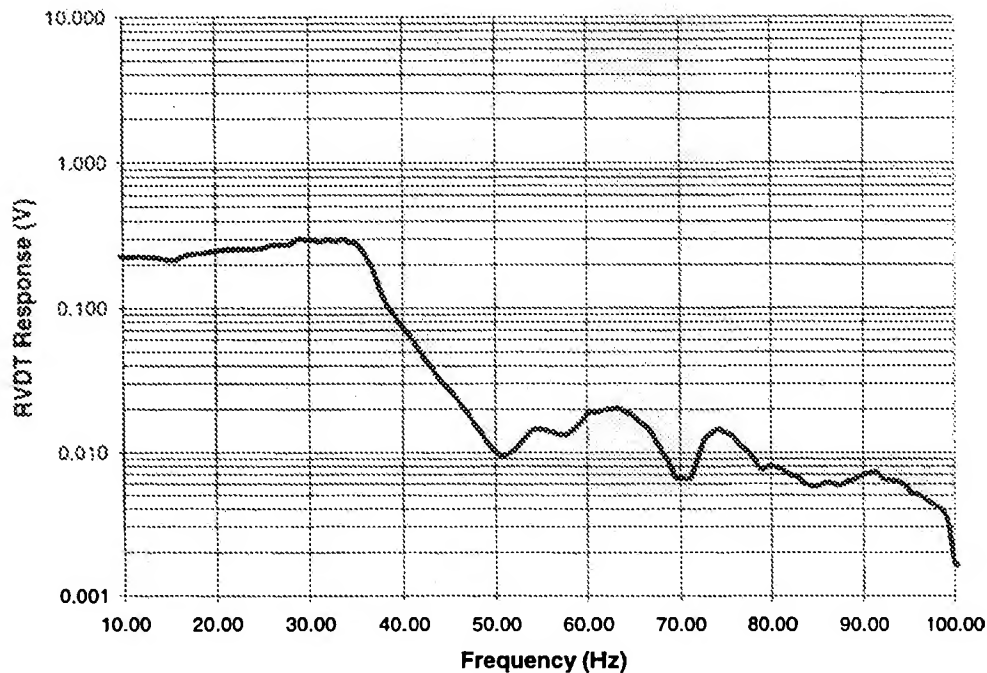


Figure 5 - Commanded signal to rudder response transfer function as measured using a RVDT

5.0 CONTROL SYSTEM GOALS AND SETUP

As one of the primary objectives for this test, Neural Predictive Control (NPC) was used to control the hydraulic actuator to actively position the rudder to reduce buffet as shown in Figure 6. A 133Mhz Pentium based PC was used to provide the processing power for the NPC digital controller running at 400Hz as well as real time data logging and graphical plotting. The PC was also equipped with a plug-in Sharc board containing 8 RISC processors useful for modeling the plant in real time. Analog-to-Digital and Digital-to-Analog boards working at ± 10 volts mounted within the PC were used for data I/O.

The test plan called for controlling only the first bending mode, then controlling only the second mode (torsion), and finally controlling both together. Root bending strain was used and the control input for the bending mode. The inboard torsion strain gauge was used for second mode control. Test time ran out before dual mode control was attempted.

Another issue to be looked at was controller performance as a function of maximum allowed deflection. It is important that buffet reduction not interfere with flight performance. Controller performance at ± 8 degrees and ± 14 degrees maximum rudder deflection was examined.

The neural controller was trained at one specific static AOA for each band of interest. This NPC model was also used to control the rudder during transient maneuver testing. In future developments, the neural controller will be able to adapt from one flight conditions to the next based on historical knowledge. The neural controller will train on the response during each condition and use Mach No., dynamics pressure, AOA, and pitch rate as additional state variables.

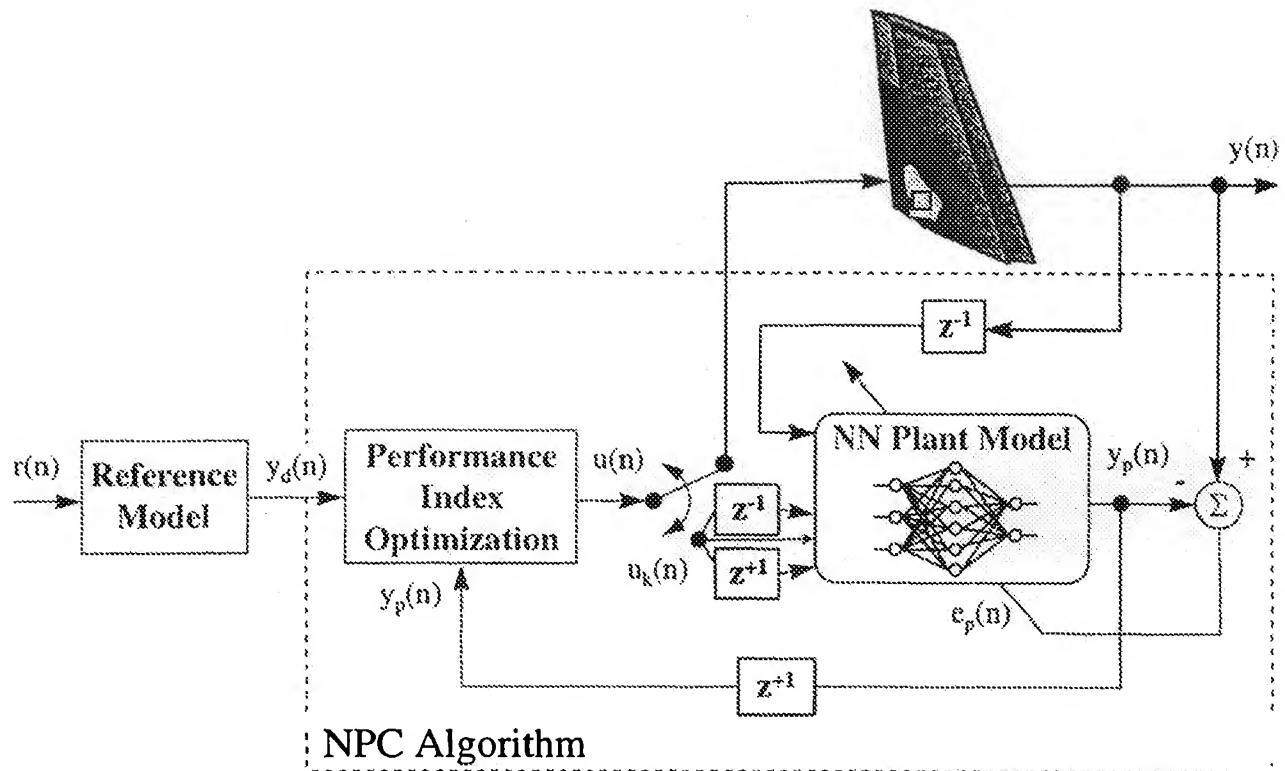


Figure 6 - Neural Predictive Control Buffet Load Alleviation System

6.0 THE NEURAL NETWORK MODEL

A key component of NPC is a neural network model of the system to be controlled. A neural network can be defined as a massively parallel, highly interconnected collection of simple processing units that receives inputs (sensor output and input history), passes them through its network of weights and nonlinearities, and transforms them into outputs (future state predictions). This technology is useful for linear and non-linear data modeling, and is especially adept at handling complex, noisy data. These models can be created with much less effort than first principle models and can capture real world effects. Figure 7 shows a typical architecture for capturing plant dynamics. Both past states and past controls applied at discrete instances of time are used along with the candidate future control to predict the future state of the system¹³.

The neural network that was used for modeling the plant is known as a Multi-Layer-Perceptron (MLP) trained with backpropagation¹⁴. This type of neural network is a universal approximator, able to learn any function to any degree of accuracy. It has the advantage of being the most compact of all neural network architectures, as well as providing excellent generalization. The major disadvantages of this type of network involves its longer than average training times and the fact that the number of nodes in each layer and the number of layers must be determined either by an experienced modeler or by trial and error. For linear systems, a linear version of the network may be used by employing only the input and output layers of the network and making the output transfer function linear.

In many plants, it is desirable and possible to generate modeling data under disturbance or nearly disturbance free conditions. This is normally the case for plants which rely on PZT actuators⁹, or any other operationally independent actuator. In this particular case the control surface of the rudder used aerodynamic forces to oppose aerodynamic forces. Due to this, the model to be used for control had to be created under very noisy conditions, in some cases the signal to noise ratio could be as low as 1-to-10. To complicate matters, the amount of authority available due to aerodynamic forces is a nonlinear function of

Q and AOA as is implied by Figure 3. It was postulated that a suitable model for control could be developed at each Q given that data was collected at a low enough angle of attack to limit the amount of noise due to buffet.

To model the rudder-to-strain transfer function, the scale aircraft was positioned to an angle of attack of 7 degrees, where buffeting is almost nonexistent. The plant is modeled by driving the hydraulic actuator with uniformly distributed random excitation at the bandwidth of the anticipated control rate of 200Hz (a sample rate of 400Hz). Feedback from the strain sensor is digitized and fed into the inputs of the neural network and passed through a digital tapped-delay-line for m past time steps. A similar process is used for feeding the current and past controls into the network inputs. The output from the network is compared to actual sensor output and any difference between the two is backpropagated through the network to modify its learning parameters (weights).

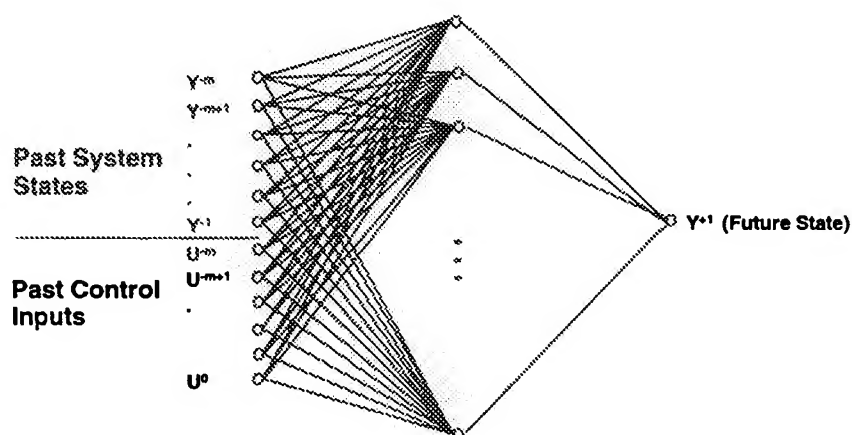


Figure 7 - A Neural Network Plant Model

7.0 PREDICTIVE CONTROL IMPLEMENTATION

After a neural network model of the plant has been trained, it is then ready to be used within the predictive control framework. Figure 6 diagrams the basic algorithm. Current state information is fed into the neural network as well as the first proposed control input. The D/A board has possible output voltages ranging between ± 10 volts and the first proposed control input may be chosen as any value in that range. In the Multi-Step Horizon Look Ahead block, the effect of this input is projected n steps into the future. The value of n is approximately determined both by the modes of the plant and the control rate, and is then empirically perturbed. The n steps into the future is known as the horizon and normally ranges between 1 and 20 time steps.

The horizon is then passed to the Performance Index block. As shown in Figure 6, the performance index is a cost function comprised of: the future predictions of the neural network model, its derivatives, and the proposed control signal magnitude. Each of these parameters can be weighted to form a cost performance index tailored to a particular system⁹.

Finally, the cost is passed from the Performance Index block to the Search Strategy block. In most conventional linear predictive control schemes, an entire series of optimal future controls can be solved for analytically and only the most recent one is used. This approach is known as using a receding horizon and is powerful for linear systems but is limited by its inability to work on nonlinear systems. For a controller to be broadly applicable, no assumptions can be made about the nonlinear aspects of a plant. For predictive control to achieve this goal an exhaustive search strategy can be employed. In this approach, a comprehensive set of possible control inputs (a control horizon) is presented to the neural network model and out of the lowest cost horizon the first input of the horizon is selected. The advantage of this method is that the search is guaranteed to work on any system, regardless of complexity. The disadvantage of an exhaustive search lies in its long computation time, it is actually computationally impossible to select independent future controls with a modest horizon due to combinatorial explosion. The simplifying assumption which makes exhaustive searching possible and in no way relies on

any plant information is that all future inputs remain at the same value. This assumption approaches truth when the ratio of control rate to modal frequency is very high. One additional technique which reduces generality but dramatically decreases search time is incorporating plant information into the search strategy. Assuming near linearity for example, can reduce the amount of model evaluations to less than five.

8.0 PERFORMANCE AND TEST RESULTS

As discussed in section 5.0 above, the bending mode (mode 1) was the first to be controlled. Because dynamic fatigue life is determined chiefly by root-mean-square (RMS) vibration levels, control success was measured by examining percent reduction in RMS vibration levels at a particular flight condition as compared to open loop. Band 1 is defined as the RMS vibration level occurring between 10 and 20 Hz. This band was chosen to single out mode 1 effects and was set wide enough to capture any frequency shifts caused by the controller and different flight conditions. Figure 8 shows the performance of the NPC controller on RMS root bending strain against open loop results. These curves are based on average value across the Q spectrum on all runs. Table 1 and Table 2 show values of RMS vibration reduction at discrete values of AOA and Q for the two levels of rudder authority. While looking at the data represented in these tables and charts, the following rule of thumb should be kept in mind. *A 10% reduction in RMS vibration corresponds to a doubling in the fatigue life of a structure.* For band 1 reductions with full 14 degree rudder authority, NPC/rudder vibration control shows averages of close to 40% and individual instances of over 50%. This level of performance is very substantial. Figure 9 is a PSD showing band 1 response reduction using NPC. Note that in this plot the NPC controller was trained only to work on band 1.

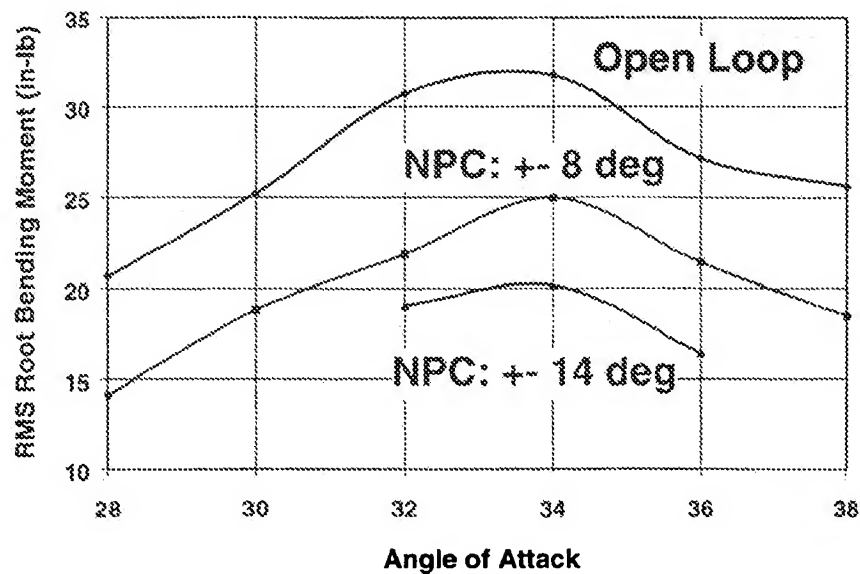


Figure 8 - NPC Reduction in RMS root bending moment with hard limits on rudder deflection

Maximum Actuated Deflection = +/- 8 deg							
Dynamic Pressure	Angle of Attack						
	26	28	30	32	34	36	38
Q=2.3(psf)	40.1%	24.4%					
Q=2.7(psf)		31.3%	27.3%	6.99%			
Q=3.1(psf)			22.8%	26.1%	19.5%		
Q=3.5(psf)		31.5%	25.4%	28.7%	21.3%	21.1%	27.8%

Table 1 - Band 1 RMS vibration reduction at measured Q/AOA conditions with an 8° hard rudder limit

Maximum Actuated Deflection = +/- 14 deg							
Dynamic Pressure	Angle of Attack						
	26	28	30	32	34	36	38
Q=2.3(psf)		50.53%	42.1%				
Q=2.7(psf)			43.9%	39.1%	38.1%		
Q=3.1(psf)				38.0%	36.4%	39.4%	
Q=3.5(psf)				53.9%	52.7%		

Table 2 - Band 1 RMS vibration reduction at measured Q/AOA conditions with an 14° hard rudder limit

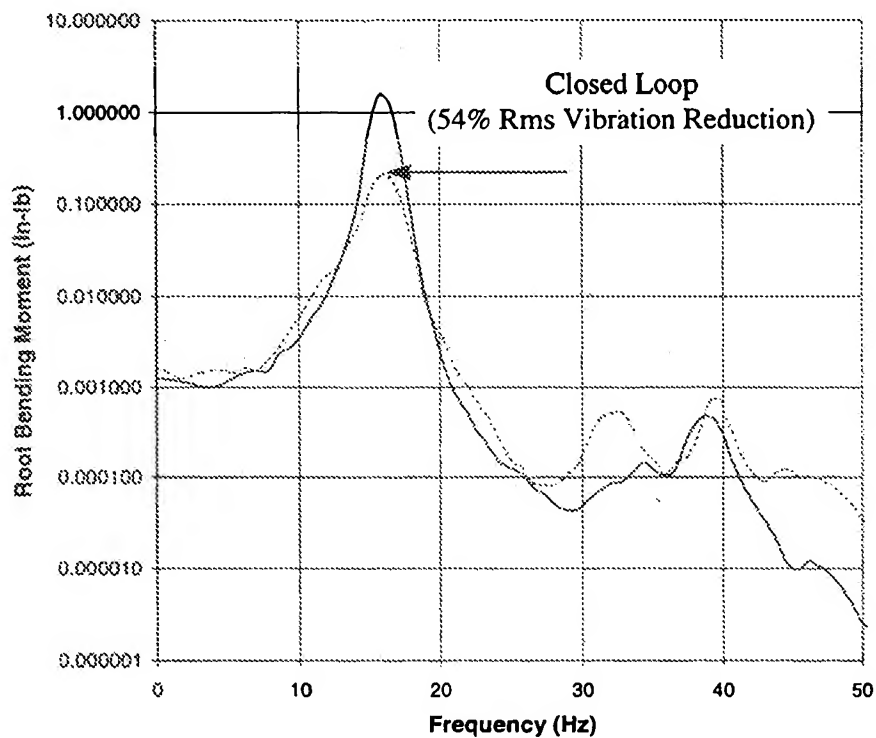


Figure 9 - PSD showing Band 1 response reduction using NPC

Band 2 is defined as the RMS vibration level occurring between 30 and 40 Hz. This is principally a torsion mode strongly coupled to a bending mode and can be measured with an outboard bending strain gauge. This band was chosen to single out mode 2 effects and was chosen wide enough to capture any frequency shifts caused by the controller. Table 3 shows performance of 20% to 37% achieved by the NPC controller on RMS outboard bending strain as a reduction in RMS vibration percentage. This table shows values of RMS vibration reduction at discrete values of AOA and Q. Very few cases were run at this extreme condition due to possible severe damage occurring to the tail while open loop measurements were being made.

Maximum Actuated Deflection = +/- 14 deg		
Dynamic Pressure	Angle of Attack	
	20	24
Q=10.0(psf)	20%	37%

Table 3 - Band 2 RMS vibration reduction at measured Q/AOA conditions with an 14° hard rudder limit

9.0 ISSUES AND FUTURE WORK

There are issues that need be examined for both rudder based vibration reduction and on the NPC system. Work on improving NPC is currently progressing on two issues. The first is determining the correct cost function. Currently these parameters must be chosen by trial and error with the engineer choosing the parameters, observing the effect on the plant, and trying new parameters. Not only is this a tedious process, but the selected parameters have no guarantee of being optimally chosen. Even considering this fact however, it is far faster to produce a working NPC control system than to design a more conventional controller. Some progress has been made in this area and will be featured in future papers. The second issue is expanding NPC from a single input/single output system (SISO) to a multiple input/multiple output (MIMO) system. Although it appears to be difficult to handle very many input/outputs, as many as four input/ four output systems appear to be feasible.

One important rudder based control issue is to examine the effect of using the rudder for vibration suppression concurrently with using it for flight control. Future efforts will focus on MIMO control, other actuator options such as PZT, and affordability and cost issues. These issues will need to be addressed in future work.

10.0 CONCLUSIONS

The use of NPC based active control along with an active rudder appears to be a very powerful way of alleviating the effects of the buffeting environment on structural fatigue. Considering that a 10% reduction in RMS vibration corresponds to a doubling in the fatigue life of a structure, this scheme appears to provide breakthrough performance on extending the life and the maintenance cost of current and future aircraft.

11.0 REFERENCES

1. Frasier, R.A. and Duncan, W.J., "The Accident Investigation Sub-committee on the Accident to the Aeroplane G-AAZK at Meopham, Kent, England on July 21, 1930," *British R&M 1360*, January 1931. July 21, 1903
2. Russel, A., "A Span of Wings," *Airlife Publishing*, Shrewsbury, England, 1992.
3. Bean, D.E., Greenwell, D.I. and Wood, N.J., "A Vortex Control Technique for the Attenuation of Fin Buffet," *ICAS-92-4.10.3*.
4. Ashley, H., Rock, S.M., Digumarthi, R., Chaney, K., and Eggers, A.J. Jr., "Active Control For Fin Buffet Alleviation," *WK-TR-93-3099*, January 1994.
5. Moses, R.W., "Vertical Tail Buffeting Alleviation Using Piezoelectric Actuators - Some Results of the Actively Controlled Response of Buffet-Affected Tail (ACROBAT) Program", *Proceeding of the SPIE Smart Structures and Materials Conference*, 1997.
6. Moses, R.W., "Vertical Tail Buffeting Alleviation Using Piezoelectric Actuators And Rudder", *High Angle of Attack Technology Conference* September 17-19, 1996 NASA LaRC, Hampton VA
7. M. Morari. "Model Predictive Control: Multivariable Control Technique of Choice in the 1990s?," *Advances in Model-Based Predictive Control*, Oxford University Press Inc., New York, 1994.
8. R. Soeterboek, *Predictive Control - A Unified Approach*. p. 51, Prentice Hall , Cambridge, Great Britain, 1992.
9. Pado L.E., Damle R.D., "Predictive Neuro Control of vibration in Smart Structures", *Proceedings of the SPIE 1996 Symposium on Smart Structures and Materials*, San Diego, CA, 1996.

10. Lichtenwalner, P. F., Little, G. R., Pado, L. E., and Scott, R. C., "Adaptive Neural Control for Active Flutter Suppression," ASME 1996 IMEC&E Conference Proceedings," Atlanta, GA, Nov. 1996.
11. Soloway, D. and Haley, P. J., "Neural Generalized Predictive Control - A Newton-Raphson Implementation," 1996, *NASA Technical Memorandum 110244*.
12. Draeger, A., Engell, S., and Ranke, H., 1995, "Model Predictive Control Using Neural Networks," *IEEE Control Systems*, Vol. 15, No. 5, pp. 61-66.
13. K.S. Narendra,, "Identification and Control of Dynamical Systems Using Neural Networks," *IEEE Transactions on Neural Networks*, Vol 1, No. 1, March 1990.
14. D.E. Rumelhart, J.L. McClelland, and the PDP Research Group, (1986) *Parallel Distributed Processing*, vol. 1, Foundations. Cambridge, MA: MIT Press, Ch. 8

Set	Items	Description
S1	7252	CRITICAL() (CODE? ? OR CODING) OR (NEST??? OR INNER?) () LOOP? ? OR ATOMIC() EXECUT?
S2	379	S1(5N) (DETERMIN? OR COMPAR? OR ASCERTAIN? OR ANALY? OR IDE- NT? OR CHECK? OR VERIF? OR JUDGE? ? OR JUDGING?)
S3	98	S1(5N) (MONITOR? OR EXAMIN? OR DETECT? OR UNCOVER? OR REVEA- L? OR ASSESS? OR EVALUAT? OR INSPECT? OR DISCOVER?)
S4	439	S1(5N) (REPLAC? OR SUBSTITUT? OR PLACE() "OF" OR REWRIT? OR - RE() WRIT??? OR MODIF? OR REVIS??? OR CHANG??? OR UPDATING? OR UP() (DATE? ? OR DATING) OR UPGRAD? OR CUSTOMI? OR ALTER??? OR OPTIMI?)
S5	48185	(CALL??? OR INVOK? OR INVOC?) (3N) (FUNCTION? OR COMMAND? OR INSTRUCT? OR PROCEDURE? ?)
S6	6356	S5(5N) (USE? ? OR USING OR UTILI? OR APPLY? OR APPLIE? ? OR EMPLOY? OR IMPLEMENT? OR "WITH")
S7	46	(COMPIL? OR RUN OR RUNS OR RUNNING) (7N) S4
S8	0	S2:S3 AND S4 AND S5:S6
S9	29	S2:S3 AND S4
S10	20	RD (unique items)
S11	15	S10 AND PY=1978:2003
S12	0	S4 AND S6
S13	16	S1 AND (REPLAC? OR REWRIT? OR RE() WRIT????) AND CRITICAL? (-) (CODE? ? OR CODING)
S14	16	S13 NOT S11
S15	13	S14 AND PY=1978:2003
S16	7	RD (unique items)
S17	22	S11 OR S16
S18	11	S1 AND EXTEN? (7N) COMPIL?
S19	10	S18 NOT (S9 OR S13)
S20	9	S19 AND PY=1978:2003
S21	9	RD (unique items)
S22	31	S17 OR S21
S23	31	RD (unique items)
File	2:INSPEC 1898-2007/Nov W2	(c) 2007 Institution of Electrical Engineers
File	6:NTIS 1964-2007/Dec W2	(c) 2007 NTIS, Intl Cpyrght All Rights Res
File	8:EI Compendex(R) 1884-2007/Nov W3	(c) 2007 Elsevier Eng. Info. Inc.
File	34:SciSearch(R) Cited Ref Sci 1990-2007/Nov W4	(c) 2007 The Thomson Corp
File	35:Dissertation Abs Online 1861-2007/Jul	(c) 2007 ProQuest Info&Learning
File	56:Computer and Information Systems Abstracts 1966-2007/Oct	(c) 2007 CSA.
File	60:ANTE: Abstracts in New Tech & Engineer 1966-2007/Nov	(c) 2007 CSA.
File	62:SPIN(R) 1975-2007/Nov W2	(c) 2007 American Institute of Physics
File	65:Inside Conferences 1993-2007/Nov 26	(c) 2007 BLDSC all rts. reserv.
File	95:TEME-Technology & Management 1989-2007/Nov W3	(c) 2007 FIZ TECHNIK
File	99:Wilson Appl. Sci & Tech Abs 1983-2007/Sep	(c) 2007 The HW Wilson Co.
File	111:TGG Natl.Newspaper Index(SM) 1979-2007/Nov 15	(c) 2007 The Gale Group

File 144:Pascal 1973-2007/Nov W2
(c) 2007 INIST/CNRS
File 239:Mathsci 1940-2007/Nov
(c) 2007 American Mathematical Society
File 256:TecInfoSource 82-2007/Dec
(c) 2007 Info.Sources Inc
File 434:SciSearch(R) Cited Ref Sci 1974-1989/Dec
(c) 2006 The Thomson Corp
File 583:Gale Group Globalbase(TM) 1986-2002/Dec 13
(c) 2002 The Gale Group

Set	Items	Description
S1	7252	CRITICAL() (CODE? ? OR CODING) OR (NEST??? OR INNER?) () LOOP? ? OR ATOMIC() EXECUT?
S2	379	S1(5N) (DETERMIN? OR COMPAR? OR ASCERTAIN? OR ANALY? OR IDE- NT? OR CHECK? OR VERIF? OR JUDGE? ? OR JUDGING?)
S3	98	S1(5N) (MONITOR? OR EXAMIN? OR DETECT? OR UNCOVER? OR REVEA- L? OR ASSESS? OR EVALUAT? OR INSPECT? OR DISCOVER?)
S4	439	S1(5N) (REPLAC? OR SUBSTITUT? OR PLACE() "OF" OR REWRIT? OR - RE() WRIT??? OR MODIF? OR REVIS??? OR CHANG??? OR UPDATING? OR UP() (DATE? ? OR DATING) OR UPGRAD? OR CUSTOMI? OR ALTER??? OR OPTIMI?)
S5	48185	(CALL??? OR INVOK? OR INVOC?) (3N) (FUNCTION? OR COMMAND? OR INSTRUCT? OR PROCEDURE? ?)
S6	6356	S5(5N) (USE? ? OR USING OR UTILI? OR APPLY? OR APPLIE? ? OR EMPLOY? OR IMPLEMENT? OR "WITH")
S7	46	(COMPIL? OR RUN OR RUNS OR RUNNING) (7N) S4
S8	0	S2:S3 AND S4 AND S5:S6
S9	29	S2:S3 AND S4
S10	20	RD (unique items)
S11	15	S10 AND PY=1978:2003
S12	0	S4 AND S6
S13	16	S1 AND (REPLAC? OR REWRIT? OR RE() WRIT???) AND CRITICAL? (-) (CODE? ? OR CODING)
S14	16	S13 NOT S11
S15	13	S14 AND PY=1978:2003
S16	7	RD (unique items)
S17	22	S11 OR S16
S18	11	S1 AND EXTEN? (7N) COMPIL?
S19	10	S18 NOT (S9 OR S13)
S20	9	S19 AND PY=1978:2003
S21	9	RD (unique items)
S22	31	S17 OR S21
S23	31	RD (unique items)
File	2:INSPEC 1898-2007/Nov W2	(c) 2007 Institution of Electrical Engineers
File	6:NTIS 1964-2007/Dec W2	(c) 2007 NTIS, Intl Cpyrght All Rights Res
File	8:Ei Compendex(R) 1884-2007/Nov W3	(c) 2007 Elsevier Eng. Info. Inc.
File	34:SciSearch(R) Cited Ref Sci 1990-2007/Nov W4	(c) 2007 The Thomson Corp
File	35:Dissertation Abs Online 1861-2007/Jul	(c) 2007 ProQuest Info&Learning
File	56:Computer and Information Systems Abstracts 1966-2007/Oct	(c) 2007 CSA.
File	60:ANTE: Abstracts in New Tech & Engineer 1966-2007/Nov	(c) 2007 CSA.
File	62:SPIN(R) 1975-2007/Nov W2	(c) 2007 American Institute of Physics
File	65:Inside Conferences 1993-2007/Nov 26	(c) 2007 BLDSC all rts. reserv.
File	95:TEME-Technology & Management 1989-2007/Nov W3	(c) 2007 FIZ TECHNIK
File	99:Wilson Appl. Sci & Tech Abs 1983-2007/Sep	(c) 2007 The HW Wilson Co.
File	111:TGG Natl. Newspaper Index(SM) 1979-2007/Nov 15	(c) 2007 The Gale Group

File 144:Pascal 1973-2007/Nov W2
 (c) 2007 INIST/CNRS
File 239:Mathsci 1940-2007/Nov
 (c) 2007 American Mathematical Society
File 256:TecInfoSource 82-2007/Dec
 (c) 2007 Info.Sources Inc
File 434:SciSearch(R) Cited Ref Sci 1974-1989/Dec
 (c) 2006 The Thomson Corp
File 583:Gale Group Globalbase(TM) 1986-2002/Dec 13
 (c) 2002 The Gale Group

Set	Items	Description
S1	3042	CRITICAL?() (CODE? ? OR CODING) OR (NEST??? OR INNER?) () LOOP? ? OR ATOMIC() EXECUT?
S2	301	S1(5N) (DETERMIN? OR COMPAR? OR ASCERTAIN? OR ANALY? OR IDENT? OR CHECK? OR VERIF? OR JUDGE? ? OR JUDGING?)
S3	98	S1(5N) (MONITOR? OR EXAMIN? OR DETECT? OR UNCOVER? OR REVEAL? OR ASSESS? OR EVALUAT? OR INSPECT? OR DISCOVER?)
S4	195	S1(5N) (REPLAC? OR SUBSTITUT? OR PLACE() "OF" OR REWRIT? OR RE() WRIT??? OR MODIF? OR REVIS??? OR CHANG??? OR UPDATING? OR UP() (DATE? ? OR DATING) OR UPGRAD? OR CUSTOMI? OR ALTER??? OR OPTIMI?)
S5	44312	(CALL??? OR INVOK? OR INVOC?) (3N) (FUNCTION? OR COMMAND? OR INSTRUCT? OR PROCEDURE? ?)
S6	10854	S5(5N) (USE? ? OR USING OR UTILI? OR APPLY? OR APPLIE? ? OR EMPLOY? OR IMPLEMENT? OR "WITH")
S7	3	(COMPIL? OR RUN OR RUNS OR RUNNING) (7N) S4
S8	0	S2:S3(100N) S4(100N) S5:S6
S9	11	S2:S3(100N) S4
S10	7	S1(100N) EXTEN? (7N) COMPIL?
S11	18	S9:S10(100N) (CRITICAL?() (CODE? ? OR CODING) OR (NEST??? OR INNER?) () LOOP? ?)
S12	9	S11 AND PY=1978:2003
S13	11	S11 AND (AC=US OR AC=US/PR) AND AY=1978:2003
S14	12	S12:S13
S15	0	S4(100N) S6
S16	13	S4(100N) S5
S17	11	S16 NOT S9:S14
S18	11	S17(100N) (CRITICAL?() (CODE? ? OR CODING) OR (NEST??? OR INNER?) () LOOP? ?)
S19	8	S18 AND PY=1978:2003
S20	10	S18 AND (AC=US OR AC=US/PR) AND AY=1978:2003
S21	10	S19:S20
File 348:EUROPEAN PATENTS 1978-2007/ 200744		
(c) 2007 European Patent Office		
File 349:PCT FULLTEXT 1979-2007/UB=20071122UT=20071115		
(c) 2007 WIPO/Thomson		

Set	Items	Description
S1	3042	CRITICAL?() (CODE? ? OR CODING) OR (NEST??? OR INNER?()) LOOP? ? OR ATOMIC()EXECUT?
S2	301	S1(5N) (DETERMIN? OR COMPAR? OR ASCERTAIN? OR ANALY? OR IDENT? OR CHECK? OR VERIF? OR JUDGE? ? OR JUDGING?)
S3	98	S1(5N) (MONITOR? OR EXAMIN? OR DETECT? OR UNCOVER? OR REVEAL? OR ASSESS? OR EVALUAT? OR INSPECT? OR DISCOVER?)
S4	195	S1(5N) (REPLAC? OR SUBSTITUT? OR PLACE() "OF" OR REWRIT? OR -RE()WRIT??? OR MODIF? OR REVIS??? OR CHANG??? OR UPDATING? OR UP() (DATE? ? OR DATING) OR UPGRAD? OR CUSTOMI? OR ALTER??? OR OPTIMI?)
S5	44312	(CALL??? OR INVOK? OR INVOC?) (3N) (FUNCTION? OR COMMMAND? OR INSTRUCT? OR PROCEDURE? ?)
S6	10854	S5(5N) (USE? ? OR USING OR UTILI? OR APPLY? OR APPLIE? ? OR EMPLOY? OR IMPLEMENT? OR "WITH")
S7	3	(COMPILE? OR RUN OR RUNS OR RUNNING) (7N) S4
S8	0	S2:S3(100N) S4(100N) S5:S6
S9	11	S2:S3(100N) S4
S10	7	S1(100N) EXTEN? (7N) COMPILE?
S11	18	S9:S10(100N) (CRITICAL?() (CODE? ? OR CODING) OR (NEST??? OR INNER?()) LOOP? ?)
S12	9	S11 AND PY=1978:2003
S13	11	S11 AND (AC=US OR AC=US/PR) AND AY=1978:2003
S14	12	S12:S13
S15	0	S4(100N) S6
S16	13	S4(100N) S5
S17	11	S16 NOT S9:S14
S18	11	S17(100N) (CRITICAL?() (CODE? ? OR CODING) OR (NEST??? OR INNER?()) LOOP? ?)
S19	8	S18 AND PY=1978:2003
S20	10	S18 AND (AC=US OR AC=US/PR) AND AY=1978:2003
S21	10	S19:S20

File 348:EUROPEAN PATENTS 1978-2007/ 200744

(c) 2007 European Patent Office

File 349:PCT FULLTEXT 1979-2007/UB=20071122UT=20071115

(c) 2007 WIPO/Thomson